Design of Rare-Earth Organometallic Complexes Stabilized by Novel Cyclopentadienyl-Phosphazene and Modified Dialkylbenzylamine Ligand Regimes

Dissertation

zur

Erlangung des Doktorgrades

der Naturwissenschaften

(Dr. rer. nat.)

dem

Fachbereich Chemie

der Philipps-Universität Marburg

vorgelegt von

Alexander R. Petrov

aus

Yakutsk, Russland

Marburg/Lahn

2008

Die vorliegende Dissertation entstand in der Zeit von Oktober 2002 bis August 2008 am Fachbereich Chemie der Philipps-Universität Marburg in der Arbeitsgruppe und unter Betreuung von Herrn Prof. Dr. Jörg Sundermeyer und Herrn Dr. Konstantin A. Rufanov (Chemistry Department, M. V. Lomonosov State University of Moscow).

Vom Fachbereich Chemie der Philipps-Universität Marburg
als Dissertation am _____ angenommen.

Erstgutachter: Herr Prof. Dr. Jörg Sundermeyer
Zweitgutachter: Herr Prof. Dr. Martin Bröring

Wissenschaftlicher Betreuer: Herr Dr. Konstantin A. Rufanov

Tag der mündlichen Prüfung am 12.8.2008

to my parents

Those who aspire not to guess and divine, but discover and know,
who propose not to devise mimic and fabulous worlds of their own,
but to examine and dissect the nature of this very world itself,
must go to the facts themselves for everything.

F. Bacon, 1620

Articles:

A. Petrov, K. A. Rufanov, V. V. Kotov, F. Laquai, J. Sundermeyer
A Lutetium Cyclopentadienyl-Phosphazene Constrained Geometry Complex (CGC): First Isolobal Analoues of group 4 Cyclopentadienyl-Silylamino CGC Systems.
Eur. J. Inorg. Chem. **2005**, 3805–3807.

A. R. Petrov, K. A. Rufanov, B. Ziemer, P. Neubauer, V. V. Kotov, J. Sundermeyer
P-Amino-cyclopentadienylidene-phosphoranes *versus P*-cyclopentadienyl-iminophosphoranes – tautomeric protic forms of a new bidentate *CpPN* ligand system.
Dalton Trans. **2008**, 909–915.

K. A. Rufanov, B. Ziemer, **A. R. Petrov**, K. Harms, J. Sundermeyer
Organophosphorus(V) ligands for coordination and organometallic chemistry. Part 7: Synthesis and Molecular Structures of a Series of New Cyclopentadienyl-Phosphazene Constrained-Geometry Complexes of Rare-Earth Metals.
Dalton Trans, **2008**, *submitted.*

A. R. Petrov, K. A. Rufanov, K. Harms, J. Sundermeyer
Re-investigation of *ortho*-Metallated Dimethylbenzylamine Complexes of Rare-Earth Metals. First Structurally Characterized Nd and Gd *tetrakis*-Arylates.
J. Organomet. Chem. **2008**, *submitted.*

A. R. Petrov, J. Möbus, K. Harms, J. Sundermeyer
Synthesis and Chemistry of a New Highly Sterically Crowdered Cyclopentadienyl-Phosphane.
J. Organomet. Chem. **2009**, *in preparation.*

Reports:

A. R. Petrov, K. A. Rufanov, J. Sundermeyer;
Rare-Earth Constrained-Geometry Complexes (*CGC*) with a New Cyclopentadienylidene-*P*-Aminophosphorane (*CpPN*) Ligand System.
18th Workshop on Rare Earth Chemistry: *Terrae Rarae*.
Universität zu Köln, Köln (Bonn-Röttgen), November **2005**.

A. R. Petrov, K. A. Rufanov, J. Sundermeyer;
Exploration of Lanthanide (II, III) – *CpPN* – Complexes: Synthesis and Reactivity Studies,
19th Workshop on Rare Earth Chemistry, Terrae Rarae.
Universität Oldenburg, Oldenburg, November **2006**.

Poster Presentations:

K. A. Rufanov, **A. Petrov**, J. Sundermeyer
New Iminophosphonamide Ligands on the Basis of BINAMIN & TADDAMIN Auxiliaries.
Proceedings of the 12th Conference of the Inorganic Chemistry Division (Wöhler-Vereinigung für Anorganische Chemie) of the GDCh
Philipps-Univeristät Marburg, Marburg, September **2004**, P-048.

K. A. Rufanov, **A. R. Petrov**, J. Sundermeyer
New concept of ligand design for rare-earth and lanthanide organometallics.
Keynote lecture, 17th Workshop on Rare Earth Chemistry and 1. Berichtskolloquium im Rahmen des SPP 1166
Universität Bayreuth, Bayreuth, December **2004**.

K. A. Rufanov, **A. Petrov**, J. Sundermeyer
Synthesis, Structures and Reactivity of a New Family of Cyclopentadienyl-Phospahazene (*"CpPN"*) Constrained-Geometry Complexes (*CGC*)
of the Rare-Earth Metals (Sc, Y, Nd, Lu).
Proceedings of the Symposium of the Graduiertenkolleg 352.
Technische Universität Berlin, Berlin, November **2005**.

K. A. Rufanov, **A. Petrov**, J. Sundermeyer
Rare-Earth Constrained-Geometry Complexes (*CGC*) with a New Cyclopentadienylidene-*P*-Aminophosphorane (*"CpPN"*) Ligand System.
Proceedings of the 18th Workshop on Rare Earth Chemistry.
Universität zu Köln, Köln (Bonn-Röttgen), December **2005**.

A. Petrov, K. A. Rufanov
Lanthanide *tris*- and *tetrakis*- Aryl Complexes with pendant Dialkylamino Arms.
Proceedings of the 18th Workshop on Rare Earth Chemistry.
Universität zu Köln, Köln (Bonn-Röttgen), December **2005**.

A. R. Petrov, J. Sundermeyer
Neue Herausforderungen in der metallorganischen Chemie mit Elementen der Gruppe 3 und Lanthanoide. Cyclopentadienyl-Iminophphosphoran Constrained-Geometry Komplexe (*CGC*) der Lanthanoiden.
GdCh Jahrestagung
Heinrich Heine Universität Düsseldorf, Düsseldorf, September **2005**

K. A. Rufanov, **A. R. Petrov**
New hydroamination catalysts on the basis of tris- and tetrakis-aryl complexes of lanthanides with chelating dialkylamino groups (*in Russian*).
International Symposium Advanced Science in Organic Chemistry (ACOS in Crimea 2006)
Sudak, Crimea, June **2006**.

A. R. Petrov, O. Thomas, J. Sundermeyer
New, Homoleptic *tris*-Aryl Complexes of the Rare Earth Metals.
20th Workshop on Rare Earth Chemistry, Terrae Rarae,
Universität zu Köln, Köln (Bonn-Röttgen), November, **2007**.

Acknowledgements

I would like to acknowledge everyone who extended their support and help during the course of this work. My deep sense of gratitude goes to:

- Prof. Dr. Jörg Sundermeyer for a great opportunity to perform my PhD work in the one of the best universities of Germany under his supervision and for establishing an interesting research topic.
- Dr. Konstantin Rufanov for his introduction in practical organometallic chemistry to me, interesting discussions all around chemistry as well as for a nice time in and out side of laboratory.
- Prof. Dr. Andreas Seubert, Prof. Dr. Gerhard Hilt and Prof. Dr. Martin Broering that they kindly agreed to familiarized themselves with my Thesis and to express their opinion as scientific referees.
- Prof. (Emeritus) Manfred Meisel for his manificient support during my stay at his research group in the Institut für Chemie der Humboldt-Universität zu Berlin.
- Dr. Klaus Harms for all X-ray structures he determined and solving computer problems arose.
- Gertraud Geiseler for her patient and preparation of my very ″important″ crystals.
- Burkhard Ziemer and Petra Neubauer from the Institut für Chemie der Humboldt-Universität zu Berlin for X-ray structure determination of crystals with the lowest R-factor ever been seen at the department.
- Dr. Thomas Linder and Michael Elfferding for fast solution and refinement of a numerous crystal data.
- Dr. Xiulan Xie for being ready to help to hold the stand-by modus on NMR spectrometers.
- All colleagues of analytical laboratories of the department for spectroscopic measurements even at holidays.
- My AFP colleagues – Drs. Christian Kleeberg and Thomas Linder – during the time of inorganic practicum for precise organization and time management.
- Irene Barth for being actively involved in decision of any questions with respect to the lab management – patience in preparation of huge amounts of the solvents needed and holding order in our really big lab.

▫▪▫ Drs. Marat M. Khusniyarov and Katya Gauotchenova for their help in the creation of reliable chemical database, typing and labeling of many thousands chemicals in our laboratory.

▪▫▪ Dr. Daniel Gaess for instant holding of all three glove-boxes in running regime.

▫▪▫ Jan Döring for his grateful help in any kind of problems with Microsoft© and PC's, that ones saved a part of the work presented below.

▪▫▪ Konstantin I. Smolko† for interesting discussions in chemistry.

▪▫▪ All present and past PhD students I worked with: Marik, Alexey&Katja, Denis, Nuri, Jan, Daniel, Thomas, Andi, Udo, Ralf, Wael, Fuming.

▪▫▪ All new PhD students that give start of the ″new age″ in our laboratory: Marion, Michael, Wolf, Olli, Nina and Kristina, Benjamin.

▫▪▫ All students worked with me during their AFP practicum for their patience in complete analysis of a mass of new compounds synthesized.

▫▪▫ All my old and new friends I found in Moscow and Marburg.

▪▫▪ My mother Anastasia – who never prohibited my ″research″ work in my ″hood″ at -50 °C and good chemical books and journals.

▫▪▫ My father Robert – who showed me that the world is bigger than a village and gave me inspiration to believe on ″what would happen, if we …″

Table of Content

CHAPTER III

P-Amino-Cyclopentadienylidene-Phosphoranes

versus

P-Cyclopentadienyl-Imino-Phosphoranes

Development and Investigation of *CpPN*-Ligand System

CHAPTER IV

Synthesis and Chemistry of a New Highly Crowded Cyclopentadienyl-Phosphane

CHAPTER V

Rare-Earth Metal Cyclopentadienyl-Phosphazene-Complexes
A New Dimension for *Constrained-Geometry-Catalysts* Variability

List of Abbreviations

Ad	1-adamantyl group
Alk	aliphatic substituent
Ar	aromatic substituent
Bu	butyl group
Cp	cyclopentadienyl (C_5H_5)
C5	cyclopentadienyl ring
dec.	decomposition temperature
Dip	2,6-di-*iso*-propylphenyl group
DME	dimethoxyethane
EI	electron ionization
ESI	electrospray ionization
Flu/FluH	fluorenilydene/fluorenyl group
Ind/IndH	indenylidene/indenyl group
Hal	halogene (F, Cl, Br, I)
M.p.	melting point
m/z	mass-to-charge ratio
MAO	methylalumoxane
Me	methyl group
Mes	mesityl, 2,4,6-trimethylphenyl group
MS	mass spectrometry
NMR	nuclear magnetic resonance
Ph	phenyl group
pmdeta	*N,N,N',N",N"*-pentamethyl-diethylene-diamine
iso-Pr	*iso*-propyl
Py	pyridine
R	organic substituent
SSC	single-site-catalyst
TACN	N,N-dimethyl-1,3,6-triazacyclononane
THF	tetrahydrofurane
TMEDA	*N,N,N',N'*-tetramethyl-ethylenediamine
TMS	tetramethylsilane
TON	turn-over-number
xs	excess
Z	centroid of cyclopentadienyl ring

List of Compounds and their Numbering

In the presented work several different classes of compounds are disclosed. For symplisity the numbering system is ordered according to the substance class. To each class of compounds discussed in the work, a two-digit symbol ([**A**][**n**]) is assigned. The symbols consist of a letter ([**A**]) followed by a number ([**n**]). In the following table the correspondence of the first symbol and the substance class is given. Compounds denoted with (*) are new.

Substance class	*First symbol*
ortho-lithiated benzylamine-type **R**eagents	**R__**
Homoleptic aryl-rare earth complexes	**H__**
diorganyl-cyclopentadienyl-**P**hosphanes	**P__**
diphenyl-**F**ulvenyl-phosphanes	**F__**
CpPN-type **L**igands	**L__**
CpPN-lanthanide **C**omplexes	**C__**
remaining **S**ubstances [§)]	**S__**

[§)] Compounds not belonging to any above mentioned substance class.

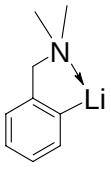

R1

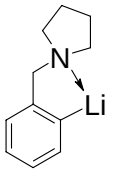

R2*

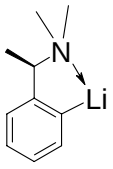

R3

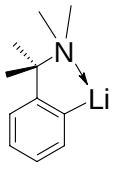

R4*

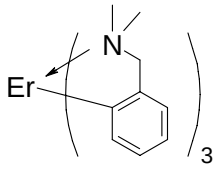

H1

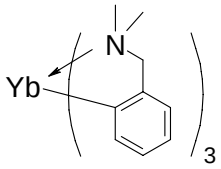

H2

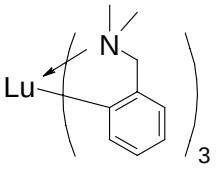

H3

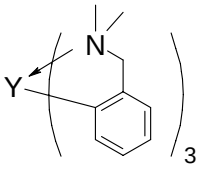

H4

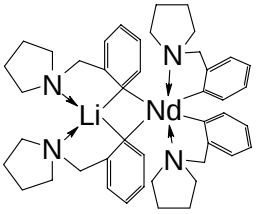

H5*

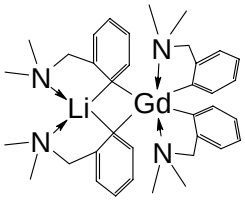

H6*

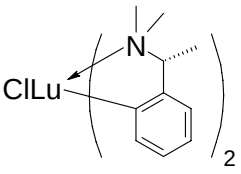

H7' *

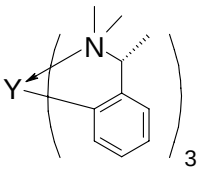

H8*

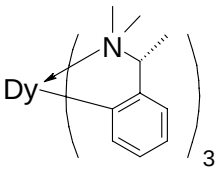

H9*

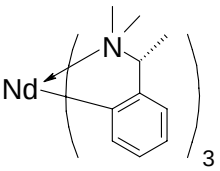

H10*

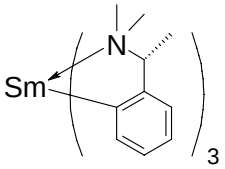

H11*

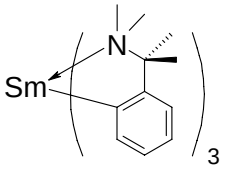

H12*

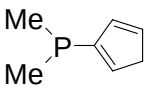

P1

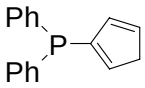

P2

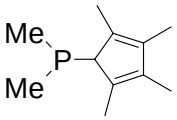

P3

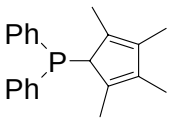

P4

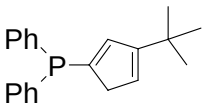

P5

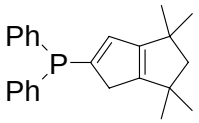

P6*
($Ph_2PCp^{TM}H$)

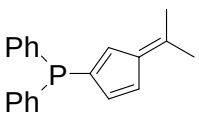

F1*

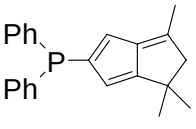

F2*

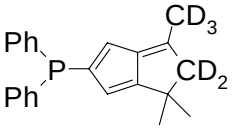

F3*

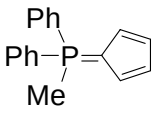

S1

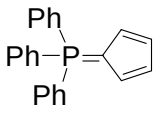

S2

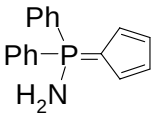

S3[*]

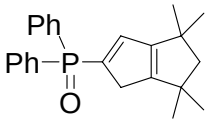

S4[*]

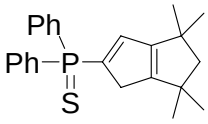

S5[*]

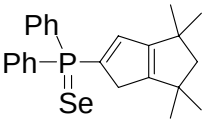

S6[*]

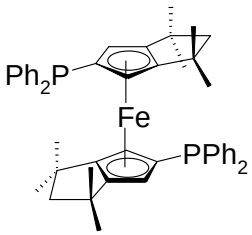

S7[*] (dppf[TM])

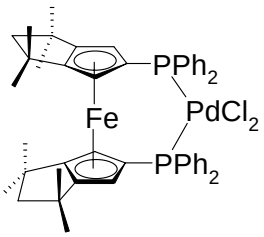

S8[*]

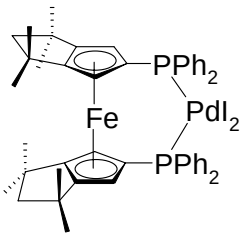

S9[*]

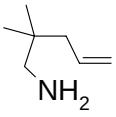

S10

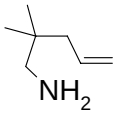

S11

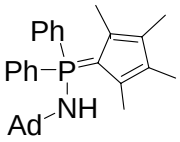

S12

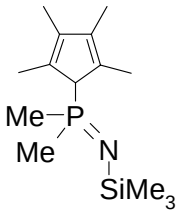

L1[*]

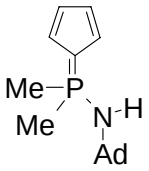

L2[*]

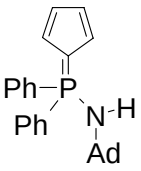

L3[*]

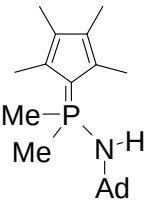

L4[*]

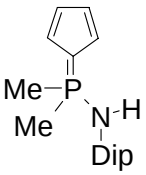

L5[*]

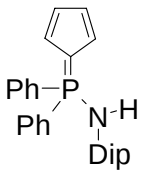

L6[*]

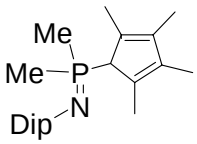

L7[*]

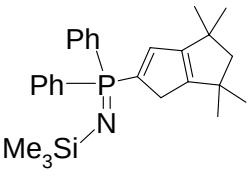

L8[*]

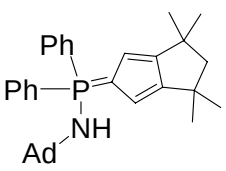

L9[*]

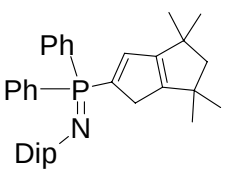

L10[*]

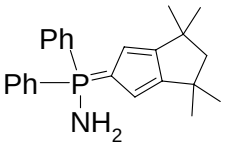

L11[*]

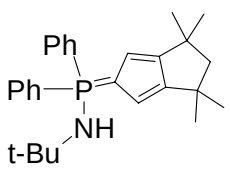

L12[*]

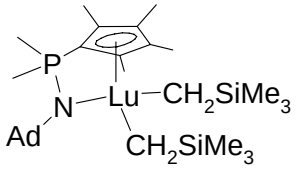

C1[*]

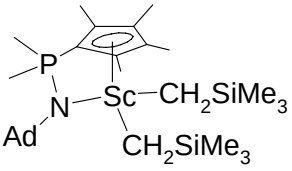

C2[*]

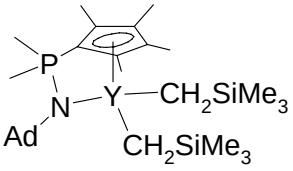

C3[*]

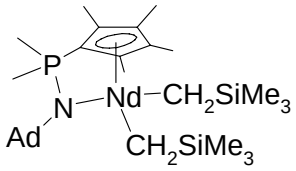

C4[*]

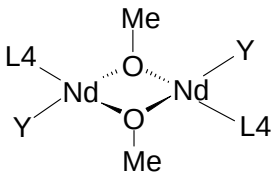

C5[*]
(Y = CH_2SiMe_3)

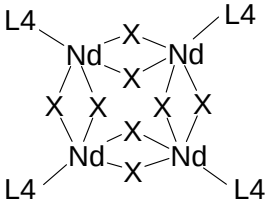

C6[*]
(X = OH)

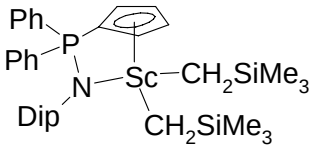

C7[*]

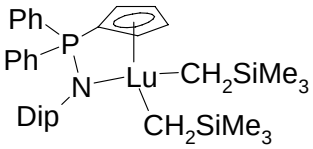

C8[*]

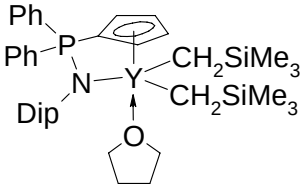

C9[*]

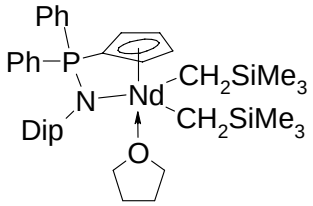

C10[*]

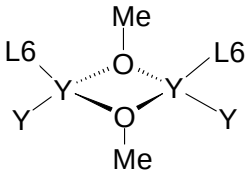

C11[*]

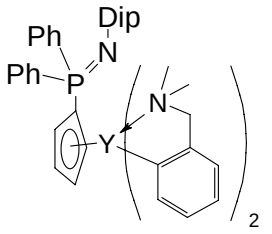

C12[*]

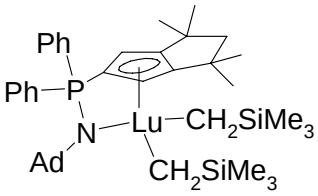

C13[*]

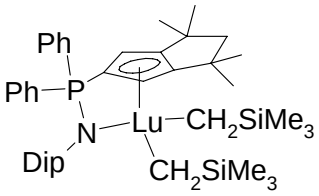

C14

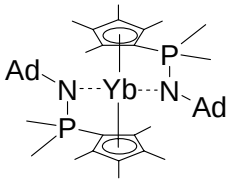

C15[*]

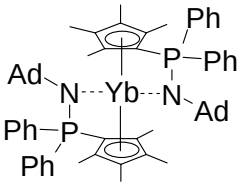

C16[*]

GENERAL INTRODUCTION

Low density polyethylene had been formed during high-pressure radical polymerization experiments with ethylene by ICI scientists *R. O. Gibson* and *E. W. Fawcett*.[1] Since then classic polyolefines (polyethylene, polypropylene) and polystyrene became most important commodities of our daily life with more than 130×10^6 tons of their annual world-wide production.[2]

Today, most polyethylene and polypropylene is produced by transition metal catalysts. Two main discoveries are standing in the background: 1) the pioneer works of *Ziegler*[3] and *Natta*[4] demonstrated a real possibility to polymerize ethylene and propylene even at low pressure in the presence of $TiCl_4/Et_2AlCl$ catalytic system and 2) the discovery of chromium based Phillips catalysts by *Hogan* and *Banks*.[5] A major disadvantage of these classic catalytic systems is the heterogeneous nature of the catalysts that prevented a thorough characterization of their active sites and for a long time left many questions open concerning concrete mechanisms involved in polymer growth.[6,7,9,10]

The development of well-defined, homogeneous metallocene catalysts (single-site-catalysts, SSC) and suitable cocatalysts such as methylalumoxane (MAO) in the early 1980s raised high expectations for industrial applications of new, tailor-made polymers.[7] The first generation of SSCs is represented by bent metallocenes, mainly titanocenes and zirconocenes. Already in the late 1980s and further during the last decade of the XXth century the researchers' interest was more and more drawn to the other types of pre-catalysts. Among them there were *ansa*-metallocenes bearing sophisticated modifications in the ligand framework, achieved at the central laboratories of *Hoechst AG* (Scheme 1, **A**),[8] half-sandwich complexes of groups 3 and 4 metals with the linked (cyclopentadienylsilyl)amido ligand framework, better known as "*constrained-geometry catalysts*" (*CGC*) and almost simultaneously developed by two groups of academic[15,16] and two groups of industrial[9] researches (Scheme 1, **B**) and finally the late transition metal complexes with chelating tri- and diazene-type ligands (Scheme 1, **C** and **D**) also achieved independently by several researches[10,11,12] thus culminating the paradigm change from metallocene to non-metallocene catalysts.

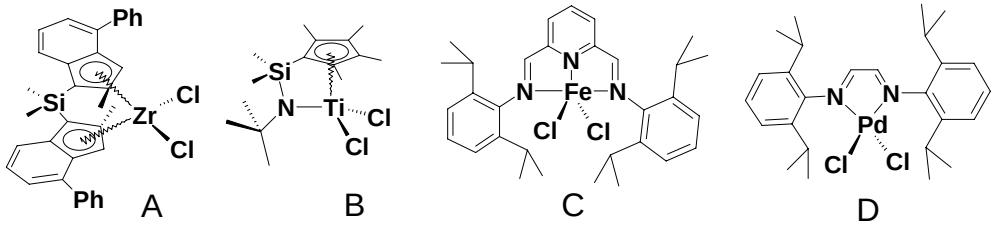

Scheme 1. Examples of olefin polymerization pre-catalysts

When compared to metallocenes these new generation catalysts showed improved stabilities towards high temperatures and MAO and remarkably increased incorporation rates of higher olefins in copolymerizations with ethylene.

The term "*constrained-geometry*" complex was originally coined by *Stevens* for complexes in which a π-bonded moiety (e.g. cyclopentadienyl or a derivative) is linked to one of the other ligands on the same metal centre in such a way that the angle at this metal between the centroid of the π-system and the additional ligand is smaller than in comparable un-bridged complexes. *Stevens et al*. claimed in their patent, that such a strain inducing link would improve catalyst performance. Their thesis was supported by a comparison of the polymerization performance of a series of silanediyl and disilanediyl bridged cyclopentadienyl amido complexes.[13]

The superiority of *CGC*s for copolymerization of ethylene and α-olefins when compared to metallocenes is generally ascribed to (i) a less crowded coordination sphere, (ii) a by 25–30° smaller Cp(centroid)–M–N bite angle compared to Cp(centroid)–M–Cp'(centroid) in (*ansa*)-metallocenes and (iii) a decreased tendency of the bulk polymer chain to undergo chain transfer reactions. Another advantage is the higher thermal stability of alkyl and dialkyl *CGC*s when compared to related metallocenes[14] that allows higher polymerization temperatures.

Obviously, the scope of the definition given by *Stevens* goes far beyond *ansa*-bridged cyclopentadienyl amido complexes and was accordingly used in connection with other more or less related ligand systems, including (i) other *ansa*-complexes with η^5,η^1-coordination, where at least one of the coordinating fragments of bridged cyclopentadienyl-amido complexes is replaced by an isolobal fragment, (ii) other *ansa*-complexes with η^5,η^1-coordination, where at least one of the coordinating fragments is not isolobal to the formally replaced fragments of bridged cyclopentadienyl-amido complexes and (iii) other *ansa*-complexes with a coordination mode different from η^5,η^1-coordination.

The first group III and IV constrained geometry catalyst were synthesized by *Bercaw* and *Shapiro*[15] (scandium) and *Okuda*[16] (titanium) in 1990 *via the salt metathesis* route by the metallation of the doubly deprotonated ligand {(C_5Me_4)$SiMe_2$(NH-*tert*-Bu)} with appropriate metal chlorides (Scheme 2).

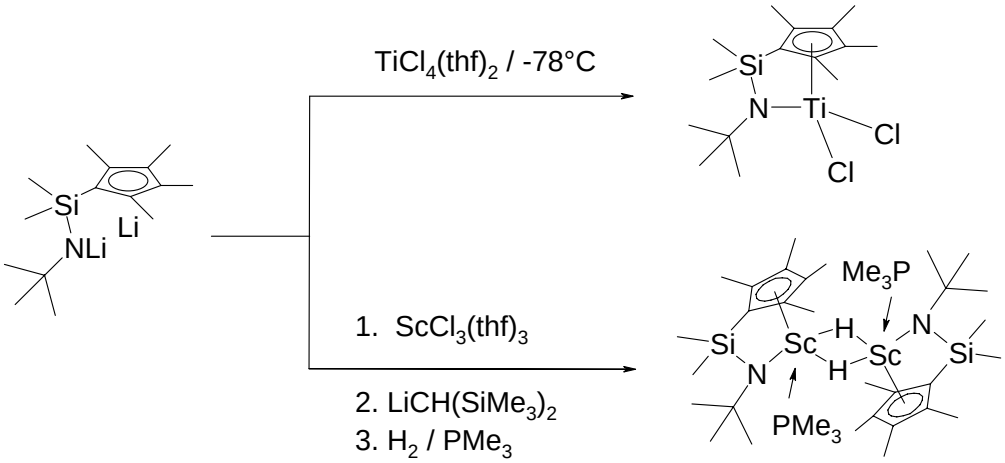

Scheme 2. Synthesis of the first reported "*constrained-geometry*" complexes (*CGC*)

The cyclopentadienyl-silylamido (*CpSiN*) ligands belong to one of the best developed classes of chelating cyclopentadienyl-amido early transition metal complexes, because of their numerous industrial application as single-site olefin polymerization catalysts.

The diversity of *CGC* systems can be achieved by variation of the substituents at the C5-ring ($C_5Me_{5-n}H_n$, indenyl, fluorenyl, etc.), donor-atom linked to the bridging motiv (N, C, P, O) and the bridging unit itself. The most detailed analysis of the chemistry of *CGC*s are presented in reviews of *Braunschweig* and *Brightling*[17] and *Cano* and *Kunz*.[18]

Besides silicon, only a few other elements have been used to connect the respective ligand fragments in *ansa*-cyclopentadienyl amido complexes by a short, single atom bridge (Scheme 3). These include boron (R_2NB),[19] carbon in both the sp^2 (H_2C=C) [20,21] or sp^3 (RHC, R= Akl, Ar) [22,23] hybridized forms and phosphorous(III) (*tert*-BuP).[24]

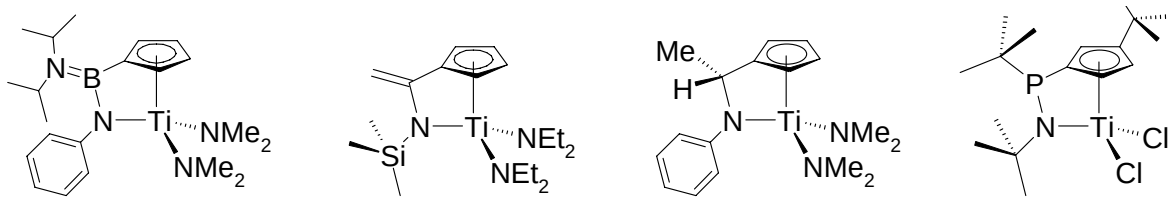

Scheme 3. *CGC*s with non-silicon single atom bridges

Beyond their application in polymerization reactions, *CGC*s experience increasing relevance in the catalysis of various other transformations.

In a comparative study, *Teuben* and co-workers demonstrated the catalytic activity of some group 4 *CGC*s, namely [{η^5,η^1-(C_5H_4)(CH_2)$_3$NMe}MR_2] (MR_2 = $TiMe_2$, $Zr(BH_4)_2$, $ZrBn_2$), for the hydroboration of 1-hexene with catecholborane (Scheme 4). These *CGC*s showed a much lower catalytic activity than the benchmark catalyst [{η^5-C_5Me_5}$_2$LaCH($SiMe_3$)$_2$], but a better stability under the reaction conditions applied.[25]

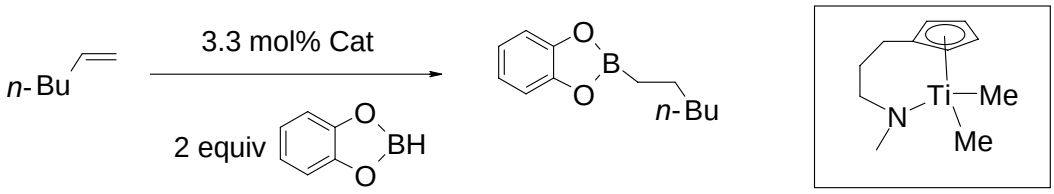

Scheme 4.

Okuda et al. showed that [{η^5,η^1-(C_5Me_4)$SiMe_2$(NR*)}$TiCl_2$] (R* = optically pure chiral alkyl group) can efficiently catalyze the hydrogenation of imines, e.g. acetophenone *N*-benzylimine, upon activation with two equivalents of *n*-BuLi (Scheme 5).

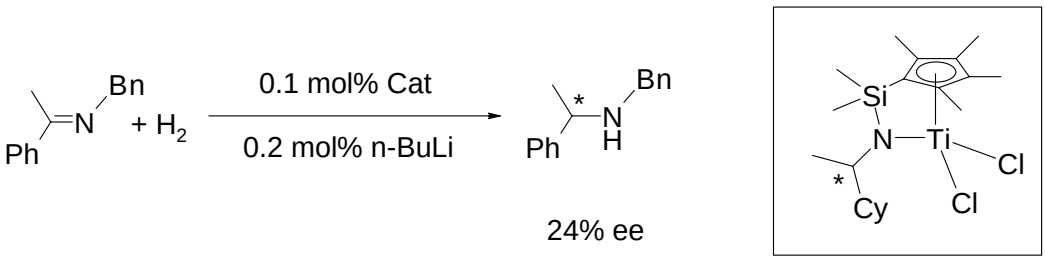

Scheme 5.

Marks and co-workers reported the high efficiency of lanthanide and actinide *CGC*s[26,27] for the intramolecular hydroamination/cyclization reaction of various *ω*-alkylamines (Scheme 6)

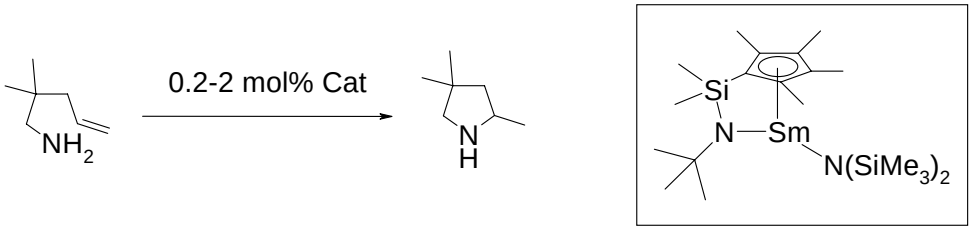

Scheme 6.

Okuda and *Trifonov* applied [{η^5,η^1-(C_5Me_4)CH_2SiMe_2N(*tert*-Bu)}Y(thf)(μ-H)]$_2$ and [{η^5,η^1-(C_5Me_4)$SiMe_2$(N-*tert*-Bu}Y(thf)(μ-H)]$_2$ in the hydrosilylation of olefins with good results. Thus, the former catalyst quantitatively converted 1-decene in the presence of $PhSiH_3$ to the *anti-Markovnikov* product *n*-$C_{10}H_{21}SiH_2Ph$ (Scheme 7).[28]

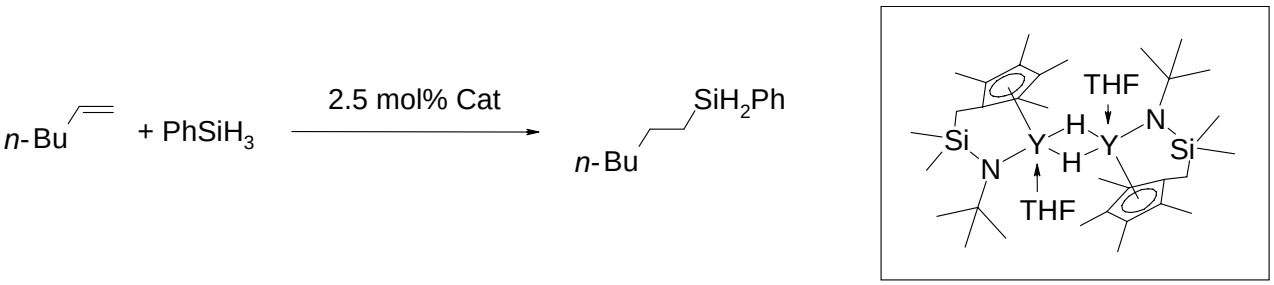

Scheme 7.

Waymouth and co-workers applied catalytic amounts of titanium *CGC* [{η^5,η^1-(C_5Me_4)$SiMe_2$(N-*tert*-Bu)}$TiMe_2$] / $[Ph_3C]^+[B(C_6F_5)_4]^-$ in the presence of $AlMe_3$ or $AlEt_3$ for the carboalumination of a variety of α-olefins (Scheme 8). Strong evidence that supports a mechanism involving olefin insertion into a Ti–C bond followed by transmetalation was given in the report. Catalytic amounts of a chiral titanium *CGC*s [{η^5,η^1-(Ind)$SiMe_2$N(CHMePh)}$TiCl_2$] were also used in asymmetric carbometallation of α-olefins with $AlEt_3$.[14]

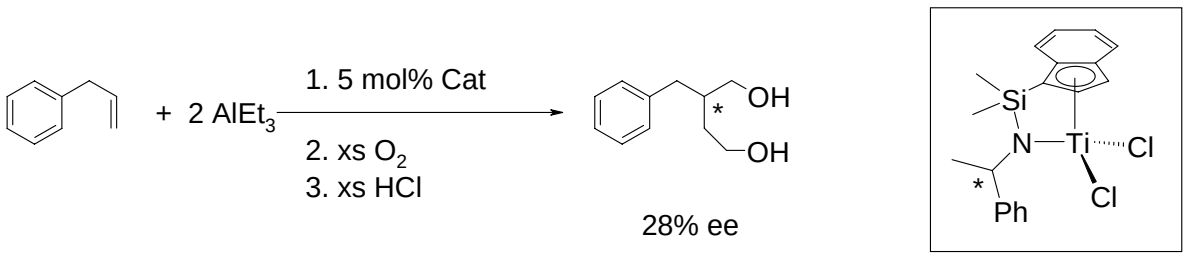

Scheme 8.

Furthermore, complexes [{η^5,η^1-(C_5Me_4)$SiMe_2$NR}M(CH_2SiMe_3)$(thf)_n$] (M = Y, Yb, Lu; R = *tert*-Bu, Ph, 2,4,6-$Me_3C_6H_2$; n = 1, 2) were found to catalyze dimerization of various termi nal alkynes with high activity (Scheme 7). Almost exclusively *head-to-head*-(Z)-dimerization products were formed, exhibiting a high degree of regio- and stereoselectivity (Scheme 9).[29] In fact, this reaction presents the first example of such selectivity for aromatic alkynes.[27c] The reaction proceeds cleanly and tolerates the presence of carbon-halogen bonds that are known to be highly susceptible to reductive cleavage by transition metals.[29]

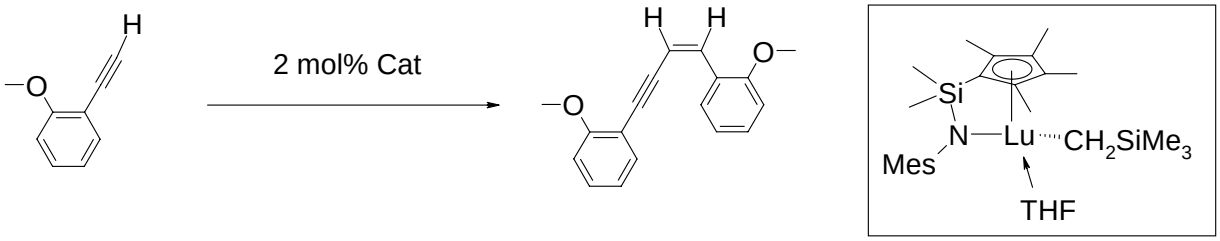

Scheme 9.

Research targets

The target of this Thesis was to develop new class of half-sandwich complexes for further investigation as potentially active catalytic system that might become an alternative to the known group 4 transition metals constrained-geometry catalysts. The approach chosen to reach this target consisted in the principle of isolobal analogy (Scheme 10). From a conceptual point of view, three-valent complexes on the basis of monoanionoc *CpPN* type ligands are isolobal, in case of group 3 metals even isoelectronic, to tetra-valent group 4 transition metal complexes with dianionic *CpSiN* type ligands.

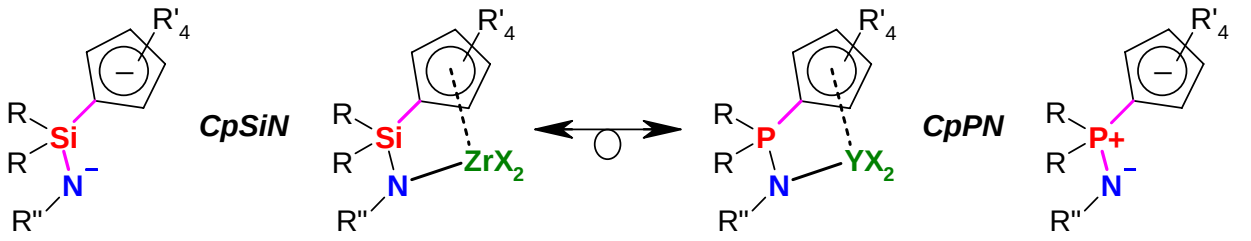

Scheme 10.

Having in mind this concept and the greater diversity of rare-earth metals the PRINCIPAL GOALS in this approach were defined as follows:

- to develop a convenient synthetic protocol for a large variety of the *CpPN* type ligands with different substituents at the N-, P-atoms and the C5-ring;
- to develop a convenient synthetic protocol to the group 3 and lanthanide complexes of *CpPN* ligands based on a representative pool of rare earth metals;
- to study reactivity, molecular structures and spectroscopic properties of both these new classes of organoelement compounds and organometallic complexes thereof.

In the course of these studies there were a lot of general problems both in ligand synthesis, precursor availability and organometallic chemistry appeared. For this reason the following aspects became FURTHER GOALS of this Thesis:

- synthesis of new rare-earth metal salts solvates as inorganic precursors for further synthetic applications;
- synthesis of new homoleptic lanthanide *tris*-aryl complexes with pendant tertiary amine arms as interesting organometallic precursors;
- synthesis of new cyclopentadienyl-phosphanes, as highly promising sterically hindered ligand precursors.

To what extent and how good or bad all these goals has been achieved is described below.

REFERENCES

[1] a) E. W. Fawcett, R. O. Gibson, M. W. Perrin, J. G. Paton, E. G. Williams (Imperial Chemical Industries Ltd.), GB 471,590, **1936**.

[2] PlasticsEurope Deutschland (Eds.), *Plastics Business Data and Charts*, Frankfurt, **2005**, http://www.vke.de.

[3] a) K. Ziegler, E. Holzkamp, H. Breil, H. Martin, *Angew. Chem*. **1955**, *67*, 541–647; b) K. Ziegler, *Angew. Chem*. **1964**, *76*, 545–553.

[4] a) G. Natta, P. Corradini, *Atti. Accad. Naz. Lincci Mem. Cl. Sci. Fis. Mat. Nat. Sez. II* **1955**, *5*, 73; b) G. Natta, *Angew. Chem*. **1956**, *68*, 393–403; c) G. Natta, *Angew. Chem.* **1964**, *76*, 553–566.

[5] a) J. P. Hogan, R. L. Banks, Belg. Patent 530,617 **1955**; b) M. P. McDaniel, *Adv. Catal*. **1985**, *33*, 47–98.

[6] B. M. Weckhuysen, R. A. Schoonheydt, *Catal. Today* **1999**, *51*, 215–221.

[7] H.-H. Brintzinger, D. Fischer, R. Mülhaupt, B. Rieger, R. Waymouth, *Angew. Chem.* **1995**, *107*, 1255–1283; *Angew. Chem., Int. Ed. Engl.* **1995**, *34*, 1143–1170.

[8] W. Spaleck, F. Kueber, A. Winter, J. Rohrmann, B. Bachmann, M. Antberg, V. Dolle, E. F. Paulus, *Organometallics* **1994,** *13*, 954–963.

[9] a) J. C. Stevens, F. J. Timmers, G. W. Rosen, G. W. Knight, S. Y. Lai (Dow Chemical Co.), Eur. Pat. Appl. EP0416815A2, **1991**; b) J. A. Canich (Exxon Chemical Co.), Eur. Pat. Appl. EP0420436A1, **1991**.

[10] G. J. P. Britovsek, V. C. Gibson, D. F. Weiss, *Angew. Chem.* **1999**, *111*, 448–468; *Angew. Chem. Int. Ed.* **1999**, *38*, 428–447.

[11] S. D. Ittel, L. K. Johnson, M. Brookhart, *Chem. Rev*. **2000**, *100*, 1169–1204.

[12] L. K. Johnson, C. M. Killian, M. Brookhart, *J. Am. Chem. Soc.* **1995**, *117*, 6414–6415.

[13] P. N. Stevens, F. J. Timmers, D. R. Wilson, G. F. Schmidt, P. N. Nickias, R. K. Rosen, G. W. Knight, S. Lai, *Eur. Pat. Appl*. EP 416815-A2, **1991**.

[14] a) P.-J. Sinnema, L.v.d. Veen, A. L. Spek, N. Veldman, J. H. Teuben, *Organometallics* **1997**, *16*, 4245–4247; b) D. B. Millward, A. P. Cole, R. M. Waymouth, *Organometallics* **2000**, *19*, 1870–1878.

[15] a) P. J. Shapiro, E. Bunel, W. P. Schaefer, J. E. Bercaw, *Organometallics* **1990**, *9*, 867–869. W. E. Piers, P. J. Shapiro, E. E. Bunel, J. E. Bercaw, *Synlett 1990*, 74–84; b) P. J. Shapiro, W. D. Cotter, W. P. Schaefer, J. A. Labinger, J. E. Bercaw, *J. Am. Chem. Soc*. **1994**, *116*, 4623–4640.

[16] J. Okuda, *Chem. Ber*. **1990**, *123*, 1649–1651.

[17] H. Braunschweig, F. M. Breitling, *Coord. Chem. Rev.* **2006**, *250*, 2691–2720.

[18] J. Cano, K. Kunz, *J. Organomet. Chem.* **2007**, *692*, 4411–4423.

[19] a) H. Braunschweig, C. von Koblinski, U. Englert, *Chem. Commun*. **2000**, 1049–1050; b) H. Braunschweig, F. M. Breitling, C. von Koblinski, A. J. P. White, D. J. Williams, *Dalton Trans*. **2004**, 938–943; c) H. Braunschweig, F. M. Breitling, K. Radacki, F. Seeler, *J. Organomet. Chem*. **2005**, *690*, 5000–5005; d) H. Braunschweig, F. M. Breitling, C. Burschka, F. Seeler, *J. Organomet. Chem.* **2006**, *691*, 702–710.

[20] L. Duda, G. Erker, R. Fröhlich, F. Zippel, *Eur. J. Inorg. Chem*. **1998**, 1153–1162.

[21] A. Bertuleit, M. Könemann, L. Duda, G. Erker, R. Fröhlich, *Top. Catal*. **1999**, *7*, 37–44.

[22] K. Kunz, G. Erker, S. Döring, R. Fröhlich, G. Kehr, *J. Am. Chem. Soc*. **2001**, *123*, 6181–6182.

[23] K. Kunz, G. Erker, S. Döring, S. Bredeau, G. Kehr, R. Fröhlich, *Organometallics* **2002**, *21*, 1031–1041.

[24] V. V. Kotov, E. V. Avtomonov, J. Sundermeyer, K. Harms, D. A. Lemenovskii, *Eur. J. Inorg. Chem*. **2002**, 678–691.

[25] E. A. Bijpost, R. Duchateau, J. H. Teuben, *J. Mol. Catal. A: Chem*. **1995**, *95*, 121–128.

[26] B. D. Stubbert, C. L. Stern, T. J. Marks, *Organometallics* **2003**, *22*, 4836–4838.

[27] a) V. M. Arredondo, S. Tian, F. E. McDonald, T. J. Marks, *J. Am. Chem. Soc.* **1999**, *121*, 3633–3639; b) S. Tian, V. M. Arredondo, C. L. Stern, T. J. Marks, *Organometallics* **1999**, *18*, 2568–2570; c) A. M. Seyam, B. D. Stubbert, T. R. Jensen, J. J. O'Donnell III, C. L. Stern, T. J. Marks, *Inorg. Chim. Acta* **2004**, *357*, 4029–4035.

[28] A. A. Trifonov, T. P. Spaniol, J. Okuda, *Organometallics* **2001**, *20*, 4869–4874.

[29] M. Nishiura, Z. Hou, Y. Wakatsuki, T. Yamaki, T. Miyamoto, *J. Am. Chem. Soc*. **2003**, *125*, 1184–1185.

– CHAPTER I –

Contributions to the Starting Material Synthesis. The new Route Towards Solvated Lanthanide Tribromides

Abstract

A new, convenient one-pot protocol towards the synthesis of anhydrous ether-solvated lanthanide tribromides using the water-catalyzed reaction of lanthanide(III) oxide and Me_3SiBr has been developed. Further optimization of this protocol lies in generation of highly reactive Me_3SiBr *in situ* from easily available Si_2Me_6 and Br_2. Thus, four solvated tribromides of neodymium and samarium – $[NdBr_3(dme)_2]$, $[NdBr_3(thf)_4]$, $[SmBr_3(dme)_2]$ and $[SmBr_3(thf)_2]$ were successfully synthesized in high yields.

1. INTRODUCTION

Due to the lanthanide contraction the atomic radii in the row of the lanthanides gradually decrease from 1.07 Å for Ce to 0.86 Å for Lu.[1] The atomic radius of the first element is almost 1.25 times larger than that of the last one in the period! Consequently, it is obvious that the chemistry of early and late lanthanide complexes differs markedly.

Conventionally, lanthanides have been subdivided into three groups – early (La – Sm), middle (Eu – Ho) and late (Er – Lu) lanthanides (Scheme 1). Outstanding is the lanthanide chemistry of the only radioactive one, namely promethium. This subdivision takes not only the structural and reactivity differences of the organolanthanide compounds into account, but also has large consequences for the synthetic accessibility of the starting materials.

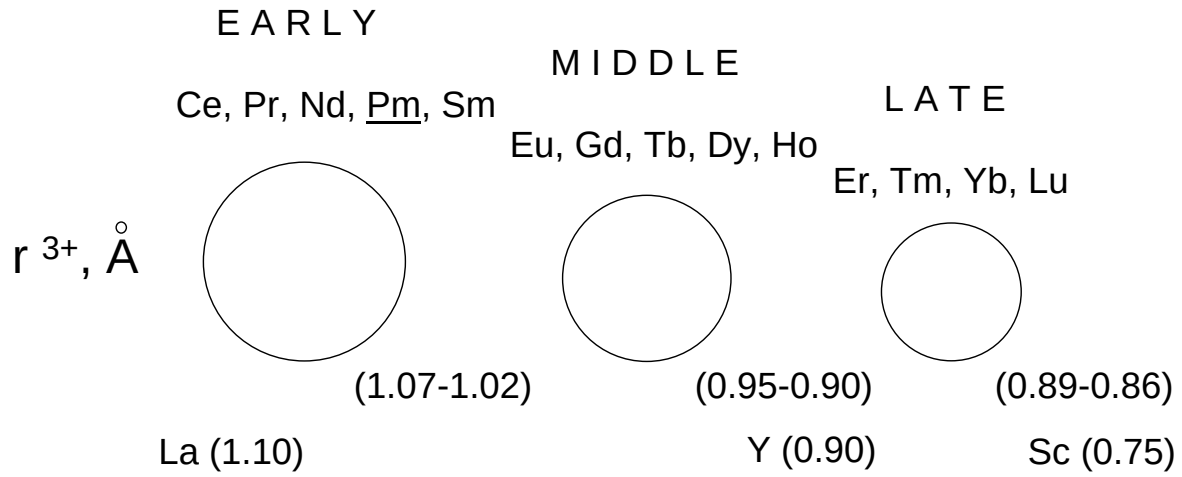

Scheme 1.

1.1. *Common Synthetic Routes and Starting Materials in Lanthanide Chemistry*

Among synthetic routes towards lanthanide organometallics there are only three which are rather common to all these metals. The most commonly used synthetic route is the *silylamine elimination route* based on *Brønsted* acid/base-type reactions of the homoleptic lanthanide *tris*-disilylamides. The second approach is based on protolysis of lanthanide alkyl or aryl complexes by the protonated form of appropriate ligand. For reason of simplicity this way will be called *alkane elimination route*. The good old *salt metathesis route* cannot be entirely substituted by the above mentioned modern elimination routes. The *salt metathesis route* is actually used for the synthesis of these amide and alkyl precursors (Scheme 2).[2]

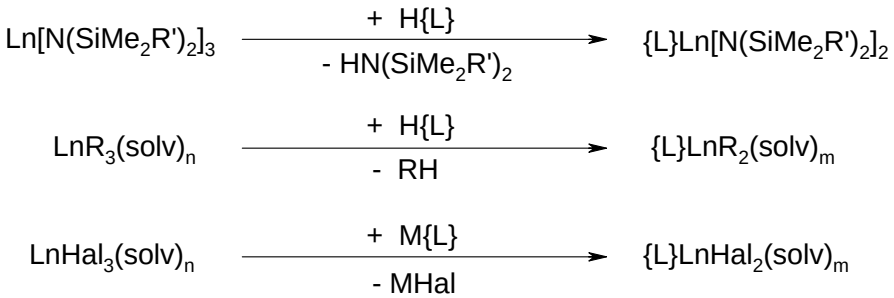

Ln = Sc, Y, La - Lu;
R' = H, Me, Ph;
solv = coordinating solvent molecule;
n, m = 0 - 4;

R = Alk, Ar;
{L} = ligand;
Hal = halogen atom;
M = alkali metal ion.

Scheme 2.

The key to a successful synthesis of lanthanide complexes is the right choice of an appropriate starting material. Although the Ln^{3+} ions in inorganic salts are in common very close in their properties (that for years has been plaguing good separation of lanthanides in pure elemental forms), their organometallic derivatives reveal much stronger dissimilarities. Therefore almost for any single case a careful decision on the suitable synthetic route should be made: on the one hand it depends on the nature of lanthanide, its electronic configuration, and ionic radius, on the other hand the nature of the applied ligand has to be considered. Consequently, precise physicochemical properties of the desired derivative, its solubility, thermal or hydrolytic stability, susceptibility to oxidation, reduction or to any other spontaneous reactions should be taken into account.

The homoleptic *tris*-disilylamides can be synthesized for all lanthanides; their isolation and purification is easily achieved by high-vacuum sublimation. These starting materials, which, in recent decades, have become commercially available, are commonly employed in the syntheses of organolanthanide complexes through *silylamine elimination route*.

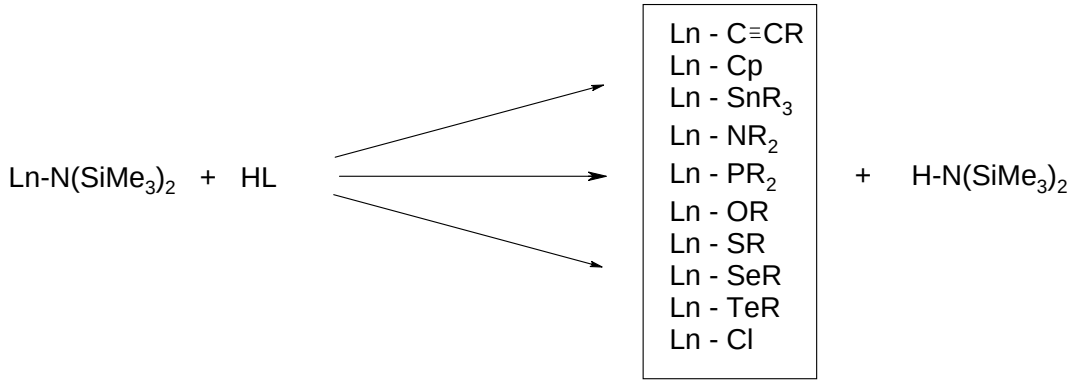

Scheme 3.

The overall redox stability of the lanthanide cations and the chemical robustness of the silylamide ligand has resulted in numerous ligand exchange reactions involving substrates of increased *Brønsted* acidity such as acetylenes,[3a] cyclopentadienes,[3b] stannanes,[3c] amines,[3d] phosphanes,[3g] phenols,[3e] alcohols,[3f] halcogenides[4a,4b] and chlorides[5] as listed in Scheme 3.

The main aspect that makes the *silylamide route* superior to traditional *salt metathesis* reactions is the high solubility of the monomeric metal amides in non-coordinating solvents that allows the use of homogeneous reaction conditions. Easy removal of the released amine (b.p. $HN(SiMe_3)_2$: 125°C) together with the solvent under vacuum yields the desired pure product by a one-pot protocol.

A limiting factor of this specific *amine elimination route* is the bulkiness of $N(SiMe_3)_2$ ligand that not only lacks reactivity in case of ligands with low proton acidity, but also decreases reaction rates with similarly bulky ligands such as C_5Me_5H,[6] $HOC(tert\text{-}Bu)_3$[7] or highly substituted phosphanes.[8] In order to cope better with such sterically suppressed ligand exchange reactions *Anwander* has introduced the alternative silylamide precursor $[Ln\{N(SiHMe_2)_2\}_3(thf)_2]$, which can be prepared in high yields for all lanthanides. The *bis*-(dimethylsilylamide) ligand $\{N(SiHMe_2)_2\}$ not only favours the attack of protic reagents due to the decreased steric bulk, but also affects the amine elimination by a decreased silylamide basicity, easier workup procedures (b.p. $HN(SiHMe_2)_2$: 93 – 99°C) and the presence of an excellent spectroscopic marker ("Si–H"). According to this *extended silylamide route,* catalytically relevant complexes involving salen,[9] (substituted) linked-indenyl,[10] and sulfonamide ligands[11] have been synthesized.

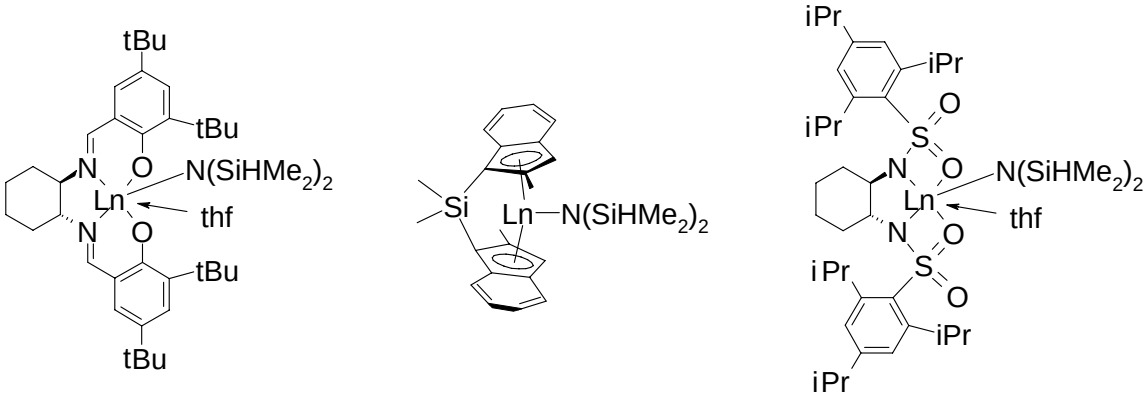

Scheme 4.

Such controlled ligand associations, which are proposed as proceeding *via* THF dissociation, are not obtained with the $[Ln\{N(SiMe_3)_2\}_3]$ precursors.

The *alkane elimination route* is particularly attractive because it can be applied under very mild reaction conditions; it leads to formation of unreactive alkane or arene and allows easy purification of the desired organolanthanide complexes. The applied alkyl/aryl precursors are highly reactive species and can also be generated *in situ*.

Most attention was paid to reactive alkyl-lanthanides. With the smallest organic ligand – methanide – only two compounds $[LnMe_3]$ (Ln = Y, Lu) are established.[12] Remarkably, both compounds are thermally stable at ambient temperature (dec. > 80°C). Most of the homoleptic lanthanide alkyls are thermally not robust and predominantly limited to complexes of late lanthanides and group 3 elements (Sc, Y), which have lower formal coordination numbers. Structurally characterized non-*ate* complexes are stable at low temperatures and include *tris*-silylmethanide complexes of the type $[Ln(CH_2SiMe_3)_3(thf)_n]$ (Ln = Sc, Y,[13] Sm, Er, Lu,[14]

Yb[15]). The complexes of late lanthanides are widely used in the synthesis of complexes as starting materials (Scheme 5).

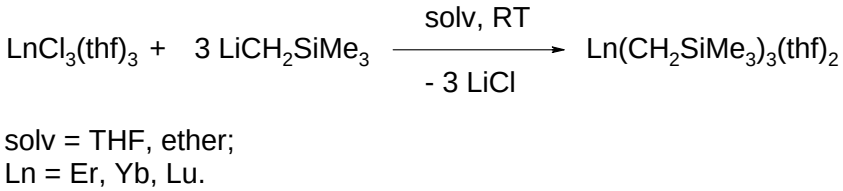

Scheme 5.

Other known homoleptic alkyl complexes are $[Yb(CH_2CMe_3)_3(thf)_2]$[16] and $[ScPh_3(thf)_2]$[17] as well as the thermally more robust complex $[Sc(CH_2SiMe_2Ph)_3(thf)_2]$.[18] All listed homoleptic complexes were synthesized from corresponding anhydrous THF solvated chlorides $[LnCl_3(thf)_n]$.

Exploration of disilylmethanide as ligand granted access to the homoleptic solvent-free complexes of early lanthanides of the type $[Ln\{CH(SiMe_3)_2\}_3]$ (Ln = La, Sm).[19]

The success in synthesis of the complexes was achieved by developing of the so-called "*phenolate route*" based on the use of 2,6-disubstituted *tris*-phenoxy-lanthanides as starting material (Scheme 6).

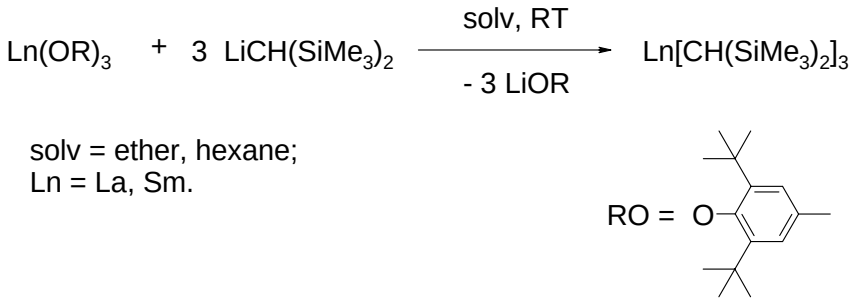

Scheme 6.

The choice of the precursor is essential because the use of lanthanum chloride, for example, together with the same reactant in the presence of pmdeta, leads to the formation of an *ate* complex of the type $[Ln\{CH(SiMe_3)_2\}_3]\times LiCl(pmdeta)$.[20]

Interestingly, some organic nitriles do not react with the disilylmethanide complexes of Ce or Y; only addition products were obtained: $[Ln\{CH(SiMe_3)_2\}_3(NCR)_n]$ for Ln = Y (n = 2) and Ce (n = 1), R = *tert*-Bu, Ph.[21]

Lanthanum possesses the largest ionic radius within the lanthanide series and shows the highest tendency to form *ate* complexes. With regard to lanthanum chemistry, benzylic complexes are the most studied species: $[Ln(CH_2C_6H_4NMe_2\text{-}o)_3]$ (Ln = Y, La),[22] $[La(CH_2C_6H_4\text{-}4\text{-}R)_3(thf)_3]$ (R = H, Me).[23]

$$LnBr_3(thf)_3 + 3\,KCH_2Ph \xrightarrow[-\,3\,KBr]{THF,\ 0°C} Ln(CH_2Ph)_3(thf)_3$$

Scheme 7.

The thermal stability was also enhanced by employing a mixed coordinating solvent environment $[Lu(CH_2SiMe_3)_3(thf)(dme)]$,[24] cyclic coordinating molecules like crown ethers $[Ln(CH_2SiMe_3)_3(12\text{-crown-}4)]$ (Ln = Sc, Y, Sm, Gd – Lu)[25] or cyclic permethylated amines and neutral *tris*-(methylpyrazolyl)methanes.[26]

Traditionally, divalent lanthanide chemistry has been limited to four elements – Sm, Eu, Tm and Yb. The choice of precursors for divalent lanthanides is also restricted. The most explored starting materials have been the lanthanide diiodides: $[YbI_2(thf)_2]$ and stock solutions of samarium diiodide in THF. Though there are many crystallographically characterized examples of solvated lanthanide dihalides, which differ by coordinated solvent molecules and by coordination mode, loss of coordinated solvent by drying in vacuum yields samples with sub-stoichiometric amounts of solvent. For example, though crystalline $[SmI_2(dme)_3]$[27] is known, it is rarely applied in the synthesis.

For all four divalent lanthanides disilylamides of the type $[Ln\{N(SiMe_3)_2\}_2]$ are known.[28] From reactive dialkyl species, the *bis*-alkyl complexes $[Ln\{C(SiMe_3)_3\}_2]$ (Ln = Yb,[29] Sm[30]) have been described. Though the latter compounds are highly reactive, they have not been well studied due to the tedious synthesis of the starting alkyllithium $[Li\{C(SiMe_3)_3\}]$ and very high solubility of the *bis*-alkyl complexes.

The *salt metathesis route* is the third general route towards the complex synthesis in lanthanide chemistry. Limitations are caused by the fact that early and middle lanthanides tend to have higher coordination numbers. Moreover *ate* complexes, instead of the desired neutral complexes, or mixture of products that are difficult to separate are usually obtained. Anhydrous lanthanide halides are convenient starting materials for the synthesis of many types of amido-, alkoxo-, phenoxo- and organo-lanthanoid complexes. Though anhydrous lanthanide trihalides (Hal = Cl, Br and I) are commercially available, high purity compounds are rather expensive. Due to the pronounced oxophilic nature of lanthanides typical impurities

in their trihalides are oxohalides (LnOHal) as well as aqua halide complexes. Even though there are several general methods for preparation of anhydrous lanthanide halides, preparation of pure anhydrous lanthanide trihalides is not a trivial exercise.

1.2. *Synthesis of Lanthanide Trichlorides*

The most general synthetic protocol towards the pure anhydrous trichlorides is based on dehydratation of their hydrates [$LnCl_3 \times nH_2O$] (n = 2, 6, 7).[31] It can be achieved with the help of NH_4Cl since the latter counteracts hydrolysis (Scheme 8).[32,31] The expelling of water is complete at 100°C in vacuum (approx. 10^{-2} torr); to sublime off NH_4Cl, the temperature have to be slowly arised to approx. 400°C. The time program is very important for the obtaining of high purity product and depends on the respective rare-earth metal and the amount of the substance to be processed.

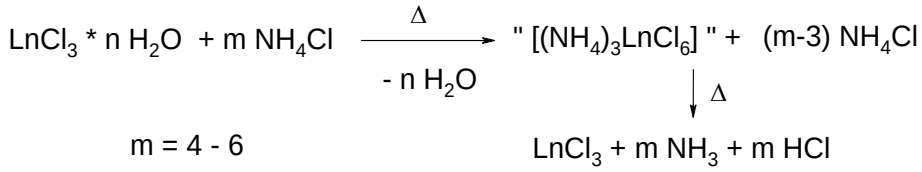

Scheme 8.

This method can be applied for the synthesis of all anhydrous lanthanide trichlorides as well as of scandium, yttrium and lanthanum.

The anhydrated chlorides of various lanthanides can be also prepared by heating with thionyl chloride.[31,33] The method is rather simple; however, a high purity product is not guarantied without a subsequent sublimation.

Commonly, THF-solvated lanthanide halides are employed.[31] They can be easily prepared from anhydrous non-solvated trichlorides by *Soxlet* extraction or by use of an excess of $SOCl_2$ as dehydrating agent in THF (Scheme 9).[34]

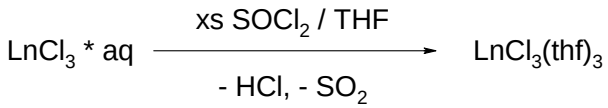

Scheme 9.

We have successfully applied this known protocol[34] for the syntheses of THF-solvated late lanthanide trichlorides (Sc, Y, Er, Yb, Lu). Whereas the standard dehydratation procedure of hydrated lanthanides chlorides with excess of thionyl chloride in THF as solvent was successfully employed for neodymium and samarium,[35] our attempts to apply the very same method to the synthesis of the solvated chlorides of the "closest" neighbours gadolinium and praseodymium failed. The result was a darkening of the reaction mixture and formation of a syrup like mass; no defined products were obtained even at low temperatures (-30 – (-80)°C).

The use of DME instead of THF allows the synthesis of analogous DME-solvated lanthanide trichlorides – $[LnCl_3(dme)_n]$, e.g. Ln = Ce, Pr, Nd (n =1, 2); Tb, Ho, Tm, Yb, Lu (n = 2).[36]

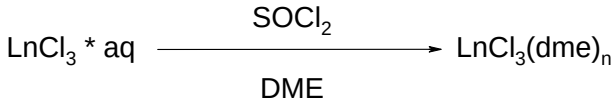

Ln = Ce, Pr (n = 1, 2),
Tb, Tm, Er, Ho, Yb, Lu (n = 2).

Scheme 10.

The same work group reported also a synthesis of DME-solvated lanthanide trichlorides directly from their oxides (Ln = La and Nd). This method consist in the use of HCl solution in DME, generated *in situ* from H_2O and a large excess of $SOCl_2$ (Scheme 11).[36]

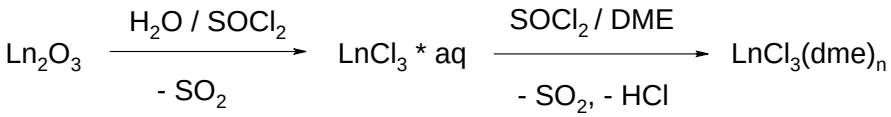

Ln = La, Nd (n = 1, 2).

Scheme 11.

The DME-solvated lanthanide trichlorides $[LnCl_3(dme)_2]$ (Ln = La, Er, Yb) can also be obtained by crystallization of corresponding THF-solvated salts from DME.[37]

▫ ▪ ▫

The solvates of early lanthanide trichlorides (La – Sm) are only rarely employed as precursors due to their very low solubility in ethers, caused by their polymeric nature.

1.3. *Synthesis of Lanthanide Tribromides and Triiodides*

As synthetic precursors for the *salt metathesis route*, the tribromides and triiodides of the early and middle lanthanides are superior to the corresponding trichlorides. However, since the bromides and even more the iodides have a higher tendency to undergo hydrolysis compared to the chlorides, special attention has to be paid to preventing it. Dehydratation of $[LnBr_3 \times nH_2O]$ and $[LnI_3 \times nH_2O]$ with ammonium halide, to form the pure anhydrous tribromides and triiodides, is less general and can be easily achieved only for lanthanum to samarium (Scheme 12). The method necessitates the use of an excess of NH_4Hal (up to 14 equiv); the reaction must be performed especially slowly.[32b]

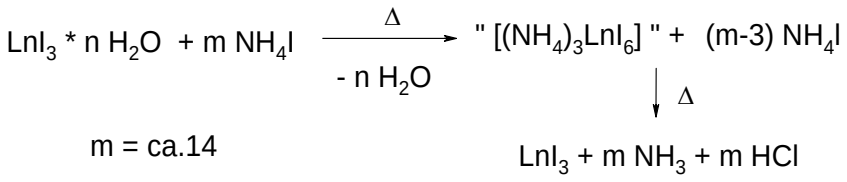

Scheme 12.

A following sublimation is always recommended if high purity desired. The method requires a special equipment (dry Ar atmosphere, tungsten or tantalum boats and protective tubes, vacuum/thick-walled quartz apparatus) and therefore the bromides are only available on *semi* gram scale.[31]

Alternatively, the syntheses of solvent-free lanthanide triiodides from metals can be performed from elemental iodine[38,31] or HgI_2[39] as oxidants (Scheme 13). Both syntheses proceed under considerably harsh conditions and require special equipment (dry Ar atmosphere, tungsten or tantalum boats and protective tubes, vacuum/thick-walled quartz apparatus) and subsequent prolonged sublimation in vacuum (10^{-5} mm Hg).

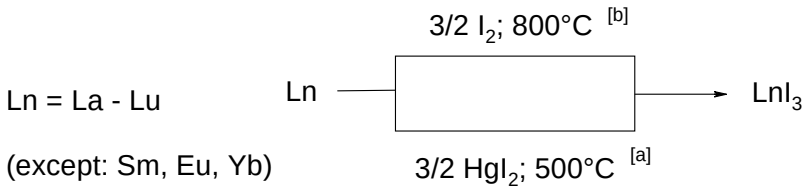

Scheme 13.

The methods are unsuitable for syntheses of samarium, europium and ytterbium triiodides.

The anhydrous ether-solvated lanthanide trihalides can be better prepared from the lanthanide metal powder and organic *vic*-/*gem*-dihalides (Scheme 14).[37,40]

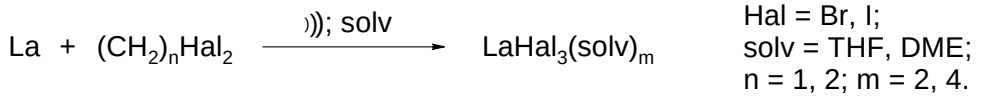

Scheme 14.

This heterogenic reaction is known to be accelerated by ultrasonic irradiation. The generality of the method was demonstrated by *Deacon* in the synthesis of the following lanthanide tribromides $[LaBr_3(thf)_4]$, $[LaBr_3(dme)_2]$, $[YbBr_3(thf)_3]$, $[YbBr_3(dme)_2]$ and lanthanum triiodide $[LaI_3(thf)_4]$ (the use of hexachloroethane results in the formation of the solvated lanthanide chlorides $[LnCl_3(dme)_2]$, Ln = Er, Yb).[37]

For the lanthanide triiodides, *i*-PrOH-solvated complexes of the type $[LnI_3(i\text{-}PrOH)_3]$, where Ln = La, Ce and Nd, were reported (Scheme 15).[41,42] On the example of $[NdI_3(i\text{-}PrOH)_4]$ were demonstrated, that this solvate can be easily converted into the corresponding THF-solvate $[NdI_3(thf)_x]$ by trituration with THF.[42] The microcrystalline material, obtained directly from THF solution, has the composition $[NdI_3(THF)_4]$.[43] The desolvatation and loss of THF begins as soon as supernatant solution is removed (x = 2.6 after several months storing in a Glove-box).

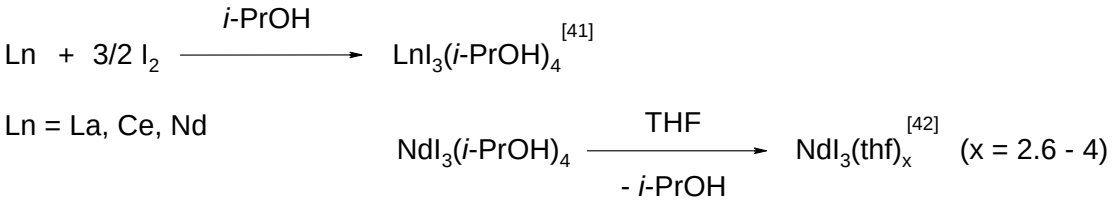

Scheme 15.

The drawback of most reported methods is the use of the still expensive metallic precursors (La (99.9%, powder) – \$450 per mole; Sm (99.9%, powder) – \$750 per mole),[44] that especially preclude their application for preparation of the middle and late lanthanide trihalides (Eu (99.9%, pieces) – \$7600 per mole; Yb (99.9%, powder) – \$3500 per mol).[44]

2. RESULTS AND DISCUSSION

Because of the difficulties described above in the synthesis of both anhydrous and solvated early and middle lanthanide tribromides on the one hand and their preferred use in the *salt metathesis route* on the other, we decided to develop a alternative protocol towards solvated lanthanide tribromides.

It has to be emphasized that during our study a related method was reported in the patent literature.[45] CHEMETALL claims an efficient synthesis of solutions of anhydrous lanthanide trichlorides using lanthanide(III) oxides as precursors and $SiCl_4$ as the chlorine source in the corresponding ethereal solvent.

With respect to the syntheses of solvated lanthanide tribromides, we have developed an alternative protocol starting from lanthanide(III) oxides (Ln = Nd, Sm) and stoichiometric amount of Me_3SiBr (Scheme 16).

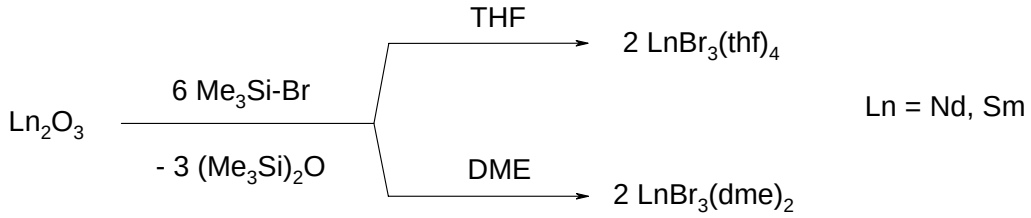

Scheme 16.

The addition of bromotrimethylsilane to a slurry of oxide (Nd_2O_3, Sm_2O_3) in an ethereal solvent (THF, DME) results in the dissolution of the compact oxide accompanied by the appearance of a voluminous precipitate that was identified as corresponding $[LnBr_3(thf)_4]$ or $[LnBr_3(dme)_2]$ by elemental analysis.

It seems that catalytic amounts of water – present in all commercially available lanthanide(III) oxides – act as promotor and thus play a decisive role in this convenient *one-pot* synthesis. We postulate a reaction mechanism comprising the hydrolysis of Me_3SiBr by catalytic amounts of water, under liberation of hydrobromic acid (Scheme 17). The latter reacts with the oxide reforming a steady state concentration of water and the corresponding solvated lanthanide tribromide.

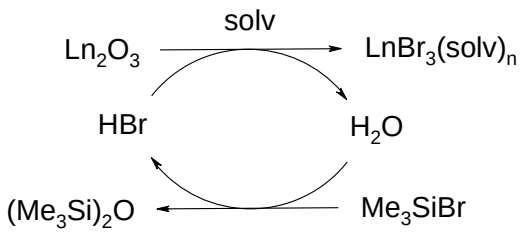

Scheme 17.

Instead of using highly corrosive bromotrimethylsilane, it was proposed to generate this reagent *in situ* from easily available hexamethyldisilane ($Me_3Si\text{-}SiMe_3$) and elemental bromine. To ensure the reaction proceed a catalytic amount of water (ca. 2.5 mol%) have to be added to the reaction mixture. (Scheme 18).

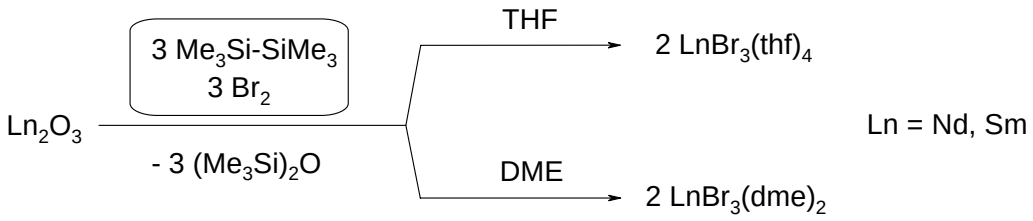

Scheme 18.

Thus, an effective *one-pot* synthesis of anhydrous ether-solvated lanthanide bromides was developed. Using this protocol, two series of solvated lanthanides tribromides – $[NdBr_3(thf)_4]$, $[NdBr_3(dme)_2]$, $[SmBr_3(thf)_4]$ and $[SmBr_3(dme)_2]$ – were prepared. These compounds were obtained as amorphous pale blue and yellow substances, respectively. According to the elemental analysis the composition of these compounds is nearly stoichiometric and corresponds to the compounds containing 2 DME or 4 THF molecules per lanthanide atom. The obtained products were slightly contaminated by the starting oxides. Their further purification was achieved by simple extraction with methylene chloride containing small amounts (10 vol%) of the solvent corresponding to that in the solvated tribromide. It is worth to note that the compounds themselves possess only poor solubility in THF or DME. After subsequent filtration and solvent removal crystalline products were obtained in yields varying within 64 - 88%.

The solubility of the tribromides in methylene chloride results from their molecular structure: All these compounds contain a seven-coordinated lanthanide atom and have binuclear molecular structure in the solid state as reported for $[NdBr_3(dme)_2]$,[46] $[NdBr_3(thf)_4]$,[47] $[SmBr_3(dme)_2]$ and $[SmBr_3(thf)_2]$.[48] The high solubility in methylene chloride was reported only for the THF-solvated yttrium trichloride $[YCl_3(thf)_3]$.[49]

3. CONCLUSIONS

A new and very convenient *one-pot* protocol for the synthesis of anhydrous ether-solvated lanthanide tribromides directly from their oxides has been developed. The high purity DME- and THF-solvated tribromides of neodymium and samarium were obtained in 64 – 88% isolated yields. The complexes show significant solubility in methylene chloride that allows their efficient purification from traces of the non-converted oxide precursors.

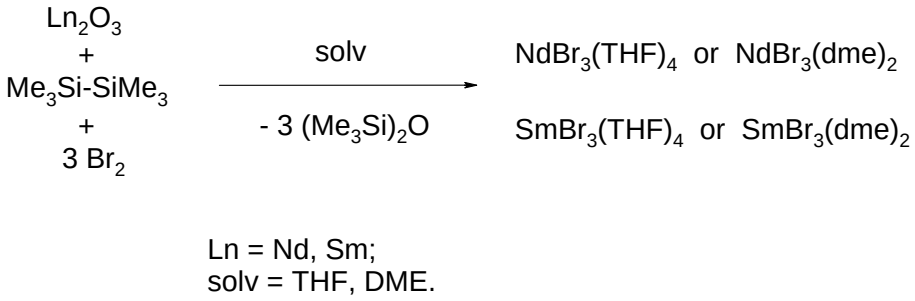

Ln = Nd, Sm;
solv = THF, DME.

4. EXPERIMENTAL PART

General considerations. All manipulations were performed under purified argon or nitrogen using standard high vacuum or *Schlenk*-tube techniques. Solvents were dried and distilled under argon employing standard drying agents. All organic reagents were purified by conventional methods.[50] Elementary analyses were performed at the Analytical Laboratory of the Chemistry Department / Philipps-Universität Marburg. Starting materials Sm_2O_3, Nd_2O_3 (99.9% purity) were purchased from *Chempur*, Si_2Me_6 from *Acros*.

4.1. *Synthesis of [$NdBr_3(thf)_4$]:* To a stirred suspension of Nd_2O_3 (2.00 g, 5.9 mmol) in 100 mL THF with Si_2Me_6 (9.0 mL, 6.4 g, 44 mmol, 7.5 equiv) one drop of water was added. Bromine (2.0 mL, 40 mmol, 6.6 equiv) was added drop wise. A slightly exothermic reaction occurs. The reaction mixture was heated to 50°C for further 20 min, whereupon the cloudy, heavy precipitate transforms in a compact, pale blue crystalline mass. It was separated by filtration, washed with THF (2×10 mL) and dried in vacuum. 5.60 g of the crude mixture of the product contaminated with small amount of unreacted oxide was obtained.

For isolation of the tribromide from this obtained crude product 100 mL 1:1 mixture of CH_2Cl_2/THF (v/v) was added. After almost complete dissolution, the pale blue cloudy solution was filtered through a Celite©-pad and the solvent was removed in vacuum. The product was obtained as a sky blue, crystalline solid. Yield: 64% (5.1 g).

Anal. Calcd. for $C_{16}H_{32}Br_3NdO_4$ (672.39): C 28.58, H 4.80, Br 35.65.
Found: C 28.70, H 4.85, Br 35.46.

4.2. *Synthesis of [$NdBr_3(dme)_2$]:* The similar procedure as for synthesis of [$NdBr_3(thf)_4$] in DME instead of THF was used. After purification the product was obtained as a sky blue, microcrystalline solid. Yield: 76% (5.0 g).

Anal. Calcd for $C_8H_{20}Br_3NdO_4$ (564.19): C 17.03, H 3.57, Br 42.49.
Found: C 16.93, H 3.63, Br 42.55.

4.3. *Synthesis of [$SmBr_3(thf)_4$]:* The same procedure as for synthesis of [$NdBr_3(thf)_4$], starting from 2.00 g Sm_2O_3 (5.7 mmol), was used. After the addition of bromine the reaction mixture was heated under reflux for 1 h. The product was obtained as a yellow, microcrystalline solid. Yield: 84% (6.5 g)

Anal. Calcd for $C_{16}H_{32}Br_3SmO_4$ (678.51): C 28.32, H 4.75, Br 35.33.

Found: C 28.39, H 4.63, Br 35.10.

4.4. *Synthesis of [$SmBr_3(dme)_2$]:* The similar procedure as for synthesis [$SmBr_3(thf)_4$] was used. DME was used instead of THF. The product was obtained as a yellow, microcrystalline solid. Yield: 88% (5.7 g)

Anal. Calcd for $C_8H_{20}Br_3SmO_4$ (570.32): C 16.85, H 3.53, Br 42.03;

Found: C 17.04, H 3.31, Br 41.81.

5. REFERENCES

[1] R. D. Shannon, *Acta Cryst. Sec. A32* **1976**, 751–767.

[2] R. Anwander: "Principles in Organolanthanide Chemistry", *Top. Organomet. Chem.* **1999**, *2*, 1–61.

[3] a) L. N. Bochkarev, S. B. Shustov, T. V. Guseva, S. F. Zhil'tsov *J. Gen. Chem. USSR* **1988**, *58*, 819–821; *Zh. Obshch. Khim.* **1988**, *58*, 923–924. b) Y. Mu, W. E. Piers, M.-A. MacDonald, M. J. Zaworotko, *Can. J. Chem.* **1995**, *73*, 2233–2237. c) G. A. Razuvaev, G. S. Kalinina, E. A. Fedorova, *J. Organomet. Chem.* **1980**, *190*, 157–165. d) W. J. Evans, M. A. Ansari, J. W. Ziller, S. I. Khan, *Inorg. Chem.* **1996**, *35*, 5435–5444. e) H. A. Stecher, A. Sen, A. L. Rheingold, *Inorg. Chem.* **1989**, *28*, 3280–3282. f) M. J. McGeary, P. S. Coan, K. Folting, W. E. Streib, K. G. Caulton, *Inorg. Chem.* **1991**, *30*, 1723–1735. g) H. C. Aspinall, D. C. Bradley, K. D. Sales, *J. Chem. Soc., Dalton Trans.* **1988**, 2211–2213.

[4] a) Y. F. Rad'kov, E. A. Fedorova, S. Y. Khorshev, G. S. Kalinina, M. N. Bochkarev, G. A. Razuvaev, *J. Gen. Chem. USSR* **1986**, *55*, 1911–1914; b) D. R. Cary, J. Arnold, *J. Am. Chem. Soc.* **1993**, *115*, 2520–2521.

[5] A. R. Strzelecki, C. L. Likar, B. A. Helsel, T. Utz, M. C. Lin, P. A. Bianconi, *Inorg. Chem.* **1994**, *33*, 5188–5194.

[6] a) M. Booij, N. H. Kiers, H. J. Heeres, J. H. Teuben, *J. Organomet. Chem.* **1989**, *364*, 79–86; b) S. D. Stults, R. A. Andersen, A. Zalkin, *Organometallics* **1990**, *9*, 115–122.

[7] W. A. Herrmann, R. Anwander, F. C. Munck, W. Scherer, V. Dufaud, N. W. Huber, G. R. J. Artus, *Z. Naturforsch.* **1994**, *B49*, 1789–1797.

[8] M. Allen, H. C. Aspinall, S. R. Moore, M. B. Hursthouse, A. I. Karvalov, *Polyhedron* **1992**, *11*, 409–413.

[9] O. Runte, T. Priermeier, R. Anwander, *Chem. Commun.* **1996**, 1385–1386.

[10] W. A. Herrmann, J. Eppinger, M. Spiegler, O. Runte, R. Anwander, *Organometallics* **1997**, *16*, 1813–1815.

[11] H. W. Görlitzer, M. Spiegler, R. Anwander, *Eur. J. Inorg. Chem.* **1998**, 1009–1014.

[12] a) H. M. Dietrich, Ch. Meermann, K. W. Törnroos, R. Anwander, *Organometallics* **2006,** *25,* 4316–4321; b) H. M. Dietrich, G. Raudaschl-Sieber, R. Anwander, *Angew. Chem.* **2005**, *117*, 5437–5440; *Angew. Chem. Int. Ed.* **2005**, *44*, 5303–5306.

[13] M. F. Lappert, R. Pearce, *J. Chem. Soc., Chem. Commun.* **1973**, 126–127.

[14] H. Schumann, J. Müller, *J. Organomet. Chem.* **1979**, *169*, C1–C4. H. Schumann, D. M. M. Freckmann, S. Dechert, *Z. Anorg. Allg. Chem*. **2002**, *628*, 2422–2426.

[15] M. Niemeyer, *Acta Cryst. Sec. E* **2001**, *57*, m553–m555.

[16] M. Niemeyer, *Z. Anorg. Allg. Chem.* **2000**, *626*, 1027–1029.

[17] M. A. Putzer, G. P. Bartholomew, *Z. Anorg. Allg. Chem.* **1999**, *625*, 1777–1778.

[18] D. J. H. Emslie, W. E. Piers, M. Parvez, R. McDonald, *Organometallics* **2002**, *21*, 4226–4240.

[19] P. B. Hitchcock, M. F. Lappert, R. G. Smith, R. A. Bartlett, P. P. Power, *J. Chem. Soc., Chem. Commun.* 1988, 1007–1009.

[20] J. L. Atwood, M. F. Lappert, R. G. Smith, H. Zhang, *J. Chem. Soc., Chem. Commun.* **1988**, 1308–1309.

[21] A. G. Avent, C. F. Caro, P. B. Hitchcock, M. F. Lappert, Z. Li and X.-H. Wei, *Dalton Trans.* **2004**, 1567–1577.

[22] S. Harder, *Organometallics* **2005**, *24*, 373–379.

[23] S. Bambirra, A. Meetsma, B. Hessen, *Organometallics* **2006**, *25*, 3454–3462.

[24] K. Rufanov, D. M. M. Freckmann, H. J. Kroth, S. Schutte, H. Schumann, *Z. Naturforsch.*, **2005**, *60b*, 533–537.

[25] S. Arndt, P. P. Zeimentz, T. P.Spaniol, J. Okuda, M. Honda, K. Tatzumi, *Dalton Trans.* **2003**, 3622–3627.

[26] C. S. Tredget, S. C. Lawrence , B. D. Ward, R. G. Howe, A. R. Cowley, P. Mountford, *Organometallics* **2005**, *24*, 3136–3148.

[27] a) M. Hakansson, M. Vestergren, B. Gustafsson, G. Hilmersson, *Angew. Chem.***1999**, *111*, 2336–2338; *Angew. Chem. Int. Ed.* **1999**, *38*, 2199–2201; b) T. Grob, G. Seybert, W. Massa, K. Dehnicke, *Z. Anorg. Allg. Chem.* **1999**, *625*, 1897–1903; c) W. J. Evans, R. N. R. Broomhall-Dillard, J. W. Ziller, *Polyhedron* **1998**, *17*, 3361–3370.

[28] a) W. J. Evans, D. K. Drummond, H. Zhang, J. A. Atwood, Inor. Chem.1988, 27, 575–579; b) B. Cetinkaya. P. B. Hitchcock, M. F. Lappert, R. G. Smith, J. Chem. Soc., Chem. Commun. 1992, 932–934.

[29] C. Eaborn, P. B. Hitchcock, K. Izod, J. D. Smith, *J. Am. Chem. Soc.* **1994**, *116*, 12071–12072.

[30] G. Qi, Y. Nitto, A. Saiki, T. Tomohiro, Y. Nakayama, H. Yasuda, *Tetrahedron* **2003**, *59*, 10409–10418.

[31] F. T. Edelmann, P. Poremba, in: *Synthetic Methods of Organometallic and Inorganic Chemistry*, (W. A. Herrmann, ed.), Vol. 6, Georg Thieme Verlag, Stuttgart, **1997**.

[32] a) M. Taylor, P. C. Carter, *J. Inorg. Nucl. Chem.* **1962**, *24*, 387–391; b) J. Kutscher, A. Schneider, *Inorg. Nucl. Chem. Lett.* **1971**, *733*, 815–819.

[33] J. H. Freeman, M. L. Smith, *J. Inorg. Nucl. Chem.* **1958**, *7*, 224–227.

[34] N. C. Burton, F. G. N. Cloke, P. B. Hitchcock, H. C. de Lemos, A. A. Sameh, *Chem. Commun.* **1989**, 1462–1464.

[35] N. C. Burton, *D. Phil. Thesis*, University of Sussex, **1991**.

[36] U. Baisch, A. Dell, B. Daniela, F. Calderazzo, R. Conti, L. Labella, F. Marchetti, E. A. Quadrelli, *Inorg. Chim. Acta* **2004**, *357*, 1538–1548.

[37] G. B. Deacon, T. Feng, P. C. Junk, G. Meyer, N. M. Scott, B. W. Scelton, A. H. White, *Aust. J. Chem.* **2000**, *53*, 853–865.

[38] L. F. Druding, J. D. Corbett, *J. Am. Chem. Soc*. **1961**, *83*, 2462–2467.

[39] a) L. B. Asprey, T. K. Keenan, F. H. Kruse, *Inorg. Chem.* **1964**, *3*, 1137–1141; b) L. B. Asprey, F. H. Kruse, *J. Inorg. Nucl. Chem.* **1960**, *13*, 32–35.

[40] P. N. Hazin, J. C. Huffman, J. W. Bruno, *Organometallics* **1987**, *6*, 23–27.

[41] D. M. Barnhart, T. M. Frankcom, P. L. Gordon, N. N. Sauer, J. A. Thompson, J. G. Watkin, *Inorg. Chem.* **1995,** *34,* 4862–4867.

[42] D. L. Clark, J. C. Gordon, B. L. Scott, J. G. Watkin, *Polyhedron* **1999**, *18*, 1389–1396.

[43] H. Schumann, J. A. Meese-Marktscheffel, L. Esser, *Chem. Rev*. **1995**, *95*, 865–986.

[44] Catalogue, *Chempur*, (Feinchemikalien und Forschungbedarf GmbH), **2003**.

[45] U. Lischka, J. Röder, U. Wietelmann (Chemetall GmbH), DE 10 2005 059 940 A1, **2006**.

[46] G. Zi, H.-W. Li, Z. Xie, *Organometallics* **2002,** *21,* 1136–1145.

[47] W. Chen, Z. Jin, Y. Xing, *Inorg. Chim. Acta* **1987**, *130*, 125–129.

[48] S. Petriček, *Polyhedron* **2004**, *23*, 2293–2301.

[49] P. Sobota, J. Putko, S. Szafert, *Inorg. Chem.* **1994**, *33*, 5203–5206.

[50] W. L. F. Armarego, D. D. Perrin, *Purification of laboratory chemicals*, 4 Ed., Butterworth-Heinemann, **1996**.

— CHAPTER II —

Synthesis of σ-Aryl Lanthanide Complexes with *ortho*-Metallated Benzylamine Pendant Ligands

Abstract

A series of homoleptic aryl complexes of early (Nd, Sm), middle (Gd, Dy) and late (Er, Yb) lanthanides with chelating *ortho*-donor functionality at the aryl ligand is described.

The *tris*-aryl complexes of Y, Er and Yb with *ortho*-metallated dimethyl-benzylamine ligand (dmba) were crystallographically characterized. In the case of Nd and Gd, homoleptic lithium ate complexes of the type $Li[Ln(dmba)_4]$ were isolated. It was shown that the success in the synthesis of the Nd and Gd complexes strongly depends on the choice of the lanthanide precursor, e.g. $[GdCl_3(dme)_2]$ or $[NdCl_3(dme)]$, and the reaction conditions such as THF-free working conditions.

For early (Nd, Sm) and middle (Gd, Dy) lanthanides, it was shown for the first time that a modification of the (dmba)-type aryl ligand, in particular replacing benzylic protons by methyl groups, leads to an increase of thermal and kinetic stability. Thus, so far unknown *tris*-aryl complexes of the larger lanthanide cations have been synthesized and characterized. These complexes can be stored at -30°C for months without decomposition.

1. INTRODUCTION

1.1. *Aryl Complexes with ortho-Metallated Benzylamine Ligand*

The bidentate monoanionic *ortho*-metallated *N,N*-dimethylbenzylamine ligand (dmba) found broad application in the organometallic chemistry. Complexes with this ligand are known for almost every transition metal. Ligands having this structural motif are also widely used for the complex synthesis. The ligand may be introduced using the aryllithium reagent 2-lithio-*N,N*-dimethylbenzylamine Li(dmba) (**R1**) which itself is conveniently prepared by lithiation of *N,N*-dimethylbenzylamine.

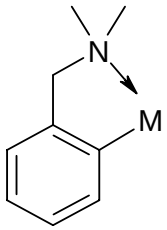

M(dmba)

This ligand can perfectly provide kinetic stabilization of its metal complexes.

The bidentate ligand has a strongly σ-donating dimethylamino-group and therefore can stabilize complexes of low-valent metals. Some examples are shown below in Scheme 1.

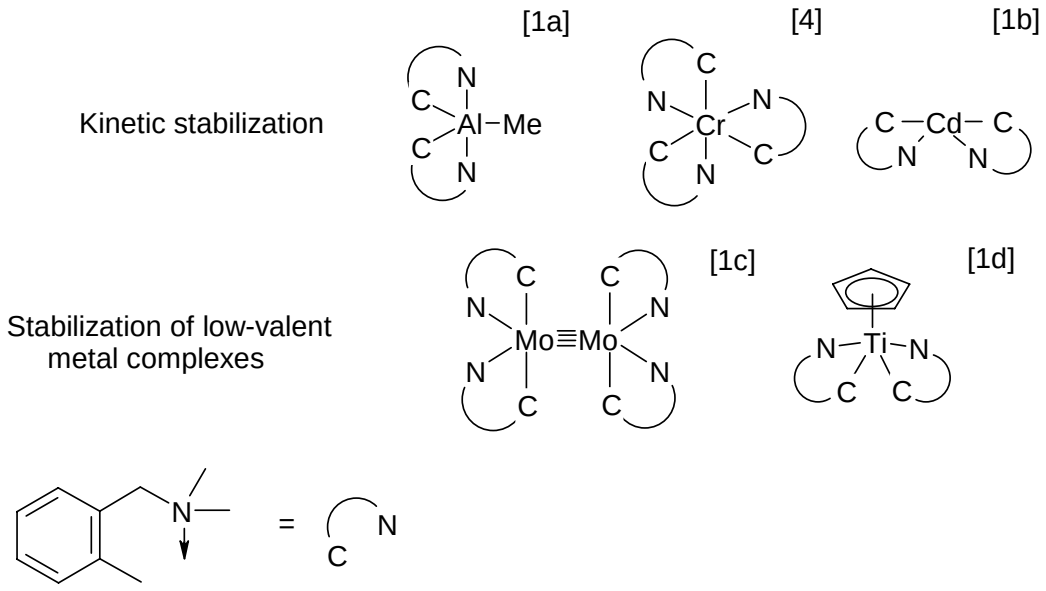

Scheme 1.

1.2. *Tris-Aryl Complexes of Late Lanthanides as well as Sc and Y*

In the early 1984 *Wayda et al.* [2] have reported that molecular complexes of lanthanides stabilized by (dmba) as ligand can only be obtained for the lanthanides with smaller ionic radii, *e.g.* Er (**H1**), Yb (**H2**) and Lu (**H3**). Since that time only one homoleptic *tris*-aryl lanthanide complex, namely [Lu(dmba)$_3$], was crystallographically characterized. Complexes of erbium and ytterbium reported by the group of *Wayda* were characterized solely by elemental analysis and IR spectroscopy.

For the early and middle lanthanides all attempts to isolate molecular *tris*-(dmba) complexes or *tetrakis*-(dmba) ate complexes failed and resulted in formation of uncharacterizable mixtures of products.[2] While the first attempts on isolation of *tetrakis*-phenyl-ate complexes Li[LaPh$_4$] and Li[PrPh$_4$] were reported in 1970,[3] no complete analysis or structural confirmation by physical methods was given.

Homoleptic *tris*-aryl complex of the group 3 elements – [Sc(dmba)$_3$] and [Y(dmba)$_3$] – have been reported early.[4,5] Both complexes are not crystallographically characterized. The scandium complex is not commonly used as precursor since it shows very low solubility in common organic solvents and therefore no crystalline product suitable for crystallographic characterization was obtained so far.

Nowadays, the homoleptic diamagnetic *tris*-aryl complexes of yttrium [Y(dmba)$_3$] (**H4**) and lutetium [Lu(dmba)$_3$] (**H3**) with the (dmba) ligand find broad application as precursors in the organolanthanide chemistry.[6]

1.3. *Considerations of Possible Degradation Pathways of (dmba) Ligand*

The enhanced *Lewis* acidity of the metal center combined with the high *Brønsted* basicity of the aryl ligands cause the high reactivity of lanthanide complexes and their low thermal stability. Compared to the late lanthanides that have sterically unsaturated ligands, the early and middle lanthanides reveal higher coordination numbers which provides an enhanced tendency to coordinate molecules with donor functionalities (ether solvents, amines). The following ligand activation can cause rapid degradation reactions.

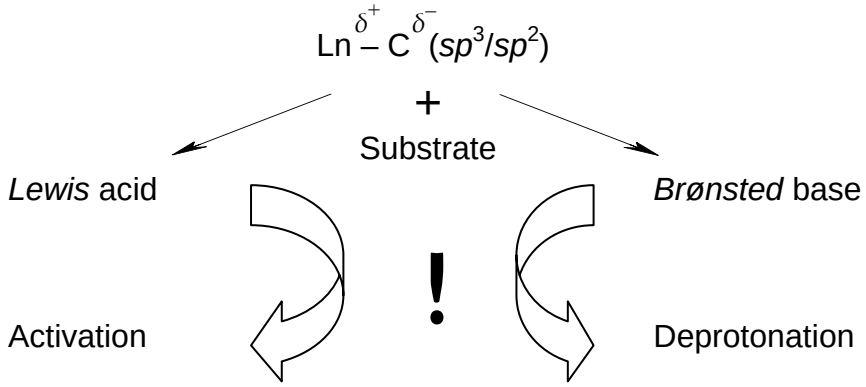

The common decomposition pathways of the sterically unsaturated lanthanide complexes are often indicated by solvent-,[7] ligand-degradation,[8] and/or occurrence of secondary agostic interactions.[9]

In the case of the (dmba)-ligand there are three possible pathways of degradation of the formed aryl complexes (Scheme 2): (i) decomposition of coordinated solvent molecules or ligand deprotonation on (ii) benzylic- or (iii) dimethylamino-positions. Deprotonation pathways can proceed *via* an *inter*- or *intra*-molecular mechanism.

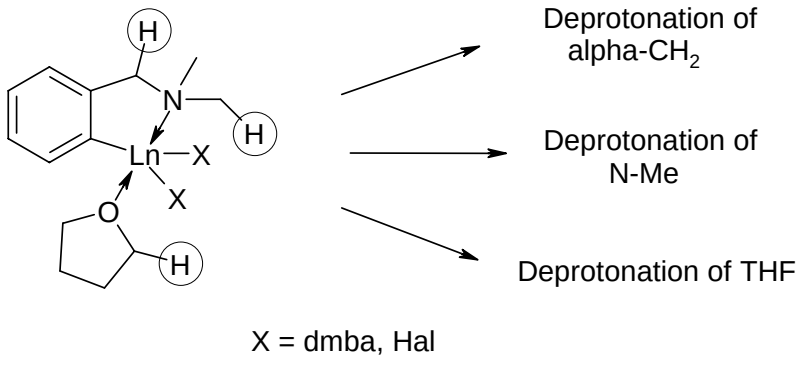

Scheme 2. Possible degradation pathways of complexes with (dmba) as ligand.

Decomposition of coordinated solvent molecules, especially of THF, is not unusual in the lanthanide chemistry.[10] The possibility of working under THF-free conditions put hard limitations on the choice of appropriate starting materials and acceptable solvents for reactions. An application of alternative high polarity solvents instead of THF, like dimethoxyethane (DME) or diethoxymethane (DEM) is highly promising. The latter has recently become commercially available in solvent quantities.[11] Astonishingly, up to now there are no reports on the application of anhydrous DME-solvated lanthanide trihalides. Almost all dme-solvated lanthanide trihalides were characterized by X-ray diffraction in 2004 with the aim to understand structural aspects.[12]

Ligand degradation is strongly affected by the ligand skeletonand can be demonstrated for example of by a lanthanum complex with a modified 4,7-dimethyl-1,4,7-triazacyclononane (Me_2TACN) ligand (Scheme 3).

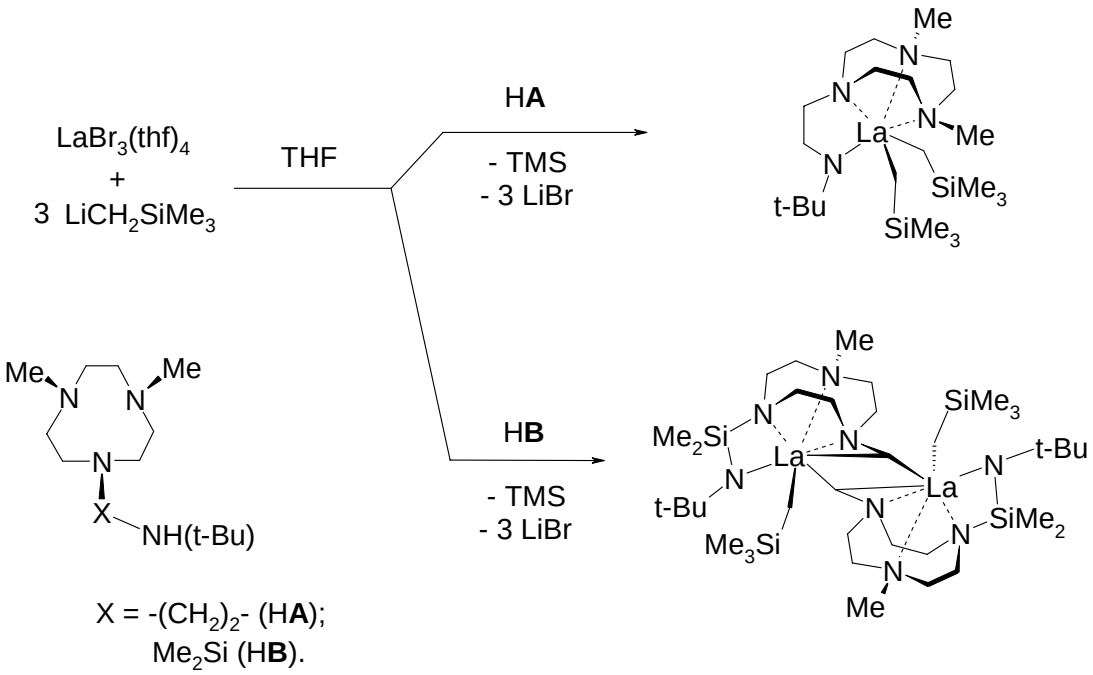

Scheme 3.

Two ligand systems based on Me_2TACN with different bridging amino side arms $(CH_2)_2$N(H)-*tert*-Bu (H**A**) and Si$(Me)_2$N(H)-*tert*-Bu (H**B**) were investigated.[13] The stability of the resulting dialkyl species strongly depends on the nature of the spacer between TACN and the amide side arm. In the case of the ethylene bridged ligand H**A** the mononuclear dialkyl complex [{**A**}La$(CH_2SiMe_3)_2$] was isolated. The complex is stable at ambient temperature. In the case of Me_2Si-bridged ligand H**B** the dinuclear lanthanum complex [{**B**'}La$(CH_2SiMe_3)_2$] was isolated as the only organometallic product, even when the

reaction was performed at -10°C. This product is the result of the metallation of one of the methyl substituents at the TACN ligand moiety, followed by dimerization.

Direct α-deprotonation pathways of dimethylamino groups are rarely reported in the literature. Two examples of deprotonation are described. The first comprises an *ortho*-dirigating effect of a carbonyl group in conjugation to the nitrogen atom (Scheme 4). The method is applied for the derivatization of carbonic acid amides. The second example describes double deprotonation of several aminales (R = Me, *i*-Pr, Cy) with *tert*-BuLi in pentane.[14]

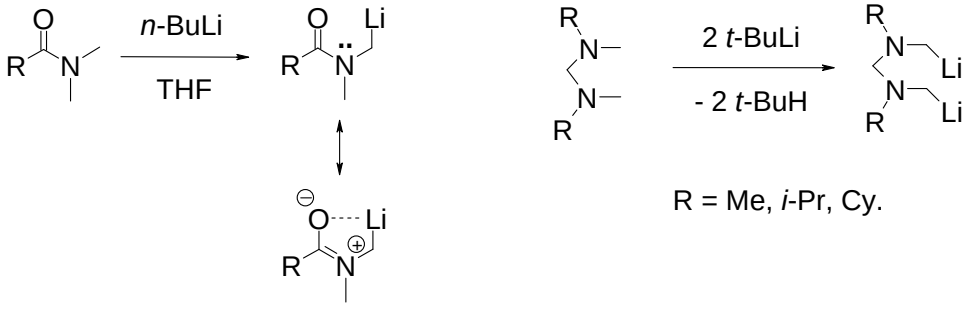

Scheme 4. α-Deprotonation of methylamino species.

For synthetic purposes pure α-lithiated amines are generated by transmetallation reaction (tin/lithium exchange).[15] The compounds were used for investigation of coordination of aluminum and gallium complexes (Scheme 5).

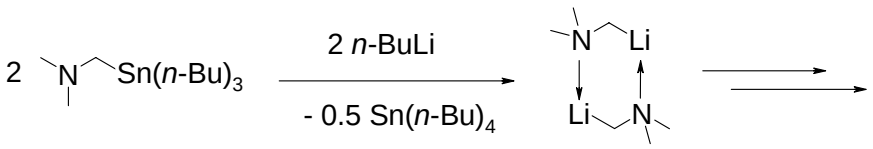

Scheme 5. Synthesis of α-lithio-trimethylamine by tin/lithium exchange reaction.

1.4. *Alkaline Metal Aryl Complexes with (dmba) Ligand*

Deprotonation of *N,N*-dimethylbenzylamine with *n*-BuLi in ether takes place exclusively at the *ortho*-position of the phenyl ring yielding only one isolated product (Scheme 6).[21]

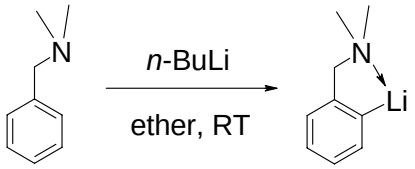

Scheme 6. Deprotonation of *N,N*-dimethylbenzylamine with *n*-BuLi in ether.

However, intermediate formation of the α-lithio species of the type [PhCH(Li)R], deprotonated at the benzylic position, followed by isomerization into *ortho*-lithiated species cannot be excluded. Indeed, when alkylsodium compounds, (*e.g.* *n*-BuNa or *n*-AmNa) suspended in hexane at 25 – 30°C are used, the deprotonation of *N,N*-dimethylbenzylamine also occurs at the *ortho*-position (Scheme 7). However, the resulting *ortho*-sodio derivative is unstable and isomerizes into a red α-sodio species within 20 h.[16] The stability of the α-sodio derivative in non-ethereal solutions is high: the compound is stable in a boiling benzene-octane mixture (85°C) for 24 h, whereas in ethereal solvent it decomposes within 45 h at 45°C forming the starting amine in 92% yield.

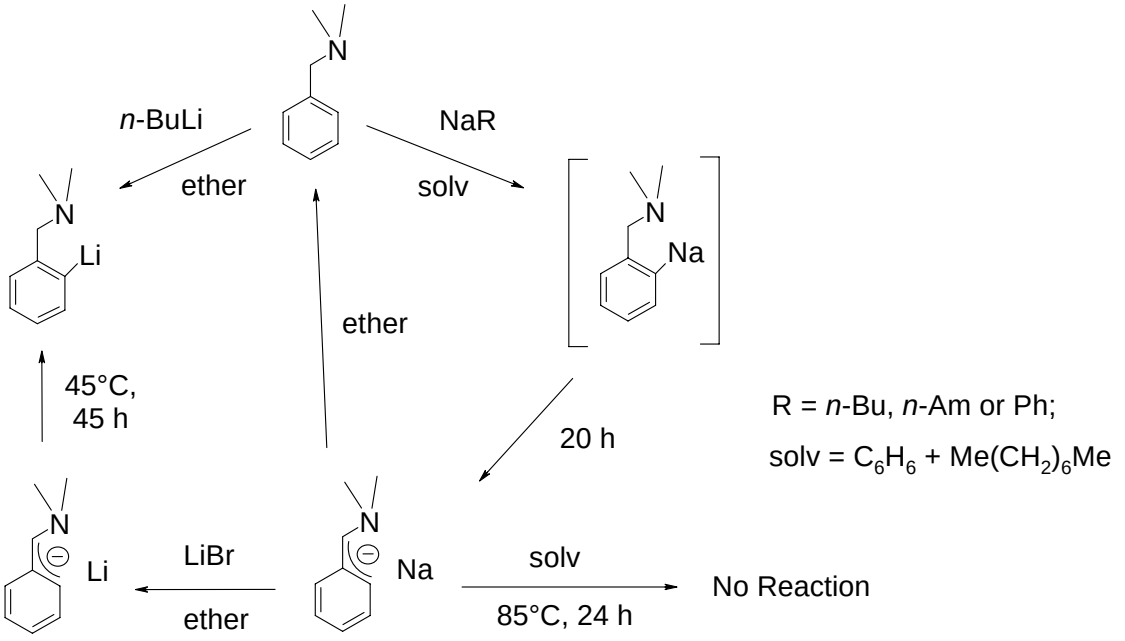

Scheme 7. Deprotonation of *N,N*-dimethylbenzylamine with lithio- and sodio-organyls and their following transmetallation/isomerization reactions.

The α-lithio derivative is stable at 25 – 30°C for at least 24 h. It was prepared from the α-sodio compound by metathesis with lithium bromide in ether-benzene-octane mixture. Interestingly, at higher temperatures (45°C / 45 h) this species slowly isomerizes forming the *ortho*-lithio derivative.

Obviously, deprotonation of the *ortho*-aryl position is the result of a kinetically controlled reaction, whereas deprotonation of the benzylic α-position is the result of the thermodynamically controlled reaction. It further seems that there is no general tendency valid for any metal.

Organometallic potassium compounds rarely possess mononuclear structures and commonly crystallize in polymeric chains. The crystallographically characterized potassio derivatives possessing benzyl anions are usually highly aggregated where the aryl rings bridged to the neighboring unit. This tendency to form coordination polymers is attributed to the larger coordination sphere of K^+ and its strong preference for binding softer delocalized π-ligands. This is also observed in few other crystallographically characterized structures of benzylpotassium derivatives: $[PhCH_2K(pmdta)]_\infty$,[17] $[PhCH_2K(thf)]_\infty$,[18] $[Ph(Me_3Si)_2CK]_\infty$[19] and $[Me_2NC_6H_4CHSiMe_3K(thf)]$.[20]

In this chapter achievements in the stabilization of early and middle lanthanide complexes by fine tuning of the architecture of the aryl ligand containing *N*-donor functionalities is reported.

2. RESULTS AND DISCUSSION

2.1. *Lanthanide Tris-Aryl Complexes with (dmba)- and (pyba)-Ligands*

Searching for novel and versatile precursors for the organolanthanide chemistry we have reinvestigated the reactions of *ortho*-lithiated *N,N*-dimethylbenzylamine (**R1**) with different lanthanide and group 3 element trihalides. Additionally, the chemistry of the structurally similar new *ortho*-lithiated amine *N*-benzylpyrrolidine Li(pyba) **R2**[21] was investigated.

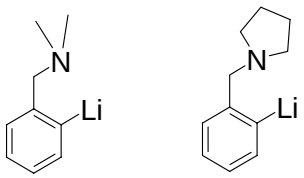

Li(dmba) Li(pyba)

R1 **R2**

The *salt metathesis* reactions of $[LnCl_3(thf)_3]$ or $[LnCl_3(dme)_2]$ (Ln = Er, Yb, Y) with the aryllithium reagent Li(dmba) **R1** are straightforward and furnish the corresponding *tris*-aryl complexes of analytical purity (Scheme 8).

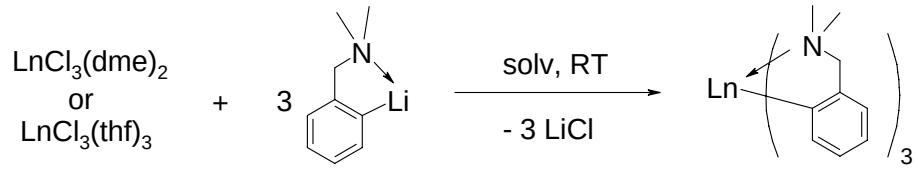

R1

Ln = Er (**H1**),
Yb (**H2**),
Y (**H4**).

solv = THF, DME, ether, toluene.

Scheme 8. Synthesis of the homoleptic complexes $[M(dmba)_3]$, M = Er (**H1**), Yb (**H2**) and Y (**H4**).

The ^{1}H NMR spectrum of the paramagnetic erbium complex **H2** in C_6D_6 at 23°C reveals three moderately upfield shifted, relatively "sharp" resonances at -9.1 ($\nu_{½}$ = 100 Hz), -17.7 ($\nu_{½}$ = 23 Hz) and -31.9 ppm ($\nu_{½}$ = 45 Hz) as well as a highly upfield shifted broad resonance at -99.1 ppm ($\nu_{½}$ = 360 Hz) (Figure 1). The latter resonance should to be assigned to the *ortho*-Ar proton, since it is the closest to the paramagnetic center. The assignment of other aromatic resonances is non-trivial. Furthermore, two very broad resonances downfield shifted to the values of 29.5 and 101 ppm ($\nu_{½}$ = ca. 1900 Hz and ca. 1200 Hz, resp.) at an integral ratio 2:6 were observed. Whereas the signals at 29.5 and 101 ppm can without any doubt be assigned to the protons of the side-arm CH_2NMe_2-group

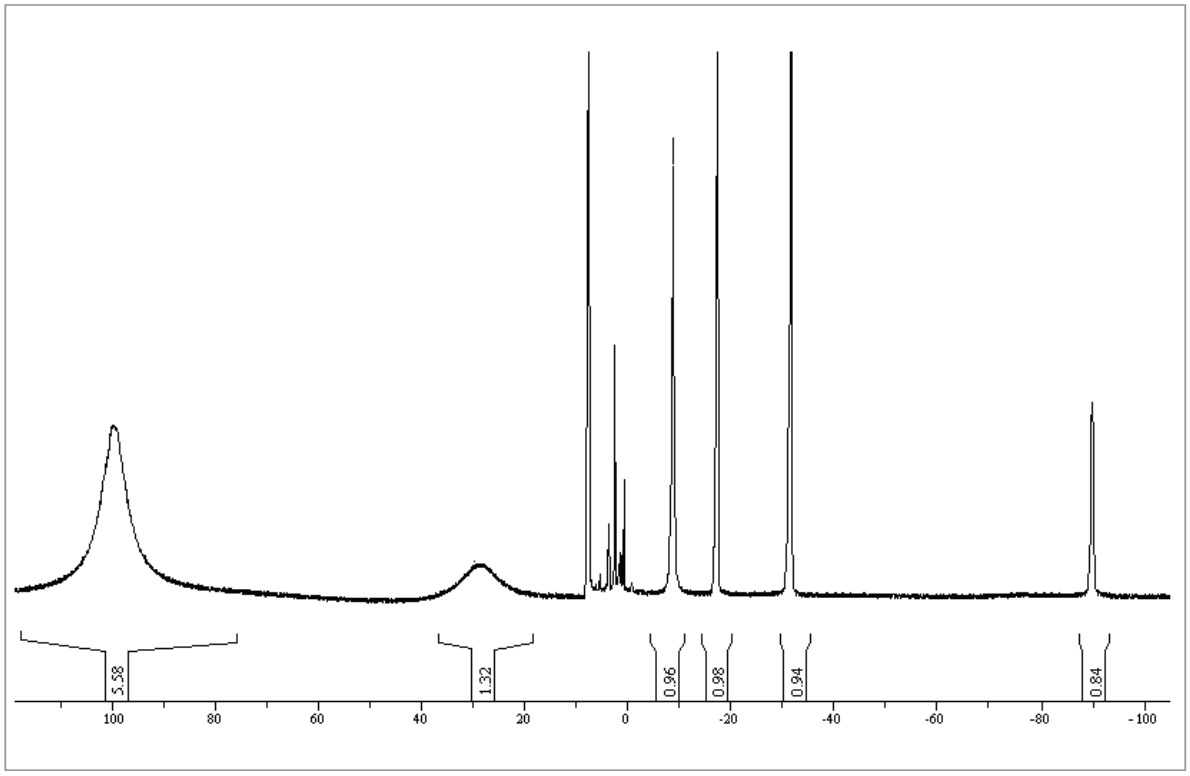

Figure 1. The ^{1}H NMR spectrum (300.1 MHz) of ytterbium complex [Yb(dmba)$_3$] **H2** dissolved in C_6D_6 at +25°C.

Due to efficient paramagnetic relaxation, caused by the Er^{3+} metal center, the NMR spectroscopy was not informative for the complex [Er(dmba)$_3$] **H1**.

The ^{1}H NMR spectrum of the yttrium complex [Y(dmba)$_3$] **H4** in toluene-d_8 reveals two sharp resonances in the aliphatic region at 3.37 and 2.12 ppm at an integral ratio of 2:6 assigned to benzylic methylene and Me_2N-groups. The low temperature NMR investigation reveals very weak temperature dependence and shows no resonance broadening down to 230 K. The slow broadening of resonances occurs beneath that temperature, but no complete splitting of resonances was observed down to 200 K. Such behavior in solution is a result of a high conformational flexibility of (dmba)-ligands.

Among the whole series of homoleptic (dmba)-lanthanide complexes a molecular structure analysis has only been reported for the [Lu(dmba)$_3$] **H3** so far. In the course of the study it was managed to get single crystals and perform X-ray crystal structure determination for the erbium- (**H1**), ytterbium- (**H2**) and yttrium-(dmba) (**H4**) complexes. Despite of the fact that **H4** is used as precursor,[6] until now this complex has not been crystallographically characterized.

All these complexes crystallize in the monoclinic space group *C*2/*c* with one asymmetric unit (Z = 8) – similar to the known Lu-analog (**H3**). The rare-earth metal atoms reveal a six-fold coordination by three *σ*-bound aryl groups and three nitrogen atoms of the (dmba)-ligands in a distorted octahedral geometry (Figure 2). Interestingly, *ipso*-carbon atoms as well as the nitrogen atoms give a *pseudo*-meridional arrangement. The selected bond lengths and angles, compared with those of [Lu(dmba)$_3$] **H3**, are presented in Table 1. The metal atoms are very close to the planes formed by three *ipso*-carbon atoms (CCC-plane) and three nitrogen atoms (NNN-plane). These distances vary in the range from 0.250(1) – 0.259(1) Å in the case the CCC-plane and from 0.297(1) – 0.305(1) Å in the case the NNN-plane. The *pseudo*-meridional arrangement is also supported by the values of C–M–C and N–M–N angular sums which are close to 360° for all investigated complexes.

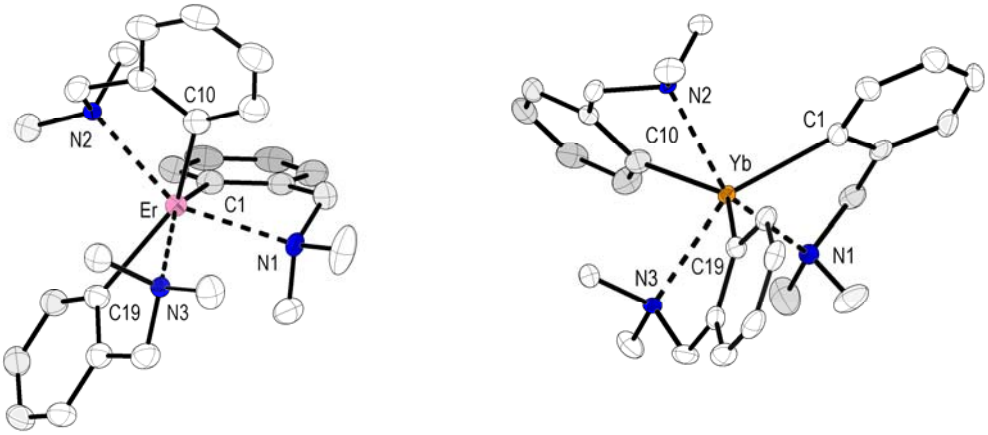

Figure 2. The molecular structures of [Ln(dmba)$_3$], Ln = Er (**H1**) and Yb (**H2**). Hydrogen atoms have been omitted for clarity.

The Er–C bond lengths in the erbium complex [Er(dmba)$_3$] **H1** are in the range of 2.456(3) – 2.483(2) Å. The Er–N bond lengths, also like in the structure reported for **H3**, fit to the "two-short, one-long" pattern:[2] 2.496(2), 2.505(2), 2.594(2) Å. Essentially the same pattern was found for the ytterbium complex **H2**: 2.433(7) – 2.453(7) Å for the Yb–C bond lengths and 2.481(5), 2.488(5), 2.565(5) Å for the Yb–N bond lengths; for the yttrium complex **H4**:[22] 2.475(4) – 2.504(3) Å for the Y–C bond lengths and 2.514(3), 2.525(3) Å and 2.601(3) Å for the Y–N bond lengths.

Table 1. Selected bond lengths (Å) and angels (°) in the homoleptic complexes [M(dmba)$_3$] of Y (**H4**), Er (**H1**) and Yb (**H2**), compared with those, found in [Lu(dmba)$_3$] (**H3**).

	H4 (M = Y)[22]	**H1** (M = Er)	**H2** (M = Yb)	**H3** (M = Lu)[2]
M–N1	2.601(3)	2.505(2)	2.488(5)	2.588
M–N2	2.525(3)	2.496(2)	2.481(5)	2.478
M–N3	2.514(3)	2.594(2)	2.565(5)	2.468
M–C1	2.475(4)	2.457(2)	2.433(7)	2.427
M–C10	2.479(4)	2.483(3)	2.453(7)	2.425
M–C19	2.504(4)	2.456(2)	2.434(7)	2.456
C1–M–C10	96.4(1)	121.0(1)	120.4(2)	140.2(3)
C10–M–C19	121.4(2)	138.8(1)	140.0(2)	119.9(3)
C1–M–C19	138.7(1)	96.7(1)	96.1(2)	96.6(2)
$\Sigma(C_A–M–C_B)$	356.5(4)	356.5(3)	356.5(6)	356.6(7)
N1–M–N2	91.8(1)	148.2(1)	148.8(2)	114.0(2)
N2–M–N3	147.9(1)	115.0(1)	114.6(1)	149.8(3)
N1–M–N3	115.0(1)	91.4(1)	91.4(2)	91.2(2)
$\Sigma(N_A–M–N_B)$	354.8(3)	354.6(2)	354.8(5)	355.0(7)
M···CCC	0.259(1)	0.256(1)	0.250(1)	0.247(1)
M···NNN	0.304(1)	0.305(1)	0.297(1)	0.289(1)

The origin of the "two-short, one-long" bond length pattern around the metal center can be explained by packing effects in the solid state. Analysis of the packing in the unit cell reveals that molecules are arranged with respect to a center of inversion, as shown below on the example of the compound **H4** (Figure 3).

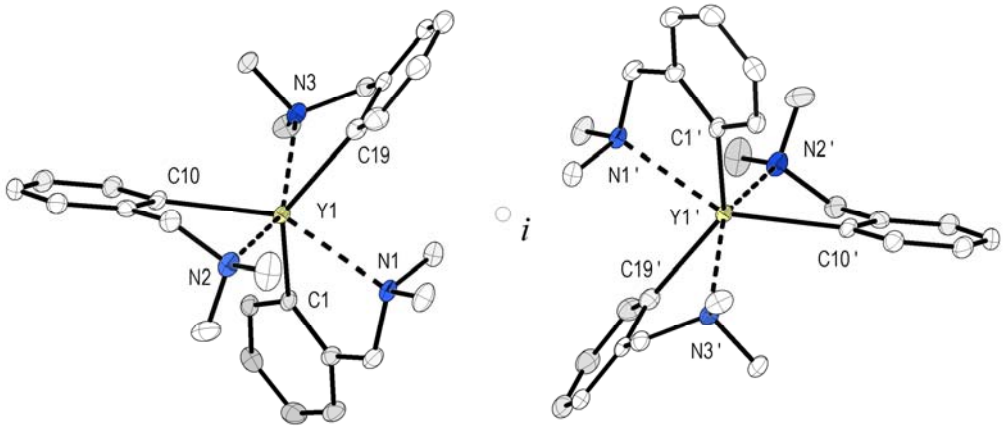

Figure 3. The molecular structure of [Y(dmba)$_3$] **H4**.[22] Hydrogen atoms have been omitted for clarity.

Consequently, one among three M–C σ-bonds and one among three M–N bonds in these (dmba)-ligands has been found to be ca. 0.2 Å and 0.8 Å longer than two other corresponding M–C and M–N bonds.

The arrangement of molecules in the unit cell is depicted in Figure 4.

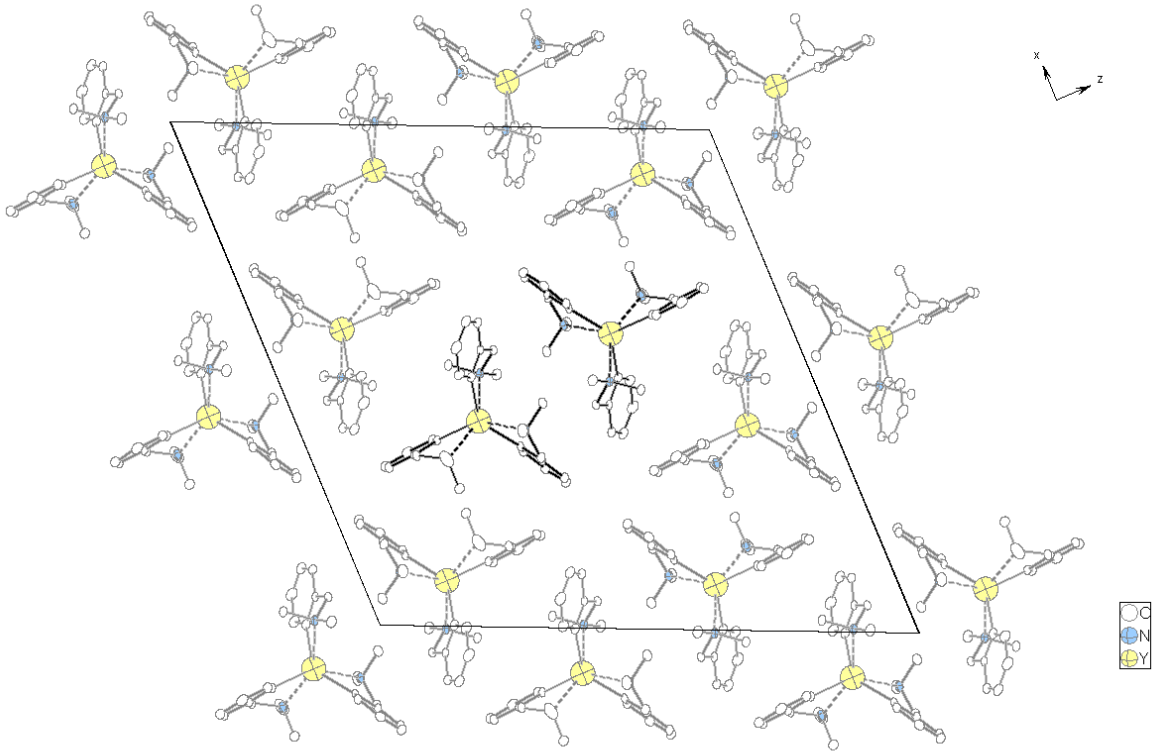

Figure 4. The molecular view of molecules arrangement in [Y(dmba)$_3$] **H1** along the crystallographic y-axis.

The Y^{3+} ion by its size (0.90 Å) has to be associated with the middle lanthanides' sub-group and this is the largest ion in the series that shows formation of stable *tris*-aryl complexes with the unmodified (dmba)-ligand. According to *Wayda* and from our own experience, early (Pr, Nd, Sm) and middle (Gd, Tb, Dy) lanthanides either with the lithium reagents Li(dmba) **R1** or with Li(pyba) **R2** give no stable *tris*-aryl complexes.

2.2. *Lanthanide Tetrakis-Aryl-ate Complexes with (dmba)- and (pyba)-Ligands*

These earlier observations denote the crucial role of coordinated solvent in the lanthanide precursors $[LnCl_3(solv)_n]$ on the nature of the transmetallated products. It was found that the use of $[NdCl_3(dme)]$ or $[GdCl_3(dme)_2]$ instead of their THF-solvated analogs allows the isolation of highly air-sensitive, crystalline products in moderate yields (Scheme 9). Both compounds were identified as molecular binuclear lithium ate complexes of gadolinium $Li[Gd(dmba)_4]$ **H6** and neodymium $Li[Nd(pyba)_4]$ **H5**. The compounds appear as a colorless and a pale green, microcrystalline solid respectively.

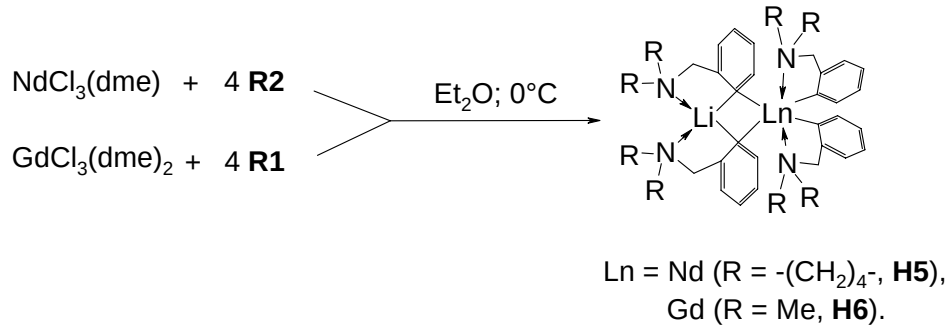

Scheme 9. Synthesis of the lithium ate complexes $Li[Nd(pyba)_4]$ **H5** and $Li[Gd(dmba)_4]$ **H6**.

The composition of these complexes was confirmed by elemental analysis. The molecular structures have been determined by X-ray diffraction.

It is worth to mention that the isolation of these complexes from their solutions should be performed at possibly low temperatures (< 0°C) although in the solid state the substances are much more stable. They can be stored at -30°C without decomposition for several months.

Crystals of **H5** and **H6** suitable for X-ray diffraction analysis were obtained by cooling of their concentrated toluene and ether solutions respectively. The molecular structures are depicted in Figure 5.

The compound **H5** crystallizes with additional two toluene molecules per unit cell. Both **H5** and **H6** are heterobinuclear and crystallize in the monoclinic ($P2_1/n$) and triclinic ($P\bar{1}$) space groups respectively.

In their structures a slightly distorted propeller-like arrangement of ligands around each metal with *pseudo*-C_2-rotation axis through lithium and lanthanide atoms is observed. In both structures terminal and bridging aryl groups are present. The geometry of the six-fold coordinated lanthanide atom is best described as distorted octahedral. Both terminal aryl groups with their dialkylamino-groups routinely coordinate in κ^2-fashion. The bridging aryl

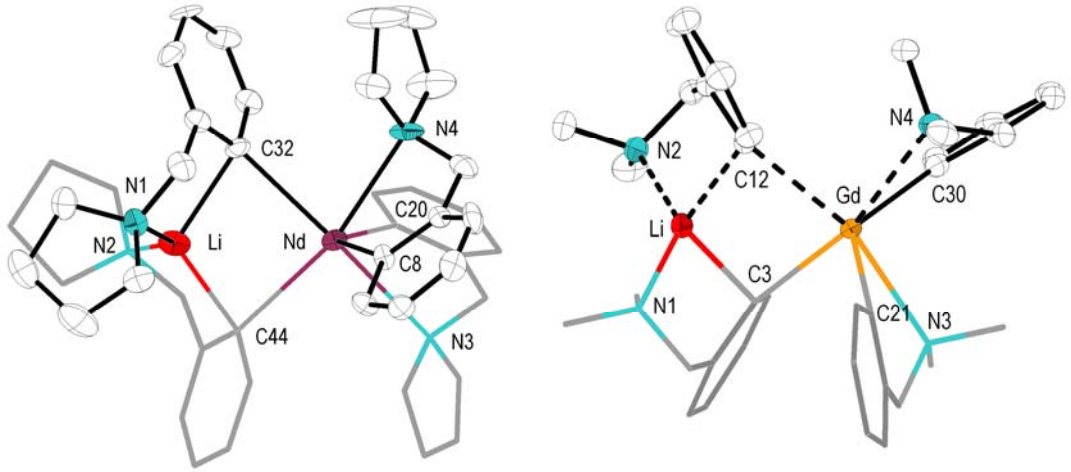

Figure 5. The molecular structures of Li[Nd(pyba)$_4$] **H5**×½PhCH$_3$ (left) and Li[Gd(dmba)$_4$] **H6** (right) drawn with 50% probability Toluene molecules in compound **H5**×½PhCH$_3$, as well as all hydrogen atoms, have been omitted for clarity. For simplicity, some ligand molecules have been drawn in wires and sticks model.

groups coordinate to lithium and lanthanide atoms forming an almost planar heterobimetallic [Li{μ-C$_6$H$_4$(CH$_2$NMe$_2$)}Ln] unit with Li–μ-C$_{Ar}$–Ln–μ-C$_{Ar}$' torsion angles of 4.2(5)° and 6.5(2)°. The lithium atoms are tetra-coordinated by the bridging aryl groups and their dialkylamino-groups. Due to the steric bulk of the aryl groups, the terminal aryl groups occupy antiperiplanar positions relative to dialkylamino-groups coordinated to the lithium atom: The C–Ln–Li–N torsion angles are close to 180° (**H5**: 167.2(5)°, 160.9(5)°; **H6**: 162.7(2)°, 169.9(2)°). The selected bond lengths and angles are given in Table 2.

As expected, the C$_{Ar}$–Ln bond lengths of bridging aryl ligand in **H5** and **H6** (av. 2.630 Å and av. 2.596 Å resp.) are essentially longer than those of the terminal ones (av. 2.573 Å and av. 2.518 Å resp.). These bond lengths are in good agreement with those ones found in the heteroleptic complex {Li(dme)$_3$}[PhNd(μ^5-C$_5$H$_5$)$_3$][23] (av. 2.60(1) Å).

Table 2. Selected bond lengths (Å) and angles (°) for the lithium ate complexes **H5**×½PhMe and **H6**.

	H5×½PhMe (Ln = Nd)	**H6** (Ln = Gd)
Ln–C$_{Ar}$	2.567(9), 2.578(7)	2.521(3), 2.517(3)
Ln–μ-C$_{Ar}$	2.626(9), 2.634(10)	2.597(3), 2.594(3)
Li–μ-C$_{Ar}$	2.250(18), 2.144(16)	2.180(5), 2.185(6)
Ln–NR$_2$	2.739(9), 2.734(13)	2.694(2), 2.629(2)
Li–NR$_2$	2.124(15), 2.091(15)	2.063(6), 2.068(5)
μ-C$_{Ar}$–Ln–μ-C$_{Ar}$'	87.2(3)	87.3(1)
μ-C$_{Ar}$–Li–μ-C$_{Ar}$'	111.3(6)	110.3(3)
(N–CH$_2$–C$_{Ar}$)$_{Ln}$	112.8(8), 111.4(11)	112.9(3), 112.4(3)
(N–CH$_2$–C$_{Ar}$)$_{Li}$	112.5(8), 111.6(8)	109.7(3), 109.9(3)
C$_{Ar}$–Ln–Li–N$_{Ar}$'	167.2(5), 160.9(5)	162.7(2), 169.9(2)
Li–C$_{Ar}$–Ln–C$_{Ar}$'	4.2(5)	6.5(2)

These slight modification of the ligand framework (dmba → pyba) has allowed for the first time to stabilize one of the early lanthanide metals (Nd) in the form of its *tetrakis*-aryl ate complex. Best to our knowledge, this is the first homoleptic crystallographically characterized lithium ate complex, that has "pure" δ-C(sp^3)–Nd bonding.

The attempted reactions of aryllithium reagents **R1** and **R2** with [$PrCl_3$(dme)] under the same conditions was not successful any more – a progressive darkening of the reaction mixture was observed immediately after the beginning of the reaction, even at 0°C.

2.3. *Lanthanide Tris-Aryl Complexes with (tmba)- and (cuda)-Ligands*

2.3.1. *Synthesis of (tmba)- and (cuda)-Ligands*

As shown before by the example of the alkaline earth metals (Na, K) the deprotonation of the α-benzylic-position is the most probable side reaction that might be responsible for the quick degradation of the coordinated (dmba)- and (pyba)-ligands. Therefore, we decided to modify the (dmba)-ligand by introducting either one or two methyl groups into the α-benzylic position.

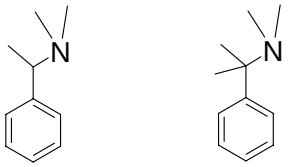

tmba cuda

These α-mono- and α,α-dimethyl derivatives of *N,N*-dimethylbenzylamine are *N,N,*α-trimethylbenzylamine (tmba)H and cumyl-*N,N*-dimethylamine (cuda)H. Both amines were synthesized according to the literature procedure from the commercial (*S*)-phenylethylamine[41] and *tert*-cumylamine by the standard protocol of exhaustive methylation under *Eschweiler-Clark* conditions.[24] The intermediate *tert*-cumylamine was prepared in 60% yield[25] by electrophilic addition of hydrazoic acid to α-methylstyrol followed by reduction of cumylazide with Raney-Ni in *iso*-PrOH. The crude cumylazide was reduced without purification (Scheme 10).[26]

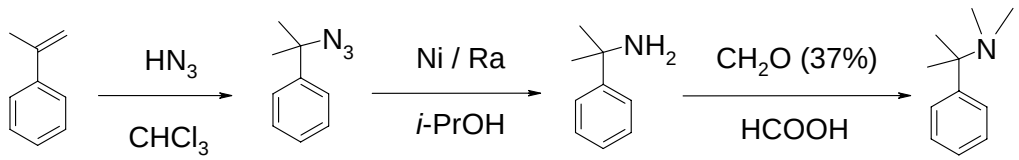

Scheme 10. Synthesis of cumyl-*N,N*-dimethylamine from α-methylstyrol.

The apparently simpler *one-pot* synthesis of *tert*-cumilamine from *α*-methylstyrol under the *Ritter* reaction conditions (MeCN / conc. H_2SO_4) was reported to be inefficient and leads selectively to 1,1,3-trimethyl-3-phenyl-indane.[27]

2.3.2. *Synthesis of Starting Aryllithium Reagents Li(tmba) (**R3**) and Li(cuda) (**R4**)*

The synthesis and properties of aryllithium reagent Li(tmba) (**R3**) were first reported in 2004 by *van Koten et al*.[28] It was shown that the appearance, reactivity and physicochemical properties of *ortho*-lithiated racemic and enantiopure amine differ dramatically. Therefore, the metallation was investigated with (*S*)-phenylethylamine instead of the racemate. The synthesis of the aryllithium reagent **R3** was performed using *tert*-BuLi as deprotonating agent in pentane at room temperature.[28] It was reported that in case were *n*-BuLi was applied as deprotonating agent the mixed complex of the type [{Li(tmba)}$_2$(*n*-BuLi)$_2$(tmba)$_2$] forms.[29]

The second aryllithium reagent – *ortho*-lithiated cumyl-*N,N*-dimethylamine, Li(cuda) (**R4**) – was first time *in situ* generated by transmetallation of (*o*-BrC_6H_4)$C(Me)_2NMe_2$ with *n*-BuLi and further used for a following reaction in boron chemistry. No isolation or characterization of the compound was attempted (Scheme 11). [30]

R = Me, Et, *n*-Pr, *i*-Pr Yields: ca. 40 % (R = *i*-Pr)
ca. 5 % (R = Me, Et, *n*-Pr)

Scheme 11.

We have synthesized Li(cuda) **R4** by deprotonation of *N,N*-dimethyl-cumylamine with *tert*-BuLi in multigram scale and completely characterized for the first time. The product shows higher solubility in ethereal and aliphatic solvents analogous to Li(tmba). The isolation of lithium reagent **R4** was achieved by storing its pentane solution at -30°C. The product was isolated in 55% yield. From an ether solution an etherate of the composition Li(cuda)×½Et_2O can be isolated. The attempts to remove the coordinated ether molecule by drying this etherate in vacuum at 10^{-2} Torr/20°C were unsuccessful.

This stable etherate was used as a convenient precursor for the further syntheses.

In the aliphatic region of the ^{1}H NMR spectrum, broad resonances for Me_2C- and Me_2N-groups were observed at 1.42 and 1.76 ppm respectively, as well as sharp resonances of the coordinated ether molecule (0.92 and 3.13 ppm). This findings reflect the fluxional behavior of the (cuda)-ligands in solution (C_6D_6).

From the attempted reaction of [$LaCl_3$(dme)] with three equivalents of Li(cuda)×½Et_2O in ether at room temperature, a colorless, crystalline solid was isolated. Analysis of crystals by X-ray diffraction shows that a binuclear complex with coordinating solvent formed. Both ether and DME molecules are present at the ratio of 0.68/0.32. The molecular structure of [Li_2(cuda)$_2$(Et_2O)$_{0.68}$(dme)$_{0.32}$] is presented below (Figure 6).

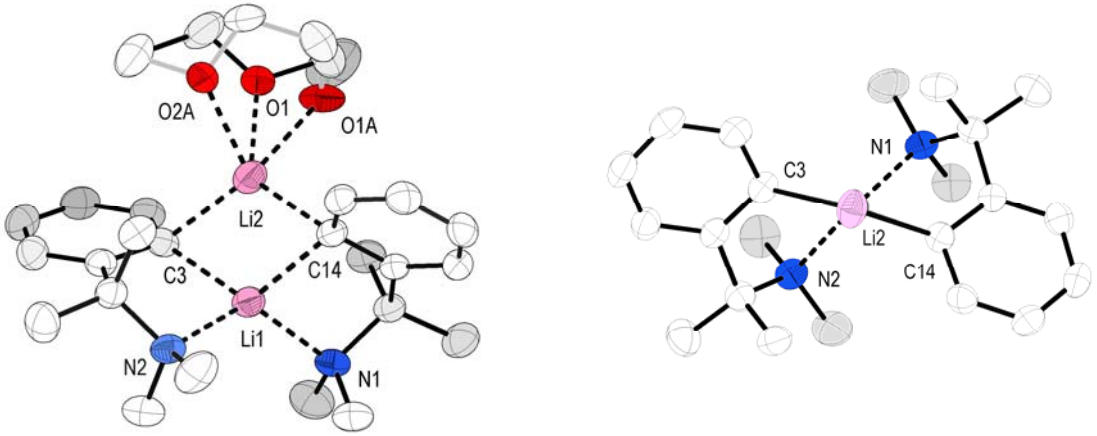

Figure 6. The molecular structures of [Li_2(cuda)$_2$(Et_2O)$_{0.68}$(dme)$_{0.32}$] **R4**: side view (right) and view along the *pseudo*-C_2-axis through Li1···Li2 axis. Hydrogen atoms have been omitted for clarity. In the right picture ether molecules have also been omitted. Selected bond lengths (Å) and angles (°): Li1–C3 2.188(3), Li1–C14 2.207(3), Li2–C3 2.181(4), Li2–C14 2.173(3), Li1–N1 2.120(3), Li1–N2 2.087(3), Li2–O1 1.851(4), Li2–O1A 2.326(7), Li2–O2A 2.105(5), L1–C3–Li2 66.3(1), Li1–C13–Li2 66.1(1), C3–Li1–C13 112.8(1), C3–Li2–C13 114.5(2), N1–Li1–N2 121.3(1).

In the solid state the compound adopts an approximately C_2-symmetric, propeller-like structure, in which two lithium atoms are bridged by the *ipso*-carbon atoms of the aryl groups thus forming a nearly planar Li_2C_2-ring. The Li2 atom is coordinated by Et_2O and DME molecules. The coordination around the Li1 atom is distorted as tetrahedral by the additional interaction with two coordinated Me_2N-groups of the (cuda)-ligand.

2.3.3. *Lanthanide Complexes with (tmba)-Ligand*

In first experiment on transmetallation with the aryllithium reagent Li(tmba) **R3**, the synthesis of the homoleptic lutetium complex [Lu(tmba)$_3$] (**H7**) was attempted. The *salt metathesis* reaction of the aryllithium reagent **R3** with [$LuCl_3(thf)_3$] in 3:1 stoichiometry resulted in the formation of a clear solution and precipitation of LiCl (Scheme 12). After getting rid of LiCl by filtration, the isolated compound was identified as the first in this series heteroleptic *bis*-aryl-chlorocomplex [(tmba)$_2$LuCl] (**H7'**). The composition of the complex was confirmed by elemental analysis. Prolongation of the reaction time (24 d at 20°C) did not result in the substitution of the third chlorine atom in this complex pointing out the fact that only *bis*-aryl complexes can be obtained *via salt metathesis* reaction.

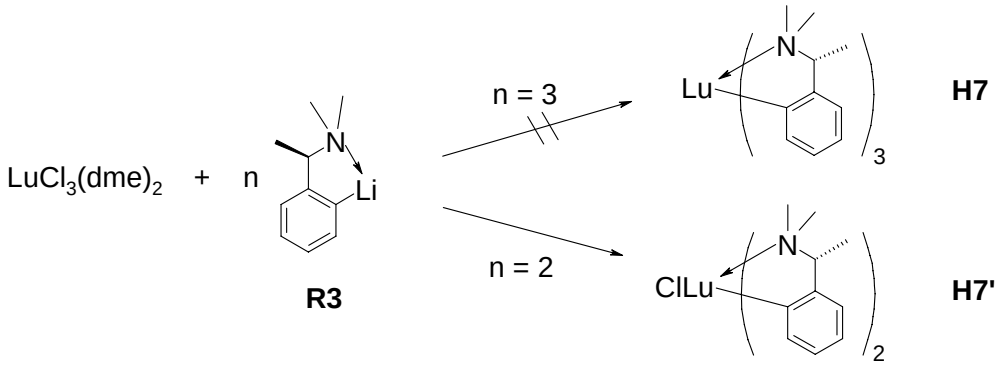

Scheme 12. The attempted synthesis of the complex [Lu(tmba)$_3$] **H7**.

In the aliphatic region of the ^{1}H NMR spectrum, three broad resonances were observed. It is believed, that the complex **H7'** has in the solid state a binuclear structure, bridged over the chlorine atoms.

Thus, the introduction of only one methyl substituent at the benzylic position results in a dramatic increase of the steric bulk of the ligand and no further insertion of the third aryl ligand at this late lanthanide atom was observed.

By its size, the Y^{3+} ion occupies exactly the boarder position between middle and late lanthanides, therefore the transmetallation of Li(tmba) **R3** with middle rare-earth metal trihalides (Y and Dy) using the same procedure was applied for the attempted synthesis of complex **H7**.

It was observed, that in both cases the formation of the corresponding *tris*-aryl complexes proceeds without side reactions and in high yields (Scheme 13).

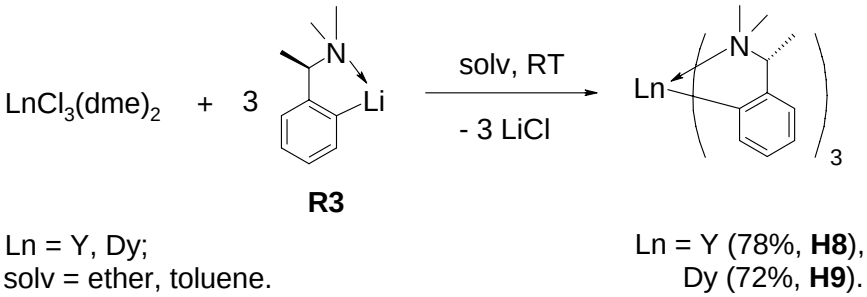

Scheme 13. Synthesis of the homoleptic complexes [Y(tmba)$_3$] **H8** and [Dy(tmba)$_3$] **H9**.

The colorless [Y(tmba)$_3$] (**H8**) and yellowish [Dy(tmba)$_3$] (**H9**) complexes were isolated by crystallization from ether and hexane respectively. Both complexes possess a high thermal stability and show high solubility in aromatic solvents; they can be crystallized by cooling of hot saturated hexane solutions.

The complex [Y(tmba)$_3$] (**H8**), which contains three chiral ligands, crystallizes in the monoclinic space group $P2_1$ with two independent molecules in the unit cell. The molecular structure is presented in Figure 7, selected bond lengths and angles in Table 3.

The molecular architecture is similar to the pattern found in the homoleptic complexes **H1** – **H4** with the ligands which also arranged in "two-short, one-long" pattern. Comparison with the related yttrium complex [Y(dmba)$_3$] **H4** reveals similarities in the values for angles, but some differences in the Y–N and Y–C bond lengths. In general all Y–N bond lengths are slightly longer (ca. 0.5 Å) than in complex **H4**. Surprisingly, both "long" Y–C bond lengths in both independent molecules of **H8** (2.468(8) and 2.471(8) Å resp.) not only shorter than the "long" one (2.504(3) Å) in the parent **H4**, but even shorter than both "short" ones (2.475(2), 2.479(4) Å).

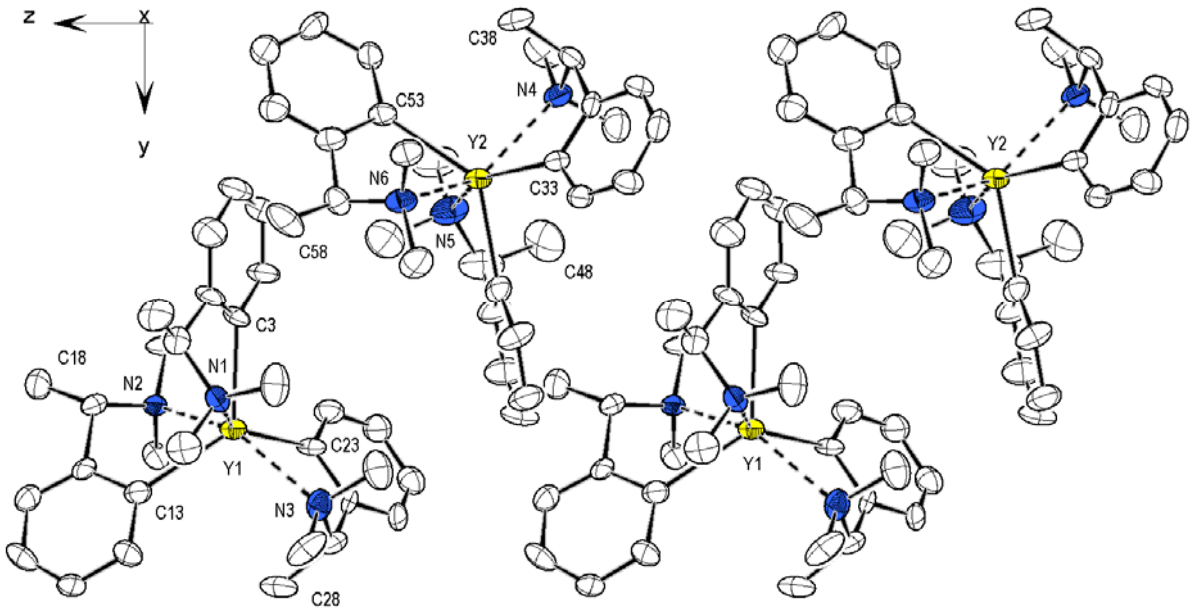

Figure 7. The molecular structure of the complex [Y(tmba)$_3$] **H8**: view along the crystallographic x-axis. All hydrogen atoms have been omitted for clarity.

The sum of C_{Ar}–Y–C_{Ar} angles at the metal center are smaller (349.5(8) and 353.7(9)°) compared to [Y(dmba)$_3$] **H4**. Consequently, deviation of metal center from the CCC-plane is also larger (0.457(1) and 0.350(1) Å).

In order to understand these findings, the impact of benzylic methyl-substituents on conformation was analyzed.

Table 3. Selected bond lengths (Å) and angles (°) for the homoleptic complexes **H8** and **H9**.

	H8 (M = Y)		**H9** (M = Dy)	
	Molecule 1	Molecule 2	Molecule 1	Molecule 2
M–N1	2.666(6)	2.587(7)	2.548(7)	2.611(7)
M–N2	2.580(7)	2.599(7)	2.666(9)	2.570(7)
M–N3	2.569(7)	2.568(8)	2.566(8)	2.606(8)
M–C1	2.435(7)	2.422(9)	2.518(7)	2.453(7)
M–C10	2.459(8)	2.468(10)	2.450(11)	2.508(9)
M–C19	2.468(8)	2.471(8)	2.450(8)	2.483(8)
C1–M–C10	124.0(2)	99.4(3)	134.1(3)	124.7(3)
C10–M–C19	121.7(3)	132.6(3)	99.5(3)	134.4(3)
C1–M–C19	103.8(3)	121.7(3)	116.2(3)	94.9(3)
$\Sigma(C_A–M–C_B)$	349.5(8)	353.7(9)	349.8(9)	354.0(9)
N1–M–N2	125.2(2)	94.1(2)	116.8(3)	140.3(2)
N2–M–N3	144.1(2)	119.7(2)	88.6(3)	117.4(2)
N1–M–N3	87.3(2)	140.0(3)	151.1(1)	94.1(1)
$\Sigma(N_A–M–N_B)$	356.6(6)	353.8(7)	356.5(7)	351.8(5)
M···CCC*)	0.457(1)	0.350(1)	0.343(4)	0.447(4)
M···NNN*)	0.255(1)	0.352(1)	0.244(4)	0.408(1)

*) M···CCC and M···NNN denotes the distance of metal with respect to the plane defined by atoms N1, N2, N3 and C1, C10, C19 respectively.

The chiral (tmba)-ligand coordinated at a metal center can exhibit two conformations in the solid state: the methyl-substituent is orientated either nearly parallel to the orthogonal vector defined by the aromatic ring plane and not located on the plane (*out-of-plane* conformation, $\varphi \rightarrow 90°$, Scheme 14) or it is oriented nearly coplanar to the aromatic ring (*in-plane-*, $\varphi \rightarrow 0°$).

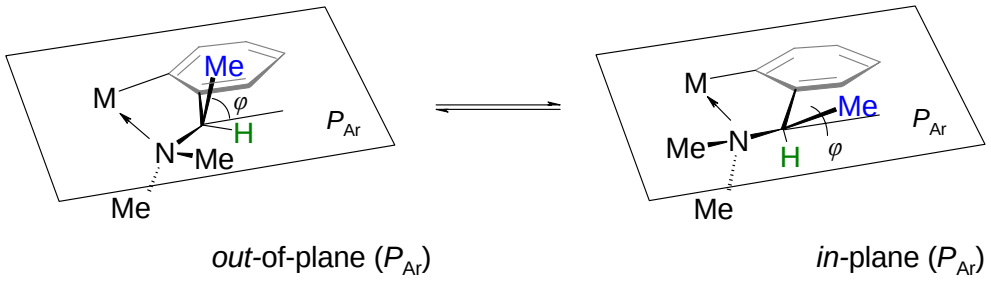

Scheme 14. The *out-* and *in*-of-plane conformations of the (tmba)-ligand in its complexes. The φ-angle is defined as the angle between the C–Me bond and the Ar-plane.

According to this definition, the independent molecules of [Y(tmba)$_3$] **H8** have different conformations of the (tmba)-ligands. One molecule in the unit cell has mixed *in-in-out*-(tmba)-ligand conformations with the φ-angles of 10.4(7), 8.1(6) and 82.6(4)° respectively. The other independent molecule has *out-out-in*-conformations with the φ-angles of 82.3(5), 87.5(7) and 8.9(6)° respectively.

Unlike all previously crystallographically characterized complexes, the homoleptic dysprosium complex [Dy(tmba)$_3$] **H9** crystallizes in the orthorhombic space group $P2_12_12_1$ (Figure 8). The complex **H9**, which features a slightly larger Dy^{3+} metal center, crystallizes also with two independent molecules in the unit cell. The selected bond lengths and angles are given in Table 3.

The Dy–C bond lengths vary from 2.450(8) – 2.518(7) Å. No crystallographical reference structures containing Dy–(sp^2-C) bond was found in the Cambridge Crystallographical Data Base. Two crystallographically characterized structures containing Dy–(sp^3-C) are listed. The Dy–C bonds in silyl- and disilylmethanide complexes [{η^5-$Me_3SiC_5Me_4$)}-Dy(CH_2SiMe_3)$_2$(thf)] (Dy–C: 2.410(3) and 2.373(2) Å)[31] and [{η^5,η^5-$C_5H_4SiMe_2Flu$}-DyCH($SiMe_3$)$_2$] (Dy–C: 2.364(9) Å)[32] are significantly shorter than av. 2.48 Å found in the homoleptic complex [Dy(tmba)$_3$] **H9**.

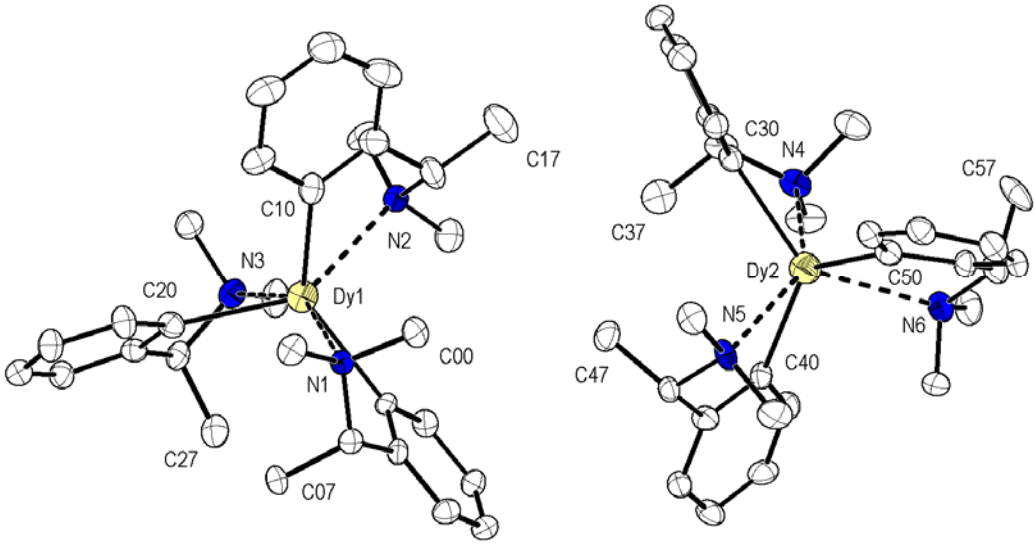

Figure 8. The molecular view of two independent molecules in the dysprosium complex [Dy(tmba)$_3$] **H9** in the unit cell. All hydrogen atoms have been omitted for clarity.

The most interesting feature of this structure is that the conformations of the benzylic methyl-substituents differ significantly from the picture shown by the yttrium analog **H8**. Both independent molecules of **H9** have predominantly *out*-conformations in the solid state. In the one molecule all three (tmba)-ligands have *out*-conformations with φ-angles of 85.5(5), 84.9(4) and 89.2(8)° and in the other – two *out*- and one *in*-conformations with the φ-angles of 86.0(4), 88.9(7) and 1.4(6)°. Moreover, the angles are closer to the extremes of 90° and 0° in comparison to compound **H8**.

Impressed by these successful syntheses, the reaction of Li(tmba) (**R3**) with the early lanthanide trihalides (Nd and Sm) was studied. Both reactions started at 0°C in ether/toluene (1:1, v/v) solvent mixture proceed quickly with formation of light-green (Nd) or deep yellow (Sm) solutions and precipitation of LiCl (Scheme 15). It is essential to work-up at low temperatures (<0°C), because at ambient temperature a swift brown coloration of the reaction mixtures and obvious decomposition of the early formed complexes [Nd(tmba)$_3$] (**H10**) and [Sm(tmba)$_3$] (**H11**) takes place.

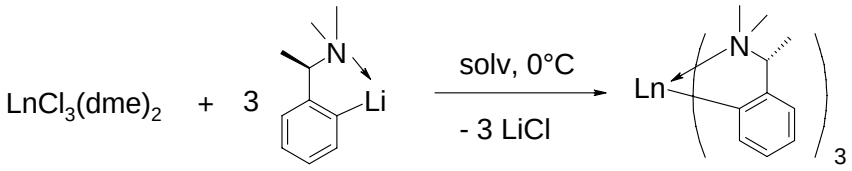

R3

Ln = Nd, Sm;
solv = ether, toluene.

Ln = Nd (**H10**);
Sm (**H11**).

Scheme 15. Synthesis of complexes [Nd(tmba)$_3$] (**H10**) and [Sm(tmba)$_3$] (**H11**).

Both complexes were isolated by storing of their concentrated hexane solutions at -30°C for several days. Good elemental analysis was obtained for both complexes. For the neodymium complex **H10** we succeeded to obtain crystals, suitable for X-ray analysis.

Also like the dysprosium complex **H9**, the neodymium complex [Nd(tmba)$_3$] **H10** crystallizes in the orthorhombic space group $P2_12_12_1$. The molecular structure is depicted in Figure 9.

Unexpectedly, two independent molecules found in the structure have odd occupancy ratio of 0.603:0.397. Although this ratio is very close to 3:2, all attempts of structure refinement were unsuccessful.

The molecules differing by conformation of only one of three (tmba)-ligands – the positions of other two ligands and even the position of the metal center in the lattice are identical. The common (tmba)-ligands have *out*- and *in*-conformations, the "odd"-ligand has predominantly *in*-conformation with occupancy of 0.603. The φ-angles of 79.7(2) and 6.5(3)° were found for both common ligands and of 3.4(3) and 88(1) for *in*- and *out*-conformations of the third.

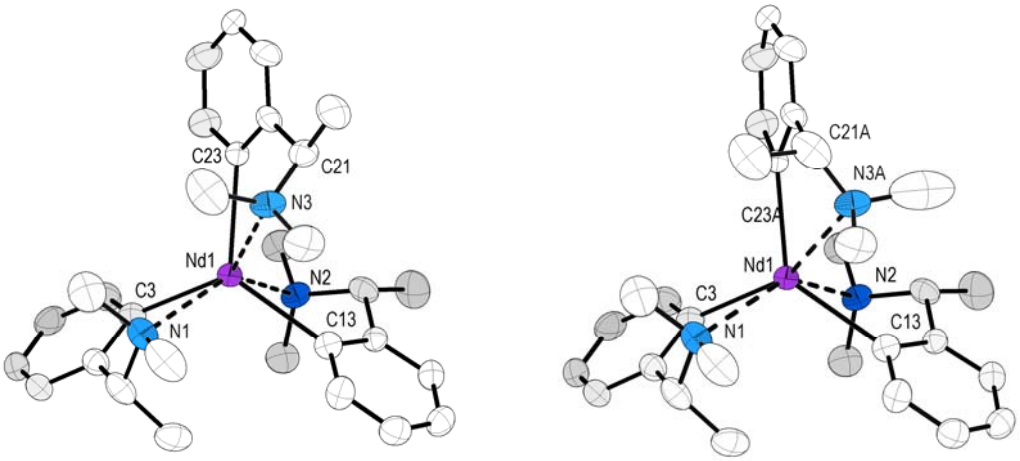

Figure 9. The molecular structures of two independent molecules in neodymium complex [Nd(tmba)$_3$] (**H10**): *out-in-in*-conformation (left) and *out-in-out*-conformation (right). All hydrogen atoms have been omitted for clarity. Selected bond lengths (Å) and angles (Å): Nd1–N1 2.678(1), Nd1–N2 2.653(1), Nd1–N3 2.750(1), Nd–N3A 2.789(1), Nd–C3 2.565(5), Nd–C13 2.557(5), Nd–C23 2.589(4), Nd–C23A 2.440(14), N1–Nd1–N2 139.4(1), N2–Nd1–N3 126.6(1), N3–Nd1–N1 89.8(1), N2–Nd1–N3A 111.5(1), N3A–Nd1–N1 103.2(1), C3–Nd1–C13 120.7(2), C13–Nd1–C23 122.7(1), C23–Nd1–C13 106.4(1), C13–Nd1–C23A 130.4(1), C23A–Nd1–C13 101.7(1); for *out-in-in*-conformer (left): $\Sigma(N_A–Nd1–N_B)$, 355.8(3), $\Sigma(C_A–Nd1–C_B)$ 349.8(5), Nd1···CCC 0.474(1), Nd1···NNN 0.303(1); for *out-in-out* conformer (right): $\Sigma(N_A–Nd1–N_B)$ 354.1(3), $\Sigma(C_A–Nd1–C_B)$ 352.8(3), Nd1···CCC 0.384(1), Nd1···NNN 0.364(1).

The packing in the unit cell is presented in Figure 10. In this figure one can clearly see, that the molecules are arranged in periodic stacks along the crystallographic y-axis, whereas the disordered (tmba)-ligands forming an endless "tunnels of disordering". This, obviously, is a result in low conformational barrier between *in*- and *out*-conformations in this complex.

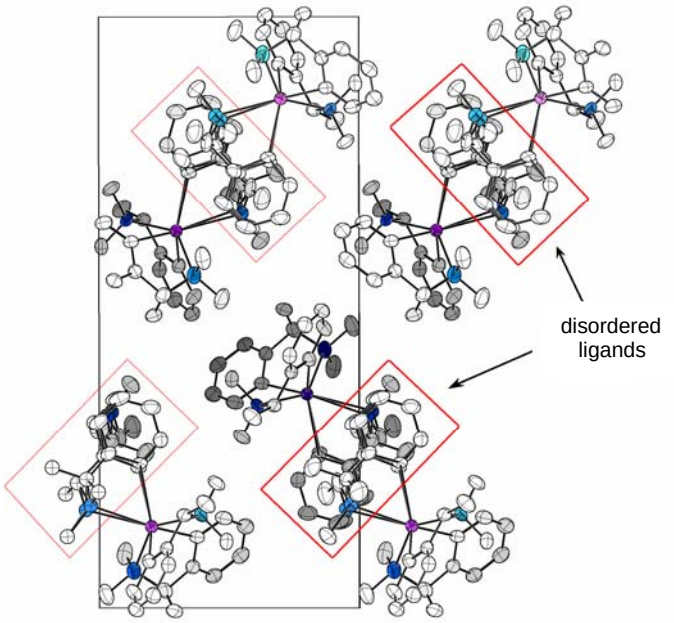

Figure 10. The lattice structure of complex [Nd(tmba)$_3$] (**H10**): view along the crystallographic y-axis. All hydrogen atoms have been omitted for clarity.

2.3.4. *Lanthanide Complexes with (cuda)-Ligand*

Finally, we attempted the synthesis of samarium complex [Sm(cuda)$_3$] **H12** starting from [SmCl$_3$(dme)$_2$] and Li(cuda) **R4** in ether/toluene mixture (1:1, v/v). As in the case of [Sm(tmba)$_3$] (**H11**) the reaction proceeds quickly at 0°C with formation of deep yellow solution and a precipitation of LiCl (Scheme 16). However, in this case, it was found, that upon warming to ambient temperature no (detectable) decomposition takes place.

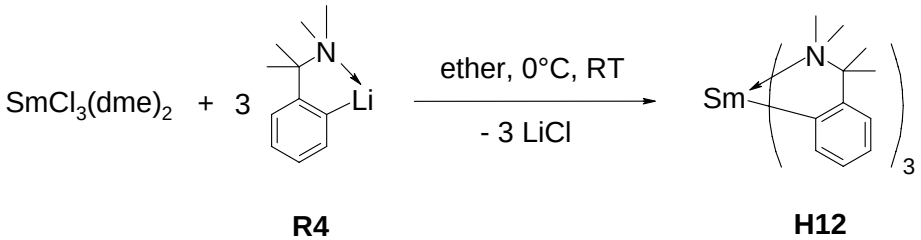

R4 **H12**

Scheme 16. Synthesis of samarium complex [Sm(cuda)$_3$] **H12**.

Simple filtration of the precipitated LiCl followed by extraction with toluene and low temperature crystallization yields a bright yellow, microcrystalline powder that is rather stable for several houses even at ambient temperature. It can be stored at -30°C without decomposition for at least three months (!) Very good elemental analysis was obtained for this complex. The compound is highly reactive and decomposes when reacted with THF forming a colorless solution. Single crystals, suitable for X-ray diffraction, were obtained by crystallization from the saturated diethyl ether solution at -30°C. The molecular structure of **H12** is depicted in Figure 11.

The complex crystallizes in the monoclinic space group $P2_1/c$ with only one asymmetric unit/molecule (Z = 4). The coordination is similar to those of the late and middle lanthanide complexes and also best described as a distorted *pseudo*-octahedral. The Sm–C bond lengths vary from 2.489(5) – 2.550(4) Å; the Sm–N bond lengths from 2.628(3) – 2.709(3) Å. Comparison with neutral mononuclear complexes reveals that the Sm–C bond lengths fall into the region of reported ones in $[\{o\text{-}(o\text{-}MeOC_6H_4)_2C_6H_3\}Sm\{N(SiHMe_2)_2\}_2]$[33] (2.483 Å), $[(\eta^5\text{-}Me_5C_5)_2SmPh(thf)]$[34] (2.511 Å), $[(o\text{-}C_4H_3N\text{-}C_6H_4)Sm(\eta^5\text{-}C_5Me_5)_2]$[35] (2.527 Å), $[\{o\text{-}Mes_2C_6H_3\}Sm(\eta^8\text{-}C_8H_8)(thf)]$ (2.529 Å), $[(o\text{-}(o\text{-}MeOC_6H_4)_2C_6H_3)Sm(\eta^8\text{-}C_8H_8)(thf)]$[36] (2.543 Å), $[(o\text{-}Mes_2C_6H_3)SmCl_2(ImMe)_2(thf)]$[37] (2.532 Å), $[(o\text{-}Mes_2\ C_6H_3)SmCp]$[38] (2.536 Å).

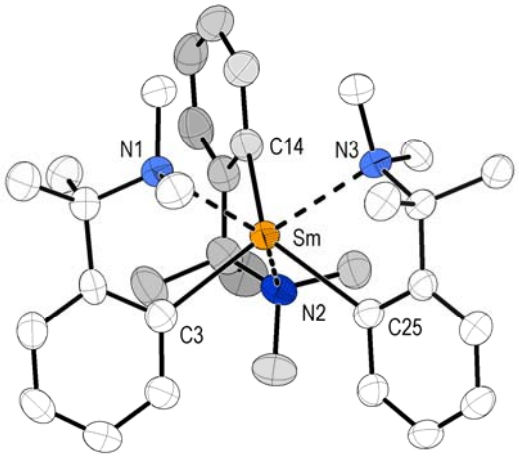

Figure 11. The molecular structure of samarium complex $[Sm(cuda)_3]$ **H12**. All hydrogen atoms have been omitted for clarity. Selected bond lengths (Å) and angles(°): Sm–C3 2.489(5), Sm–C14 2.528(5), Sm–C25 2.550(4), Sm–N1 2.710(4), Sm–N2 2.628(3) Sm–N3 2.709(3); C3–Sm–C14 117.6(2), C14–Sm–C25 136.0(2), C25–Sm–C3 99.4(2), N1–Sm–N2 136.1(1), N2–Sm–N3 119.0(1), N3–Sm–N1 97.6(1); $\Sigma(C_A\text{–}Sm\text{–}C_B)$ 353.0(6), $\Sigma(N_A\text{–}Sm\text{–}N_B)$ 352.7(3); Sm···CCC 0.374(1), Sm···NNN 0.402(1).

3. CONCLUSIONS

The results achieved are summarized in Table 4. The sterically less demanding ligands (dmba) and (pyba), that contain a benzylic CH_2-groups, do not stabilize early lanthanide complexes of the type [$LnAr_3$] (Ln = Ce – Sm, La). The largest rare-earth cation forming homoleptic *tris*-aryl complexes with (dmba) or (pyba) is yttrium followed by the late lanthanide cations (Er^{3+}, Yb^{3+}, Lu^{3+}). On the other hand (dmba) and (pyba) ligands form interesting lithium ate complexes with the early (Nd) and middle (Gd) lanthanide cations, whereas this could not be verified for the late lanthanides. Stabilization of early homoleptic Ln^{3+} complexes was achieved when the benzylic CH_2-group in the (dmba) ligand is replaced by CHMe (tmba) or Me_2C (cuda). The mismatch leads either to unstable species of early and middle lanthanides with less crowded ligands, or to incomplete substitution and formation of heteroleptic [$Lu(tmba)_2Cl$] complex. Up to date, the formation of stable complexes [$Ln(tmba)_3$] with the larger late lanthanides (Er, Tm) or [$Ln(cuda)_3$] with the middle lanthanides (Eu – Ho) cannot be excluded, but remains unverified. Stabilization of *tris*-aryl complexes of the smaller late lanthanides with (cuda) ligand is fairly improbable. Synthesis and structural characterization of novel Li[$LnAr_4$] species was verified for one early lanthanide metal [$LiNd(pyba)_4$]×½PhMe and one middle lanthanide metal [$LiGd(dmba)_4$], but remains unverified for the sterically demanding (tmba) and (cuda) ligands.

Table 4.

		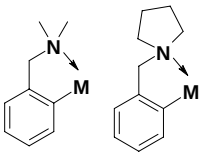 **M(dmba)** **M(pyba)**	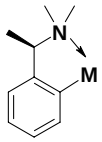 **M(tmba)**	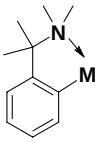 **M(cuda)**
Early lanthanides complexes (Ce – Sm & La)	$LnAr_3$	unstable for Ce – Sm	fairly stable for Nd and Sm	stable for Sm
	Li[$LnAr_4$]	stable for Nd	unverified	
Middle lanthanides complexes (Eu – Ho & Y)	$LnAr_3$	unstable for Gd, Tb, Dy stable for Y only	stable for Y and Dy	unverified
	Li[$LnAr_4$]	stable for Gd	unverified	
Late lanthanides complexes (Er – Lu & Sc)	$LnAr_3$	stable for Er, Yb & Lu	unverified; only Ar_2LuCl stable	improbable
	Li[$LnAr_4$]	unverified	improbable	

4. EXPERIMENTAL PART

General considerations. Starting lanthanide chlorides [$LnCl_3 \times 6H_2O$] were synthesized by dissolving their oxides in conc. hydrochloric acid (p. a.) followed by continuous evaporation in an evaporating dish at 90°C. 1,2-Dimethoxyethane (DME) was purified by conventional methods.

Composition of solvated lanthanide trichlorides was determined by dissolution of a weighted amount of sample (ca. 0.5 g) in dist. water and determination of chloride with an excess of aqueous $AgNO_3$ (filtration of AgCl followed by repeated washing with dist. H_2O and MeOH) and lanthanide by complexometric titration with EDTA in the presence of xylenol orange as indicator (violet → pure yellow).[39] Elemental analyses (CHN) were performed in microanalytical laboratory at chemistry department of Philipps-Universität Marburg

Following compounds were synthesized as reported in the literature: $PhC(Me)_2NH_2$,[25] Li(dmba)[40] (**R1**), (*S*)-$PhCH(Me)NMe_2$,[41] Li(tmba)[42] (**R3**), [$Er(dmba)_3$][2] (**H1**), [$Yb(dmba)_3$] (**H2**).[2] Following reagents – $PhCH_2NMe_2$, benzaldehide, pyrrolidine, formic acid, 37% aq. formaldehyde and *tert*-BuLi (15% solution in pentane) – were used as supplied (Acros, Aldrich).

4.1. *Synthesis of Starting Materials*

4.1.1. *Synthesis of N-benzylpyrrolidine (pyba)H*

Although many literature procedures toward the synthesis of this amine are described,[43] it was found, that the reaction of pyrrolidine and benzaldehyde amine under Leuckart-Wallach conditions[44] (with formic acid as reducing agent) is the best, rapid and upscalable approach.

To ice bath cooled formic acid (23.0 mL, 27.6 g, 0.60 mol) pyrrolidine (25.0 mL, 21.5 g, 0.30 mol) was added drop by drop (*Caution! Pyrrolidine is very corrosive and trace amounts can invoke allergic reaction*). After addition was complet freshly distilled benzaldehyde (20.0 mL, 20.6 g, 0.19 mol) was added and the reaction mixture slowly heated to 100° C (*Caution! Vigorous CO_2 evolution*). The reaction mixture was refluxed additionally for 1 h. Water (100 mL) was added and the solution was cooled to 0°C. After addition of NaOH (10 g) the amine separates as yellow oil, that was extracted with hexane (2×30 mL). The organic phase was

washed with water (3×50 mL) and brine (50 mL) and dried over Na_2SO_4 and than over $LiAlH_4$. The solvent was carefully evaporated at 0°C. Bulb-to-bulb distillation of the crude product gives 28.2 g (0.175 mol) of *N*-benzylpyrrolidine as a colorless liquid (Yield: 92 %).
^{1}H NMR ($CDCl_3$, 200.1 MHz): δ = 1.76 (m, 4 H, NCH_2CH_2), 2.49 (m, 4 H, NCH_2CH_2), 3.59 (s, 2 H, $PhCH_2$), 7.30 (m, 4 H, *Ph*) ppm.
$^{13}C\{^1H\}$ NMR (C_6D_6, 50.0 MHz): δ = 23.3 (NCH_2CH_2), 54.1(NCH_2CH_2), 60.7 ($PhCH_2$), 126.8 (*p-Ph*), 128.1, 128.8 (*m-/o-Ph*), 139.3 (*ipso-Ph*) ppm.

4.1.2. *Synthesis of cumyl-N,N-dimethylamine (cuda)H*

Although this amine was reported in literature,[45] it was synthesized by a multistep procedure with low yield (21%). The amine can be easily synthesized, analogue to that of in Ref. 41, by exhaustive methylation of cumylamine under Eschweiler-Clarck conditions.[24]
Cumylamine (5.0 g, 37 mmol) was added carefully to an ice cooled mixture of formic acid (11.1 mL, 0.3 mol, 8 equiv) and formaldehyde (37%, 13.9 mL, 122 mmol, 3.3 equiv). The mixture was brought to ambient temperature and further warmed to 70°C whereupon an exothermic reaction with gas evolution began. After the vigorous gas evolution seazed, the reaction mixture was refluxed for 1 h. It was cooled with an ice bath, extracted twice with ether (2×30mL) and was made alkaline by addition of excess of 50% solution of NaOH. The separated organic phase was separated and the aqueous phase was extracted with ether (3×50 mL). The combined organic phases were successively dried with Na_2SO_4 and CaH_2 followed by removal of solvent in vacuum. The substance was purified by vacuum distillation (83°C / 16 mm). A colorless liquid was obtained in 75% yield (4.5 g, 27 mmol).
^{1}H NMR ($CDCl_3$, 300.1 MHz): δ = 1.35 (s, 6 H, CMe_2), 2.16 (s, 6 H, NMe_2), 7.19 (t, $^3J_{HH}$ = 7.1 Hz, 1 H, *p-Ph*), 7.30 (t, $^3J_{HH}$ = 7.8 Hz, 2 H, *m-Ph*), 7.50 (d, $^3J_{HH}$ = 7.5 Hz, 2 H, *o-Ph*) ppm.
$^{13}C\{^1H\}$ NMR (C_6D_6, 75.5 MHz): δ = 23.4 (CMe_2), 39.0 (NMe_2), 59.5 ($PhCMe_2$), 126.1 (*p-/m-Ph*), 127.9 (*o-Ph*), 148.7 (*ipso-Ph*) ppm.

4.1.3. *Synthesis of o-(N-pyrrolidylmethyl)-phenyllithium (Li(pyba),* ***R2****)*

To *N*-benzylpyrrolidine (10.0 g, 62.1 mmol) in ca. 120 mL ether, solution of *n*-BuLi (46 mL, 1.6M in hexane, 75 mmol, 1.2 equiv) was added at ambient temperature and stirred for 48 h. The precipitated solid was filtered off from deep yellow mother liquor and thoroughly

washed with hexane (3×50 mL). The product was obtained as colorless, crystalline solid in 94% yield (9.8 g).

^{1}H NMR (C_6D_6, 300.1 MHz): δ = 0.70 (s br, 1H,), 1.09 (s br, 1H,), 1.24 (s br, 2H), 1.57 (dd, 1H, J = 8.4 Hz, J = 17.2 Hz), 1.81 (dd, 1H, J = 8.5 Hz, J = 17.4 Hz), 2.27 (m. br, 1H), 2.71 (m br, 1H,), 3.19 (d, J = 13.1 Hz, 1H), 4.48 (d, J = 13.0 Hz, 1H,), 7.20 (m, *Ar*, 4H), 8.38 (d, J = 5.3 Hz, 1H, *o-Ar*) ppm.

^{13}C{^{1}H} NMR (C_6D_6, 75.5 MHz): δ = 22.6, 23.5 (NCH_2CH_2), 54.1, 55.1 (NCH_2CH_2), 67.7 ($ArCH_2N$), 125.3 (*Ar*), 126.1 (*Ar*), 126.7 (*Ar*), 139.3 ($C2_{Ar}$), 152.8 ($C6_{Ar}CH_2$), 174.7 (br s, $C1_{Ar}$) ppm.

Anal. Calcd. for $C_{11}H_{15}NLi$ (168.19): C 78.56, H 8.99, N 8.33.

Found: C 77.94, H 8.92, N 8.24.

4.1.4. *Synthesis of o-(α,N,N-trimethylaminomethyl)phenyllithium (Li(tmba),* ***R3****)*[28]

To a solution of (*S*)-PhCH(Me)NMe_2 (3.0 g, 20.1 mmol) in 100 mL hexane, solution of *tert*-BuLi (16 mL, 1.5M in hexane, 24.1 mmol, 1.2 equiv) was added at ambient temperature and the reaction mixture was stirred over night. The precipitate formed was filtered off, wached with hexane (2×15 mL) and dried in vacuum. The product was obtained as a colorless crystalline solid in yield of 64% (2.0 g).

^{1}H NMR (C_6D_6, 300.1 MHz): δ = 1.14 (br s, $\nu_{½}$ = 15 Hz, 3H, ArH*Me*), 1.61, 1.79 (2 × br s, $\nu_{½}$ = 20 Hz, 2×3H N*Me*$_2$), 3.35 (br s, $\nu_{½}$ = 34 Hz, 1H, Ar*H*Me), 7.06 (d, $^3J_{HH}$ = 7 Hz, 1H, *Ar*), 7.26 (m, 2H, *Ar*), 8.51 (br s, $\nu_{½}$ = 16 Hz, 1H, *o-Ar*) ppm.

^{13}C{^{1}H} NMR (C_6D_6, 75.5 MHz): δ = 17.7 (br s, ArCH*Me*), 39.8, 44.5 (br s, N*Me*$_2$), 70.2 (br s, Ar*C*HMe), 125.0 (*Ar*), 125.5 (*Ar*), 125.7 (*Ar*), 141.9 ($C6_{Ar}$CHMe), 157.8 ($C2_{Ar}$), 177.2 ($C1_{Ar}$) ppm.

Anal. Calcd. for $C_{10}H_{14}NLi$ (155.17): C 77.40, H 9.10, N 9.03.

Found: C 76.24, H 9.03, N 9.02.

4.1.5. *Synthesis of o-(α,α,N,N-tetramethyl-aminomethyl)phenyllithium (Li(cuda),* ***R4****)*[30]

This aryllithium reagent was in situ generated by transmetallation of (o-BrC_6H_4)C(Me)$_2$NMe_2 with n-BuLi and further used for a following reaction in boron chemistry. No isolation or characterization of the substance was reported.

To a solution of cumyl-*N,N*-dimethylamine (4.0 g, 25 mmol) in 40 mL hexane, *tert*-BuLi (21 mL, 1.5M in hexane, 32 mmol, 1.3 equiv) was added in one portion at room temperature.

The color of the reaction mixture changes *via* over yellow into orange. The reaction mixture was stirred for 48 h, whereupon a colorless crystalline precipitate forms. It was filtered off and dried in vacuum. The product was obtained as colorless solid in yield of 55%. (2.3 g). Crystallization from ether yields **R4**×½Et_2O.

^{1}H NMR (C_6D_6, 300.1 MHz): δ = 1.34 (s, 6H, *Me*$_2$C), 1.68 (s, 6H, *Me*$_2$N), 7.16 (m, 3H, *m-/p-Ph*), 8.22 (d, $^3J_{HH}$ = 5.5 Hz, 1H, *o-Ph*) ppm.

Data for **R4**×½Et_2O: ^{1}H NMR (C_6D_6, 300.1 MHz): δ = 0.92 (t, $^3J_{HH}$ = 7.0 Hz, 3H, *Et*$_2$O) 1.42 (br s, $\upsilon_{½}$ = 26 Hz, 6H, *Me*$_2$C), 1.76 (br s, $\upsilon_{½}$ = 23 Hz, 6H, *Me*$_2$N), 3.14 (q, $^3J_{HH}$ = 7.0 Hz, 2H, *Et*$_2$O) 7.27 (m, 3H, *m-/p-Ph*), 8.26 (m, 1H, *o-Ph*) ppm.

^{13}C{^{1}H} NMR (C_6D_6, 75.5 MHz): δ = 38.3 (br s, *Me*$_2$C), 38.3 (*Me*$_2$N), 63.4 (Me$_2$*C*), 122.3 (*Ar*), 125.0 (*Ar*), 125.6 (*Ar*), 140.5 (*ipso-C*6$_{Ar}$CMe$_2$), 161.1 (*C*2$_{Ar}$), 178.4 (*ipos-C*$_{Ar}$Li) ppm.

Anal. Calcd. for $C_{11}H_{16}NLi$ (169.23): C 78.07, H 9.53, N 8.28.

Found: C 78.75, H 9.33, N 8.54.

4.1.6. *Synthesis of [PrCl$_3$(dme)]*

Modification of the method earlier reported by Petriček[12b]

A suspension of [$PrCl_3$×$6H_2O$] (13.0 g, 36 mmol) in 100 mL DME was allowed to stir overnight. Thionyl chloride (25 mL, 340 mmol, 9.4 equiv) was added during 0.5 h. The reaction mixture was heated 2 h at 70°C till no gas evolution observed. The solid formed was filtered off, washed thoroughly with ether (5×20 mL) and dried in vacuum. A light green, voluminous solid was obtained in 93% yield (11.4 g).

Anal. Calcd. for $C_4H_{10}Cl_3O_2Pr$ (338.38): Cl 31.43, Pr 41.76.

Found: Cl 31.40, Pr 41.80.

4.1.7. *Synthesis of [NdCl$_3$(dme)]:*[12b] The same procedure as for [$PrCl_3$(dme)] starting from [$NdCl_3$×$6H_2O$] (12.1 g, 34 mmol) and thionyl chloride (20 mL, 270 mmol, 8.0 equiv) in ca. 150 mL DME was followed. Since the reaction is only slightly exothermic, thionyl chloride was added in portions (4×5 mL). The product was obtained as light blue, compact microcrystalline solid in 86% yield (10.1 g).

Anal. Calcd. for $C_4H_{10}Cl_3NdO_2$ (340.71): Cl 31.21, Nd 42.34.

Found: Cl 30.85, Nd 42.28.

4.1.8. *Synthesise of [$SmCl_3(dme)_2$]:*[12b] The same procedure as for [$PrCl_3 \times 6H_2O$] starting from [$SmCl_3 \times 6H_2O$] (10 g, 27.4 mmol) and thionyl chloride (18 mL, 245 mmol, 9 equiv) in 150 mL DME was followed. A colorless, microcrystalline solid was obtained in 93% yield (11.1 g).

Anal. Calcd. for $C_8H_{20}Cl_3SmO_4$ (436.96): Cl 24.34, Sm 34.41.

Found: Cl 24.31, Sm 34.36.

4.1.9. *Synthesis of [$GdCl_3(dme)_2$]:*[12b] The same procedure as for [$PrCl_3$(dme)] starting from [$GdCl_3 \times 2H_2O$] (10.0 g, 33 mmol) with thionyl chloride (20 mL, 270 mmol, 8.0 eq) in 100 mL DME was followed (Inversed addition of [$GdCl_3 \times 2H_2O$] to DME causes formation of lumps that proofed difficult to be crushed). The reaction mixture was stirred at ambient temperature for 15 h. An off-white, compact microcrystalline solid was obtained in 92% yield (13.6 g).

Anal. Calcd. for $C_8H_{20}Cl_3GdO_4$ (443.85): Cl 23.96, Gd 35.43.

Found: Cl 23.95, Gd 35.28.

4.1.10. *Synthesis of [$YCl_3(dme)_2$]:*[12b] The same procedure as for [$PrCl_3$(dme)] starting from [$YCl_3 \times 6H_2O$] (12.0 g, 40 mmol) with thionyl chloride (25 mL, 0.36 mol, 9.0 equiv) in ca. 120 mL DME was followed. The reaction mixture was stirred at ambient temperature for 15 h. A colorless, compact microcrystalline solid was obtained in 97% yield (14.5 g).

Anal. Calcd. for $C_8H_{20}Cl_3YO_4$ (375.50): Cl 28.32, Y 23.68.

Found: Cl 28.40, Y 23.71.

4.2. *Synthesis of Aryl Complexes*

4.2.1. *Synthesis of [$Er(dmba)_3$][2] (**H1**):* The erbium complex **H1** was synthesized as reported in the literature. Crystallization from ether yields a pink, microcrystalline solid in yield of 69%.

Crystallographic data for the erbium complex **H1**: Monoclinic, space group *C*2/*c*, a = 24.177(2) Å, b = 9.344(1) Å, c = 23.860(2) Å, β = 113.57(1)°, V = 4940.4(5) Å^3, Z = 8, D_c = 1.532 g/cm^3, μ = 3.415 mm^{-1}, F(000) = 2296.

Anal. Calcd for $C_{27}H_{36}N_3Er$ (569.87): C 56.91, H 6.37, N 7.37.

Found: C 56.80, H 6.51, N 7.24.

4.2.2. *Synthesis of [Yb(dmba)$_3$][2] (**H2**):* The ytterbium complex **H2** was synthesized as reported in the literature. Crystallization from ether yields a bright yellow, microcrystalline solid in yield of 87%.

^{1}H NMR (C_6D_6, 400.1 MHz): δ = 101 (br s, $\nu_{½}$ = ca. 1200 Hz, 6H, N*Me*$_2$), 29.5 (br s, $\nu_{½}$ = ca. 1900 Hz, 2H, C*H*$_2$NMe$_2$), -9.1 (br s, $\nu_{½}$ = 50 Hz, 1H, *H*C3$_{Ar}$), -17.7 (s, 1H, *H*C4$_{Ar}$), -31.9 (s, 1H, *H*C5$_{Ar}$), -99.2 (br s, $\nu_{½}$ = 170 Hz, 1H, *H*C6$_{Ar}$) ppm.

^{13}C{^{1}H} NMR (C_6D_6, 100.1 MHz): δ = -7.6 (br s, *C*H$_2$NMe$_2$), 54.1 (s, C5$_{Ar}$), 76.6 (CH$_2$N*Me*$_2$), 82.1 (s, C4$_{Ar}$), 143 (br s, C3$_{Ar}$), 210 (br s, C5$_{Ar}$), 372 (br s, C2$_{Ar}$) ppm.

Crystallographic data for the ytterbium complex **H2**: Monoclinic, space group *C*2/*c*, *a* = 24.098(11) Å, *b* = 9.312(4) Å, *c* = 26.247(9) Å, β = 123.880(3)°, *V* = 4890(3) Å^3, *Z* = 8, D_c = 1.564 g/cm^3, μ = 3.843 mm^{-1}, *F*(000) = 2312.

Anal. Calcd for $C_{27}H_{36}N_3Yb$ (575.65): C 56.34, H 6.30, N 7.30.

Found: C 56.21, H 6.61, N 7.35.

4.2.3. *Synthesis of [Y(dmba)$_3$][5] (**H4**):* The yttrium complex **H4** was synthesized as reported in the literature. Crystallization from hot hexane yields an off-white, crystalline solid in yield of 91%.

^{1}H NMR (C_7D_8, 400.1 MHz): δ = 2.12 (s, 6 H, *Me*$_2$N), 3.37 (s, 2 H, C$_{Ar}$C*H*$_2$), 6.83 (d, $^2J_{HH}$ = 7.3 Hz, *H*C5$_{Ar}$), 7.10 (t, $^3J_{HH}$ = 7.0 Hz, *H*C4$_{Ar}$), 7.20 (t, $^3J_{HH}$ = 7.0 Hz, *H*C3$_{Ar}$), 8.06 (d, $^3J_{HH}$ = 6.6 Hz, *H*C2$_{Ar}$) ppm.

^{13}C{^{1}H} NMR (C_6D_6, 100.1 MHz): δ = 45.9 (*Me*$_2$N), 69.7 (C$_{Ar}$CH$_2$), 124.8 (*Ar*), 125.2 (*Ar*), 125.7 (*Ar*), 138.7 (*C*2$_{Ar}$), 146.8 (*C*6$_{Ar}$CHMe), 186.9 (d, $^1J_{CY}$ = 44 Hz, *C1*$_{Ar}$Y) ppm.

Crystallographic data for the yttrium complex **H3**: Monoclinic, space group *C*2/*c*, *a* = 24.170(3) Å, *b* = 9.362(1) Å, *c* = 23.880(2) Å, β = 113.47(1)°, *V* = 4955.9(8) Å^3, *Z* = 4, D_c = 1.317 g/cm^3, μ = 2.372 mm^{-1}, *F*(000) = 2064.

Anal. Calcd. for $C_{27}H_{36}N_3Y$ (491.52): C 65.98, H 7.38, N 8.55.

Found: C 64.48, H 7.55, N 8.34.

4.2.4. *Synthesis of [LiNd(pyba)$_4$] (**H5**):* To a suspension of Li(pyba) **R2** (620 mg, 4.00 mmol) in 20 mL of ether [$NdCl_3$(dme)] (340 mg, 1.00 mmol) was added. The obtained green suspension was stirred for 10 min at ambient temperature and the solution over white precipitate of LiCl was decantated into a flask pre-cooled to 0°C. Stirring for ½ h resulted in

formation of blue green crystalline precipitate that was filtered off and dried in vacuum. A sky blue, microcrystalline solid was obtained in 13% yield (96 mg). The complex is stable at ambient temperature for couple of days and therefore was stored at -30°C.

^{1}H NMR (C_6D_6, 300.1 MHz): δ = -0.4 (br s, $\nu_{½}$ = 780 Hz), 11.4 (br s, $\nu_{½}$ = 1000 Hz), 29.5 (br s, $\nu_{½}$ = 1300 Hz) ppm.

Crystallographic data for the neodymium complex **H5**: Monoclinic, space group $P2_1/n$, a = 12.599(1) Å, b = 24.326(2) Å, c = 13.631(1) Å, β = 95.34(1)°, V = 4159.6(6) Å^3, Z = 4, D_c = 1.338 g/cm^3, μ = 1.285 mm^{-1}, F(000) = 1744.

Anal. Calcd for $C_{44}H_{56}N_4LiNd$ (792.14): C 66.72, H 7.13, N 7.07.

Found: C 64.32, H 6.81, N 6.82.

4.2.5. *Synthesis of Li[Gd(dmba)$_4$] (**H6**):* To a stirred suspension of Li(dmba) **R1** (668 mg, 4.0 mmol) in 40 mL ether, solid [$GdCl_3(dme)_2$] (442 mg, 1.0 mmol) was added at ambient temperature. The color of the reaction mixture turned slowly yellowish depositing a white heavy microcrystalline solid. It was filtered off and dried in vacuum. This solid was triturated with toluene (20 mL) whereupon LiCl precipitates. The solution was filtered through a Celite®-pad and the filtrate was concentrated to 20% of the original volume. Addition of ether (20 mL) at 0°C causes formation of white crystalline solid. It was filtered off and dried in vacuum. Yield: 56% (450 mg, 0.56 mmol).

Crystallographic data for the gadolinium complex **H6**: Triclinic, space group P-1, a = 9.760(1) Å, b = 12.083(2) Å, c = 15.836(2) Å, α = 82.54(1)°, β = 75.10(1)°, γ = 70.26(1)°, V = 1696.6(4) Å^3, Z = 2, D_c = 1.372 g/cm^3, μ = 1.983 mm^{-1}, F(000) = 718.

Anal. Calcd for $C_{44}H_{56}N_4GdLi$ (805.15): C 65.64, H 7.01, N 6.96.

Found: C 63.89, H 6.83, N 7.02.

4.2.6. *Synthesis of [Lu(tmba)$_2$Cl] (**H7'**):* To a stirred mixture of Li(tmba) **R2** (346 mg, 2.23 mmol, 2.0 equiv) and [$LuCl_3(thf)_3$] (538 mg, 1.08 mmol) 20 mL ether was added at ambient temperature. The slightly turbid solution formed was stirred for 18 h. After that the solvent was removed in vacuum and the product was extracted with toluene (20 mL). The reaction mixture was filtered through a Celite®-pad and the solvent was completely removed in vacuum to give colorless foam. Addition of hexane (25 mL) causes a spontaneous crystallization of the product. The product was filtered off and dried in vacuum. An air-

sensitive, colorless, microcrystalline solid was isolated in 69% yield (380 mg). The complex is highly soluble in aromatic solvents, ether and almost insoluble in hexane.

^{1}H NMR (300.1 MHz, C_6D_6): δ = 1.19 (br s, 3 H, *Me*CH), 2.20 (br s, 6 H, *Me*$_2$N), 3.40 (br s, 1 H, MeC*H*), 7.03 (d, $^3J_{HH}$ = 7.6 Hz, 1 H, Ar), 7.24 (dt, J = 1.5 Hz, J = 7.4 Hz, 1 H, Ar), 7.38 (t, J_{HH} = 7.0 Hz, 1 H, Ar), 8.38 (br s, 1 H, *o*-Ar) ppm.

^{13}C{^{1}H} NMR (75.5 MHz, C_6D_6): δ = 20.7 (*Me*$_2$C), 43.3 (H*C*NMe$_2$), 44.7 (br s, *Me*$_2$N), 124.4, 125.1, 125.8, 140.1 (4×*Ar*), 154.1 (*ipso*-C_{Ar}-CHMe), 196.3 (*ipso*-C_{Ar}–Lu) ppm.

Anal. Calcd. for $C_{20}H_{28}N_2LuCl$ (506.88): C 47.39, H 5.57, N 5.53.

Found: C 46.54, H 5.59, N 5.49.

4.2.7. *Synthesis of [Y(tmba)$_3$] (**H8**):* To a suspension of [YCl_3(dme)$_2$] (1.40 g, 3.7 mmol) in 40 mL ether, solid Li(*tmba*) **R3** (1.75 g, 11.3 mmol) was added at ambient temperature. The reaction mixture was stirred for 15 min, after that the solvent was completely removed in vacuum to yield a foamy residue. Benzene (10 mL) was added and precipitated LiCl was filtrated off through a Celite®-pad and washed twice with the same solvent (2×5 mL). The filtrate was concentrated in vacuum to 2–3 mL followed by addition of hexane (50 mL) whereupon a white solid precipitates. It was collected by filtration and washed with hexane (2×10 mL). A colorless, microcrystalline solid was obtained in 78% yield.

^{1}H NMR (300.1 MHz, C_6D_6): δ = 1.13 (d × br s, $^3J_{HH}$ = 6.5 Hz, $\nu_{½}$ = 10 Hz, 3 H, PhC*Me*), 2.22 (br s, $\nu_{½}$ = 60 Hz, 6 H, N*Me*$_2$), 3.16 (br s, $\nu_{½}$ = 44 Hz, 1 H, PhC*H*), 6.97 (d, $^3J_{HH}$ = 7.5 Hz, *m-Ph*), 7.11 (dt, $^3J_{HH}$ = 1.2 Hz, $^3J_{HH}$ = 7.4 Hz, *p-Ph*), 7.20 (t, $^3J_{HH}$ = 7.2 Hz, *m-Ph*), 8.18 (br s, $\nu_{½}$ = 27 Hz, *o-Ph*)ppm.

^{13}C{^{1}H} NMR (75.5 MHz, C_6D_6): δ = 22.1 (br s, ArCH*Me*), 45.0 (br s, N*Me*$_2$), 73.5 (br s, Ar*C*HMe), 124.2 (*Ar*), 124.9 (*Ar*), 125.8 (*Ar*), 138.8 (*C*2$_{Ar}$), 153.9 (br s, *C*6$_{Ar}$CHMe), 185.9 (d, $^1J_{CY}$ = 44 Hz, *C*1$_{Ar}$) ppm.

Crystallographic data for the yttrium complex **H8**: Monoclinic, space group $P2_1$, a = 10.376(1) Å, b = 23.851(2) Å, c = 11.104(1) Å, β = 90.32(1)°, V = 2747.8(4) Å^3, Z = 4, D_c = 1.290 g/cm^3, μ = 2.144 mm^{-1}, F(000) = 1128.

Anal. Calcd for $C_{30}H_{42}N_3Y$ (533.59): C 67.53, H 7.93, N 7.88.

Found: C 66.51, H 7.94, N 7.67.

4.2.8. *Synthesis of [Dy(tmba)$_3$] (**H9**):* The dysprosium complex **H9** was synthesized analogous to [Y(tmba)$_3$] (**H8**) starting from [DyCl$_3$(dme)$_2$] (821 mg, 1.83 mmol) and Li(tmba) **R3** (853 mg, 5.48 mmol). Crystallization from hot hexane yields a yellowish, microcrystalline solid in yield of 83%.

Crystallographic data for the dysprosium complex **H9**: Orthorhombic, space group $P2_12_12_1$, a = 9.130(2) Å, b = 22.055(6) Å, c = 27.588(6) Å, V = 5555(2) Å^3, Z = 4, D_c = 1.452 g/cm^3, μ = 2.712 mm^{-1}, F(000) = 2472.

Anal. Calcd for $C_{30}H_{42}N_3Dy$ (602.19): C 59.34, H 6.97, N 6.92.

Found: C 58.23, H 7.12, N 6.45.

4.2.9. *Synthesis of [Nd(tmba)$_3$] (**H10**):* To a stirred suspension of [NdCl$_3$(dme)] (681 mg, 2.0 mmol) in 20 mL ether suspension of Li(tmba) **R3** (929 mg, 6.0 mmol, 3 equiv) in toluene (10 mL) was gradually added at 0°C. The reaction mixture was stirred for 0.5 h after that it was concentrated in vacuum to the one half of the original volume. The precipitated LiCl was filtered off and washed with toluene (5 mL) to yield pale blue solution. All volatiles were removed in vacuum followed by hexane (10 mL) addition. The pale blue, heavy precipitate was isolated by filtration and was dried in vacuum. The product was obtained as a pale blue, microcrystalline solid in 28% yield (328 mg).

Crystallographic data for the neodymium complex **H10**: Orthorhombic, space group $P2_12_12_1$, a = 10.485(1) Å, b = 11.214(1) Å, c = 23.796(2) Å, V = 2797.7(4) Å^3, Z = 4, D_c = 1.398 g/cm^3, μ = 1.877 mm^{-1}, F(000) = 1212.

Anal. Calcd for $C_{30}H_{42}N_3Nd$ (588.93): C 61.18, H 7.19, N 7.13.

Found: C 58.91, H 7.00, N 6.84.

4.2.10. *Synthesis of [Sm(tmba)$_3$] (**H11**):* The samarium complex **H11** was synthesized analogous to [Nd(tmba)$_3$] **H10** starting from [SmCl$_3$(dme)$_2$] (873 mg, 2.0 mmol) and Li(tmba) **R3** (931 mg, 6.0 mmol, 3 equiv). A yellow, crystalline solid was obtained in 56% yield (666 mg).

Anal. Calcd for $C_{30}H_{42}N_3Sm$ (595.09): C 60.55, H 7.11, N 7.06.

Found: C 57.72, H 6.51, N 7.89.

4.2.11. *Synthesis of [Sm(cuda)$_3$] (**H12**):* To a stirred suspension of [$SmCl_3(dme)_2$] (437 mg, 1.00 mmol) in 20 mL ether, Li(cuda) **R4** (500 mg, 2.95 mmol) was added in portions at 0°C. The bright yellow suspension formed immediately. It was stirred for additional 0.5 h at the same temperature. The LiCl formed was filtered off through a Celite©-pad and the solvent was completely removed in vacuum leaving bright yellow foam. Treatment with hexane (25 mL) causes dissolution of the foam and immediate precipitation of lustrous, bright yellow, microcrystalline solid. It was filtered off and dried in vacuum. It is highly soluble in benzene, methylcyclohexane rather than in hexane. It reacts reversibly with toluene with appearance of brown coloration and decomposes in THF. Yield: 38 % (240 mg).

Crystallographic data for the samarium complex **H12**: Monoclinic, space group $P2_1/c$, a = 15.207(1) Å, b = 11.730(1) Å, c = 17.165(1) Å, β = 90.82(1)°, V = 3061.4(3) Å^3, Z = 4, D_c = 1.382 g/cm^3, μ = 1.943 mm^{-1}, $F(000)$ = 1316.

Anal. Calcd for $C_{33}H_{48}N_3Sm$ (637.13): C 62.21, H 7.59, N 6.60.

Found: C 61.18, H 7.92, N 6.49.

5. REFERENCES

[1] a) C. Boker, M. Noltemeyer, H. Gornitzka, B. O. Kneisel, M. Teichert, R. Herbst-Irmer, A. Meller, *Main Group Metal Chem.* **1998**, *21*, 565–578; b) O. F. Z. Khan, D. M. Frigo, P. O'Brien, A. Howes, M. B. Hursthouse, *J. Organomet. Chem*. **1987**, *334*, C27–C30; c) F. A. Cotton, G. N. Mott, *Inorg. Chem*. **1981**, 20, 3896–3899; d) L. E. Manzer, R. C. Gearhart, L. J. Guggenberger, J. F. Whitney, *J. Chem. Soc., Chem. Comm*. **1976**, 942–943.

[2] a) A. L. Wayda, J. L. Atwood, W. E. Hunter, *Organometallics* **1984**, *3*, 939–941; b) A. L. Wayda, R. D. Rogers, *Organometallics* **1985**, *4*, 1440–1444.

[3] F. A. Hart, A. G. Massey, M. S. Saran, *J. Organomet. Chem.* **1970**, *21*, 147–154.

[4] L. E. Manzer, *J. Am. Chem. Soc.* **1978**, *100*, 8068–8073.

[5] M. Booij, N. H. Kiers, H. J. Heeres, J. H. Teuben, *J. Organomet. Chem.* **1989**, 364, 79–86.

[6] a) K. C. Hultzsch, F. Hampel, T. Wagner, *Organometallics* **2004**, *23*, 2601–2612; b) K. A. Rufanov, B. H. Müller, A. Spannenberg, U. Rosenthal, *New J. Chem*. **2006**, *30*, 29–31.

[7] a) W. J. Evans, L. R. Chamberlain, T. A. Ulibarri, J. W. Ziller, *J. Am. Chem. Soc.* **1988**, *110*, 6423–6432; b) H. Schumann, M. Glanz, H. Hemling, F. H. Görlitz, *J. Organomet. Chem.* **1993**, *462*, 155–161.

[8] M. E. Thompson, S. M. Baxter, A. R. Bulls, B. J. Burger, M. C. Nolan, B. D. Santarsiero, W. P. Schaefer, J. E. Bercaw, *J. Am. Chem. Soc*. **1987**, *109*, 203–219.

[9] a) W. T. Klooster, V. Brammer, C. J. Schaverien, P. H. M. Budzelaar, *J. Am. Chem. Soc.* **1999**, *121*, 1381–1382; b) W. Scherer, G. S. McGrady, *Angew. Chem.* **2004**, *116*, 1816–1842; *Angew. Chem., Int. Ed.* **2004**, *43*, 1782–1806.

[10] W. E. Evans, *Inorg. Chem.* **2007**, *46*, 3435–3449.

[11] N. W. Boaz, B. Venepalli, *Org. Proc. Res. Dev.* **2001**, *5*, 127–131; b) about commercial product 3M MeLi-solution in DEM: www.chemetalllithium.com.

[12] a) U. Baisch, A. Dell, B. Daniela, F. Calderazzo, R. Conti, L. Labella, F. Marchetti, E. A. Quadrelli, *Inorg. Chim. Acta* **2004**, *357*, 1538–1548. b) S. Petriček, *Polyhedron* **2004**, *23*, 2293–2301.

[13] C. G. J. Tazelaar, S. Bambirra, D. van Leusen, A. Meetsma, B. Hessen, J. H. Teuben *Organometallics* **2004,** *23*, 936–939.

[14] a) N. N. Smith, *Adv. Chem. Ser.* **1974**, *130*, 23–55; b) H. H. Karsch, K.-A. Schreiber, M. Reisky, *Organometallics* **1998**, *17*, 5052–5060.

[15] a) E. W. Abel, R. J. Rowley, *J. Chem. Soc., Dalton Trans.* **1975**, 1096–1099; b) C. W. Fong, G. Wilkinson, *J. Chem. Soc., Dalton Trans.* **1975**, 1100–1104.

[16] a) W. H. Puterbaugh, C. R. Hauser, *J. Org. Chem.* **1963**, *28*, 2467–2470; b) W. H. Puterbaugh, C. R. Hauser, *J. Org. Chem.* **1963**, *28*, 3465–3467.

[17] D. Hofmann, W. Bauer, F. Hampel, N. J: R. van Eikema Hommes, P. v. R. Schleyer, P. Otto, U. Pieper, D. Stalke, D. S. Wright, R. Snaith, *J. Am. Chem. Soc.* **1994**, *116*, 528–536.

[18] M. Westerhausen, W. Schwarz, *Z. Naturforsch.* **1998**, *B53*, 625–627.

[19] F. Feil, S. Harder, *Organometallics* **2000**, *19*, 5010–5015.

[20] F. Feil, S. Harder, *Organometallics* **2001,** *20,* 4616–4622.

[21] a) H. J. Reich, W. S. Goldenberg, B. O. Gudmundsson, A. W. Sanders, K. J. Kulicke, K. Simon, I. A. Guzei, *J. Am. Chem. Soc.* **2001**, *123*, 8067–8079; b) A. Spector, S. R.Wilson, P. A. Zucker, US 5,128,365 **1994**.

[22] O. Thomas, *Diploma Thesis*, Philipps-Universität Marburg, **2008**.

[23] H. Gao, Q. Shen, J. Hu, S. Jin, Y. Lin, *J. Organomet. Chem*. **1992**, *427*, 141–149.

[24] R. N. Icke, B. B. Wisegarver, G. A. Alles, *Org. Synth.* **1945**, *25*, 89–92.

[25] D. Balderman, A. Kalir, *Synthesis* **1978**, *1*, 24–26.

[26] H. Kämmerer, L. Horner, H. Beck, *Chem. Ber.* **1958**, *91*, 1376–1379.

[27] L. H. Welsh, N. L. Drake, *J. Am. Chem. Soc.* **1938**, *60*, 59–62.

[28] C. M. P. Kronenburg, E. Rijnberg, J. T. B. H. Jastrzebski, H. Kooijman, A. L. Spek, G. van Koten, *Eur. J. Org. Chem.* **2004**, 153–159.

[29] C. M. P. Kronenburg, E. Rijnberg, J. T. B. H. Jastrzebski, H. Kooijman, M. Lutz, A. L. Spek, A. Gossage, G. van Koten, *Chem. Eur. J.* **2005**, *11*, 251–261.

[30] a) M. Asakura, M. Oki, S. Toyota, *Organometallics* **2000**, *19*, 206–208; b) S. Toyota, M. Asakura, T. Futawaka, M. Oki, *Bull. Chem. Soc. Jpn.* **1999**, *72*, 1879–1885.

[31] D. Cui, M. Nishiura, Z. Hou, *Macromolecules* **2005**, *38*, 4089–4095.

[32] C. Qian, W. Nie, J. Sun, *Organometallics* **2000,** *19*, 4134–4140.

[33] G. W. Rabe, M. Zhang-Presse, F. A. Riederer, G. P. A. Yap, *Inorg. Chem.* **2003**, *42*, 3527–3533.

[34] W. J. Evans, I. Bloom, W. E. Hunter, J. L. Atwood, *Organometallics* **1985**, *4*, 112–119.

[35] N. S. Radu, S. L. Buchwald, B. Scott, C. J. Burns, *Organometallics* **1996**, *15*, 3913–3915.

[36] G. W. Rabe, M. Zhang-Presse, F. A. Riederer, J. A. Golen, C. D. Incarvito, A. L. Rheingold, *Inorg. Chem.* **2003**, *42*, 7587–7592.

[37] G. W. Rabe, B. Rhatigan, J. A. Golen, A. L. Rheingold, *Acta Cryst., Sect. E* **2003**, *E59*, m99–m101.

[38] M. Niemeyer, S.-O. Hauber, *Z. Anorg. Allg. Chem.* **1999**, *625*, 137–140.

[39] J. L. Atwood, W. E. Hunter, A. L. Wayda, W. J. Evans, *Inorg. Chem*. **1981**, *20*, 4115–4119.

[40] a) F. N. Jones, M. F. Zinn, C. R. Hauser, *J. Org. Chem.* **1963**, *28*, 663–665; b) A. C. Cope, R. N. Gourley, *J. Organomet. Chem.* **1967**, *8*, 527–533; c) J. B. H. Jastrzebski, G. van Koten, M. F. Lappert, D. R. Hankey, *Inorg. Synth.* **1989**, *26*, 150–152.

[41] W. D. Ollis, M. Rey, I. O. Sutherland, *J. Chem. Soc., Perkin Trans. 1* **1983**, 1009–1027.

[42] C. M. P. Kronenburg, E. Rijnberg, J. T. B. H. Jastrzebski, H. Kooijman, A. L. Spek, G. van Koten, *Eur. J. Org. Chem.* **2004**, 153–159.

[43] R. O. Hutchins, M. Markowitz, *J. Org. Chem.* **1981**, *46*, 3571–3574; b) P. Froyen, P. Juvvik, *Tetrahedron Lett.* **1995**, *36*, 9555–9558; c) J. M. Flaniken, C. J. Collins, M. Lanz, B. Singaram, *Org. Lett.* **1999**, *1*, 799–801; d) Z. Li, H.-J. Feiten, J. B. Van Beilen, W. Duetz, B. Witholt, *Tetrahedron: Asymmetry* **1999**, *10*, 1323–1333; e) H. Alinezhad, M. Tajbakhsh, R. Zamani, *Synlett* **2006**, 431–434.

[44] a) M. L: Moore, *Org. Reactions* **1949**, *5*, 301–330; b) B. M. Bogoslovskij, *Reakcii i Metody Issledovanija org. Soedinenij* **1954**, *3*, 253–314; c) F. Möller, R. Schröter in: Houben-Weil Bd. **1957**, *11/1*, 648–664.

[45] H. M. Taylor, C. R. Hauser, *J. Am. Chem. Soc.* **1960**, *82*, 1960–1965.

— Chapter III —

P-Amino-Cyclopentadienylidene-Phosphoranes *versus* *P*-Cyclopentadienyl-Imino-Phosphoranes Development and Investigation of *CpPN*-Ligand System

Abstract

The *Staudinger* reaction of the cyclopentadienyl-phosphanes $C_5H_5PMe_2$ (**P1**), $C_5H_5PPh_2$ (**P2**), $HC_5Me_4PMe_2$ (**P3**) and $HC_5Me_4PPh_2$ (**P4**) with the azides Me_3SiN_3, AdN_3 and $DipN_3$ has been studied. The nature of the products depends largely on the substituents at the C5-ring and the nitrogen atoms; dependence on the substituents at the phosphorus atom is less pronounced. A series of new *P*-amino-cyclopentadienylidene-phosphoranes **L2** – **L6** and **L8** was synthesized by the reactions of **P1** – **P4** with AdN_3 (**L2** – **L4**, **L8**) and $DipN_3$ (**L5** – **L7**). Contrastingly, the *P*-cyclopentadienyl-iminophosphoranes **L1** and **L7** were obtained as predominant tautomers by reaction of the less CH-acidic **P3** with Me_3SiN_3 (**L1**) and $DipN_3$ (**L7**). Both tautomers are protonated forms of potentially chelating constrained-geometry ligands for elements of group 3 and lanthanides. The molecular structures of six members of the *CpPN-ligand* family – **L3**, **L4**, **L5**, and **L6** – are characterized by X-ray diffraction studies. The procedure for the synthesis of the Cp-substituted aminophosphoranes **L2**, **L3**, **L5** and **L6** was investigated in detail.

1. INTRODUCTION

In the framework of collaborative studies of our group in the field of coordination chemistry of transition and rare-earth metals with functionalized ambident donor organophosphorus(V) ligands we focused our efforts on the synthetic development of two particular systems – cyclopentadienyl-phosphoranylidenes (**B**)[1] and *P*-amino-cyclopentadienyliden-phosphoranes (**C**). The corresponding dianion of **B** and monoanion of **C** are isoelectronic to the chelating dianionic cyclopentadienyl-silylamido ligand systems (**A**, Scheme 1), which in the recent decades became one of the best developed classes of chelating cyclopentadienyl-amido complexes of the early transition metals,[2] the so-called "constrained-geometry catalysts" (**A**).[3]

In 2005 we reported on the syntheses and structures of the first type **C** ligand – $Me_2P(C_5Me_4)NHAd$ and the first lutetium complex thereof: $[(\eta^5\text{-}C_5Me_4PMe_2NAd)\text{-}Lu(CH_2SiMe_3)_2]$.[4] From a conceptual point of view three-valent lanthanide or group 3 metal complexes on the basis of type **C** ligands are isolobal with tetra-valent group 4 transition metal complexes of type **A** ligands. Having this concept and the greater diversity of rare-earth metals in mind, we set out our goal to develop a convenient and reliable synthetic protocol for a large variety of type **C** ligands with different substituents at the N-, P- and C-atoms. Here we describe our efforts on the development and further optimization of the general synthetic approach towards this type **C** ligand precursors (*CpPN*), studies on their physicochemical and NMR properties as well as on their molecular structures in detail.

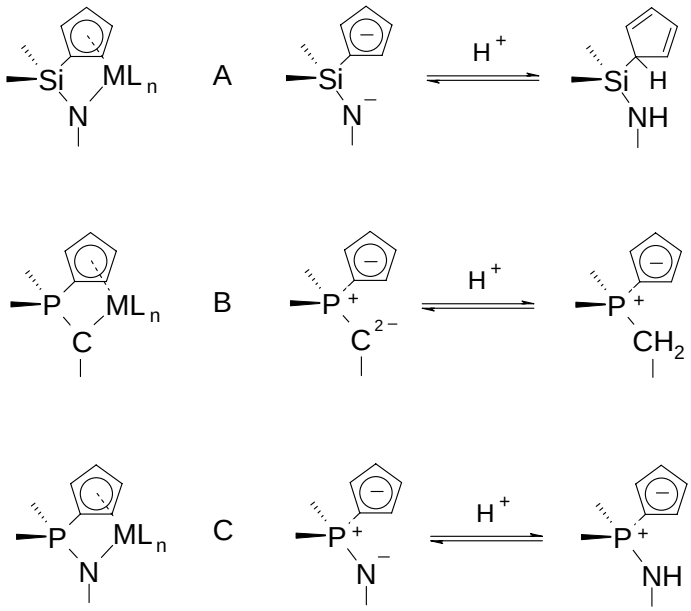

Scheme 1. Isolobally related "constrained-geometry" complexes and corresponding ligand systems.

2. RESULTS AND DISCUSSION

2.1. *General Considerations*

There are two general strategies toward the synthesis of modified Cp-transition metal-complexes. The first one consists in the modification of the Cp-core when the ligand is already attached to the metal in the complex. This pathway found wide application in the ferrocene chemistry and allowed to design many interesting ligands for powerful catalysts. The second strategy implies that the Cp-ligand has to be modified before it is attached to the metal in the desired complex. Nevertheless this rather complicated approach is superior to the first one which is easily applied to the stable Cp-complexes only when any side reaction – except for those upon the Cp-ligand – can be excluded. In our design of the *CpPN*-ligands we followed the second synthetic strategy.

In general, the protonated form of the *CpPN*-ligand system can show two tautomeric forms (Scheme 2).

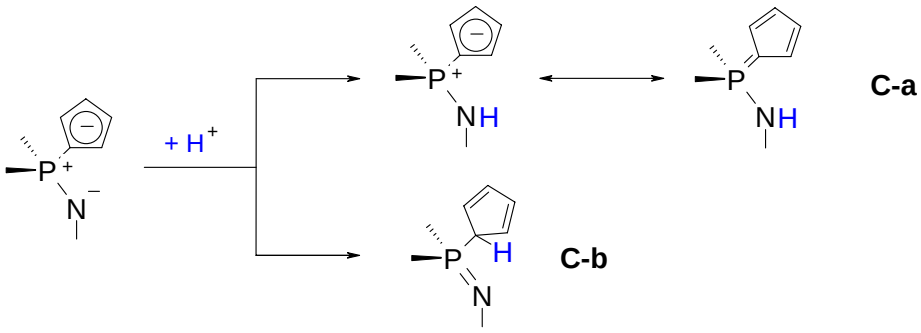

Scheme 2.

It is known that σ-bounded cyclopentadienyl compounds of main group elements show dynamic behavior and undergo prototropic and/or elementotropic re-arrangements. Therefore, a conceivable appearance of two additional isomers is expected for the **C-b** form.[5]

In 1974 *Kolodyazhnyi* showed that some *P*-iminophosphoranes, upon formation by *Staudinger* reaction, isomerizes into the corresponding aminophosphoranes (Scheme 3).[6]

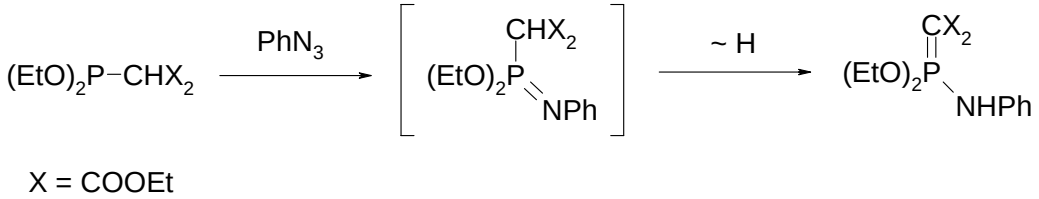

Scheme 3.

It was also found that both tautomers can occur in equilibrium. Depending on the nature of substituents at the nitrogen and carbon atoms the tautomeric equilibrium could be forced in both directions. If C*H* and N*H* acidities are comparable, the proton migration will become reversible. (Scheme 4)[7]

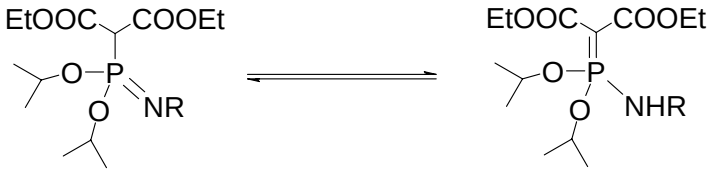

R = Me	10%	90%
R = 2,4-$(NO_2)_2C_6H_3$	85%	15%

Scheme 4.

The latter is highly stabilized by the presence of two electron withdrawing groups (X = COOEt). In our case, the presence of an energetically stabilized aromatic C5-ring could stabilize the *CpPN*-ligands in their **C-a** form (Scheme 2).

2.2. *Retrosynthetic Analysis of CpPN-Ligand System*

In Table 1 our retrosynthetic analysis of the *CpPN-ligand* system is summarized. Five retrosynthetic strategies (*routes A – E*) have been foreseen and synthetically tested.

Table 1. Retrosynthetic strategies toward the *CpPN-ligand* system

Route	Synthon(s)	1st Reagent	2nd Reagent
A	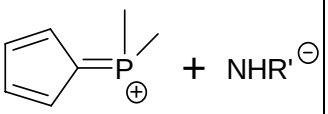	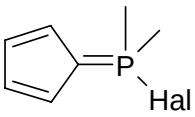	$R'NH_2$ / R'NHM (M = Li, Na)
B	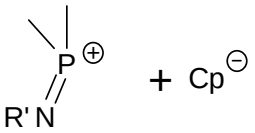	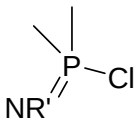	LiCp, NaCp or $MgCp_2$
C	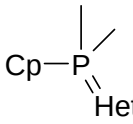 (through metathesis)	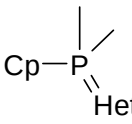 (Het = O, S)	R'-NSO or R'-NCO
D	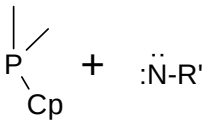	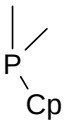	1. R'NHHal 2. Base
E			$R'N_3$

Routes A and *B* concern a heterolytic disconnection of the target molecule (TM) upon a single bond of the corresponding **C-a** or **C-b** tautomeric form. In *route C* a metathesis with the known $R_2P(S)Cp$ (R = Me, Ph) and organic isocyanates or sulfinylamines is followed. Furthermore the use of an oxidative addition of nitrene-synthones, derived either from primary monohaloamines (*route D*) or from organic azides (*route E)* to the Cp-phosphanes was studied.

– Route A –

Following the procedure developed by *Kolodiazhnyi et al.*[8] the reaction of the *in situ* prepared cyclopentadienyliden-phosphoric acid chloride with benzylamine was tested (TM = target molecule, Scheme 5):

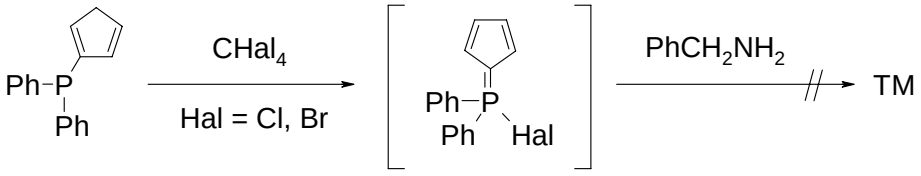

Scheme 5.

The absence of a reaction with both CCl_4 and CBr_4 was confirmed by ^{31}P NMR spectroscopy of the reaction mixture. The application of the reaction seems to be limited only to highly stabilized ylides having strong electron-withdrawing groups like CN or COOR.

– Route B –

P-Chloro-*N*-(2,6-diisopropylphenyl)-diphenyl-iminophosphorane (**S1**) – the key precursor for this route – was easily synthesized from Ph_2PCl and $DipN_3$ in yield of 96% (Scheme 6).

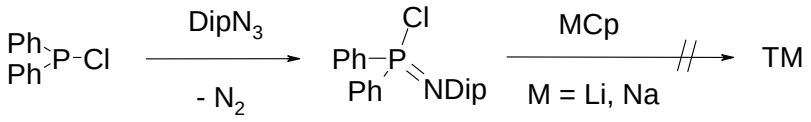

Scheme 6.

Though this new *P*-chloro-iminophosphorane is ***very*** sensitive toward air moisture, surprisingly, it does not react with either LiCp or NaCp (**!**). All variations of experimental conditions – temperature, organic solvent and/or reaction duration as well as the use of $MgCp_2$ as Cp-source – appeared to be unsuccessful. Only unchanged starting materials were recovered after workup.

– Route C –

Although $Ph_2P(O)C_5H_5$ would better fit in this route as a starting material, it appeared to be fairly inaccessible. Simple oxidation of unsubstituted cyclopentadienyl-diphenyl-phosphanes with oxygen or aqueous hydrogen peroxide – as described in literature – did not lead to the desired compound, but solely to a complex mixture of isomers of *Diels-Alder* products (Scheme 7).[9] This unusual behavior upon *P*-oxidation could be explained by a significant discrepancy in the electronic density of double bonds in reagent and product caused by electron donating nature of P(III) and electron withdrawing of P(V) in phosphine oxides. In this particular case the Cp-moiety of the electron rich Cp-phosphane acts as a diene component, while the Cp-moiety of the phosphine oxide (oxidation product) – as a dienophile, yielding – upon further oxidation – a complex mixture of isomeric $Me_2P(O)$-substituted dicyclopentadienes.

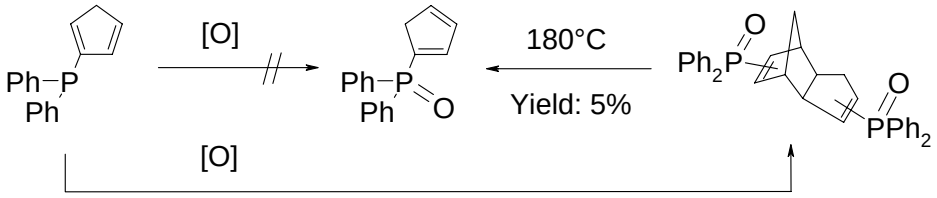

Scheme 7. Oxidation of $Me_2PC_5H_5$ leading to dimeric product $(Me_2P(O)C_5H_5)_2$.

The phosphine oxide $Ph_2P(O)C_5H_5$ was obtained by the *retro-Diels-Alder* reaction with overall isolated yield of only 5%.[9]

Generally, the oxidation reaction of Cp-phosphanes to Cp-phosphanesulfides is more selective and the stability of these compounds allows obtaining them in better yields.[9] As reported[9] the *Diels-Alder* dimerization occurs only at elevated temperatures (EtOH, reflux, 4 h). We tried the reaction of $Ph_2P(S)C_5H_5$ with PhNCO and DipNSO. However, it appeared to be rather unselective, yielding a complex mixture of unidentified products according to ^{31}P NMR spectroscopy data of the crude reaction mixture (Scheme 8).

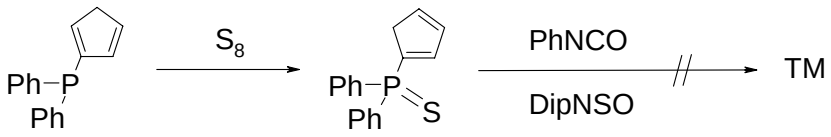

Scheme 8.

Additionally, no metathesis reaction was observed between $Ph_2P(O)Cl$ and DipNSO in DME, even after 48 h at 60°C as shown by ^1H and ^{31}P NMR spectroscopy.

– Route D –

The reaction of the phosphane Ph_2PCp and *N*-brom-adamantylamine, obtained by the stoichiometric metathetical reaction of adamantylamine and *N*-bromsuccinimide,[10] in the presence of base (Et_3N) results in the formation of a colorless precipitate. ^{31}P NMR spectroscopy in $CDCl_3$ shows the presence of two main resonances at 48.3 and 34.1 ppm with an integral ratio of 22:78. A comparison with values of known cyclopentadienyl-phosphoranes which vary in a region from 26.1 to -1.2 ppm – and particularly with closely related $Ph_3PC_5H_4$ (δ = 17.4 ppm) – indicate an unusual downfield shift. ^1H and ^{13}C NMR spectra confirm the complex composition of the products. However, it is known that stable monohalogenamines can disproportionate in solution giving an equimolar mixture of a free amine and dihalogenamine.[48] It strongly depends on the nature of amine, halogen and solvent used. We found that in THF solution of *N*-brom-adamantylamine quantitatively disproportionates. Furthermore, ^{13}C NMR spectroscopy in $CDCl_3$ reveals a significant broadening of resonances for α-, β- and γ-carbon atoms in *N*-bromadamantane verifying its dynamic behavior in solution. It is believed that there are too many generated species involved in the reaction leading to a mixture of salt-like products (Scheme 9).

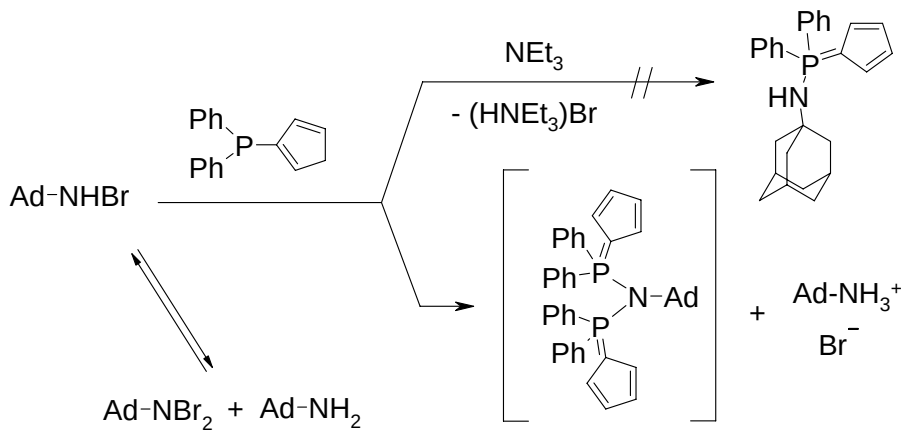

Scheme 9.

We speculate that *N,N*-diphosphorane-amine species (or its protonated form) might exist in the product mixture (Scheme 2), but the only isolated compound in this reaction was 1-adamantylammonium bromide, that was crystallographically characterized.

– Route E –

The next tested route was the *Staudinger* reaction. For our preliminary investigation a highly reactive phosphane $HC_5Me_4PMe_2$ stable against *Diels-Alder* dimerization was chosen. It was allowed to react with a stoichiometric amount of adamantyl-1 azide (Scheme 10).

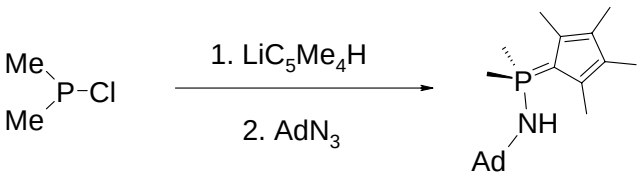

Scheme 10.

Immediately upon addition of that azide to a THF solution of freshly obtained phosphane $HC_5Me_4PMe_2$ an exothermic reaction with gas evolution takes place. In the beginning, the reaction mixture is yellow and turns into dark brown after stirring for 4 h at ambient temperature and ceasing of the gas evolution. The removal of all volatiles in vacuum yields a light brown foamy residue, which was treated and washed with hexane and dried in vacuum giving an air-sensitive white powder. The product was characterized by ^{1}H, ^{13}C and ^{31}P NMR spectroscopy, elemental analysis and mass spectrometry. The molecular composition determination was confirmed by X-ray structure analysis (*vide infra*).

The success in *route E* prompted us to explore its scope and limitations in detail.

2.3. *Synthesis of CpPN-H Compounds*

2.3.1. *Scope and Limitations*

Reactions of a series of the cyclopentadienyl-phosphanes of increasing thermal stability – $C_5H_5PMe_2$ (**P1**), $C_5H_5PPh_2$ (**P2**), $HC_5Me_4PMe_2$ (**P3**) and $HC_5Me_4PPh_2$ (**P4**) – have been studied with three representative azides – silyl azide Me_3SiN_3, alkyl azide AdN_3 and aryl azide $DipN_3$ (Scheme 11).

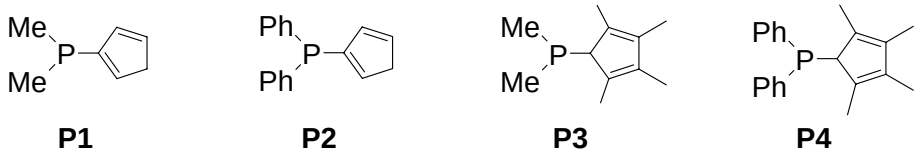

P1 **P2** **P3** **P4**

Scheme 11. Representative objects chosen for the studies.

It is worth to note that the phosphanes **P1** and **P2** exist predominantly in their vinilic forms,[9] whereas **P3**[13] and **P4**[41] in exclusively their allilic one.

Success in the synthesis of *CpPN*-H compounds depends crucially on the relative reactivity of the applied phosphanes and azides.

The results of our studies on the reactivity of the cyclopentadienyl-phosphanes **P1** – **P4** towards the above mentioned azides are summarized in Table 2. All studied phosphanes are fairly air-sensitive oils.

Table 2. Isolated yields of the *CpPN*-compounds in the studied reactions. Except of compounds denoted with (*), which have *P*-cyclopentadienyliden-iminophosphorane form, all other have *P*-amino-cyclopentadienyliden-phosphorane form; NR = no reaction.

	$Me_2PC_5H_5$ (**P1**)	$Ph_2PC_5H_5$ (**P2**)	$Me_2PC_5Me_4H$ (**P3**)	$Ph_2PC_5Me_4H$ (**P4**)
Me_3SiN_3	NR	NR	**L1**,*) 86%	NR
AdN_3	**L2**, traces	**L3**, 69%	**L4**, 95%	**L8**, 78 %
$DipN_3$	**L5**, 75%	**L6**, 85%	**L7**,*) 60%	NR

In general, the reaction with the least reactive azide Me_3SiN_3 requires higher temperatures, which are undesirable for the thermally labile phosphanes **P1** and **P2,** which are prone to undergo *Diels-Alder* type dimerization.[9] Although the reaction of $Me_2PC_5H_5$ (**P1**) with AdN_3, which is more reactive than Me_3SiN_3, leads to the formation of the desired *P*-amino-cyclopentadienyliden-phosphorane $Me_2P(C_5H_4)NHAd$ (**L2**), only traces of analytically pure

compound can be isolated after further purification (Scheme 12). The reaction with the most reactive azide ($DipN_3$) decreases the yield of product $Me_2P(C_5H_4)NHAd$ (**L5**) to 75%.

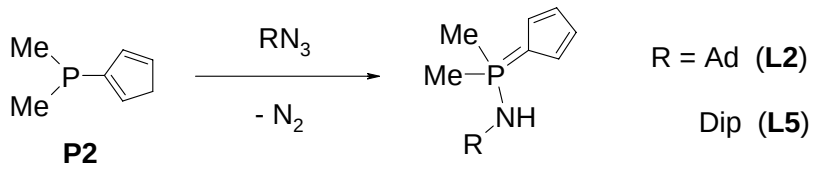

Scheme 12. Reactions of phosphane $Ph_2PC_5H_5$ (**P1**) with AdN_3 and $DipN_3$.

The phosphane $Ph_2PC_5H_5$ (**P2**) is less labile with respect to oxidative *Diels-Alder* type dimerization and gives smoothly the ligand **L3** and **L6** upon reaction with AdN_3 and $DipN_3$ in yield up to 69% and 85% respectively (Scheme 13).

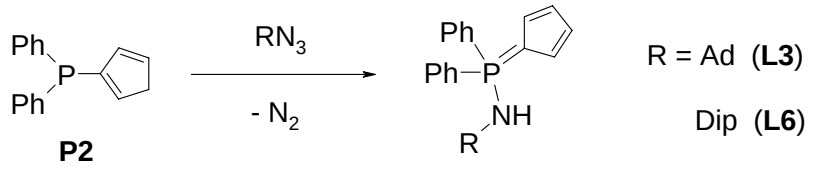

Scheme 13. Reactions of phosphane $Ph_2PC_5H_5$ (**P2**) with AdN_3 and $DipN_3$.

Formation of $Me_2P(C_5H_4)NHAd$ (**L4**) from thermally stable $Me_2PC_5Me_4H$ (**P3**) is nearly quantitative (Scheme 10). For the synthesis of its Ph-analog $Ph_2P(C_5H_4)NHAd$ (**L8**) prolonged heating under reflux temperature is required (5 – 10 d depending on solvent).

This synthetic approach may be extended to other cyclopentadienyl-phosphanes and azides. However, in some of our experiments we experienced its limitation. Reactions of the sterically demanding and less nucleophilic phosphane $C_5Me_4HPPh_2$ (**P4**) with the less reactive azide Me_3SiN_3 did not lead to the desired ligand in any acceptable yield (Scheme 14). Surprisingly, no *CpPN-H* compound was obtained with the most reactive azide $DipN_3$.

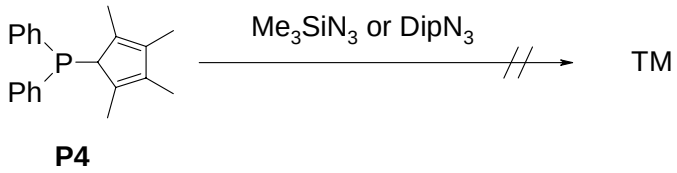

Scheme 14. Attempted reaction of phosphane $Ph_2PC_5Me_4H$ (**P4**) with Me_3SiN_3 and $DipN_3$.

Monitoring of the reaction mixtures by ^{31}P NMR spectroscopy shows only the formation of the corresponding *Staudinger* adduct (*cf.* Chapter IV, Part 2.6). This result can be explained by unfavorable steric reasons – two Ph-groups at the phosphorus atom and highly demanding

Dip-substituent at the nitrogen atom preclude the reachable transition state for intramolecular formation of the type **II** species and nitrogen extrusion.

We also failed to obtain any (isolated) product from the *Staudinger* reaction with indenyl-diphenylphosphane (Δ_1-Ind)PPh_2. Instead, intensively green-colored waxes with complex ^{31}P NMR spectra were obtained (Scheme 15). Initially, we explained this by the dipolar 1,3-cycloaddition of azide to the activated double bond of the indenyl-phosphane or indenyl-iminophosphorane as one of the side reactions.

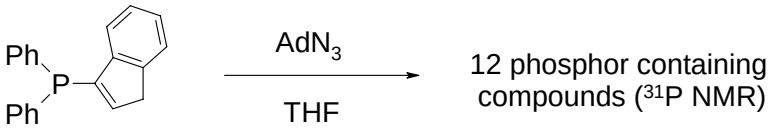

Scheme 15. Attempted reaction of (Δ_1-Ind)PPh_2 with AdN_3 in THF.

However, very recently the synthesis of these *IndPN*-ligands has been demonstrated by *Bourissou*.[11] The key to the success was employing dichloromethane instead of THF as solvent. Yet, this synthetic route is limited by reactions of phosphanes with low reactivity toward dichloromethane.

In the reaction of $Ph_2PC_5H_5$ (**P2**) with *tert*-BuN_3 (Scheme 16) the only isolated product was identified as *P*-amino-cyclopentadienyliden-phosphorane $Ph_2P(C_5H_4)NH_2$ (**S3**) without *tert*-Bu-substituent at the nitrogen atom.

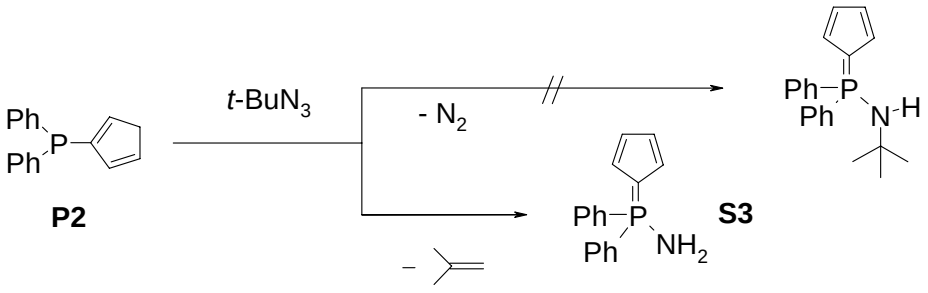

Scheme 16. Reaction of $Ph_2PC_5H_5$ (**P4**) with *tert*-BuN_3 leading to $Ph_2P(C_5H_4)NH_2$ (**S3**).

This unexpected result is explained by a different – compared to the other cases – mechanism of degradation of the intermediately formed *Staudinger* adduct. Compared to AdN_3 (and certainly to $DipN_3$ and Me_3SiN_3), *tert*-BuN_3 is the only one that able to take part in a β-elimination reaction, which – we assume – can attend degradation of the *Staudinger* adduct yields not only nitrogen, but also *iso*-butene and the product **S3** (Scheme 17). The formation of *iso*-butene was not investigated.

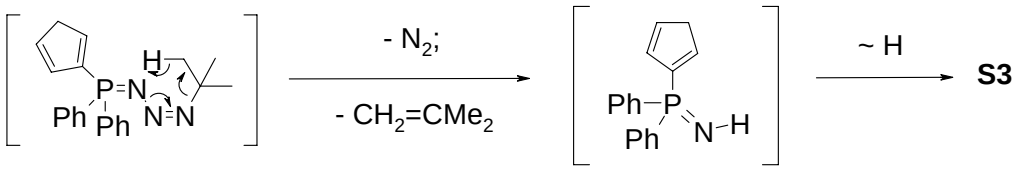

Scheme 17. Mechanism of the intramolecular way of decompositions of the *Staudinger* adduct.

We also tried to modify the substitution at the N-atom (Scheme 18). The compound **S3** was allowed to react with Me_3SiCl in $(Me_3Si)_2NH$ as solvent. No reaction was observed after 10 h at 100°C:

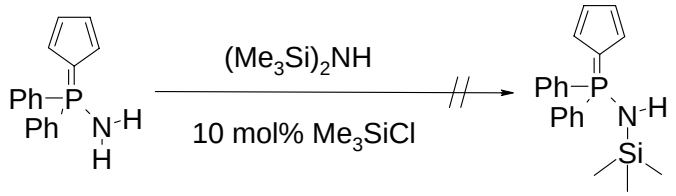

Scheme 18. Attempted reaction of $Ph_2P(C_5H_4)NH_2$ (**S3**) with $(Me_3Si)_2NH$ in the presence of Me_3SiCl.

As it was found later, the hydrolysis of *N*-silylated cyclopentadienyl-iminophosphoranes proceeds much more easily (*vide infra*).

2.3.2. *Syntheses of Starting Phosphanes **P1** – **P4***

The phosphanes **P1** and **P2** are thermally unstable substances and they were prepared *in situ* from CpTl and the corresponding chlorodiorganylphosphanes (Me_2PCl and Ph_2PCl) at 0°C and immediately involved in the following reactions.

Though CpTl is highly toxic compound, this reagent is highly advantageous Cp-synthon:

- the reactions proceed very quickly (5 – 15 min) and even at low temperatures (-30°C);
- easier work up – simple filtration without a Celite® pad;
- high purity of products (no detectable amounts of impurities by ^1H NMR);
- CpTl can be handled without inert atmosphere technique.

When common anionic Cp-synthons (CpM, M = Li, Na) are applied for the Cp-phosphane syntheses, the following *Staudinger* reaction leads to a complex mixtures of dark colored products, from which only trace amounts of the target substances can be isolated. It is believed that this unselective reaction pathway takes place due to the presence of basic impurities. Such difficulties have been recently reported for the syntheses of cyclopentadienyliden phosphoranes, obtained *via* anionic Cp-synthons.[12]

With highly sterically demanding chlorophosphane (*tert*-Bu)$_2$PCl no reaction with CpTl was observed even after 48 h at ambient temperature.

The phosphane $HC_5Me_4PMe_2$ (**P3**) was synthesized by a slightly modified literature procedure[13] from a stock solution of Me_2PCl and C_5Me_4HLi in an ether/hexane mixture. Recently, it was found, that the highly reactive C_5Me_4HLi is prone to nucleophilic ring-opening of THF at ambient temperature.[14] Therefore the usage of this solvent mixture instead of THF/hexane allows a rapid and simpler isolation of highly pure phosphane **P3** in nearly quantitative yield. Use of a stock solution of Me_2PCl in toluene (ca. 1.5 – 2.0M solution) is an advantage in hading of this aggressive substance. Another achievement in the manipulation with Me_2PCl was the procedure of neutralization of the exceedingly unpleasant odor of air-degradation products of the phosphane. This could be achieved by the use of a mixture of aqueous Na_2CO_3 solution and acetone (v/v = 1:10). This procedure is based on the ability of chlorophosphanes to react with aqueous acetone under basic conditions with formation of odorless, high melting α-hydroxy-phosphine oxides.

2.3.3. *Detailed Synthetic Aspects*

The typical protocol employed for the synthesis of *CpPN*-ligands consists in the reaction of 0.1 – 0.6 molar THF solutions of the phosphanes **P1** – **P4** with the corresponding azides for 12 – 16 h at ambient temperature, in the case of AdN_3 and $DipN_3$. Reactions with Me_3SiN_3 and the reaction of sterically crowded, less reactive phosphane **P4** with AdN_3 require refluxing and longer reaction times (2 – 10 d), as monitored by ^{31}P NMR spectroscopy.

In the case of the Cp-phosphanes **P1** and **P2** the choice of the solvent is very important. The *Staudinger* reactions in ether, hexane or toluene as solvent did not proceed selectively and only brown intractable semisolid masses could be obtained: the solvent of choice appears to be THF or its mixture with ether.

With the sterically demanding phosphane $Ph_2PC_5Me_5H$ (**P3**) the *Staudinger* reactions take place also in dichloromethane and diethyl ether and proceed with higher selectivity as shown by ^{31}P NMR spectroscopy of the reaction mixture. Though reactions with Me_3SiN_3 could be performed in THF under reflux, the use of toluene at 110°C was found to be superior. Compared to **P3** the thermally stable phenyl analog $Ph_2PC_5Me_4H$ (**P4**) is less reactive and reacts slowly only with AdN_3 by heating in THF. Interestingly, in the reaction of **P4** with either Me_3SiN_3 or $DipN_3$ in refluxing THF no products were obtained. Complete evaporation of the solvent after the reaction yields light-brown powders or oils. In the case of crystalline products purification was afforded by repetitive washing with ether or hexane or re-crystallization to give the desired compounds in yields of 60 – 95% (Table 2). The *P*-methyl family of ligands – **L2**, **L4** and **L5** appears as white air-sensitive, microcrystalline substances, readily soluble in THF, $CHCl_3$, DMSO and C_6H_6, moderately soluble in ether and insoluble in hexane, while the *P*-phenyl-substituted derivatives – **L3**, **L6** and **L8** – are less air-sensitive yellowish powders that are less soluble in C_6H_6 and ether at ambient temperature and could be crystallized from hot aromatic solvents. Interestingly, the compound **L5** which is moderate stable in the solid state is highly air-sensitive in solution and turns its color into brown within seconds.

It is known that in some cases the *Staudinger* reaction can be catalyzed by *Lewis* acids. The promotion of the *Staudinger* reaction by catalytic amounts of $AlCl_3$ was demonstrated in the synthesis of $(tert\text{-}Bu)_3P{=}NSiMe_3$.[15a] However, so far no acceleration has been documented by the addition of *Brønsted* acids.

In fact, we have found an indirect proof of such a *Brønsted* acid catalysis during the study of the *Staudinger* reaction with $Ph_2PC_5H_5$ (**P2**), obtained from HCl-free carefully purified by

a "bulb-to-bulb" vacuum distillation Ph_2PCl. The yields of *CpPN-ligands* ***dropped twice*** (!), compared to the syntheses with **P2,** obtained from the technical grade chlorophosphane that typically contains some HCl. The influence of catalytic amounts of organic bases was also investigated: neither acceleration nor deceleration of the *Staudinger* reaction by addition of small amounts of amines (Et_3N, Py) was observed. This suggests that catalysis by ammonium salts, though it can be foreseen, is rather doubtful.

All attempts of exploration of fairly unstable $PhP(C_5H_4)_2$ – synthesized by reaction of equimolar amounts of TlCp with $PhPCl_2$ in diethyl ether – in reaction with $DipN_3$, even at low temperatures (-30°C) were unsuccessful.

2.3.4. *Mechanistic and Tautomeric Equilibrium Aspects*

The mechanism of the *Staudinger* reaction of cyclopentadienyl-phosphanes with azides is schematically presented in Scheme 19. The first step of the *Staudinger* reaction leads to the formation of a so-called *„Staudinger adduct"* (**I**),[16] which can be sometimes observed in an experiment in the form of a colorless precipitate if the reaction is carried out in low polarity solvents at low temperatures (< 0°C). The second step is commonly fast and it has most probably an intramolecular character: extrusion of N_2 leads to the formation of iminophosphorane **II**, that may tautomerize to the *P*-amino-cyclopentadienyliden-phosphorane **III.**

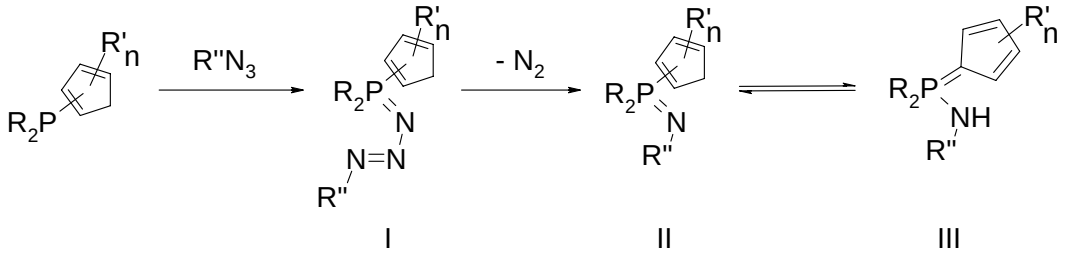

Scheme 19. General mechanism of the *Staudinger* reaction.

Because the relative *Brønsted* acidity of the protons in unsubstituted Cp–*H* is higher compared to that one of all RN–*H* protons, the compounds **L2** – **L6** and **L8** exist in the thermodynamically more stable form of type **III** tautomers (Scheme 19). Contrastingly, the hexane highly soluble oily $Me_2P(NSiMe_3)C_5Me_4H$ (**L1**) has been identified as a mixture of three isomeric *P*-cyclopentadienyl-iminophosphoranes **L1a** – **L1c** in a ratio of approximately 7:2:1 with predominance of the *P*-allylic regioisomer **L1a** (Scheme 20). Due to the low *N*-

basicity and low C*H*-acidity, type **II** isomers **L1a** – **L1c** did not tautomerize to the type **III** *P*-amino-cyclopentadienylidene-phosphorane **L1d**.

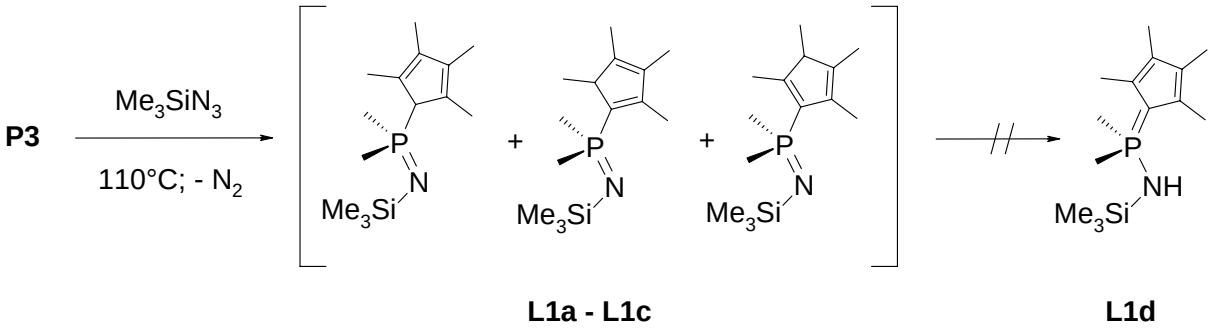

Scheme 20. The C5-ring isomers observed for the compound **L1**.

Also like the compound **L1**, the semi-solid product of the *Staudinger* reaction of $Me_2PC_5Me_4H$ (**P3**) with $DipN_3$ – $Me_2P(NDip)C_5Me_4H$ (**C7**) – comprises at most the type **II** tautomer as the *P*-allylic regioisomer in solution. According to more precise ^{1}H and ^{31}P NMR spectroscopic investigation it comprises a mixture of the type **II** and **III** tautomers – *P*-cyclopentadienyl-iminophosphorane (**L7a**) and *P*-amino-cyclopentadienylidene-phosphorane (**L7b**) – in an *approx.* 8:1 ratio. Again, the *P*-allylic regio-isomer is the predominant species of the major tautomer L**7a** (Scheme 21).

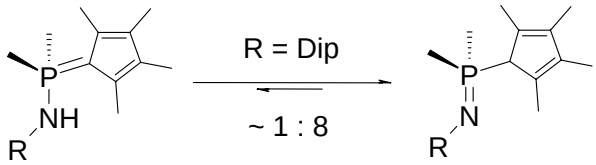

Scheme 21. The tautomeric equilibrium observed for the compound **L7**.

As one might anticipate, the increasing of N-basicity of the iminophosphorane shifts the tautomeric equilibrium towards the cyclopentadienylidene-phosphorane form **III**. In the case of the compound $Me_2P(C_5Me_4)NHAd$ (**L4**), with four methyl groups at the C5-ring, the pK_a of the tetramethyl substituted C5-ring becomes smaller than that one of the AdN-group, therefore in the *P*-amino-cyclopentadienylidene-phosphorane **L4** the only one type **III** tautomer was observed. This fact underlines the strong N-basicity and expected donor strength of these ambident cyclopentadienyl-iminophosphorane ligands, in particular, when C5-ring-, P- and N-substituents are alkyl groups. As expected, the favored isomer of the tautomeric equilibrium can be easily rationalized by the relative acidity of both Me_4C_5–*H* and N–*H* protons.

2.4. *NMR Studies*

All isolated complexes **L1** – **L8** were characterized by multinuclear NMR spectroscopy. Noticeably, the tautomeric appearance of compounds strongly affects the chemical shifts of *CpPN*-H compounds, especially of ^{31}P NMR spectra, and therefore they are discussed further according to their tautomeric appearance. The prototropic (for **L1**) and tautomeric (for **F7**) equilibrium was studied by the ^{1}H and ^{31}P NMR spectrometry.

2.4.1. *^{31}P NMR Spectroscopy of P-Aminophosphoranes **L2** – **L6** & **L8***

In ^{31}P NMR resonances of **L2** – **L6** and **L8** span the range from 15 to 29 ppm, confirming their cyclopentadienylidene-phosphorane structural motif (Table 3).[17] In each case only *one* distinct signal was observed, assuming the absence of tautomeric equilibrium.

The comparison of ^{31}P NMR resonances of **L2** – **L6** and **L8** with the known compounds, having cyclopentadienylidene-phosphorane moieties, is limited to a few representative examples. The highest values of resonances are comparable with those of $Ph_3P(C_5H_4)$ (17.4 ppm) and of $Me_2P(Ind)IndH$ (16.9 ppm).[18] All resonances of other electron rich cyclopentadienylidene-phosphoranes are significantly upfield shifted to the values 10.8 ppm for $Me_2P(Fl)(FlH)$,[19] 8.0 ppm for $Ph_2P(C_5H_4)Me$, 6.2 ppm for $Me_2P(C_5H_4)CH_2PMe_2$ and 4.0 for $Me_3P(C_5H_4)$.[20] Curiously, diisopropyl derivatives $(iso\text{-}Pr)_2P(C_5H_4)R$ are all downfield shifted with the values 24.7 ppm for R = Me, Et and 26.1 ppm for R = *iso*-Pr.[21]

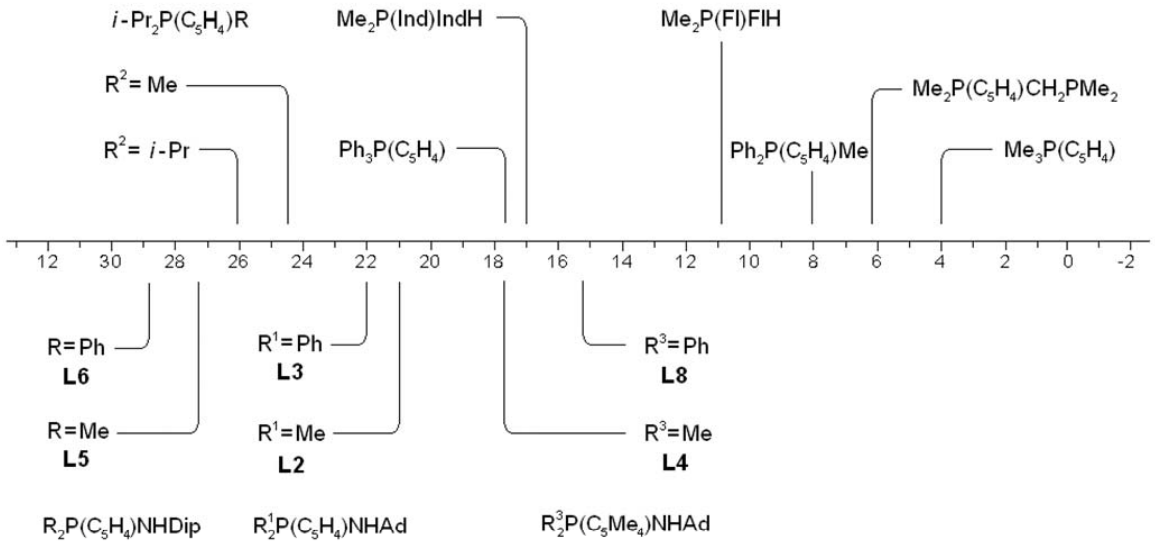

Figure 1. Comparison of chemical shifts of **L2** – **L8** with reported values of cyclopentadienylidene-phosphoranes reported in the literature.

It is interesting to note, that the chemical shifts of the studied aminophosphoranes **L2**, **L3** and **L5**, **L6** are depending more strongly on the nature of substituents at the nitrogen atom than those at the phosphorus atom (*i.e.* Me_2P and Ph_2P). The resonances of compounds with Ph-substituents at the phosphorus atom (**L3** and **L6**) are slightly downfield shifted (~ 1–2 ppm) compared with the counterparts with Me-groups. This could be explained by the electron withdrawing effect of phenyl groups. The shielding of the phosphorus atom congruently correlates with electronegativity and basicity of substituents at the nitrogen atom and the C5-ring. The ^{31}P NMR resonances of **L2** and **L3**, both carrying adamantyl moiety at the nitrogen atom, arise at 21.0 and 22.0 ppm respectively. The compounds **L5** and **L6**, having a less electron donating substituent (*Dip*NH), are most deshielded and downfield shifted to the values of 27.4 and 28.9 ppm. The ^{31}P NMR resonance of the compound **S2**, which has no organic substituents at the nitrogen atom, appears exactly between resonances of compounds **L3** and **L6** and of 26.4 ppm.

Interestingly, for aminophosphoranes **L4** and **L8** the reversed effect was observed. The resonances of the electron rich **L4** and **L8** are most high field shifted in the aminophosphorane series and appear at 17.6 and 15.2 ppm respectively.

2.4.2. *^{31}P NMR Spectroscopy of P-Cyclopentadienyl-Iminophosphoranes **L1** & **L7***

In contrast to the *P*-aminophosphoranes, the ^{31}P NMR spectra of **L1** and **L7** reveal several resonances. The careful assignment of ^{1}H, ^{31}P and ^{13}C NMR resonances shows, that the distribution of resonances is in accordance with a number of isomers present: three isomers for **L1** or two tautomers for **L7** (*vide supra*). The predominant species of both **L1** and **L7** are *P*-cyclopentadienyl-iminophosphoranes with ^{31}P NMR resonances in the δ_P range -20 – 0 ppm characteristical for iminophosphoranes.[22] As a criterion for their purity deprotonation of both substances either with *n*-BuLi or benzylpotassium (BnK) has been used. This leads to the quantitative formation of metallated compounds (Scheme 22) with only one ^{31}P NMR signal (for **L1** in THF-d_8: δ_P(K-salt) = 7.3 ppm; δ_P(Li-salt) = 8.5 ppm). Interestingly, although deprotonation of **L1** was performed in THF, no product with coordinated solvent was obtained, suggesting that these salts exist as "head-to-tail" polymer or dimer. Both salts are highly air-sensitive and, as expected, soluble only in high polarity solvents. They were characterized by NMR spectroscopy in THF-d_8 and elemental analysis.

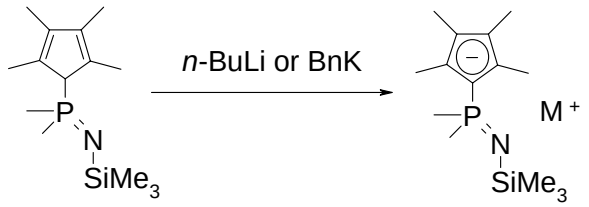

Scheme 22. Deprotonation of the compound $Me_2P(NSiMe_3)C_5Me_4H$ (**L1**) with *n*-BuLi or BnK. Only one isomer of **L1** is depicted.

Using the ^{31}P NMR spectroscopy, the distribution of the **L1** isomers has been determined more precisely (Scheme 23). The ratio **L1a**:**L1b**:**L1c** was estimated to be of 69:22:9 with the major allylic isomer **L1a** (1.1 ppm) and two minor vinylic iminophosphoranes **L1b** (5.6 ppm) and **L1c** (-10.1 ppm).

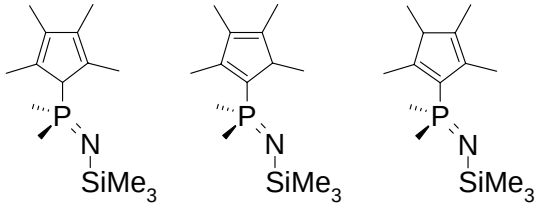

	L1a	**L1b**	**L1c**
isomeric ratio	69	22	9

Scheme 23. Distribution of the isomers of compound **L1** after the equilibaration in solution (C_6D_6).

The ^{31}P NMR chemical shift of the predominant allylic isomer **L7a** (δ = -3.1 ppm) was completed only on the basis of its characteristic shifts observed in the analogous fluorenyl-iminophosphorane ligands $Ph_2P(=NR)(FluH)$, R = Mes (δ = -1.7 ppm), Dip (δ = -1.9 ppm).[11] Signal assignment for the minor *P*-aminophosphorane tautomer **L7b** was not achieved. All attempts to obtain analytically pure sample of one of these isomers of **L7** by repeated crystallization from hexane failed due to the high solubility of the compound and their impurities even at low temperatures (-78°C).

2.4.3 *^{1}H and ^{13}C NMR Spectroscopy of P-Aminophosphoranes **L2** – **L6** & **L8***

All spectra were recorded in C_6D_6 at +25°C except those of compounds **L3** and **L6** showing low solubility in benzene at +25°C (Table 3). Therefore their spectra were recorded in $CDCl_3$, although they appear to react slowly with chloroform, while the solutions slowly darkened. Complete signals' assignment in all spectra has been supported with COSY ^{1}H/^{1}H and ^{1}H/^{13}C experiments. In ^{1}H NMR spectra no *P*-allylic C5-ring protons were observed rather than slightly broadened N*H* resonances appearing as doublets with two-bond ^{1}H–^{31}P scalar coupling varying from 4.8 – 7.2 Hz. The coupling constants of N*H* protons of electron rich compounds **L2** and **L4** were not defined, since the signals overlap with aliphatic proton resonances. The ^{1}H and ^{13}C NMR signals of the C_5H_4-mojety in **L2**, **L3**, **L5** and **L6** correlate perfectly with those, found in related cyclopentadienylidene-triphenylphosphorane $Ph_3P(C_5H_4)$ (**S2**). These spectroscopic data also in very good agreement with those of $Ph_2P(C_5H_4)NH_2$ (**S3**), albeit the latter was not crystallographically characterized.

Finally, the one-bond ^{31}P–^{13}C scalar coupling of the C5-ring of av. 120 Hz are in very large and comparable with those of the *P*-phenyl groups found in $Ph_2P(C_5H_4)$NHAd (**L3**) and $Ph_2P(C_5H_4)$NHDip (**L6**). This finding additionally indicates the sp^2-hybridization of the *ipso*-C5-ring carbon atom.

Table 3. Selected ^{1}H, ^{13}C and ^{31}P NMR spectroscopic data [a] for *P*-amino-phosphoranes **L2** – **L6** and $Ph_2P(C_5H_4)NH_2$ (**S3**) compared with $Ph_3P(C_5H_4)$ (**S2**).

^{1}H	**L2**	**L3**[c]	**L4**	**L5**	**L6**[c]	**L8**	**S3**	**S2**
*H*C5	6.66	6.35	--	6.74	6.37	--	6.27	6.32
	6.95	6.39		6.99	6.49		6.37	6.50
Me_2P	1.21	--	1.25	--	--	--	--	--
($^{2}J_{H,P}$)	(13.2)		(10.1)					
N*H*	1.57[b]	2.71	1.35	3.21	4.53	2.41	3.21	--
($^{2}J_{H,P}$)		(5.8)	(ca. 6)[b]	(6.6)	(7.2)	(4.8)	(br s)	
$^{13}C\{^{1}H\}$								
C_{C5}	113.1	113.8	117.9	113.6	114.5	119.4	114.8	114.2
($J_{C,P}$)	(17.6)	(16.8)	(18.0)	(16.0)	(18.9)	(16.0)	(18.9)	(18.0)
	114.4	116.5	119.7	114.9	116.9	122.3	116.4	116.8
	(18.7)	(16.8)	(19.0)	(19.3)	(17.4)	(19.1)	(17.0)	(15.0)
P-C_{C5}	86.7	84.0	77.8	83.1	83.1	72.1	84.6	77.9
($^{1}J_{C,P}$)	(126)	(126)	(125)	(133)	(133)	(127)	(126)	(112)
$^{31}P\{^{1}H\}$	21.0	22.0	17.6	27.4	28.9	15.2	26.4	26.4

a) The spectra were recorded in C_6D_6 at 25°C; b) The $^{2}J_{H,P}$ coupling constant of NH was not observed since this signal overlaps with aliphatic protons; c) because of low solubility in C_6D_6, the spectra were recorded in $CDCl_3$.

2.4.4. *^{1}H and ^{13}C NMR Spectroscopy of P-Cyclopentadienyl-Iminophosphoranes* ***L1*** *&* ***L7***

The selected ^{1}H and ^{13}C NMR spectroscopic characteristics are represented in Table 4 (for compounds **L1** and **L7** values of main isomers are given). All spectra were recorded in C_6D_6 at +25°C. Formulation of **L1** and **L7** as iminophosphoranes is strongly supported by characteristic one-bond $^{13}C–^{31}P$ scalar coupling of av. 12 Hz constants for the Me_2P-group that is considerably smaller compared to those of cyclopentadienylidene-phosphoranes **L2** – **L6** (av. 120 Hz). The ^{1}H and ^{13}C chemical shifts of the Me_4C_5-moiety correlate greatly not only with those of the phosphane $Me_2PC_5Me_4H$ (**P3**), but, moreover, with the ^{13}C resonances of the parent 1,2,3,4-tetramethylcyclopenta-1,3-diene (!)[23] The *ipso-H*C resonances of C5-rings in the main isomers of **L1** and **L7** are significantly closer to each other (2.98 and 3.36 ppm resp.). This result is in a good agreement with those found in *bis*-(2,3,4,5-tetramethylcyclopenta-2,4-dienyl)-selenium $(Me_4C_5H)_2Se$ (δ_H(Se-*H*C$_{C5}$) = 3.29 ppm).[24] For the minor isomers of **L1** only partial assignment can be achieved (see Experimental Part). The only reliable assignment of isomeric ratio could be made by the deconvolution of the $SiMe_3$-group resonances.

Table 4. Selected ^{1}H, ^{13}C and ^{31}P NMR spectroscopic data for *P*-cyclopentadienyl-iminophosphoranes **L1** and **L7** in comparison with Ph_2P(FluH)N(Ph) and $Me_2PC_5Me_4H$ (**P3**) in C_6D_6.

^{1}H	**L1**[a)]	**L7** [a)]	Ph_2P(FluH)NPh	**P3**
Me–C_5	1.64	1.65	--	1.72
	1.93	1.97	--	1.92
Me$_2$P ($^{2}J_{H,P}$)	0.95 (12.6)	1.02 (11.7)	--	0.83 (4.7)
*ipso-H*C$_{C5}$ ($^{2}J_{H,P}$)	2.98 (25.5)	3.36 (26.8)	5.09 (24.0)	2.79
$^{13}C\{^{1}H\}$				
C_{C5} ($^{2}J_{C,P}$)	131.3 (4.0)	131.4 (3.7)	--	133.6 (2)
C_{C5} ($^{3}J_{C,P}$)	139.2 (6.8)	140.0 (7.4)	--	136.2 (3)
ipso-C$_{C5}$ ($^{1}J_{C,P}$)	63.8 (58)	63.0 (62)	49.8 (75.5)	57.9 (23)
$^{31}P\{^{1}H\}$	1.1	-3.1	7.8	-34.8

[a)] NMR data of the main isomer; [b)] The $^{3}J_{H,P}$ and $^{2}J_{C,P}$ coupling constant recorded at 50.1 MHz.

2.5. *Molecular Structures*

2.5.1. *Molecular Structures of P-Amino-Cyclopentadienylidene-Phosphoranes **L3** – **L6***

The molecular structures of the *P*-amino-cyclopentadienylidene-phosphoranes **L3** – **L6** appear to be rather similar. Certain differences – particularly the lattice packing effect – are worth discussing. Suitable crystals for X-ray structure analysis of **L3** and **L6** were obtained upon crystallization at room temperature from chloroform; crystals of **L4** and **L5** were obtained from less polar solvents such as benzene and toluene. The molecular structures of **L4** and **L5** with thermal ellipsoids of 50% probability are shown in the figure below.

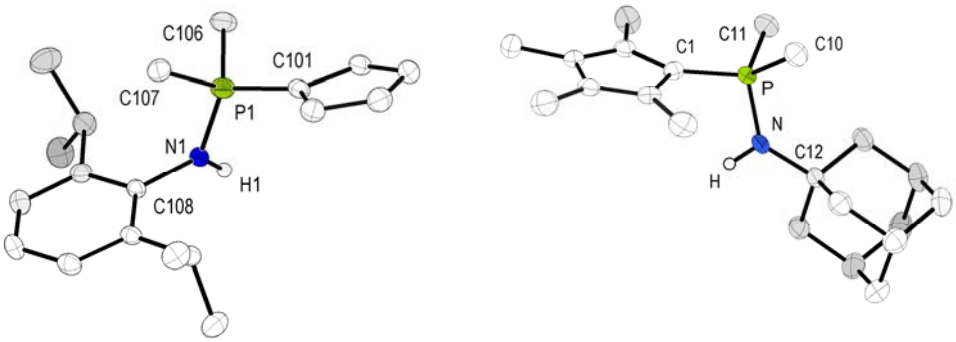

Figure 2. The molecular structures of **L5** (left) and **L4** (right); all hydrogen atoms, except of N–H **L5** have been omitted for clarity.

In all molecular structures the phosphorus atom has a tetrahedral environment. The angular sum around the nitrogen atoms is very close to 360° and hence shows sp^2-hybridization. In the compounds **L5** and **L6**, having the di-*ortho*-substituted aromatic ring at the nitrogen (Dip), the P–N bond is almost perpendicular to the aromatic ring. Therefore the lone pair at the nitrogen atom is not conjugated with the aromatic ring like in anilines. As a consequence, the nitrogen atom has enhanced basicity, compared to the parent $Ph_3P{=}NPh$ (pK_a(MeCN) = 16.74), a significantly shortened P–N bond length and high field shifted ^{31}P NMR resonances. This reflects the ability of compound **L5** and **L6** not to participate in a tautomeric equilibrium as it was observed for the *N*-$SiMe_3$ and *N*-Dip substituted **L1** and **L7**.

The P–C_{Ph} bond lengths in **L3** and **L6** vary within 1.808(2)–1.823(2) Å and are almost equal with those in $Ph_3P(C_5H_4)$ (**S2**: 1.802(2) – 1.808(2) Å).[25] Other parameters like average C_{C5}–P–C_{Ph} angles (114.3°, 110.1°) or C_{Ph}–P–$C_{Ph'}$ (105.73°, 106.94°) angles for *P*-phenyl substituted **L3** and **L6** are also similar to those observed in **S2** (110.2°–112.6° and 105.8°–109.2°).

The P–Me bond lengths within one and the same molecule in **L4** (1.803(2), 1.805(2) Å) and **L5** (1.775(3), 1.785(6) Å) are almost equivalent to each over and comparable with those in $Me_2P(Fl)(FlH)$ (1.793(2), 1.795(2) Å)[19] and $Ph_2P(C_5H_4)Me$ (in the solid state the substance has two independent molecules with P–Me bond lengths of 1.799(2) and 1.792(2) Å).[12]

In all these compounds the P–C_{C5} and P–N bond lengths are similar (Table 5). The P–C_{C5} bond lengths lie in the narrow range of 1.720(1) – 1.735(2) Å and are only slightly longer than that one in the parent phosphoranes $Ph_3P(C_5H_4)$ (**S2**: 1.718(2) Å),[25] $Ph_2P(C_5H_4)Me$ (**S1**: av. 1.727(5) Å)[13] or $\{(i\text{-}Pr)_2N\}_2P(Flu)Cl$ (1.698(7) Å),[26] but significantly longer than in the $Ph_3P{=}CH_2$ (1.66 Å),[27] a typical example of non-resonance-stabilized ylide.

The P–N bond distances in all crystallographically characterized *P*-aminophosphoranes are similar and vary within a range of 1.642(5) – 1.659(2) Å. These bond lengths are significantly longer compared not only to the closely related iminophosphoranes $PhN{=}PPh_3$ (1.602(3) Å),[28] $(2,6\text{-}Me_2C_6H_3)N{=}PPh_3$ (1.553(2) Å)[29] and $Ph_3P{=}N(tert\text{-}Bu)$ (1.543(2) Å)[33] but also to phosphinic acid amides $Ph_2P(O)NH_2$ (1.623(4) – 1.639(4) Å)[30] or to $(tert\text{-}Bu)_2P(O)NH_2$ (1.628(1), 1.641(1) Å).[31] Similar unusually elongated bond lengths were found in newly characterized $1\sigma^4,3\sigma^3$-diphosphaallen $Ph_2P\{N(i\text{-}Pr)_2\}{=}C{=}P\{N(i\text{-}Pr)_2\}$ (1.673(4), 1.675(4) Å)[32] and in phosphonium salts $[Ph_3P\{NMe(tert\text{-}Bu)\}]I$ (1.646(3) Å), $[Ph_3P\{NH(tert\text{-}Bu)\}]I$ (1.621(3) Å),[33] and $(tert\text{-}Bu)_3P{=}NH$ (1.652(1) Å).[49]

Table 5. Selected bond distances (Å), angles and torsion angles (°) for **L3** – **L6**.

	L3	**L4**	**L5** × ¼ PhMe[36]	**L6**
P–$C_{Ph/Me}$,	1.814(2)	1.805(2)	1.774(3)–1.787(3)	1.808(2)
P–$C_{Ph'/Me'}$	1.813(2)	1.803(2)		1.823(2)
P–C_{C5}	1.735(2)	1.724(2)	1.720(3)–1.723(3)	1.720(2)
P–N	1.649(2)	1.659(2)	1.637(3)–1.645(3)	1.648(2)
N–C	1.493(2)	1.482(2)	1.441(3)–1.451(4)	1.445(2)
C_{C5}–P–N	115.43(8)	108.23(7)	112.7(1), 116.4(1)–116.7(1)	109.0(1)
$C_{Ph/Me}$–P–N	103.9(1)	109.6(1)	104.9(1)–105.6(1)	106.4(1)
$C_{Ph'/Me'}$–P–N	108.5(1)	109.6(1)	109.0(1)–112.7(2)	114.4(1)
P–N–C	128.0(1)	133.8(1)	124.7(2)–129.3(2)	125.9(1)
C_{C5}–P–N–C	72.8(2)	167.8(2)	126.9(2)–141.9(2)	153.3(2)

These findings propose that such elongation of the P–N bond lengths in the studied *P*-aminophosphoranes is reflected by the presence of the stabilized ylide moiety. The sufficient charge distribution leads to a shortening of the P–C_{C5} bond length and to an elongation of all other X–P bond lengths. This situation is really experimentally observed on the P–C_{C5} and P–N bonds in the studied *P*-aminophosphoranes. According to the reported DFT studies for cyclopentadienylidene-phosphoranes $Ph_2P(C_5H_4)Me$ (**S1**)[12] and $Ph_3P(C_5H_4)$ (**S2**)[34] a significant charge distribution between the phosphorus atom and the C_5H_4-ring. In the case of the compound **S1** it was reported that the C_5H_4-ring carries a charge of about -0.5 independent of the type of calculation (the Mulliken charges were computed at the B3LYP, RHF, and MP2 levels of computation), the phenyl rings and the methyl group are nearly uncharged, and the charge on phosphorus is between +0.4 and +0.7, depending on the levels of computation. As a result the nature of this compound has to be better described as zwitterionic phosphonium cyclopentadienide form **S1-b**, rather than cyclopentadienylidene form **S2-a** (Scheme 9). Somewhat similar results were also found for $Ph_3P(C_5H_4)$ (**S2**).[34]

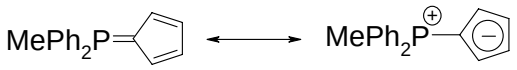

S1-a **S1-b**

Scheme 24.

Conformational analysis in the solid state can be explained by electronic and steric properties in a single molecule, but description would be incomplete without consideration of the packing effects, which are discussed in the following Chapter.

The P–N bonds in the compounds **L4** and **L6** have nearly *anti*-orientation of the C5-rings and *N*-substituents (C_R–N–P–C_{C5} = 167.8(1) and 153.1(1)° resp.). On the one hand, in compound **L4**, the N–*H* position lies nearly under the Me_4C_5-ring and the AdN-group occupies the *gauche*-conformation with respect to Me-groups (CMe–P–N–C = 19.4(1)°). On the other hand, the Ad–N group in **L3** has *anti*-orientation to one of the phenyl substituents (C_{Ph}–P–N–C = 164.8(2)°) and occupies the *gauche*-conformation between the C5-ring and Ph-group.

In the crystal structure of the compound **L5**, four molecules form asymmetric units with significantly different angles and intermolecular distances. Because of the more complicated packing situation, the analysis of the structure will best described in the following Chapter.

2.5.2. *Analysis of Packing of P-Aminophosphoranes* ***L3*** *–* ***L6*** *in Unit Cell*

The compound $Me_2P(C_5Me_4)NHAd$ (**L4**) crystallizes in the monoclinic space group $P2_1/c$. The analysis of the closest intermolecular distances reveals an interesting packing modus: molecules are arranged in periodic stacks (Figure 3). In the stacks the molecules are arranged in endless zigzag chains. The high basicity of the nitrogen atom in the compound **L4**, due to strong donating Ad-, Me_2P and polymethyl substituted C5-ring, is reflected by weak intermolecular interactions. The intermolecular distance between the nitrogen atoms and the centroid of the C5-ring is 4.446(2) Å – significantly longer (ca. 1 Å) than those observed in solid state structures of **L3**, **L5**[36] and **L6**.

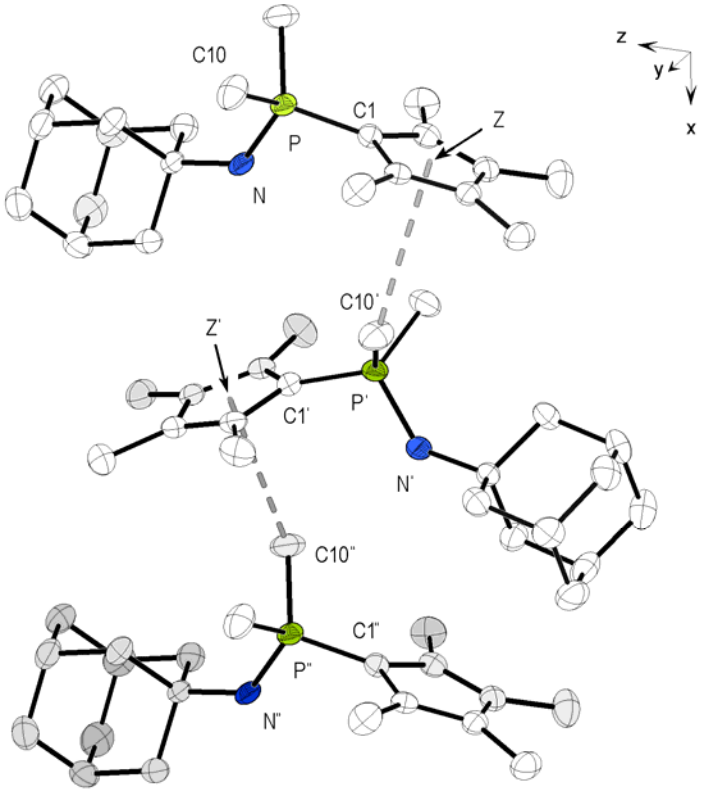

Figure 3. The lattice structure of chains of the compound $Me_2P(C_5Me_4)NHAd$ (**L4**). All hydrogen atoms have been omitted for clarity. Selected closest intermolecular distances are depicted by dashed lines (Å): N–C1'= 4.446(2), Z–C10' = 3.430(2).

The compounds $Ph_2P(C_5H_4)NHAd$ (**L3**) and $Ph_2P(C_5H_4)NHDip$ (**L6**) show outstanding properties – such as decreased air-sensitivity, lower solubility in aromatic solvents, decomposition without melting point reached, NMR spectroscopic features (significantly downfield shift in ^{31}P NMR spectra). Differentiations from the other *CpPN*-H compounds having aminophosphorane structure were found also in their molecular structures and packing in the lattice.

The compounds **L3** and **L6** are isostructural and crystallize in the monoclinic space group $P2_1/c$. The X-ray diffraction studies reveal that in the solid state both possess head-to-tail dimeric units (Figure 4). In the dimeric structure of compound **L6** the molecules are arranged around an inversion center. The N–H bond has its direction to one of the α-carbon atoms of C5 ring in the case of compound **L3** and to the centroid of C5-ring in the case of compound **L6**. The closest intermolecular C–Z distance in **L6** of 3.296(2) Å is somewhat shorter that those found in compound **L3** (3.505(2) Å) – presumably due to the decreased basicity of the NDip-group. No other short intermolecular distances (d < 4.0 Å) in the structure of compound **L6** were observed.

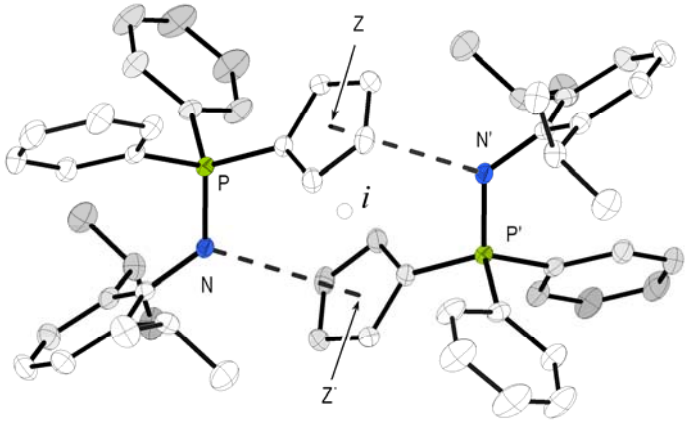

Figure 4. Molecular view of the dimeric unit in compound $Ph_2P(C_5H_4)NHDip$ (**L6**). All hydrogen atoms have been omitted for clarity. The closest intermolecular distance (Å): N···Z' = 3.486(1), N···C_{C5} 3.296(2).

The hydrogen bonding, measured as the closest distance between donor atom (D–H; D = donor) and acceptor (X), *i.e.* d(X···D) for this compounds, lye close to crucial value of 3.0 Å. For example, in highly polar diphenylphosphinic acid amide $Ph_2P(O)NH_2$, that forms dimeric molecules *via* hydrogen bonds, which again are associated *via* hydrogen bonds in infinite double chains,[31] the intermolecular N···O distances are short and varying within the region 2.951(6) – 3.033 Å.

At the first view, the compounds **L3** and **L6** differ insignificantly – compound **L3** comprises also dimeric units in the solid state. The high density of **L3** (1.238 g/cm^3) calculated by X-ray crystallography really stands out. The typical calculated density values are varying from 1.098 – 1.171 g/cm^3 for **L4**, **L5**×¼C_6H_6[36] and **L6**. The careful analysis of the closest intermolecular distances reveals that a slightly different crystal packing situation is realized.

Two neighboring dimeric units, appear to interact with each over by means of two additional T-shape stackings, forming zigzag-like columns along the x-axis. Except of the C5···NH' contact, the C5-ring interacts with two Ph-groups, forming inter- and intramolecular contacts, whereas the intermolecular contact (d(*m*-HC···Ph) = 3.525(2) Å), is comparable with the intermolecular C_{C5}···NH' contact (d(C8···N') = 3.505(2) Å).

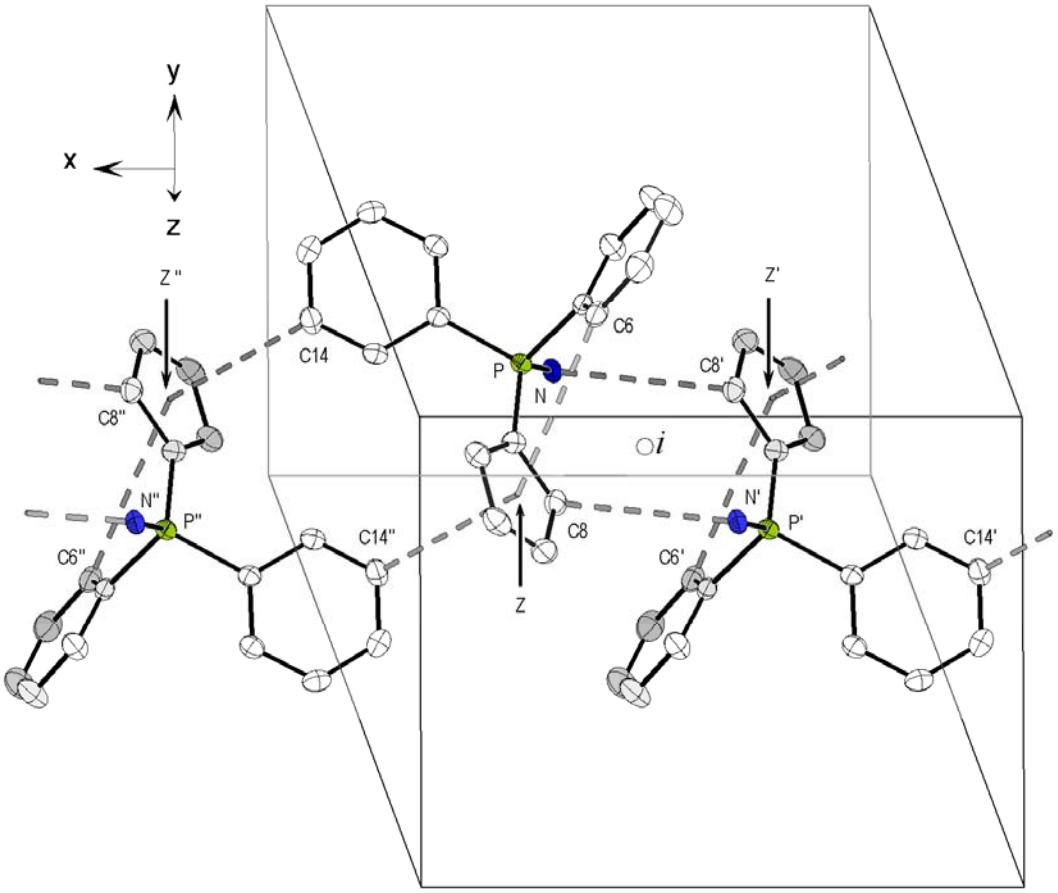

Figure 5. Molecular structure of the zigzag chain along the x-axis in compound $Ph_2P(C_5H_4)NHAd$ (**L3**). Hydrogen atoms and Ad-groups have been omitted for clarity. The closest intermolecular distances are depicted by dashed lines (Å): C8···N' = 3.505(2), C6···Z1 = 3.789(2), Z1···C14' = 3.525(2).

The ability to build such strong interactions in the solid state is obviously responsible for their physico-chemical properties, such as lower solubility and higher melting points.

The T-shape C–H···C(π) stacking was observed in the whole series of crystallographically characterized aminophosphoranes.

The classical example of this interaction is the benzene *herringbone structure*.[35] The T-shape stacking was found not only in structures of neutral molecules, but more offen in structures consisting ionic C5-ring fragments. For example, in the ionic tetra-*n*-butylammonium salt $[(n\text{-Bu})_4N]^+$ $[C_5H_5]^-$ the closest intermolecular C–H···C(π)' distances vary from 3.58–3.72 Å and the closest intermolecular C–H···Z' distance was found to be 3.44 Å (Z = centroid of C5-ring). In closely related systems like the bulky phosphonium salt $[Ph_4P]^+$ $[C_5H_5]^-$, the closest intermolecular C–H···C(π)' distances were found to be 3.59–3.88 Å, while an intermolecular C–H···Z' distance was found to be of 3.57 Å. There are two arguments, favoring the consideration of T-shape stacking: these values are very close to the established for the classical arene, C(π)···C(π)-stacking, usually varying from 3.2 – 3.6 Å; the reduced solubility is in accordance with the ability of the molecules to form multiple T-shaped hydrogen bridges in the crystal state.

The compound **L5** crystallizes from toluene solution and containing one molecule of toluene per four molecules of $Me_2P(C_5H_4)NHDip$.[36] Unlike the compounds **L3**, **L4** and **L6** in the compound **L5** an asymmetric tetrameric unit was realized. Here, the precise analysis of the molecular structure and the packing in the unit cell is accomplished. The molecular view of the tetrameric unit is shown in Figure 7.

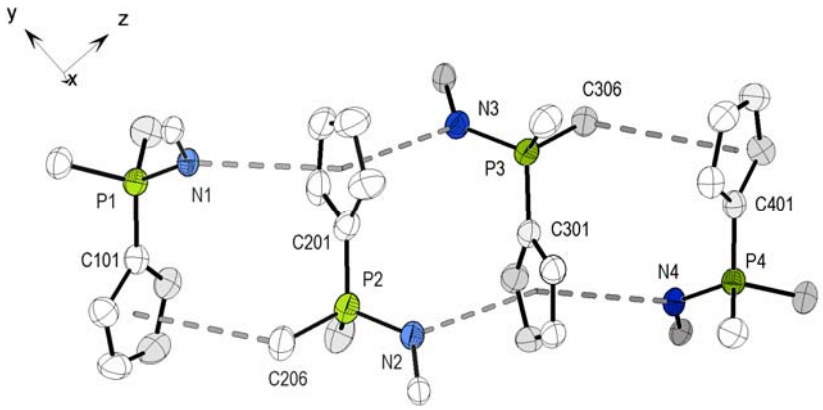

Figure 6. The molecular structure of the asymmetric tetrameric unit of **L5** × ¼ PhMe.[36] All hydrogen atoms and aromatic rings, except of the *ipso*-carbon atoms of the Dip-group, are omitted for clarity. Z2 and Z3 are centroids of the C5-rings of the second and third units. The closest intermolecular distances are depicted by dashed lines (Å): N1···Z2 = 3.352(2), Z1···C206 = 3.632(2), Z2···N3 = 3.316(2), N2···Z3 = 3.439(2), Z3···N4 = 3.383(2), C306···Z4 = 3.548(3).

The four independent molecules are ordered in a chair-like head-to-tail tetrameric structural arrangement. Moreover, both inner C5-rings are coordinated from both sides by the NH-groups of the neighboring molecules, whereas the outer C5-rings are coordinated only from one side by a PC–H group of the inner molecule. The four closest Z···N' intermolecular distances were found to vary from 3.316(2) – 3.439(2) Å. Also two C···Z' distances (3.632(2) and 3.548(3) Å) could be defined and they are slightly longer than those found in the structure of compound **L4**.

Because of an overall complexity in the description of the tetrameric unit, first, the invariants observed within the unit were determinated (Figure 7).

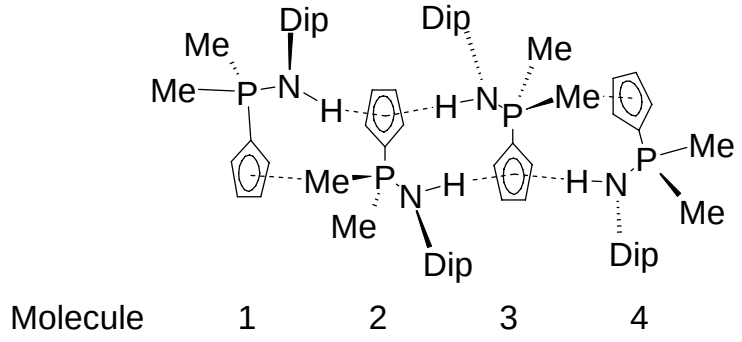

Figure 7. Numeration of the molecules in the tetrameric unit of compound $Me_2P(C_5H_4)NHDip$ (**L5**×¼Tol).

It was interesting to find that the MeP-groups of the inner molecules being located directly above the C5-ring of the outer core molecules. There is only a little deviation of 2.9(1) and 1.8(1)° between the vector orthogonal to the C5-ring and the vector from the centroids Z1/Z4 directed to the P–Me groups of the inner molecules.

No similar alignment was found between the C5-plane-orthonormal vectors and vectors, between the other centroids and nitrogen atoms (for Z2: 10.8° and 17.1(1)°, for Z3: 20.5(1)° and 14.3(1)°).

The most interesting feature found in the structure is, that in the inner core of the unit, both phosphorus atoms are also located almost directly over the counter positioned C5-rings and deviating by values of 4.7(1)° and 1.8(1)°.

These structural findings undoubtedly show the high degree of intermolecular attraction of the negatively charged C5-rings and the positively charged phosphorus atom or hydrogen atoms $P^{\delta-}$–$CH^{\delta+}$ respectively.

Recently, the working group of *Baird* reported the solid structure of $MePh_2PC_5H_4$.[12] This yellowish, air-stable compound has two independent molecules in the unit cell. The bond lengths and angles for each molecule were reported. The more detailed analysis of the closest distances in the unit cell shows a fascinating picture that was not pointed out by the authors. This compound has a column structure in the solid state (Figure 8), similar to those found in the compounds **L3** and **L4**, but differs by the presence of a second layer.

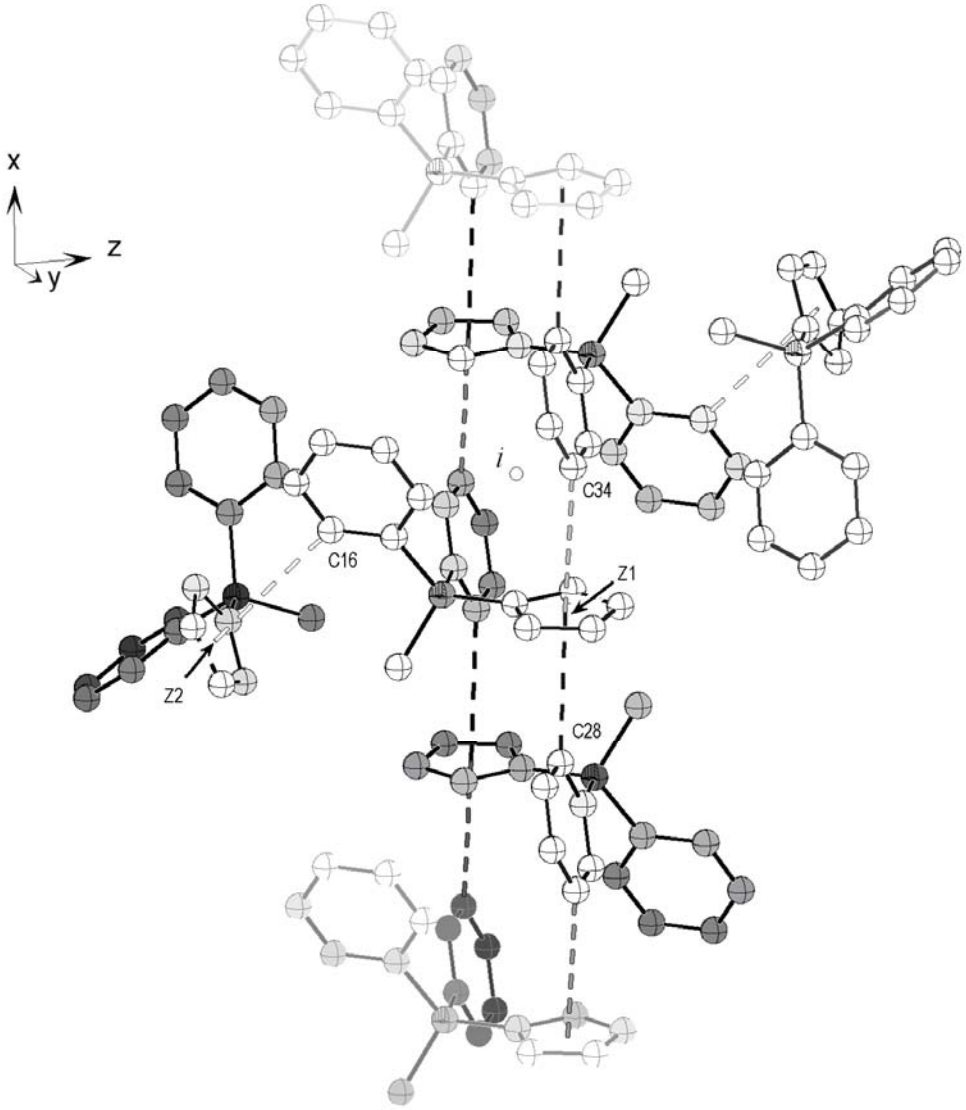

Figure 8. The molecular view of the columns in $MePh_2PC_5H_4$. All hydrogen atoms have been omitted for clarity. The closest intermolecular distances are depicted with dashed lines (Å): Z1···C28 = 3.389(2) (black), Z1···C34 = 3.579(2) (gray), Z2···C16 = 3.662(2) (white).

One part of molecules builds a zigzag-like core column along the x-axis; another part completes the outer second sphere of the column. All closest distances have the same T-shape stacking nature as found for the compounds **L3** – **L6**. The calculated density of this compound, found by X-ray crystallography, is, again, significantly high (1.205 g/cm^3).

Table 6. Crystallographic data and structure refinement details for *P*-aminophosphoranes **L3** – **L6**.

	L3	**L4**	**L5** × ¼ PhMe[36]	**L6**
formula	$C_{27}H_{30}NP$	$C_{21}H_{34}NP$	$C_{19}H_{28}NP$	$C_{29}H_{32}NP$
Fw	399.49	331.46	301.41	425.53
cryst system	monoclinic	orthorhombic	triclinic	monoclinic
space group	$P2_1/c$	$P2_12_12_1$	$P\bar{1}$	$P2_1/c$
a, Å	11.418(2)	10.582(2)	10.304(2)	9.781(2)
b, Å	9.773(2)	13.135(3)	17.697(2)	23.416(2)
c, Å	19.444(3)	13.845(2)	23.576(3)	10.692(3)
α, °	90.0	90.0	101.48(1)°	90.0
β, °	99.07(2)	90.0	100.78(1)°	99.73(2)
γ, °	90.0	90.0	105.49(1)°	90.0
V, Å^3	2142.5(5)	1924.5(6)	3926.5(8)	2413.6(9)
Z	4	4	2	4
ρ calcd., g/cm^3	1.238	1.144	1.098	1.171
T, K	180(2)	180(2)	173(2)	180(2)
refl. collected	13689	12951	39332	16846
unique refl.	3872	3468	7011	4597
GoF[b]	0.861	0.995	0.760	1.029
R_1 ($F^2>2\sigma(F^2)$)[a]	0.0343	0.0270	0.0424	0.0396
wR_2 (F^2)[c]	0.0646	0.0611	0.0944	0.1014

a) Observation criterion: $I > 2\sigma(I)$. $R1 = \Sigma||F_0|-|F_c||/\Sigma|F_0|$. b) Goodness of fit (GoF) = $[\Sigma\{w(F_0^2-F_c^2)^2\}/(n-p)]^{1/2}$.
c) $wR2 = [\Sigma\{w(F_0^2-F_c^2)^2\}/\Sigma\{w(F_0^2)^2\}]^{1/2}$, where $w = 1/\sigma^2(F_0^2)+(aP)^2+bP$ and $P = (F_0^2+2F_c^2)/3$.

3. CONCLUSIONS

In this chapter we have reported on the first synthesis of phosphorus(V) compounds having a *CpPN*-motive. This class of mono-anionic ligands has been deliberately designed for the further application to the synthesis of "*constrained-geometry*" complexes (*CGC*) of the rare-earth metals, isolobal with the well studied class of the group 4 metal CGC with the dianionic *CpSiN* ligand regime.

The *Staudinger* reaction of cyclopentadienyl-phosphanes with organic azides turned out the best synthetic strategy among other tested reactions. A series of the cyclopentadienyl-phosphanes of increasing thermal stability – $C_5H_5PMe_2$ (**P1**), $C_5H_5PPh_2$ (**P2**), $HC_5Me_4PMe_2$ (**P3**) and $HC_5Me_4PPh_2$ (**P4**) – in the *Staudinger* reaction with three azides – Me_3SiN_3, AdN_3 and $DipN_3$ – of increased reactivity was investigated. The *CpPN*-H compound syntheses starting from the thermally labile phosphanes $C_5H_5PR_2$ (R = Me, Ph) were optimized by application of CpTl as a Cp-synthon and THF as a solvent. Due to the low reactivity of Me_3SiN_3, only the *Staudinger* reaction thermally stable and sufficient nucleophilic phosphane **P3** made a *N*-silylated derivative of a *CpPN*-ligand, namely $Me_2P(NSiMe_3)C_5Me_4H$ (**L1**), available in high yield. With one exception – for steric reasons no reaction between **P4** and $DipN_3$ has been observed – the *CpPN*-family of new ligands was synthesized and characterized by multinuclear and 2D NMR spectroscopy, mass spectrometry, XRD analysis and microanalysis.

It was found that two tautomeric forms of protonated *CpPN*-ligands can exist. The position of the tautomeric equilibrium depends on the substituents at the nitrogen atom and the C5-ring:

– all studied *CpPN*-H compounds bearing Ad-group at the nitrogen atom (**L2** – **L4**, **L8**) along with those ones (**L5**, **L6**), having at the same time a *N*-Dip-group and an unsubstituted C5-ring moiety in the molecule, adopt the *P*-amino-cyclopentadienylidene-phosphorane form both in solution and in the solid state;
– the tautomeric *P*-cyclopentadienyl-iminophosphorane form is realized only in a limited number of representatives of this *CpPN*-ligand family (**L1**, **L7**) revealing a low CH-acidity and at the same time a low N-basicity. Apart from the predominant iminophosphorane form negligible amounts of C5-ring isomers of **L1** or *N*-amino-tautomer of **L7** were observed to be present in solution equilibrium.

Four novel compounds of the whole *CpPN*-ligand family (**L3** – **L6**) were also characterized by X-ray crystallography.

4. EXPERIMENTAL PART

General considerations. All manipulations were performed under purified argon or nitrogen using standard high vacuum or *Schlenk*-tube techniques, or in a glovebox. Solvents were dried and distilled under argon employing standard drying agents. All organic reagents were purified by conventional methods. NMR spectra were recorded at +25°C on a Bruker ARX200, Bruker AMX300, and Bruker AVANCE DRX400. ^{1}H NMR spectra were referenced (in ppm) to the residual proton signals $CDCl_3$ (7.26 ppm) and C_6D_6 (7.16 ppm). $^{13}C\{^{1}H\}$ NMR spectra were referenced (in ppm) to the residual carbon signals $CDCl_3$ (77.16 ppm) C_6D_6 (128.00 ppm). ^{31}P NMR spectra were referenced (in ppm) to the external standard 85 % H_3PO_4. Abbreviations used are: s = singlet, d = doublet, t = triplet, m = multiplet.

Elemental analyses were performed at the Analytical Laboratory of the Chemistry Department / Philipps-Universität Marburg. Mass spectra were obtained on a Varian MAT CH7A spectrometer (70 eV, EI). Starting materials AdN_3,[37] $DipN_3$,[38] LiC_5Me_4H[39], TlCp,[40] $C_5Me_4HPMe_2$,[13] $HC_5Me_4PPh_2$,[41] $C_5H_5PPh_2$ and $C_5H_5PMe_2$[9] AdNHBr[42] were generated with slight modifications to published methods. Following compound were synthesized according to the literature proceduras: Me_2PCl,[43] *tert*-BuN_3.[44] The following chemicals were used as supplied: 1,2,3,4-tetramethylcyclopenta-1,3-dien (Acros), Ph_2PCl (95%, techn., Acros), (*tert*-Bu)$_2$PCl (Acros) and Me_3SiN_3 (Merck).

X-ray Crystallographic Data Collection and Refinement of Structures.

Crystals of **L3**, **L4** and **L6** were coated with inert perfluoropolyether oil, picked up with a glass fibre and mounted in the cold nitrogen stream of diffractometer STOE IPDS 2. Intensity data were collected at 180 K using graphite monochromated Mo-*K*α radiation (λ = 0.71073 Å). Data collection was performed by hemisphere runs taking frames at every 1.0° in ω. Final cell constants were obtained from a least squares fit of a subset of several thousand strong reflections. All structures have been solved by the direct method SHELXS-97 and refined using the full matrix least squares refinement procedure of SHELXL97.[45]. All non-hydrogen atoms were treated anisotropically, H atoms were places at the calculated positions and refined using the rigid model with $U_{iso}(H) = 1.2U_{eq}(C)$. Crystallographic data of compounds are listed in Table 6.

4.1. Modified Literature Protocols for Synthesis of Starting Materials

4.1.1. *Lithium Tetramethylcyclopentadienid (LiC_5Me_4H):*[40] To a solution of 1,2,3,4-tetramethylcyclopenta-1,3-dien (10.2 g, 84 mmol) in ether/hexane = 1:3 mixture (400 mL) *n*-BuLi was added (60 mL, 1.56 M in hexane, 94 mmol, 1.56 equiv) in three portion within 1 h at RT (weakly exothermic reaction occurs at the beginning). The white suspension gradually formed was stirred with effective magnetic stirrer. After stirring for 3 h the precipitate was filtered off (Ø 80 mm, Glass filter (Por. 3), *filtration is very slow – max. overpressure and min. vacuum*) and was repeatedly eluted with hexane (3×60 mL). Drying in vacuum for 2 h at 50°C gives 9.90 g of off-white crumbly substance (*crushing with a spatula during drying in vacuum is recommended*). Yield: 92% (78 mmol).

4.1.2. *Thallium Cyclopentadienid (TlCp):*[41] Crystalline $TlNO_3$ (25.8 g, 97 mmol) was dissolved in water (320 mL) followed by addition of KOH pellets (14 g, 250 mmol, 2.5 equiv). To the suspension formed a mixture of freshly "cracked" cyclopentadiene (15 g, 230 mmol, 2.3 equiv) and EtOH (50 mL) was added within 5 min. The reaction mixture was stirred with an effective magnetic stirrer for 0.5 h. The pale yellow precipitate was filtered off, successively washed with water (3×100 mL) and ethanol (2×50 mL) and dried in HV for 4 h at RT. Further purification was performed by sublimation in HV (in 3 - 4 g portions; 130°C / 10^{-2}). A pale yellow needle-like crystalline substance was obtained in 97% yield.

Anal. Calcd. for C_5H_5Tl (269.50): C 22.28, H 1.87.
Found: C 22.24, H 1.82.

4.1.3. *Upscaling of 1-Adamantylazide Synthesis (AdN_3):*[46]

Caution!!! *Though we have worked with purified AdN_3 over the course of 3 years without incident, caution is advised in handle and storage of organic azides with M_r<100, which are potentially explosive.*[47] *The further scaling up of the reaction may be hazardous.*

To an ice bath cooled solution of 1-adamantylazide (34.0 g, 158 mmol) and Me_3SiN_3 (22.0 g, 191 mmol, 1.2 equiv) in 250 mL chloroform, $SnCl_4$ (15.0 mL, 128 mmol, 0.8 equiv) was added within 5 min. No significant exothermic reaction was observed. The reaction mixture was brought to RT and left to stir overnight; after that it was cooled to 0°C again and crushed ice was added in small portions. The formed white precipitate was dissolved by

addition of water (ca. 250 mL). The organic phase was separated and washed successively with water, conc. Na_2CO_3 solution and brine. The solvent was completely removed at a rotary evaporator and residue was dried in high vacuum for 0.5 h. Purification of a crude product (yield: 66%, 18.5 g, 104 mmol) was performed by flash chromatography (Ø 100 mm, H 35 mm) with hexane (ca. 150 mL) giving 15.5 g of an off-white product, having a pleasant terpene-like. TLC: R_f (hexane) = 0.7; I_2 vapors as detection). This compound, unlike previously reported,[48] found to be stable under artificial light, not hygroscopic and therefore was stored in a normal transparent flask. *This protocol allows synthesis of high purity AdN_3 in 100 mmol scale. Upon ignition of small amounts of AdN_3 in a Bunsen burner flame no detonation but calm burning was observed. Impacts from a hammer did not cause detonation.*

M.p. = 81.0 – 81.5°C

^{1}H NMR (300.1 MHz, $CDCl_3$): δ = 1.67 (m, 6H, $H_2C(CH)_2$), 1.80 (d, J_{HH} = 3.0 Hz, 6H, CH_2CN_3), 2.15 (m, 3H, $HC(CH_2)_3$) ppm.

$^{13}C\{^1H\}$ NMR (75.5 MHz, $CDCl_3$): δ = 29.92 (*γ-Ad*), 36.02 (*δ-Ad*), 41.63 (*β-Ad*), 59.11 (*α-Ad*) ppm; (75.5 MHz, C_6D_6): δ = 30.03 (*γ-Ad*), 35.90 (*δ-Ad*), 41.56 (*β-Ad*), 58.81 (*α-Ad*) ppm.

4.1.4. *Modified Procedure of 2,6-Di-iso-propylphenylazide Synthesis ($DipN_3$):*[49]

Caution!!! *Though we have worked with purified $DipN_3$ over the course of 3 years without incident, caution is advised in handling and storage of organic azides with M_r<100, which are potentially explosive.*[46] *The further scaling up of the reaction may be hazardous.*

The 2,6-di-*iso*-propylamine (20.0 g, 0.10 mol) was added drop-wise to conc. hydrochloric acid (50 mL) cooled to -30°C. To thus formed thick white slurry conc. aq. solution of $NaBF_4$ (20.4 g, 0.24 mol) was added in one portion, followed by a drop-wise addition of solution of $NaNO_2$ (7.7 g, 0.11 mol in 25 mL H_2O) at the same temperature. *The temperature control is very important.* Thus obtained yellow to orange reaction mixture was further stirred at -30°C for 0.5 h and then filtered quickly in air. The intermediate aryldiazonium tetrafluoroborate was washed twice with ice cold H_2O and transferred with a glass spatula to an ice cooled solution of NaN_3 (19.8 g, 0.31 mol) in 150 mL H_2O covered with 100 mL hexane. When the gas evolution ceased (*ca*. 1 h), the organic phase was separated and an aqueous phase was extracted with hexane (3×50 mL). The combined organic phases were washed with brine and dried over Na_2SO_4. Purification of the azide was performed by flash chromatography (Ø 100 mm, H 50 mm) with hexane. Major amount of the solvent was removed in vacuum at RT; traces of solvent in HV at 0°C. Pale yellow oily substance was obtained in 80% yield (16.5 g).

The substance appears to be slightly photosensitive, continuously developing a brown coloration, and therefore has to be best stored in the dark.
^{1}H NMR (300.1 $CDCl_3$): δ = 1.17 (d, $^{3}J_{HH}$ = 7.0 Hz, 12H, *Me*$_2$CH), 3.37 (sept, $^{3}J_{HH}$ = 7.0 Hz, 2H, Me_2C*H*), 7.01 (m, 3H, *m-/p-Dip*) ppm.
^{13}C{^{1}H} NMR (75.5 MHz, $CDCl_3$): δ = 23.6 (*Me*$_2$CH), 28.9 (Me_2*C*H-), 124.3 (*m-Dip*), 127.3 (*p-Dip*), 136.0 (*ipso-Dip*), 143.4 (*o-Dip*) ppm.

*4.2. Modified Syntheses of Starting Cp-Phosphanes **P1** – **P4***

4.2.1. *Cyclopentadienyl-dimethylphosphane (**P1**):*[9] To a suspension of TlCp (4.47 g, 16.6 mmol) in 80 mL ether, stock solution of Me_2PCl (10 mL of 1.83 M solution in toluene, 18.3 mmol, 1.1 equiv) was added per syringe at 0°C. The reaction mixture was stirred for 30 min. The precipitated white TlCl was filtered off and washed twice with 15 mL of THF. Additional amount of THF (80 mL) was added and the solvent mixture was concentrated in vacuum to one third of the original volume (Et_2O was replaced by THF). This solution of **P1** in THF was immediately introduced in the following reactions.

4.2.2. *Cyclopentadienyl-diphenylphosphane (**P2**):*[9] To a stirred suspension of TlCp (2.81 g, 10.4 mmol) in 40 mL ether, pure Ph_2PCl (2.20 g, ca. 10 mmol, ca. 0.95 equiv) was added per syringe at 0°C (*Caution!!! Ph_2PCl can freeze at temperatures < 0°C*). The reaction mixture was stirred for 1 h. The precipitated TlCl was filtered off and washed twice with 15 mL of ether. The solvent was completely removed in vacuum leaving 2.37 g of a viscous pale-yellow oil. Yield: 95%. The compound **P1** is somewhat unstable at room temperature therefore it has to be introduced in the following reactions as soon as possible.

4.2.3. *Dimethyl-(2,3,4,5-tetramethylcyclopentadien-2,4-yl)-phosphane (**P3**):*[13] To a stirred suspension of C_5Me_4HLi (1.9 g, 14.7 mmol) in 120 mL of 1:2 THF/hexane mixture, a solution of Me_2PCl (1.5 g, 15.5 mmol) in 10 mL THF was added during ½ h at –78 °C. The reaction mixture was allowed to stir overnight warming up to room temperature; LiCl was filtered off and the solution was concentrated to ¼ of the original volume in vacuum. The residual solvent was carefully removed at 0°C in vacuum. The product was obtained as a light-yellow oil in a yield of 83% (2.2 g, 12.1 mmol).

^{1}H NMR (300.1 MHz C_6D_6): δ = 0.83 (d, $^{2}J_{H,P}$ = 4.7 Hz, 6H, *Me*$_2$P), 1.72 (s, 6H, *Me*–C5), 1.92 (s, 6H, *Me*–C5), 2.79 (s, 1H, *all-H*-C5) ppm.

^{13}C{^{1}H} NMR (75.5 MHz, C_6D_6): δ = 9.5 (d, $^{1}J_{CP}$ = 19 Hz, *Me*$_2$P), 11.2 (s, β-C_{C5}-*Me*), 14.3 (d, $^{3}J_{CP}$ = 8.3 Hz, α-C_{C5}-*Me*), 57.4 (d, $^{1}J_{CP}$ = 23 Hz, *all-C*$_{C5}$), 133.6 (d, *J* = 2 Hz, C_{C5}), 136.2 (d, *J* = 3 Hz, C_{C5}) ppm; (50.3 MHz, $CDCl_3$): δ = 9.6 (d, $^{1}J_{CP}$ = 18 Hz), 11.0 (s, β-C_{C5}-*Me*), 14.2 (d, $^{3}J_{CP}$ = 8.1 Hz, α-C_{C5}-*Me*), 57.6 (d, $^{1}J_{CP}$ = 23 Hz, *all-C*$_{C5}$), 133.8 (d, *J* = 2 Hz, C_{C5}), 136.4 (d, *J* = 3 Hz, C_{C5}) ppm.

^{31}P{^{1}H} NMR (81.0 MHz, C_6D_6): δ = -35.1 ppm; (81.0 MHz, $CDCl_3$): δ = -34.8 ppm.

EI-MS: m/z (%) = 182.5 (65.9) [M^+], 167.5 (100) [M^+ - Me], 120.3 (45.9) [$Me_4C_5^+$], 105.3 (42.6) [$Me_3C_5^+$].

4.2.4. *Diphenyl-(2,3,4,5-tetramethylcyclopentadien-2,4-yl)-phosphane (**P4**):*[41] For the preparation of the highly reactive, finely dispersed reagent, a suspension of C_5Me_4HLi (2.56 g, 20.0 mmol) in 100 mL ether was stirred overnight. To this suspension pure Ph_2PCl (4.63 g, 21 mmol, 1.05 equiv) was added at ambient temperature. The reaction mixture was allowed to stir overnight. After addition of 100 mL hexane the precipitated LiCl was filtered off and the solution was concentrated in vacuum to yield viscous yellowish oil that was dried in high vacuum for 2 h. Yield: 87% (5.3 g, 17.4 mol).

^{1}H NMR (300.1 MHz C_6D_6): δ = 1.50 (s, 6H, *Me*–C5), 1.75 (s, 6H, *Me*–C5), 3.64 (d, 1H, $^{2}J_{H,P}$ = 1.4 Hz, 1H, *all-H*-C5), 7.00 (m, 6H, *m-/p-Ph*), 7.42 (m, 4H, *o-Ph*) ppm.

^{13}C{^{1}H} NMR (75.5 MHz, C_6D_6): δ = 11.5 (s, β-C_{C5}-*Me*), 14.5 (d, $^{3}J_{CP}$ = 6.5 Hz, α-C_{C5}-*Me*), 57.4 (d, $^{1}J_{CP}$ = 27 Hz, *all-C*$_{C5}$), 128.4 (d, $^{4}J_{CP}$ = 5.5 Hz, *Ph*), 133.9 (d, *J*= 20 Hz, *Ph*), 134.1 (d, *J* = 3.5 Hz, C_{C5}), 137.2 (d, *J* = 20 Hz, *Ph*), 137.7 (d, *J* = 3 Hz, C_{C5}) ppm.

^{31}P{^{1}H} NMR (81.0 MHz, C_6D_6): δ = 1.6 Hz

EI-MS: m/z (%) = 306.4 (77.2) [M^+], 229.3 (9.7) [M^+- Ph], 185.3 (45.7) [Ph_2P^+], 120.2 (100) [$C_5Me_4^+$], 105.2 (24.6) [$C_5Me_3^+$].

4.2.5. *Attempted synthesis of bis-(tert-butyl)-P-cyclopentadienylphosphane:* To a suspension of TlCp (1.4 g, 5.2 mmol) in 30 mL ether chloro-*bis*-(*tert*-butyl)-phosphane (0.9 g, 5.0 mmol) was added drop-wise. Proceeding of the reaction was monitored by ^{31}P NMR spectroscopy. No reaction was observed after stirring for 24 h. The reaction does not take place in THF as well.

4.3. Syntheses of P-amino-cyclopentadienylidene-phosphoranes

4.3.1. *P-Amino-diphenyl-cyclopentadienylidene-phosphorane (**S3**):* To a solution of the phosphane **P2** was synthesized from Ph_2PCl (2.15 g, 9.8 mmol) and TlCp (2.70 g, 10.0 mmol) in 20 mL THF (see Part 4.2.2), *tert*-BuN_3 (1.60 g, 16.2 mmol, 1.65 equiv) was added in one portion. Gas evolution was observed and the reaction mixture gradually turns yellow and further brown. After 24 h at ambient temperature, all volatiles were stripped off in vacuum yielding a light brown solid. Addition of 20 mL ether results in complete dissolution of the solid and formation of small amount of red-violet oil at the walls of flask. The solution was *quickly* decanted from the oil in an other flask, whereupon spontaneous crystallization occurs. A creamy colored microcrystalline substance was filtered off and dried in vacuum. Yield: 61 % (1.56 g, 5.89 mmol). An analytically pure sample was obtained by crystallization from boiling benzene (40 mg/1.0 mL). M.p. = 166°C (dec.). The substance shows high solubility in THF, CH_2Cl_2, $CHCl_3$, but fair solubility in benzene, toluene, ether and hexane.

^{1}H NMR (300.1 MHz, $CDCl_3$): δ = 3.21 (br. s., 2H, N*H*$_2$) 6.27 (m, 2H, C_5*H*), 6.34 (m, 2H, C_5*H*), 7.47 (m, 4H, *m-Ph*), 7.58 (m, 2H, *p-Ph*), 7.73 (dd, $^3J_{HP}$ = 12.4 Hz, $^3J_{HH}$ = 7.4 Hz, 4H, *o-Ph*) ppm.

^{13}C{^{1}H} NMR (75.5 MHz, $CDCl_3$): δ = 84.6 (d, $^1J_{CP}$ = 126 Hz, *ipso*-C_5H_4), 114.8 (dd, J_{CP} = 2.4 Hz, J_{CP} = 18.9 Hz, C_5H_4), 116.4 (d, J = 17 Hz, C_5H_4), 128.8 (d, $^3J_{CP}$ = 12.7 Hz, *m-Ph*), 129.4 (d, $^1J_{CP}$ = 104 Hz, *ipso-Ph*), 132.3 (J_{CP} = 11.0 Hz, *o-Ph*), 132.6 (d, J_{CP} = 2.4 Hz, *p-Ph*) ppm.

^{31}P{^{1}H} NMR (121.5 MHz, $CDCl_3$): δ = 26.4 ppm.

EI-MS: m/z (%) = 265 (100) [M^+], 188 (31) [M^+ – Ph].

Anal. Calcd. for $C_{17}H_{16}NP$ (265.30): C 76.97, H 6.08, N 5.28.

Found: C 77.12, H 5.91, N 5.15.

4.3.2. *Attempted reaction of $Ph_2P(C_5H_4)NH_2$ (**S3**) with Me_3SiCl in $(Me_3Si)_2NH$:* To a suspension of the *P*-aminophosphorane **S3** (260 mg, 1.00 mmol) in $(Me_3Si)_2NH$ (5.0 mL, 29.0 mmol, 29 equiv) Me_3SiCl (0.2 mL, 1.56 mmol) was added and the reaction mixture was stirred at 100°C. After 2 and 10 h ^{31}P NMR spectroscopy of the solution shows no additional resonances except for that one of the starting **S2**.

*4.3.3. N-Trimethylsilyl-P-(2,3,4,5-Tetramethylcyclopenta-2,4-dienyl)-dimethyl-iminophosphorane (**L1**):* Phosphine $Me_2PC_5Me_4H$ (**P3**) was generated from LiC_5Me_4H (1.61 g, 12.6 mmol) and stock solution of Me_2PCl in toluene (7.2 mL of 1.83M, 13.2 mmol, 1.05 equiv) according the procedure described in Part 4.2.3. The phosphane **P3** was obtained in a yield of 90% (2.05 g, 11.3 mmol). It was dissolved in toluene (20 mL) and Me_3SiN_3 (2.6 g, 22.6 mmol, 2.0 equiv) was added. The reaction mixture was stirred for 48 h at 60°C. Slow evolution of N_2 was observed. All volatiles were removed in vacuum (60°C for 2 h) furnishing 2.6 g (9.7 mmol) of **L1** as a highly air-sensitive pale yellow oil in 86% yield.

^{1}H NMR (300.1 MHz, C_6D_6): Isomer **L1a**: δ = 0.35 (s, 9H, *Me*$_3$Si), 0.95 (d, $^2J_{H,P}$ = 12.6 Hz, 6H, P*Me*$_2$), 1.64 (s, 6H, *α–Me–*C5), 1.93 (s, 6H, *β–Me–*C5), 2.98 (d, $^2J_{H,P}$ = 26 Hz, 1H, *all-H*C$_{C5}$) ppm. Isomer **L1b**: 0.36 (s, *Me*$_3$Si), (d, $^2J_{HP}$ = 12Hz, Me_2P), 1.65, 1.67 (2×dd, $^3J_{HH}$ = 1.6 Hz, $^4J_{HP}$ = 25 Hz, C(H)*Me*), 2.50, 2.52 (2×d, $^3J_{HP}$ = 27 Hz, P–C–C(*H*)Me) ppm. Isomer **L1c**: 0.38 (s, *Me*$_3$Si), 1.25, 1.27 (2×d, $^2J_{HP}$ = 12.5 Hz, Me_2P), 2.76 (dq, $^4J_{HP}$ = 7.3 Hz, $^3J_{HH}$ =1.7 Hz, *H*C(Me)–(CMe)$_2$) ppm.

^{13}C{^{1}H} NMR (75.5 MHz, C_6D_6): Isomer **L1a**:δ = 4.73 (s, *Me*$_3$Si), 11.3 (d, $^3J_{CP}$ = 1.7 Hz, *α–Me–*C5), 14.7 (s, *β–Me–*C5), 17.5 (d, $^1J_{C,P}$ = 66 Hz, *Me*$_2$P), 63.8 (d, $^1J_{C,P}$ = 58 Hz, *all-C*$_{C5}$), 131.3 (d, *J* = 4.0 Hz, *C*$_{C5}$), 139.2 (d, *J* = 6.8 Hz, *C*$_{C5}$) ppm; Isomer **L1b**: 4.69 (s, *Me*$_3$Si), 22.02, 22.13 (2×d, $^1J_{C,P}$ = 70 Hz, *Me*$_2$P), 59.2 (d, $^1J_{CP}$ = 62 Hz, P–C–*C*H(C)–Me), 131.3 (P–C–*C*(H)Me) ppm; Isomer **L1c**: 4.80 (s, *Me*$_3$Si), 18.4 (d, $^1J_{C,P}$ = 61 Hz, *Me*$_2$P), 52.3 (d, $^1J_{CP}$ = 13.3 Hz, *C*H(CMe)$_2$) ppm.

^{31}P{^{1}H} NMR (81.0 MHz, C_6D_6): δ = 1.1 (**L1a**), 5.6 (**L1b**), -10.1 (**L1c**);

L1a: L1b: L1c = 69:22:9.

EI-MS: m/z (%) = 269 (4.5) [M^+], 149 (63.2) [$M^+ - C_5Me_4$], 148 (12.6) [$M^+ - C_5HMe_4$], 134 (77.5) [$M^+ - Me - C_5Me_4$].

Anal. Calcd. for $C_{14}H_{28}NPSi$ (269.5): C 62.41, H 10.47, N 5.20.

Found: C 62.87, H 10.62, N 4.78.

*4.3.4. N-Trimethylsilyl-(2,3,4,5-tetramethylcyclopenta-2,4-dienyl)-dimethyl-iminophosphoranid potassium [{**L1**}K]:* To a stirred solution of compound **L1** (2.00 g, 7.42 mmol) in 80 mL THF, a deep red solution of benzylpotassium (0.94 g 7.21 mmol, 0.97 equiv) in 50 mL THF was slowly added at -60°C. The red color of benzylpotassium disappears soon and a slightly green solution of the K-salt was evaporated. The semisolid residue was triturated with pentane

(5×10 mL) to remove traces of **L1** and dried in vacuum yielding 1.9 g (6.2 mmol) of slightly green solid. Yield: 84% M.p. > 200°C (dec).

^{1}H NMR (THF-d_8, 300.1 MHz): δ = -0.07 (s, 9H, *Me*$_3$Si), 1.59 (d, 6H, $^{2}J_{HP}$ = 12.3 Hz, *Me*$_2$P), 1.91 (s, 6H, *α-Me*–C5), 2.14 (s, 6H, *β-Me*–C5) ppm.

^{13}C{^{1}H} NMR (THF-d_8, 75.5 MHz): δ = 5.1 (d, $^{4}J_{CP}$ = 3.4 Hz, *Me*$_3$Si), 11.9 (d, $^{3}J_{CP}$ = 1.7 Hz, *α-Me*–C5), 14.4 (s, *β-Me*–C5), 24.3 (d, $^{1}J_{CP}$ = 54.8 Hz, *Me*$_2$P), 114.0 (d, $^{2}J_{PC}$ = 14.7 Hz, *α-C*$_{C5}$), 114.4 (d, $^{3}J_{CP}$ = 16.4 Hz, *β-C*$_{C5}$) ppm.

^{31}P{^{1}H} NMR (THF-d_8, 81.0 MHz): δ = 7.3 ppm.

EI-MS: m/z (%) = 269 (33) [M^+ - K], 149 (84) [$M^+ - C_5Me_4$], 134 (100) [M^+ – Me – C_5Me_4].

Anal. Calc for $C_{14}H_{27}NPKSi$ (307.53): C 54.7, H 8.9, N 4.6.

Found: C 53.5, H 8.7, N 4.7.

*4.3.5. P-(1-Adamantylamino)-dimethyl-cyclopentadienylidene-phosphorane (**L2**):* To a stirred solution of phosphane $Me_2PC_5H_5$ (**P1**) synthesized from TlCp (2.16 g, 8.02 mmol, 1.05 eq) and Me_2PCl (0.75 g, 7.78 mmol) in 50 mL THF (see Part 4.2.1), solid AdN_3 (1.65 g, 9.34 mmol, 1.2 equiv) was added at once. The reaction mixture was allowed to stir for 12 h at room temperature, diluted with 30 mL ether furnishing yellow precipitate that was filtered off and washed with ether (3×25 mL) yielding 0.55 g of a beige powder. Yield of the crude product: 10 – 15%. Repeated crystallization from toluene gives a small crop of analytically pure sample.

^{1}H NMR (300.1 MHz, C_6D_6): δ = 1.21 (d, $^{2}J_{H,P}$ = 13.2 Hz, 6H, P*Me*$_2$), 1.36 (m, 6H, *Ad*), 1.41 (m, 6H, *Ad*), 1.57 (m, 1H, N*H*), 1.76 (m, 3H, *Ad*), 6.66 (m, 2H, *H*Cp), 6.95 (m, 2H, *H*Cp) ppm.

^{13}C{^{1}H} NMR (75.5 MHz, C_6D_6): δ = 16.5 (d, $^{1}J_{C,P}$ = 71 Hz, *Me*$_2$P), 29.9 (s, *C*H$_2$(CH-)$_2$), 36.0 (s, *C*H(CH$_2$-)$_3$), 44.8 (d, $^{3}J_{C,P}$ = 3.9 Hz, -C*C*H$_2$CH-), 52.9 (d, $^{2}J_{C,P}$ = 3.9 Hz, -N*C*(CH$_2$)$_3$-), 86.7 (d, $^{1}J_{C,P}$ = 126 Hz, *ipso-C*$_{Cp}$), 113.1 (d, *J* = 17.6 Hz, *C*$_{Cp}$), 114.4 (d, *J* = 18.7 Hz, *C*$_{Cp}$) ppm.

^{31}P{^{1}H} NMR (81.0 MHz, C_6D_6): δ = 21.0 ppm.

EI-MS: m/z (%) = 275 (100) [M^+], 141 (11.1) [M^+ + H - Ad], 135 (20) [Ad^+].

Anal. Calcd. for $C_{17}H_{26}NP$ (275.4): C 74.14, H 9.44, N 5.08.

Found: C 73.81, H 9.05, N 5.32.

*4.3.6. P-(1-Adamantylamino)-diphenyl-cyclopentadienylidene-phosphorane (**L3**):* Phosphane $Ph_2PC_5H_5$ (**P2**), synthesized from TlCp (1.70 g, 6.5 mmol) and Ph_2PCl (1.42 g, 6.4 mmol) in 50 mL THF, solid AdN_3 (1.4 g, 7.1 mmole, 1.2 equiv) was added at once. A slightly exothermic reaction occurs with the formation of a yellow solution and gas evolution. The reaction mixture was stirred overnight. It was diluted with ether and the colorless precipitate formed was filtered off, washed with ether (2×10 mL) and dried in vacuum to give 1.80 g of **L3** in form of white powder. Yield: 69%. Compound is soluble in THF, $CHCl_3$, not soluble in benzene, ether and hexane. M.p. > 175 (dec.)

^{1}H NMR (400.1 MHz, $CDCl_3$): δ = 1.52 (m, 6H, *Ad*), 1.72 (s, 6H, *Ad*), 1.96 (s, 3H, *Ad*), 2.71 (d, $^2J_{H,P}$ = 5.8 Hz, 1H, N*H*), 6.35 (m, 2H, *H*Cp), 6.39 (m, 2H, *H*Cp), 7.56 (m, 6H, *Ph*), 7.97 (m, 4H, *o-Ph*) ppm.

^{13}C{^{1}H} NMR (100.6 MHz, $CDCl_3$): δ = 29.6 (s, *C*H_2(CH-)$_2$), 35.6 (s, *C*H(CH_2-)$_3$), 44.7 (d, $^3J_{C,P}$ = 4.3 Hz, -C*C*H_2CH-), 54.1 (d, $^2J_{C,P}$ = 3.5 Hz, -N*C*(CH_2-)$_3$), 84.0 (d, $^1J_{C,P}$ = 126 Hz, *ipso-*C_{Cp}), 113.8 (d, *J* = 18.1 Hz, C_{Cp}), 116.5 (d, *J* = 17.2 Hz, C_{Cp}), 128.4 (d, *J* = 12.9 Hz, *Ph*), 129.6 (d, *J* = 104 Hz, *Ph*), 132.1 (d, *J* = 2.6 Hz, *Ph*), 132.9 (d, *J* = 10.4 Hz, *Ph*) ppm.

^{31}P{^{1}H} NMR (81.0 MHz, $CDCl_3$): δ = 22.0 ppm.

EI-MS: m/z (%) = 399 (100) [M^+], 335 (3) [$M^+ - C_5H_4$], 265 (82) [M^+ – Ad – H].

Anal. Calcd. for $C_{27}H_{30}NP$ (399.5): C 81.17, H 7.57, N 3.51.

Found: C 81.38, H 7.55, N 3.58.

*4.3.7. P-(1-Adamantylamino)-dimethyl-tetramethylcyclopentadienylidene-phosphorane (**L4**):*

Phosphane $Me_2PC_5Me_4H$ (**P3**) (2.2 g, 12.1 mmol) was dissolved in 10 mL THF and treated with a solution of AdN_3 (2.2 g, 12.4 mmol) in the same amount of THF at ambient temperature. The obtained yellow solution was allowed to stir with a gas-overpressure controller. While gas (N_2) liberation, the reaction solution gradually deepened in color and after 4 h became dark-brown. For completing the reaction it was warmed up to 50°C for additional 30 min. THF was removed in vacuum yielding light-brown residue that was treated with hexane (50 mL) and thoroughly washed with the same solvent (4×50 mL) to give a highly air-sensitive white powder of **L4**. Yield 3.8 g (95% based on the phosphane **P3**).

M.p. = 153.0 – 153.5°C.

^{1}H NMR (300 MHz, C_6D_6): δ = 2.44, 2.39 (2×s, 2×6H, *Me*C5), 1.71 (br s, 3H, C*H*(CH_2)$_3$), 1.40 (br d, 6H, N–C(C*H*$_2$)$_3$), 1.35 (br s, 1H, N*H*). 1.30 (br m, 6H, C*H*$_2$(CH)$_2$), 1.25 (d, $^1J_{CP}$ = 10 Hz, 6H, *Me*$_2$P) ppm.

$^{13}C\{^1H\}$ NMR (75.5 MHz, C_6D_6): δ = 14.9, 12.1 (2×s, *Me*C5) 19.2 (d, Me_2P, $^1J_{CP}$ = 70 Hz), 36.0 (s, $CH_2(CH_2)_2$), 29.9 (s, $CH(CH_2)_3$), 44.7 (d, $^3J_{CP}$ = 4 Hz, $NC(CH_2)_3$), 52.4 (d, $^2J_{CP}$ = 4 Hz, N*C*), 77.8 (d, $^1J_{CP}$ = 125 Hz, PC_{C5}), 119.7, 117.5 (2×d, J_{CP} = 19 Hz, J_{CP} = 18 Hz, α-/β-MeC_{C5}) ppm.

$^{31}P\{^1H\}$ NMR (121.5 MHz, C_6D_6): δ = 17.6 ppm.

EI-MS: m/z (%) = 331 (36 %) [M^+], 316 (5%) [$M^+ - CH_3$], 286 (11%) [$M^+ - 3\ CH_3$], 196 (20%) [M^+ – Ad].

Anal. Calcd. for $C_{21}H_{34}NP$ (331.46): C 76.09, H 10.34, N 4.23.

Found: C 75.85, H 10.99, N 4.25.

*4.3.8. P-(2,6-Di-iso-propylphenylamino)-dimethyl-cyclopentadienylidene-phosphorane (**L5**):*

To a stirred solution of phosphane $Me_2PC_5H_5$ (**P1**), synthesized from TlCp (2.65 g, 9.9 mmol, 1.04 equiv) and Me_2PCl (0.92 g, 9.5 mmol) according the procedure described in Part 4.2.1, $DipN_3$ (1.8 g, 10.2 mmol, 1.1 equiv) was added and the reaction mixture was stirred overnight. Removing of solvent yields an intractable oil, that, after trituration with ether, gives 2.14 g (7.1 mmol) of the product in form of a slightly yellow powder in a yield of 75%.

Compound is soluble in THF, $CHCl_3$, sparingly in benzene and ether; not soluble in hexane. The compound is air-stable in solid state and as suspension in hexane, but decomposes in solutions within minutes. M.p. = 142.4 – 143.0°C.

^1H NMR (300.1 MHz, C_6D_6): δ = 1.08 (d, $^3J_{H,H}$ = 6.9 Hz, 6H, Me_2CH-), 1.13 (d, $^2J_{H,P}$ = 13.0 Hz, 6H, Me_2P), 3.21 (d, $^1J_{H,P}$ = 6.6 Hz, 1H, N*H*), 3.43 (sept, $^3J_{H,H}$ = 6.9 Hz, 2H, Me_2CH-), 6.74 (m, 2H, *H*Cp), 6.99 (m, 2H, *H*Cp), 6.95 (m, 1H, *p-Dip*), 7.05 (m, 2H, *m-Dip*) ppm.

$^{13}C\{^1H\}$ NMR (75.5 MHz, C_6D_6): δ = 13.8 (d, $^1J_{C,P}$ = 72 Hz, Me_2P), 24.2 (s, Me_2CH-), 28.3 (s, Me_2*C*H-), 83.1 (d, $^1J_{C,P}$ = 133 Hz, *ipso*-C_{Cp}), 113.6 (d, *J* = 16.0 Hz, C_{Cp}), 114.9 (d, *J* = 19.3 Hz, C_{Cp}), 124.1 (d, *J* = 1.7 Hz, *Dip*), 127.8 (s, *Dip*), 132.2 (d, *J* = 5.5 Hz, *Dip*), 148.5 (d, *J* = 2.6 Hz, *Dip*) ppm.

$^{31}P\{^1H\}$ NMR (81.0 MHz, C_6D_6): δ = 27.4 ppm.

EI-MS: m/z (%) = 301 (100) [M^+], 286 (96) [$M^+ - CH_3$], 258 (79) [$M^+ - C_3H_7$].

Anal. Calcd. for $C_{19}H_{28}NP$ (301.4): C 75.71, H 9.36, N 4.65.

Found: C 75.39, H 9.33, N 4.70.

*4.3.9. P-(2,6-Di-iso-propylphenylamino)-diphenyl-cyclopentadienylidene-phosphorane (**L6**):*
The same procedure as for **L3** from TlCp (1.43 g, 5.3 mmol, 1.04 equiv), Ph_2PCl (1.13 g, 5.1 mmol) and $DipN_3$ (1.2 g, 5.9 mmol, 1.2 equiv) was followed. 1.84 g (4.3 mmol) of product in form of a white powder was isolated. Yield: 85%. The compound **L6** is soluble in THF, $CHCl_3$; sparingly in benzene; not soluble in ether, hexane. M.p. > 170°C (dec.).
^{1}H NMR (300.1 MHz, $CDCl_3$): δ = 0.81 (d, $^3J_{H,H}$ = 6.9 Hz, 12H, *Me*$_2$CH-), 3.25 (sept, $^3J_{H,H}$ = 6.9 Hz, 2H, Me$_2$C*H*-), 4.53 (d, $^2J_{H,P}$ = 7.2 Hz, 1H, N*H*), 6.37 (m, 2H, *H*Cp), 6.49 (m, 2H, *H*Cp), 7.01 (d, *J* = 7.8 Hz, 2H, *m-Dip*), 7.21 (t, *J* = 7.8 Hz, 1H, *p-Dip*), 7.36 (m, 6H, *m-/p-Ph*), 7.53 (m, 4H, *o-Ph*) ppm.
^{13}C{^{1}H} NMR (75.5 MHz, $CDCl_3$): δ = 23.0 (s, *Me*$_2$CH-), 28.6 (s, Me$_2$*C*H-), 83.1 (d, $^1J_{P,C}$ = 133 Hz, *ipso-C*$_{Cp}$), 114.5 (d, *J* = 18.9 Hz, *C*$_{Cp}$), 116.9 (d, *J* = 17.4 Hz, *C*$_{Cp}$), 123.9 (s, *Dip*), 126.8 (s, *ipso-Dip*), 128.1 (d, *J* = 12.4 Hz, *Ph*), 128.4 (s, *Dip*), 131.6 (d, *J* = 5.9 Hz, *Ph*), 132.5 (d, *J* = 2.9 Hz, *Ph*), 133.5 (d, *J* = 10.9 Hz, *Ph*), 148.4 (d, *J* = 2.5 Hz, *Dip*) ppm.
^{31}P{^{1}H} NMR (81.0 MHz, $CDCl_3$): δ = 28.9 ppm.
EI-MS: m/z (%) = 425 (100) [M^+], 410 (48) [$M^+ - CH_3$], 382 (47) [$M^+ - C_3H_7$].
Anal. Calcd. for $C_{29}H_{32}NP$ (425.6): C 81.85, H 7.58, N 3.29.
Found: C 82.08, H 7.68, N 3.27.

*4.3.10. N-(2,6-Di-iso-propylphenyl)-P-(2,3,4,5-tetramethylcyclopenta-2,4-dienyl)-dimethyl-iminophosphorane (**L7**):* The same procedure as for **L1** from $Me_2PC_5Me_4H$ **P3** (2.05 g, 11.3 mmol) and $DipN_3$ (2.52 g, 12.4 mmol, 1.1 eq) was followed. The purification was achieved by repetitive crystallization from hexane at -80°C giving a pale rose colored powder. Compound **L7** is very air-sensitive; highly soluble in all custom solvents. The NMR data of the main tautomer (**L7a**) are presented (ca. 90% by ^{31}P NMR).
^{1}H NMR (300.1 MHz, C_6D_6): δ = 1.02 (d, $^2J_{H,P}$ = 11.7 Hz, 6H, *Me*$_2$P), 1.34 (d, $^3J_{H,H}$ = 7.0 Hz, 12H, *Me*$_2$CH-), 1.65 (m, 6H, *Me*–Cp), 1.97 (s, 6H, *Me*–Cp), 3.37 (d, $^2J_{H,P}$ = 26.8 Hz, 1H, *all-H*Cp), 3.65 (sept, $^3J_{H,H}$ = 7.0 Hz, 2H, Me$_2$C*H*-), 7.10 (m, 1H, *p-Dip*), 7.24 (m, 2H, *m-Dip*) ppm.
^{13}C{^{1}H} NMR (75.5 MHz, C_6D_6): δ = 11.4 (s, *Me*–Cp), 13.8 (d, $^1J_{C,P}$ = 62 Hz, *Me*$_2$P), 14.7 (s, *Me*–Cp), 24.2 (s, *Me*$_2$CH-), 28.9 (s, Me$_2$*C*H-), 63.0 (d, $^1J_{C,P}$ = 62 Hz, *ipso-C*$_{Cp}$), 119.4 (d, *J* = 3.2 Hz, *Dip*), 123.0 (d, *J* = 2.5 Hz, *Dip*), 131.4 (d, *J* = 3.7 Hz, *C*$_{Cp}$), 140.0 (d, *J* = 7.4 Hz, *C*$_{Cp}$), 142.2 (d, *J* = 7.1 Hz, *Dip*), 145.9 (d, *J* = 3.4 Hz, *Dip*) ppm.
^{31}P{^{1}H} NMR (81.0 MHz, C_6D_6): δ = -3.1 (major isomer), 32.5 (minor isomer) ppm.
EI-MS: m/z (%) = 357 (1.3) [M^+], 253 (10.9) [$M^+ - C_3H_7 - 4\ CH_3$], 237 (1) ($M^+ - C_5Me_4$).

Anal. Calcd. for $C_{23}H_{36}NP$ (357.5): C 77.27, H 10.15, N 3.92.
Found: C 77.69, H 10.23, N 3.90.

*4.3.11. P-(1-Adamantylamino)-diphenyl-tetramethylcyclopentadienylidene-phosphorane (**L8**):* Phosphane $Ph_2PC_5Me_4H$ **P4** (5.3 g, 17.4 mol) was dissolved in 50 mL THF and solid AdN_3 (5.3 g, 26.1 mmol) was added. The reaction mixture was heated under reflux for 10 d. The proceeding of the reaction was monitored by the ^{31}P NMR spectroscopy of the sample from the reaction mixture (δ_P(THF) = 1.9 (**P4**), -23.5 (Phosphazide), 13.3 (**L8**) ppm). After the completing of the reaction, all volatiles were removed in vacuum yielding a brown, sticky residue. It was triturated with hexane (100 mL) whereupon a yellow solid appears. The precipitate was filtered off, washed with hexane (2×50 mL) and dried in vacuum. A yellow solid was obtained in a yield of 45% (3.56 g).

^1H NMR (300.1 MHz, C_6D_6): δ = 1.50 (s, 6H, CH_2(CH)$_2$), 1.89 (m, 9H, C*H*, PC(CH_2)$_3$), 2.24 (s, 6H, *Me*–C5), 2.41 (d, $^2J_{HP}$ = 4.8 Hz, 1H, N*H*), 2.58 (s, 6H, *Me*–C5), 7.15 (m, 6H, *p-/m-Ph*), 7.92 (m, 4H, *o-Ph*) ppm.

$^{13}C\{^1H\}$ NMR (75.5 MHz, C_6D_6): δ =12.3 (s, *Me*–C5), 15.6 (s, *Me*–C5), 30.3 (s, *C*H(CH$_2$)$_3$), 36.2 (s, *C*H$_2$(CH)$_2$), 44.9 (d, $^3J_{CP}$ = 3.4 Hz, PC(*C*H$_2$)$_3$), 50.1 (d, $^2J_{CP}$ = 10.2 Hz, N*C*), 72.1 (d, $^1J_{CP}$ = 127 Hz, *ipso*-C_{C5}), 119.4 (d, J_{CP} = 16 Hz, Me–C_{C5}), 122.3 (d, J_{CP} = 19 Hz, Me–C_{C5}), 131.1 (s, *Ph*), 132.4 (d, $^2J_{CP}$ = 10.7 Hz, *o-Ph*), 134.0 (d, $^1J_{CP}$ = 102 Hz, *ipso-Ph*) ppm.

$^{31}P\{^1H\}$ NMR (81.0 MHz, C_6D_6): δ = 15.2 ppm.

Anal. Calcd. for $C_{31}H_{38}NP$ (455.63): C 81.72, H 8.41, N 3.07.
Found: C 81.27, H 8.58, N 3.27.

5. REFERENCES

[1] K. A. Rufanov, B. Ziemer, M. Hummert, S. Schutte, *Eur. J. Inorg. Chem.* **2004**, 4759–4763.

[2] *a*) P. J. Shapiro, E. E. Bunel, W. P. Schaefer, J. E. Bercaw, *Organometallics* **1990**, *9*, 867–869; *b*) P. J. Shapiro, W. D. Cotter, W. P. Schaefer, J. A. Labinger, J. E. Bercaw, *J. Am. Chem. Soc.* **1994**, *116*, 4623–4640; *c*) W. E. Piers, P. J. Shapiro, E. E. Bunel, J. E. Bercaw, *Synlett* **1990**, *2*, 74–84; *d*) J. Okuda, *Chem. Ber*. **1990**, *123*, 1649–1651; e) J. Okuda, *Top. Curr. Chem*. **1991**, *160*, 97–145.

[3] a) J. C. Stevens, F. J. Timmers, G. W. Rosen, G. W. Knight and S. Y. Lai (Dow Chemical Co.), *Eur. Pat. Appl.* EP 0 416 815 A2, **1991** (filed August 30, 1990); b) J. A. Canich (Exxon Chemical Co.), *Eur. Pat. Appl.* EP 0 420 436 A1, **1991** (filed September 10, 1990); c) J. C. Stevens, *Stud. Surface Sci. Cat.* **1996**, *101*, 11–18; d) A. L. McKnight and R. M. Waymouth, *Chem. Rev.* **1998**, *98*, 2587–2598.

[4] K. A. Rufanov, A. R. Petrov, V. V. Kotov, F. Laquai, J. Sundermeyer, *Eur. J. Inorg. Chem.* **2005**, 3805–3807.

[5] a) P. Jutzi, *Chem. Rev.* **1986**, *86*, 983–996; b) P. Jutzi, *J. Organomet. Chem.* **1990**, *400*, 1.

[6] O. I. Kolodyazhnyi, L. A. Repina, Yu. G. Gololobov, *Zh. Obshch. Khim.* **1974**, *44*, 1275–1282.

[7] O. I. Kolodyazhnyi, V. P. Kukhar, *Zh. Obshch. Khim.* **1979**, *49*, 1992–2001.

[8] O. I. Kolodiazhnyi, V. P. Kukhar, *J. Gen. Chem.* **1975**, *45*, 2509–2510; *J. Org. Chem. USSR* **1977**. 13, 248–250. O. I. Kolodiazhnyi, V. P. Kukhar, *J. Gen. Chem.* **1979**, *49*, 1752–1759.

[9] F. Mattey J.-P. Lampin, *Tetrahedron* **1975**, *31*, 2685–2690.

[10] H. Stetter, E. Smulders, *Chem. Ber.* **1971**, *104*, 917–923.

[11] P. Oulié, C. Freund, N. Saffon, B. Martin-Vaca, L. Maron, D. Bourissou, *Organometallics* **2007**, *26*, 6793–6804.

[12] a) J. H. Brownie, M. C. Baird, H. Schmider, *Organometallics* **2007**, *26*, 1433–1443. b) J. H. Brownie, *PhD Thesis*, Kingston, Ontario, Canada, **2007**.

[13] M. Visseaux, A. Dormond, M. M. Kubicki, C. Moïse, D. Baudry, M. Ephritikhine, *J. Organomet. Chem.* **1992**, *433*, 95–106.

[14] N. Hillesheim, *Diploma Thesis*, Philipps Universität Marburg, Germany, **2007**.

[15] a) Synthesis of (*tert*-Bu)$_3$PNSiMe$_3$: W. Buchner, W. Wolfsberger, *Z. Naturforsch.* **1974**, *29b*, 328–334. b) M. Elfferding, *Diploma Thesis*, Philipps Universität Marburg, Germany, **2007**.

[16] Y. G. Gololobov, L. F. Kasukhin, *Tetrahedron* **1992**, *48*, 1353–1406.

[17] S. O. Grim, W. McFarlane, T. J. Marks, *Chem. Comm.* **1967**, 1191–1192.

[18] K. A. Rufanov. *Private communication*.

[19] E. D. Brady, T. P. Hanusa, M. Pink, V. G. Young, Jr., *Inorg. Chem.* **2000**, *39,* 6028–6037.

[20] W. Simanko, W. Tesch, V. N. Sapunov, K. Mereiter, R. Schmid, K. Kirchner, *Organometallics* **1998,** *17*, 5674–688.

[21] E. Ortega, N. Kleigrewe, G. Kehr, G. Erker, R. Fröhlich, *Eur. J. Inorg. Chem.* **2006**, 3769–3774.

[22] a) E. M. Briggs, G. W. Brown, P. M. Cairus, J. Jiricny, M. F. Meidine, *Org. Magn. Reson.* **1980**, *13*, 306–307; b) J. Bödeker, P. Köckritz, H. Köppel, R. Radeglia, *J. prakt. Chem.* **1980**, *322*, 735–741; c) M. Pomerantz, D. S. Marynick, K. Rajeshwar, W.-N. Chou, L. Throckmorton, E. W. Tsai, P. C. Y. Chen, T. Cain, *J. Org. Chem.* **1986**, *51*, 1223–1230.

[23] ^{13}C NMR (75.5 MHz, $CDCl_3$): δ = 11.6, 14.4, 48.2, 132.0, 136.0 ppm.

[24] S. Ford, M. Hofmann, C. P. Morley, J. L. Roberts, M. Di Vaira, *Org. Biomol. Chem.* **2005**, *3*, 3990–3995.

[25] H. L. Ammon, G. L. Wheeler, P. H. Watts, *J. Amer. Chem. Soc.* **1973**, *95*, 6158–6163.

[26] J. A. Dobado, H. Martínez-García, J. M. Molina, M. R. Sundburg, *J. Am. Chem. Soc.* **2000**, *122*, 1144–1149.

[27] J. C. J. Bart, *J. Chem. Soc. B* **1969**, 350–366.

[28] E. Boehm, K. Dehnicke, J. Beck, W. Hiller, J. Strähle. A. Maurer, D. Fenske, *Z. Naturforsch.* **1988**, *43*, 138–144.

[29] K. T. K. Chan, L. P. Spencer, J. D. Masuda, J. S. J. McCahill, P. Wei, D. W. Stephan, *Organometallics* **2004**, *23*, 381–390.

[30] S. Schlecht, S. Chitsaz, B. Neumüller, K. Dehnicke, *Z. Naturforsch., B: Chem. Sci.* **1998**, *53*, 17–22.

[31] M. Nieger, D. Hansgen, W. Roos, *Contribution from Department of Inorganic Chemistry, University of Bonn, Germany* **2002**, CCDC Refcode: XIVQEY.

[32] a) D. Martin, H. Gornitzka, A. Baceiredo, G. Bertrand *Eur. J. Inorg. Chem.* **2005**, 2619–2624; b) D. Martin, F. S. Tham, A. Baceiredo, G. Bertrand, *Chem. Eur. J.* **2006**, *12*, 8444–8450.

[33] C. Imrie, T. A. Mordo, P. H. van Rooyen, C. C. P. Wagener, K. Wallace, H. R. Hudson, M. McPartlin, J. B. Nasirun, L. Powroznyk *J. Phys. Org. Chem.* **1995**, *8*, 41–46.

[34] P. Laavanya, B. S. Krishnamoorthy, K. Panchanatheswaran, M. Manoharan, *J. Mol. Struct.* THEOCHEM **2005**, *716*, 149–158.

[35] W. L. Jorgensen D. L. Severance *J. Am. Chem. Soc.* **1990**, *112*, 4768–4774.

[36] M. Elffeding, *Diploma Thesis*, Philipps-Universität Marburg, **2007**.

[37] G. K. S. Prakash, M. A. Stephenson, J. G. Shih, G. A. Olah, *J. Org. Chem.* **1986**, *51*, 3215–3217.

[38] L. P. Spencer, R. Altwer, P. Wei, L. Gelmini, J. Gauld, D. W. Stephan, *Organometallics* **2003**, *22*, 3841–3854.

[39] A. Antiñolo, M. Fajardo, S. Gómez-Ruiz, I. López-Solera, A. Otero, S. Prashar, A. M. Rodríguez, *J. Organomet. Chem.* **2003**, *683*, 11–22.

[40] H. Meister, *Angew. Chem.* **1957**, *16*, 533–534; G. V. B. Madhavan, J. C. Martin, *J. Org. Chem.* **1986**, *51*, 1287–1293.

[41] J. Szymoniak, J. Besançon, A. Dormond, C. Moïse, *J. Org. Chem.* **1990**, *55*, 1429–1432.

[42] M. Paulshock, J. C. Watts, NL P. Appl. 6403, 294, **1965**, Du Pont de Nemours.

[43] G. W. Parshall, *Inorg. Synth.* **1974**, *15*, 191–193.

[44] J. C. Bottaro, P. E. Penwell, R. J. Schmitt, *Synth. Comm.* **1997,** *27,* 1465–1466.

[45] G. M. Sheldrick, *Program for solution of crystal structures, SHELXS-97*, Universität Göttingen, **1997**; G. M. Sheldrick, *Program for the refinement of crystal structures, SHELXL-97*, Universität Göttingen, **1997**.

[46] G. K. S. Prakash, M. A. Spephenson, J. G. Shih, J. A. Olah, *J. Org. Chem.* **1986**, *51*, 3215–3217.

[47] "Rule of thumb". About an explosion of MeN_3: Ch. Grundmann, H. Haldenwanger, *Angew. Chem.* **1950**, *62A*, 410.

[48] Sigma-Aldrich Catalogues: sigmaaldrich.com.

[49] Modification of the protocol of L. P. Spencer, R. Altwer, P. Wei, L. Gelmini, J. Gauld, D. W. Stephan, *Organometallics* **2003**, *22*, 3841–3854.

[48] W. Gottardi, *Monatsh. Chem.* **1973**, *104*, 1681–1689.

[49] D. W. H. Rankin, H. E. Robertson, R. Seip, H. Schmidbaur, G. Blaschke, *J. Chem. Soc. Dalton Trans.* **1985**, 827–830.

— Chapter IV —

Synthesis and Chemistry of a New Highly Crowded Cyclopentadienyl-Phosphane

Abstract

A pyrrolidine catalyzed condensation of diphenyl-cyclopentadienyl-phosphane $Ph_2PC_5H_5$ (**P2**) with a stoichiometric amount (1 equiv) of acetone leads to 3-diphenylphosphino-6,6-dimethylfulvene (**F1**). Contrastingly, with an excess of acetone an unusual bicyclic-[3,3,0]-fulvenyl-phosphane derivative (**F2**) was isolated and identified. Carbometallation of this new fulvene **F2** with MeLi in ether or hexane leads to an anionic form of a new cyclopentadienyl ligand bearing a highly sterically demanding annelated 1,1,3,3-tetramethyl-cyclopentane moiety and a Ph_2P-group in anti position of the cyclopentadiene-ring. This new ligand $Ph_2PCp^{TM}H$ (**P6**) appears to be a colorless, air-stable, crystalline solid; its molecular structure was confirmed by a X-ray structure analysis. Oxidation reactions with H_2O_2, S_8 or Se led to the corresponding phosphine chalcogenides **S4** – **S6**. Reactions with the organic azides AdN_3, *tert*-BuN_3 or $DipN_3$ and Me_3SiN_3 lead to *P*-amino-cyclopentadienylidenes $Ph_2P(Cp^{TM})NHAd$ (**L9**), $Ph_2P(Cp^{TM})NH$(*tert*-Bu) (**L12**) or *P*-cyclopentadienyl-iminophosphoranes $Ph_2P(NDip)Cp^{TM}H$ (**L10**) and $Ph_2P(NSiMe_3)Cp^{TM}H$ (**F8**) respectively. The compound **L10** represents the first *P*-cyclopentadienyl-iminophosphorane characterized by X-ray diffraction analysis. For all characterized compounds only one isomer was observed; the compounds do not possess any detectable prototropic or elementotropic isomers. Hydrolysis of **L8** with wet MeCN leads to the novel *P*-amino-cyclopentadienyl-phosphorane ligand $Ph_2P(NH_2)Cp^{TM}H$ (**L11**). Transmetallation of the potassium salt of **P6** with $FeCl_2$ leads to the formation of the corresponding ferrocene (**S7**), analogous to the known dppf-ligand. Its X-ray diffraction analysis reveals the strictly *anti*-orientation of substituents at both cyclopentadienyl rings. $PdCl_2$ forms 1:1 complex with **S7**, namely $[(dppf^{TM})PdCl_2]$ (**S8**), that undergoes halogen exchange by reaction with NaI forming $[(dppf^{TM})PdI_2]$ (**S9**). Both complexes are monomeric in C_6D_6 solution as was shown by NMR spectroscopy. The complex **S9** was also characterized by X-ray diffraction analysis.

1. INTRODUCTION

For the synthesis of *CpPN*-ligands *via Staudinger* reaction, the following pool of Cp-phosphanes was used: $Me_2PC_5H_5$, $Ph_2PC_5H_5$, $Me_2PC_5Me_4H$ and $Ph_2PC_5Me_4H$ (**P1** – **P4**). The syntheses of all these phosphanes is reported in the literature. The first two phosphanes are thermally unstable and undergo gradually ($Ph_2PC_5H_5$) or rush ($Me_2PC_5H_5$) dimerization at ambient temperature by *Diels-Alder* reaction. The stabilities of the phosphanes **P3** and **P4** are comparatively high due to kinetic stabilization by four methyl groups with respect to *Diels-Alder* dimerization. It was found, that the last phosphane is too unreactive in the *Staudinger* reaction with alkyl- and arylazides.

In order to enhance the thermal stability and diversity of Cp-phosphanes we attempted to synthesize C5-alkylated Cp-phosphanes.

Sterically hindered derivatives of cyclopentadienyl-anions ($C_5H_{5-n}R_n$; R = Me, Et, *iso*-Pr, *tert*-Bu, Bn, Ph, $SiMe_3$; n = 1 – 5) are useful building blocks, widely used in organometallic chemistry. Introduction of sterically demanding groups at the C5-ring generally changes the physicochemical properties of the respective parent unsubstituted compound. Thus, it becomes possible to obtain monomeric organometallic species, which, in the cases of use a simple C_5H_5-ligand are often unattainable or exist predominantly as polymeric species.

Generally, there are two established routes towards the synthesis of poly-alkylated cyclopentadienes: the stepwise alkylation of the cyclopentadienyl anions with R-X electrophiles and hydro- or carbometallation of fulvenes, the so-called “fulvene route”. Both methods were already established in the 1930s[1] with more general applications appearing in the early 1960s.[2] The first method allows the introduction of a wide range of alkyl groups (Scheme 1).

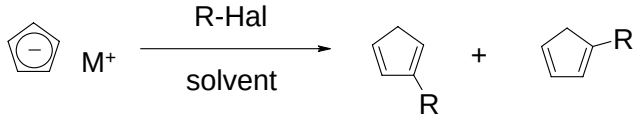

M = Na, K, MgBr;
R = Me, Et, *n*-Pr, All, *t*-Bu, $PhCH_2$,
$-(CH_2)_n$-Hal (n = 5 - 8, 12, 14, 16, 18);
solvent = ether, THF, PhH, NH_3.

Scheme 1. Examples of syntheses of mono-substituted cyclopentadienes.

A main drawback of the method is given by difficulties at the isolation step, where the desired compound should be separated from the mixture of products usually forming.

The second method – the fulvene route – is considerably more general and wider applied for the ligand design in organometallic chemistry. This route is based on the facile condensation of aldehydes and ketones with CpH to form a variety of fulvenes. The cyclopentadienyl ligands are obtained therefrom by reduction with metal hydrides or by carbometallation with anionic organometallics (Scheme 2).

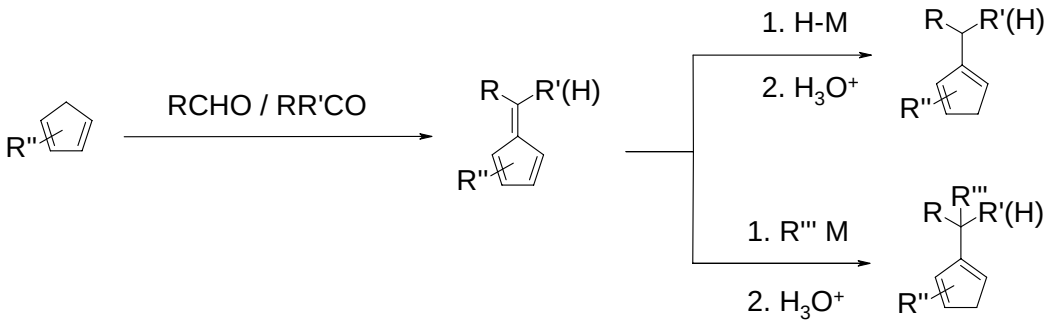

Scheme 2. Preparation of substituted cyclopentadienes by the fulvene route**.**

Historically, the fulvene syntheses were presented by two general approaches – according to *Thiele* and *Little/Stone* methodologies. Both methods consist in the base catalyzed condensation of cyclopentadienes with carbonyl compounds. The methods differ by the choice of the base and solvent. The synthesis according to *Thiele* comprises the use of NaOH or KOH in water or alcohols such as MeOH, EtOH as solvents. Generally, the yields are moderate. The method of *Little/Stone* uses an organic *sec*-amine, usually pyrrolidine (pyrr), as catalyst (5 mol%) in high polarity solvents, usually methanol. The reaction is highly chemoselective. As a rule high yields of the mono-condensation product are reported.[3,8]

Both methods differ significantly in their selectivity of isolated products: whereas the synthesis under *Little/Stone* conditions yields exclusively the mono-condensation product 6,6-dimethylfulvene, the reaction under *Thiele* conditions can give either a double condensation product of one CpH with two acetone molecules, 2-(*iso*-propenyl)-6,6-dimethylfulvene, (Scheme 3) or even a double condensation product of two fulvene molecules (Scheme 4).

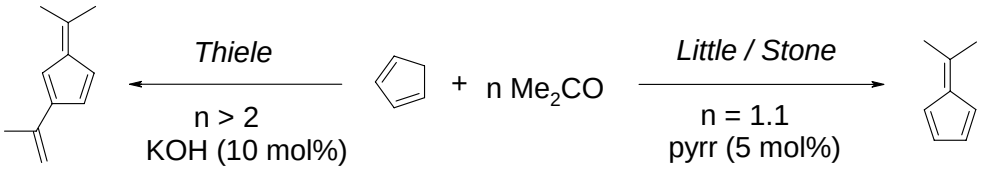

Scheme 3. Dependence of product formation in the reaction of C_5H_6 with acetone according to the *Tiele* and *Little/Stone* conditions.

Indeed, the acidity of methyl groups at the 6-position of 6,6-dimethylfulvene is enhanced by stabilization as aromatic *iso*-propenyl-cyclopentadienide form. Therefore, deprotonation of 6,6-dimethylfulvene with bases such as KOEt or even KOH in MeOH or THF is easily achieved. Thus, intermediately formed *iso*-propenyl-cyclopentadienide reacts further with either another molecule of acetone or with the starting 6,6-dimethylfulvene, that has high electrophilicity at the 6-position. First reaction gives 2-(*iso*-propenyl)-6,6-dimethylfulvene,[4a] while the second one leads to *bis*-cyclopentadiene.[4b, 4c]

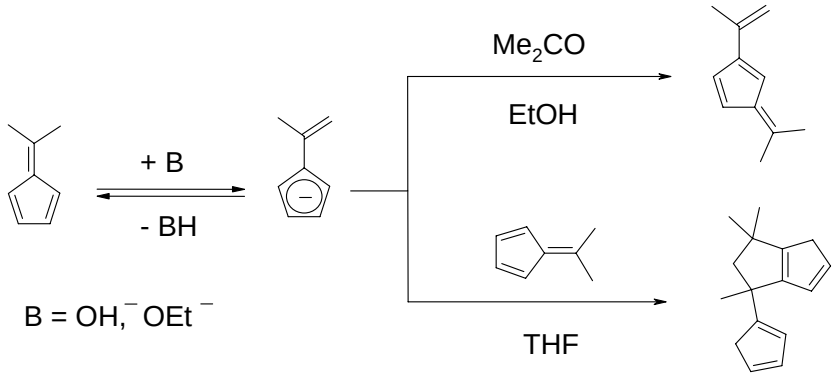

Scheme 4. Formation of different products of condensation under the *Thiele* conditions depending on the solvent used.

Our original goal was the synthesis of the phosphane $Ph_2PC_5H_4$(*tert*-Bu) by this earlier developed fulvene route (Scheme 5) and its further use for the *CpPN*-ligand synthesis.

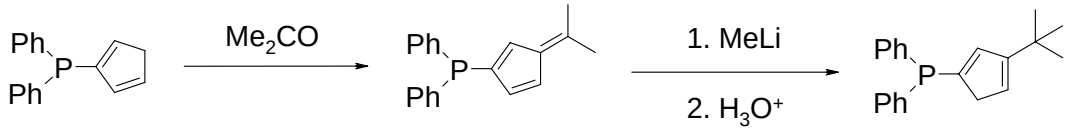

Scheme 5. The intended synthesis of $Ph_2PC_5H_4$(*tert*-Bu).

2. RESULTS AND DISCUSSION

2.1. *Synthesis and Characterization of $Ph_2PC_5H_5$ (**P2**)*

The starting material required for the synthesis of 3-diphenylphosphino-6,6-dimethylfulvene is cyclopentadienyl-diphenylphosphane ($Ph_2PC_5H_5$).

The first synthesis of pure $Ph_2PC_5H_5$ (**P2**) was achieved by *Mattey* and *Lampin* in 1975.[5] They found that high-purity **P2** can only be obtained under non-basic conditions by reaction between Ph_2PCl and freshly sublimed TlCp. Along with **P2** the syntheses of its oxide, sulfide and their dimerization products were reported. All stable compounds were characterized solely by mass spectrometry and low field ^1H NMR spectroscopy (60 and 100 MHz). Only the major vinylic isomers of **P2** and their derivatives were characterized.

This reaction can be performed within large temperature range (-30 – 30°C). According to our observation the reaction conducted at lower temperatures (< 0°C) results in appearance of a colorless solution at first; at room temperature the color of the reaction mixture progressively turns yellowish. The ^{31}P NMR spectroscopic investigation of the sample, immediately after the reaction has completed, reveals three resonances at an integral ratio of 44:50:6, clearly demonstrating the presence of all three isomers. It is obvious that after the nucleophilic addition of Cp^- the allylic Cp-phosphane with a sp^3-hybridized P–C_{C5} linkage is formed (Scheme 6, isomer **A**: δ_P = -8.2 ppm). Additional signals were assigned to the reported[5] vinylic isomer **B** (δ_P = -16.9 ppm) and small amounts of vinylic isomer **C** (δ_P = -18.6 ppm).

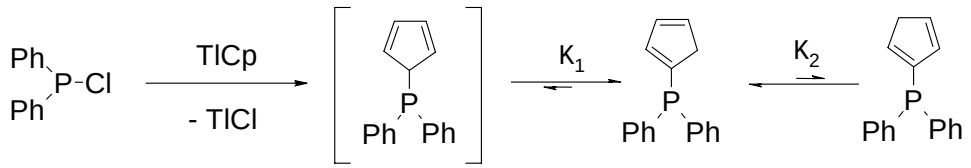

	A	**B**	**C**
immediately after preparation	44	50	6
upon equilibrium reached	2	71	27

Scheme 6. Synthesis of $Ph_2P(C_5H_5)$ (**P2**) and the distribution of isomers, immediately after preparation and upon prototropic equilibrium has been reached respectively.

The phosphane **A** isomerizes quickly at ambient temperature. The color of the solution gradually turns yellow accompanied by changing of the integral distribution of isomers. After

the equilibrium has been reached (ca. 2 h at +25°C), only trace amount of the initially formed phosphane **A** (2%) and significant quantities of **B** (71%) and **C** (27%) were observed by the ^{31}P NMR spectroscopy (125 MHz). For the first equilibrium the free standard enthalpy ΔG_1^o of -8.8 kJ/mol was established ($\Delta G_i^o = -RT\ln K_i$) and for second one the free standard enthalpy was estimated to be of -2.4 kJ/mol.

2.2. *Synthesis and Characterization of Fulvenyl-Phosphanes **F1** – **F3***

The condensation of $C_5H_5PPh_2$ (**P2**) with acetone under *Little/Stone* conditions[3] was studied in three different solvents: ether, methanol and acetone. No reaction was observed in ether, while in MeOH the expected fulvenyl-phosphane (**F1**) forms in nearly quantitative yield as shown by ^{31}P NMR spectroscopy of the crude reaction mixture.

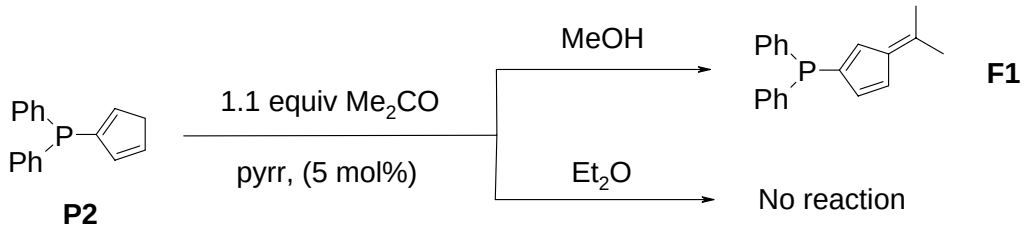

Scheme 7. Synthesis of compound **F2**.

The bright yellow, crystalline compound **F1** was obtained in 67% of isolated yield. An intensive yellow color is consistent with the formation of the fulvene system. The compound melts at 82.5°C and is only slightly air-sensitive in the solid state. It shows high solubility in organic solvents like hexane or THF, but is only sparingly soluble in cold MeOH or acetonitrile. The ^{31}P NMR resonance is somewhat upfield shifted compared to Ph_3P (δ_P = -5.1 ppm) and appears at -17.2 ppm. This indicates a slightly increased electron density at the C5-ring due to the charge distribution in the fulvene system. As expected, ^{1}H NMR spectroscopy reveals two singlets at 1.59 and 1.67 ppm, assigned to methyl group protons at the 6-position of the fulvene and the resonances in olefinic region according to the C5-ring protons together with the phenyl group resonances (Figure 1).

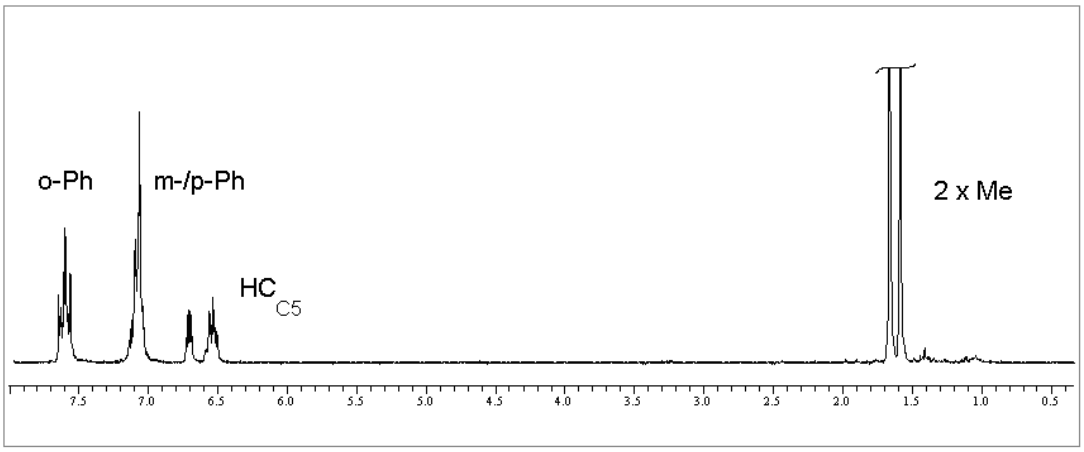

Figure 1. The ^{1}H NMR spectrum (300.1 MHz) of compound **F1** dissolved in C_6D_6 at +25°C.

In the aromatic region, the ^{13}C NMR spectrum shows four resonances of the phenyl group and six resonances of low intensity assigned to the fulvenyl group. In the aliphatic region, unlike the ^{1}H NMR spectrum, only one resonance for both methyl groups was observed.

Accomplishing this reaction in pure acetone seemed us to be highly promising, because the solvent acts as reagent and solvent at the same time. The course of the reaction was monitored by ^{31}P NMR spectroscopy of the crude reaction mixture. The solvent grade acetone was used without drying or other purification. According to the ^{31}P NMR spectra complete consumption of the starting phosphane was achieved after 14 h and formation of a compound with a single resonance (δ_P = -14.9 ppm), very similar to that one found in **F1** (δ_P = -17.2 ppm), was observed.

Further characterization showed that the ^{1}H and ^{13}C NMR resonances are not consistent with those of **F1**. The ^{1}H NMR spectrum is shown in Figure 2. Contrary to compound **F1**, ^{1}H NMR spectroscopy shows only <u>two</u> resonances in the olefinic region (integrals at the ratio of 1:1) and only <u>one</u> methyl group resonance at the 6-position of the fulvene (δ_H = 1.59 ppm). Moreover, in the aliphatic region, methylene (δ_H = 2.43 ppm) and methyl proton (δ_H = 1.12 ppm) resonances at the integral ratio of 6:2 were observed.

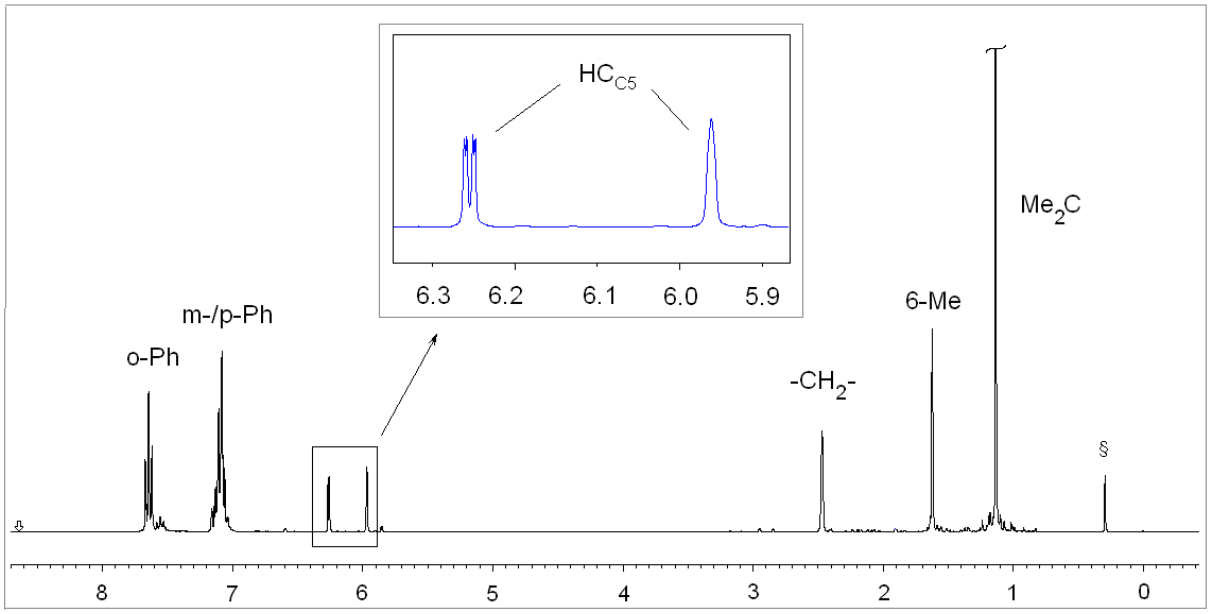

Figure 2. The ^{1}H NMR spectrum (300.1 MHz) of compound **F2** dissolved in C_6D_6 at +25°C. The resonance denoted with (§) is assigned to the silicon grease.

Mass spectrometry reveals the molecular peak of 330 and indicates the formation of the double condensation product.

The molecular composition of the fulvenyl-phosphane (**F2**) was determined by ^{13}C, ^{31}P and 2D HMQC NMR spectroscopy as well as elemental analysis. As a result of the analyses the formation of a compound with a bicyclic-[3,3,0]-moiety (Scheme 8) was proposed.

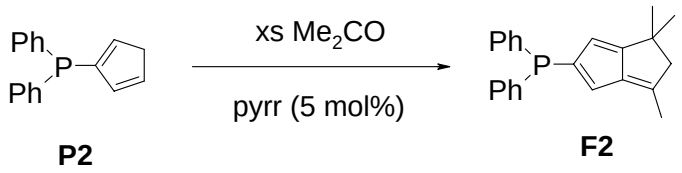

P2 **F2**

Scheme 8. Pyrrolidine (pyrr) catalyzed reaction of **P2** with excess of acetone.

There are only few compounds with a similar structural motive known. Generally, the compounds formed unexpectedly in reactions where the product of mono-condensation was expected.[6]

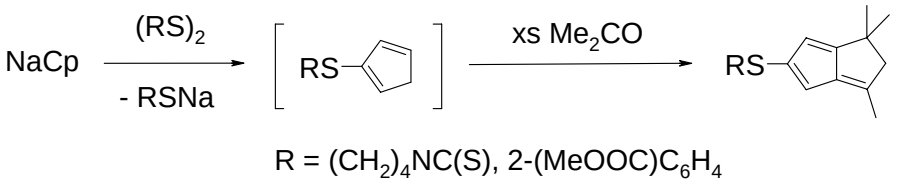

R = $(CH_2)_4NC(S)$, 2-$(MeOOC)C_6H_4$

Scheme 9. Synthesis of sulfur-analogs of compound **F3**.

Another example of unexpected formation of the double condensation product is shown in Scheme 10. With the aim to obtain fused bicyclic-[5,3,0]-system (**D**) in an attempted reaction of cyclopentadiene with phorone was found, that except of desired product another side product (**E**) formed, that was identified as tricyclic-[$6^{2,6}$,5,0]-compound.[7]

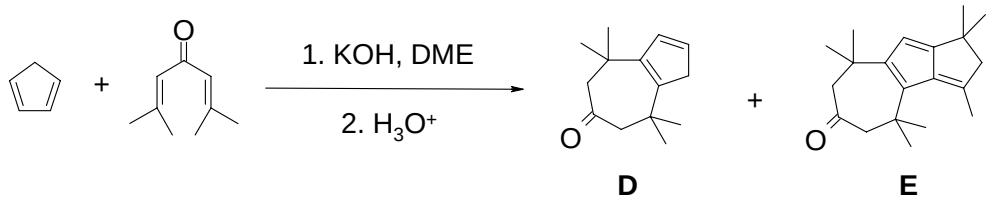

Scheme 10. Different products in reaction of cyclopentadiene with phorone.

▪ ▫ ▪

This simple formation of fulvenyl-phosphane **F2** opens an access towards a new more sterically crowded phosphane ligand system. Compared to (*tert*-Bu)Cp, this new annelated 1,1,3,3-tetramethylcyclopentyl-cyclopentadiene (Cp^{TM}) is higher both by its steric hindrance and symmetry. Because of these reasons it was decided to study this attractive ligand system in more detail (Scheme 11). Moreover, with the Ph_2P-group it possesses a great potential for further application in the synthesis of the *CpPN*-ligand systems and generally for the organometallic chemistry.

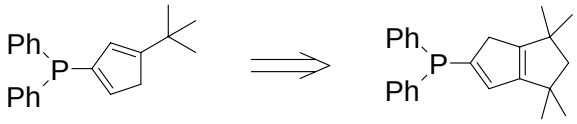

Scheme 11. The initial and aspired target compound.

2.3. *Mechanistic Aspects of Formation of Fulvenyl-Phosphane (**F2**)*

Whereas the first step of condensation of a carbonyl compound with cyclopentadienes is well known and widely investigated for fulvene synthesis,[2,8] the mechanism of the second step of condensation is not obvious. Annelated, unsaturated bicyclic-[3,3,0]-systems were commonly reported for hydrocarbons.[9] They were generally synthesized by reaction of *α,β*-unsaturated carbonyl compounds with cyclopentadienes under basic reaction conditions. The reaction pathways depend largely on the nature of the *α,β*-unsaturated carbonyl component.

There are two possible pathways: stepwise addition of acetone with the final cyclization into bicyclic-[3,3,0]-system and the addition of diacetone or mesityloxide, formed by the base catalyzed self-condensation of acetone molecules, to the C5-ring of the phosphane **P2**.

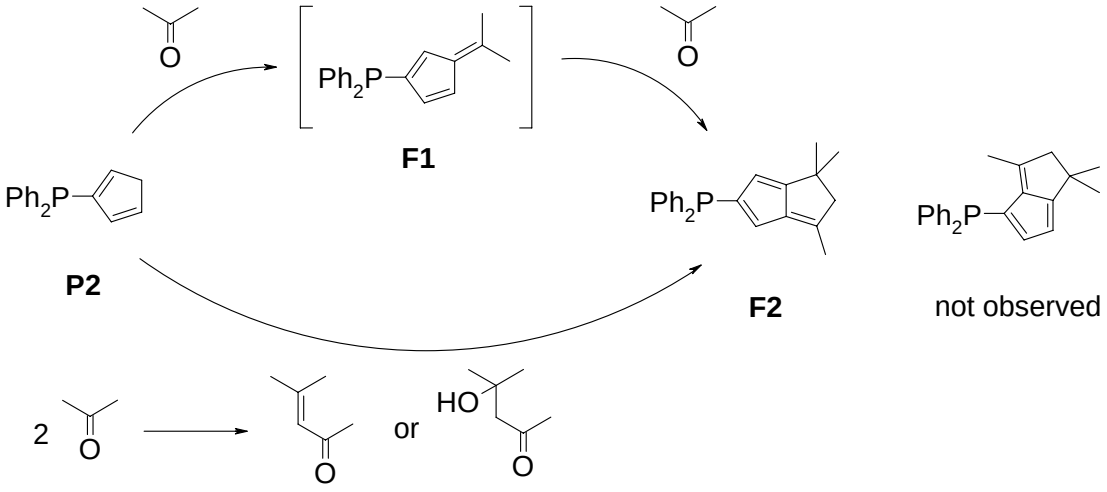

Scheme 12. Two amenable reaction pathways towards the formation of compound **F2**.

It was found that the reaction of the previously isolated fulvenyl-phosphane **F1** with further molecule Me_2CO into **F2** is very selective and proceeds without formation of intermediates that could be observed by ^{31}P and ^{1}H NMR spectroscopy. This is an indirect proof that the mechanism does not proceed *via* addition of diacetone or mesityloxide. Thus, an NMR scale condensation reaction of fulvenyl-phosphane **F1** in acetone-d_6 as solvent and reagent was performed. The reaction was also catalyzed by pyrrolidine (5 mol%). The analysis of ^{1}H NMR spectrum clearly shows the presence of only $\underline{Me_2}C$-group resonance in the aliphatic region and olefinic HC_{C5}-resonances at the integral ratio of 6:2. Bridging methylene and methyl group resonances at the 6-position have not been observed in the ^{1}H NMR spectrum. Thus, the 2nd condensation step includes an attack of pyrrolidine-enamine of

deuterated acetone at the 6-position of fulvenyl-phosphane (Scheme 13), followed by intramolecular cyclization and pyrrolidine elimination.

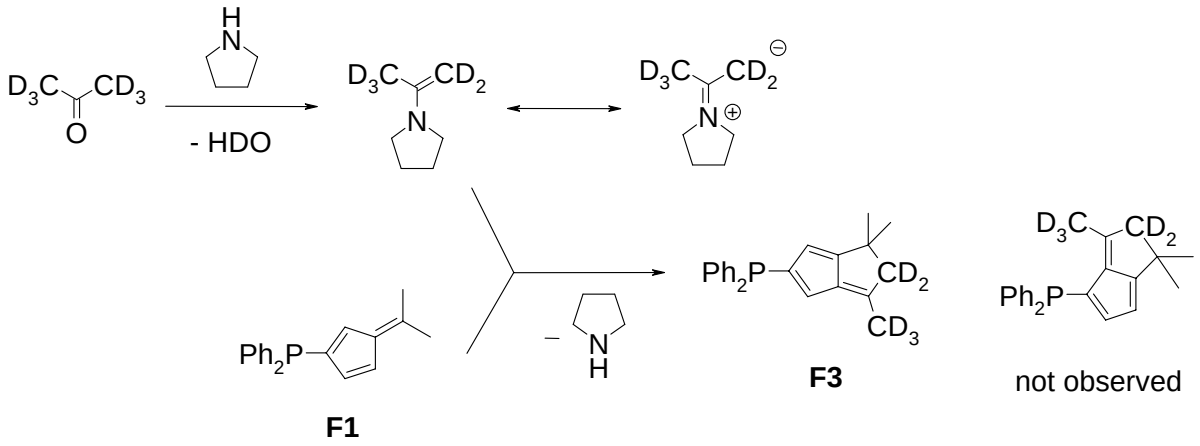

Scheme 13. The reaction compound **F1** with acetone-d_6 leading to the formation of the partly deuterated fulvenyl-phosphane **F3**.

Despite two possible condensation products amenable, according to the ^{1}H NMR spectroscopy, that confirms the absence of the three bond H–H scalar coupling of neighboring H_{C5}-atoms, only one isomer forms. The formation of the other isomer is disfavored by high steric repulsion within the transition state.

Mass spectrometry of the partly deuterated **F3** gave the expected molecular peak of 335.

2.4. *Synthesis of Cyclopentadienyl-Phosphane $Ph_2PCp^{TM}H$ (**P6**)*

To obtain the desired cyclopentadienyl-phosphane $Ph_2PCp^{TM}H$ (**P6**) a carbometallation of fulvenyl-phosphane **F3** with MeLi was studied in various solvents: THF, ether and hexane.

The ^{31}P NMR spectrum of the reaction mixture, immediately after the addition of MeLi to a THF-solution of **F2**, reveals complete consumption of the starting **F2** accompanied by appearance of a new signal (δ_P(THF) = 17.3 ppm). However, the following aqueous work-up leads to a recovery of the starting phosphane **F2** in 85% yield. No formation of other products was detected. This result suggests that in THF a deprotonation of Me-group on the side chain of the fulvene **F2** rather than its carbometallation takes place (Scheme 14).

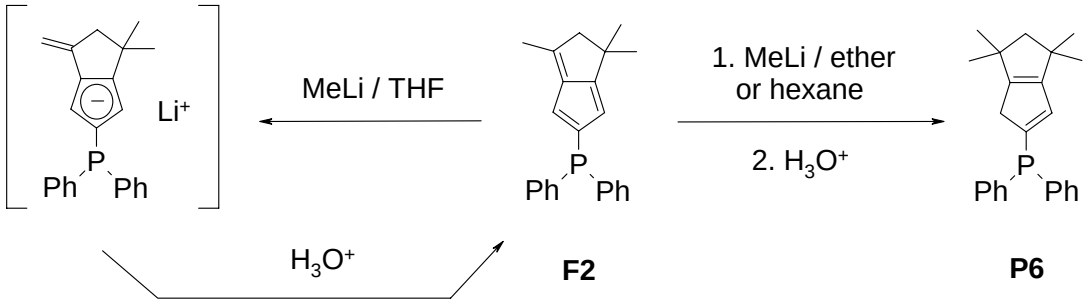

Scheme 14. The reaction of **F2** with MeLi/ether in solvents of different polarity.

When the same reaction is conducted in less polar solvents such as ether or hexane, the quenching of the reaction mixture released an almost colorless product of successful carbometallation of **F2**. The formulation of the cyclopentadienyl-phosphane $Ph_2PCp^{TM}H$ (**P6**) was confirmed by multinuclear NMR, mass spectrometry as well as elemental analysis.

The isolated yield of **P6** varies in a range of 73 – 92%, depending on the solvent used. Higher yields of **P6** were obtained when the methylation was performed in hexane. The purification of **P6** was performed by preparative flash-chromatography under unaerobic conditions (~ 0.15M solution of **P6**; eluent: ether:hexane = 1:2 (v/v)). In a solid state, **P6** comprises a pale yellow, needle-like microcrystalline material with a faint phosphine-like odor. It is fairly air-stable in the solid state and can be handled under air atmosphere for days without noticeable decomposition, but its solutions oxidize rather easily. Thus, storing of **P6** under inert atmosphere is recommended. Its solubility in common organic solvents is very high that makes its crystallization either from less polar hexane at < -30°C or from higher polar CH_3CN and low alcohols (MeOH, EtOH) rather problematic and accompanied by the considerable loss of the material. The highest purity colorless material was obtained by

crystallization from tetramethylsilane (TMS) at -30°C. The precisely determined melting point of **P6** was in a narrow range of 109.0–109.3°C.

In contrast to the closely related Ph_2PIndH and the starting phosphane **P2** ^{31}P NMR spectroscopy of **P6** reveals one single resonance at δ_P = -13.6 ppm. The chemical shift indicates coordination of the phosphorus atom to the sp^2-hybridized *ipso*-C atom of the C5-ring. This value is in a good agreement with those, known for diphenyl(alkenyl)phosphanes $Ph_2PCH{=}CH_2$ (δ_P = -11.7 ppm) and *trans*-$Ph_2PCH{=}C(H)Me$ (δ_P = -14.2 ppm).

In comparison to the parent fulvene **F2**, the ^1H NMR spectrum of **P6** shows only one resonance in the olefinic region at 6.76 ppm (dt, $^3J_{HP}$ = 5.1 Hz, $^4J_{HH}$ = 1.5 Hz, 1H) and an additional triplet of allylic CH_2-group of the C5-ring at 2.88 ppm (t, $^4J_{HH}$ = 1.5 Hz, 2H). In the aliphatic region there are two sharp resonances of the Me-group at 1.05 and 1.12 ppm, and one of the bridging CH_2-group at 1.95 ppm at their integral ratio of 6:6:2.

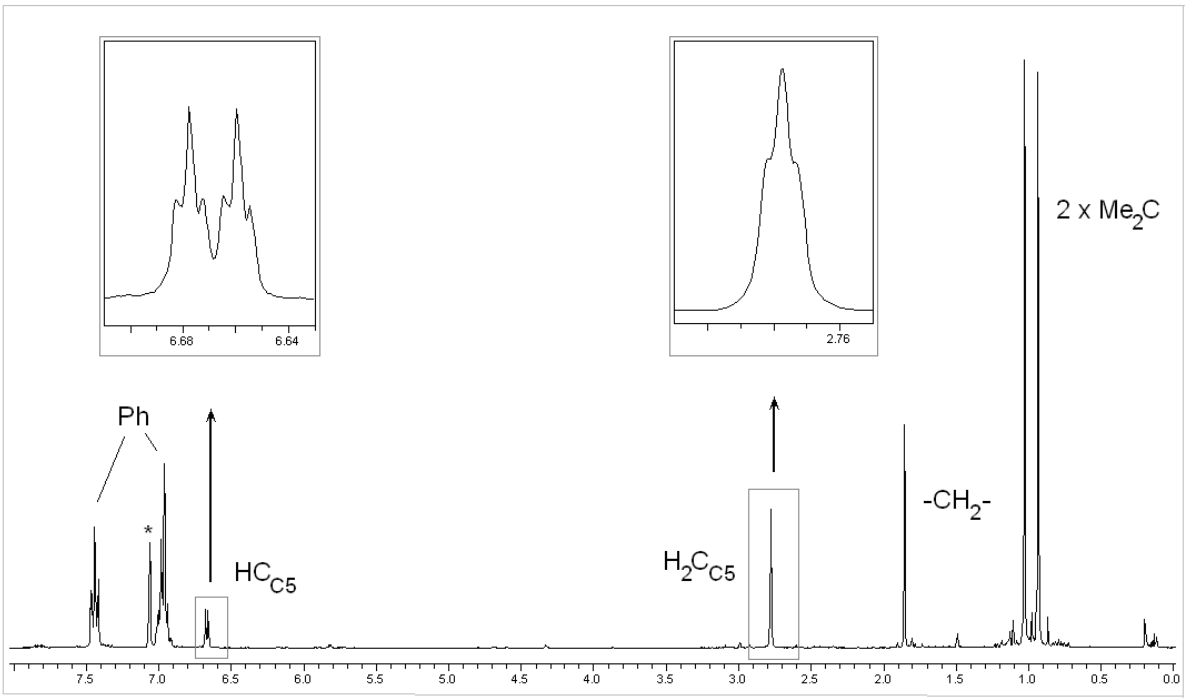

Figure 3. The ^1H NMR spectrum (300.1 MHz) of compound **P6** dissolved in C_6D_6 at +25°C. The resonance denoted with (*) is assigned to the residual protons of C_6D_6.

Of three possible isomers (**P6a** – **P6c**, Scheme 15), only one of them can deliver such pattern. The reason for an absolute predominance of the isomer **P6a** in the contrast to the parent **P2** isomers has to be reduction of the ring-strain of the annelated aliphatic C5-ring.

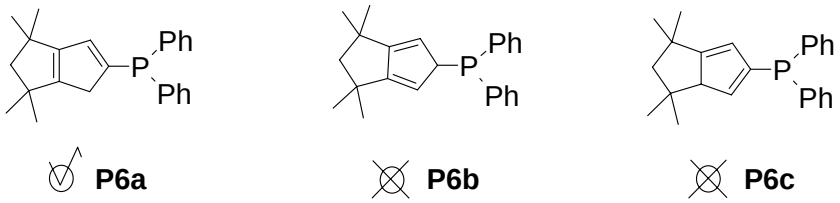

Scheme 15. Structures of the three possible isomers of the compound **P6**.

The complete assignment of the ^{13}C NMR resonances was achieved by 2D HMQC spectroscopy.

Crystals of the compound **P6**, suitable for X-ray diffraction analysis, were obtained by slow cooling of its hot concentrated ethanol solution. It crystallizes in the monoclinic space group $P2_1/c$ with four molecules per cell unit. In the structure the bridging H_2C-group of the aliphatic ring is disordered with occupancies of 0.49/0.51; only one position is shown in Figure 4.

As expected, the phosphorus atom is three-fold coordinated by two phenyl groups and a $Cp^{TM}H$-moiety – all are twisted in a propeller like arrangement. The unsaturated C5-ring is essentially planar. The maximal deviation from the C5-ring plane of 0.002(2) Å was found at the C8 atom. The C4 and C6 atoms of the aliphatic ring deviate only by values of 0.053 and

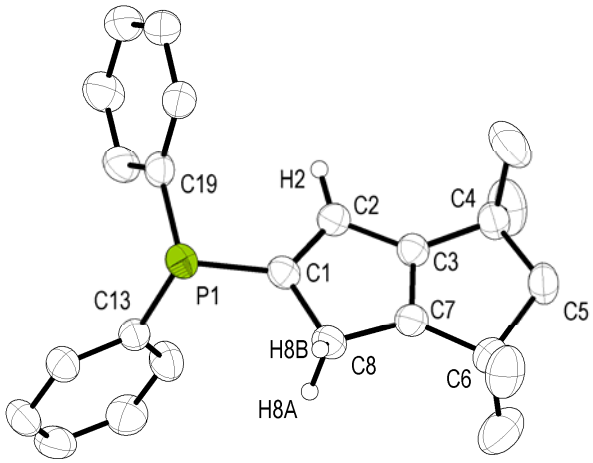

Figure 4. Molecular structure of compound **P6**. All hydrogen atoms, except of the ones at the unsaturated C5-ring, have been omitted for clarity. Selected bond lengths (Å) and angles (°): P1–C1 1.807(2), P1–C13 1.832(2), P1–C19 1.833(2), C1–C2 1.348(2), C2–C3 1.475(2), C3–C7 1.334(2), C7–C8 1.487(2), C1–C8 1.517(2); C1–P1–C13 103.1(1), C13–P1–C19 102.3(1), C19–P1–C1 100.7(1), C1–C8–C7 102.7(1), C3–C2–C1–C8 0.2(2), C2–C3–C7–C8 0.2(2).

0.073(2) Å from the $Cp^{TM}H$-ring plane. Both *ipso*-C_{Ph}–P bond lengths (av. 1.832(3) Å) have essentially the same values as in Ph_3P (av. 1.828 Å).[10] However, the P–C_{C5} bond length is slightly shorter (1.807(2) Å). The olefinic C1–C2 and C3–C7 bonds are significantly shorter (1.348(2) and 1.334(2)Å resp.) then other ones in the Cp-ring (C2–C3 1.475(2), C7–C8 1.487(2), C1–C8 1.517(2)Å). All C–P–C angles (100.7(1), 102.3(1) and 103.1(1) Å) lies in the typical range reported for triarylphosphanes.[11]

To the best of our knowledge, $Ph_2PCp^{TM}H$ (**P6**) is the first crystallographically characterized cyclopentadienyl-phosphane.

2.5. *Synthesis of Chalcogenides $Ph_2P(X)Cp^{TM}H$ (X = O (**S4**), S (**S5**), Se (**S6**))*

Further, the oxidation of **P6** to its chalcogenide derivatives was studied. Earlier *Mattey* and *Lampin* described the tendency of the unsubstituted $Ph_2P(X)C_5H_5$ (X = O, S) to dimerize in the *Diels-Alder* reaction manner.[5] On the contrary, it is not the case for the sterically hindered phosphane **P6**.

The oxidation of phosphane **P6** was performed by H_2O_2 (30% solution in water) in THF, elemental sulfur in toluene and red selenium in $CHCl_3$. The corresponding phosphine chalcogenides were obtained in high yields (72 – 96%).

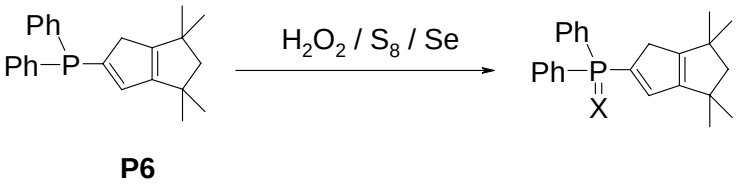

P6

Yields:

X = O (**S4**), 89%
S (**S5**), 72%
Se (**S6**). 96%

Scheme 16. Oxidation of **P6** into phosphine chalcogenides.

All chalcogenide compounds appear as crystalline, air-stable solids. Whereas the compounds **S4** and **S6** are colorless, the sulfide **S5** is a yellow solid. The melting point of the phosphine oxide **S4** (162.9 – 163.3°C) is significantly higher that of **P6** (108 – 109°C), that is typical for phosphanes. For example, the melting points of Ph_3PO and (*tert*-Bu)$_3$PO (150 – 157 and 77°C resp.)[12] are significantly higher those ones of the parent phosphanes: Ph_3P and (*tert*-Bu)$_3$P (79 – 81 and 30°C resp.).[13] The melting points of **S5** and **S6** are lower than those of **S4** (134.4 – 134.7 and 147.7 – 148.0°C resp.).

Selected physicochemical properties and ^{1}H and ^{31}P NMR spectroscopic data for phosphine chalcogenides **S4** – **S6** are given in the Table 1. The NMR spectra of all three chalcogenides are very similar and are consistent with their formulations.

Table 1. Physicochemical properties and selected ^{1}H and ^{31}P NMR spectroscopic data for phosphine chalcogenides $Ph_2P(X)Cp^{TM}H$ (**S4** – **S6**) and the phosphane **P4**.

	P4	**S4** (X = O)	**S5** (X = S)	**S6** (X = Se)
appearance	pale-yellow	colorless	yellow	colorless
m.p., °C	109.0 – 109.3	162.9 – 163.3	134.4 – 134.7	147.7 –148.0
^{1}H NMR, ppm				
H_2C_{C5}	2.89	3.10	3.19	3.25
HC_{C5} ($^{3}J_{HP}$, Hz)	7.76 (5.4)	6.95 (8.7)	6.94 (9.5)	6.94 (9.8)
$^{31}P\{^{1}H\}$ NMR, ppm	-14.5	18.1	31.4	22.3[a)]

a) The one-bond P–Se scalar coupling constant is of 710 Hz.

The ^{1}H and ^{31}P NMR studies of compounds **S4** – **S6** confirm that there is no equilibrium between the amenable cyclopentadienylidene- and *P*-cyclopentadienyl-forms in solutions (Scheme 17).

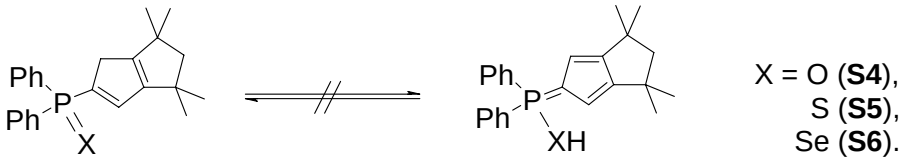

Scheme 17.

The σ-donating property of phosphanes is routinely estimated by the ^{77}Se NMR spectroscopy of their selenides. The chemical shift (δ_{Se}) and the one-bond coupling constant ($^{1}J_{SeP}$) strongly depends on the constitution and electronic properties of the substituents at the phosphorus atom.[14]

The ^{77}Se NMR spectrum of the phosphine selenide **S6** reveals a doublet at δ_{Se} = -260.8 ppm with the one-bond scalar coupling ($^{1}J_{SeP}$) of 741 Hz. These characteristics are very close to those of Ph_3PSe ($^{1}J_{SeP}$ = 735 Hz).[15] The best comparison can be made with the slightly donating 2-thienyl-substituted diphenylphosphine selenide $Ph_2P(Se)(2\text{-}C_4H_3S)$ with $^{1}J_{SeP}$ = 743 Hz.[37]

2.6. *Reactions with Organic Azides*

The most interesting study was the reactions of the phosphane **P6** with organic azides. Four organic azides differing by constitution and reactivity have been studied: AdN_3, $DipN_3$, *tert*-BuN_3 and Me_3SiN_3.

As it was previously shown (*cf.* Chapter III, part 2.3.), among this series of azides the aromatic $DipN_3$ is the most reactive one in the *Staudinger* reaction. Indeed, the reaction between the phosphane **P6** and $DipN_3$ was complete within 14 h at room temperature and gave **L10** in 78% of isolated yield after crystallization from cold MeCN. Compound **L10** was found to be highly soluble also in hexane.

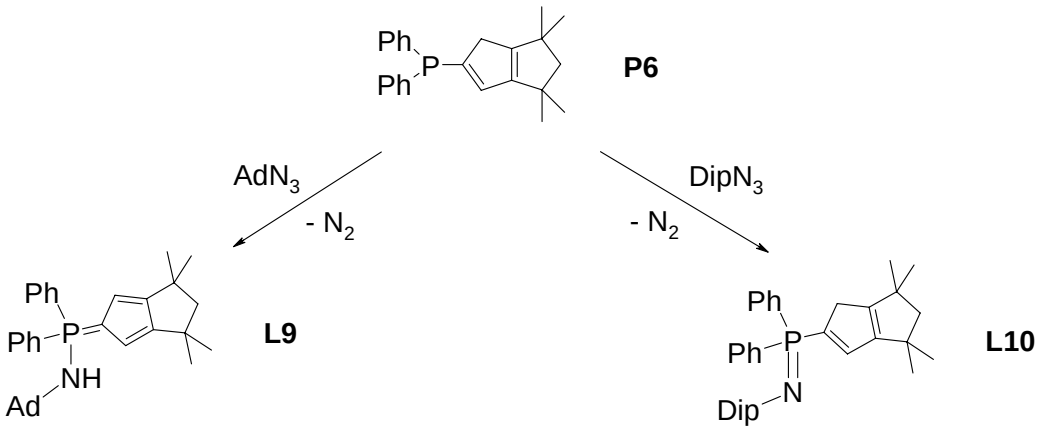

Scheme 18. The synthesis of compounds **L9** and **L10** by the *Staudinger* reaction of phosphane **P6** with AdN_3 and $DipN_3$.

Contrastingly, the *Staudinger* reaction of **P6** with of AdN_3 (1.10 equiv) proceeds unexpectedly slowly and yields **L9** after 10 d in refluxing THF in only 46% isolated yield (Table 2). Further, it was found that the reaction is highly facilitated by heating. The reaction was complete after 1 – 2 d at reflux temperature (toluene, 110°C) and the compound **L9** was isolated in 75% yield.[40]

For a better understanding of the decreased reactivity, a model reaction of Ph_3P with AdN_3 was studied.[16] We found, the reaction to be reversible and leading only to the *Staudinger* adduct Ph_3P=N–N=NAd, also known as phosphazide (δ_P values of those are usually 10 – 20 ppm upfield shifted). As was shown by ^{31}P NMR monitoring of the reaction mixture, no formation of the desired iminophosphorane product Ph_3P=NAd was detected – even after 72 h heating under reflux (THF, 65°C). Moreover, the equilibrium between Ph_3P and phosphazide is temperature dependent (^{31}P NMR integral ratio [phosphazide]/Ph_3P = 0.73 (65°C) and 0.33 (25°C)).

The formation of compound **L9** was monitored by ^{31}P NMR spectroscopy. The phosphane **P6** (δ_P = -14.6 ppm) forms, in the first place, an intermediate phosphazide (δ_P = -29.1 ppm) that slowly decomposes with N_2-evolution to form **L9** (δ_P = 17.0 ppm). A similar behavior is known for the phosphazides of the Ar_3PN_3Ar' type: usually the first reaction step of their formation was found to be reversible.[17] We observed that equilibrium is achieved after 2 d (THF, reflux, 60°C) when the integral ratio of [phosphazide]/**P6** remains constant (K = 0.77). This undoubtedly confirms that the phosphazide decomposition is the rate-determining step in this particular case. Similar observations were earlier reported for Ph_3PN_3R with sterically demanding and/or electron withdrawing/donating groups (for R = *n*-Bu, dec. 106 – 108°C;[18a] R = 2,4,6-$(NO_2)_3C_6H_2$ dec. 131°C;[18b]) and for $(Me_2N)_3P{=}N{-}N{=}NMe$, dec. r.t.[18c]

Acceleration of the *Staudinger* reaction by addition of *Lewis* acids is though well documented, but rarely applied protocol. It was shown that the catalysis with 5 mol% $AlCl_3$ under the same conditions shortens the reaction time by 50% (Table 2). Although the conversions after 3 h in the catalyzed and uncatalyzed reactions are almost the same (ca. 70%), the uncatalyzed reaction needs 10 d at reflux temperature to proceed the reaction.

Table 2. The ^{31}P NMR spectroscopic monitoring (THF) of the reaction proceeding between P6 and AdN_3 (1.10 equiv) in THF (0.12M) at 60°C (uncatalyzed (left) and catalyzed with 5 mol% $AlCl_3$ (right)).

Reaction duration, d	Product formation, %	Reaction duration, d	Product formation, %
1	26	1	41
3	55	4	73
4	71	5	93
5	80		
8	88		
10	92		

Compared to **L10**, which is a highly air-sensitive substance with melting point of 142.4 – 143.0°C and a high solubility in hexane, compound **L9** is only moderately air-sensitive, has a considerably higher melting point (176.5 – 177.0°C) and shows a very low solubility in hexane. Further investigations by means of NMR spectroscopy and single crystal X-ray diffraction analysis reveal that the compound **L9** occurs in the *P*-amino-cyclopentadienyl-phosphorane form, while compound **L10** exists in the other tautomeric form *P*-cyclopentadienyl-iminophosphorane. No tautomerization or isomerization for both **L9** and **L10** could be observed by the multinuclear NMR spectroscopy.

The reaction of **P6** with the least reactive Me_3SiN_3 was found to be extremely slow. This reaction does not proceed to completeness even with 3 equiv of the azide (0.1M solution in

THF, reflux, 5 d). The formation of the *N*-trimethylsilyl-iminophosphorane **L8** was approved by a monitoring of the reaction mixture only by ^{31}P NMR spectroscopy (Figure 5).

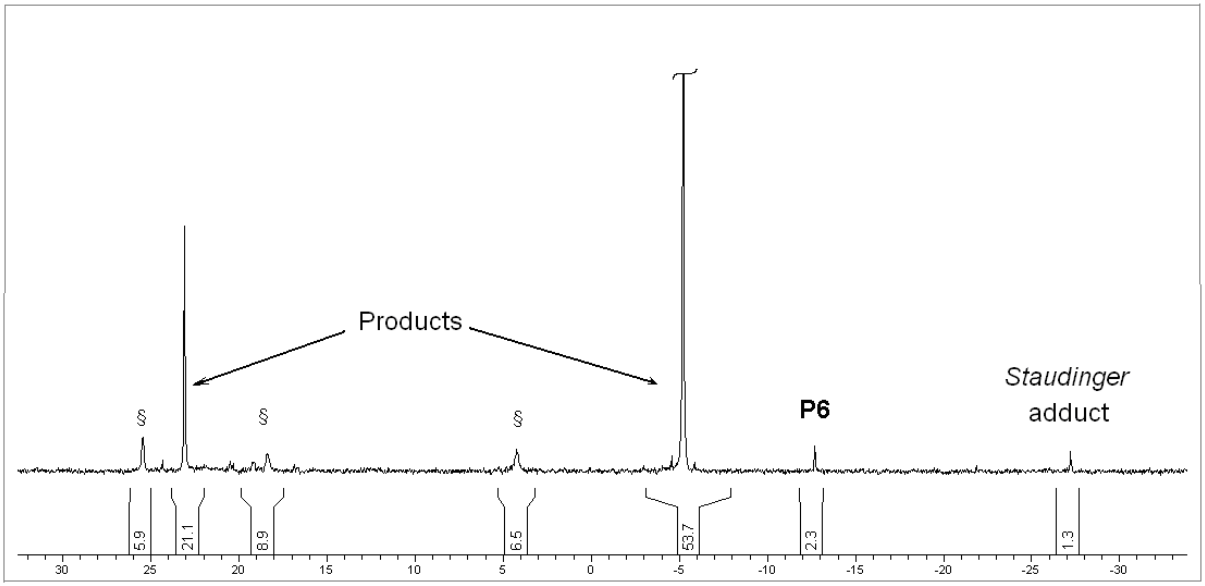

Figure 5. The ^{31}P NMR spectrum (81.0 MHz) of the crude reaction mixture from reaction of **P6** with Me_3SiN_3 in THF. The resonances denoted with (§) are assigned to unidentified impurities.

When reaction is conducted in Me_3SiN_3 as a solvent (1.0M solution, ca. 7.5 equiv of the reagent) at the reflux temperature (ca. 100°C) it results in dissolution of the phosphane **P6** and formation of the pale green solution accompanied by a moderate N_2 evolution. The ^{31}P NMR monitoring the reaction mixture after 14 h of heating reveals absence of both starting **P6** and its *Staudinger*-adduct. Two new signals were observed at ca. -5 and 23 ppm. The main resonance appears in the characteristic *P*-iminophosphorane region and belongs to the target *N*-trimethylsilyl derivative **L8**. The minor signal, observed at ca. 23 ppm, appears in the characteristic *P*-aminophosphorane region. The feasible *P*-aminophosphorane in this reaction system can be the corresponding tautomeric form of the phosphazide. The formation of free *P*-aminophosphorane $Ph_2P(Cp^{TM})NH_2$ is not exclueded (Scheme 19). The *P*-aminophosphoranes are known to be less soluble in hexane, therefore, extraction the reaction mixture with hexane was used to purify the main product **L8**. After solvent removal a pale brown microcrystalline solid was obtained. The routine analyses confirm the formation of the desired *N*-silylated iminophosphorane **L8** that comprises highly air-sensitive, comparatively low-melting crystalline solid (94.5 – 94.7°C).

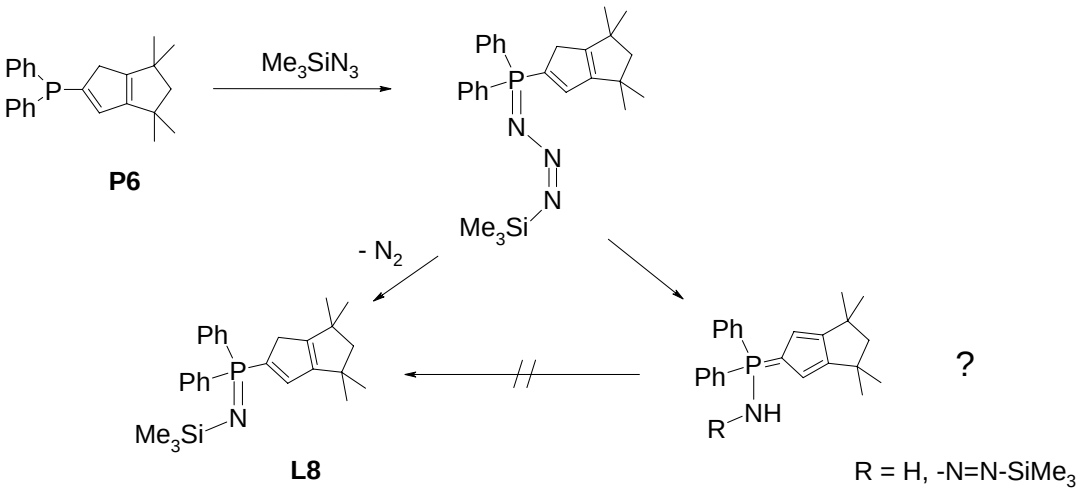

Scheme 19. The synthesis of compounds **L8** by the *Staudinger* reaction of phosphane **P6** with Me_3SiN_3.

Unexpectedly, it was found that Me_3Si-substituated *P*-iminophosphorane **L8** is easily subjected to hydrolysis that proceeds in two steps and gives, depending on the reaction conditions, two decomposition compounds. The first step of hydrolysis furnishes, after tautomerization, *N*-unsubstituted *P*-amino-cyclopentadienyliden-phosphorane **L11** (Scheme 20). The further hydrolysis of **L11** by air moisture causes the P–C bond degradation and results in release of the free $Cp^{TM}H$ ligand and precipitation of a crystalline solid, which was identified as diphenylphosphinic acid amide $Ph_2P(O)NH_2$.[38]

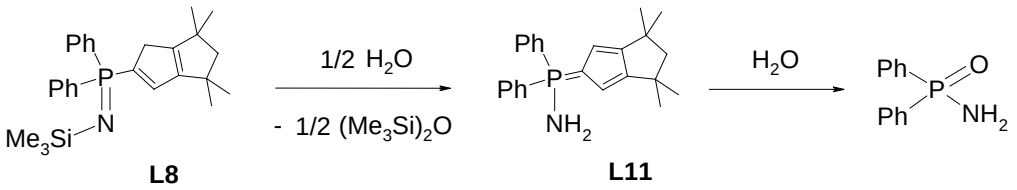

Scheme 20. Two-step hydrolysis of **L8** to **L11** and further to $Ph_2P(O)NH_2$.

The compound **L11** was isolated as a gray, microcrystalline solid, which has the highest melting point (172.0 – 173.5°C) in the whole series of the investigated *P*-aminophosphoranes (**L3** – **L5, L8**) and comparable with those of **L9**. The compound shows high solubility in aromatic solvents and THF; it is only slightly soluble in ether.

Earlier we found, that in the *Staudinger* reaction of the Ph_2PCp with *tert*-BuN_3, the latter served as a NH-synthon (*cf.* Chapter III, part 2.3.). Therefore it was attempted to obtain *N*-unsubstituted compound **L11** by the similar reaction principle. However, unlike the reaction with AdN_3, it proceeds already at ambient temperature yielding a yellow, microcrystalline solid that was isolated by crystallization from MeCN in moderate yield of 35%. Upon

characterization of this compound by multinuclear NMR spectroscopy and mass spectrometry we were surprised that the reaction product represents the regular product of the *Staudinger* reaction **L12** rather than expected *N*-unsubstituted *P*-aminophosphorane **L11**. The reason, why in this particular case no elimination of isobutene takes place, was not further studied.

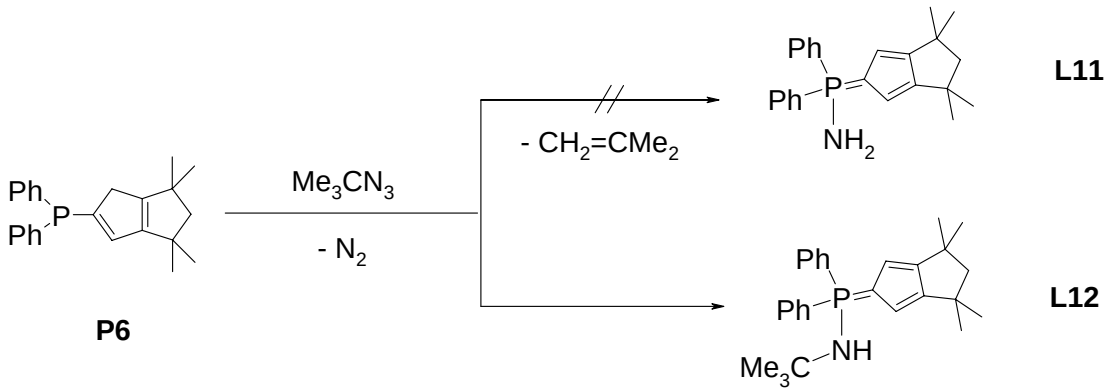

Scheme 21. The *Staudinger* reaction of phosphine **P6** with *tert*-BuN_3.

*2.7. NMR Spectroscopic Characterization of Compounds **L9** – **L12***

The ^{1}H NMR spectrum of compound **L9** is depicted in Figure 6. In the aliphatic region, apart of the adamantyl group multiplets, one doublet ($^2J_{HP}$= 5.0 Hz) and two singlets were assigned to the NH-group, methylene and four methyl groups respectively. The highly upfield shifted NH-group proton resonance indicates on its low acidity.

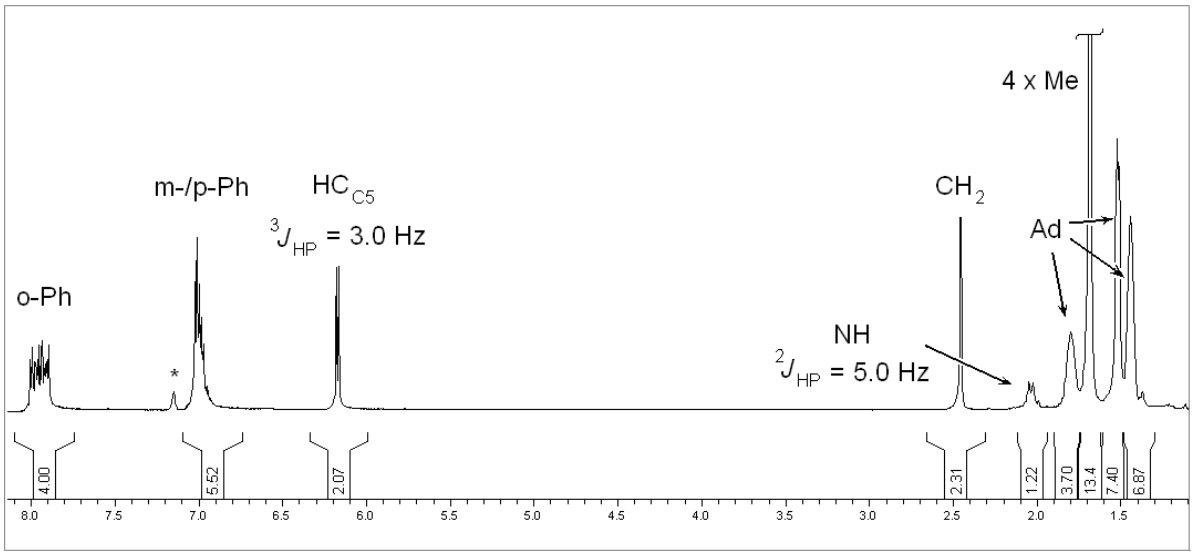

Figure 6. The ^{1}H NMR spectrum (300.1 MHz) of compound **L9** dissolved in C_6D_6 at +25°C. The resonance denoted with (*) is assigned to the residual protons of C_6D_6.

The original position of NH-proton in **L9** was established by the HMQC spectroscopy – the resonance at 2.04 ppm does not correlate with any carbon atom in the molecule.

Essentially similar spectrum was obtained for compound **L12**, where instead of the three resonances of the Ad-group one sharp resonance of the *tert*-Bu group protons appears at 0.90 ppm. The resonance of the NH-group appears also as an upfield shifted doublet ($^2J_{HP}$ = 5.1 Hz) at 2.06 ppm.

Unlike **L9** compound **L10** shows in the aliphatic region, besides of resonances of *iso*-Pr protons at 1.18 and 3.66 ($^3J_{HH}$ = 7.0 Hz), four resonances at 1.00, 1.03, 1.91 and 3.08 ($^4J_{HH}$ = 1.5 Hz). This pattern is very similar to that one of the parent phosphane **P6**. This finding confirms its appearance in solution in the iminophosphorane form. In the aromatic region well resolved resonances assigned to the Dip- and Ph-groups, together with one C5-ring proton are observed. The latter resonance appears as a doublet of triplets ($^4J_{HH}$ = 1.5 Hz, $^3J_{HP}$ = 3.4 Hz) also confirming an existence of the iminophosphorane motif.

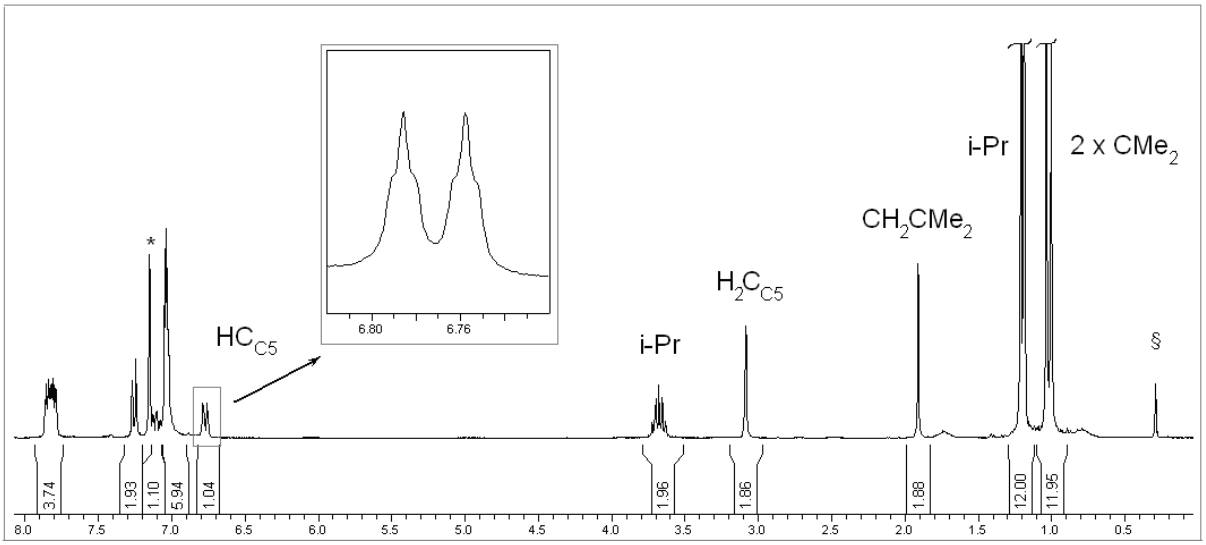

Figure 7. The ^{1}H NMR spectrum (300.1 MHz) of compounds **L10** dissolved in C_6D_6 at +25°C. The resonances denoted with (*) and (§) are assigned to the residual protons of C_6D_6 and silicon grease respectively.

The ^{1}H NMR spectrum of compound **L11** is the simplest one. In its aliphatic region there are two sharp resonances (1.66, 2.42 ppm), which can be undoubtedly assigned to two $\underline{Me}_2$C- and CH_2-groups, as well as a broad resonance (2.10 ppm), assigned to the NH_2-group protons, at the integral ratio of 12:2:2. In the aromatic region, apart of typical pattern of phenyl group, a doublet ($^3J_{HP}$ = 3.4 Hz), assigned to the protons of the C5-ring, at the integral ratio of 2 was observed. In the ^{31}P NMR spectrum, compound **L11** shows <u>one</u> downfield shifted resonance at 22.1 ppm. This value is in a good agreement with those of **L9** and *P*-aminophosphorane **L3** $Ph_2P(C_5H_4)NHAd$ both existing in the *P*-aminophosphorane form.

The ^{31}P NMR resonances of **L9** and of **L12** (17.8 and 17.1 ppm respectively) appears essentially at the same δ_P as those ones of *CpPN*-ligands **L4** $Me_2P(C_5Me_4)NHAd$ (17.6 ppm) and **L8** $Ph_2P(C_5Me_4)NHAd$ (17.8 ppm) (*cf.* Chapter III, part 2.4.3.1.).

Thus it can postulate that the steric demand and the basicity of phosphane **P6** are comparable with those of the phosphane $Me_2PC_5Me_4H$ (**P3**).

Contrastingly to $Me_2P(NSiMe_3)(C_5Me_4H)$ **L1** and $Me_2P(NDip)(C_5Me_4H)$ **L7**, the corresponding *P*-iminophosphorane derivatives **L10** and **L8** show single sharp resonances at -9.5 and -7.8 ppm respectively assuming the absence of any elementotropic and prototropic shifts or tautomeric equilibrium in solution (C_6D_6) at ambient temperature. The chemical shifts of **L10** and **L8** are in good agreement with those reported by *Bouressou et al.* for main vinylic isomers of $Ph_2IndP{=}NPh$ (δ_P = -8.3 ppm) and $Ph_2IndP{=}NDip$ (δ_P = -16.5 ppm).[19]

2.8. *Molecular Structures of Compounds **L9** & **L10***

The compound **L9** crystallizes from benzene with two molecules of solvent molecules per unit cell.[41] Compound **L10** crystallizes without incorporated solvent molecules. Both compounds are monomeric in the solid state and crystallize in the monoclinic crystal system (space groups $P\bar{1}$ and $P2_1/c$ resp.). The molecular structures of compounds **L9** and **L10** are depicted in Figure 9. In the structures of both compounds two phenyl groups and Cp^{TM}-moiety are arranged in typical propeller-like pattern. The C5-rings are essentially planar (Δ_{max} = 0.004(2) and 0.006(2) Å resp.). The selected bond lengths and angles are summarized in Table 2.

In both structures the substituents at the nitrogen atoms occupy *gauche*-conformation between one phenyl ring and Cp^{TM}-moiety with respect to P–N axis (C1–P1–N1–C25 = 37.5(2) and 17.5(2)° resp). It was found that in the structure of **L9** the P–C_{C5} bond length (1.703(2) Å) is the shortest one among the whole series of the cyclopentadienylidene-*P*-aminophosphoranes crystallographically characterized in this work. This value indicates a high conjugation degree of the Cp^{TM}-moiety with the phosphorus atom.

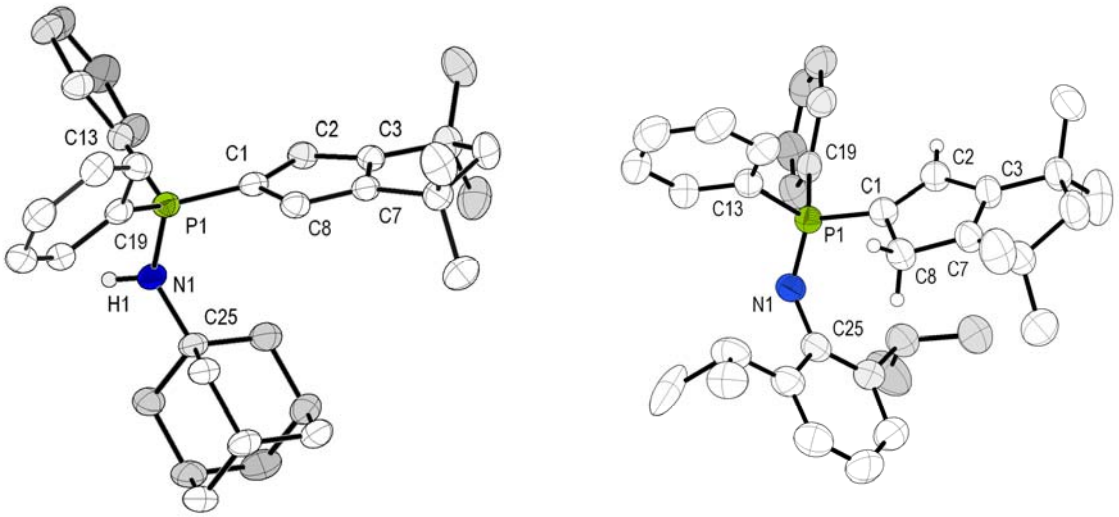

Figure 9. The molecular structures of **L9** × 2 C_6H_6 (left)[41] and **L10** (right). Solvent molecules and hydrogen atoms, except of N–H (left) and of the C5-ring (right), have been omitted for clarity.

The P–N bond length is long (1.653(2) Å) and is in good agreement with those ones found in the structures of compounds **L3** – **L6** (see Chapter III, part 2.4.4.1.). This bond length can also be better compared with those ones found in crystallographically characterized phosphonium salts $[Ph_3P(NMePh)][P,P\text{-}(p\text{-}NO_2C_6H_4)P_2N_2(S)_4]$ (1.643(2) Å)[20] and $[Ph_3PNH(iso\text{-}Pr)]Br$ (1.621(3) Å).[22]

The structure of **L10** is unexceptional with a short P1–N1 bond length of 1.556(2) Å, typical for iminophosphoranes $Ph_3P{=}NMes$ (1.553(2) Å)[21] and $Ph_3P{=}N(tert\text{-}Bu)$ (1.543(2) Å).[22] The alternating order and the bond lengths in the Cp^{TM}-moiety are similar to those found in the parent phosphine $Ph_2PCp^{TM}H$ (**P6**) and lies in ranges typical for cyclopentadiene-compounds.[23] The P1–C1 bond length is significantly larger (1.788(2) Å) than those ones found in the structures of *P*-aminophosphoranes **L3** – **L6** and **L9**. Moreover, this value is much closer to $P–C_{Ph}$ bond lengths having the $C(sp^2)$–P bonding.

Table 2. Selected bond lengths (Å) and angles (°) for **L9** and **L10**.

	L9	**L10**		**L9**	**L10**
P1–N1	1.653(2)	1.556(2)	C1–C2	1.440(3)	1.358(3)
P1–C1	1.703(2)	1.788(2)	C2–C3	1.387(3)	1.462(3)
P1–C13	1.800(2)	1.819(2)	C3–C7	1.407(3)	1.336(3)
P1–C19	1.801(2)	1.806(2)	C7–C8	1.376(3)	1.490(3)
N1–C25	1.496(3)	1.408(2)	C1–C8	1.443(3)	1.512(3)
C1–P1–N1	115.5(1)	115.2(1)			
C19–P1–N1	110.0(1)	110.1(1)	C1–P1–N1–C25	37.5(2)	17.5(2)
C13–P1–N1	102.6(1)	113.2(1)			

2.9. *Synthesis of Ferrocene* ***S7*** *(dppf^{TM})*

There is a great diversity of homo- and hetero-substituted ferrocenes bearing different phosphanyl groups. These bidentate phosphanes are broadly applied as ligands in Pd-catalyzed coupling reactions; therefore, we were attracted by the idea to synthesize the corresponding **P6**-derived ferrocene (**S7**), named in direct analogue with its well-known parent – dppf^{TM} ligand and to study its complexation with Pd(II) halides.

In the first experiment we have attempted to synthesize **S7** using probably too mild conditions reported for synthesis of the simple ferrocene (Scheme 22).[24] The phosphane **P6** was added to a stirred mixture of ferrous chloride and excess of Et_2NH or pyrrolidine in THF. Unfortunately, no reaction took place, even after prolonged reaction times (72 h) at 65°C.

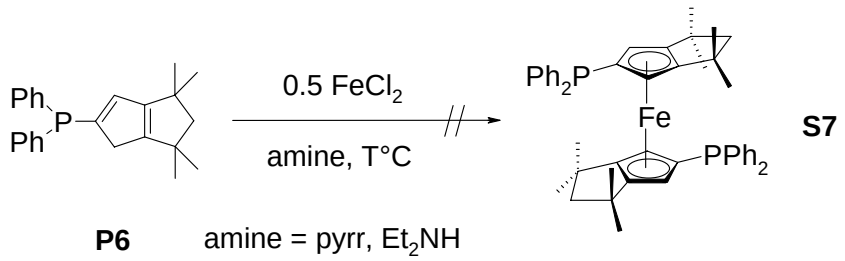

Scheme 22. Attempted reaction of the phosphine **P6** with $FeCl_2$.

Further, a direct transmetallation of the lithiated **P6** by ferrous chloride was performed. This method gave the desired **S7** in 28% isolated yield only (Scheme 23). A possible explanation for such a poor yield might be a partial deprotonation of $Ph_2PCp^{TM}H$ because of its too low kinetic CH-acidity compared to the parent unsubstituted $Ph_2PC_5H_5$ (**P2**).

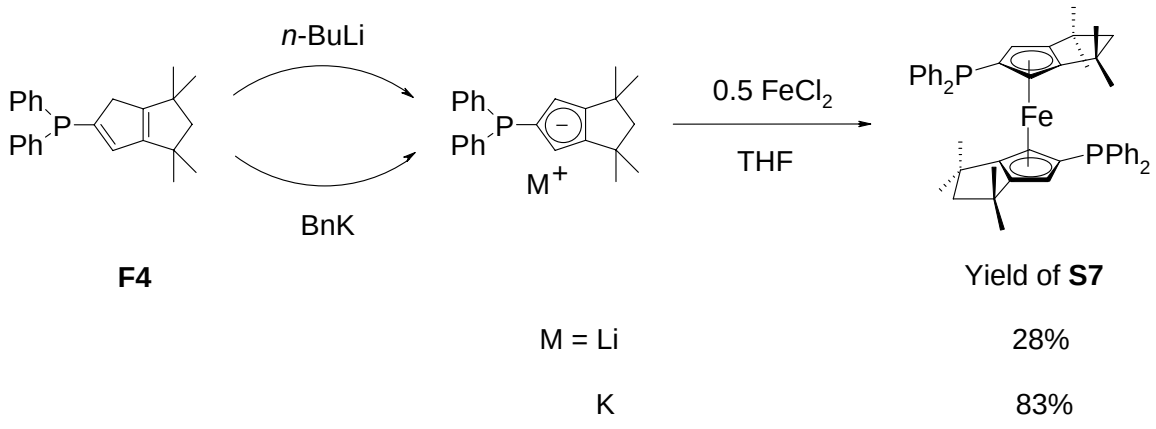

Scheme 23. Dependence of yield of the ferrocene **P6** on the deprotonation conditions (*n*-BuLi, BnK).

Benzylpotassium (BnK) is known to be a stronger base and compared to *n*-BuLi is an advantageous deprotonating reagent. The reaction was performed at 0°C in THF. The drop-wise addition of a deep-red colored THF solution of BnK to the cooled solution of the phosphane **P6** leads to immediate decoloration of the potassium reagent. Subsequent addition of the solid ferrous chloride to thus obtained yellow solution causes instantaneous precipitation of KCl and the reaction mixture turns red. After aqueous work-up the obtained red solid was purified by column chromatography giving an orange, powdery product in 83% of isolated yield. Their formulation was confirmed by microanalysis and NMR spectroscopy.

Thus obtained ferrocene ligand **S7** (dppf^{TM}) comprises an orange, non-volatile, air-stable solid. It crystallizes from MeCN in form of bright-orange crystals with melting point of 180.4°C. The melting point is very close to one of the unsubstituted dppf (183–184°C).[25] The ferrocene dppf^{TM} shows very high solubility in common organic solvents and moderate solubility in high polarity solvents (MeCN, low alcohols).

The ^{31}P NMR spectroscopy (C_6D_6, 300.1 MHz) reveals single upfield shifted resonance at -15.8 ppm (*cf.* unsubstituted dppf:[26] $\delta(CDCl_3)$ = -15.1 ppm). The ^{1}H NMR spectrum is depicted in Figure 10.

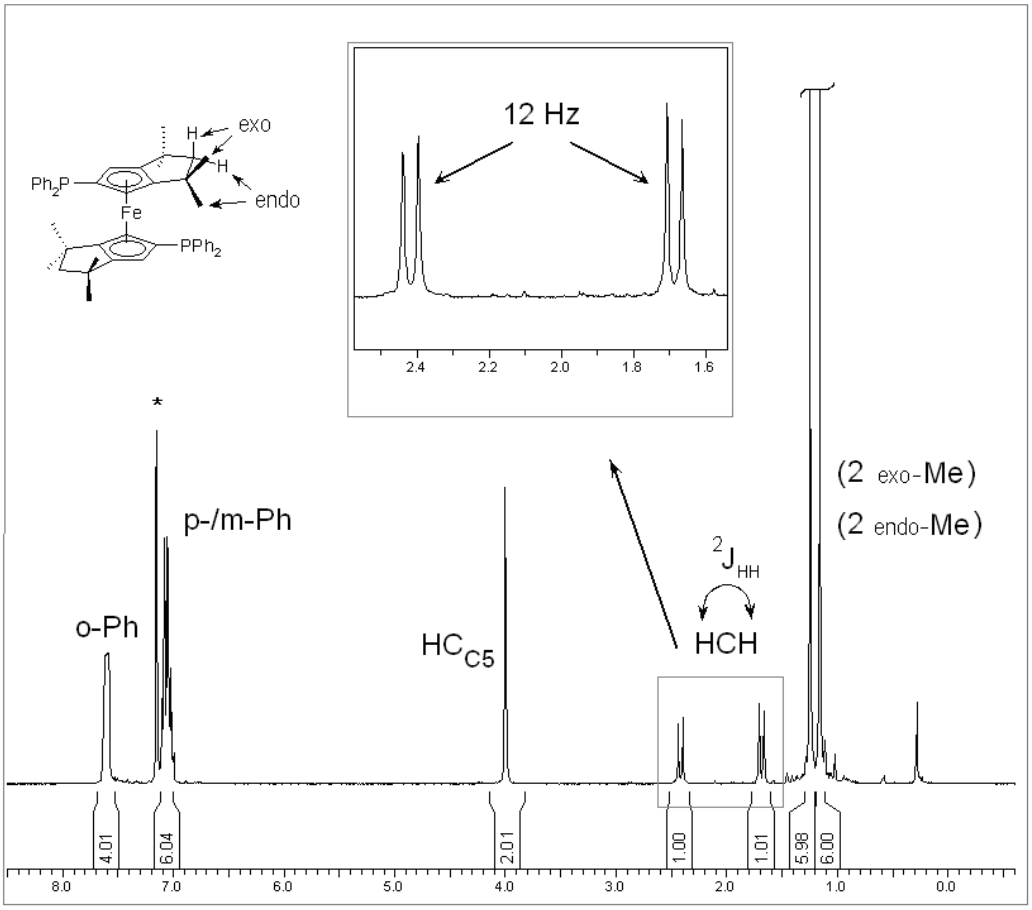

Figure 10. The ^{1}H NMR spectrum (300.1 MHz) of compound **S7** dissolved in C_6D_6 at +25°C. The resonance denoted with (*) is assigned to the residual protons of the C_6D_6.

For the hydrogen atoms at the C5-rings of the ferrocene a very small $^{3}J_{HP}$ coupling constant of ca. 1 Hz was observed. The geminal protons of the aliphatic CH_2-group appear as a AX-pattern ($^{2}J_{HH}$ = 12 Hz) and the diastereotopic methyl groups appear as singlets at 1.16, 1.25 ppm corresponding to their *endo*-/*exo*-positions.

In the aromatic region of the ^{13}C NMR spectrum four resonances of the phenyl groups were observed (Figure 11). The resonances at 134.6 and 141.2 ppm, which were assigned to *ortho*- and *ipso*-Ph protons, show a *pseudo*-triplet pattern ($|^{2}J_{CP} + {}^{5}J_{CP'}|$ = 10.5 Hz, $|^{1}J_{CP} + {}^{4}J_{CP'}|$ = 6.8 Hz resp.). This coupling pattern is in contrast to those reported for the unsubstituted ferrocene (dppf), which shows for these resonances doublets with the coupling constants of 20 and 9.9 Hz respectively. The unusual pattern found in the ^{13}C NMR spectrum of compound **S7** has to be the result of the conformational rigidity in solution.

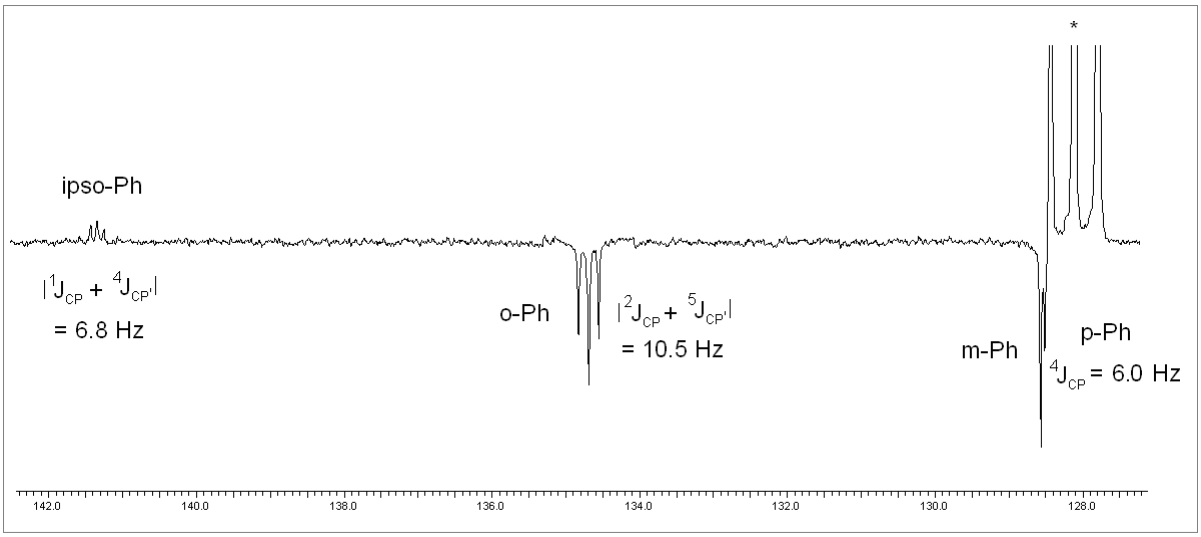

Figure 11. The aromatic part of the ^{13}C NMR spectrum (75.0 MHz) of compound **S7** dissolved in C_6D_6 at +25°C. The resonance denoted with (*) is assigned to the residual solvent protons.

The resonance of the α-carbon atom of the C5-ring has very low intensity and it occurs at 79.0 ppm as a *pseudo*-triplet ($|^{1}J_{CP} + {}^{3}J_{CP'}|$ = 13.8 Hz). HMQC spectroscopy allows individual assignment of the carbon resonances and offers further confirmation of the proton assignments. A selected part of the HMQC spectrum of compound **S7** is shown in Figure 12. The resonance of the β-carbon atom of the C5-ring correlates with the C*H*-group and appears at 63.7 ppm also as a *pseudo*-triplet ($|^{2}J_{CP} + {}^{3}J_{CP'}|$ = 7.6 Hz). The extremely downfield shifted singlet resonance at 109.5 ppm, which does not correlate with any of the carbon resonances, has to be assigned to the γ-carbon atom of the C5-ring.

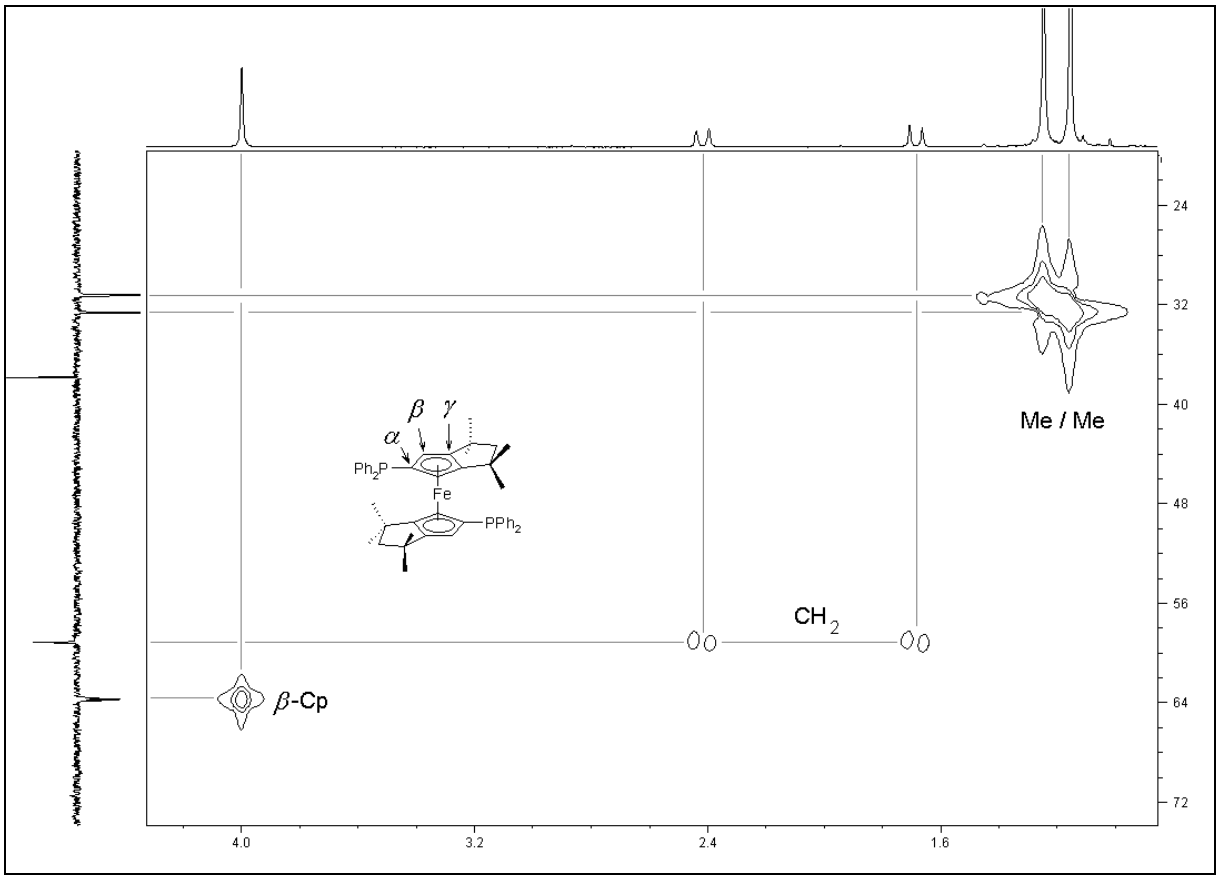

Figure 12. Selected region of the HMQC spectrum of compound **S7** dissolved in C_6D_6 at +25°C.
The 1D ^{1}H NMR spectrum (300.1 MHz) is shown at the top and ^{13}C NMR spectrum (75.1 MHz) is shown on the left edge of the contour plot.

The large, orange crystals of compound **S7**, suitable for X-ray structure determination, were grown by slow cooling of its concentrated alcohol solution. Compound **S7** crystallizes in the triclinic space group $P\bar{1}$ with one molecule in the unit cell. The molecular structure of ferrocene with ellipsoids of 50% of probability is presented in Figure 13. The iron atom lies on the crystallographic inversion center, the molecule as a whole is centrosymmetric. The molecule has a strictly *anti*-conformation of substituents at both C5-rings. Crystallographic analysis delivers the dihedral angle P1–Z1–Z2–P1 of 180.00(2)°. The distance between the iron atom and centroid (Z) of the C5-ring (1.682(1)°) is slightly longer than those in $[(C_5H_4PPh_2)_2Fe]$ (1.646(5) Å),[27] $[(Me_4C_5PPh_2)_2Fe]$ (1.653(1) Å).[28] Bond lengths and angles involving the phosphorous atoms compare well with the values in triphenylphoshine, $[(C_5H_4PPh_2)_2Fe]$[27] and $Ph_2PCp^{TM}H$ (*vide supra*). Two of three C–P1–C angles are somewhat smaller (99.7(1), 100.1(1)°) than the last (101.2(2)°). All Fe1–C_{C5} distances lie in the narrow range and varying from 2.064(1) – 2.088(1) Å.

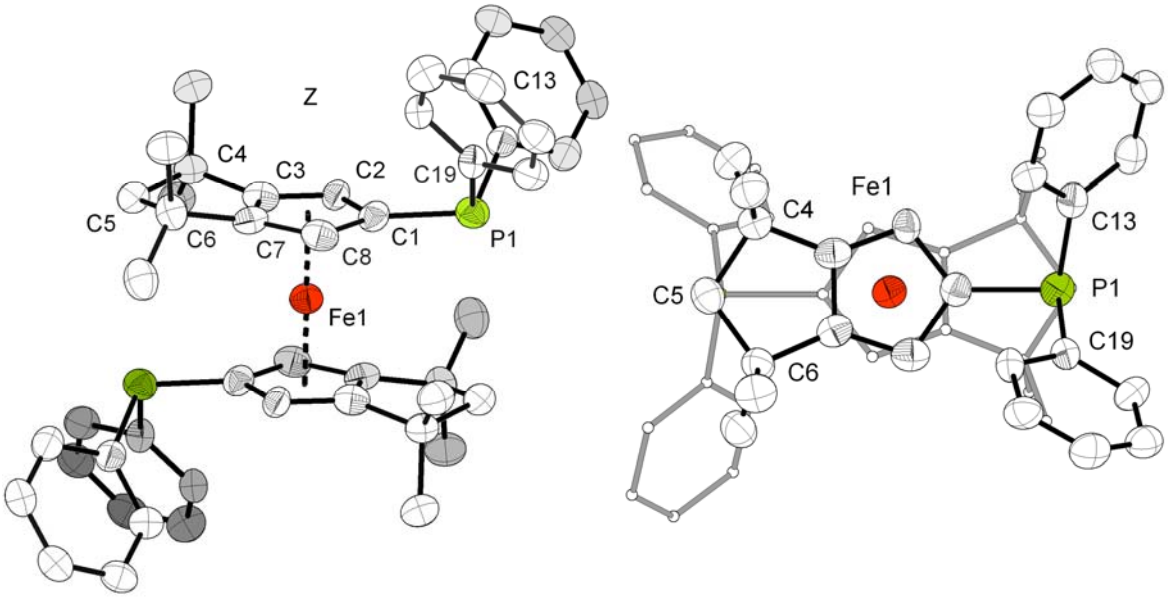

Figure 13. The molecular views of the ferrocene **S7**: side view (left), view along Z–Fe–Z' (right). Hydrogen atoms have been omitted for clarity. Selected bond lengths (Å) and angles (°) for **S7**: P1–C1 1.832(1), P1–C13 1.833(1), P1–C19 1.853(1), C1–C2 1.441(1), C2–C3 1.406(1), C3–C7 1.400(1), C7–C8 1.427(1), C8–C1 1.437(1), C5···Fe1 1.682(1), Fe1–C1 2.084(1), C1–P1–C13 101.2(2), C13–P1–C19 99.7(2), C19–P1–C1 100.1(1), C8–C1–P1–C19 46.6(1), C2–C1–P1–C13 24.5(1).

The intramolecular distance P···CH_2 is comparatively long (3.678(1) Å) and neither in the ^{1}H nor in ^{13}C NMR spectra through-space coupling of the CH_2-group with the phosphorus atom was observed.

The transoid conformation in the solid state is not unusual and known for the structures of many C_2-symmetrical 1,1'-*bis*-(diphenylphosphino)-ferrocene complexes (Figure 14).

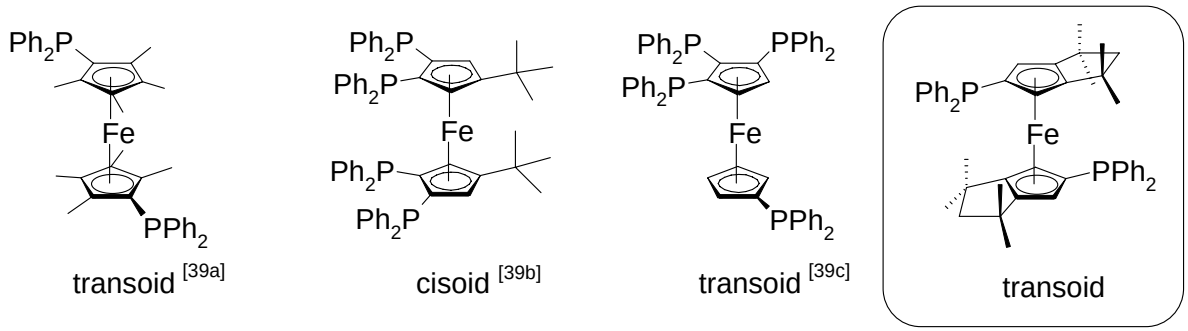

Figure 14. Comparisons of conformations of C_2-symmetrically substituted 1,1'-*bis*-(diphenylphosphino)-ferrocenes in the solid state.

Only the case of super-bulky combination of two *ortho*-diphenylphosphino and one *meta*-*tert*-Bu substituents in each C5-ring renders the cisoid conformation preferential over the

transoid one. Despite of the transoid conformation of Ph_2PCp^{TM}-ligands in $dppf^{TM}$ their potential to act as chelate ligand was investigated.

*2.10. Synthesis and Characterization of [(dppf^{TM})PdX$_2$], (X = Cl (**S8**), I (**S9**))*

Addition of $[PdCl_2(CH_3CN)_2]$ to a slight excess of $dppf^{TM}$ in THF followed by stirring the reaction mixture overnight at ambient temperature gives an orange-purple, lustrous microcrystalline solid of $[(dppf^{TM})PdCl_2]$ (**S8**) in 66% yield. Further halogen exchange was achieved by reaction with an excess of NaI in MeOH. Thus, $[(dppf^{TM})PdI_2]$ (**S9**) was isolated as a deep purple microcrystalline solid in 87% of yield that is far superior to the recently reported analogous synthesis of the $[(dppp)PdI_2]$ complex.[29]

Identification of both compounds was done by microanalysis and multinuclear NMR spectroscopy.

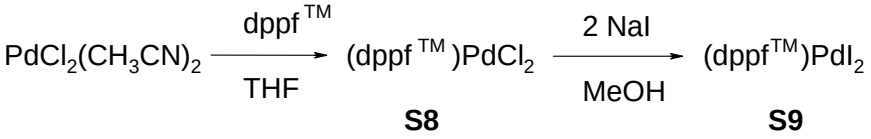

Scheme 24. Synthesis of palladium complexes **S8** and **S9**.

Compounds **S8** and **S9** have very similar NMR spectroscopic characteristics, therefore, only the spectra of compound **S8** will be discussed further.

As expected, in the ^{1}H NMR spectrum the diastereotopic protons of the aliphatic methylene group have similar as $dppf^{TM}$ AX-pattern ($^2J_{HH}$ = 13.4 Hz). Interestingly, four resonances for methyl groups were observed (Figure 15). Unlike the free ligand, the protons at the C5-ring appears as two resonances at 3.64 (s) and 4.11 (d, $^3J_{HP}$ = 2.5 Hz) ppm. These findings confirming the molecule is rigid and adopts the chiral (*racemic*), presumably of the helical nature, (*d, l*)-form; it does not dissociates or inverts in its mirror counterpart in solution.

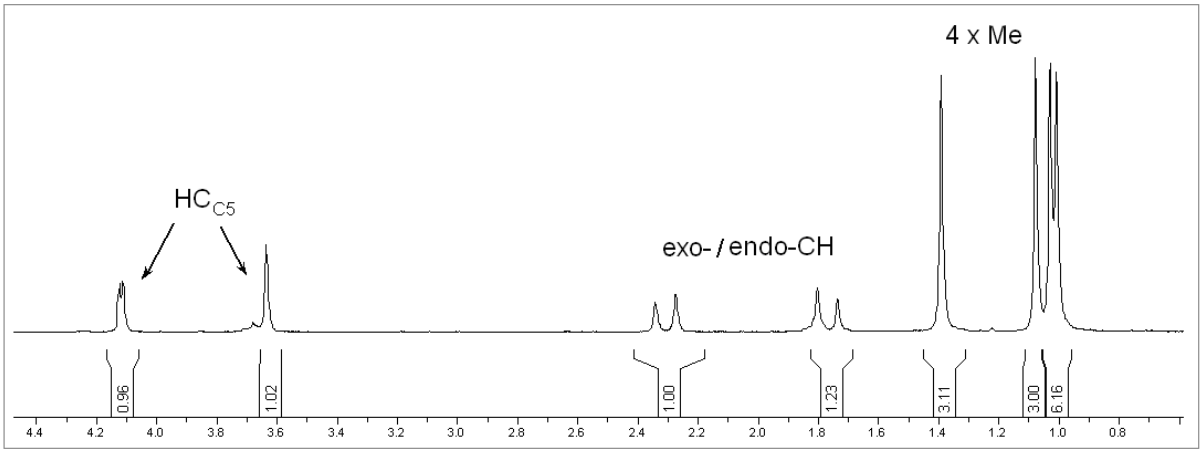

Figure 15. Selected region of the ^{1}H NMR spectrum (300.1 MHz) of compound **S8**.

In the aromatic region of the ^{13}C NMR spectrum (Figure 16), two sets of resonances for each remoted carbon atom of the phenyl group were obtained, whereas in the spectrum of the closely related [(dppf)PdI_2] only one set of resonances was reported.[29]

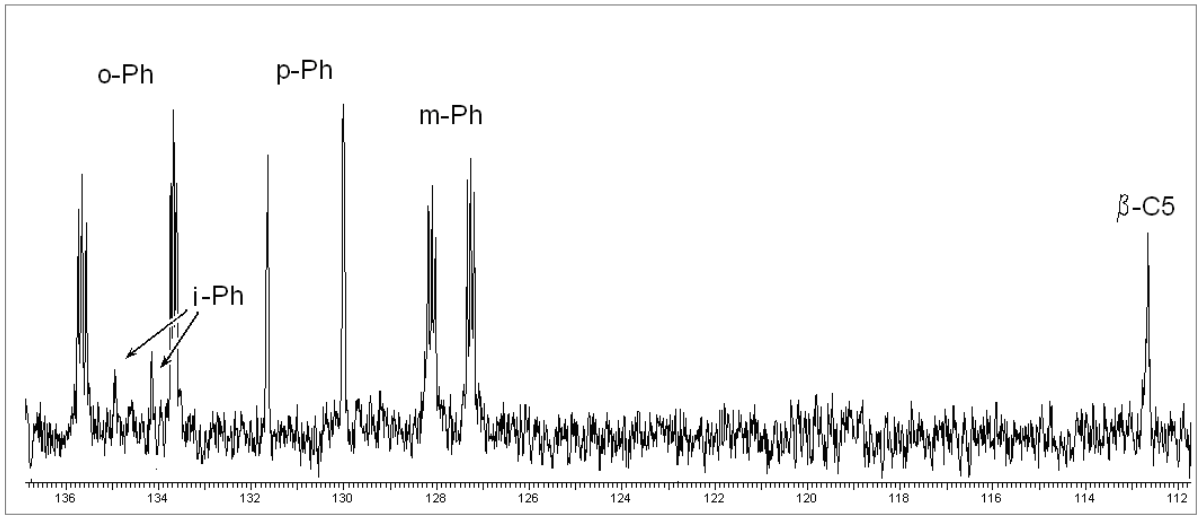

Figure 16. Selected region of the ^{13}C NMR spectrum (75.0 MHz) of compound **14** dissolved in CD_2Cl_2 at +25°C.

Ortho- and *meta*-protons at the phenyl rings show *pseudo*-triplet multiplicities ($|^{2}J_{CP} + {}^{4}J_{CP}|$ = 4.6, 6.4 Hz and $|^{3}J_{CP} + {}^{5}J_{CP}|$ = 5.5, 6.1 Hz), while *para*- and *ipso*-protons have very decreased coupling constants and appears as singlets at 130.0, 131.6 and 134.1, 134.9 ppm respectively. Theses findings reflect that the phenyl groups attached at each phosphorus atom are diastereotopic.

The accurate assignment of the ^{13}C NMR resonances was accomplished by the HMQC spectroscopy. The selected region of the spectrum is depicted in Figure 17.

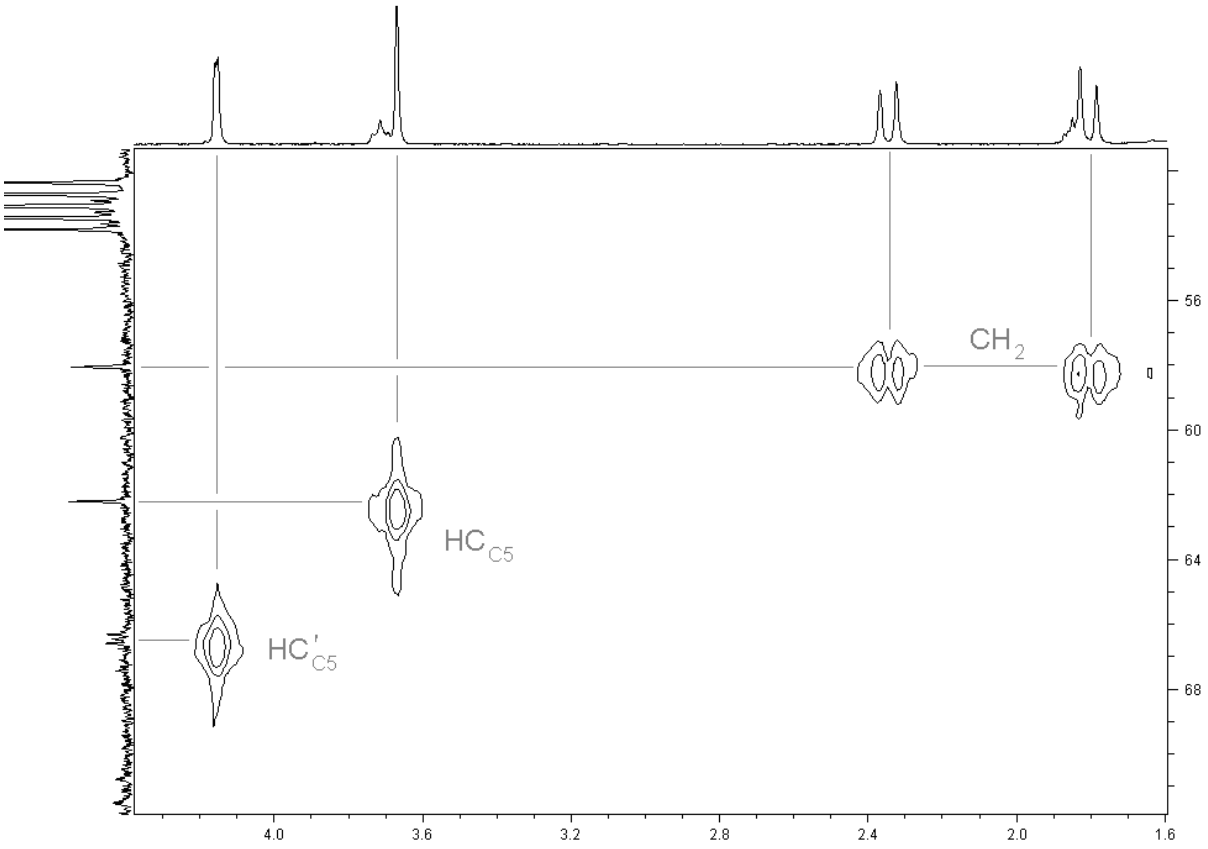

Figure 17. Selected region of the HMQC spectrum of compound **S8** dissolved in CD_2Cl_2 at +25°C. The 1D ^1H NMR spectrum (300.1 MHz) is shown at the top and ^{13}C NMR spectrum (75.0 MHz) is shown on the left edge of the contour plot.

Single crystals of palladium complex **S9**, suitable for X-ray diffraction analysis, were obtained by a slow evaporation of its chloroform solution. The compound crystallizes in the orthorhombic space group *Pca*2_1 with four molecules per unit cell. The molecular structure of **S9** is presented in Figure 18. The palladium atom has a distorted square planar geometry. The similar distortion was reported for complexes [(dppf)PdI_2] (Hal = Br, I).[30]

The P1–Pd1–P2 bite angle is of 99.3(1)° and comparable with those of in series [(dppf)$PdHal_2$] (Hal = Cl – I: 98.9 – 99.9°). The I1–Pd1–I2 angle is slightly larger and of 90.2(1)° (Hal = Cl – I: 87.2 – 87.8°).[29,31] The most interesting feature is the dramatic distortion of both C5-rings in the molecule. The Z–Fe–Z1 angle of 172.0(1)° is the lowest value in the whole series of the [(dppf)$PdHal_2$] (Hal = Cl: 179.5(1)°, Br 177.8(1), I: 178.3(1)°).[29,30]

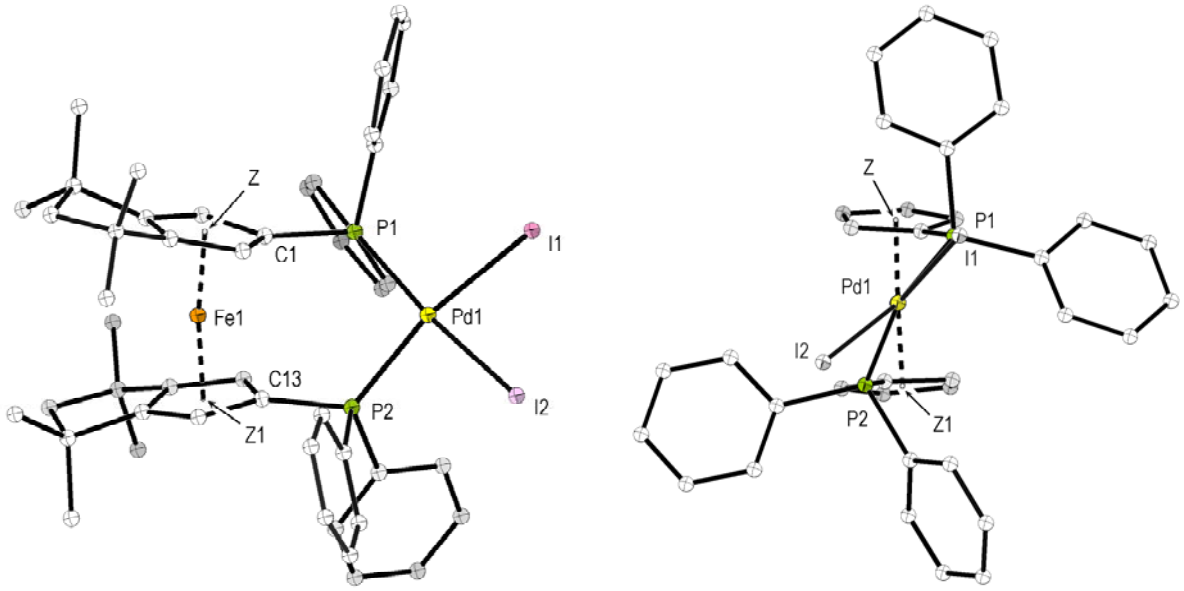

Figure 18. The molecular structere of [(dppf^{TM})PdI_2] (**S9**): side view (left), view along Pd–Fe1 axis (right). All H-atoms and alkylated rings at the right figure have been omitted for clarity. Selected bond lengths (Å) and angles (°) for **S9**: Pd1–I1 2.639(2), Pd1–I2 2.652(2), Pd1–P1 2.293(1), Pd1–P2 2.298(1), P1–C1 1.808(2), P2–C13 1.801(2), Fe–Z 1.683(1), Fe–Z1 1.675(1), I1–Pd1–I2 90.2(1), P1–Pd1–I1 86.3(1), P2–Pd1–I2 86.3(1), P1–Pd1–P2 99.3(1), Z–Pd1–Z1 172.0(1).

Unfortunately, attempts to obtain the single crystals of the corresponding chloride complex **S8** from different solvent or solvent combinations as – THF, $CHCl_3$ and DCM – as well as the layering method (ether/DCM) – failed, yielding only needle-like, very thin fibers.

3. CONCLUSIONS

In this chapter the synthesis of sterically demanding cyclopentadienyl-phosphane via the fulvene route was investigated. We were fascinated to discover that substitution of methanol as solvent by acetone as both solvent and reagent and in the synthesis of the fulvene **F1** as a key precursor unintentionally led to a novel fulvene **F2** that turned out to be an even more attractive one. Using deuterated acetone as labeled reagent confirmed the assumption that **F1** acts an intermediate in the mechanism of **F2** formation. Subsequent carbometallation of **F2** with MeLi resulted in development of a convenient protocol towards the first air-stable, sterically highly crowded cyclopentadienyl-phosphane **P6** having in its backbone an annelated 1,1,3,3-tetramethyl-cyclopentyl ring. This cyclopentadienyl-phosphane ($Ph_2PCp^{TM}H$) appeared to be thermodynamically very stable and it is the first one that has been crystallographically characterized. As highly promising starting material for both *CpPN*-ligand design and for the organometallic chemistry in general it was investigated in more detail.

The oxidation reactions of $Ph_2PCp^{TM}H$ with H_2O_2, S_8 and selenium yield exclusively the corresponding chalcogenides $Ph_2P(X)Cp^{TM}H$, X = O (**S4**), X = S (**S5**), X = Se (**S6**).

The *Staudinger* reactions of $Ph_2PCp^{TM}H$ with AdN_3 and $DipN_3$ lead to the *P*-amino-cyclopentadienylidene-phosphorane $Ph_2P(Cp^{TM})NHAd$ (**L9**) and *P*-cyclopentadienyl-iminophosphorane $Ph_2P(NDip)Cp^{TM}H$ (**L10**) with high selectivities and in good yields. Each of **L9** and **L10** appeared to exist in it own fixed tautomeric form that was approved by all common analytical methods, including X-ray diffraction analysis.

The *Staudinger* reaction with Me_3SiN_3 leads to formation of chemically very labile $Ph_2P(NSiMe_3)Cp^{TM}H$ (**L8**) that, upon hydrolysis by air-moisture, followed by tautomerization forms a new *N*-unsubstituted *P*-amino-cyclopentadienylidene-phosphorane $Ph_2P(Cp^{TM})NH_2$ (**L11**). An attempt of using *tert*-BuN_3 as "NH"-synthon in direct synthesis of **L11** by reaction with $Ph_2PCp^{TM}H$ gave a regular *Staudinger* reaction product $Ph_2P(Cp^{TM})NH$(*tert*-Bu) (**L12**).

Finally, ferrocene [(η^5-$Cp^{TM}PPh_2)_2Fe$] (**S7**) was synthesized by metallation of $Ph_2PCp^{TM}H$ with BnK and transmetallation with $FeCl_2$. It was named in analogy to its known predecessor dppf, $dppf^{TM}$. The ferrocene **S7** has been applied as a bidentate phosphane ligand for the synthesis of palladium complexes [($dppf^{TM}$)$PdCl_2$] (**S8**) and [($dppf^{TM}$)PdI_2] (**S9**). Both complexes **S7** and **S9** have also been characterized by X-ray diffraction.

4. EXPERIMENTAL PART

General considerations. All manipulations were performed under purified argon or nitrogen using standard high vacuum or *Schlenk* or glovebox techniques. Solvents were dried and distilled under argon employing standard drying agents.[32] All organic reagents were purified by conventional methods. NMR spectra were recorded at +25°C on a Bruker ARX200 and Bruker AMX300. ^{1}H NMR spectra are referenced to residual proton signals C_6D_6 (7.15 ppm) and CD_2Cl_2 (5.32 ppm). ^{13}C NMR spectra are referenced to ^{13}C signals of C_6D_6 (128.0 ppm) and CD_2Cl_2 (53.1 ppm). Elemental analyses were performed at the Analytical Laboratory of the Chemistry Department / Philipps-Universität Marburg. EI-Mass spectra were obtained on a Varian MAT CH7A spectrometer (70 eV). Melting points were determined using Büchi Melting point B-540 apparatus. All melting points are corrected.

Starting materials AdN_3,[33] $DipN_3$,[34] were generated with minor modifications to published methods. The anhydrous metal salts $FeCl_2$[35] and $PdCl_2(MeCN)_2$[36] were prepared according to the literature procedures. Ph_2PCl and Me_3SiN_3 were used as supplied from Merck and Acros.

4.1.1. *Synthesis of diphenyl-(6,6-dimethylfulven-3-yl)-phosphane (**F1**):* To a stirred solution of CpLi (240 mg, 3.33 mmol, 1.05 equiv) in 10 mL ether a solution of Ph_2PCl (700 mg, 3.17 mmol) in 10 mL hexane was slowly added at ambient temperature and stirred for 0.5 h whereupon a yellow suspension forms. After that the reaction mixture was concentrated to 50% of its original volume in vacuum; LiCl was filtered off through a Celite®-pad and washed with hexane (2×5 mL). Evaporating the solvent from filtrate in vacuum leaves yellowish oil (745 mg, 2.98 mmol, yield based on Ph_2PCl: 94%). Thus obtained $Ph_2PC_5H_5$ (**P2**) was dissolved in 10 mL methanol and 0.24 mL (3.72 mmol, 1.1 equiv) of acetone and 0.1 mL (ca. 1.3 mmol, ca. 5 mol%) of pyrrolidine were added. The reaction mixture progressively turns deep yellow. The solution was stirred for 4 h at ambient temperature whereupon a bright yellow microcrystalline precipitate forms. It was filtered off and was dried in vacuum for 4 h. The product can be crystallized from hexane at -30°C. Yield: 59% (510 mg, 1.76 mmol). M.p. = 83.0 – 83.5°C.

^{1}H NMR (300.1 MHz, C_6D_6): δ = 1.59, 1.67 (2×s, 2×3H, 2×*Me*), 6.52 (m, 1H, C*H*), 6.56 (m, 1H, C*H*), 6.71 (m, 1H, C*H*), 7.07 (m, 6H, *Ph*), 7.55 – 7.64 (m, 4H, *o-Ph*) ppm.

$^{13}C\{^{1}H\}$ NMR (75.5 MHz, C_6D_6): δ = 22.6 (s, 2×*Me*), 122.4 (d, J_{PC} = 4.1 Hz, C_{C5}), 128.7 (d, $^{3}J_{CP}$ = 7.0 Hz, *m-Ph*), 128.7 (s, *p-Ph*), 129.0 (d, J_{PC} = 22 Hz, PC_{C5}), 133.6 (d, J_{PC} = 12.8 Hz, *ipso-Ph*), 134.0 (d, $^{2}J_{PC}$ = 19.4 Hz, *o-Ph*), 138.5 (d, $^{1}J_{PC}$ = 11.1 Hz, C_{C5}), 140.9 (d, J_{PC} = 10.3 Hz, C_{C5}), 143.8, 149.6 (2×d, J_{PC} = 7.8 Hz, J_{PC} = 2.5 Hz, *C*=*C*Me_2) ppm.

$^{31}P\{^{1}H\}$ NMR (81.0 MHz, C_6D_6): δ = -16.8 ppm.

EI-MS: m/z (%) = 290 (100) [M^+], 275 (1) [M^+ – Me], 213 (1) [M^+ – Ph].

$C_{20}H_{19}P$ (290.35): calcd. C 82.73, H 6.60; found C 80.91, H 6.63.

4.1.2. *Synthesis of diphenyl-(4,4,6-trimethyl-4,5-dihydropentalen-2-yl)-phosphane (**F2**):* To a suspension of 2.00 g (27.8 mmol, 1.05 equiv) CpLi in 120 mL ether/ hexane (1:1, v/v) a mixture of 5.85 g (26.5 mmol) Ph_2PCl and 5 mL hexane was added at ambient temperature. A slightly exothermic reaction takes place giving a bright yellow solution and LiCl-precipitate. The reaction mixture was stirred for additional 0.5 h at the same temperature and the solvent was stripped to 1/3 of original volume. Reaction mixture was filtered through a Celite®-pad and LiCl was washed with hexane (2×10 mL). The solvent was completely removed in vacuum giving 6.20 g (24.8 mmol, 94% based on Ph_2PCl) of **P2** as highly air-sensitive, pale yellow oil. Thus obtained **P2** was dissolved in acetone (40 mL) and pyrrolidine (0.5 mL, 6.4 mmol, 25 mol%) was added. The reaction mixture turned gradually yellow to deep orange. After 4 h all volatiles were removed in vacuum and resulting viscous orange oil was dried for 4 h at 60°C under high vacuum. Thus obtained crude product was re-crystallized twice from 20 ml hexane at -30°C to give the desired **F3** as bright yellow, microcrystalline solid in 44% yield (4.0 g, 12.1 mmol).

M.p. = 93 – 94°C.

^{1}H NMR (300.1 MHz, C_6D_6): δ = 1.12 (s, 6H, Me_2C), 1.59 (q, $^{4}J_{HH}$ = 1.2 Hz, 3H, *Me*C=C), 2.44 (s, 2H, CH_2), 5.97 (s, 1H, C*H*), 6.27 (dd, $^{3}J_{HP}$ = 3.0 Hz, $^{4}J_{HH}$ = 1.2 Hz, 1H, C*H*), 7.09 (m, 6H, *Ar*), 7.65 (m, 4H, *Ar*) ppm.

$^{13}C\{^{1}H\}$ NMR (75.5 MHz, C_6D_6): δ = 16.4 (s, *Me*C=C), 29.2 (s, Me_2C), 37.7 (Me_2C), 61.3 (s, CH_2), 115.7 (d, $^{2}J_{PC}$ = 17.6 Hz, H*C*), 117.3 (d, $^{2}J_{PC}$ = 17.1 Hz, H*C*), 128.6 (s, *Ph*), 128.7 (s, *Ph*), 134.3 (d, $^{2}J_{PC}$ = 19.8 Hz, *o-Ph*), 138.4 (d, $^{1}J_{PC}$ =11.3 Hz, *ipso-Ph*), 148.7 (d, J_{PC} = 8.1 Hz, *Flv*), 151.3 (d, J_{PC} = 13.6 Hz, *Flv*), 153.2 (d, J_{PC} = 3.0 Hz, *Flv*), 161.6 (d, J_{PC} = 5.8 Hz, *Flv*) ppm.

$^{31}P\{^{1}H\}$ NMR (81.0 MHz, C_6D_6): δ = -13.9 ppm.

ESI-MS: m/z (%) = 331 (22.5) [M^+ + H], 330 (100) [M^+], 315 (18.6) [$M^+ - CH_3$], 253 (8.3) [M^+ – Ph].

$C_{23}H_{23}P$ (330.41): calcd. C 83.61, H 7.02; found C 83.01, H 6.14.

4.1.3. *Reaction of **F1** with aceton-d_6: Synthesis of diphenylphosphino-(4,4-dimethyl-6-trideuteromethyl-5,5-dideutero-4,5-dihydropentalen-2-yl)-phosphane (**F3**):* To a solution of the fulvenyl-phosphane **F1** (33 mg, 114 μmol) in 0.6 mL of acetone-d_6 pyrrolidine (1.0 μL, ca. 0.5 mg, ca. 10 mol%) was added by means of a micro-syringe . The proceeding of the reaction was monitored by ^1H and ^{31}P NMR spectrometry. After the reaction was accomplished (ca. 8 h) the solvent was removed in vacuum. A bright yellow amorphous solid of **F3$_d$** was obtained in approx. 31% yield by crystallization from hexane at -30°C.

^1H NMR (300.1 MHz, Me_2CO-d_6): δ = 1.22 (s, 6H, Me_2C), 5.70 – 5.71 (m, 1H, HC_{C5}), 6.00 (dd, $^3J_{HP}$ = 3.5 Hz, $^4J_{HH}$ = 1.0 Hz, 1H, HC_{C5}), 7.40 (5H, *Ph*) ppm.

$^{31}P\{^1H\}$ NMR (81.0 MHz, Me_2CO-d_6): δ = -19.1 ppm.

EI-MS: m/z (%) = 335.

4.1.4. *Synthesis of diphenyl-(4,4,6,6-tetramethyl-1,4,5,6-tetrahydropentalen-2-yl)-phosphane (**P6**):* To a solution of the fulvenyl-phosphane **F2** (5.28 g, 16.0 mmol) in ether (50 mL) MeLi-solution (1.6 M in ether, 15 mL, 24 mmol) was added at 0°C during 15 min followed by stirring at room temperature for 1 h. The reaction mixture was quenched with 3.5 mL of methanol and solution was decantated from the sticky slurry of LiOMe. From the filtrate all volatiles were removed in vacuum and the residue was taken up into hexane (100 mL). The solution was filtered through Celite®-pad again. Cooling the solution to -80°C over night leaves a pale yellow, crystalline material, which was isolated by low temperature filtration and dried in vacuum for 1 h. If the purity is insufficient the product has to be repeatedly crystallized from hexane. A pale yellow, crystalline solid was obtained in yield of 91% (5.04 g, 14.6 mmol). M.p. = 108 – 109°C. Almost colorless compound can be obtained by crystallization from $SiMe_4$ at -30°C. M.p. = 109.0 – 109.3°C.

^1H NMR (300.1 MHz, C_6D_6): δ = 1.02 (s, 6H, Me_2C), 1.11 (s, 6H, Me_2C), 1.94 (s, 2H, $CH_2(CMe_2)_2$), 2.89 (t, $^4J_{HH}$ = 1.5 Hz, 1H, H_2C_{C5}), 7.76 (dt, $^3J_{PH}$ = 5.4 Hz, $^4J_{HH}$ = 1.5 Hz, 1H, HC_{C5}), 7.05 (m, 6H, *Ar*), 7.53 (m, 4H, *Ar*) ppm.

$^{13}C\{^1H\}$ NMR (75.5 MHz, C_6D_6): δ = 30.0, 30.4 (2×s, 2×CMe_2) 37.6 (d, $^2J_{CP}$ = 9.8 Hz, H_2CC_{5}), 40.2, 41.8 (2×s, 2×CMe_2), 61.6 (s, $CH_2(CMe_2)_2$), 128.6 (m, *m-/p-Ph*), 133.7 (d, $^1J_{CP}$ =

19.7 Hz, *ipso-Ph*), 139.0 (d, $^2J_{CP}$ = 24.1 Hz, *o-Ph*), 139.4 (d, J_{CP} = 10.9 Hz, C_{C5}), 145.8 (d, J_{CP} = 14.8 Hz, C_{C5}), 155.8 (d, J_{CP} = 8.2 Hz, C_{C5}), 160.6 (s, C_{C5}) ppm.

$^{31}P\{^1H\}$ NMR (81.0 MHz, C_6D_6): δ = -14.5 ppm.

EI-MS: m/z (%) = 347 (1.4) [M^+ + H], 346 (34.5) [M^+], 331 (100) [M^+ – Me], 269 (1) [M^+ – Ph].

$C_{24}H_{27}P$ (346.45): calcd. C 83.21, H 7.86; found C 83.38, H 7.79.

4.1.5. *Synthesis of phosphine oxide $Ph_2P(O)Cp^{TM}H$ (**S4**)*: To a stirred solution of **P6** (490 mg, 1.42 mmol) in 10 mL THF aq. H_2O_2 (ca. 30%, ca. 1.6 mmol) was added in one portion at r.t. An exothermic reaction takes place. Stirring was continued for 0.5 h after that the volatiles were completely removed in vacuum. The traces of water were removed by azeotropic drying with 50 mL toluene. After removal of the toluene in vacuum, the solid residue was washed twice with 5 mL cold hexane, crystallized from hot heptane and dried in vacuum. Yield: 71% (365 mg, 0.40 mmol) of colorless, microcrystalline solid.

M.p. = 162.9 – 163.3°C

^1H NMR (300.1 MHz, C_6D_6): δ = 0.97, 1.02 (2×s, 2×6H, 2×Me_2C), 1.90 (s, 2H, CH_2(CMe_2)$_2$), 3.10 (s, 2H, H_2C_{C5}), 6.95 (d, $^3J_{CP}$ = 8.7 Hz, 1H, HC_{C5}), 7.05 (m, 6H, *m-/p-Ph*), 7.89 (m, 4H, *o-Ph*) ppm.

$^{13}C\{^1H\}$ NMR (75.5 MHz, C_6D_6): δ = 29.8, 30.1 (2×s, 2×Me_2C), 36.8 (d, $^2J_{CP}$= 12.6 Hz, H_2C_{C5}), 40.1, 41.8 (2×s, 2×Me_2C), 61.4 (s, $CH_2(CMe_2)_2$), 128.5 (m, *m-/p-Ph*), 131.1 (d, J_{CP} = 2.7 Hz, C_{C5}), 132.2 (d, J = 10.9 Hz, *o-Ph*), 141.6 (d, J = 9.8 Hz, HC_{C5}) , 155.0 (d, $^3J_{CP}$ = 14.8 Hz, $C_{C5}CMe_2$), 164.2 (s, $C_{C5,}$ $C_{C5}CMe_2$) ppm.

$^{31}P\{^1H\}$ NMR (81.0 MHz, C_6D_6): δ = 18.1 ppm.

EI-MS: m/z (%) = 362 (19) [M^+], 347 (87) [M^+ – Me].

Anal. calcd for $C_{24}H_{27}OP$ (362.4): C 79.53, H 7.51; found C 79.78, H 6.98.

4.1.6. *Synthesis of phosphine sulfide $Ph_2P(S)Cp^{TM}H$ (**S5**)*: Sulfur powder (340 mg, 1.33 mmol, 1 eq.) was added to a stirred solution of $Ph_2PCp^{TM}H$ (460 mg, 1.33 mmol) in 12 mL toluene at r.t. A slightly exothermic reaction with dissolution of the sulfur was observed. Reaction mixture was stirred at r.t. for additional 2 h. The solvent was removed in vacuum and the solid residue obtained was triturated with hexane. The formed precipitate was filtered off and washed with small amount of hexane. Yield 72% (360 mg) of yellow powder with the melting

point of 133 – 134°C. The sample of the analytical purity was obtained by crystallization from hot heptane solution: yellow, crystalline solid.

M.p. = 134.4 – 134.7°C.

^{1}H NMR (300.1 MHz, C_6D_6): δ = 0.96, 1.00 (2×s, 2×6H, *Me*$_2$C), 1.87 (s, 2H, C*H*$_2$(CMe$_2$)$_2$), 3.20 (s, 2H, H$_2$*C*$_{C5}$), 6.94 (d, $^{3}J_{CP}$ = 9.5 Hz, 1H, *H*C$_{C5}$), 7.01 (m, 6H, *m-/p-Ph*), 7.97 (m, 4H, *o-Ph*) ppm.

^{13}C{^{1}H} NMR (75.5 MHz, C_6D_6): δ = 29.8, 30.1 (2×s, 2×*Me*$_2$C), 36.8 (d, $^{2}J_{CP}$= 12.6 Hz, H$_2$*C*$_{C5}$), 40.1, 41.8 (2×s, 2×Me$_2$*C*), 61.4 (s, *C*H$_2$(CMe$_2$)$_2$), 128.5 (m, *m-/p-Ph*), 131.1 (d, J_{CP} = 2.7 Hz, *C*$_{C5}$), 132.2 (d, *J* = 10.9 Hz, *o-Ph*), 141.6 (d, *J* = 9.8 Hz, *H*C$_{C5}$) , 155.0 (d, $^{3}J_{CP}$ = 14.8 Hz, *C*$_{C5}$CMe$_2$), 164.2 (s, *C*$_{C5,}$ *C*$_{C5}$CMe$_2$) ppm.

^{31}P{^{1}H} NMR (81.0 MHz, C_6D_6): δ = 31.4 ppm.

EI-MS: m/z (%) = 378 (55) [M$^+$], 363 (65) [M$^+$ – Me]

Anal. calcd for $C_{24}H_{27}PS$ (378.5): C 76.16, H 7.19; found C 76.46, H 7.13.

4.1.7. *Synthesis of phosphine selenide Ph$_2$P(Se)Cp^{TM}H (**S6**)*: Red selenium powder (119 mg, 1.55 mol, 1.07 eq.) was added to a solution of Ph$_2$PCp^{TM}H (**P6**) (498 mg, 1.44 mmol) in chloroform (5 mL). The heterogenic reaction mixture was further heated under reflux for 5 h, whereupon the selenium amount diminished. The excess of red selenium was removed by filtration through a Celite®-pad. Removal of the solvent from the filtrate gives a brown foamy solid. Yield: 96% (588 mg of) of brown solid with the melting point of 143 – 144°C. The sample of the analytical purity was obtained by slow crystallization from hot heptane. Colorless, crystalline solid.

M.p. = 147.7 – 148.0°C.

^{1}H NMR (300.1 MHz, C_6D_6): δ = 0.95, 1.00 (2×s, 2×6H, 2×*Me*$_2$C), 1.86 (s, 2H, C*H*$_2$(CMe$_2$)$_2$), 3.25 (s, 2H, *H*$_2$C$_{C5}$), 6.94 (d, $^{3}J_{CP}$ = 9.8 Hz, 1H, *H*C$_{C5}$), 6.99 (m, 6H, *m-/p-Ph*), 7.97 (m, 4H, *o-Ph*) ppm.

^{13}C{^{1}H} NMR (75.5 MHz, $CDCl_3$): δ = 30.0, 30.5 (2×s, 2×*Me*$_2$C), 36.8 (d, $^{2}J_{CP}$= 12.7 Hz, H$_2$*C*$_{C5}$), 40.2, 42.1 (2×s, 2×Me$_2$*C*), 61.3 (s, *C*H$_2$(CMe$_2$)$_2$), 128.6 (d, $^{3}J_{CP}$ = 12.1 Hz, *m-Ph*), 131.5 (d, $^{4}J_{CP}$ = 3.3 Hz, *p-Ph*), 132.4 (d, $^{2}J_{CP}$ = 11.0 Hz, *o-Ph*), 132.5 (d, $^{1}J_{CP}$ = 78 Hz, *ipso-Ph*), 138.3 (d, $^{1}J_{CP}$ = 83 Hz, P*C*$_{C5}$), 143.2 (d, $^{2}J_{CP}$ = 9.9 Hz, H*C*$_{C5}$), 154.9 (d, $^{3}J_{CP}$ = 15.4 Hz, *C*$_{C5}$CMe$_2$), 165.0 (d, $^{3}J_{CP}$ = 7.2 Hz, *C*$_{C5}$CMe$_2$) ppm.

^{31}P{^{1}H} NMR (81.0 MHz, C_6D_6): δ = 22.3 ($^{1}J_{SeP}$ = 710 Hz) ppm.

^{77}Se{^{1}H} NMR (76 MHz, C_6D_6): δ = -260.8 (d, $^{1}J_{SeP}$ = 741 Hz) ppm.

EI-MS m/z (%): 426 (32.8) [M^+], 265 (84.5) [$M^+ - Cp^{TM}$].
Anal. calcd for $C_{24}H_{27}PSe$ (425.41): C 67.76, H 6.40; found C 68.06, H 6.87.

4.1.8. *Synthesis of N-adamantyl-aminophosphorane $Ph_2P(Cp^{TM})NHAd$ (**L9**)*: To a stirred solution of phosphane **P6** (2.50 g, 7.22 mmol) in 60 mL of toluene AdN_3 (1.41 g, 7.94 mmol, 1.10 equiv) was added and stirred at 100°C over night. The color of the reaction mixture progressively turns yellow and afterwards it becomes deep brown. The reaction proceeding was monitored by ^{31}P spectroscopy. The solvent was completely removed in vacuum and the brown, foamy residue was triturated with 15 mL of hexane yielding in formation of the brown, clear solution. A sonication of hexane solution precipitates yellowish powder. It was filtered off, washed twice with 10 mL of hexane and dried in vacuum. Cooling the mother liquor to 8°C delivers some additional amount of the product. The isolated yield: 35% (1.23 g) of yellow powder. The compound has very high solubility in aromatic solvents; it is moderately stable in air (a week), but oxidizes faster in solutions.
M.p. = 176.5 – 177.0°C.
^1H NMR (300.1 MHz, C_6D_6): δ = 1.44 (m, 6H, *Ad*), 1.52 (m, 6H, *Ad*), 1.68 (s, 12H, Me_2C), 1.80 (m, 3H, $CH(CH_2)_3$), 2.04 (d, $^2J_{PH}$ = 4.8 Hz, 1H, N*H*), 2.45 (s, 2H, $CH_2(CMe_2)_2$), 6.15 (d, $^3J_{PH}$ = 3.2 Hz, 2H, HC_{C5}), 7.00 (m, 6H, *m-/p-Ph*), 7.89 – 8.00 (m, 4H, *o-Ph*) ppm.
$^{13}C\{^1H\}$ NMR (75.5 MHz, C_6D_6): δ = 30.4 (s, $CH(CH_2)_2$), 33.4 (2×s, 2×CMe_2), 36.2 (s, *Ad*), 39.3 (d, $^4J_{PC}$ = 1.3 Hz, CMe_2), 44.5 (d, J_{CP} = 4.0 Hz, Ad), 54.0 (d, $^2J_{PC}$ = 2.3 Hz, $NC(CH_2)_3$), 65.0 (s, $CH_2(CMe_2)_2$), 80.8 (d, $^1J_{PC}$ = 116 Hz, *ipso-*C_{C5}), 106.5 (d, $^2J_{PC}$ = 16.2 Hz, HC_{C5}), 128.5 (d, $^3J_{PC}$ = 12.3 Hz, *m-Ph*), 131.7 (d, $^4J_{PC}$ = 2.3 Hz, *p-Ph*), 131.9 (d, $^1J_{PC}$ = 105 Hz, *ipso-Ph*), 132.9 (d, $^2J_{PC}$ = 10.5 Hz, *o-Ph*), 146.8 (d, $^3J_{PC}$ = 18.5 Hz, Me_2CC_{C5}) ppm.
$^{31}P\{^1H\}$ NMR (81.0 MHz, C_6D_6): δ = 17.8 ppm.
EI-MS: m/z (%) = 495 (70) [M^+], 480 () [M^+ – Me], 466 () [M^+H – 2 Me].
Anal. calcd for $C_{34}H_{42}PN$ (495.69): C 82.38, H 8.54; found C 82.03, H 8.55.

4.1.9. *Synthesis of N-(2,6-diisopropylphenyl)-iminophosphorane $Ph_2P(NDip)Cp^{TM}H$ (**L10**)*: To a stirred solution of phosphane **P6** (6.59 g, 19.0 mmol) in 75 mL of THF $DipN_3$ (4.46 g, 22 mmol, 1.1 equiv) was added and stirred over night at room temperature, whereupon N_2-evolution occurs. After that the solvent was removed in vacuum to yield a foamy residue. The compound was crystallized from acetonitrile at ambient temperature. Yield: 75% (7.51 g) of a pale rose, crystalline solid.
M.p. = 142.5 – 143.0°C.

^{1}H NMR (300.1, MHz, C_6D_6): δ = 1.00, 1.03 (2×s, 2×6H, 2×*Me*$_2$C), 1.18 (d, $^{3}J_{HH}$ = 7.0 Hz, 12H, 2×(C*H*$_3$)$_2$CH), 1.91 (s, 2H, C*H*$_2$(CMe$_2$)$_2$), 3.08 (s, 2H, H$_2$*C*$_{C5}$), 3.66 (sept, $^{3}J_{HH}$ = 7.0 Hz, 2H, (CH$_3$)$_2$C*H*), 6.77 (d, $^{3}J_{CP}$ = 8.5 Hz, 1H, H*C*$_{C5}$), 7.04 (m, 6H, *m-/p-Ph*), 7.08 (m, 1H, *p-Dip*), 7.85 (m, 4H, *o-Ph*) ppm.

^{13}C{^{1}H} NMR (75.5 MHz, C_6D_6): δ = 24.0 (s, *Me*$_2$CH), 29.0 (s, Me$_2$C*H*), 29.8, 30.2 (2×s, 2×*Me*$_2$C), 37.0 (d, $^{2}J_{CP}$ = 11 Hz, H$_2$*C*$_{C5}$), 39.6, 41.7 (2×s, 2×Me$_2$*C*), 61.6 (s, *C*H$_2$(CMe$_2$)$_2$), 119.9 (d, $^{5}J_{CP}$ = 3.3 Hz, *p-Dip*), 132.2 (d, $^{4}J_{CP}$ = 2.1 Hz, *m-Dip*), 128.5 (s, *p-Ph*), 131.0 (d, $^{4}J_{CP}$ = 2.4 Hz, *p-Ph*), 132.2 (d, $^{2}J_{CP}$ = 9.1 Hz, *o-Ph*), 134.5 (d, $^{1}J_{CP}$ = 106 Hz, *ipso-Ph*), 140.7 (d, $^{2}J_{CP}$ = 10 Hz, *C*H$_{C5}$), 142.5 (d, $^{1}J_{CP}$ = 100 Hz, *ipso-C5*), 143.0 (d, $^{2}J_{CP}$ = 6.9 Hz, *ipso-Dip*), 145.5 (s, *o-Dip*), 155.2 (d, $^{3}J_{CP}$ = 13.9 Hz, *C*CMe$_2$CH$_2$), 163.2 (d, $^{3}J_{CP}$ = 6.4 Hz, *C*CMe$_2$CH$_2$) ppm.

^{31}P{^{1}H} NMR (81.0 MHz, C_6D_6): δ = -14.9 ppm.

EI-MS m/z (%): 521 (47.0) [M$^+$], 506 (31.6) [M$^+$ – Me], 185 (56.2) [Ph$_2$P$^+$].

$C_{36}H_{44}NP$ (521.73): calcd. C 82.88, H 8.50, N 2.68; found C 83.11(82.53), H 8.57, N 2.88.

4.1.10. *Synthesis of N-trimethylsilyl-iminophosphorane Ph$_2$P(NSiMe$_3$)Cp^{TM}H (**L8**):* To the solid phosphane **P6** (334 mg, 0.96 mmol) Me$_3$SiN$_3$ (1.0 mL, ca. 7.5 mmol, ca. 7.5 equiv) was added and stirred at 100°C for 18 h, whereupon slow N_2-evolution takes place. The reaction mixture turns progressively brown. The proceeding of the reaction was performed by ^{31}P NMR spectroscopy of the crude reaction mixture in $CDCl_3$. After the reaction proceeded to 87% it was terminated. Removal of the all volatiles in vacuum yields a light brown semisolid mass, which was taken into 10 mL hexane. Filtration from a small amount amorphous solid followed by removal of the solid results in the formation of the light brown crystalline product (M.p = 94.0 – 94.5°C) The moisture and air-sensitive compound **L8** shows very high solubility in all aprotic common solvents, except of acetonitrile. The sample of the analytical purity was obtained by crystallization from acetonitrile.

M.p. = 94.5 – 94.7°C.

^{1}H NMR (300.1, MHz, C_6D_6): δ = 0.39 (s, 9H, Si*Me*$_3$), 1.00, 1.04 (2×s, 2×6H, 2×*Me*$_2$C), 1.91 (s, 2H, C*H*$_2$(CMe$_2$)$_2$), 3.03 (dd, $^{3}J_{HP}$= 1.0 Hz, $^{4}J_{HH}$ = 1.7 Hz, 2H, *H*$_2$C$_{C5}$), 6.95 (dt, $^{4}J_{HH}$ = 1.7 Hz, $^{3}J_{CP}$ = 9.0 Hz, *H*C$_{C5}$), 7.05 (m, 6H, *m-/p-Ph*), 7.80 – 7.90 (m, 4H, *o-Ph*) ppm.

^{13}C{^{1}H} NMR (75.5 MHz, C_6D_6): δ = 4.5 (d, $^{2}J_{CP}$ = 3.3 Hz, Si*Me*$_3$), 29.9, 30.3 (2×s, 2×C*Me*$_2$), 36.6 (d, $^{2}J_{CP}$ = 12.7 Hz, H$_2$*C*$_{C5}$), 40.0, 41.7 (2×s, 2×*C*Me$_2$), 61.6 (s, *C*H$_2$(CMe$_2$)$_2$), 128.2 (d, *m-Ph*), 130.7 (d, $^{4}J_{CP}$ = 2.8 Hz, *p-Ph*), 131.9 (d, $^{2}J_{CP}$ = 10.5 Hz, *o-Ph*), 136.8 (d, $^{1}J_{CP}$

= 104 Hz, *ipso-Ph*), 140.3 (d, $^{2}J_{CP}$ = 11 Hz, *C*H$_{C5}$), 144.6 (d, $^{1}J_{CP}$ = 108 Hz, PC$_{C5}$). 155.5 (d, $^{3}J_{CP}$ = 14.9 Hz, C_{C5}CMe$_2$), 162.7 (d, $^{3}J_{CP}$ = 6.6 Hz, C_{C5}CMe$_2$) ppm.

^{31}P{^{1}H} NMR (81.0 MHz, C_6D_6): δ = -7.8 ppm.

ESI-MS m/z (%): 433 (34) [M^+], 360 (100) [M^+ – SiMe$_3$].

Anal. calcd for $C_{27}H_{36}NPSi$ (433.65): calcd. C 74.78, H 8.37, N 3.23; found C 73.71, H 8.36 N 3.16.

4.1.11. *Synthesis of diphenylphosphino-(4,4,6,6-tetramethyl-1,4,5,6-tetrahydropentalen-2-ylidene)-P-aminophosphorane (**L11**)*: The compound was isolated accidentally as a small amount of colorless precipitate by crystallization attempt from wet acetonitrile. Therefore, the synthesis of compound **L11** was not optimized.

M.p. = 172.0 –173.0°C.

^{1}H NMR (300.1 MHz, C_6D_6): δ = 1.66 (s, 12H, 4×*Me*), 2.10 (br. s., 2H, N*H*$_2$), 2.42 (s, 2H, C*H*$_2$(CMe$_2$)$_2$), 5.68 (d, $^{3}J_{CP}$ = 3.4 Hz, 2H, *H*C$_{C5}$), 6.87-7.03 (m, 6H, *Ph*), 7.48-7.56 (m, 4H, *Ph*) ppm.

^{13}C{^{1}H} NMR (50.1 MHz, C_6D_6): δ = 33.2 (s, 4×*Me*), 39.5 (s, 2×*C*Me$_2$), 64.8 (s, *C*H$_2$(CMe$_2$)$_2$), 82.0 (d, $^{1}J_{CP}$ = 110 Hz, *ipso*-*C*$_{C5}$), 104.8 (d, $^{2}J_{CP}$ = 17.8 Hz, H*C*$_{C5}$), 128.3 (d, $^{3}J_{CP}$ = 12.6 Hz, *m-Ph*), 131.1 (d, $^{1}J_{CP}$ = 102 Hz, *ipso-Ph*), 131.7 (d, $^{4}J_{CP}$ = 2.5 Hz, *p-Ph*), 132.4 (d, $^{2}J_{CP}$ = 10.7 Hz, *o-Ph*), 146.0 (d, $^{3}J_{CP}$ = 19.3 Hz, Me$_2$C*C*$_{C5}$) ppm.

^{31}P{^{1}H} NMR (81.0 MHz, C_6D_6): δ = 22.1 ppm.

ESI-MS m/z (%): 361 (100) [M^+], 284 (32) [M^+ – Ph].

Anal. calcd for $C_{24}H_{28}NP$ (361.47): C 79.75, H 7.81, N 3.88; found C 80.30, H 8.18, N 3.98.

4.1.12. *Synthesis of N-tert-butyl-aminophosphorane Ph$_2$P(Cp^{TM})NH(tert-Bu) (**L12**)*: To a pale yellow solution of the phosphane **P6** (360 mg, 1.04 mmol) in 10 mL of THF *tert*-BuN$_3$ (500 mg, 5.0 mmol, 5.0 equiv) was added at ambient temperature. The reaction mixture was stirred over 5 h. The proceeding of the reaction was performed by ^{31}P NMR spectroscopy of the crude reaction mixture. After the reaction proceeded, all volatiles were removed in vacuum and the solid residue was triturated with acetonitrile whereupon a yellow precipitate forms. The latter was filtered off and dried in vacuum. Yield: 41% (170 mg) of a yellow, microcrystalline solid. M.p. = 165.5 – 166.5°C. The sample of the analytical purity was obtained by crystallization from conc. hot acetonitrile solution (M.p. = 166.3 – 166.7°C). The

compound has high solubility in aromatic solvents, THF; it is weakly soluble in acetonitrile, ether and aliphatic solvents.

^{1}H NMR (300.1 MHz, C_6D_6): δ = 0.90 (s, 9H, *tert-Bu*), 1.69 (s, 12H, 2×C*Me*$_2$), 2.07 (d, $^{2}J_{HP}$ = 5.1 Hz, 1H, N*H*), 2.47 (s, 2H, CH_2(CMe$_2$)$_2$), 6.16 (d, $^{3}J_{CP}$ = 4.0 Hz, 2H, CH_{C5}), 7.03 (m, 6H, *m-/p-Ph*), 7.83 – 7.90 (m, 4H, *o-Ph*) ppm.

^{13}C{^{1}H} NMR (75.5 MHz, C_6D_6): δ = 31.4 (d, $^{3}J_{CP}$ = 3.9 Hz, NC*Me*$_3$), 33.3 (s, 2×C*Me*$_2$), 39.6 (d, $^{4}J_{PC}$ = 1.7 Hz, *C*Me$_2$), 53.1 (d, $^{2}J_{CP}$ = 2.2 Hz, *C*Me$_3$), 64.9 (s, *C*H$_2$(CMe$_2$)$_2$), 80.5 (d, $^{1}J_{CP}$ = 118 Hz, *ipso-C5*), 106.1 (d, $^{2}J_{CP}$ = 16 Hz,*C*H$_{C5}$) 128.5 (d, $^{3}J_{CP}$ = 12 Hz, *m-Ph*), 131.5 (d, $^{1}J_{CP}$ = 105 Hz, *ipso-Ph*), 131.7 (d, $^{4}J_{CP}$ = 2.8 Hz, *p-Ph*), 133.9 (d, $^{2}J_{CP}$ = 9.9 Hz, *o-Ph*), 146 ($^{3}J_{CP}$ = 18.7 Hz, Me$_2$C*C*$_{C5}$) ppm.

^{31}P{^{1}H} NMR (81.0 MHz, C_6D_6): δ = 17.0 ppm.

ESI-MS m/z (%): 417 (100) [M$^+$], 340 (70) [M$^+$ – Ph], 412 (25) [M$^+$ – Me].

Anal. calcd for $C_{28}H_{36}PN$ (417.56): calcd. C 80.54, H 8.69, N 3.35; found C 80.25, H 8.57, N 3.38.

4.1.13. *Synthesis of ferrocene dppf^{TM} [(η^5-Cp^{TM}PPh$_2$)$_2$Fe] (**S7**)*

a) *Deprotonation with n-BuLi*: To a solution of **P6** (690 mg, 2.0 mmol) in 25 mL ether 1.6 M solution *n*-BuLi in hexane (1.4 mL, ca. 1.1 equiv) was added at r.t in 4 portions. The pale yellow reaction mixture turns colorless. The addition of solid $FeCl_2$ (126 mg, 1.0 mmol) to a stirred solution of lithium salt cases the formation of a dark brown solution, that was stirred for another 2 h. After that all volatiles were removed in vacuum and residue was extracted with hexane; solvent was stripped off yielding a brown-orange foamy residue. Treatment of acetonitrile solution with ultrasonic causes the precipitate of an orange-rose product, which was filtered off and dried in vacuum. Yield: 28% (209 mg) of an orange, amorphous solid.

b) *Deprotonation with BnK*: The reaction was provided and purified in the same manner as described for the *method a)* from a solution of **P6** (690 mg, 2.0 mmol, 2.05 equiv) in 20 mL of THF and a solution of BnK (255 mg, 0.98 mmol) in 10 mL THF. The slow addition on BnK- solution was performed at 0°C and results an immediate decoloration of the red BnK-solution.

The reaction was followed by addition of solid $FeCl_2$ (64 mg, 0.50 mmol) and stirring 1 h at ambient temperature. Yield: 83% (620 mg) of an orange powder. Compound **S7** is highly soluble in hydrocarbons, aromatic solvents, ethers and ethanol and virtually insoluble in methanol and acetonitrile.

M.p. = 180.5°C (dec. > 188°C).

^{1}H NMR (300.1 MHz, C_6D_6): δ = 1.16 (s, 6H, *Me*), 1.25 (s, 6H, *Me*), 1.68 (d, $^{2}J_{HH}$ = 12.8 Hz, 1H, Me_2C–C*H*–CMe_2), 2.42 (d, $^{2}J_{HH}$ = 12.8 Hz, 1H, Me_2C–C*H*–CMe_2), 4.00 (s, 2H, *H*C_{C5}), 7.06 (m, 6H, *p-/m-Ph*), 7.60 (m, 4H, *o-Ph*) ppm.

^{13}C{^{1}H} NMR (75.5 MHz, C_6D_6): δ = 31.3 (s, *Me*), 32.7 (s, *Me*), 37.9 (*C*Me_2), 59.2 (*C*H_2), 63.7(qt, $^{2}J_{CP}$ =7.6 Hz, H*C*$_{C5}$), 109.6 (*C*$_{C5}$C$(Me)_2$), 128.4, 128.7 (2×s, *m-/p-Ph*), 134.6 (qt, $^{2}J_{CP}$ = 10.4 Hz, *o-Ph*), 141.2 (qt, $^{1}J_{CP}$ = 6.8 Hz, *ipso-Ph*) ppm.

^{31}P{^{1}H} NMR (81.0 MHz, C_6D_6): δ = -16.7ppm.

ESI-MS: m/z (%) = 748 (100) [M^+].

$C_{48}H_{52}FeP_2$ (746.7): calcd. C 77.21, H 7.02; found C 76.62, H 7.13.

4.1.14. *Synthesis of palladium dichloride complex [(dppf^{TM})PdCl$_2$] (**S8**)*: To an orange solution of dppf^{TM} (500 mg, 0.67 mmol, 1.07 equiv) in THF (10 mL) $PdCl_2(MeCN)_2$ (160 mg, 0.63 mmol) was added and reaction mixture was stirred further for 24 h. During that period a purple-orange microcrystalline precipitate forms. It was filtered off and dried in vacuum. Yield: 66% (395 mg). The air-stable substance shows very good solubility in CH_2Cl_2, only low solubility in THF; not soluble in aromatic solvents, hexane, ether, acetone, low alcohols. M.p. > 250°C.

^{1}H NMR (300.1 MHz, C_6D_6): δ = 1.00, 1.03, 1.08, 1.39 (s, 4×3H, 4×Me), 1.76, 2.30 (2×d, AB-system, $^{2}J_{HH}$ = 13.4 Hz, 2×1H, *exo-/endo*-C*H*$_2$), 3.64 (s, 1H, C*H*$_{C5}$), 4.11 (d, $^{3}J_{HP}$ = 2.5 Hz, 1H, C*H*$_{C5}$), 7.33 – 7.65 (m, 8H, *Ph*), 8.11 (m, 2H, *Ph*) ppm.

^{13}C{^{1}H} NMR (75.5 MHz, C_6D_6): δ = 29.4, 30.4, 31.7, 32.7 (s, 4×*Me*), 36.3, 38.1 (s, 2×*C*Me_2), 58.1 (s, *C*$H_2(CMe_2)_2$), 62.2 (s, *C*H$_{C5}$), 66.5 (pst, $|^{2}J_{CP} + {}^{4}J_{CP}|$ = 20.2 Hz, *C*H$_{C5}$), 71.1 (dd, $^{1}J_{CP}$ = 56 Hz, $^{3}J_{CP}$ = 4 Hz, P*C*$_{C5}$), 112.6 (pst, $|^{3}J_{CP} + {}^{5}J_{CP}|$ = 5.4 Hz, *C*$_{C5}$CMe_2), 127.2, 128.1 (2×pst, $|^{3}J_{CP} + {}^{5}J_{CP}|$ = 11.0 Hz, $|^{3}J_{CP} + {}^{5}J_{CP}|$ = 11.6 Hz, 2×*m-Ph*), 130.0, 131.6 (2×s, 2×*p-Ph*), 133.7 (pst, $|^{2}J_{CP} + {}^{4}J_{CP}|$ = 9.2 Hz, *o-Ph*), 134.6 (d, $^{1}J_{CP}$ = 60 Hz, *ipso-Ph*), 135.6 (pst, $|^{2}J_{CP} + {}^{4}J_{CP}|$ = 12.4 Hz, *o-Ph*) ppm.

^{31}P{^{1}H} NMR (121.0 MHz, CD_2Cl_2): δ = 30.3 ppm.

ESI-MS: m/z (%): 927.2 (92) [M^+], 964.3 (100) [M^+ + Cl].

$C_{48}H_{52}Cl_2FeP_2Pd$ (924.07): calcd. C 62.39, H 5.67; found C 62.05, H 5.81.

4.1.15. *Synthesis of palladium diiodide complex [(dppf^{TM})PdI$_2$] (**S9**)*: To a mixture of the complex (dppf^{TM})PdCl$_2$ (166 mg, 0.18 mmol) and sodium iodide (660 mg ,4.4 mmol, ca. 24 equiv) 30 mL MeOH was added and the reaction mixture was refluxed for 10 min. After that the reaction mixture was cooled to room temperature and major amount of inorganic salts by removed by the centrifugation. The filtrate was collected by decantation and the solid was extracted in the same way three times. The solvent from the combined organic phases was removed in vacuum and the brown residue was extracted with CH_2Cl_2. The subsequent removal of the solvent yields a deep purple, microcrystalline solid in yield of 87%. The compound has very high solubility in CH_2Cl_2; marginally soluble in THF and insoluble in MeCN and Et_2O.

M.p. > 250°C.

^{1}H NMR (300.1 MHz, $CDCl_3$): δ = 1.01, 1.06, 1.039 (3×s, 3H, 6H, 3H, 4×*Me*), 1.75, 2.30 (2×d, AB-system, $^2J_{HH}$ = 12.6 Hz, 2×1H, *exo-/endo*-C*H*$_2$), 3.55 (s, 1H, *H*C$_{C5}$), 3.94 (d, $^2J_{HP}$ = 3.3 Hz, 1H, *H*C$_{C5}$), 7.30 – 7.44 (m, 5H, *Ph*), 7.51 – 7.63 (m, 3H, *Ph*), 8.00 – 8.06 (m, 2H, *Ph*) ppm.

^{13}C{^{1}H} NMR (75.5 MHz, $CDCl_3$): δ = 30.0, 31.2, 32.4, 33.5 (s, 4×*Me*), 36.8, 38.5 (s, 2×*C*Me$_2$), 58.7 (s, *C*H$_2$(CMe$_2$)$_2$), 62.7 (s, *C*HC$_{C5}$), 67.0 (pst, $|^2J_{CP} + {}^4J_{CP}|$ = 21 Hz, *C*HC$_{C5}$), 73.9 (dd, $^1J_{CP}$ = 47 Hz, $^3J_{CP}$ = 6 Hz, P*C*$_{C5}$) , 112.4 (d, $^3J_{CP}$ = 6.6 Hz,*C*$_{C5}$CMe$_2$), 112.5 (pst, $|^3J_{CP} + {}^5J_{CP}|$ = 2.2 Hz, *C*$_{C5}$CMe$_2$), 127.4, 128.2 (2×pst, 2×$|^3J_{CP} + {}^5J_{CP}|$ = 11.6 Hz, *m-Ph*), 130.3, 131.6 (2×s, 2×*p-Ph*), 132.2 (d, $^1J_{CP}$ = 54 Hz, *ipso-Ph*), 134.8, 135.9 (2×pst, $|^2J_{CP} + {}^4J_{CP}|$ = 9.4 Hz, $|^2J_{CP} + {}^4J_{CP}|$ = 12.5 Hz, 2×*o-Ph*), 136.6 (d, $^1J_{CP}$ = 55 Hz, *ipso-Ph*) ppm.

^{31}P{^{1}H} NMR (81.0 MHz, $CDCl_3$): δ = 19.9 ppm.

ESI-MS: m/z (%): 1106.4 (91) [M$^+$].

$C_{48}H_{52}I_2FeP_2Pd$ (1106.97): calcd. C 52.08, H 4.74; found C 52.53, H 4.65.

5. REFERENCES

[1] a) K. Ziegler, W. Schafer, *Justus Liebigs Ann. Chem.* **1934**, *511*, 101–109; b) K. Alder, H. Holzrichter, *Justus Liebigs Ann. Chem.* **1936**, *524*, 145–180.

[2] a) K. Hafner, K. H. Häfner, C. König, M. Kreuder, G. Ploss, G. Schulz, E. Surm, K. H. Vöpel, *Angew. Chem., Int. Ed. Engl.* **1963**, *2*, 123–134; b) R. Riemschneider, *Z. Naturforsch. B.* **1963**, 641–645.

[3] K. J. Stone, P. D: Little, *J. Org. Chem.* **1984**, *49*, 1849–1853.

[4] a) D. M. Fenton, M. J. Hurwitz, *J. Org. Chem.* **1963**, *28*, 1646–1651; b) (4) P. Kronig, M. Slongo, M. Neuenschwander, *Makromol. Chem.* **1982**, *183*, 359–361; c) L. Atovmyan, S. Mkoyan, I. Urazowski, R. Broussier, S. Ninoreille, P. Perron, B. Gautheron, *Organometallics* **1995**, *14,* 2601–2604.

[5] F. Mattey J.-P. Lampin, *Tetrahedron* **1975**, *31*, 2685–2690.

[6] a) K. Hartke, G. Ashry, *Scientia Pharmaceutica* **1996**, *64*, 407–420; K. Hartke, C. Timpe, *Justus Liebigs Ann. Chem.* **1994**, 183–187; b) K. Hartke, C. Timpe, *Heterocycles* **1993**, *35*, 77–80.

[7] N. B. Ivchenko, P. V. Ivchenko, I. E. Nifant'ev, I. A. Kashulin, I. V. Taidakov, L. G. Kuz'min, *Russ. Chem. Bull.* **2000**, *49* (4), 724–727.

[8] I. Erden, F.-P. Xu, A. Sadoun, W. Smith, G. Sheff, M. Ossun, *J. Org. Chem.* **1995**, *60*, 813–820.

[9] A. G. Griesbeck, *J. Org. Chem.* **1989**, *54*, 4981–4982.

[10] The average C–P distance for [Ph_3P] is 1.828 Å: J. J. Daly, *J. Chem. Soc.* **1964**, 3799–3810; for [P(*o*-$EtC_6H_4)_3$] is 1.840 Å: N. Fey, J. A. S. Howell, J. D. Lovatt, P. C. Yates, D. Cunningham, P. McArdle, H. Gottlieb, S. J. Coles, *Dalton Trans.* **2006**, 5464–; for [P(2,6-$Me_2C_6H_3)_3$] is 1.83 Å**:** R. A. Shaw, M. Woods, T. S. Cameron, B. Dahlen, *Chem. Ind. (London)* **1971**, 151–152; and of 1.842 Å: A. N. Sobolev, L. A. Chetkina, I. P. Romm, E. N.Gur'yanova, *Zh. Strukt. Khim.* **1976**, *17*, 103–105.

[11] for [Ph_3P]: B. J. Dunne, A. G. Orpen, *Acta Crystallogr., Sect. C* **1991**, *47*, 345–347; for [P(*m*-$MeC_6H_4)_3$]: T. S. Cameron, K. D. Howlett, K. Miller, *Acta Crystallogr., Sect. B* **1978**, *34*, 1639–1644.

[12] [Ph_3PO][31]; for [(*tert*-$Bu)_3PO$]: H. Schmidbaur, *Z. Naturforsch., Teil B* **1978**, *33*, 1556–1558.

[13] [Ph_3P][31]; for [P(*tert*-$Bu)_3$]: W. Wolfsberger, *Z. Naturforsch., Teil B* **1978**, *33*, 1452–1456.

[14] J. A. Iggo, *NMR Spectroscopy in Inorganic Chemistry*, Oxford University press, **2000**.

[15] W. McFarlane, D. S. Rycroft, *J. Chem. Soc.*, *Dalton Trans.* **1973**, *20*, 2162–2166.

[16] The iminophosphorane AdN=PPh_3 was reported can be synthesized in a two-step reaction by the *Kirsanov* reaction: a) A. O. Chong, K. Oshima, K. B. Sharpless, *J. Am. Chem. Soc.* **1977**, *99*, 3420–3426; b) H. Zimmer, M. Jayawant, P. Gutsch, *J. Org. Chem.* **1970**, *35*, 2826–2828.

[17] J. E. Löffler, R. D. Temple, *J. Am. Chem. Soc.* **1967**, *89*, 5235–5246.

[18] a) L. Horner, A. Gross, *Liebigs Ann.* **1955**, *591*, 117–134; b) G. Wittig, K. Schwarzenbach, *Liebigs Ann.* **1961**, *650*, 1–20; c) H. Goldwhite, P. Gysegem, St. Schow, Ch. Swyke, *J. Chem. Soc., Dalton Trans*. **1975**, 16–18.

[19] P. Oulié, C. Freund, N. Saffon, B. Martin-Vaca, L. Maron, D. Bourissou, *Organometallics* **2007**, *26*, 6793–6804.

[20] F. Aasen, D. Wulff-Molder, M. Meisel, *Contribution from PhD Thesis*, Institute of Inorganic Chemistry, Humboldt-Universität zu Berlin **2001**.

[21] K. T. K. Chan, L. P. Spencer, J. D. Masuda, J. S. J. McCahill, P. Wei, D. W. Stephan, *Organometallics* **2004**, *23,* 381–390.

[22] C. Imrie, T. A. Mordo, P. H. van Rooyen, C. C. P. Wagener, K. Wallace, H. R. Hudson, M. McPartlin, J. B. Nasirun, L. Powroznyk, *J. Phys. Org. Chem.* **1995**, *8*, 41–46.

[23] a) M. P. Thornberry, C. Slebodnick, P. A. Deck, F. R. Fronczek, *Organometallics* **2000**, *19*, 5352–5369; b) V. K. Belsky, N. N. Zemlyanskii, I. V. Borisova, N. D. Kolosova, I. P. Beletskaya, *Cryst. Struct. Commun*. **1982**, *11*, 497–499.

[24] R. Gelius, W. Uhlmann, W. Sperling, *Z. Chem.* **1966**, 227–228.

[25] J. J. Bishop, A. Davison, M. L. Katcher, D. W. Lichtenberg, R. E. Merrill, J. C. Smart, *J. Organomet. Chem.* **1971**, *27*, 241–249.

[26] M. B. Gholivand, A. Babakhanian, M. Joshaghani, *Anal. Chim. Acta* **2007**, *584*, 302–307.

[27] U. Casellato, D. Ajo, G. Valle, B. Corain, B. Longato, R. Graziani, *J. Crystallogr. Spectrosc. Res.* **1988**, *18*, 583–588.

[28] G. Trouve, R. Broussier, B. Gautheron, M. M. Kubicki, *Acta Crystallogr., Sect. C: Cryst. Struct. Commun.* **1991**, *47*, 1966–1967.

[29] J. Barkely, M. Ellis, S. J. Higgins, M. K. McCart, *Organometallics* **1998**, *17*, 1725–1731.

[30] T. J. Colacot, H. Qian, R. Cea-Olivares, S. Hernandez-Ortega, *J. Organomet. Chem.* **2001**, *637–639*, 691–697.

[31] T. Hayashi, M. Konishi, Y. Kobori, M. Kumada, T. Higuchi, K. Hirotsu, *J. Am. Chem. Soc.* **1984**, *106*, 158–163.

[32] W. L. F. Armarego, D. D. Perrin, *Purification of Laboratory Chemicals*, 4th Ed., Butterworth-Heinemann, **1996**.

[33] G. K. S. Prakash, M. A. Stephenson, J. G. Shih, G. A. Olah, *J. Org. Chem.* **1986**, *51*, 3215–3217.

[34] L. P. Spencer, R. Altwer, P. Wei, L. Gelmini, J. Gauld, D. W. Stephan, *Organometallics* **2003**, *22*, 3841–3854.

[35] P. Kovacic, N. O. Brace, *Inorg. Synth.* **1960**, *6*, 172–173.

[36] Ch. J. Mathews, P. J. Smith, T. Welton, *J. Mol. Catal. A: Chemical* **2003**, *206*, 77–82.

[37] D. W. Allen, B. F. Taylor, F. Brian, *J. Chem. Soc., Dalton Trans.* **1982**, 51–54.

[38] S. Schlecht, S. Chitsaz, B. Neumüller, K. Dehnike, *Z. Naturforsch.* **1998**, *53*, 17–22.

[39] a) G. Trouve, R. Broussier, B. Gautheron, M. M. Kubicki, *Acta Cryst.* **1991**, *C47*, 1966–1967; b) R. Broussier, E. Bentabet, P. Mellet, O. Blacque, P. Boyer, M. M. Kubicki, B. J. Gautheron, J. Organomet. Chem. **2000**, *598,* 365–373; c) D. A. Thomas, V. V. Ivanov, I. R. Butler, P. N. Horton, P. Meunier, J.-C. Hierso, *Inorg. Chem.* **2008**, *47*, 1607–1615.

[40] N. Hangaly, *Diploma Thesis* **2008**, Phillips University Marburg, in preparation.

[41] M. Elfferding, *Diploma Thesis* **2007**, Phillips University Marburg.

– Chapter V –

Rare-Earth Metal Cyclopentadienyl-Phosphazene-Complexes A New Dimension for *Constrained-Geometry-Catalysts* Variability

Abstract

A series of the rare-earth metal *CGC*-type complexes with the cyclopentadienyliden-*P*-aminophosphorane ligands – $Me_2P(C_5Me_4)NHAd$ (**L4**), $Ph_2P(C_5H_4)NHDip$ (**L6**), $Ph_2P(Cp^{TM})NHAd$ (**L9**) and $Ph_2P(NDip)Cp^{TM}H$ (**L10**), the so-called *CpPN* ligand family is synthesized and structurally characterized, namely mononuclear complexes $[\{\mathbf{L4}\}Ln(CH_2SiMe_3)_2]$ for Ln = Sc, Y, Lu, Nd, $[\{\mathbf{L6}\}Ln(CH_2SiMe_3)_2(thf)_x]$ for Ln = Sc, Lu (x = 0) and Y, Nd (x = 1), $[\{\mathbf{L9}\}Lu(CH_2SiMe_3)_2]$ and $[\{\mathbf{L10}\}Ln(CH_2SiMe_3)_2]$ for Ln = Lu and Y. The complexes reveal different thermostablility. Among structurally charaterized decomposition products there are binuclear heteroleptic complexes – $[\{\mathbf{Lig}\}Ln(OMe)(CH_2SiMe_3)]_2$ for **Lig** = **L4**, Ln = Nd and **Lig** = **L6**, Ln = Y formed by ether cleavage and $[\{\mathbf{L4}\}Nd(OH)_2]_4$ formed upon partial hydrolysis.

Reaction of $[Y(dmba)_3]$ (dmba = *N,N*-dimethylbenzylamine) with one equivalent of ligand **L6** affords the corresponding half-sandwich complex $[\{\eta^5\text{-}\mathbf{L6}\}Y(dmba)_2]$. Its structure in solution was studied by NMR spectroscopy.

Divalent ytterbium complexes with the ligand **L4** and its phenyl analog $Ph_2P(C_5Me_4)NHAd$ of the type $[Yb\{CpPN\}_2]$ were synthesized. Coordination of the ligand, its geometry around the yttrium atom in solution and solid state were studied by NMR spectroscopy and X-ray diffraction analysis.

The reactivity of complexes **C1** –**C4** in the intramolecular hydroamination-/ cyclization reactions of penten-4-ylamines was studied.

1. INTRODUCTION

The cyclopentadienyl-silylamido (*CpSiN*) type ligand system has been developed to the most promising classes of chelating cyclopentadienyl-amido early transition metal complexes, [1,11] the so-called "*Constrained-Geometry-Catalysts*" *CGC*.[2,3] These complexes became famous because of their industrial application as single-site olefin polymerization catalysts. In the previous chapters we have described the new type of chelating *P*-amino-cyclopentadienylidene-phosphorane (*CpPN*) ligands that are isoelectronic with the chelating dianionic cyclopentadienylsilylamido (*CpSiN*) ones.

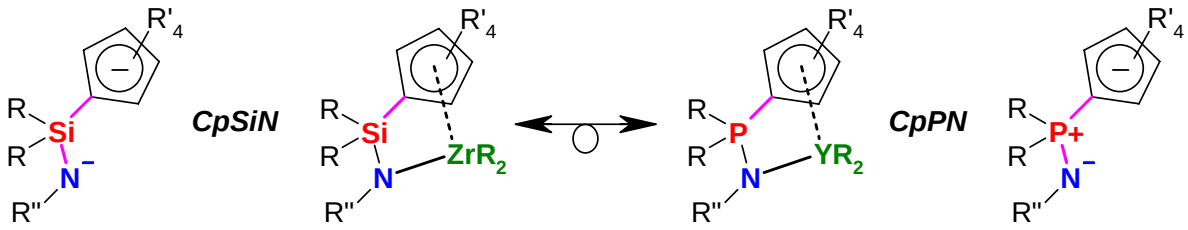

From a conceptual standpoint of view, three-valent lanthanide or group 3 metal complexes on the basis of monoanionic *CpPN*-type ligands are isolobal with tetra-valent group 4 transition metal complexes with dianionic *CpSiN* ligands. Having developed convenient syntheses for a large variety of *CpPN*-ligands with different substituents at N-, P- and C-atoms we have focused on the development of coordination and organometallic chemistry of *CpPN* ligands with rare-earth metals as a promising approach towards new CG-catalysts with a new dimension of ligand variability.

General Remarks to Synthesis of Lanthanide-Cp Complexes

Since the beginning of the organometallic chemistry of cyclopentadienyl complexes, compared to relatively quick developed chemistry of the early transition (bent-)metallocenes $[Cp_2MX_n]$ (n = 0, 1, 2), less attention had been paid towards their one-decked counterparts – $[CpMX_n]$ (n = 2, 3, 4). Extreme in this respect was the situation with lanthanides: before 1989 their chemistry has been limited mainly to *bis*- and rare *tris*-cyclopentadienides, the most studied were bent-metallocenes $[\{Me_5C_5\}_2LnX]$. One-decked $[\{C_5R_5\}LnX_2]$ (R = H, Me; X = Hal, Alk, Ar) were only little explored. The latter tend to undergo further ligand metathesis: thus, homoleptic rare-earth metal amides $[M\{N(SiMe_3)_2\}_3]$ (M = Y, La, Ce) were found to react with highly basic C_5Me_5H in THF yielding only *bis*-substituted complexes and half an equivalent of the unreacted starting material (Scheme 1). No isolable amount of the one-decked species was detected.[46]

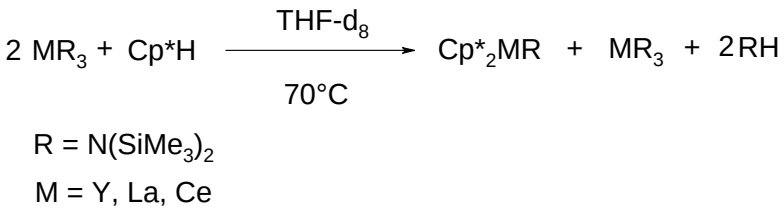

Scheme 1. Reaction of homoleptic rare-earth metal amides $[M\{N(SiMe_3)_2\}_3]$ (M = Y, La, Ce) with C_5Me_5H.

This was explained by low basicity of the used amides. However, reactions using more basic homoleptic alkyl lanthanide complexes proceed also unselectively, e.g. the reactions of $[Ln\{CH(SiMe_3)_2\}_3]$ (Ln = La, Ce)[4] with C_5Me_5H in C_6D_6 give the mixtures of $[\{\eta^5\text{-}C_5Me_5\}Ln\{CH(SiMe_3)_2\}_2]$ and $[\{\eta^5\text{-}C_5Me_5\}_2Ln\{CH(SiMe_3)_2\}]$ complexes along with unreacted precursor (Scheme 2).

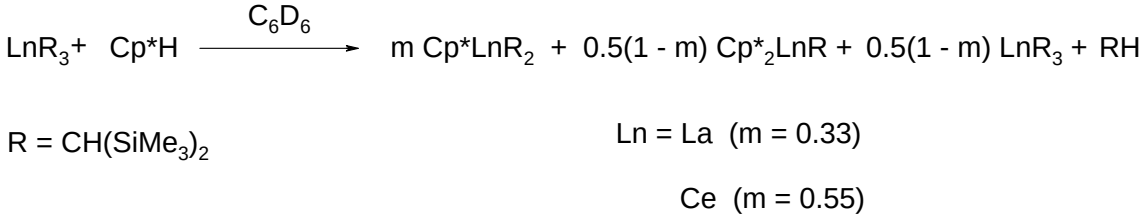

Scheme 2. Reaction of $[Ln(CH\{SiMe_3\}_2)_3]$ with C_5Me_5H (Cp*H) leading to a mixture of products.

The main problem in the synthesis on this type of one-decked complexes is their more pronounced ionic character compared to more covalent transition metal counterparts on the one hand and less thermodynamic and kinetic stability compared to double-decked bent complexes on the other hand.

Among three general synthetic methods towards preparation of rare-earth metal complexes discussed in Chapter I we have studied the *alkane elimination* and its combination with the *salt metathesis* protocol. For the syntheses of the lutetium complexes we used the easy to handle, sufficiently thermally stable, homoleptic lutetium complex $[Lu(CH_2SiMe_3)_3(thf)_2]$.[5] In other cases the *combined protocol* (Scheme 3) has been applied.

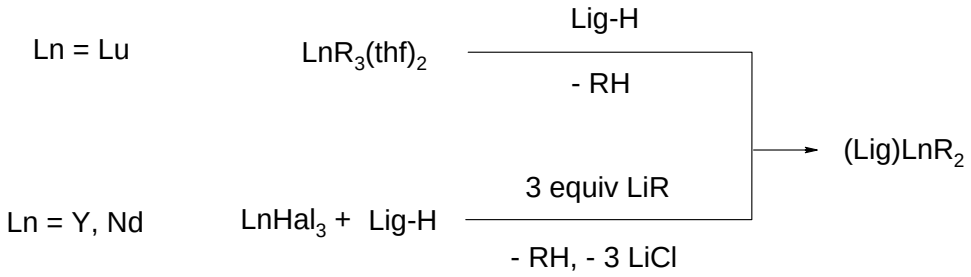

Scheme 3.

2. Results and Discussion

2.1. *Synthesis of CpPN-Dialkyl Complexes of Rare-Earth Metals*

2.1.1. *Synthesis of Complexes with Ligand **L4***

Initial experiments were focused on the development of a direct protocol of *CpPN* metallation with lanthanide *tris*-alkyl complexes. Thus, the first lutetium complex in the series (**C1**) was synthesized by drop wise addition of a benzene solution of the ligand **L4** to a solution of $[Lu(CH_2SiMe_3)_3(thf)_2]$ in the same solvent.[7] The reaction proceeds with high selectivity, as was shown by multinuclear NMR spectroscopy. After the evaporation of the solvent in the Glove-box complex **C1** was isolated as a pale-red, crystalline solid in almost quantitative yield of 96%. The presence of intensively colored oxidation products of the ligand is responsible for the pale-red color. However among the conventional *tris*-alkyl precursors this is the only one with sufficient thermal stability that allows stocking it and using it in multiple syntheses. Therefore, we were forced to develop an alternative synthetic protocol of *in-situ* transmetallation of an equimolar mixture of the **L4** ligand and a rare-earth metal halide source with 3 equivalents of $LiCH_2SiMe_3$ (Scheme 4).

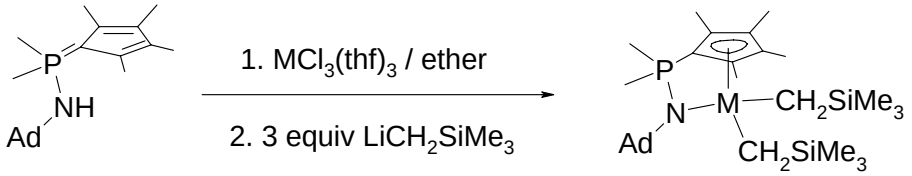

L6

M = Lu (**C1**), Sc (**C2**),

Y (**C3**), Nd (**C4**).

Scheme 4.

The developed synthesis comprises in addition of alkyl lithium ($LiCH_2SiMe_3$) to a stirred suspension of the mixture of appropriate ligand (*CpPN*-H) and lanthanide trihalides in ether/hexane (1:1, v/v) at 0°C. Thus, starting from **L4** and $[MCl_3(thf)_3]$ (M = Sc, Lu), $[YCl_3(dme)_2]$ or $[NdCl_3(dme)]$ this protocol led after an appropriate work-up (solvent removal, extraction with toluene and crystallization) the desired complexes **C1** – **C4**. These show moderate solubility in saturated hydrocarbons and high solubility in ethers (Et_2O, THF) and aromatic solvents. Crystallization succeeds at low temperature from concentrated hexane

solutions and affords air-sensitive pale blue [{**L4**}Nd(CH_2SiMe_3)$_2$] (**C4**) and colourless complexes [{**L4**}M(CH_2SiMe_3)$_2$], M = Lu (**C1**), Sc (**C2**) and Y (**C3**), as microcrystalline, analytically pure and stable at room temperature substances in 50 – 90% yields. The neodymium complex **C4** decomposes gradually at 25°C, and fully in ca. 6 h at 50°C to turn light green, but it is stable enough at -30°C for months. This simple protocol allows a highly efficient and quick synthesis of partly stabilized reactive lanthanide alkyl complexes.

2.1.2. *Multinuclear NMR Spectroscopy of Complexes **C1** – **C4***

According to the ^{1}H and ^{13}C NMR spectroscopy, the complexes **C1** – **C4** with the sterically demanding ligand **L4** crystallize without coordinated solvent molecules. Compared with the free ligand (**L4**: δ = 17.6 ppm), the ^{31}P NMR spectra of diamagnetic **C1** – **C3** complexes are up-field shifted and appear in the narrow region (δ = 9.6, 12.0 and 9.0 resp.).

All ^{1}H NMR spectra of the diamagnetic complexes **C1** – **C3** are very similar and therefore only the spectrum of representative complex [{**L4**}Y(CH_2SiMe_3)$_2$] (**C3**) will be further considered (Figure 1).

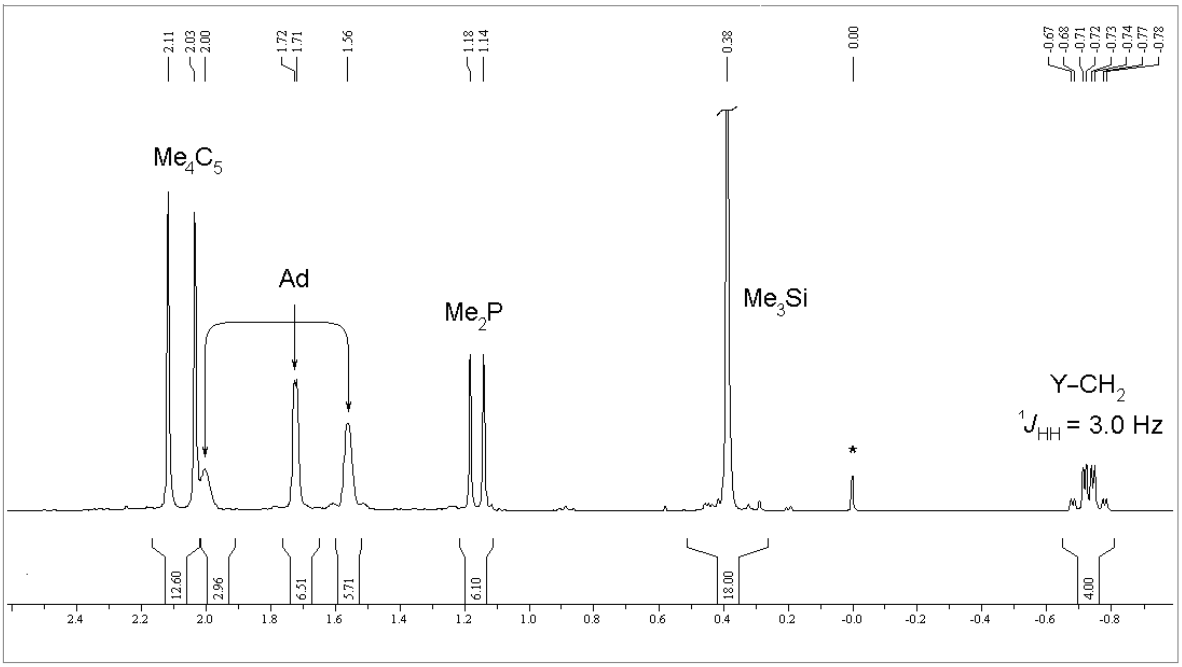

Figure 1. The ^{1}H NMR spectrum (300.1 MHz) of complex [{**L4**}Y(CH_2SiMe_3)$_2$] (**C3**) dissolved in C_6D_6 at +25°C. The resonance denoted with (*) is assigned to TMS.

The room temperature ^{1}H NMR spectrum of **C3** is rather simple, showing two resonances at 2.03 and 2.12 ppm assigned to the pairs of methyl protons of the C_5Me_4-moiety, a typical

set of adamantyl signals at 1.56, 1.71 and 2.00 ppm with the integral ratio of 6:6:3 together with the doublet of the Me_2P-protons at 1.13 ppm ($^2J_{HP}$ = 12.5 Hz).

Diastereotopic silylmethylene protons are magnetically non-equivalent and appear as two multiplet sets at -0.70 and -0.75 ppm with ABX pattern ($^2J_{HH}$ = 11 Hz, $^1J_{HY}$ = 3.0 Hz) at +25°C in solution. $^1J_{HY}$ scalar coupling constant clearly shows that this signal is that of the linked to the yttrium atom CH_2SiMe$_3$-moiety. Thus, in an analogous homoleptic complex [Y(AlMe$_4$)$_3$] the bridging methyl groups appearing at -0.05 ppm with the $^2J_{HY}$ coupling constant of 2.5 Hz.[] ^{1}H NMR spectra of lutetium (**C1**) and scandium (**C2**) complexes with these smaller ionic radii rare-earth metals also show AB-pattern for the diastereotopic methylene protons of CH_2SiMe$_3$-groups at 0.95, -0.89 and -0.40, -0.37 ppm respectively.

The ^{13}C APT spectrum (75.5 MHz) of the complex **C3**, shown in Figure 2, reveals narrow resonances typical for the ligand system: two resonances of *Me*C$_{C5}$ at 11.4 and 13.8 ppm, one doublet of Me_2P at 21.9 ppm ($^1J_{CP}$ = 55 Hz), characteristic four resonances of the Ad-moiety at 30.2 (s), 36.3 (s), 47.5 (d), 54.3 (d) ppm and two doublets at 121.8 and 123.7 ppm (J_{CP} = 13.2 Hz, J_{CP} = 14.3 Hz), which are assigned to the Me*C*$_{C5}$-moiety. The resonance of the *ipso*-carbon atom of the C5-ring was not observed due to the low intensity of the latter. The resonance of the Me_3Si-group appears at 4.7 ppm. The assignment of the methylene group was performed by HMQC spectroscopy; it appears as a doublet of very low intensity at 31.5 ppm with the one-bond ^{13}C–^{89}Y scalar coupling of 41 Hz.

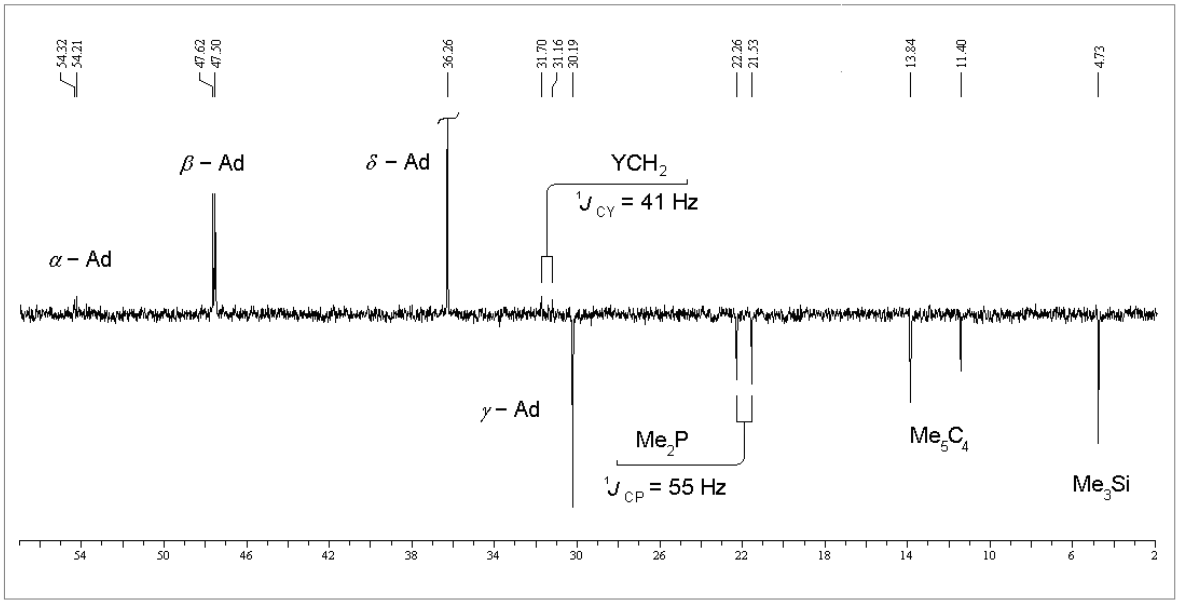

Figure 2. The ^{13}C APT spectrum (75.0 MHz) of the complex [{**L4**}Y(CH$_2$SiMe$_3$)$_2$] (**C3**) dissolved in C$_6$D$_6$ at +25°C.

Although the ^{1}H and high resolution ^{13}C NMR spectra of the paramagnetic neodymium complex **C4** are also showing well resolved picture, the signals assignment was non-trivial. The ^{1}H NMR spectrum of **C4** in C_6D_6 at 25°C (Figure 3) spans the range 30 to -22 ppm and shows narrow resonances for trimethylsilyl groups and almost all ligand protons together with two broad resonances for methylene protons of the silylmethyl groups (Figure 4).

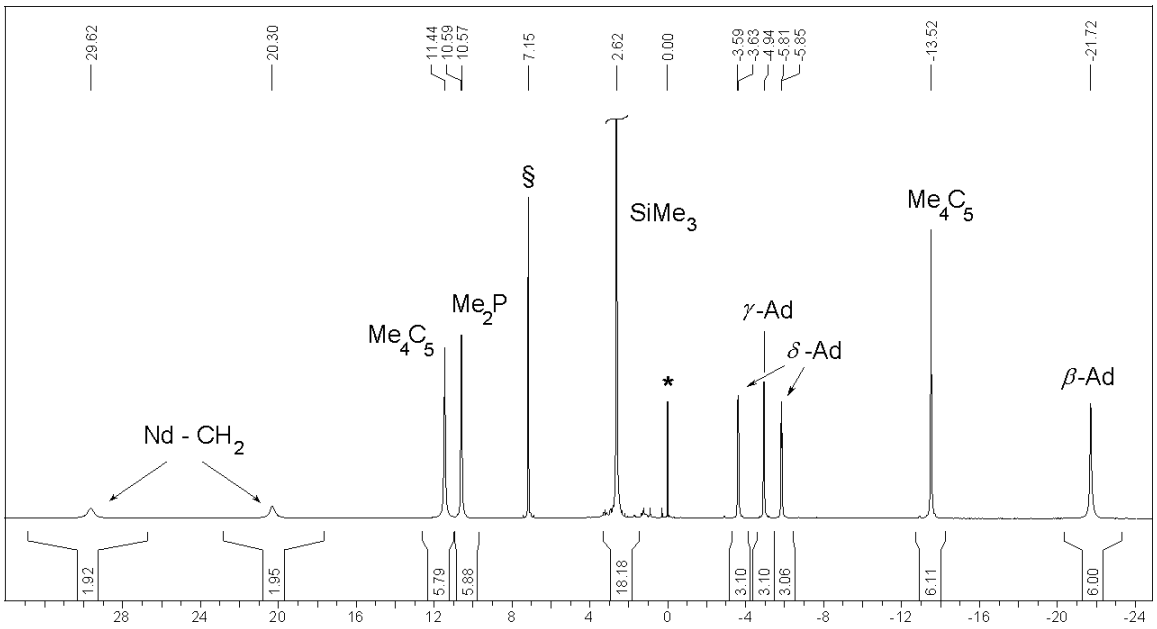

Figure 3. The ^{1}H NMR spectrum (300.1 MHz) of complex [{**L4**}Nd(CH_2SiMe_3)$_2$] (**C4**) dissolved in C_6D_6 at +25°C. Signal denoted with (*) and (§) are assigned to TMS and the residual protons of C_6D_6.

Two sets of methyl protons of Me_4C_5 moiety are low and upfield-shifted (11.45 and -13.52 ppm). This correlates greatly with the proton resonances of methyl groups in closely related homoleptic complex [Nd{C_5Me_4H}$_3$] (16.64 and -16.68 ppm).[6] All resonances of the adamantyl moiety protons are shifted up-field: the diastereotopic geminal *exo*- and *endo*-δ-methylene protons appear at -3.61 and -5.83 ppm respectively as two duplets ($^{2}J_{HH}$ = 11 Hz). The chemical shift of the γ-methyne protons is almost of the same order (-4.94 ppm) due to the nearly same distance to the paramagnetic metal center. The resonance at -21.72 ppm, which has to be assigned to the β-methylene protons (*vide infra*), is somewhat broader ($\nu_{½}$ = ca. 30 Hz). By manual extrapolation of ^{1}H NMR spectrum of the β-methylene protons with two *Gauss*-curves (-21.79 and -21.82 ppm (both $\nu_{½}$ = ca. 30 Hz) the two-bond ^{1}H–^{1}H scalar coupling constant was estimated to be of 10±3 Hz.

The resonances of the Me_3SiCH_2-group are significantly downfield-shifted to the values of 20.4 ($\nu_{½}$ = 84 Hz) and 29.7 ($\nu_{½}$ = 102 Hz) ppm. The comparable deep downfield-shifted resonance (38.23 ppm), however two-bond remote, was reported for the HC_{C5}-proton in the

complex [Nd{C_5Me_4H}$_3$].[6] The extrapolation with *Gauss*-curves give acceptable coupling constant 14±2 Hz for both resonances (Figure 4).

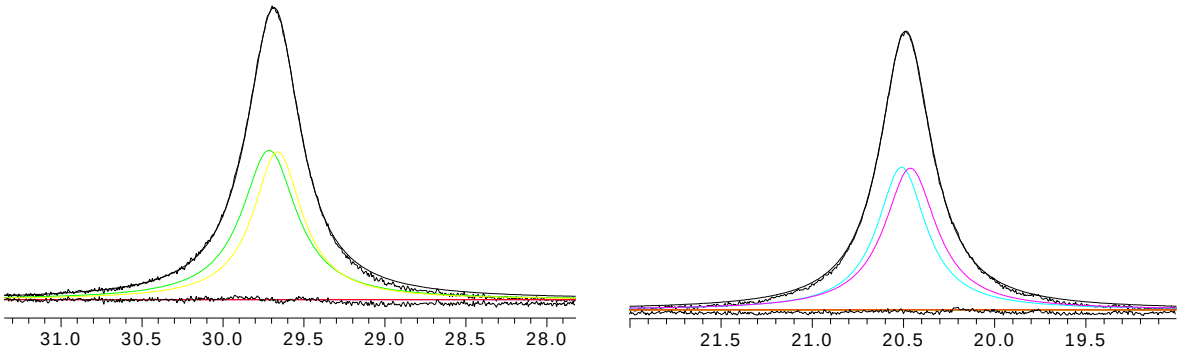

Figure 4. Deconvolution results of ^{1}H NMR (300.1 MHz) silylmethyl proton resonances at 20.4 and 29.7 ppm (both $\nu_{½}$ = ca. 30 Hz) with *Gauss*-curves.

Conformational rigidity in solution at the NMR time scale points out also diastereotopic methylene protons of C*H*$_2$SiMe$_3$-groups. That was accomplished by various temperature ^{1}H and ^{31}P NMR spectroscopy – no significant resonance broadening, but the gradual downfield-migration of resonances was observed down to 190 K.

Interestingly, the ^{31}P resonance of the paramagnetic neodymium complex **C4** (80.1 MHz, C_6D_6) is not broadened, but was observed as a sharp signal at 22.1 ppm.

So far, there is no detailed analysis of the ^{13}C resonance assignment for Nd-organometallics in the literature; hence it was attempted to analyze their distribution on the example of our compound. The high resolution ^{13}C NMR spectrum (125.5 MHz, C_6D_6) of the neodymium complex is depicted in Figure 5. The assignment of resonances was completed by the analysis of 2D HMBC and HMQC spectra (*vide infra*). Thus, there are three narrow resonances at 103.1 (s), 107.3 (d) and 146.2 (s) ppm in the aromatic region, that have been assigned to the C5-ring carbon atoms. The *ipso*-carbon atom of the C5-ring appears as a doublet with the one-bond ^{13}C–^{13}P scalar coupling of 118 Hz.

In the aliphatic region eight well resolved resonances have been observed spanning the region from -40 to 35 ppm. Two pairs of Me-groups of the Me_4C_5-ring are significantly downfield shifted (-37.3 (br s), -15.1), the Ad-group protons appear at -13.1, 19.8, 27.2 and 29.5 ppm, Me-protons of Si*Me*$_3$ and PMe$_2$ groups, which both are three-bond remote from the paramagnetic center, are unusually downfield shifted and appear at 30.6 (SiMe$_3$), 34.9 (d, $^1J_{CP}$ = 53 Hz, *Me*$_2$P) respectively. Unfortunately, the assignment of ^{13}C resonances of the methylene-protons of the CH_2SiMe_3-groups was not possible.

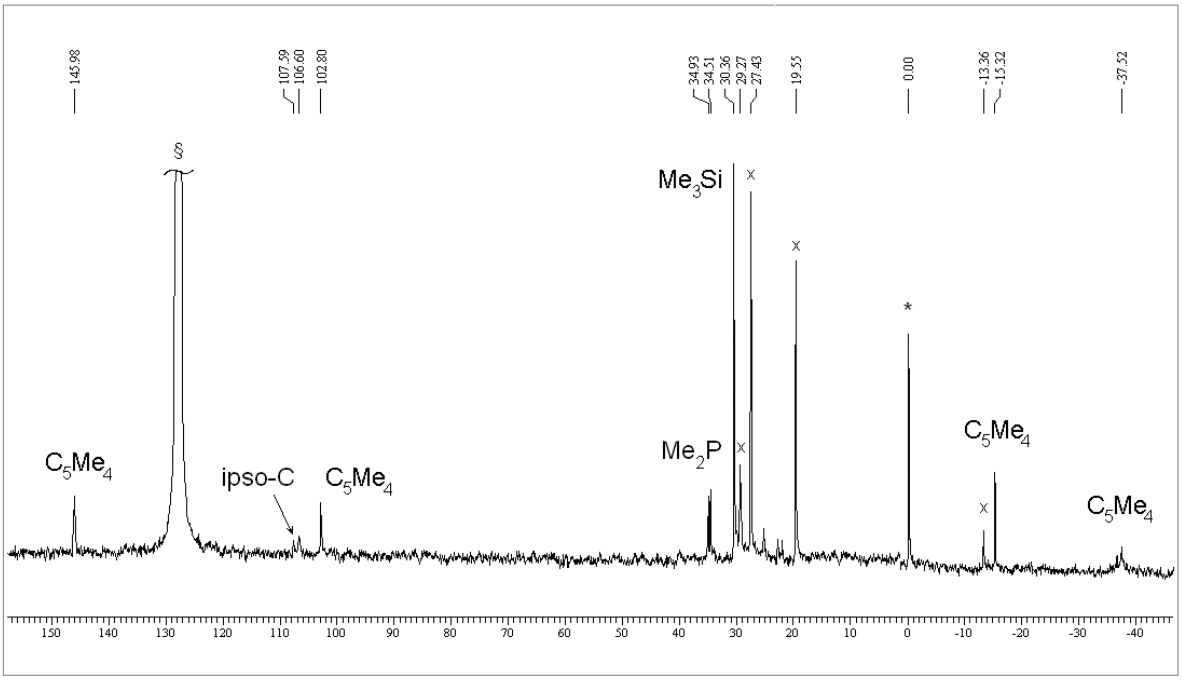

Figure 5. The ^{13}C NMR (125.5 MHz) spectrum of complex [{**L4**}Nd(CH_2SiMe_3)$_2$] (**C4**) dissolved in C_6D_6 at +25°C. Signal denoted with (*) and (§) are assigned to the residual protons of TMS and C_6D_6 respectively. Signal denoted with (x) is assigned to the resonances of 1-adamantyl moiety.

In the HMQC spectrum, shown in Figure 6, the resonance of the $SiMe_3$-group protons correlates with the resonance at 30.4 ppm. Both doublets at -3.61 and -5.83 ppm reveal cross-peaks with a resonance at 27.4 ppm and are the unambiguously assigned of the δ-Ad-group.

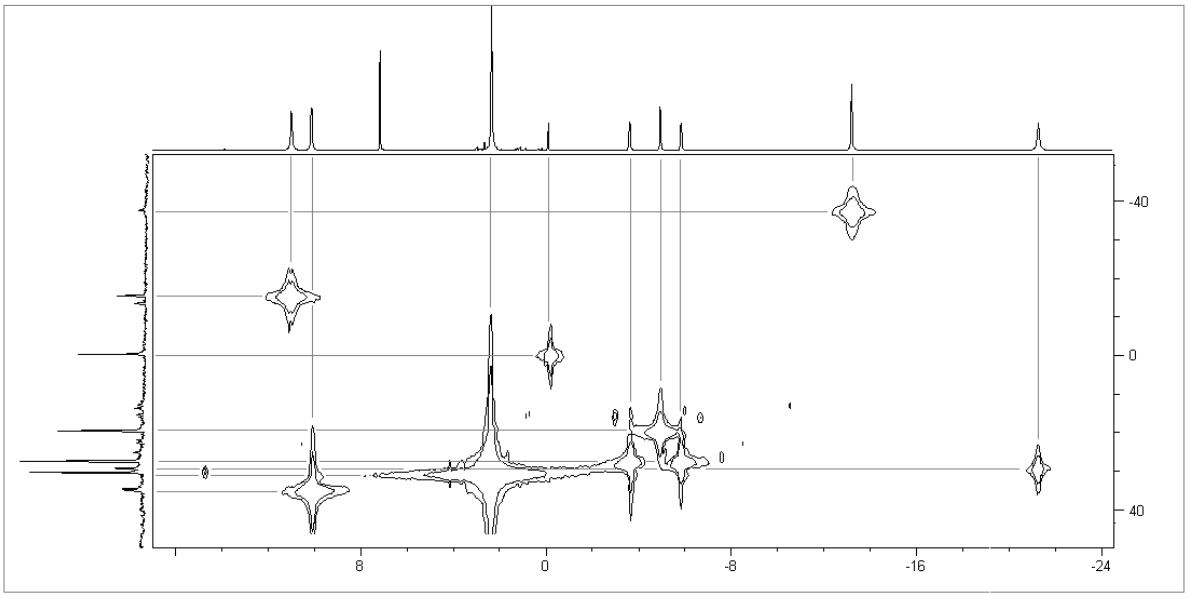

Figure 6. The HMQC spectrum of complex [{**L4**}Nd(CH_2SiMe_3)$_2$] (**C4**) dissolved in C_6D_6 at 25°C. The 1D ^{1}H NMR spectrum (500.1 MHz) is shown at the top and ^{13}C NMR spectrum (125.1 MHz) is shown on the left edge of the contour plot.

The HMBC spectrum showed long range coupling of the α-Ad-carbon atom at -13.36 ppm to β-carbon atom (Figure 7). Finally the resonance at 29.3 ppm has to be assigned to the β-carbon atom. The resonance of the Me-group of the C5-ring at -13.52 ppm shows clear cross-peaks with both the C5-ring carbons. The similar cross-peaks of another Me-group are of very low intensity – only one cross-peak was observed in the spectrum.

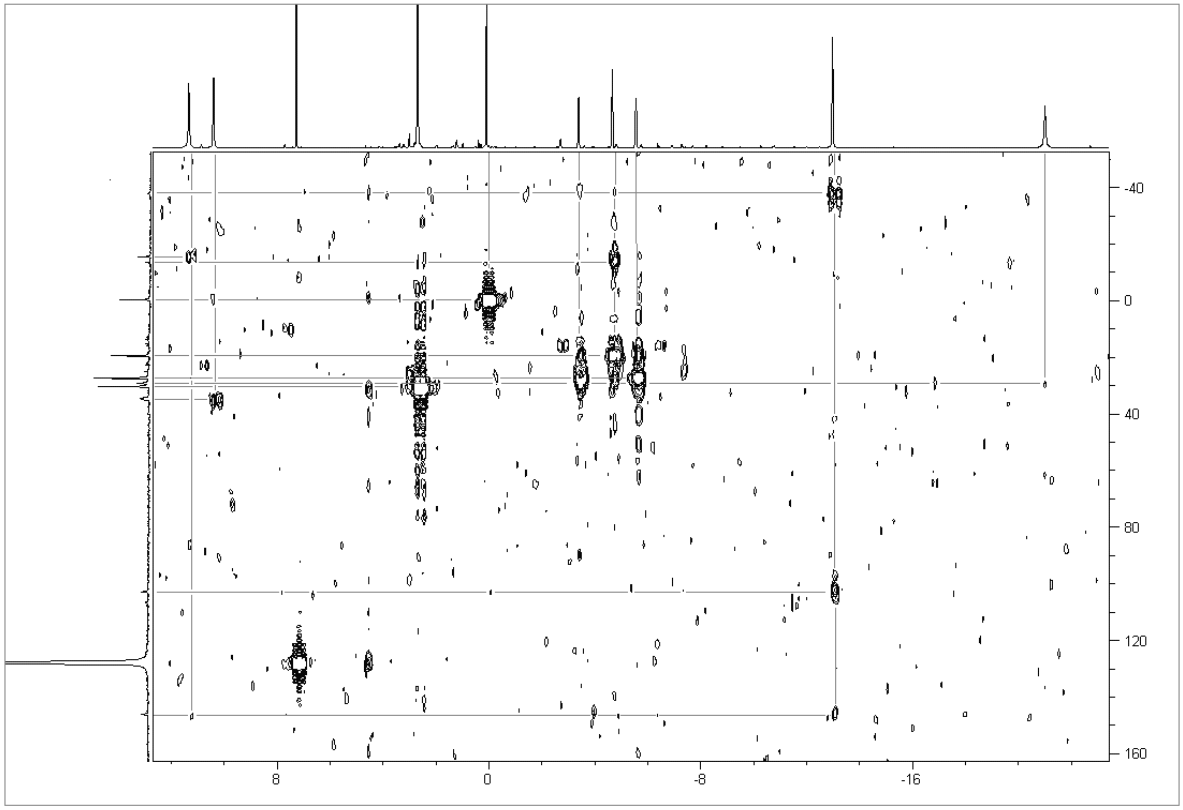

Figure 7. The HMBC spectrum of complex [{**L4**}Nd(CH_2SiMe_3)$_2$] (**C4**) dissolved in C_6D_6 at 25°C. The 1D ^{1}H NMR spectrum (500.1 MHz) is shown at the top and ^{13}C NMR spectrum (125.1 MHz) is shown on the left edge of the contour plot.

2.1.3. *Molecular Structures of* ***C1*** *–* ***C3*** *and Degradation Products of* ***C4***

In the beginning of our studies we were able to synthesize the first *CpPN* type compound $Me_2P(C_5Me_4)NHAd$ (**L4**) and its *CGC* complex [{**L4**}$Lu(CH_2SiMe_3)_2$] (**C1**). Their molecular structures were already reported by us in 2005.[7]

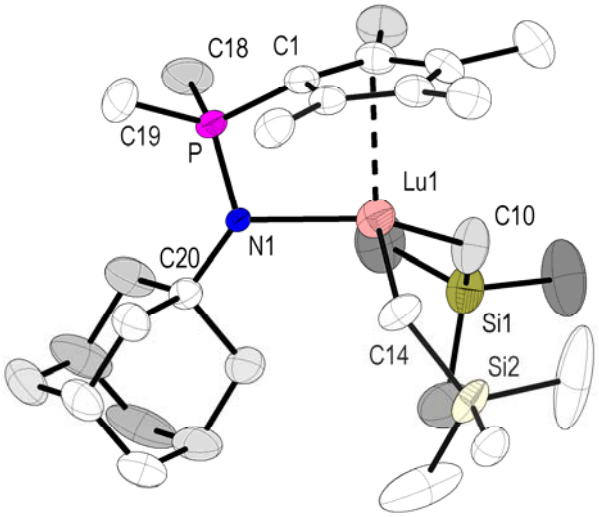

Figure 8. Molecular structure of complex [{**L4**}$Lu(CH_2SiMe_3)_2$] (**C1**). All hydrogen atoms have been omitted for clarity. Selected bond lengths (Å) and angles (°): P–C1 1.774(4), P–C17 1.812(6), P–N1 1.600(3), N1–C20 1.486(5), Lu1–C1 2.545(4), Lu1–Z 2.343(4), Lu1–N1 2.278(3), Lu1–C10 2.360(4), Lu1–C14 2.358(5), C1–P–N1 101.2(2), C1–Lu1–N1 65.2(1), N1–Lu1–Z 93.4(1), P–N1–C20 128.2(2), Lu1–N1–C20 128.0(2), P–N1–Lu1 103.7(2), N1–Lu1–C14 109.9(2), N1–Lu1–C10 115.8(2), C14–Lu1–C10 109.9(2), Lu–C10–Si1 136.6(3), Lu1–C14–Si2 126.9(2), C1–P–N1–Lu1 8.2(2).

A comparison of structures of the ligand **L4** and its complex **C1** underlines an increase of the aromatic character of the C_5Me_4 moiety coordinated to the lutetium atom: the difference in C–C bond lengths within the C_5Me_4 ring is 0.06 Å for **L4** and 0.04 Å for **C1**. The P–C_{Me} and N–C_{Ad} bonds are almost the same as in the free ligand and only 0.01 Å longer in **C1** than in **L4**. The P–C_{C5} bond in **C1** is 0.05 Å longer than in **L4**, whereas the P–N bond in **C1** is almost the same value (0.06 Å) shorter than in **L4**. The rather short Lu–N bond (2.278(3) Å) is much closer to the covalent Lu–N bond lengths (2.21 Å) than to the donor-acceptor ones (2.48 Å) found in the crystal structures of analogous lutetium complexes [{η^5-C_5Me_5}-$Lu(NHDip)CH_2SiMe_3(bipy)$] and [{$\eta^5$-$C_5Me_5$}$Lu(bipy)(NHDip)_2$].[8] The Lu–Z (2.33 Å) and the average Lu–CH_2 (2.36 Å) bond lengths lie in the typical range of lutetium η^5-C_5Me_5 and σ-alkyl moieties.[8]

The 101.2° value of the N–P–C_{C5} angle is slightly larger than that of *CpSiN*-type complexes found, for example, in the structure of ytterbium complex [{η^5,η^1-$Me_2Si(C_5Me_4)N$-^{t}Bu}Yb{$CH(SiMe_3)_2$}] (96.2(2)°).[9]

In combination with the relatively small atomic radius of lutetium, a more open coordination sphere and as a consequence a small but probably nonbonding P···Lu distance (3.08 Å) about 0.7 Å shorter than the sum of the *van der Waals* radii of these elements (3.80 Å)[10] is observed.

The molecular structures of complexes [{**L4**}$M(CH_2SiMe_3)_2$] (M = Sc (**C2**) and Y (**C3**) are rather similar (Figure 1). The complexes **C2** and **C3** crystallize in the monoclinic space groups $P2_1/c$ and $P2_1/n$ respectively with four molecules in the unit cell. In the structure of the complex **C2** the silylmethyl groups are disordered.

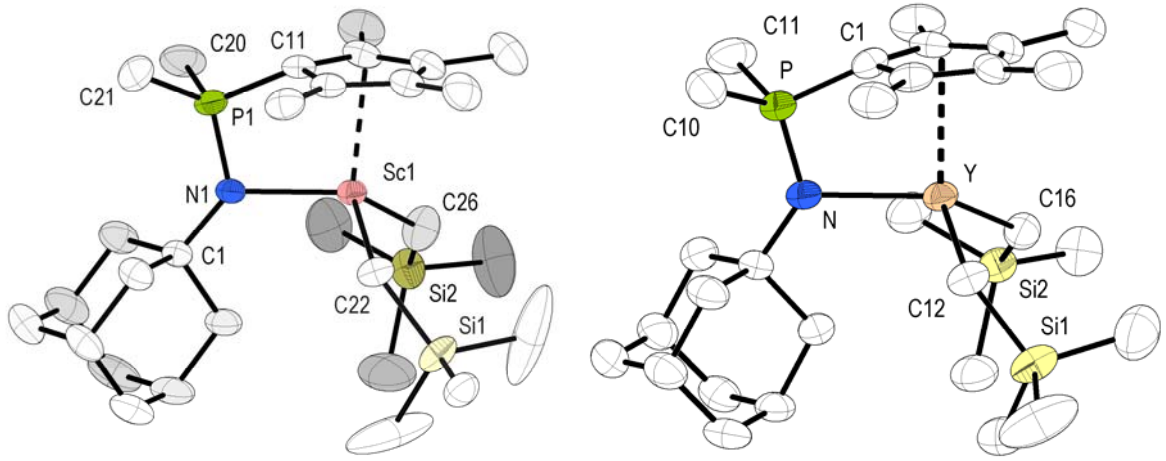

Figure 9. Molecular structures of scandium and yttrium complexes [{**L4**}$M(CH_2SiMe_3)_2$] (M = Sc (**C2,** left), Y (**C3**, right)). All hydrogen atoms have been omitted for clarity. Disordered Me_3SiCH_2-groups with lower occupancies in molecular structure of **C2** have been also omitted. Selected bond lengths (Å) and angles for **C2**: Sc1–N1 2.185(2), Sc1–C11 2.431(2), Sc1–Z 2.235(4), Sc1–C22 2.243(3), Sc1–C26 2.234(3), P1–N1 1.606(2), P1–C1 1.769(3), C11–Sc1–N1 68.0(1), N1–Sc1–Z 97.58(5), C11–P1–N1 101.1(1),C20–Sc1–N1 108.4(1), C21–Sc1–N1 114.6(1), C20–Sc1–C21 107.5(1), Sc1–C22–Si1 128.0(1), Sc1–C26–Si2 139.1(2), Sc1–N1–P1–C11 7.3(1); for **C3**: Y–N1 2.316(4), Y–C1 2.599(3), Y–Z 2.392(5), Y–C12 2.416(5), Y–C16 2.434(5), P1–N1 1.605(4), P1–C1 1.753(6), C1–Y–N1 63.3(1), Z–Y–N1 91.5(1), C12–Y–N1 106.6(2), C16–Y–N1 118.5(2), C12–Y–C16 111.6(2), Y–C12–Si1 124.6(2), Y–C16–Si2 132.4(2), Y–N–P–C1 2.1(2).

In the solid state **C2** and **C3** adopt mononuclear structures, in which metal atoms are approximately in tetrahedral coordination. The average bond length of P–C_{C5} in the complexes **C2**, **C3** are longer as in the free ligand (1.724(2) Å) and span the range 1.753 –

1.774 Å. The P–N bonds are essentially shorter (1.600 – 1.623 Å) than in the ligand (1.659(2) Å).

The Sc–N bond length of 2.185 Å is also closer to the covalent bonds represented by [{η^5,η^1-$Me_2Si(C_5Me_4)NCMe_3$}$Sc(\mu\text{-}Pr)_2]_2$[11] (2.083(5) Å) and [$Sc\{N(SiMe_3)_2\}_3$][12] (2.049 Å) than those in donor-acceptor complexes (2.456 Å in [{$Me_3SiN(CH_2CH_2NSiMe_3)_2$}-ScCl(thf)],[13] 2.467 Å in [{Me_3TACN}$Sc(CH_2SiMe_3)_3$] and av. 2.333 Å in [{Me_3TACN}$ScCl_3$][16]).The average Sc–C bond length of 2.236(6) Å lies the typical Sc–C(sp^3) bond length region (av. 2.215(10) Å in [{η^5-$C_5H_3(SiMe_3)_2$}$Sc(CH_2SiMe_3)_2$(thf)],[14] 2.252 Å [{η^5-C_5Me_5}$ScMe_2${$OP(CMe_3)_3$}][15] and av. 2.279 Å in [{Me_3TACN}-$Sc(CH_2SiMe_3)_3$][16])

In the structure of the yttrium complex [{**L4**}$Y(CH_2SiMe_3)_2$] (**C3**) the centroid(Z)–Y distance of 2.235(4) Å is almost equal to those ones in [{C_5Me_5}$ScMe_2${$OP(CMe_3)_3$}] (2.210(1) Å)[15] and in [{η^5,η^1-$Me_2Si(C_5Me_4)NCMe_3$}$Sc(\mu\text{-}Pr)_2]_2$ (2.196(1) Å).[11] The Y–N bond of 2.316(4) Å is short and also like in structures **C1** and **C2** approach the length of "pure" Y–N amide bonds. The average lengths of the amidic Y–N bond of 2.207 Å was found in [$Y(TMP)_3$],[17] 2.224 Å in [$Y\{N(SiMe_3)_2\}_3$][18] and 2.250 Å in [{η^5-C_5H_5}$_2$Y(μ-$NPPh_3)_2Y(\eta^5$-$C_5H_5)(\eta^1$-$NPPh_3)$].[19] The length of a donor-acceptor bond can be demonstrated by an average value of 2.63(7) Å determined in [{*iso*-Pr_2TACN-$CH_2CH_2N^tBu$}$Y(CH_2SiMe_3)_2$].[20]

Our attempts to get single crystals of the neodymium complex [{**L4**}$Nd(CH_2SiMe_3)_2$] (**C4**) using different ways of crystallization from a saturated toluene solution failed. Instead

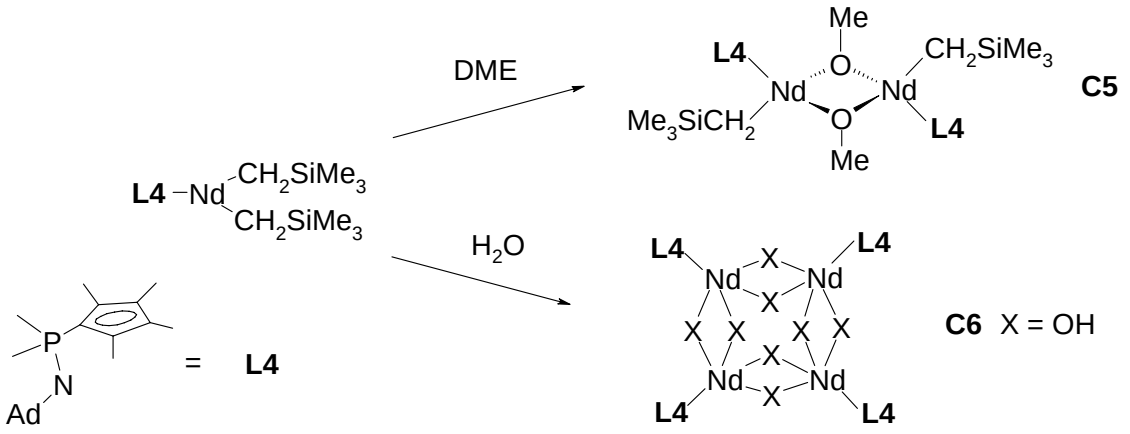

Scheme 5. Degradation pathways of complex [{**L4**}$Nd(CH_2SiMe_3)_2$] (**C4**) leading to the formation of hydroxy- (**C6**) and mixed alkyl/methoxy lanthanide complex (**C5**) .

small crops of crystalline materials of a different composition as established by X-ray diffraction analysis have been obtained. Thus, a DME-degradation product **C5** and a hydrolysis product **C6** has been identified (Scheme 5).

The complex [{**L4**}Nd(CH_2SiMe_3)(μ^2-OMe)]$_2$ (**C5**) crystallizes in the triclinic space group $P\bar{1}$ with two molecules of toluene per unit cell. The X-ray diffraction analysis reveals that the compound possesses centrosymmetrical binuclear structure. The molecular structure of the compound is depicted in Figures 10 and 11. In the binuclear structure of complex **C5** the neodymium atoms adopt a distorted trigonal bipyramidal coordination *via* two bridging MeO-groups. The distance between the neodymium atom and the plane, defined by atoms C22, O1' and the centroid of the C5-ring (Z) is of 0.0896(2) Å. The *CpPN*-ligands are coordinated in the η^5,η^1-mode. The bridging oxygen atoms of the MeO-groups form an ideal square parallelogram. All ligands in the molecule have transoid conformation. The whole molecule is symmetrically arranged around a crystallographic inversion center. The Nd1–C22 bond length (2.544(6) Å) lies in the typical Nd–C(sp^3) bond lengths region and is comparable with those found in the complex [{η^5-C_5Me_5}$_2$NdCH($SiMe_3$)$_2$],[21] (2.515 Å) and [{Me_2TACN-$(CH_2)_2$-N(*tert*-Bu)}Nd(CH_2SiMe_3)$_2$][22] (2.557, 2.569 Å). The compound [{Me_2TACN-Si$(Me)_2$-N(*tert*-Bu)}Nd(CH_2SiMe_3)$_2$][22] contain two types of Nd–N bonds – with the amido moiety (*d*(Nd–N) = 2.320 Å) and with pure σ-donor (*d*(Nd–N) = 2.664 –

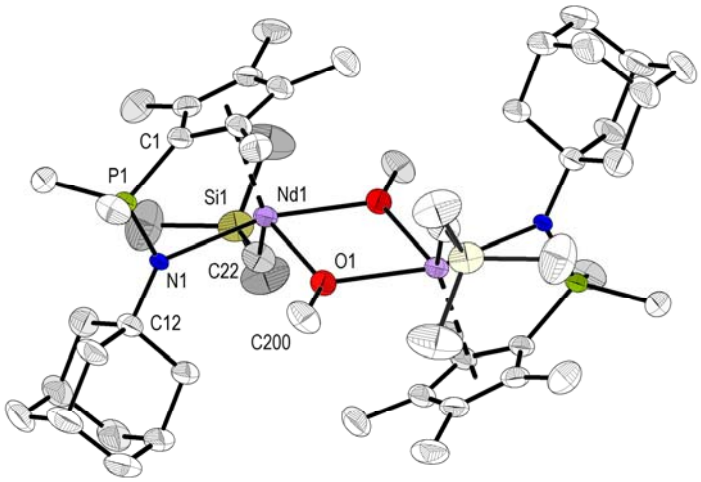

Figure 10. Molecular structure of binuclear neodymium complex [{**L4**}Nd(CH_2SiMe_3)(μ^2-OMe)]$_2$ (**C5**): view along the *pseudo*-C_2 axis (left), views of the Nd_2O_2-core (left up and down). All hydrogen atoms and Ad-groups have been omitted for clarity. Selected bond lengths (Å) and angles (°): Nd1–C22 2.544(6), Nd1–N1 2.509(4), Nd1–Z 2.554(1), Nd1–C1 2.705(5), P1–N1 1.604(4), C1–P1 1.773(4), Nd1–O1 2.319(3), Nd1–O1' 2.378(3), O1–C200 1.427(7), C10–P1–C11 100.4(3), O1–Nd1–O1' 69.5(1), 110.5(1), Z–Nd1–N1 86.8(1), C1–Nd1–N1 60.5(1), C1–P1–N1 102.3(2).

2.771 Å) nitrogen atoms. In the complex **C5** the Nd1–N1 bond length of 2.509(4) Å and is positioned essentially between both limiting values.The Nd–O bonds have slightly different lengths of 2.319(3) and 2.378(3) Å. These values lie in the range between typical Nd–O covalent bond length and pure donor-acceptor one. For example, in [{2,6-(*tert*-Bu)-4-MeC_6H_2O}$_2$Nd(CH_2SiMe_3)(thf)$_2$][23] an av. Nd–O covalent bond length is of 2.231(5) Å and the av. Nd←$O_{(thf)}$ bond length is of 2.494(5) Å, in [{$(Me_3Si)_2C(CMe_2OMe)$}Nd(μ^2-OMe)I]$_2$ the bridging Nd–O bond lengths are of 2.050(8) and 2.233(7) Å and the Nd←O bond lengths are of av. 2.485(10) Å).[24]

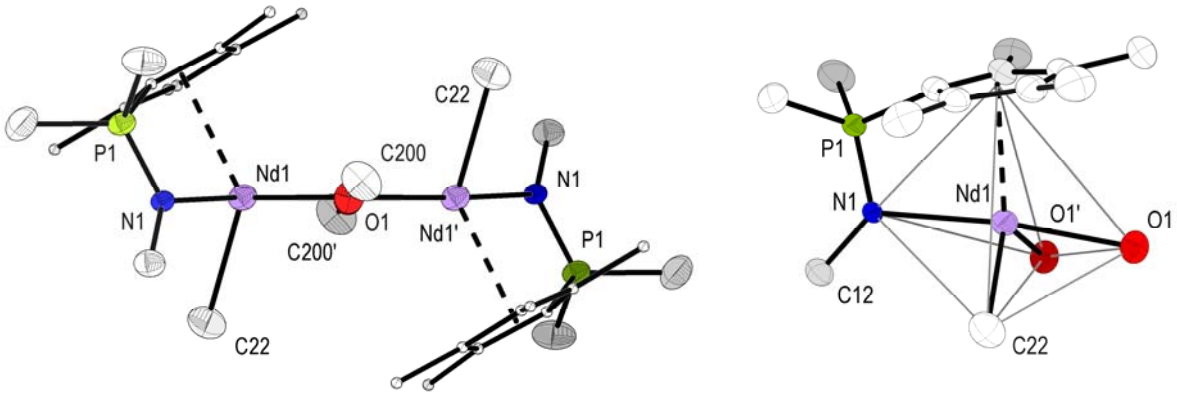

Figure 11. Molecular structure of binuclear complex [{**L4**}Nd(CH_2SiMe_3)(μ^2-OMe)]$_2$ (**C5**): View along the *pseudo*-C_2 axis (left), views of the Nd_2O_4-core (left up and down). All hydrogen atoms and Ad-groups have been omitted for clarity Selected angles and torsion angles (°): N1–Nd–O1 91.8(1), N1–Nd1–O1' 161.3(2), N1–Nd1–C22 97.7(2), O1–Nd–C22 115.0(2), O1–Nd1–Z 118.1(2), C22–Nd1–Z 126.5(2), C1–P1–N1–Nd 5.0(2), Nd1···Plane [Z,C22,O1'] 0.0896(2).

The complex [{**L4**}Nd(μ^2-OH)$_2$]$_4$ (**C6**) also crystallizes in the triclinic space group $P\bar{1}$ with one asymmetric unit ($Z = 2$) in the unit cell. Twelve toluene molecules are present in the cell unit. The molecular structures are depicted in Figure 12. According to the X-ray diffraction analysis the complex adopts an asymmetric tetra-nuclear arrangement of the neodymium atoms, which is nearly square planar. The maximal deviation of the neodymium atoms from a idealized plane formed by the four atoms is small (Δ_{max} = ±0.053(1) Å). The neodymium atoms adopt a distorted octahedral arrangement and are interconnected *via* eight bridging μ-OH-ligands forming a Nd_4O_8-core; additionally, the ligand molecules occupy the apical positions and are coordinated in the typical η^5,η^1-mode. The *CpPN*-ligands around the neodymium atoms are arranged in an *up*- and *down*-manner, so that the tetra-nuclear unit of the complex C**6** has a non-crystallographic *pseudo*-C_2 axis. As a result, the bridging hydroxy groups are tilted. This tetrameric core was also found for a closely related *tris*-(alkoxy)-

neodymium complex $[\{\eta^1\text{-NepO}\}Nd(\mu\text{-NepO})_2]_4$ [25,26] (Nep = *neo*-pentyl) obtained by protolysis of $[Nd\{N(SiMe_3)_2\}_3]$ with 3 equiv *neo*-pentyl alkohol. The average Nd···Nd distance in **C6** (3.85(1) Å) is slightly longer than in the above mentioned tetranuclear *tris*-(alkoxy)-neodymium complex (av. 3.74 Å).

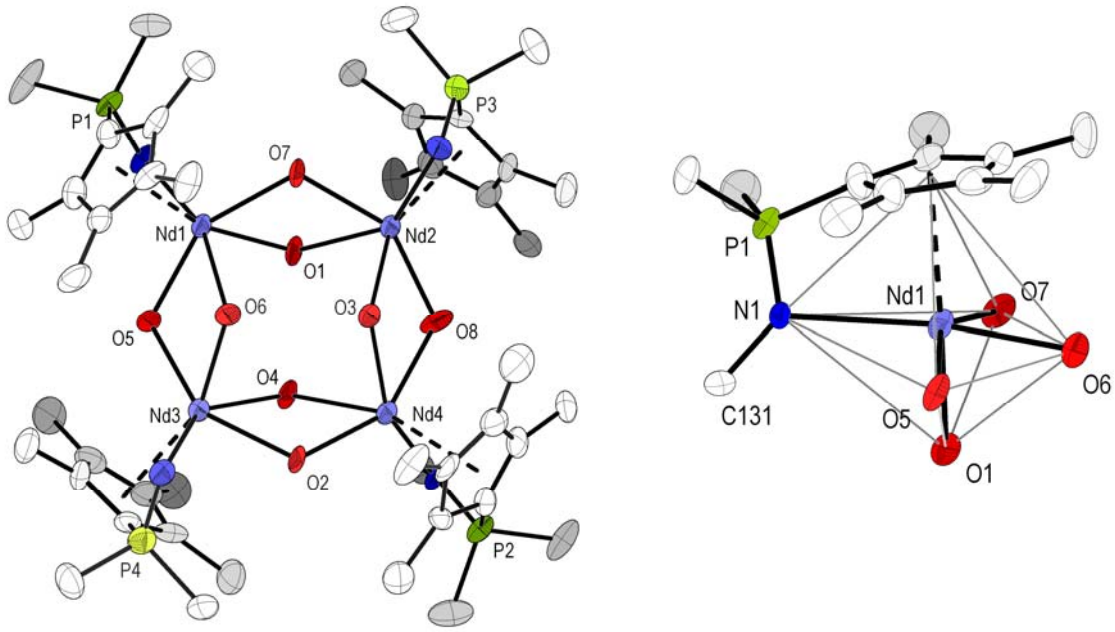

Figure 12. Molecular structure of tetranuclear neodymium complex $[\{\mathbf{L4}\}Nd(\mu^2\text{-OH})_2]_4$ (**C6**): view along the *pseudo*-C_2 axis (left), views of the Nd_4O_8-core (left up and down). All hydrogen atoms and Ad-groups have been omitted for clarity. Nd1–N2 3.871(1), Nd2–Nd4 3.846(1), Nd4–Nd3 3.858(2), Nd3–Nd1 3.825(1), P1–N1 1.570(1), P2–N2 1.585(1), P3–N3 1.570(1), P4–N4 1.601(1), P1–C102 1.746(1), P2–C203 1.744(1), P3–C302 1.755(1), P4–C401 1.773(1), Nd1–O7 2.365(1), Nd1–O1 2.374(1), Nd1–O6 2.388(1), Nd1–O5 2.353(1), Nd2–O1 2.391(1), Nd2–O7 2.366(1), Nd2–O3 2.349(1), Nd2–O8 2.332(1), Nd3–O2 2.385(1), Nd3–O4 2.355(1), Nd3–O5 2.342(1), Nd3–O6 2.334(1), Nd1–O1–Nd2 108.6(1), Nd1–O7–Nd2 109.8(1), Nd2–O3–Nd4 108.0(1), Nd2–O8–Nd4 110.8, Nd3–O4–Nd4 109.0(1), Nd3–O2–Nd4 109.5(1), Nd1–O5–Nd3 109.1(1), Nd1–O6–Nd3 108.2(1).

The Nd–O bond lengths span the range of 2.332(1) – 2.405(1) Å and are in good agreement with those ones found in the binuclear neodymium complex $[\{Phen\}_3Nd(\mu^2\text{-OH})]_2I_4\times 2Py$[27] (2.298 – 2.361 Å), in centrosymmetric complexes $[\{tert\text{-}BuC_5H_4\}_2Nd(\mu^2\text{-OH})]_2$,[28] (2.328, 2.330 Å) and $[\{H_2NCH_2CH_2NH_2\}_3Nd(\mu^2\text{-OH})]_2[Sn_2S_6]$[29] (2.325 and 2.355 Å) and also in tetra-nuclear *tris*-(alkoxy)-neodymium complex $[\{\eta^1\text{-NepO}\}Nd(\mu^2\text{-NepO})_2]_4$ (av. 2.34 Å). The P–N bond lengths span the range from 1.570(1) – 1.601(1) Å. The Nd–(μ^2-O)–Nd' angles lie in the narrow region of 108.2(1) – 110.8(1)° revealing sp^3-hybridization of the O-atoms. All other parameters of the ligand are unexceptional.

2.1.4. *Synthesis of Complexes with Ligand* ***L6***

After the successful synthesis of rare-earth metal dialkyl complexes **C1** – **C4** with sterically demanding ligand $Me_2P(C_5Me_4)NHAd$ (**L4**), it was set out to explore coordination chemistry of the less strained system. For this purpose the compound $Ph_2P(C_5H_4)NHDip$ (**L6**), which can be readily synthesized on a multi-gram scale, was chosen.

Decreased basicity and less steric bulkiness of the C5-ring resulted in formation of complexes with expected geometry only in the case of metals with small ionic radius (Sc, Lu). For the middle (Y) and early (Nd) lanthanides formation of complexes with coordinated solvent molecule (THF) was observed. Solvent decomposition products were also obtained and crystallographically characterized.

The typical synthetic procedure for complex synthesis consists in slow addition of 3 equiv of $LiCH_2SiMe_3$ dissolved in hexane to a stirred suspension of THF-solvated lanthanide trichloride and the ligand $Ph_2P(C_5H_4)NHDip$ (**L6**) in Et_2O at 0°C (Scheme 6). After the complete removal of solvent and extraction of solid residue with hexane followed by crystallization at low temperatures complexes **C7** – **C11** were obtained as analytically pure crystalline solids. It was found that the complexes with small ionic radii – Sc and Lu – did not have any coordinated ether molecules [{**L6**}$M(CH_2SiMe_3)_2$] (M = Sc (**C7**), Lu (**C8**)).

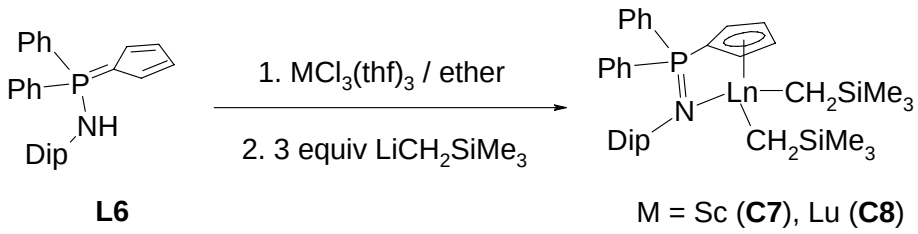

L6 M = Sc (**C7**), Lu (**C8**)

Scheme 6. Synthesis of complexes [{**L6**}$Ln(CH_2SiMe_3)_2$] (Ln = Sc (**C7**) and Lu (**C8**)).

The enhanced thermostability of these complexes is striking – they could be stored under inert atmosphere at 25°C without decomposition for at least 6 months; quick decomposition takes place at temperatures >100°C.

The complexes of yttrium and neodymium, [{**L6**}Ln(CH_2SiMe_3)$_2$(thf)] (Ln = Y (**C9**), Nd (**C10**)), having larger rare-earth metals crystallize with one coordinated THF molecule (Scheme 7). Obviously, the solvent molecule is retained from the solvated lanthanide source used. In contrast to the solvent-free complexes both are

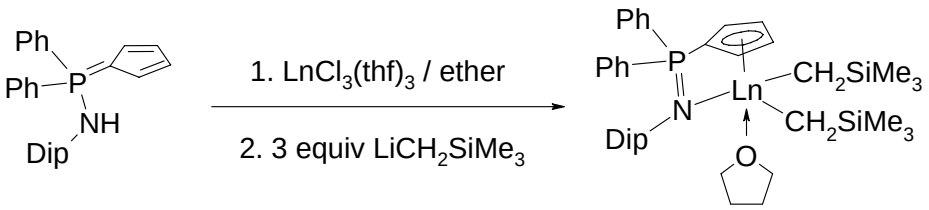

L6 Ln = Y (**C9**), Nd (**C10**).

Scheme 7. Synthesis of complexes [{**L6**}Ln(CH_2SiMe_3)$_2$(thf)] (Ln = Y (**C9**) and Nd (**C10**)).

less thermostable, presumably due to the ether-cleavage of the coordinated solvent molecule. All diamagnetic complexes were characterized by multinuclear NMR spectroscopy. The complexes **C9**, **C10** reveal unsatisfactory elemental analyses that presumably can be explained by their decomposition at ambient temperature. The complexes **C7**, **C9** and **C10** were also characterized by single crystal X-ray spectroscopy.

Easer decomposition of THF containing complexes is not unusual in the lanthanide chemistry.[30] The better results could be obtained *via* refuse of the use it as a (co)solvent or component of the lanthanide source or by use of other ethers such as Et_2O, DME.

The original goal was to find out whether an yttrium complex without coordinated THF molecule [{**L6**}Y(CH_2SiMe_3)$_2$] can be isolated. For this purpose the DME-solvated yttrium trichloride [YCl_3(dme)$_2$] was chosen as a metal source for the synthesis.

This DME-solvated yttrium trichloride [YCl_3(dme)$_2$] was first obtained as a by-product in the reaction of mixed yttrium complex [$Y_3(OCMe_3)_7Cl_2$(thf)] with [$AlMe_3$].[31] Though this DME-solvated yttrium trichloride is even crystallographically characterized, there are no described examples of its application in organometallic synthesis.

The synthesis of the starting [YCl_3(dme)$_2$] was performed as described for its THF-analogue. An exothermic reaction takes place at the addition of $SOCl_2$ to a slurry of [$YCl_3(H_2O)_6$] in DME. The composition of thus obtained compact crystalline solid was identified by elemental analysis. Unlike to [YCl_3(thf)$_3$] the coordinated DME cannot be removed from [YCl_3(dme)$_2$] in HV at ambient temperature that makes it superior as a stoichiometric metal source starting material.

The treatment of a mixture $[YCl_3(dme)_2]$ and the ligand **L6** with $LiCH_2SiMe_3$ proceeded in the mixture of ether/hexane. After filtration and removal of the solvent, extraction with hexane and crystallization a crystalline product was obtained in less than 2% yield. The crystals of high quality were further analyzed by single crystal X-ray spectroscopy. It was shown that the crystallized material is not the dialkyl complex, rather than a binuclear, mixed monoalkyl-/methoxy one $[\{\mathbf{L6}\}Y(\mu^2\text{-OMe})(CH_2SiMe_3)]_2$ (**C11**) with both yttrium atoms bridged by the methoxy groups (*vide infra*). In general, it is known that alkyllithium species (*n-/sec-/tert*-BuLi) decompose easier in DME than in THF[32] and therefore this result was not surprising.

The formation of the yttrium-alkoxy complex **C11** can be rationalized by enhanced *Lewis*-acidity of a proposed coordinativly unsaturated intermediate $[\{\mathbf{L6}\}Y(CH_2SiMe_3)_2(dme)_x]$ (x = 0.5 or 1) where an intra-molecular cleavage of a coordinated DME molecule by highly basic silylmethyl ligands takes place (Scheme 8). Existence of other intermediates, such as $[\{\eta^5\text{-}\mathbf{L6}\}Y(CH_2SiMe_3)_2(\kappa^1,\kappa^1\text{-dme})]$ or binuclear complex with bonding DME-molecule $[\{\eta^5,\eta^1\text{-}\mathbf{L6}\}Y(CH_2SiMe_3)_2]_2\{\mu\text{-}(\kappa^1,\kappa^1\text{-dme})\}$, cannot be excluded. The formation of vinylmethyl ether was not investigated.

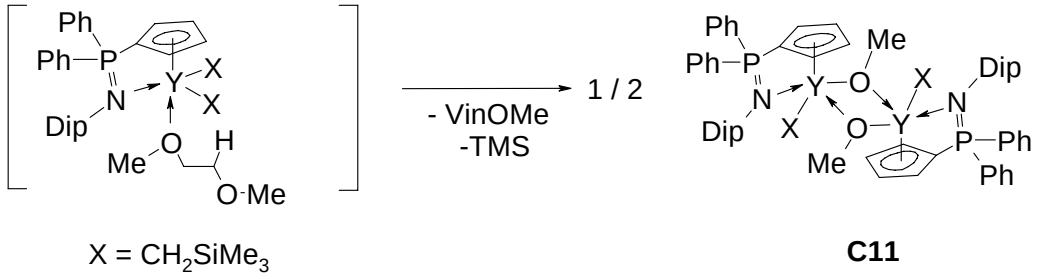

Scheme 8. Decomposition of "$[\{\mathbf{L6}\}Y(CH_2SiMe_3)_2(dme)]$" to the binuclear methoxy-/alkyl-yttrium complex $[\{\mathbf{L6}\}Y(\mu^2\text{-OMe})(CH_2SiMe_3)]_2$ (**C11**).

Although the preparative synthesis of **C11** could be performed by the treatment of the mixture containing ligand **L6**, $[YCl_3(dme)_2]$ and NaOMe in equimolar amounts with 2 equiv of $LiCH_2SiMe_3$, this protocol was not followed. It is known from the literature that even apparently simple reactions with low alkoxides can deliver several species. For example, from the reaction of $[\{\eta^5\text{-}C_5Me_5\}_2YCl(thf)]$ with MeONa or MeOK apart of desired complex $[\{\eta^5\text{-}C_5Me_5\}_2Y(\mu^2\text{-OMe})]_2$ four further different species were isolated and crystallographically characterized.[33] Moreover, it was found that the products distribution depends on many factors such as alkali metal used in the methoxide, its preparation method and particular reaction conditions.

2.1.5. *NMR Spectroscopy of Complexes **C7** – **C9***

The ^{31}P NMR spectroscopy of complexes **C7**, **C8** and **C9** reveals single sharp resonances with the chemical shifts of 12.1, 9.6 and 11.3 ppm respectively. This values are in a good agreement with those found in the complexes **C1** – **C3** having the ligand **L4**.

The ^{1}H NMR spectrum of lutetium complex [{**L6**}Lu(CH_2SiMe_3)$_2$] (**C8**) at ambient temperature, shown in Figure 13, exhibits one sharp resonance at -0.59 ppm for methylene protons of the silylalkyl groups and a somewhat broadened doublet ($\nu_{½}$ = 8 Hz, $^{2}J_{HH}$ = 6.7 Hz) for the protons of the Me_2CH-group at 0.76 ppm. Unlike to the complexes **C1** – **C4**, which reveal an AB-pattern for CH_2–M protons and adopt the frozen conformations in solution, the complex **C8** reveals a low barrier of rotation around the M–CH_2 bond. For such behaviour, the diminished steric bulkiness of the C5-ring, compared to the C_5Me_4-group, should be responsible.

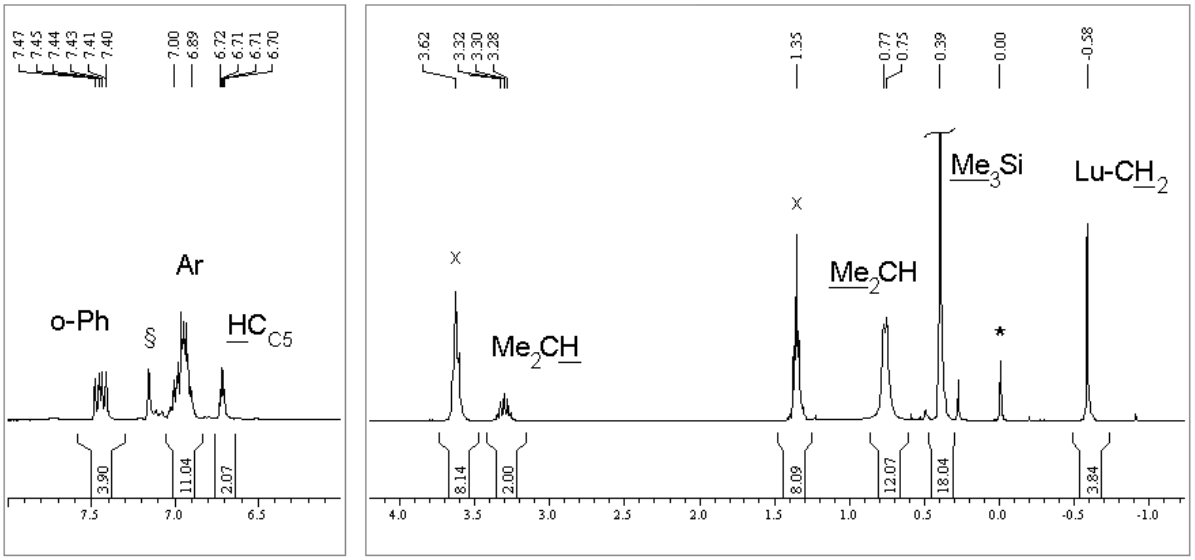

Figure 13. ^{1}H NMR spectrum (300 MHz) of complex [{**L6**}Lu(CH_2SiMe_3)$_2$] (**C8**) dissolved in C_6D_6 at +25°C. The signals denoted with (§), (*) and (x) are assigned to the residual protons of C_6D_6, TMS and uncoordinated THF.

The ^{13}C NMR spectrum of this complex is unexceptional, showing sharp signals for all carbon atoms permitting easy assignment. The Lu–CH_2 groups appear as a single resonance at 39.1 ppm.

The ^{1}H NMR spectrum of the yttrium complex [{**L6**}Y(CH_2SiMe_3)$_2$(thf)] (**C9**) clearly shows direct coordination of ligand, together with the silylmethyl ligands, which are splited with the typical one-bond ^{1}H–^{89}Y scalar coupling of 2.7 Hz.

In the ^{13}C NMR spectrum one distinct resonance for Y–$\underline{C}H_2$ was observed. The resonance appears as a doublet at 31.9 ppm with characteristic one-bond ^{13}C–^{89}Y scalar coupling of 40 ppm. No noticeable dissociation of the coordinated THF-molecule was observed in this solvent; the THF resonances appear at 24.9 and 70.1 ppm (uncoordinated THF: $\delta(^{13}C)$ = 25.72, 67.80 ppm).[34]

Surprisingly, the ^{1}H NMR spectrum of the related scandium complex **C7** is rather unusual (Figure 13). In the aliphatic region a downfield shifted broad resonance with integral ratio of only six and a complex overlapped broad resonances in the region from 0.1 – 0.4 ppm are observed. The only well resolved resonances were observed at 3.41 ppm (septet) and in the aromatic region. This indicates the presence of the *iso*-Pr-, Ph- and Dip-groups. First, we supposed that decomposition of the complex took place. Carefully repeated synthesis gave us a crystalline solid with the similar yield and same appearance. The NMR spectroscopy reveals the same chemical shifts for the complex. This adds evidence that obtained resonances in the spectrum for this compound are not an artefacts.

As a result of the manual deconvolution, depicted in Figure 14, one can show that the Me-group resonance appears as a shoulder on the sharp resonance of Me_3Si-groups that also

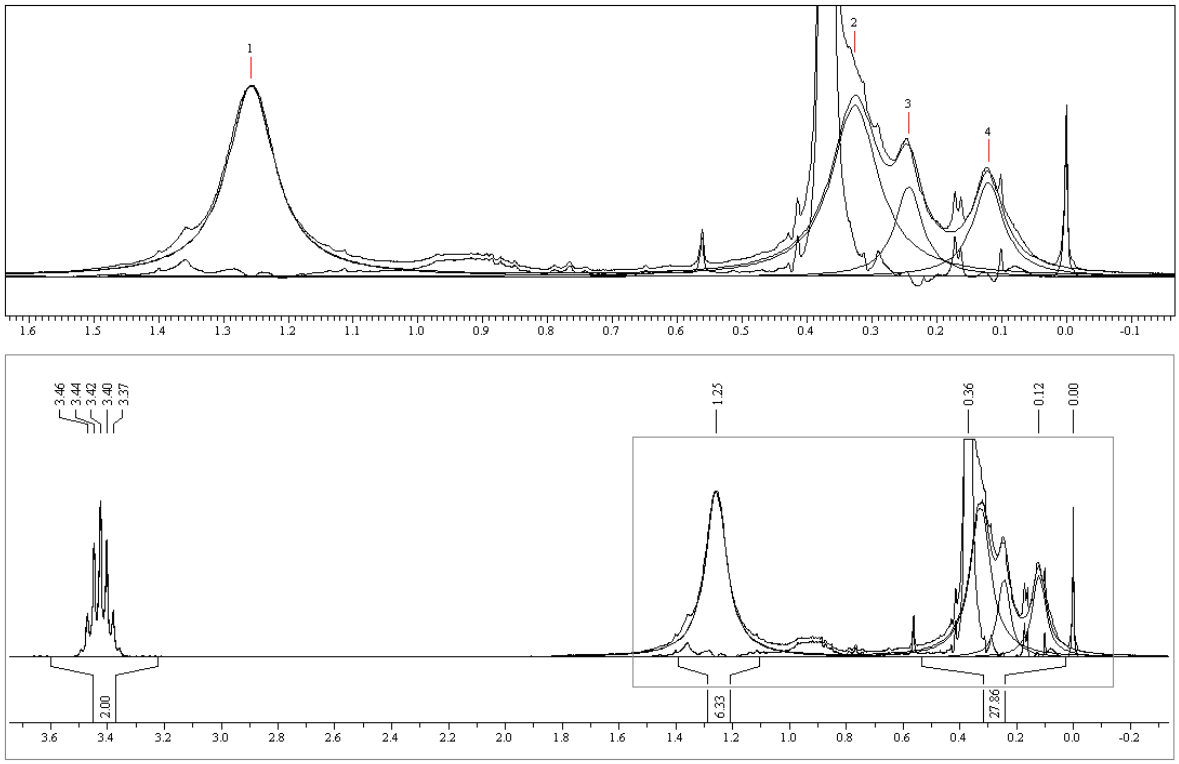

Figure 14. The selected region of the ^{1}H NMR spectrum (300.1 MHz) of complex [{**L6**}Sc(CH_2SiMe_3)$_2$] (**C7**) dissolved in C_6D_6at 25°C. The figure on the top of view shows deconvolution results of the region 0.00 – 1.40 ppm.

overlaps with ones of CH_2-group (**!**) The found integrals assigned for $\underline{Me}_3$Si-, $\underline{Me}_2$CH- and 2×C$\underline{H}_2$–Sc are in the ratio of 18:6:2:2.

The downfield shift of the methyl resonances in the *iso*-Pr-group is rather unusual. Such behaviour, albeit not of such extend, is also reported in the literature. In yttrium guanidinate complex [{$Me_2NC(NDip)_2$}$Y(CH_2SiMe_3)_2$(thf)] these methyl resonance were observed at 1.23 and 1.40 ppm.[35]

Similar up- and downfield shifts were observed in the close related aluminium complex [{$Ph_2P(C_5H_4)$NDip}$AlMe_2$],[36] in which their Me-group resonances appear as doublets at 0.49 and 1.37 ppm ($^3J_{HH}$ = 6.8 Hz).

The resonance broadening, with respect to the *iso*-Pr-group, is also observed in the ^{13}C NMR spectrum. Apart of the broad resonance found for the $Me_2\underline{C}$H-carbon atoms <u>two</u> broad resonances for methyl groups were observed.

This all indicates not only the unequivalence of the *iso*-Pr-groups, but also their slow rotation around the Ar–$CHMe_2$ bond on the NMR time scale. This feature is probably a consequence of high strain of these molecules, in which small radius metal atoms, *i.e.* aluminium and scandium, are strongly bonded to the C5-ring and the nitrogen atom resulting in an averaged C_s symmetric complexes in solution.

2.1.6. *Molecular Structures of Complexes* ***C7, C9*** – ***C11***.

All single crystals, suitable for X-ray diffraction analysis, were grown by storing of their concentrated toluene solutions at -30°C. All complexes crystallize without incorporated solvent molecules in the unit cell.

The scandium complex [{**L6**}Sc(CH_2SiMe_3)$_2$] (**C7**), with the smallest ionic radius of the whole rare-earth elements, crystallizes in the space group $P2_1/n$ with four formal units in the unit cell. In overall geometry, it is similar to the related complexes **C1** – **C4**: the metal center adopts a distorted tetrahedral environment. The silylmethyl groups attached to the scandium atom were disordered. The molecular structure is shown in Figure 15. Both alkylsilyl groups found to be disordered with occupancies of 79.5(5):20.5(5) at C30 and 61.5(5):38.5(5) at C34.

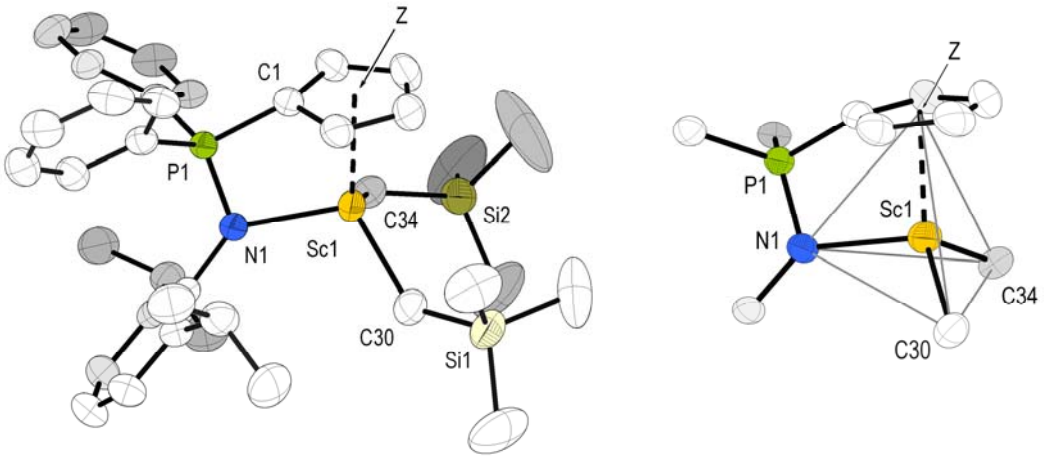

Figure 15. Molecular structure of scandium complexes [{**L6**}Sc(CH_2SiMe_3)$_2$] (**C7**). All hydrogen atoms and disordered CH_2SiMe_3-groups have been omitted for clarity. Selected bond lengths (Å) and angles(°): Sc1–N1 2.216(2), Sc1–C1 2.459(2), Sc1–Z 2.262(4), Sc1–C34 2.308(6), Sc1–C30 2.186(3), P1–N1 1.623(2), P1–C1 1.773(2), C1–Sc1–N1 66.9(1), Z–Sc1–N1 95.4(1), C30–Sc1–N1 106.7(1), C34–Sc1–N1 108.6(2), C30–Sc1–C34 104.6(2), Sc1–C30–Si1 134.2(2), Sc1–C34–Si2 125.7(3), C1–P1–N1–Sc1 16.6(1).

Compared to the complexes **C1** – **C4** with ligand $Me_2P(C_5Me_4)NHAd$ (**L4**) and in particular to the corresponding scandium complex **C2**, the dihedral C1–P1–N1–Sc1 angle of 16.6(1)° is significantly larger. Due to the high strain of the molecule, the environment around the *iso*-Pr-groups differs significantly, that reflects crucially on the NMR spectroscopy as was shown by the analysis of the ^1H and ^{13}C spectra.

The lower basicity of the ligand $Ph_2P(C_5H_4)NHDip$ (**L6**), compared to Me_2P-$(C_5Me_4)NHAd$ (**L4**), can be demonstrated by comparison of the bond Sc1–N1 and Sc1–Z_{C5} bond lengths.

Both bonding distances in the structure of complex **C7** of 2.216(2) Å for Sc1–N1 and 2.262(4) Å for Sc1–Z respectively and are longer compared to those in complex **C2** (2.185(2) and 2.235(1) Å resp.).

Single crystals of the yttrium and neodymium complexes [{**L6**}M(CH_2SiMe_3)$_2$(thf)] (M = Y (**C9**), Nd (**C10**), suitable for X-ray diffraction analysis, were obtained by storing of their saturated toluene solutions at -20°C. Both complexes crystallize in the triclinic space group $P\bar{1}$. Despite of their large difference in ionic radii ($\Delta(r^{3+})$ = 0.083 Å),[10] the molecular structures of the complexes **C9** and **C10** are very similar. They are displayed in Figure 16. The coordination at the metal centres can be best described as distorted trigonal bi-pyramidal, in which the nitrogen atom of the ligand and both silylmethyl groups occupy the equatorial positions and the coordinated THF molecules and the centroids of the C5-rings occupy the apical positions.

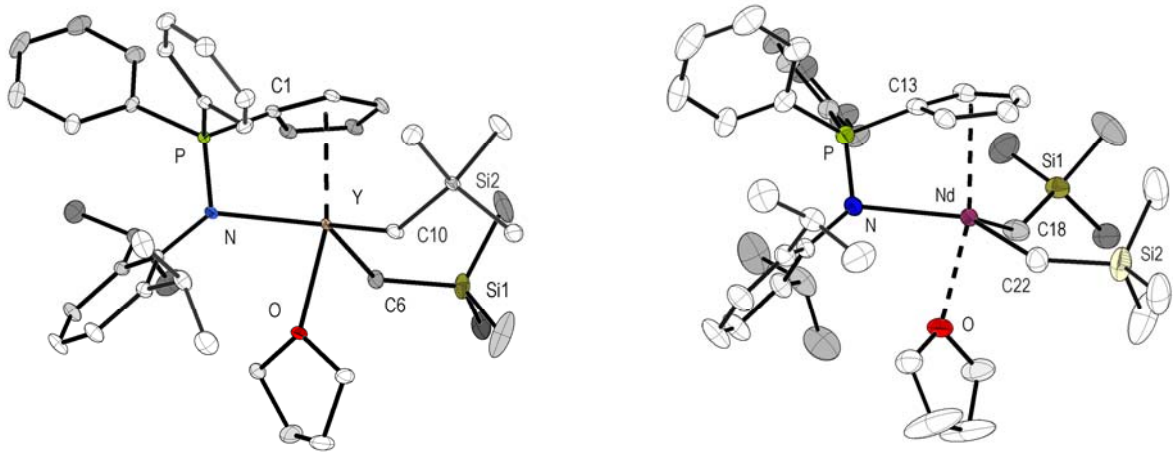

Figure 16. The molecular structures of yttrium and neodymium complexes [{**L6**}M(CH_2SiMe_3)$_2$(thf)] (M = Y (**C9**) and Nd (**C10**). All hydrogen atoms have been omitted for clarity. Selected bond lengths (Å) and angles (°) for **C9**: Y–N 2.468(1), Y–C1 2.655(2), Y–Z 2.46(1), Y–C6 2.428(1), Y–C10 2.429(1), Y–O 2.445(1), P–N 1.612(1), P–C1 1.758(1), C1–Y–N 61.0(1), Z–Y–N 87.2(1), C6–Y–N 126.6(1), C10–Y–N 116.5(1), C6–Y–C10 110.1(1), N–Y–O 79.8(1), C6–Y–O 81.5(1), C10–Y–O 83.0(1), Z–Y–O, 165.7(1), C1–P–N–Y 20.21(1); for **C10**: Nd–N 2.572(2), Nd–C13 2.729(2), Nd–Z 2.551(1), Nd–C18 2.505(2), Nd–C22 2.500(2), Nd–O 2.544(2), P–N 1.607(2), P–C13 1.767(2), C13–Nd–N 59.4(1), Z–Nd–N 85.0(1), C18–Nd–N 117.2(1), C22–Nd–N 127.4(1), C18–Nd–C22 110.2(1), N–Nd–O 81.1(1), C18–Nd–O 84.6(1), C22–Nd–O 81.8(1), Z–Nd–O 164.6(1), C13–P–N–Nd 20.1(1).

The Y–CH_2 bond lengths in the yttrium complex **C9** are of 2.428(1) and 2.429(1) Å and occupy the typical range of C(sp^3)–Y bond lengths found in the homoleptic [Y(CH_2SiMe_3)$_3$(thf)$_3$][37] (2.416, 2.429 and 2.436 Å). They are shorter than the σ-C(sp^2)–Y bond lengths of 2.506, 2.570 Å in [{η^5-C_5Me_5}Y(dmba)$_2$],[46] where (dmba) is *ortho*-Me_2NCH_2-C_6H_4), and av. 2.486(12) in [Y(dmba)$_3$] (*cf.* Chapter II, Part 2.1.).

The Nd–CH_2 bond lengths in **C10** of 2.505(2), 2.500(2) Å are in a good agreement with those found in the neodymium complex [{PhC(NDip)$_2$}Nd(CH_2SiMe_3)$_2$(thf)$_2$][38] (av. 2.504(3)) and in the structure of [Nd(tmba)$_3$] (2.52±7 Å, *cf.* Chapter II, Part 2.3.3), where (tmba) is *ortho*-deprotonated (*S*)-*N,N*-dimethyl-1-phenylethylamine.

The centroid(Z)–M–O angles in **C9** and **C10** are very similar (165.7(1) and 164.6(1)° resp.). Other ligand parameters are also very similar. The distortion of the coordinated *CpPN*-ligand presented by M–N–P–C_{C5} torsion angles is largest in the whole series of structurally characterized *CpPN*-complexes (20.1(1), 20.1(1)° resp.).

The notable structural feature is the large N–M bond lengths comparable with those of donor-acceptor bonds rather than of amidic bonds. Whereas in the yttrium complex [{**L4**}Y(CH_2SiMe_3)$_2$] (**C3**) the Y–N bond length is as short as 2.316(4) Å (*cf.* Part 2.1.3., this Chapter), in the complex **C10** the Y–N bond length is of 2.468(1) Å. The similar bonding situation was also observed in the structure of the complex **C10** (*d*(Nd–N) = 2.572(5) Å). The bond length comparison with [{κ^3-terpy}$_2$NdI$_2$]I(C_5H_5N)[39] (2.57 – 2.63 Å) and [{η^5-Flu}NdI$_2$(pyr)$_3$](thf).[40] (2.518, 2.563 and 2.590 Å) shows more donor-acceptor bonding situation, rather than amidic bonding [{Me_2TACN-R-N-(*tert*-Bu)}Nd(CH_2SiMe_3)$_2$] (R = CH_2CH_2 (2.292 Å), R = $SiMe_2$ (2.320 Å)).[22]

The most interesting feature in structures of **C9** and **C10** is the smaller centroids(Z)–M–N angle of 87.2(1) and 85.0(1)° respectively. This fact explains the coordination of the additional THF molecules.

The complex [{**L6**}Y(μ^2-OMe)(CH_2SiMe_3)]$_2$ (**C11**) crystallizes in the monoclinic space group $P2_1/n$ with four molecules of ether per unit cell. The X-ray diffraction analysis reveals that the compound possesses a binuclear structure. The molecular structure of the compound is depicted in Figure 17.

In the binuclear structure of complex **C11** the yttrium atoms are penta-coordinated. Both metal centers are bridged by oxygen atoms of MeO-ligands and form a close to C_2-symmetrical slightly distorted Y_2O_2 core. The *CpPN*-ligand molecules occupy the terminal positions and bonded in the η^5,η^1- coordination mode. The silylmethyl and *CpPN*-ligands in the molecule are arranged in cisoid conformation.

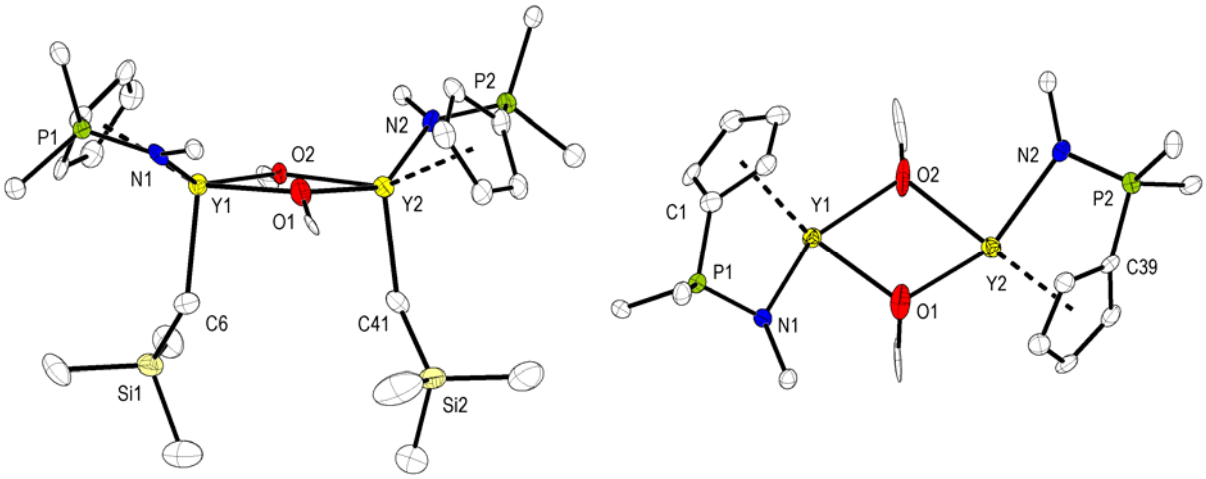

Figure 17. Molecular structure of binuclear yttrium complex [{**L6**}Y(μ^2-OMe)(CH_2SiMe_3)]$_2$ (**C11**): Side view (left) and view along the *pseudo*-C_2 axis (right); the hydrogen atoms and aromatic rings (except of *ipso*-C of Dip-group) have been omitted for clarity (in the axial view CH_2SiMe_3 groups are not depicted). Selected bond lengths (Å) and angles (°): Y1–Y2 3.731(1), Y1–N1 2.446(5), Y1–C1 2.680(8), Y1–Z1 2.499(1), Y1–C6 2.387(7), Y1–O1 2.240(7), Y1–O2 2.312(7), P1–N1 1.607(6), P1–C1 1.763(7), Y2–N2 2.471(5), Y2–C39 2.671(8), Y2–Z2 2.502(1), Y2–C41 2.419(7), Y2–O1 2.274(7), Y2–O2 2.309(8), P2–N2 1.614(6), P2–C39 1.759(7), Y1–O1–Y2 111.5(3), Y1–O2–Y2 107.7(3), O1–Y1–O2 70.6(2), O1–Y2–O2 70.1(1), C6–Y1–Y2–C41 14.3(3).

Despite of the asymmetrical bridging mode of the MeO groups, the inner Y_2O_2 core is essentially planar. The maximum deviations from the plane, formed by the yttrium and the oxygen atoms, of 0.04(1) Å and 0.07(1) Å were found for O1 and O2 respectively; the angular sums around the bridging O(1) and O(2) are 352(2) and 357(2)°. The Y–O bond lengths span the narrow range of 2.240(7) – 2.312(7) Å. Bond lengths of 2.750 and 2.290 Å were found in the binuclear, centrosymmetric [{MeC_5H_4}$_2$Y(μ-OCH=CH_2)]$_2$[41] and of 2.217(3) and 2.233(3) Å in [{C_5H_5}$_2$Y(μ-OMe)]$_2$.[33] The bonding of nitrogen atoms of the ligand **L6** is similar to the complexes **C9** and **C10** and can be ascribed to donor-acceptor type.

The coordination at the yttrium atoms can be best described as a distorted tetragonal pyramidal (Figure 18) with the bridging oxygen atoms, the nitrogen atom and the C5-ring centroid forming the pyramid basis and the alkyl carbon atom its top. Both pyramids are connected by a common basal edge formed by the oxygen atoms.

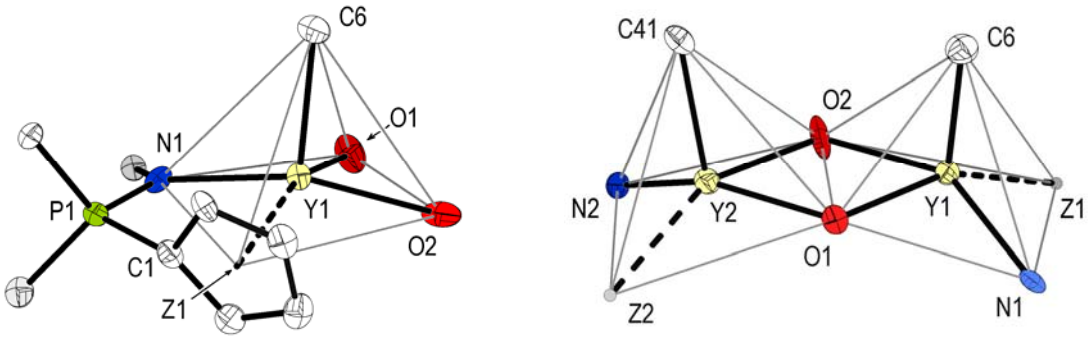

Figure 18. View of the polyhedron around the yttrium atom Y1 (left) and the edge-bonded polyhedrons in the binuclear structure of **C11**. All hydrogen atoms and bulky *CpPN*-ligand atoms have been omitted for clarity. The following planes are defined: Plane1 = [O1,O2,N1,Z1], Plane2 = [O1,O2,N2,Z2]. Selected distances (Å): Y1···Plane1 0.535(1), Y2···Plane2 0.601(1). A vector between atoms A and B is presented by the expression [A,B]. Selected angles (A^B,°): [Y1,C6]^Plane1 12.8(2), [Y2,C41]^Plane2 9.2(2), Plane1^Plane2 32.2(1).

The planes formed by atoms lying in the basis of the pyramids are essentially planar and are referred further as Plane1 and Plane2 respectively. The maximal deviation of 0.01(1) Å and 0.03(1) Å were found for O1 (Plane1) and O2 (Plane2) respectively. The angle between the planes found to be of 32.2(1)°. Both yttrium atoms are remote from the corresponding planes by values of 0.535(1) and 0.601(1) Å. Both silylmethyl groups are nearly colinear with the C6–Y1–Y2–C41 torsion angle of 14.3(3)°.

That unusual cisoid conformation, in contrary to the manifold reported structures with transoid conformation,[33,41] can be explained as follows. Such folding is advantageous for fitting the bulky Dip-groups at the one side of the molecule to the "cave" – presented by relatively "small" C_5H_4-groups; furthermore for a lower degree of steric repulsion realized by silylmethyl groups (Scheme 9).

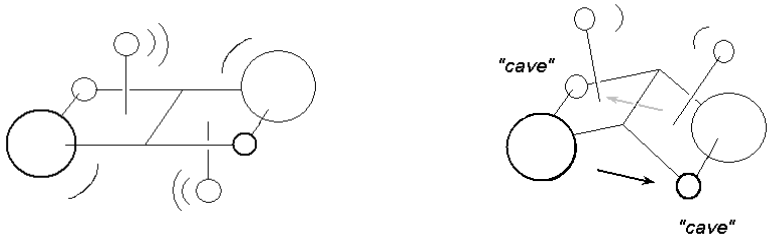

Scheme 9. Graphical explanation of the observed cisoid and unfavourite transoid conformations.

The cisoid conformation is realized in a small number of binuclear lanthanide complexes such as in $[\{\eta^5,\eta^1\text{-}(Me_4C_5SiMe_2C{\equiv}CCH{=}C(Me)O\}Y(CH_2SiMe_3)]_2$[42] and $[\{DanipO\}\text{-}Sm(C_5Me_5)]_2$[43] (Danip = 2-(*o*-anisyl)-6-(*o*-2-phenoxide)phenyl). The molecular cisoid conformation of both latter complexes can be also described well with the model discussed.

2.2. *Synthesis of CpPN-Diaryl Complex of Yttrium*

Apart from the bulky Me_3SiCH_2 group as a well established and widely used ligand for a kinetic stabilization of organometallic complexes, the chelating monoanionic (dmba) complexes (*o*-$MC_6H_4CH_2NMe_2$) are attractive starting materials as metal source for direct metallation by a *proto-dearylation* protocol.[44,45] This ligand family and its application to the chemistry of rare-earth organometallics have been discussed in more details in the Chapter II. For direct metallation of the *CpPN*-ligands we have used the "easy-to-prepare" homoleptic yttrium complex [Y(dmba)$_3$] (**H4**) and ligand **L6**.

Reaction of **H4** with an equimolar amount of the ligand **L6** in toluene afforded a colourless, microcrystalline complex [{**L6**}Y(dmba)$_2$] (**C12**). After crystallization from ether **C12** was obtained in high yield (69%). As was shown by NMR spectroscopy and microanalysis, the complex **C12** was obtained without any coordinated solvent molecules (Scheme 10), independent from which source of yttrium was used ($YCl_3(thf)_3$ or $YCl_3(dme)_2$). The 1:1 complex formation is in good agreement with the observation that [Y(dmba)$_3$] reacts with C_5Me_5H, independent on stoichiometry, under formation of the known complex [{η^5-C_5Me_5}Y(dmba)$_2$][46]

The ^{31}P NMR spectrum shows only one resonance. However, the resonance is considerably upfield shifted compared to those of **C1** – **C4**. It appears at -5.5 ppm in the characteristic region of *CpPN*-ligands having iminophosphorane tautomeric form (*cf.* ^{31}P: δ(**L10**) = -14.9 ppm)

In the ^{1}H NMR spectrum, depicted in Figure 19, two doublets for the methyl groups of the *Me*$_2$CH-group were found. Moreover, the methylene groups appear to be diastereotopic and show an AB-pattern at 3.42 and 3.61 ppm ($^2J_{HH}$ = 13.8 Hz). This is in contrast with the observation, that the CH_2-groups in [{C_5Me_5}Y(dmba)$_2$][46] or starting [Y(dmba)$_3$] both show conformational lability down to -90°C.

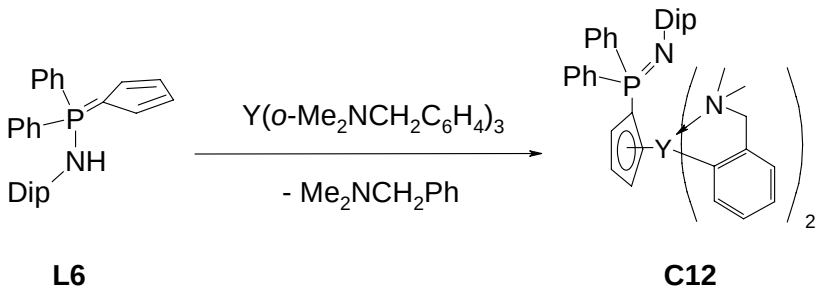

L6 **C12**

Scheme 10. Synthesis of the yttrium complex [{**L6**}Y(dmba)$_2$] (**C12**).

These findings, together with the unusual upfield shifted ^{31}P NMR resonance, can be rationalized by assumption that the *CpPN* ligand is only η^5-coordinated at the metal center; no coordination of the nitrogen atom of the ligand can be observed at the NMR time scale.

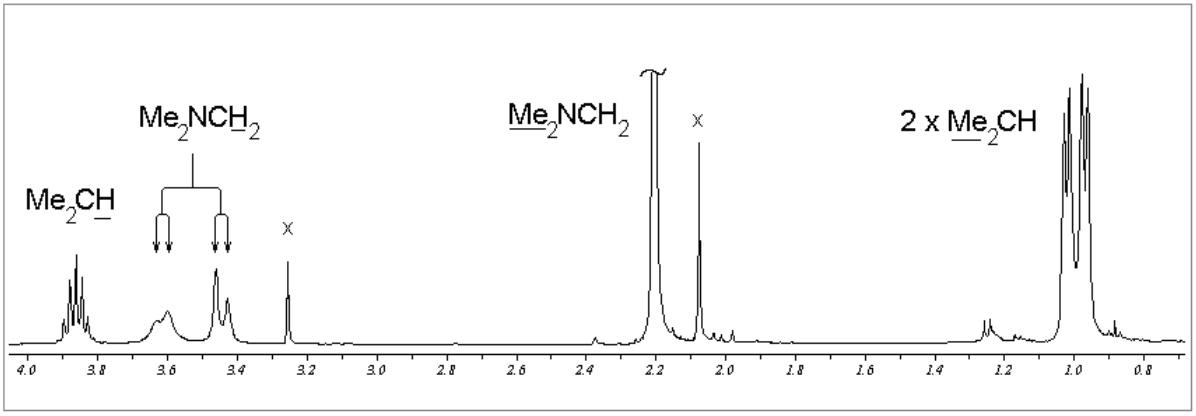

Figure 19. Selected region (0.7 – 4.0 pm) of the ^1H NMR spectrum (300.1 MHz) of the yttrium complex [{μ^5-**L6**}Y(dmba)$_2$] (**C12**) dissolved in C_6D_6 at +25°C. The resonances denoted with (x) are assigned to the Me_2N- and CH_2-groups of free *N,N*-dimethylbenzylamine

The aromatic region of the ^1H NMR spectrum exhibits plenty of resonances covering the range from 6.8 – 7.6 ppm almost without a gap. For the understanding of bonding situation, the ^{13}C NMR spectroscopy was found to be much more informative. The APT spectrum of complex **C12** dissolved in C_6D_6 is shown in Figure 20.

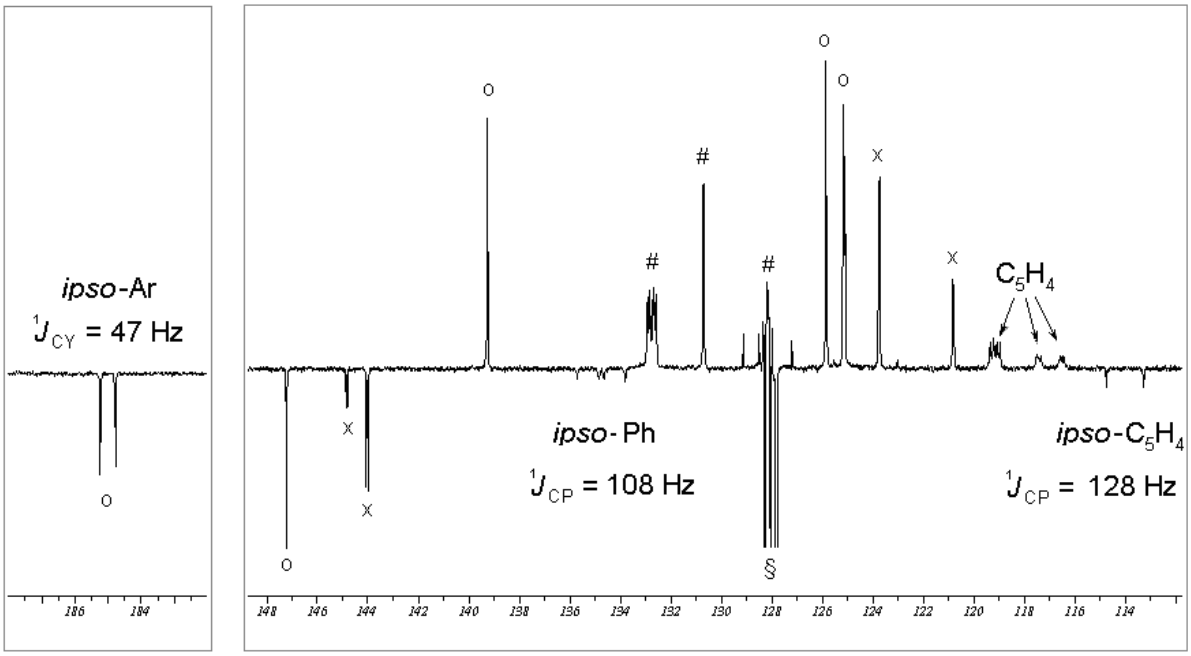

Figure 20. The ^{13}C NMR spectrum (75.5 MHz) of the yttrium complex [{μ^5- **L6**}Y(dmba)$_2$] (**C12**) dissolved in C_6D_6 at 25°C. The resonances denoted with (§), (x), (o) and (#) are assigned to residual protons of C_6D_6, Dip, (dmba) and Ph groups.

All aromatic *ipso*-carbon resonances with respect to the phosphorus atom in the *CpPN*-ligand reveal doublets with high one-bond ^{13}C –^{31}P scalar coupling of 148 Hz for the C5-ring and of 105 Hz for the Ph-groups. The carbon atoms of the Dip-group show smaller coupling constants (< 5.2 Hz).

The direct attachment of the (dmba) ligands at the yttrium atom is demonstrated by downfield shifted doublet at 185.0 ppm with one-bond ^{13}C –^{89}Y scalar coupling of 47 Hz. The comparison of the one-bond ^{13}C–^{89}Y scalar coupling of the metallated Ar-ring with those in the starting **H4** shows that $^{1}J_{CY}$ in **C12** is noticeably larger and slightly upfield-shifted. The chemical shift of 186.9 ppm was found in [Y(dmba)$_3$] (43.3 Hz), 186.2 ppm in [Y(C$_6$H$_4$C(Me)HNMe$_2$)$_3$] (42.6 Hz) (*cf.* Chapter II, Part 2.1, 2.3.3) and 186.8 ppm in [Y(C$_6$H$_4$C(Me)$_2$NMe$_2$)$_3$] (42.4 ppm).[47] This indicates that the *ipso*-carbon atom of the (dmba) ligands have, also like in the homoleptic aryl-lanthanides, "pure" sp^2-hybridized carbon-yttrium bonding.

The asymmetry of the molecule is shown by the presence of four resonances for the C5-ring together with two sets of *ipso*- and *ortho*-Ph-group resonances (Figure 21). The lack of amenable conformational rearrangements is demonstrated by presence of only one resonance for the *ipso*-C5-ring carbon atom.

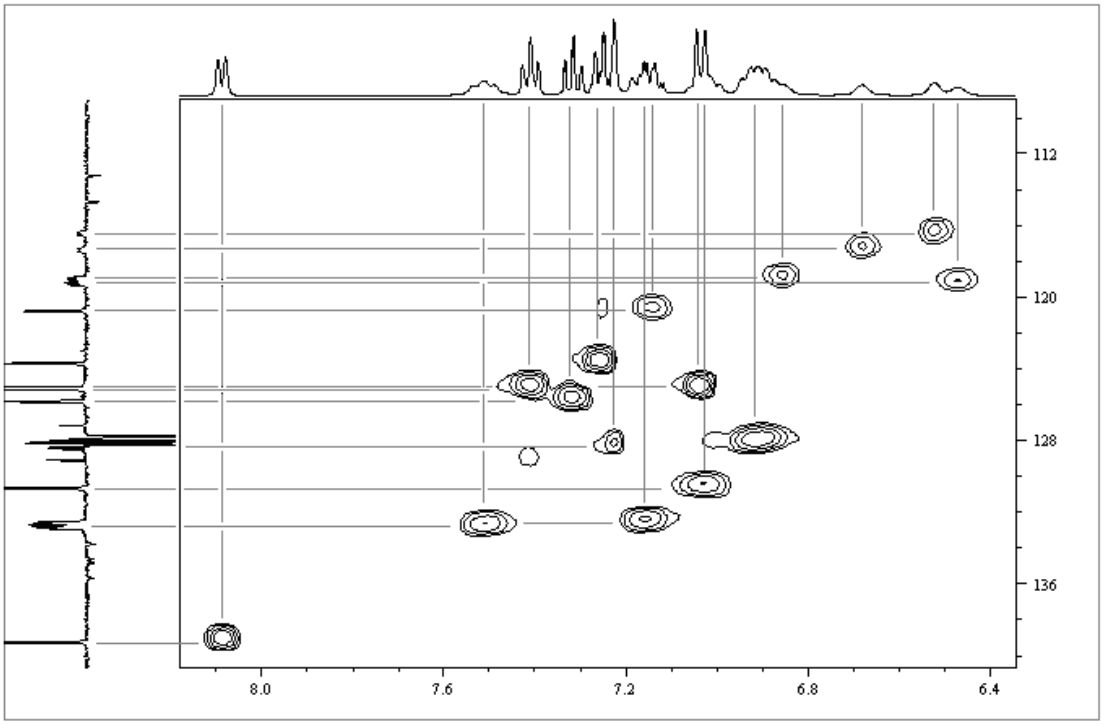

Figure 21. 2D HMQC spectrum of complex [{**L6**}Y(dmba)$_2$] (**C12**) dissolved in C_6D_6 at 25°C. The 1D ^{1}H NMR spectrum (300.1 MHz) is shown at the top and ^{13}C NMR spectrum (75.0 MHz) is shown on the left edge of the contour plot.

The complete assignment of the ^{1}H and ^{13}C NMR resonances was confirmed by the subsequent analysis of the 2D HMQC spectrum. The HMQC spectrum clearly shows four cross peaks assigned to the C5-ring indicating that the both (dmba) ligands are without a mirror plane with respect to the C5-ring. From two possible conformations of the (dmba) ligands around the yttrium atom – head-to-head and head-to-tail – the latter, that has propeller-like arrangement, is realized. This is in good agreement with the results found for the reported solid state structure of $[\{C_5Me_5\}Y(dmba)_2]$[46] and homoleptic lithium ate complexes **H5** and **H6** (*cf*. Chapter II, Part 2.2). Analysis of the cross peaks of the *ortho*-Ph–P group resonances, which appears as two doublets in the ^{13}C NMR spectrum, permit the assignment of resonances in the ^{1}H NMR spectrum. These resonances appear as downfield und upfield shifted multiplets at 7.50 and 7.16 ppm and hence appear to be diastereotopic. This behavior may be explained by an absence of rotation of the iminophosphorane moiety around the $P–C_{C5}$ bond; the Ph-groups are most probably arranged on both sides of the C5-ring.

In the light of these observations – no coordination of the iminophosphorane-arm at the yttrium atom and the propeller-like arrangement of the (dmba) ligands – one can suggest the averaged structure in solution, that is drown in Scheme 11.

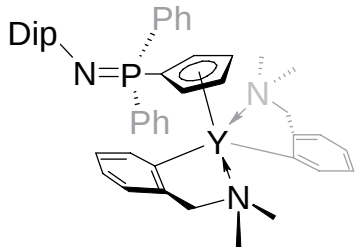

Scheme 11. The averaged solution structure of complex $[\{\eta^5$-**L6**$\}Y(dmba)_2]$ (**C12**).

In addition, it was shown that such behavior of the *CpPN*-ligand system can be attributed to the yttrium atom coordinativly saturated by two monoanionic chelating (dmba) ligands and the *CpPN* ligand.

While no single-crystal X-ray diffraction study has been made, our analysis of **C12** structure by multinuclear NMR spectroscopy and 2D HMBC experiments in solution, unambiguously confirm its “open”-structure at ambient temperature.

2.3. *Synthesis of Complexes with Ligands **L9** and **L10***

2.3.1. *Synthesis and Multinuclear NMR Spectroscopy of Complexes **C13** and **C14***

The complexes were synthesized under essentially the same reaction conditions reported for the synthesis of complexes **C1** – **C4** and were isolated in high yields as microcrystalline, highly air- and moisture-sensitive, colourless solids [{**L9**}Lu(CH_2SiMe_3)$_2$] (**C13**), [{**L10**}Lu(CH_2SiMe_3)$_2$] (**C14**) (Scheme 12). Compared to **C13**, the latter complex appears to be less stable in C_6D_6 solution.

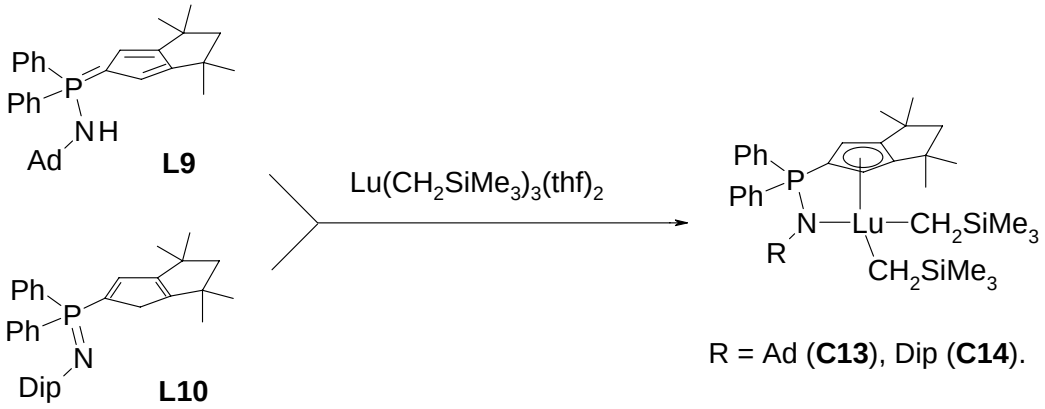

Scheme 12. Synthesis of complexes **C13** and **C14** with ligands $Ph_2P(Cp^{TM})NR$ (R = Ad (**L9**) and Dip (**L10**)).

The ^{31}P NMR resonances of complexes **C13** and **C14** appear at 8.7 and 9.3 ppm respectively. This chemical shifts most closely corresponds to those found in the diamagnetic *CpPN* complexes **C1** – **C3** and **C7** – **C9**, which span the narrow range from 9.0 – 12.1 ppm.

The ^{1}H NMR spectrum of **C13** is depicted in Figure 22. Since the C5-ring coordinated at the metal center in the η^5-mode, the methyl and protons of the methylene groups of the Cp^{TM}-moiety are diastereotopic. The methyl group resonances appear as two signals at 1.18 and 1.62 ppm. The resonances of the methylene group in the Cp^{TM}-moiety appear at 1.95 and 2.23 with $^2J_{HH}$ of 12 Hz and partly overlap with the methyne resonance of the Ad-moiety.

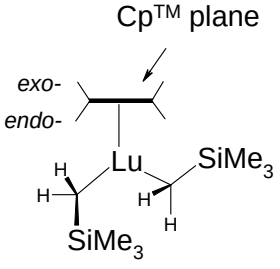

The silylmethyl group resonances, as expected, are upfield shifted and appear as pair of doublets with AB-pattern at -0.59 and -0.22 ppm with the $^2J_{HH}$ scalar coupling of 11.5 Hz. This indicates that at r.t. rotation around the Lu–CH_2 bond is frozen and the molecule adopts an averaged C_s symmetry in solution.

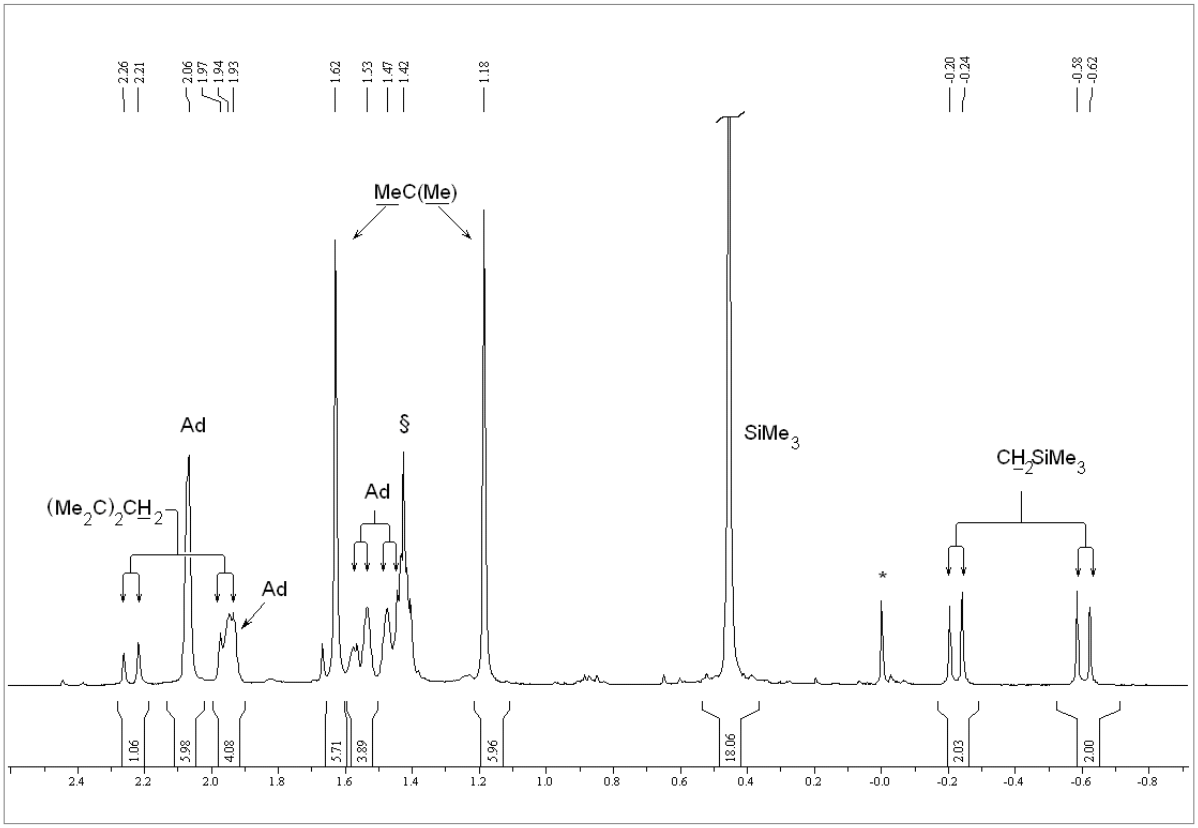

Figure 22. The ^{1}H NMR spectrum (300.1 MHz) of complex [{**L9**}Lu(CH_2SiMe_3)$_2$] (**C13**) in C_6D_6 at 25°C. The resonances denoted with (*) and (§) are assigned to TMS and uncoordinated protons of THF.

In contrast to the related complexes **C1** – **C3**, the remotest methylene protons of the Ad-moiety, which in case of **C1** – **C3** is slightly broadened, are splitted in AB-pattern with the typical for $^{2}J_{HH}$ of 12.0 Hz. This fact indicates the high degree of strain of the whole molecule and enormous bulkiness of the Cp^{TM}-moiety.

The *H*C-resonances of the C5 ring were observed at 5.94 ($^{3}J_{HP}$ = 2.8 Hz) and this is the highest value found for *CpPN*-complexes (**C7** – **C9**), which without any doubt indicates the high negative charge on the C5-ring. For instance, the ^{1}H NMR resonances of [LiC_5H_5] in THF-d_8 were observed at 5.55 ppm.[48]

The aliphatic region in the ^{13}C NMR spectrum is rich of signals and only resonances of the *Me*$_3$Si-group at 5.0 ppm can be assigned at first. In the aromatic region, except of the resonances of Ph-rings, there are three doublets of the C5-ring at 106.7 ($^{2}J_{PC}$ = 13.2 Hz,), 149.0 ($^{3}J_{PC}$ = 14.3 Hz) and 93.7 ($^{1}J_{PC}$ = 115 Hz), which were assigned to H*C*$_{C5}$, *C*$_{C5}$CMe$_2$, and P*C*$_{C5}$ respectively. The one-bond ^{13}C–^{31}P scalar coupling of the latter is larger than one of the *ipso*-Ph-groups ($^{1}J_{PC}$ = 88 Hz). The precise assignment of the ^{13}C resonances was accomplished by analysis of 2D HMQC spectrum (Figure 23).

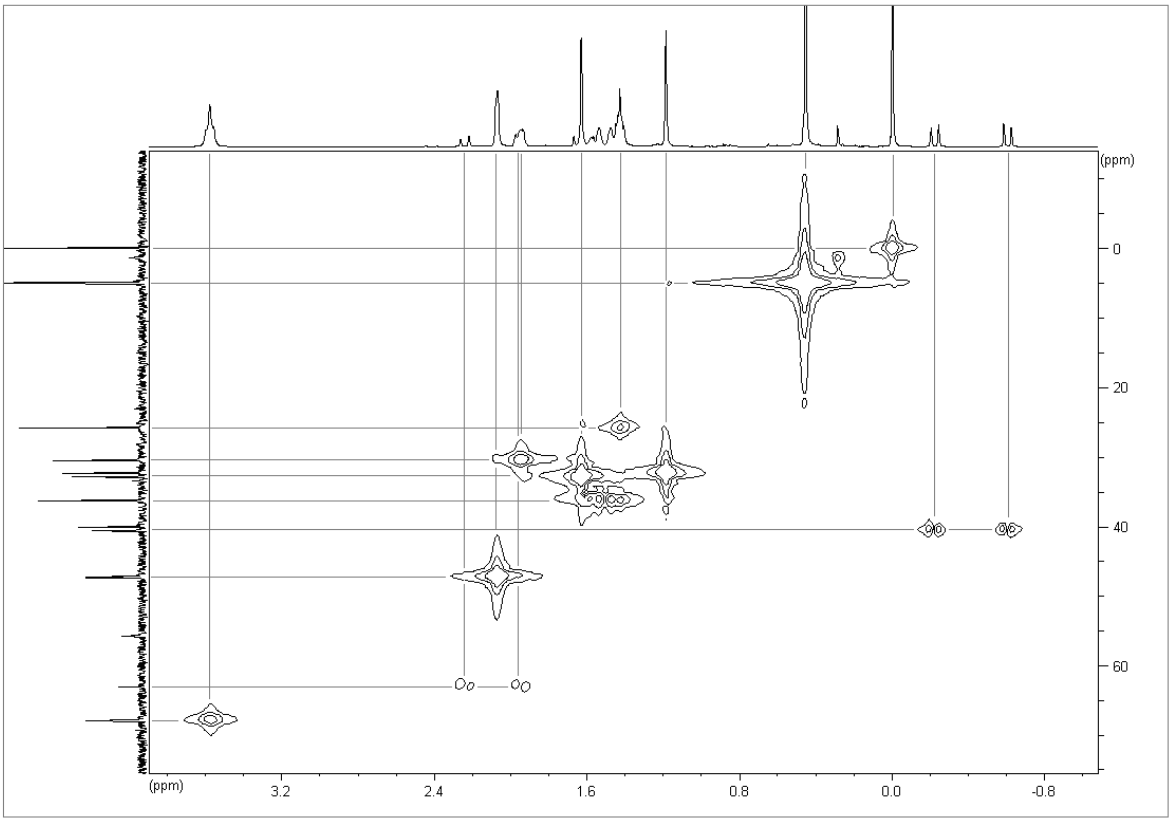

Figure 23. The HMQC spectrum of complex [{**L9**}Lu(CH_2SiMe_3)$_2$] (**C13**) dissolved in C_6D_6 at 25°C. The 1D ^{1}H NMR spectrum (300.1 MHz) is shown at the top and ^{13}C NMR spectrum (75.1 MHz) is shown on the left edge of the contour plot.

The analysis of the HMQC spectrum reveals that the resonances at 32.3 and 32.9 ppm can be easily assigned to the diastereotopic Me-groups of the Cp^{TM}-moiety, the resonance at 63.0 to *C*H$_2$(CMe$_2$)$_2$. Due to the high strain of the whole molecule, both carbon atoms of the silylmethyl groups are diastereotopic (**!**) and being magnetically non-equivalent appear as <u>two</u> signals at 40.0 and 40.6 ppm.

On the basis of the HMQC spectrum, the assignment of the proton resonances of the Ad-moiety can be easily performed: 30.5 (s, *C*H(CH$_2$)$_3$), 36.3 (s, *C*H$_2$(CH)$_2$), 47.3 (d, $^3J_{PC}$ = 8.3 Hz, PC(*C*H$_2$)$_3$), 55.7 (d, $^2J_{PC}$ = 7.2 Hz, P*C*$_{Ad}$).

The ^{1}H NMR spectrum of the dialkyl-lutetium complex [{**L10**}Lu(CH_2SiMe_3)$_2$] (**C14**) are shown in Figure 24.

In contrast to the complex **C13**, the methylene signals of the silylmethyl groups in complex **C14** are broadened; no $^{2}J_{HY}$ scalar coupling can be observed at r.t. The most unusual feature in the spectrum of **C14** is the chemical shift of the Me-groups of the Dip-moiety, which appear as a somewhat downfield shifted broad resonance at 1.40 ppm and an extremely upfield shifted broad resonance at 0.40 ppm (**!**). The latter partly overlaps with

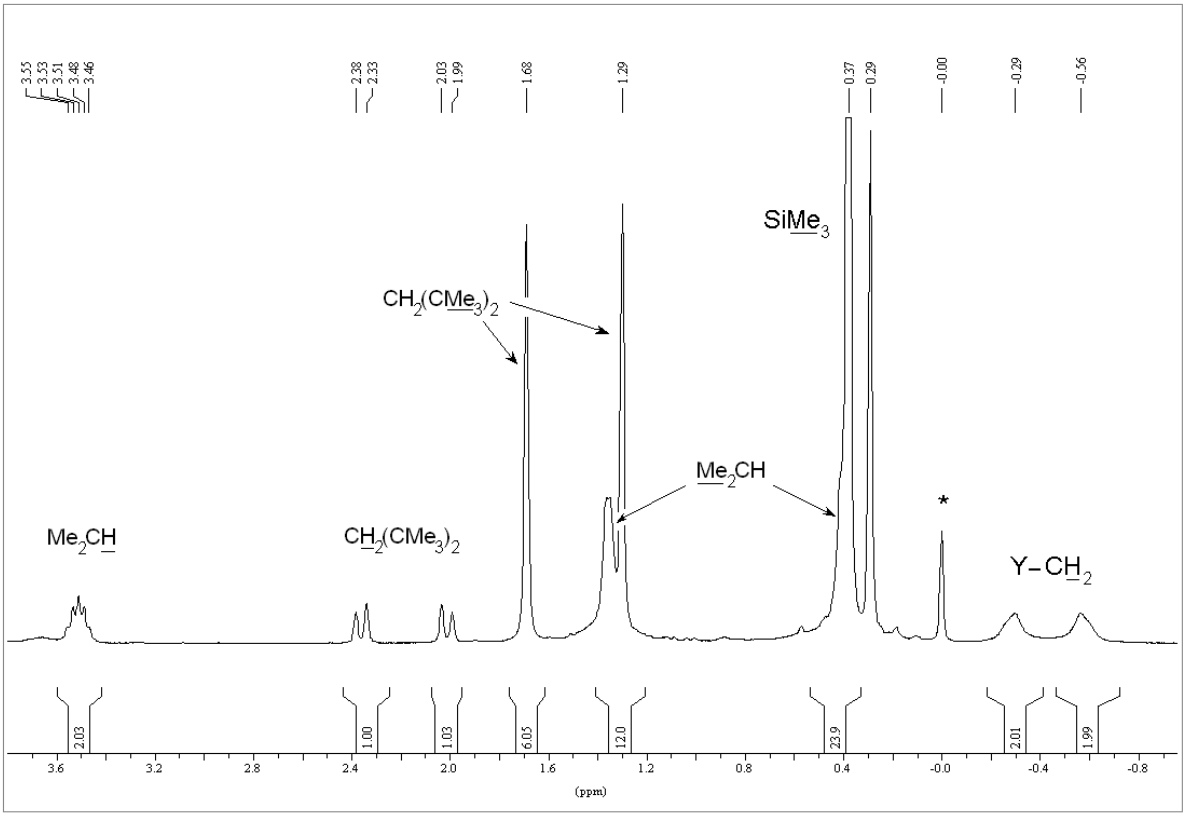

Figure 24. The ^{1}H NMR spectrum (300.1 MHz) of complex [{**L10**}Lu(CH_2SiMe_3)$_2$] (**C14**) dissolved in C_6D_6 at +25°C. The resonance denoted with (*) is assigned to TMS.

the resonance of the Me_3Si-group at 0.37 ppm. This fact, also like in the case of the scandium complex [{**L6**}Sc(CH_2SiMe_3)$_2$] (**C7**), is result of the presence of bulky groups at the metal center and therefore caused by high strain of the molecule. Due to the sterical demand of the *endo*-Me-groups of the Cp^{TM} and two silylmethyl ligands, rotational barrier within the *N*-Dip-moiety become high and the methyl groups become magnetically unequivalent. The manual deconvolution with two *Gauss*-curves gives the three-bond ^{1}H–^{1}H scalar coupling of 6.6±0.5 Hz (*cf*. $J(Me_2C\underline{H})$ = 6.8 Hz).

The assignment of the ^{13}C NMR resonances can be best made by analysis of the 2D HMQC spectrum, which depicted in Figure 25. Except of the expected cross peaks of the ligand and Me_3SiCH_2-group, in the aliphatic region, two cross-peaks assigned to the Me_{Dip}-

groups were observed. In the ^{13}C NMR spectrum they appear as <u>two</u> broad signals of very low intensity at 22.2 and 23.8 ppm. Thus, the coalescence temperature for these ^{13}C NMR signals lies above room temperature. An explanation of such anomalous behaviour of the carbon atoms of the Me_{Dip}-group signals might be the specific location of the latter. As was shown by the X-ray diffraction analysis (*vide infra*), the distance from the C_{Me}-atoms of the *iso*-Pr-groups to the centroids of the Ph-rings is only of ca. 3.15 Å (C_{Me}–Z_{Ph}, $C_{Me'}$–Z_{Ph}) and there is no conformational freedom to escape from this rather stereorigid situation.

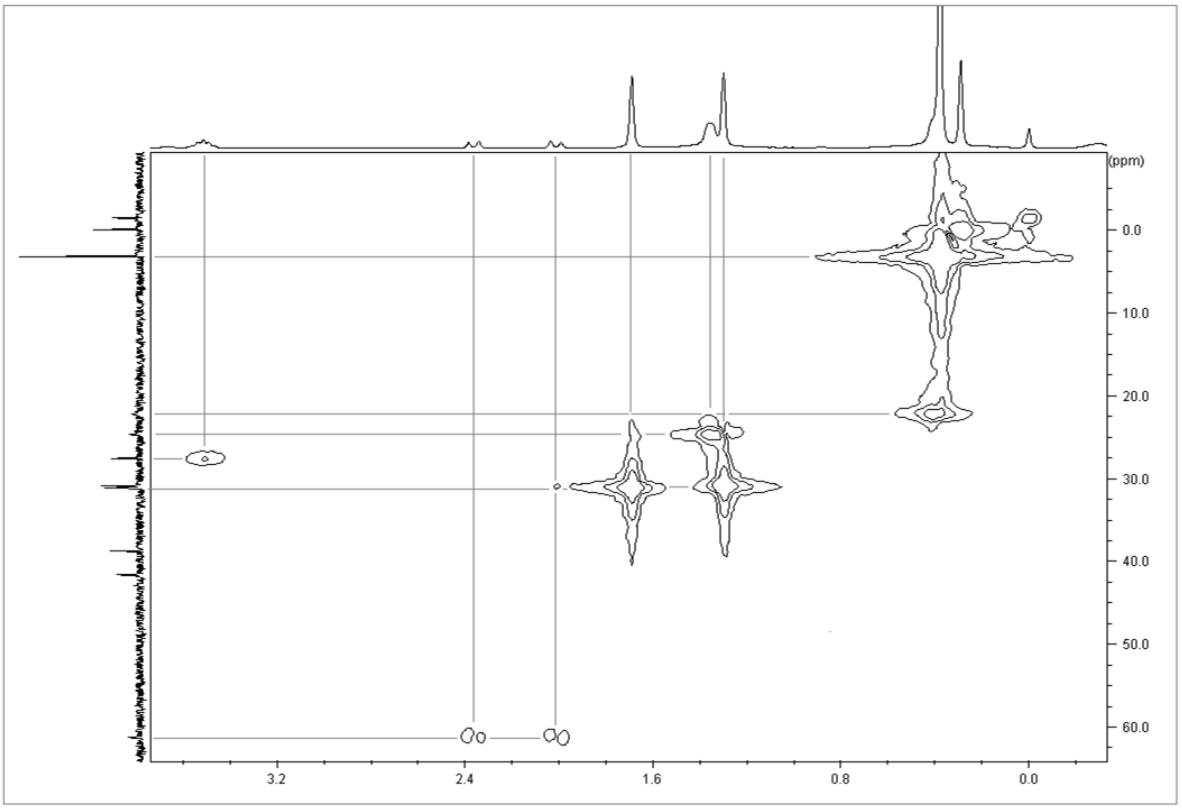

Figure 25. The HMQC spectrum of the complex [{**L10**}Lu(CH_2SiMe_3)$_2$] (**C14**) dissolved in C_6D_6 at +25°C. The 1D ^1H NMR spectrum (300.1 MHz) is shown at the top and ^{13}C NMR spectrum (75.0 MHz) is shown on the left edge of the contour plot.

2.3.2. *Molecular Structures of Complexes* ***C13*** *and* ***C14***

The complexes with *CpPN*-ligands **L9** and **L10** also confirm the coordination mode. The complex **C13** with the ligand **L9** crystallizes in the triclinic space group $P\bar{1}$ with the two formal units in the unit cell. The lutetium atom reveals a *pseudo*-tetrahedral coordination by the η^5-bonded C5-ring and the nitrogen atom of the *CpPN*-ligand together with two σ-bonded silylalkyl groups (Figure 26). The *pseudo*-tetrahedral environment around the metal center can be shown by comparison of the C39–Lu1–N1, C35–Lu1–N1, C35–Lu1–C39 angles bonds, which are all very close to 109°: 103.4(1), 112.7(1) and 107.7(1)° respectively. The Lu–C–Si angles of 124.6(1) and 129.4(1)° and greater than the ideal tetrahedral and confirming constrained arrangement of the ligands. This values are slightly less than those found in the lutetium complex **C1** (126.9(1) and 136.6(2)°). The torsion angle C1–P1–N1–Lu1 of 3.7(1)° is the lowest in the whole series of the lutetium complexes.

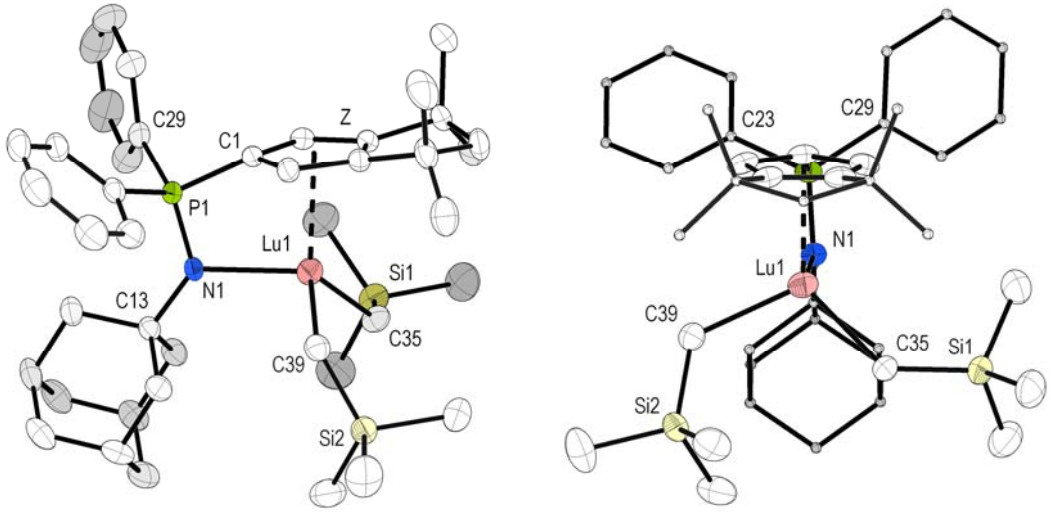

Figure 26. Molecular structure of complex [{**L9**}Lu(CH_2SiMe_3)$_2$] (**C13**): side view (left), front view (right). All hydrogen atoms and phenyl carbon atoms, except of its *ipso*-C, have been omitted for clarity. At the right figure aliphatic carbon atoms at C5-ring are shown by "ball-and-stick" model. Selected bond lengths (Å) and angles (°): Lu1–N1 2.289(2), Lu1–C39 2.348(3), Lu1–C35 2.349(2), Lu–Z 2.371(1), Lu1–C1 2.529(3), P1–N1 1.595(2), P1–C1 1.775(2), C1–Lu1–N1 66.0(1), Z–Lu1–N1 93.9(1), N1–P1–C1 102.5(1), C39–Lu1–N1 103.4(1), C35–Lu1–N1 112.7(1), C35–Lu1–C39 107.7(1), Lu1–C39–Si2 124.6(1), Lu1–C35–Si1 129.4(1), C1–P1–N1–Lu1 3.7(1).

The complex **C14** with the sterically more demanding ligand **L10** crystallizes in the orthorhombic space group *Pbca* with the eight molecules in the unit cell (Figures 27).

The coordination at the metal centers in both complexes can be described as *pseudo*-tetrahedral, but it is much less symmetric that those of **C13**. As was shown earlier, the torsion angle C_{C5}–P–N–M can be used for the evaluation of the overall strain caused by ligand

arrangement around the metal center. For this particular molecule the highest in the whole series torsion angle of 18.0(2)° was found.

This strain is reflected in the arrangement of the silylmethyl groups. Whereas one of silylmethyl groups possesses the typical parameters (Lu1–C33–Si1: 134.8(3)°), the other arranged to maximize the intramolecular distance to the *CpPN*-ligand (Lu1–C34–Si2: 147.6(3)°).

For this ligand significantly longer centroid(Z)–M distances of 2.409(1) Å was found. This value is ca. 0.07 and 0.04 Å longer in comparison to those in **C1** and even to the closely related **C13** respectively.

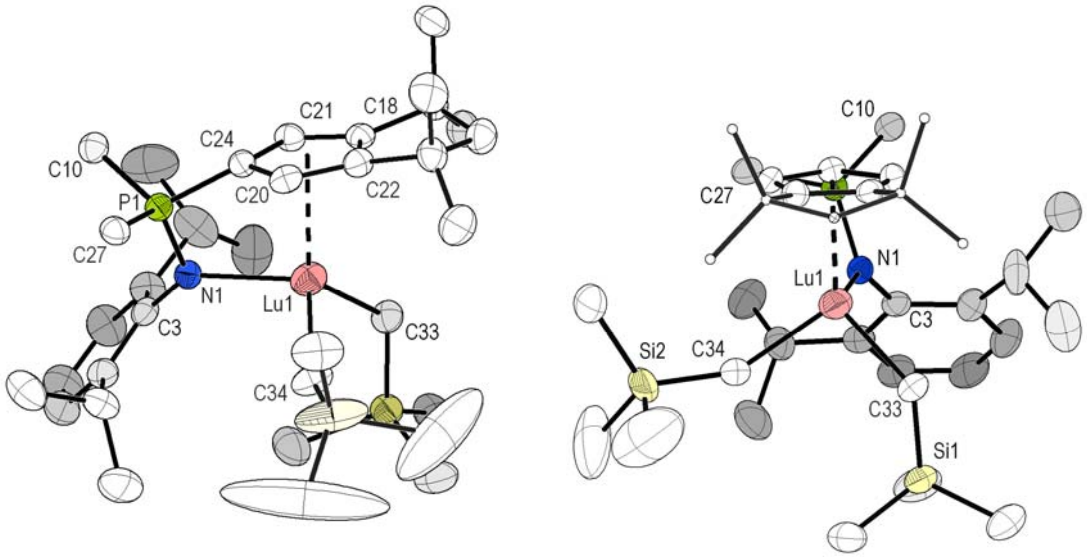

Figure 27. Molecular structure of complex [{**L10**}Lu(CH_2SiMe_3)$_2$] (**C14**): side view (left), front view (right). All hydrogen atoms and phenyl carbon atoms, except of its *ipso*-C, have been omitted for clarity. The slightly disordered Me_3Si-group at C33 has been also omitted. At the right figure aliphatic carbon atoms at C5-ring are ball-and-stick model. Selected bond lengths (Å) and angles (°): Lu1–N1 2.290(4), Lu1–C33 2.343(5), Lu1–C34 2.317(4), Lu–Z 2.409(1), Lu1–C24 2.559(4), P1–N1 1.626(4), P1–C24 1.763(4), C24–Lu1–N1 65.0(1), Z–Lu1–N1 92.3(1), N1–P1–C24 108.2(1), C33–Lu1–N1 115.1(2), C34–Lu1–N1 101.6(2), C35–Lu1–C39 100.5(2), Lu1–C33–Si1 134.8(3), Lu1–C34–Si1 147.6(3), C24–P1–N1–Lu1 18.0(2).

The P–N bond length in complex **C14** of 1.626(4) Å and is considerably elongated in comparison to the one found in **C13** (1.595(2) Å).

The decreased thermostability of the complex **C14**, in comparison with **C13**, can be attributed to the labile nature of the M–N bond that presumably leads to the cleavage of this bond followed by agglomeration and further decomposition in solutions. It is worth to note that the complexes with the ligand **L6**, which also has a Dip-group at the coordinating nitrogen atom, are less thermostable.

2.4. *Synthesis and Characterization of Divalent Ytterbium Complexes*

The syntheses of the divalent ytterbium complexes were achieved via the *salt metathesis route* from $[YbI_2(thf)_2]$ and corresponding deprotonated ligands $R_2P(C_5Me_4)NHAd$, R = Me (**L4**) and Ph (**S12**)[49] (Figure 13).

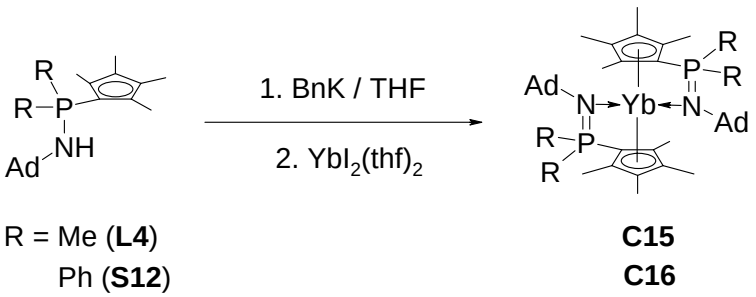

Scheme 13.

Due to very low solubility of starting $[YbI_2(thf)_2]$ in common organic solvents (ether, hexane, toluene) the syntheses were performed in THF. In a general synthetic route, to a solution of the appropriate ligand a stoichiometric amount of the BnK solution in the same solvent was added at 0°C followed by addition $[YbI_2(thf)_2]$. After stirring for a short period of time the formed colourless precipitate was filtered off. The complete removal of the solvent and subsequent crystallization yield deep-red crystalline solids in high yields.

Surprisingly, the crystalline materials are rather stable towards dioxygen for days, but hydrolyze slowly by air-moisture. The substances show high solubility in high polarity solvents like THF and pyridine; they are moderately soluble in ether and not soluble hexane. Complex **C15** is highly soluble in aromatic solvents. Whereas complex **C15** can be purified by crystallization from ether solutions, complex C**17** crystallizes from the same solvent with one molecule of ether in form of **C16**×Et_2O. By drying in vacuum (10^{-3} torr) or heating in toluene desolvatation with the formation of the solvent-free complex is observed.

The spectroscopy of both of these diamagnetic complexes is very similar; so that only the spectroscopic characterization of **C15** will be further discussed.

In the ^1H NMR spectrum of complex **C15**, depicted in Figure 28, <u>two</u> resonances for Me_2P-group were found (1.44 ($^2J_{PH}$ = 3.5 Hz), 1.48 ($^2J_{PH}$ = 3.1 Hz) ppm). Moreover, the resonances of each Me-group at the C5-ring have different chemical shift and appear as <u>four</u> singlets (2.19, 2.25, 2.27, 2.29 ppm). All CH_2-groups of the Ad-moiety appear as a single broad multiplet together at 1.70 ppm that was confirmed also by the HMQC spectroscopy.

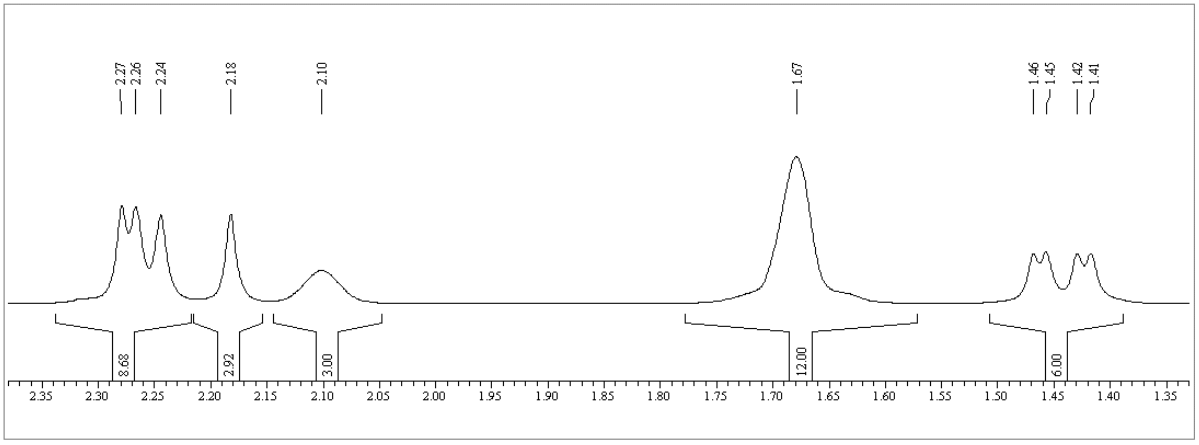

Figure 28. ^{1}H NMR spectrum (300.1 MHz) of ytterbium complex [Yb{**L4**}$_2$] (**C15**) dissolved in C_6D_6 at +25°C

These findings points out the asymmetric coordination mode of the ligands at the yttrium atom. More informative is the analysis of the ^{13}C NMR spectrum.

Two remotest of the four chemically non-equivalent Me-groups at the C5-ring appears as singlets at 13.8 and 15.8 ppm, whereas the other as set of doublets at 11.9 and 12.5 pm ($^{3}J_{CP}$ = 1.2 Hz, $^{3}J_{CP}$ = 1.5 Hz). The Ad-group signals resonate in the characteristic region. Asymmetric arrangement around the metal center was also approved by the presence of two doublets for *Me*$_2$P-group (21.3 ($^{1}J_{PC}$ = 23 Hz), 23.8 ($^{1}J_{PC}$ = 22 Hz)) and four coupled resonances for C5-ring carbon atoms (115.9 (J_{PC} = 13.2 Hz), 116.3 (J_{PC} = 12.7 Hz), 118.9 (J_{PC} = 15.4 Hz), 120.0 (J_{PC} = 14.9 Hz) ppm). For the C5-ring *ipso*-carbon atom, as expected, only one doublet at 90.6 ppm with a high one-bond coupling constant of 126 Hz was observed.

An interesting feature is the ^{31}P NMR resonance found at 0.5 ppm – in the characteristic region of *P*-cyclopentadienyl-iminophosphoranes (*cf.* **L1**, **L7** in Chapter III and **L8**, **L10** in Chapter IV).

The multinuclear NMR spectroscopy of **C15** and **C16** clearly indicates that both complexes of the bidentate *CpPN*-ligands is best described as a derivate of ytterbocene(II) and the bonding between nitrogen and the yttrium atoms is of a rather weak type. Further insight into the bonding situation is gained by X-ray diffraction analysis.

Large, deep reed crystals suitable for X-ray structure determination were grown by cooling of saturated ether solution to -10°C. Complex **C16** crystallizes in the monoclinic space group $P2_1/n$ with two independent molecules in the unit cell. The complex crystallized with one molecule of ether per ytterbium complex (**C16**×Et_2O). Its molecular structure with ellipsoids of 50% probability is presented in Figure 29. Both independent molecules can be best described as distorted tetrahedral complexes with Yb-atom falling on a crystallographic C_2-axis. Both ligands in each molecule adopt a chiral helix-like arrangement around the

ytterbium atom and therefore molecules exist as *Δ*- and *Λ*-isomers in the same crystal. Some bond lengths in both independent molecules are not equal as a result of packing effects, but in general they are nearly identical. In contrast to $[\{\eta^5\text{-}Me_5C_5\}_2Yb]_\infty$ and $[\{\eta^5\text{-}Me_4C_5H\}_2Yb]_\infty$, which both show close intermolecular contact distances (d(Yb···CC5) = 2.944(4) and 2.81(1) resp.), the molecules of **C16** are packed truly mononuclear in the solid state. Such constitution is typical for ytterbocenes with donor molecules coordinated at the metal center.

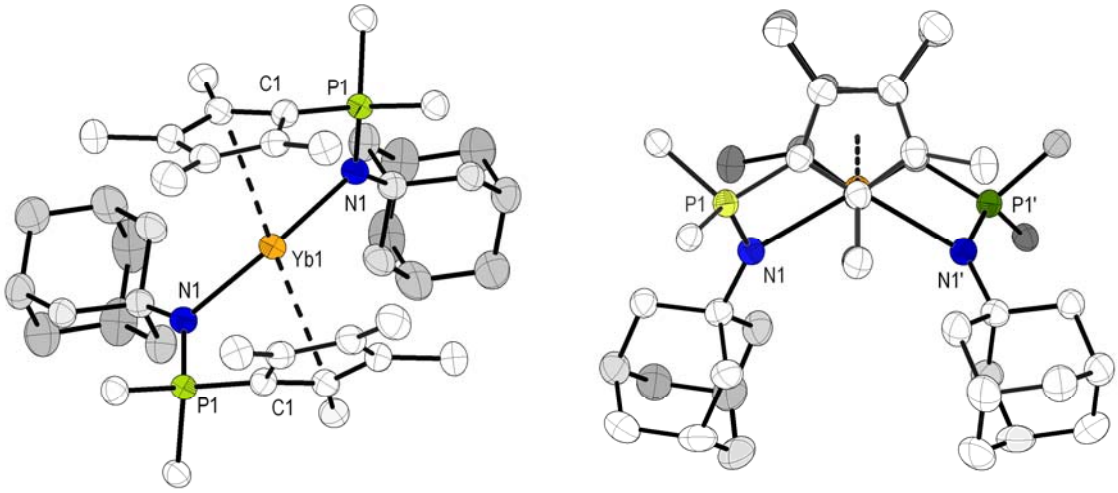

Figure 29. The molecular structures of complex C**16**×Et_2O. The *Δ*-isomer is presented; the ether molecules in the unit cell are not depicted). View along the C_2-axis (left) and the side-view (right); all hydrogen atoms and Ph-groups, except of their *ipso*-carbon atoms, have been omitted for clarity. Selected bond lengths (Å) and angles (°) for the *Δ*-isomer of **C17**×Et_2O: Yb1–N1 2.537(2), N1–P1 1.597(2), P1–C1 1.758(3), Yb1–Z 2.622(1), N1–Yb1–C1 60.2(1), N1–Yb1–Z 85.2(1), N1–P1–C1 103.1(1), N1–Yb1–N1' 122.1(1), Z–Yb1–Z' 133.6(1); for the *Λ*-isomer of **C17**×Et_2O: Yb2–N2 2.618(2), N2–P2 1.596(2), P2–C32 1.763(3), Yb2–Z 2.563(1), N2–Yb2–C32 59.6(1), N2–Yb2–Z 85.2(1), N2–P2–C32 102.7(1), N2–Yb2–N2' 127.8(1), Z–Yb2–Z' 131.5(1).

The average angle centroid(Z)–Yb–centroid(Z') is 132.6(1)°. Although both C5-rings are carrying four sterically encumbering methyl groups, the molecules are less strained, that, probably, can be explained by helix-bent-structure. For example, in the complex $[\{C_5H_5\}_2Yb(dme)]$[50] the Z–Yb–Z'angle is 134.1(1)°; whereas 129.9(2)° was found in the structure of $[\{MeC_5H_4\}_2Yb(dme)]$[51] and 133.9° in the structure of $[\{\eta^5\text{-}C_5H_4PPh_2\}_2$-Yb(dme)].[58] Further example of a sterically highly constrained molecule is the complex $[\{\eta^5\text{-}(tert\text{-}Bu)_2C_5H_3\}_2Yb(dme)]$[52] with a Z–Yb–Z' angle of 143.2(1)°. The average dihedral N–Yb–N' angle in **C16** is 125.0(1)° and it is significantly larger those ones in $[\{C_5H_5\}_2Yb(dme)]$[] and in $[\{\eta^5\text{-}C_5Me_5\}_2Yb(py)_2]$,[] where O–Yb–O' and N–Yb–N' angles are 69.3° and 85.6° respectively. However in the analogous, but, certainly, less strained $[\{\eta^5,\eta^1\text{-}C_5H_4(CH_2)_2NMe_2\}_2Yb]$[] the average dihedral N–Yb–N' angle is already 105.5°.

The molecular parameters in the *CpPN*-ligand are nearly identical with those found in structures of the *CpPN*-rare-earth metal dialkyl complexes with the same ligand (**C1** – **C3**); the average N–P bond length of 1.596(2) Å is very close to those of **C1** – **C3**, spanning the range 1.600(3) – 1.606(2) Å, and with complex **C13** (1.595(2) Å). Other molecular parameters in the ligand **L4** are unexceptional.

Further investigation of the ligand bonding mode, by comparison with the closest neighbour lutetium, shows more dissimilarities than might be expected. Even with respect of the larger ionic radius of ytterbium(II), which is 0.159 Å[Shan] greater than one of lutetium(III), the average Yb–N bond length is significantly longer (2.578(4) Å) than those in lutetium complexes **C1**, **C13** and **C14** (2.278(3), 2.289(2), 2.290(4) Å resp.) and comparable with ytterbocenes: 2.486, 2.514 Å in [{1,3-$(Me_3Si)_2C_5H_3$}$_2$Yb(Phen)],[53] 2.544, 2.586 Å in [{η^5-C_5Me_5}$_2$Yb(py)$_2$][54] and av. 2.579Å in [{η^5,η^1-$C_5H_4(CH_2)_2NMe_2$}$_2$Yb].[55] For instance, the Yb–N bond length in compounds with amidic nitrogen such as [{$(Me_3Si)_2N$}$_2$Yb(dppe)] is with 2.329 Å much shorter.[56]

The centroid(Z)–Yb distance of 2.593(2) Å is unexpectedly long and falls apart of the range typical for ytterbocenes. For instance, in ytterbocenes with the polysubstituated cyclo-pentadienyl ligands the Yb–Z distance of av. 2.466(3) Å was found in [{η^5-C_5Me_5}$_2$Yb(py)$_2$][] 2.443(2)Å in [{η^5-C_5Me_5}$_2$Yb(ter)][57] and 2.434(1) Å in [{η^5-$C_5H_4PPh_2$}$_2$Yb(dme)].[58] It worth to note that the Yb–Z distances in the complexes containing C_5H_5-moiety are in general shorter; for example, the distance of only 2.408(1) Å was found in [{η^5-C_5H_5}$_2$Yb(dme)][50] and av. 2.376(2) Å in [{η^5-C_5H_5}$_2$Yb(thf)].[59]

The elongation of the Yb–Z distance in the structure of complex **C16** could be attributed to the significant electron withdrawning –I and –M effect of the iminophosphorane-moiety. The comparison of the average P–C_{Ph} bond length (1.835(3) Å) with the closely related **S1** (av. 1.802 and 1.810 Å)[60] and **S2** (av. 1.806 Å)[61] confirm indirectly this assumption.

Presumably, this electronic effect is responsible for the unexpected enhanced air-stability of complexes **C15** and **C16**. A similar stabilization effect was observed in coinage metals: whereas the labile copper and silver complexes of the type [{C_5H_5}M(PR_3)] (M = Ag, Cu; R = Bu, Ph) are exceedingly moisture- and air-sensitive,[62] the addition of only one weakly electron withdrawing group (COOMe or Ac) at the C5-ring not only decreases sensitivity toward air, but also dramatically enhances their thermostability.[63] Unfortunately, no crystal structure determination of these crystalline compounds was provide so far.

2.5. *Catalytic Hydroamination Reactions*

The catalytic intramolecular hydroamination/cyclization of alkynes[64]1 and alkenes[65] has attracted considerable attention as a valuable method for the synthesis of nitrogenous heterocycles.[66] In a series of publications, *T. Marks* and collaborators have shown that metallocene derivatives of the lanthanide metals serve as excellent catalysts for the intramolecular hydroamination of alkenes, alkynes and allenes.[67] In addition, these investigators have demonstrated that dianionic 'constrained-geometry' half-sandwich complexes of the type [{η^5,η^1-(Me_4C_5)$SiMe_2$(N-*tert*-Bu)}Ln{$N(SiMe_3)_2$}] are catalytically quite active in this context.[9]

The catalytic activity of the rare-earth metal *CpPN*-complexes in intermolecular hydroamination/cyclization reactions was evaluated using thermostable **C1** – **C4** as precatalysts. As substrates, two typical *gem*-disubstituated *ω*-aminoalkenes – 2,2-dimethylpenten-4-ylamine (**S10**) and 2,2-diphenylpenten-4-ylamine (**S11**) – were explored (Scheme 14).

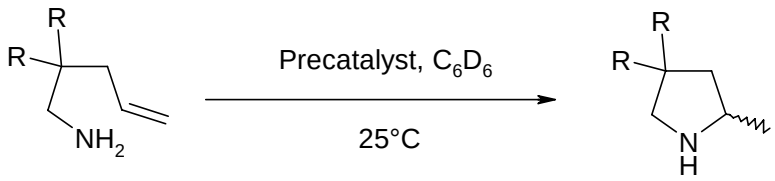

R = Me (**S10**), Ph (**S11**).

Scheme 14. Intramolecular hydroamination reaction of ω-aminoalkenes **S10** (R = Me) and **S11** (R = Ph).

The results of the intermolecular hydroamination reactions with ω-aminoalkenes with rare-earth metal *CpPN*- complexes are presented in Table 1.[36] The reactions proceeded with 4 – 5 mol% catalyst loading and monitored by ^{1}H NMR spectroscopy in C_6D_6 at +25°C.

Table 1. Intermolecular hydroamination of ω-aminoalkenes by catalysts **C1** – **C4**.[1)]

entry	precatalyst	substrate	[cat]/[s] (mol%)	time (h)	% yield[4)]	TON (h^{-1})
1	**C1**	**S10**	4.5		/[2)]	/
2	**C1**	**S11**	4.2		/[2)]	/
3	**C2**	**S10**	5.0		/[2)]	/
4	**C2**	**S11**	5.2		/[2)]	/
5	**C3**	**S10**	4.8	4.0	95	15.2
6	**C3**	**S11**	5.2	0.25	92	70.5
7	**C4**	**S10**	4.9	0.28	24	17.9
8	**C4**	**S11**	4.2	0.10	33[3)]	78.0

[1)] reaction conditions: C_6D_6, N_2 atm, +25°C; [2)] no reaction was observed after 10 h at 80°C, [3)] no further conversion was observed after additional 0.25 h. [4)] Yield by ^{1}H NMR.

The initial reaction step for complexes **C1** – **C4** is fast, showing an immediate and apparently quantitative formation of free TMS as judged by ^{1}H NMR. No hydroamination/cyclization reactions at all on both amines screened were observed in the cases of precatalysts **C1** and **C2** (Entries 1 – 4) even at +80°C for 48 h.

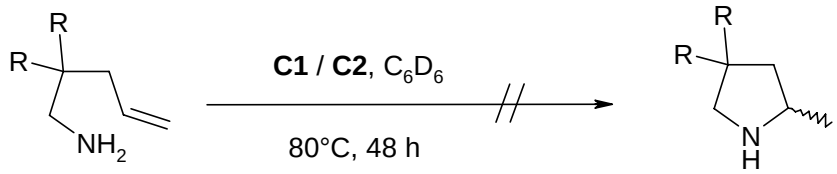

R = Me (**S10**), Ph (**S11**).

Scheme 15. Attempted cyclization reaction catalyzed by complexes of lutetium (**C1**) and scandium (**C2**).

Low activity for the complexes of the late lanthanides, such as [{μ^5-Me_5C_5}$_2$Lu{$CH(SiMe_3)_2$}] (TON < 1 h^{-1} at +80°C), was also reported in the literature (Table 2, entry 1). Replacement of this ligand environment by {η^5,η^5-$Me_2Si(Me_4C_5)_2$}[68] ligation dramatically increases the rate up to 75 h^{-1} (entry 2). Further enhancement of activity was achieved by the use of mixed dianoinic ligand {$Et_2Si(\eta^5$-$Me_5C_5)(\eta^5$-$C_5H_4)$}, where TON of 200 h^{-1} was achieved (entry 3).[69b] These results, can be rationalized by a positive effect of opening the access to the metal centre.[65b]

Table 2. π-Ancillary ligand effect on the turnover frequency (TON) for the catalytic intramolecular hydroamination/cyclyzation of substrate **S10**.

entry	Precatalyst	TON, h^{-1}
1	[{η^5-Me_5C_5}$_2$Lu{$CH(SiMe_3)_2$}][65b]	< 1 (80°C)
2	[{$Me_2Si(\eta^5$-$Me_4C_5)_2$}Lu{$CH(SiMe_3)_2$}][68]	75 (80°C)
3	[{$Et_2Si(\eta^5$-$Me_5C_5)(\eta^5$-$C_5H_4)$}Lu{$CH(SiMe_3)_2$}][69]	200 (80°C)

In the light of these observations, one can assume, that the complexes **C1** and **C2** do react with the substrates, but the catalyst formed "[{η^5,η^1-**L4**}M(NH–R)$_2$]" has filled coordination sphere to undergo the cyclization.

In the light of these observations, one can assume, that the complexes **C1** and **C2** do react with the substrates, but the catalytic species that might be formed "[{η^5,η^1-**L4**}M(NH–R)$_2$]" has probably too congested coordination sphere to undergo the cyclization.

The yttrium precatalyst [{**L4**}Y$(CH_2SiMe_3)_2$] **C3** displays high activity for the ring-closing of ω-aminoalkene **S10** at room temperature with TON of 15.2 h^{-1} (Table 1, Entry 5). This value is considerably higher than those reported for reactions, where [Y$(dmba)_3$] and [Y{$NH(SiMe_2)_2$}$(thf)_2$] were examined as precursors: these pre-catalysts show only low

activity with TON's of 2.6 at +25°C and 1.2 h^{-1} at +50°C respectively ([cat.]/[s] = 3 mol%).[70] The activity for catalytic hydroamination/cyclization of complex **C3** is comparable to one found for yttrium complex [{$MeN(CH_2CH_2NMes)_2$}Y(dmba)][70] (TON = 10 h^{-1}, [cat]/[s] = 3 mol%) and homoleptic amido catalysts [Ln{$N(SiMe_3)_2$}$_3$], where Ln = Y (TON = 11.6 h^{-1})[70] and Nd[71], for the latter complex conversion of > 95% was achieved 4 h. (The use of homoleptic amido catalysts is usually leads to low *cis/trans*-diastereomeric ratios of ca. 4:1, if a reaction proceed with an appropriate substrate.)[70]

In the most of cases, the ring-closing reaction with the substrate **S11** proceeds more rapidly.[66] So, the reactions catalyzed by yttrium complex **C3** are almost quantitative after 6 min at catalyst loading of 5.2%, resulting TON of 70.5 h^{-1} at +25°C (Entry 4).

The neodymium precatalyst **C4** is somewhat more active (Table 1, entries 7, 8) showing high TON in the beginning, but, surprisingly, the reactions do not proceed to full conversion. Highest yields obtained for both amines vary at around 30% and do not change after prolonged reaction times or at elevated temperatures (80°C). It is believed that this unusual inhibition effect could be better explained by the catalysts' decomposition, rather than by chemical inhibition, because this neodymium complex **C4** has appeared to be an extremely air- or thermosensitive compound.

The observed rate law for complex **C3** was found to be first order in substrate, but it deviates considerably at high conversions (Figure 30).

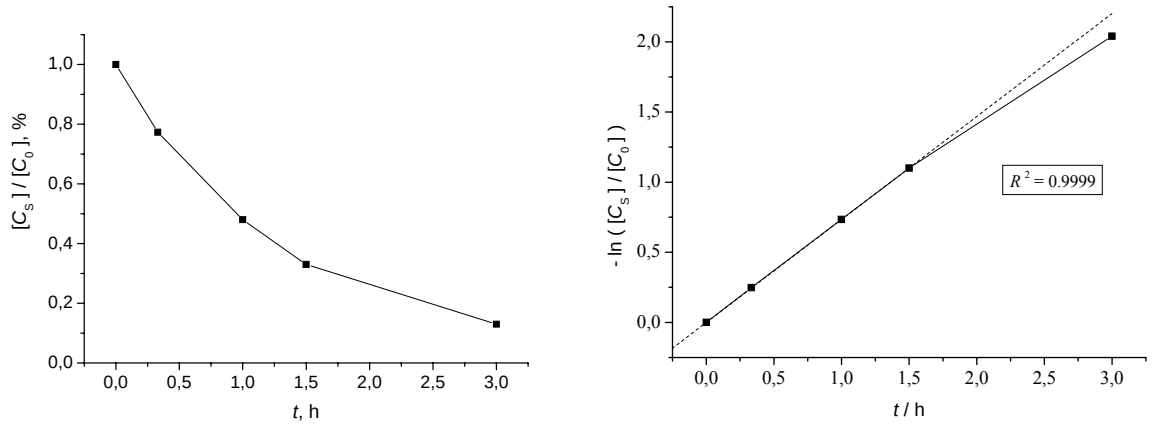

Figure 30. Plot of time dependence of substrate consuming ratio in ring-closing of the *ω*-alkylamine **S10** (left); Plot of time dependence of the rate of hydroamination (right). The dotted line through the first four data points represents the last-squares fit. Reaction conditions: [C_0] = 0.92 mol L^{-1} with **C3** (5.3 mol%) in C_6D_6 at +25°C)

The activities of the *CpPN*-lanthanide complexes of yttrium and neodymium are comparable to those *CpSiN*-lanthanide complexes recently reported by *T. Marks*.[9,72] for the same substrates **S10** and **S11** under the same reaction conditions: [{$Me_2Si(\eta^5$-$C_{13}H_{13}N)N$(*tert*-Bu)}Lu{$N(SiMe_3)_2$}(thf)] (**S10**: TON = 19.1 h^{-1}; **S11**: TON = 205 h^{-1}) and [{$Me_2Si(C_5Me_4)N$(*tert*-Bu)}Ln{$E(SiMe_3)_2$}] (**S10**: TON = 10 h^{-1}(Ln = Yb, E = CH), TON = 200 h^{-1} (Ln = Nd, E = N)).

It is worth to note, that the first order in substrate kinetic law is a rarely observed catalyst behavior. Usually, for the intra-molecular Ln-catalyzed hydroamination/cyclization, the zero order in substrate law was observed.[65b,70] A mechanism that can be proposed to explain this unusual kinetic law is given in Figure 31, but for its detailed confirmation further investigations are required.

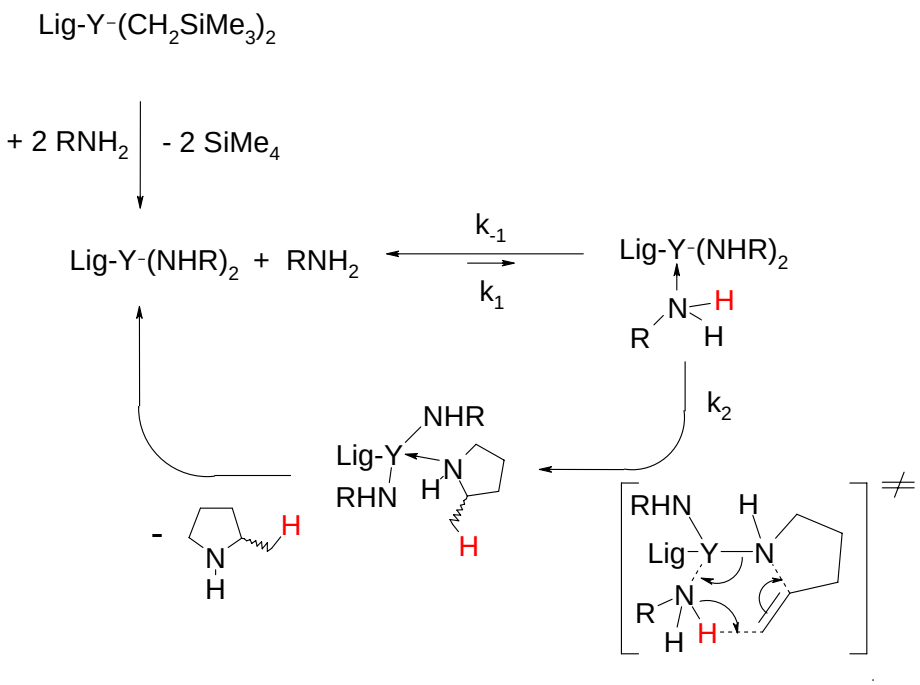

Figure 31. The proposed mechanism explaining the first order in substrate of the catalytic hydroamination/cyclization reaction with **C3** and **C4** pre-catalysts

This mechanism can explain the absence of reaction observed with the lutetium (**C1**) and scandium (**C2**) complexes. Upon formation of coordinatively saturated di-amide species [{**L4**}Ln$(NHR)_2$] of a distorted tetrahedral geometry, no further coordination of the reacting substrate becomes possible ($k_1/k_{-1} \rightarrow 0$) which results in deactivation of catalytic cycle.

3. CONCLUSIONS

In this chapter the synthesis and characterization of the rare-earth metal complexes with *CpPN* ligands is described in detail. It was shown that these monoanionic ligands form well defined 1:1 complexes of the type [(*CpPN*)LnR_2] (R = CH_2SiMe_3, dmba) and most of them were characterized by single crystal X-ray diffraction analysis (XRD). In all isolated complexes, with only one exception, the η^1,η^5-coordination mode of these new constrained-geometry ligands is realized.

The complexes were synthesized by a new one-pot protocol, which combines *deprotonation* and *salt metathesis* methods by addition of the 3 equivalents of $LiCH_2SiMe_3$ as base/ligand to a stirred mixture of corresponding THF or DME solvated rare-earth metal trihalide and appropriate *CpPN* ligand in ether. The very short synthetic protocol allows the successful isolation of the highly reactive and labile alkyl complexes of early lanthanides, which are usually prone to decompose in solution at ambient temperature. All complexes were isolated as microcrystalline solids and were completely characterized by multinuclear NMR spectroscopy and microanalysis.

The following *CpPN* ligands were investigated in this work: $Me_2P(C_5Me_4)$NHAd (**L4**), $Ph_2P(C_5H_4)$NHDip (**L6**), $Ph_2P(Cp^{TM})$NHAd (**L9**) and Ph_2P(NDip)$Cp^{TM}H$ (**L10**).

The ligand **L4** allows the synthesis of the constrained geometry dialkyl complexes [{**L4**}$M(CH_2SiMe_3)_2$] not only for the elements with smaller ionic radii (M = Lu (**C1**), Sc (**C2**), Y (**C3**)), but also for the early lanthanides (M = Nd (**C4**)). The complexes with the ligand **L4** possess high thermal stability. As it was shown by multinuclear NMR spectroscopy they are mononuclear in solution and in the solid state (XRD: **C1** – **C3**). Detailed analysis of the ^1H and ^{13}C NMR spectra was also accomplished for the paramagnetic Nd-complex **C4**.

The high reactivity of [{**L4**}$Nd(CH_2SiMe_3)_2$] (**C4**) was proven by isolation of two decomposition products – binuclear heteroleptic [{**L4**}$Nd(\mu^2$-OMe$)(CH_2SiMe_3)]_2$ (**C5**) and tetranuclear hydroxy-species [{**L4**}$Nd(\mu^2$-$OH)_2]_4$ (**C6**). Both complexes crystallize more readily than the parent complex **C4** and were analyzed by XRD. The formation of complex **C5** can be rationalized by cleavage of DME, which is introduced with the starting neodymium source [$NdCl_3$(dme)]. The **C6** complex is obviously formed upon hydrolysis of **C4**.

The dialkyl rare-earth metal complexes of yttrium (**C9**) and neodymium (**C10**) with the smaller ligand $Ph_2P(C_5H_4)$NHDip (**L6**) were isolated with an additional coordinated solvent (THF) molecule, whereas for smaller rare-earth metals – scandium (**C7**) and lutetium (**C8**) – the solvent-free complexes were obtained. The complexes **C7**, **C9** and **C10** were

characterized by XRD analysis. Distorted tetrahedral coordination was observed in the structure of the scandium complex **C7**. The complexes **C9** and **C10** are isostructural and reveal only weak coordination of the *CpPN* nitrogen atom of the ligand at the metal center.

Attempts to synthesize solvent-free yttrium complex starting from $[YCl_3(dme)_2]$ failed. A small crop of a crystalline material obtained from the crystallization was analyzed by XRD. It was found that the binuclear heteroleptic complex $[\{\mathbf{L6}\}Y(\mu^2\text{-}OMe)(CH_2SiMe_3)]_2$, with similar constitution as found in **C5**, is formed. However, unlike the complex **C5**, it possesses a cisoid arrangement of alkyl ligands.

The equimolar reaction of the ligand **L6** with homoleptic complex $[Y(dmba)_3]$ (dmba = *ortho*-metallated dimethylbenzylamine) yields selectively $[\{\mathbf{L6}\}Y(dmba)_2]$ (**C12**). The structure in solution was investigated by NMR method. The ^{31}P NMR spectrum shows a resonance in the typical for iminophosphoranes region. The accurate analysis of the ^{1}H, ^{13}C NMR and 2D spectra also confirms the formation of the "open" *CpPN* complex $[\{\eta^5\text{-}\mathbf{L6}\}Y(dmba)_2]$, in which coordination of the nitrogen atom of the ligand is not realized.

Two homoleptic ytterbium(II) complexes of the type $[Yb\{CpPN\}_2]$ with the ligands $R_2P(C_5Me_4)NHAd$, R = Me (**L4**) and Ph (**S12**) were synthesized by the *salt metathesis* route from the potassium salt of the appropriate ligand and $[YbI_2(thf)_2]$. The complexes were isolated as red-orange crystalline solids. Surprisingly both are moderately air-sensitive. The complex $[Yb\{\eta^5,\eta^1\text{-}(Me_4C_5)PPh_2(NAd)\}_2]$ was characterized by XRD analysis. In the solid state this C_2-symmetrical complex reveals distorted tetrahedral coordination with both *CpPN* ligands in a helix-like arrangement around the ytterbium atom. The analysis of the molecular structure reveals an ytterbocene(II) with rather weakly coordinated nitrogen atoms.

Hydroamination/cyclization reactions on two *gem*-substituted penten-4-ylamines were investigated. The yttrium complex **C3** was found to be the most promising catalyst in the whole series. Complexes of scandium (**C1)** and lutetium (**C2)** having the smallest ionic radii among the whole series of rare-earth metals were found to be completely inactive in hydroamination/cyclization reactions even at elevated temperatures and after prolonged heating at 80°C. The neodymium complex **C4** was found as reactive as yttrium complex **C3**, but conversions are not quantitative. A possible mechanism explaining untypical first order in substrate kinetic law found for this catalytic reaction was proposed.

4. EXPERIMENTAL SECTION

General considerations. All manipulations were performed under purified argon or nitrogen using standard high vacuum or *Schlenk*- or Glove-box techniques. Solvents were dried and distilled under argon employing standard drying agents. All organic reagents were purified by conventional methods. The NMR spectra were recorded at +25°C on a Bruker ARX200, Bruker AMX300, and Bruker AVANCE DRX400. Elemental analyses were performed at the Analytical Laboratory of the Chemistry Department / Philipps-Universität Marburg. The following starting materials were prepared according to the literature procedures: $[Lu(CH_2SiMe_3)_3(thf)_2]$,[5] $[ScCl_3(thf)_3]$, $[YCl_3(thf)_3]$, and $[NdCl_3(thf)_{1.5}]$.[72] and $[YCl_3(dme)_2]$ (Chapter II, Part 4.1). The synthesis of the ligands **C4** / **C6** and **C9** / **C10** is reported in Chapter III and IV, respectively.

*4.1. Synthesis of [{η^5,η^1-$Me_2P(C_5Me_4)NAd$}$Lu(CH_2SiMe_3)_2$] (**C1**)*: To a solution of $[Lu(CH_2SiMe_3)_3(thf)_2]$ (580 mg, 1 mmol) in 1 mL C_6D_6 a solution of the ligand **L4** (330 mg, 1 mmol) in 2 mL C_6D_6 was added at room temperature. An aliquote of 0.6 mL of thus obtained pink-colored solution was transfered into WILMAD 505-PS 7 NMR tube equipped with a *Young* teflon valve. The remaining reaction mixture was allowed to stay in a glove box for crystallization at +25°C giving after evaporation of the solvent 540 mg of **C1** in form of colourless crystals in – together with the soluble parts – close to quanitative yield.

^{1}H NMR (300 MHz, C_6D_6): δ = -0.95, -0.89 (m, AB-system, 2×$^3J_{HH}$ = 11.3 Hz, 4H, CH_2SiMe$_3$), 0.37 (s, 18H, CH$_2$SiMe_3), 1.17 (d, $^2J_{HP}$ = 12 Hz, 6H, Me_2P), 1.56 (br m, 6H, CH_2(CH)$_2$), 1.73 (br d, 6H, N–C(CH_2)$_3$), 2.01 (br s, 3H, CH$_{Ad}$), 2.04, 2.11 (2×s, 2×6H, 2×MeC$_{C5}$) ppm.

^{13}C{^{1}H} NMR (75.0 MHz, C_6D_6): δ = 4.9 (s, SiMe_3), 14.9, 12.1 (2×s, MeC$_{C5}$), 21.9 (d, $^1J_{CP}$ = 54 Hz, Me_2P), 30.2 (s, CH$_{Ad}$), 36.3 (s, CH$_2$(CH)$_2$), 38.3 (s, LuCH$_2$Si), 44.7 (d, $^3J_{CP}$ = 8 Hz, NC(CH$_2$)$_3$), 54.1 (d, $^2J_{CP}$ = 6 Hz, NC_{Ad}), 83.8 (d, $^1J_{CP}$ = 115 Hz, PC_{C5}), 121.5, 123.5 (2×d, J_{CP} = 13 Hz, J_{CP} = 14 Hz, 2×MeC_{C5}) ppm.

^{31}P{^{1}H} NMR (121.5 MHz, C_6D_6): δ = 9.6 ppm.

Anal. Calcd for $C_{29}H_{55}LuNPSi_2$ (679.88): C 51.23, H 8.15, N 2.06;
Found: C 50.56, H 8.01, N 2.32.

4.2. *Synthesis of [{η⁵,η¹-Me₂P(C₅Me₄)NAd}Sc(CH₂SiMe₃)₂] (**C2**):* To a stirred suspension of [$ScCl_3(thf)_3$] (368 mg, 1.00 mmol) and the ligand **L4** (331 mg, 1.00 mmol) in 15 mL ether, a solution of $LiCH_2SiMe_3$ (286 mg, 3.04 mmol) in 10 mL hexane was added drop by drop at 0°C. The reaction mixture was stirred at 0°C for another 0.5 h than it was concentrated in vacuum to half of the original volume and formed LiCl was filtered off through Celite®. The solvent was stripped off, whereupon a colourless foamy solid forms, which was crystallized from hexane. Storage at -30°C followed by filtration and drying in vacuum results in isolation of a white, microcrystalline solid in yield of 74% (412 mg).

^{1}H NMR (300.1 MHz, C_6D_6): δ = -0.40, -0.37 (d, AB-System, $^2J_{HH}$ = 11.2 Hz, 2H, C*H*$_2$SiMe$_3$), 0.36 (s, 18H, CH$_2$Si*Me*$_3$), 1.17 (d, $^2J_{HP}$ = 12.5 Hz, *Me*$_2$P), 1.60 (m, 6H, NC(C*H*$_2$)$_3$), 1.83 (m, 6H, C*H*$_2$(CH)$_2$), 2.01 (s, 6H, C$_5$*Me*$_4$), 2.02 (m, 3H C*H*(CH$_2$)$_3$), 2.14 (s, C$_5$*Me*$_4$) ppm.

^{13}C{^{1}H} NMR (75.0 MHz, C_6D_6): δ = 4.5 (s, Si*Me*$_3$), 12.0 (s, C$_5$*Me*$_4$), 14.4 (d, J_{CP} = 1.7 Hz, C$_5$*Me*$_4$), 21.6 (d, $^1J_{CP}$ = 55 Hz, *Me*$_2$P), 30.4 (s, *C*H(CH$_2$)$_3$), 36.5 (s, *C*H$_2$(CH)$_2$), 47.2 (d, $^3J_{CP}$ = 8.7 Hz, NC(*C*H$_2$)$_3$), 54.6 (d, $^2J_{CP}$ = 6.8 Hz, PN*C*), 84.8 (d, $^1J_{CP}$ = 114 Hz, P*C*$_{C5}$), 122.5 (d, J_{CP} = 13.3 Hz, *C*$_5$Me$_4$), 125.7 (d, J_{CP} = 14.4 Hz, *C*$_5$Me$_4$) ppm.

^{31}P{^{1}H} NMR (81.0 MHz, C_6D_6): δ = 12.0 (s) ppm

Anal. Calcd for $C_{29}H_{55}NPScSi_2$ (549.87): C 63.35, H 10.08, N 2.55;
Found: C 62.92, H 9.78, N 2.41.

4.3. *Synthesis of [{η⁵,η¹-Me₂P(C₅Me₄)NAd}Y(CH₂SiMe₃)₂] (**C3**):* The similar procedure as for the synthesis of complex **C2**, starting from [$YCl_3(dme)_2$] (188 mg, 0.50 mmol), ligand **L4** (165 mg, 0.50 mmol) in 10 mL ether and $LiCH_2SiMe_3$ (148 mg, 1.57 mmol) in 20 mL hexane, was followed. A colourless, microcrystalline solid was isolated in a yield of 83% (246 mg).

^{1}H NMR (300.1 MHz, C_6D_6): δ = -0.70, -0.75 (2×d, ABX system, $^2J_{HH}$ = 11 Hz, $^2J_{HY}$ = 3.0 Hz), 0.40 (s, 18H, Si*Me*$_3$), 1.13 (d, 6H, $^2J_{HP}$ = 12.5 Hz, *Me*$_2$P), 1.56 (m, 6H, C*H*$_2$(CH)$_2$), 1.71 (m, 6H, PC(C*H*$_2$)$_3$), 2.00 (m, 3H, C*H*(CH$_2$)$_3$), 2.03 (s, 6H, 2×*Me*C$_{C5}$), 2.12 (s, 6H, 2×*Me*C$_{C5}$) ppm.

^{13}C{^{1}H} NMR (75.0 MHz, C_6D_6): δ = 4.7 (s, Si*Me*$_3$), 11.4, 13.8 (2×s, 2×*Me*C$_{C5}$), 21.9 (d, $^1J_{CP}$ = 55 Hz, *Me*$_2$P), 30.2 (s, C*H*(CH$_2$)$_3$), 31.5 (d, $^1J_{CP}$ = 41 Hz, *C*H$_2$SiMe$_3$), 36.3 (s, H$_2$*C*(CH)$_2$), 47.5 (d, $^3J_{CP}$ = 8.8 Hz, PNC*C*H$_2$(CH)), 54.3 (d, $^2J_{CP}$ = 7.2 Hz, PN*C*$_{Ad}$), 121.8, 123.7 (2×d, J_{CP} = 13.2 Hz, J_{CP} = 14.3 Hz, 2×Me*C*$_{C5}$) ppm.

^{31}P{^{1}H} NMR (MHz, C_6D_6,): δ = 9.0 ppm

Anal. Calcd for $C_{29}H_{55}NPSi_2Y$ (593.82): C 58.66, H 9.34, N 2.36;
Found: C 59.21, H 9.71, N 2.41.

4.4. *Synthesis of [{η⁵,η¹-Me₂P(C₅Me₄)NAd}Nd(CH₂SiMe₃)₂]* (***C4***): To a mixture of $[NdCl_3(thf)_{1.5}]$ (360 mg, 1.00 mmol) and ligand **L4** (331 mg, 1.00 mmol) 10 mL of THF was added and the obtained red reaction mixture was stirred for 0.5 h. The solvent was completely removed in vacuum, then 20 mL ether were added. The obtained blue suspension was stirred for 1 h and the solvent was again removed in vacuum yielding pale blue powder. The following procedures – addition of $LiCH_2SiMe_3$ (284 mg, 3.00 mmol) – are similar to reported for the synthesis of complex **C2**, with the exception that for the extraction of complex from the reaction mixture toluene was used instead of hexane. Yield: 34% (220 mg) of a sky-blue microcrystalline solid.

^{1}H NMR (300.1 MHz, C_6D_6): δ = -21.09 (br s, 6H, *β-Ad*), -13.07 (s, 6H, *Me*$_2$C5), -5.65 (d, $^3J_{HH}$ = 11 Hz, 3H, *δ-Ad*), -4.75 (s, 3H, *γ-Ad*), -3.48 (d, $^3J_{HH}$ = 11 Hz, 3H, *δ-Ad*), 2.58 (s, 18H, Si*Me*$_3$), 10.28 (d, $^2J_{HP}$ = 7.3 Hz, *Me*$_2$P), 11.22 (s, 6H, *Me*$_2$C5), 19.75 (d, *H*CHSiMe$_3$), 28.69 (HC*H*SiMe$_3$) ppm.

^{13}C{^{1}H} (125.8 MHz, C_6D_6): *δ* = -37.5 (br s, *Me*$_2$C$_5$Me$_2$), -15.3 (Me$_2$C$_5$*Me*$_2$), -13.4 (*α-Ad*), 19.6 (*γ-Ad*), 27.4 (*δ-Ad*), 29.3 (*β-Ad*), 30.4 (Si*Me*$_3$), 34.9 (d, $^1J_{CP}$ = 53 Hz, *Me*$_2$P), 102.8 (Me*C*$_{C5}$), 107.3 (d, $^2J_{CP}$ = 118 Hz, P*C*$_{C5}$), 146.0 (Me*C*$_{C5}$), ppm.

^{31}P{^{1}H} (81.1 MHz, C_6D_6): *δ* = 22.1 ppm.

Anal. Calcd for $C_{29}H_{55}NNdPSi_2$ (649.15): C 53.65, H 8.54, N 2.16;
Found: C 53.11, H 8.21, N 2.31.

4.5. Formation of [{η⁵,η¹-Me₂P(C₅Me₄)NAd}Nd(CH₂SiMe₃)(μ-OMe)]₂ (***C5***) *and [{η⁵,η¹-C₅Me₄PMe₂(NAd)}Nd(OH)₂]₄* (***C6***)*:* These complexes were obtained by accident upon storing of concentrated benzene-d_6 solutions of complex **C4** at 8°C in NMR tubes in two independent experiments. The synthesis of **C6** was accomplished as reported for complex **C4**.

For the synthesis of compound **C5** $[NdCl_3(dme)]$ was used as the starting neodymium source. The reaction mixture was stirred over night. Single crystals were characterized by X-ray diffraction analysis.

Crystallographic data for the neodymium complex **C5**:[36] Triclinic, space group *P*-1, *a* = 11.538(2) Å, *b* = 11.812(2) Å, *c* = 13.610(2) Å, *α* = 100.31(1)°, *β* = 96.94(1)°, *γ* = 109.06(1)°, V = 1692.6(3) Å^3, Z = 1, D_c = 1.305 g·cm^3, *μ* = 1.703 mm^{-1}, *F*(000) = 694.

Crystallographic data for the neodymium compound **C6**: Triclinic, space group *P*-1, a = 15.270(2) Å, b = 19.073(2) Å, c = 20.551(3) Å, α = 78.54(2)°, β = 82.01(2)°, γ = 84.33(2)°, V = 5793.5(12) Å^3, Z = 2, D_c = 1.435 g·cm^3, μ = 1.873 mm^{-1}, F(000) = 2576.

*4.6. Synthesis of [{η^5,η^1-$Ph_2P(C_5H_4)NDip$}$Sc(CH_2SiMe_3)_2$] (**C7**):* The similar procedure as for the synthesis of complex **C2**, starting from [$ScCl_3(thf)_3$] (368 mg, 1.00 mmol), ligand **L6** (425 mg, 1.00 mmol) in 10 mL ether and $LiCH_2SiMe_3$ (284 mg, 3.00 mmol) in 20 mL hexane, was followed. Yield: 48% (330 mg) of a colourless crystalline solid.

^{1}H NMR (300.1 MHz, C_6D_6): δ = 0.12 (br s, 2H, C*H*$_2$SiMe$_3$), 0.25 (br s, 2 H, C*H*$_2$SiMe$_3$), 0.37 (s, 18 H, CH$_2$CH$_2$Si*Me*$_3$), 1.25 (br s, 12H, Me$_2$CH), 3.42 (sept, $^3J_{HH}$ = 6.8 Hz, 2 H, Me$_2$C*H*), 6.77 (m, 2H, C$_5$*H*$_4$), 8.85 – 7.09 (m, 11H, C$_5$*H*$_4$, *Ph, Dip*), 7.41 (m, 4H, *o-Ph*) ppm.

^{13}C{^{1}H} NMR (75.0 MHz, C_6D_6): δ = 3.9 (s, CH$_2$Si*Me*$_3$), 23.5 (br s, *Me*$_2$CH), 26.3 (br s, *Me*$_2$CH), 28.8 (s, Me$_2$*C*H), 42.2 (br s, *C*H$_2$SiMe3), 92.7 (d, $^1J_{CP}$ = 121 Hz, *ipso*-C$_5$H$_4$), 118.3 (d, J_{CP} = 12.9 Hz, *C*$_5$H$_4$), 119.2 (d, J_{CP} = 14.2 Hz, *C*$_5$H$_4$), 124.8 (d, J = 3.4 Hz, *m*-Dip), 125.3 (d, J_{CP} = 3.9 Hz, *p*-Dip), 127.7 (d, J = 90 Hz, *ipso*-Ph), 128.7 (d, J = 12.3 Hz, *m*-Ph), 132.8 (d, J = 2.8 Hz, *p*-Ph), 133.5 (d, J = 9.9 Hz, *o*-Ph), 139.9 (d, J_{CP} = 9.3 Hz, *ipso*-Dip), 145.8 (d, J_{CP} = 6.1 Hz, *o*-Dip) ppm.

^{31}P{^{1}H} NMR (81.0 MHz, C_6D_6): δ = 12.1 (s) ppm

Anal. Calcd for $C_{37}H_{53}NPScSi_2$ (643.94): C 69.01, H 8.30, N 2.17;
Found: C 68.71, H 8.59, N 2.10.

4.7. *Synthesis of [{η^5,η^1-$Ph_2P(C_5H_4)NDip$}$Lu(CH_2SiMe_3)_2$] (**C8**):* The same procedure as for synthesis of complex **C1**, starting from [$Lu(CH_2SiMe_3)_3(thf)_2$] (580 mg, 1.00 mmol) dissolved in 10 mL toluene and the ligand **L6** (425 mg) in 10 mL of the same solvent, was followed. Crystallization from hexane at -30°C yields a colourless solid in yield of 67% (520 mg).

^{1}H NMR (300.1 MHz, C_6D_6): δ = -0.59 (s, 4H, C*H*$_2$SiMe$_3$), 0.40 (s, 18H, CH$_2$Si*Me*$_3$), 0.76 (br d, $^3J_{HH}$ = 6.8 Hz, $\nu_{½}$ = 7.6 Hz, 12H, *Me*$_2$CH), 3.30 (sept, $^3J_{HH}$ = 6.8 Hz, 2H, Me$_2$C*H*), 6.71 (m, 2H, *H*C$_{C5}$), 7.00 (m, 11H, *m-/p-Ph, Dip, H*C$_{C5}$, *m/p-Ph*), 7.40 – 7.48 (m, 4H, *o-Ph*) ppm.

^{13}C{^{1}H} NMR (75.0 MHz, C_6D_6): δ = 4.6 (CH$_2$Si*Me*$_3$), 24.7 (*Me*$_2$CH), 28.9 (Me$_2$*C*H), 39.1 (*C*H$_2$SiMe$_3$), 93.0 (d, $^1J_{PC}$ = 124 Hz, P*C*$_{C5}$), 116.5, 118.4 (2×d, J_{PC} = 13.1 Hz, J_{PC} = 14.5 Hz, 2×H*C*$_{C5}$), 124.5 (d, $^4J_{PC}$ = 3.4 Hz, *m-Dip*), 124.7 (d, $^5J_{PC}$ = 3.6 Hz, *p-Dip*), 128.6 (d, $^3J_{PC}$ =

12.4 Hz, *m-Ph*), 128. 7 (d, $^{1}J_{PC}$ = 90 Hz, *ipso-Ph*), 132.5 (d, $^{4}J_{PC}$ = 2.9 Hz, *p-Ph*), 133.3 (d, $^{2}J_{PC}$ = 9.4 Hz, *o-Ph*), 141.4 (d, $^{2}J_{PC}$ = 9.6 Hz, *ipso-Dip*), 145.5 (d, $^{3}J_{PC}$ = 5.3 Hz, *o-Dip*).

$^{31}P\{^{1}H\}$ NMR (81.0 MHz, C_6D_6): δ = 11.3 ppm

Anal. Calcd for $C_{37}H_{51}LuNPSi_2$ (771.94): C 57.57, H 6.66, N 1.81;
Found: C 57.11, H 6.54, N 2.03.

*4.8. Synthesis of [{η^5,η^1-$Ph_2P(C_5H_4)NDip$}$Y(CH_2SiMe_3)_2(thf)$] (**C9**):* The same procedure as for **C2**, starting from [$YCl_3(thf)_3$] (412 mg, 1.00 mmol), ligand **L6** (425 mg, 1.00 mmol) in 30 mL ether and a solution of $LiCH_2SiMe_3$ (286 mg, 3.04 mmol) in 15 mL of hexane at 0°C, was followed. Crystallization at -30°C gives a colourless, microcrystalline solid in yield of 34% (231 mg).

^{1}H NMR (300.1 MHz, C_6D_6): δ = -0.48 (br d, $^{1}J_{HY}$ = 3.5 Hz, $\nu_{½}$ = 5.2 Hz, 4 H, CH_2SiMe$_3$), 0.46 (s, 18 H, CH_2Si*Me*$_3$), 0.74 (br s, $\nu_{½}$ = 107 Hz, 12 H, *Me*$_2$CH), 1.14 (m, 4 H, *THF*), 3.18 (sept, $^{3}J_{HH}$ = 6.8 Hz, 2 H, Me_2C*H*), 3.66 (m, 4 H, *THF*), 6.74 (m, 2 H, *H*C_{C5}), 6.90 – 7.00 (m, 9 H, *Ar*), 7.09 (m, 2 H, *H*C_{C5}), 7.47 (m, 4 H, *o-Ph*) ppm.

$^{13}C\{^{1}H\}$ NMR (75.0 MHz, C_6D_6): δ = 4.6 (s, CH_2Si*Me*$_3$), 24.5 (br s, *Me*$_2$CH), 24.9 (*THF*), 29.0 (C*H*Me$_2$), 31.8 (d, $^{1}J_{CY}$ = 40 Hz, CH_2SiMe$_3$), 70.1 (*THF*), 94.5 (d, *J* = 125 Hz, *ipso-*C_{C5}), 115.5 (d, *J* = 13.5 Hz, C_{C5}), 119.0 (d, *J* = 14.4 Hz, C_{C5}), 124.2 (d, $^{5}J_{CP}$= 4.0 Hz, *p-Dip*), 124.4 (d, $^{4}J_{CP}$= 3.5 Hz, *m-Dip*), 128.4 (d, $^{3}J_{CP}$= 12 Hz, *m-Ph*), 129.5 (d, $^{1}J_{CP}$ = 88 Hz, *ipso-Ph*), 132.3 (d, $^{4}J_{CP}$ = 2.9 Hz, *p-Ph*), 133.1 (d, $^{2}J_{CP}$ = 9.6, Hz, o-Ph), 141.4 (d, $^{2}J_{CP}$ = 9.8 Hz, *ipso-Dip*), 145.2 (d, $^{3}J_{CP}$ = 6.4 Hz, *o-Dip*) ppm.

$^{31}P\{^{1}H\}$ NMR (81.0 MHz, C_6D_6): δ = 9.6 (s) ppm.

Anal. Calcd for $C_{41}H_{59}NOPSi_2Y$ (757.99): C 64.97, H 7.85, N 1.85;
Found: C 64.56, H 7.80, N 1.90.

*4.9. Synthesis of [{η^5,η^1-$Ph_2P(C_5H_4)NDip$}$Nd(CH_2SiMe_3)_2(thf)$] (**C10**):* This complex was obtained upon storing of a concentrated hexane solution at -30°C, prepared as reported for **C2**, starting from equimolar amount of [$NdCl_3(thf)_{1.5}$], ligand **L6** and $LiCH_2SiMe_3$. Single crystals were characterized by X-ray diffraction analysis.

Crystallographic data for the yttrium complex **C10**: Triclinic, space group *P*-1, *a* = 10.519(2) Å, *b* = 11.456(2) Å, c = 19.097(3) Å, α = 103.11(2)°, β = 103.46(2)°, γ = 100.59(2)°, *V* = 2110.7(5) Å^3, *Z* = 2, D_c = 1.283 g·cm^3, μ = 1.354 mm^{-1}, *F*(000) = 850.

*4.10. Formation of [{η^5,η^1-$Ph_2P(C_5H_4)NDip$}$Y(CH_2SiMe_3)(\mu\text{-}OMe)]_2$ (**C11**):* This complex was obtained upon storing of a concentrated ether solution at -30°C after the attempted synthesis of solvent-free complex [{η^5,η^1-$Ph_2P(C_5H_4)(NAd)$}$Y(CH_2SiMe_3)_2$], starting from equimolar amounts of reagents [$YCl_3(dme)_2$], ligand **L6** and $LiCH_2SiMe_3$. The reaction mixture was stirred overnight. Single crystals were characterized by X-ray diffraction analysis.

Crystallographic data for the yttrium complex **C11**: Monoclinic, space group $P2_1/n$, a = 16.834(1) Å, b = 23.948(2) Å, c = 18.014(1) Å, β = 100.14(1)°, V = 7148.7(8) Å^3, Z = 4, D_c = 1.243 g·cm^{-3}, μ = 1.738 cm^{-1}, F(000) = 2824.

*4.11. Synthesis of [{η^5,η^1-$Ph_2P(C_5H_4)NDip$}$Y(C_6H_4CH_2NMe_2)$] (**C12**):* To a stirred solution of [$Y(dmba)_3$] **H4** (490 mg, 1.00 mmol) in 20 mL toluene a solution of the ligand **L6** (425 mg, 1.00 mmol) in 10 mL of the same solvent was added at 0°C drop-by-drop. The reaction mixture was brought to room temperature within 0.5 h and all volatiles were removed in vacuum yielding a foamy light yellow solid. This was taken into 20 mL ether whereupon a colourless solid forms, which was filtered off and dried in vacuum to yield the complex **C12**. The complex was obtained in form of a grey, microcrystalline solid in 52% of yield.

^{1}H NMR (300.1 MHz, C_6D_6): δ = 0.97, 1.02 (2×d, 2×$^2J_{HH}$ = 6.8 Hz, 12H, 2×*Me*$_2$CH), 2.20 (s, 12H, *Me*$_2$N), 3.45, 3.62 (d, d, AB-system, $^2J_{HH}$ = 13.8 Hz, 4H, C*H*$_2$NMe$_2$), 3.86 (sept, $^2J_{HH}$ = 6.8 Hz, Me$_2$C*H*), 6.40, 6.45, 6.61, 6.78 (4×br s, 4H, C_5H_4), 6.84 (m, 4H, *m-Ph*), 6.92 (br t, $^3J_{HH}$ = 8 Hz, 2H, *p-Ph*), 6.96 (d, $^3J_{HH}$ = 6.8 Hz, 5-C_{Ar}), 7.04 – 7.10 (m, 1H: *p-Dip*, 2H: *o-Ph*), 7.18 (dd, $^3J_{HH}$ = 7.5 Hz, $^4J_{HP}$ = 1.3 Hz, *m-Dip*), 7.24, 7.34 (2×br t, *J* = 6.5 Hz, *J* = 6.8 Hz, 2×2H, 3/4-C_{Ar}), 7.44 (m, 2H: *o-Ph*), 8.01 (d, $^3J_{HH}$ = 6.8 Hz, *o-Ar*) ppm.

^{13}C{^{1}H} NMR (75.0 MHz, C_6D_6): δ = 24.4, 24.7 (2×s, 2×Me$_{i\text{-}Pr}$), 28.3 (s, Me$_2$*C*H-), 46.8 (s, *Me*$_2$N), 69.2 (s, Me$_2$N*C*H$_2$), 114.0 (d, $^1J_{CP}$ = 148 Hz, PC_{C5}), 116.5 (d, J_{CP} = 12.1 Hz, C_{C5}), 117.4 (d, J_{CP} = 14.7 Hz, C_{C5}), 119.0 (d, *J* = 12.9 Hz, C_{C5}), 119.3 (d, *J* = 13.8 Hz, C_{C5}), 120.9 (d, $^5J_{CP}$ = 3.5 Hz, *p-Dip*), 123.7 (d, $^4J_{CP}$ = 3.4 Hz, *m-Dip*), 125.1, 125.2 (2×s, 3/5-C_{Ar}), 125.9 (s, 4-C_{Ar}), 128.2 (d, $^3J_{CP}$ = 6 Hz, *m-Ph*), 130.7 (d, $^4J_{CP}$ = 2.6 Hz, *p-Ph*), 132.7, 132.9 (2×d, 2×$^2J_{CP}$ = 9.5 Hz, 2×*o-Ph*), 134.3, 135.7 (2×s, 2×$^1J_{CP}$ = 105 Hz, *ipso-Ph*), 139.3 (s, 2-C_{Ar}), 144.0 (d, $^3J_{CP}$ = 6.5 Hz, *o-Dip*), 144.8 (d, $^2J_{CP}$ = 5.2 Hz, *ipso-Dip*),147.2 (s, C_{Ar}CHMe$_2$), 185.0 (d, $^1J_{CY}$ = 47 Hz, C_{Ar}–Y) ppm.

^{31}P{^{1}H } NMR (81.0 MHz, C_6D_6): δ = -5.5 ppm.

Anal. calcd for $C_{47}H_{55}N_3NY$ (781.86): C 72.20, H 7.09, N 5.37;

Found: C 71.65, H 7.26, N 5.51.

*4.12. Synthesis of [{η⁵,η¹-Ph₂P(Cp^TM)NAd}Lu(CH₂SiMe₃)₂] (**C13**):* To a stirred solution of [Lu(CH$_2$SiMe$_3$)$_2$(thf)$_2$] (580 mg, 1.00 mmol) in 10 mL of toluene a solution of ligand **L8** (500 mg, 1.01 mmol) in the same amount of solvent was added drop by drop at ambient temperature. After 0.5 h the solvent was completely removed in vacuum and the foamy residue was trituration with 10 mL hexane, which results in dissolution and immediate deposition of a colourless crystalline solid. It was filtered off and dried in vacuum. Additional amount of the compound can be obtained by storing the mother liquor at -30°C. Yield: 78% (combined 660 mg).

^{1}H NMR (300.1 MHz, C$_6$D$_6$): δ = -0.59, -0.22 (2×d, AB-system, 2×$^3J_{HH}$ = 11.5 Hz, 2×2H, C*H*$_2$SiMe$_3$), 0.46 (s, 18H, Si*Me*$_3$), 1.19 (s, 6H, *Me*CMe), 1.45, 1.55 (2×d, AB-system, 2×3H, PNCC(*H*)H), 1.63 (s, 6H, *Me*CMe), 1.94 (m, 3H, *H*C(CH$_2$)$_3$), 1.95 (d, $^2J_{HH}$ = 12 Hz, 1H, *H*(H)C(CMe$_2$)$_2$), 2.07 (m, 6H, PC(C*H*$_2$)$_3$), 2.23 (d, $^2J_{HH}$ = 12 Hz, 1H, *H*(H)C(CMe$_2$)$_2$), 5.94 (d, $^3J_{HP}$ = 2.8 Hz, 2H, *H*C$_{C5}$), 7.02 – 7.08 (m, 6H, *p-/m-Ph*), 7.85 (m, 4H, *o-Ph*) ppm.

^{13}C{^{1}H} NMR (75.0 MHz, C$_6$D$_6$): δ = 5.0 (s, CH$_2$Si*Me*$_3$), 30.5 (s, *C*H(CH$_2$)$_3$), 32.3, 32.9 (2×s, 2×C(Me)*Me*), 36.3 (s, *C*H$_2$(CH)$_2$), 40.0, 40.6 (s, *C*H$_2$SiMe$_3$), 47.3 (d, $^3J_{PC}$ = 8.3 Hz, PC(*C*H$_2$)$_3$), 55.7 (d, $^2J_{PC}$ = 7.2 Hz, P*C*$_{Ad}$), 63.0 (s, *C*H$_2$(CMe$_2$)$_2$), 93.7 (d, $^1J_{PC}$ = 115 Hz, P*C*$_{C5}$), 106.7 (d, $^2J_{PC}$ = 13.2 Hz, H*C*$_{C5}$), 128.6 (d, $^3J_{PC}$ = 11.6 Hz, *m-Ph*), 131.2 (d, $^1J_{PC}$ = 88 Hz, *ipso-Ph*), 132.5 (d, $^4J_{CP}$ = 2.8 Hz, *p-Ph*), 133.5 (d, $^2J_{PC}$ = 11.0 Hz, *o-Ph*), 149.0 (d, $^3J_{PC}$ = 14.3 Hz, *C*$_{C5}$CMe$_2$) ppm.

^{31}P{^{1}H} NMR (81.0 MHz, C$_6$D$_6$): δ = 8.2 ppm.

Anal. calcd for C$_{42}$H$_{63}$LuNPSi$_2$ (844.09): C 59.76, H 7.53, N 1.66;
Found: C 59.51, H 7.34, N 1.75.

*4.13. Synthesis of [{η⁵,η¹-Ph₂P(Cp^TM)NDip}Lu(CH₂SiMe₃)₂] (**C14**):* The complex was synthesized as described for **C13**, starting from [Lu(CH$_2$SiMe$_3$)$_3$(thf)$_2$] (580 mg, 1.00 mmol) and ligand **L10** (520 mg, 1.00 mmol). The reaction was performed at 0°C. Colourless, microcrystalline solid was obtained by storing the hexane solution at -30°C in a yield of 55% (480 mg).

^{1}H NMR (300.1 MHz, C$_6$D$_6$): δ = -0.30 (bs, 2H, C*H*$_2$SiMe$_3$), -0.56 (bs, 2H). 0.38 (s, 18H, Si*Me*$_3$), 1.30 (s, 6H,), 1.35 (s, 12H, *Me*$_2$CH), 1.69 (s, 6H, Me$_2$C), 2.01 (d, $^2J_{HH}$ = 13.0 Hz, 1H, HC(H)), 2.36 (d, $^3J_{HH}$ = 13.0 Hz, 1H), 3.51 (sep., 2H, Me$_2$C*H*), 6.47 (br s, 2H, *H*C$_{C5}$), 6.92 – 7.04 (m, 10H, Ar,), 7.48 – 7.54 (m, 3H, HDip) ppm.

$^{13}C\{^1H\}$ NMR (75.0 MHz, C_6D_6): δ = 3.2 (s, Si*Me*$_3$), 22.2, 24.7 (2×br s, *Me*$_2$CH), 27.6 (s, Me$_2$C*H*), 30.9, 31.1 (2×s, CH$_2$(*Me*C(*Me*))$_2$), 38.8 (CH$_2$(*C*Me$_2$)$_2$), 41.6 (s, *C*H$_2$SiMe$_3$), 61.2 (*C*H$_2$(CMe$_2$)$_2$), 98.3 (d, $^1J_{CP}$ = 82 Hz, P*C*$_{C5}$), 105.6 (d, $^2J_{CP}$ = 12.7 Hz, H*C*$_{C5}$), 123.3 (d, $^4J_{CP}$ = 3.3 Hz, *m-Dip*), 123.9 ($^5J_{CP}$ = 3.9 Hz, *p-Dip*), 127.4 (d, $^3J_{CP}$ = 12.1 Hz, *m-Ph*), 131.2 (d, $^4J_{CP}$ = 2.8 Hz, *p-Ph*), (d, $^2J_{CP}$ = 10.0 Hz, *o-Ph*), 144.3 (d, $^3J_{CP}$ = 6.6 Hz, *o-Dip*), (d, $^3J_{CP}$ = 14 Hz, *C*$_{C5}$CMe$_2$) ppm.

$^{31}P\{^1H\}$ NMR (81 MHz, C_6D_6): δ = 9.30 ppm.

Anal. calcd for $C_{44}H_{65}LuNPSi_2$ (870.13): C 68.27, H 7.53, N 1.61;

Found: C 67.76, H 7.39, N 1.80.

4.14. Synthesis of Complex [Yb{η^5*,*η^1*-Me$_2$P(C$_5$Me$_4$)NAd)}$_2$] (**C15**):* To a stirred solution of the ligand **L4** (662 mg, 2.00 mmol) in 10 mL THF a solution of BnK (250 mg 1.92 mmol) in the same solvent was added drop by drop at ambient temperature, whereupon decoloration of deep red solution takes place. To this solution of the K-salt of ligand **L4** solid YbI$_2$(thf)$_2$ (570 mg, 1.90 mmol) was added at once at ambient temperature. The deep orange suspension was stirred for 1 h. The precipitate of KCl was filtered off through Celite© and washed with THF (2×5 mL). Solvent was stripped off, yielding an orange microcrystalline substance. Yield: 82% (685 mg).

^1H NMR (300.1 MHz, C_6D_6): δ = 1.44 (d, $^2J_{PH}$ = 3.5 Hz, 3H, *Me*(Me)P), 1.48 (d, $^2J_{PH}$ = 3.1 Hz, 3H, Me(*Me*)P), 1.70 (br s, 12H, C*H*$_2$ in Ad), 2.11 (m, 3H, C*H* in Ad), 2.19, 2.25, 2.27, 2.29 (4×s, 4×3H, 4×*Me*C$_{C5}$) ppm.

$^{13}C\{^1H\}$ NMR (75.0 MHz, C_6D_6): δ = 11.9 (d, $^3J_{CP}$ = 1.2 Hz, *Me*C$_{C5}$), 12.5 (d, $^3J_{CP}$ = 1.5 Hz, *Me*C$_{C5}$), 13.8, 15.8 (2×s, 2×*Me*C$_{C5}$), 23.1(d, $^1J_{PC}$ = 23 Hz, *Me*$_2$P), 23.8 (d, $^1J_{PC}$ = 22 Hz, *Me*$_2$P), 30.8 (s, *Ad*), 37.0 (s, *Ad*), 48.8 (d, J_{PC} = 10 Hz, *Ad*), 51.8 (d, $^2J_{PC}$ = 7.4 Hz, -*C*(CH$_2$)$_3$-), 90.6 (d, $^1J_{CP}$ = 126 Hz, *ipso-C*$_{C5}$), 115.9 (d, J_{PC} = 13.2 Hz, Me*C*$_{C5}$), 116.3 (d, J_{PC} = 12.7 Hz, Me*C*$_{C5}$), 118.9 (d, J_{PC} = 15.4 Hz, Me*C*$_{C5}$), 120.0 (d, J_{PC} = 14.9 Hz, Me*C*$_{C5}$) ppm.

$^{31}P\{^1H\}$ NMR (C_6D_6, 81.0 MHz): δ = 0.5 ppm.

Anal. Calc. for $C_{42}H_{66}N_2P_2Yb$ (833.99): C 60.49; H 7.98; N 3.36;

Found: C 60.40; H 8.02; N 3.26.

*4.16. Synthesis of Complex [Yb{η^5,η^1-$Ph_2P(C_5Me_4)NAd$}$_2$] (**C16**):* The compound was synthesized as described for **C16**, starting from ligand **S12**[49] (455 mg, 1.00 mmol), BnK (130 mg 1.00 mmol) and $YbI_2(thf)_2$ (280 mg, 0.48 mmol, 0.98 equiv). Yield: 71% (385 mg) of a deep red solid. Compound crystallizes from ether with additional solvent molecule in the lattice (**C16**×Et_2O) as was shown by the X-ray diffraction analysis. By drying of the crystalline **C16**×Et_2O in high vacuum desolvatation with formation of powdery, solvent-free complex was observed. Desolvatation can be also achieved by heating its toluene solutions to 70°C. Following NMR spectroscopic data is given for the solvent-free compound.

^{1}H NMR (300.1 MHz, C_6D_6): δ = 1.72 (br s, 12H, CH_2 in Ad), 2.10 (m, 3H, C*H* in Ad), 2.23, 2.24, 2.30, 2.32 (4×s, 4×3H, 4×*Me*C_{C5}), 7.12 – 7.31(m, 6H, *m-/p-Ph*), 7.82 – 8.19 (m, 4H, *o-Ph*) ppm.

^{13}C{^{1}H} NMR (75.0 MHz, C_6D_6): δ = 12.1 (d, $^3J_{CP}$ = 0.9 Hz, *Me*C_{C5}), 12.3 (d, $^3J_{CP}$ = 1.1 Hz, *Me*C_{C5}), 14.1, 15.6 (2×s, 2×*Me*C_{C5}), 30.9 (s, *Ad*), 37.2 (s, *Ad*), 48.6 (d, J_{PC} = 10 Hz, *Ad*), 52.0 (d, $^2J_{PC}$ = 7.0 Hz, -*C*$(CH_2)_3$-), 90.7 (d, $^1J_{CP}$ = 124 Hz, *ipso-*C_{C5}), 116.1 (d, J_{PC} = 12.8 Hz, Me*C*$_{C5}$), 116.5 (d, J_{PC} = 12.6 Hz, Me*C*$_{C5}$), 121.9 (d, J_{PC} = 15.6 Hz, Me*C*$_{C5}$), 122.3 (d, J_{PC} = 16.0 Hz, Me*C*$_{C5}$), 128.3, 128.6, (4×s, 2×*p-Ph,* 4×*m-Ph*), 130.1, 131.2 (2×d, $^1J_{CP}$ = 108 Hz, $^1J_{CP}$ = 102 Hz, *ipso-Ph*), 135.0, (d, $^2J_{CP}$ = 12.2 Hz, *o-Ph*), 135.0, (d, $^2J_{CP}$ = 13.1 Hz, *o-Ph*) ppm.

^{31}P{^{1}H} NMR (81.0 MHz, C_6D_6): δ = 1.2 ppm.

Anal. Calc. for $C_{62}H_{74}N_2P_2Yb$ (1082.28): C 68.81; H 6.89; N 2.59;
Found: C 68.27; H 7.37; N 2.72.

4.17. General procedure for catalytic hydroamination/cyclization reactions: In a glovebox, a glas NMR tube was charged with the precatalyst (**C1** – **C4**) (ca. 30 μmol, 4 – 5 mol%) dissolved in C_6D_6 (0.6 mL) and the appropriate substrate (0.6 μmol) in that order. The NMR tube was then placed in the thermostated probe of the Bruker Advance 300 spectrometer. The conversion was monitored by ^{1}H NMR spectroscopy by following the disappearance of the olefinic protons of the substrate.

5. REFERENCES

[1] a) W. E. Piers, P. J. Shapiro, E. E. Bunel, J. E. Bercaw, *Synlett* **1990**, *2*, 74–84; b) J. Okuda, *Top. Curr. Chem*. **1991**, *160*, 97–145.

[2] a) J. C. Stevens, F. J. Timmers, G. W. Rosen, G. W. Knight and S. Y. Lai (Dow Chemical Co.), *Eur. Pat. Appl.* EP 0 416 815 A2, **1991** (filed August 30, 1990); b) J. A. Canich (Exxon Chemical Co.), *Eur. Pat. Appl.* EP 0 420 436 A1, **1991** (filed September 10, **1990**); c) J. C. Stevens, *Stud. Surface Sci. Cat.* **1996**, *101*, 11–18; d) A. L. McKnight and R. M. Waymouth, *Chem. Rev.* **1998**, *98*, 2587–2598.

[3] a) J. Okuda, *Chem. Ber.* **1990**, *123*, 1649–1651; b) P. J. Shapiro, E. E. Bunel, W. P. Schaefer, J. E. Bercaw, *Organometallics* **1990**, 867–871.

[4] M. Booij, N. H. Kiers, H. J. Heeres, J. H. Teuben, *J. Organomet. Chem.* **1989**, *364*, 79–86.

[5] H. Schumann, J. Müller, *J. Organomet. Chem.* **1979**, *169*, C1–C4.

[6] H. Schumann, M. Glanz, H. Hemloing, F. E. Hahn, *Z. Anorg. Allg. Chem.* **1995**, *621*, 341–345.

[7] K. A. Rufanov, P. Neubauer, A. R. Petrov, J. Sundermeyer, *Eur. J. Inorg. Chem.* **2006**, 3805–3807.

[8] T. M. Cameron, J. C. Gordon, B. L. Scott, *Organometallics* **2004**, *23*, 2995–3002.

[9] S.Tian, V. M. Arredondo, C. L. Stern, T. J. Marks, *Organometallics* **1999**, *18*, 2568–2570.

[10] R. D. Shannon, *Acta Cryst. Sec. A32* **1976**, 751–767.

[11] P. J. Shapiro, W. D. Cotter, W. P. Schaefer, J. A. Labinger, J. E. Bercaw, *J. Am. Chem. Soc.* **1994**, *116*, 4623–4640.

[12] J. S. Ghotra, M. B. Hursthouse, A. J. Welch, *J. Chem. Soc., Chem. Commun.* **1973**, 669–670.

[13] B. D. Ward, S. R. Dubberley, A. Maisse-François, L. H. Gade, P. Mountford, *J. Chem. Soc., Dalton Trans.* **2002**, 4649–4657.

[14] X. Li, J. Baldamus, Z. Hou, *Angew. Chem. Int. Ed.* **2005**, *44*, 962–965.

[15] L. D. Henderson, G. D. MacInnis, W. E. Piers, M. Parvez, *Can. J. Chem.* **2004**, *82*, 162–165.

[16] C. S. Tredget, S. C. Lawrence, B. D. Ward, R. G. Howe, A. R. Cowley, P. Mountford, *Organometallics* **2005**, *24*, 3136–3148.

[17] P. B. Hitchcock, Q.-G. Huang, M. F. Lappert, X.-H. Wei, *J. Mater. Chem.* **2004**, *14*, 3266–3273.

[18] M. Westerhausen, M. Hartmann, A. Pfitzner, W. Schwarz, *Z. Anorg. Allg. Chem.* **1995**, *621*, 837–850.

[19] S. Anfang, K. Harms, F. Weller, O. Borgmeier, H. Lueken, H. Schilder, K. Dehnicke, *Z. Anorg. Allg. Chem.* **1998**, *624*, 159–166.

[20] S. Bambirra, D. van Leusen, A. Meetsma, B. Hessen, J. H. Teuben, *Chem.Commun.* **2001**, 637–638.

[21] H. Mauermann, P. N. Swepston, T. J. Marks, *Organometallics* **1985**, *4*, 200–202.

[22] S. Bambirra, D. van Leusen, C. G. J. Tazelaar, A. Meetsma, B. Hessen, *Organometallics* **2007**, *26*, 1014–1023.

[23] J. Gromada, A. Mortreux, G. Nowogrocki, F. Leising, T. Mathivet, J.-F. Carpentier, *Eur. J. Inorg. Chem.* **2004**, 3247–3253.

[24] L. J. Bowman, K. Izod, W. Clegg, R. W. Harrington, *Organometallics* **2006**, *25*, 2999–3006.

[25] D. M. Barnhart, D. L. Clark, J. C. Gordon, J. C. Huffman, J. G. Watkin, B. D. Zwick, *J. Am. Chem. Soc.* **1993**, *115*, 8461–8462.

[26] T. J. Boyle, L. A. M. Ottley, S. D. Daniel-Taylor, L. J. Tribby, S. D. Bungea, A. L. Costello, T. M. Alam, J. C. Gordon, T. M. McCleskey, *Inorg. Chem*. **2007**, *46*, 3705–3713.

[27] C. Riviere, M. Lance, M. Ephritikhine, M. Nierlich, *Z. Kristallogr. - New Cryst. Struct.* **2000**, *215*, 239–241.

[28] W. A. Herrmann, R. Anwander, M. Kleine, K. Ofele, J. Riede, W. Scherer, *Chem. Ber.* **1992**, *125*, 2391–2397.

[29] Q. Zhao, D. Jia, Y. Zhang, L. Song, J. Dai, *Inorg. Chim. Acta* **2007**, *360*, 1895–1001.

[30] a) H. Schumann, M.Glanz, H. Hemling, F. H. Gorlitz, *J. Organomet. Chem.* **1993**, *462*, 155–161; b) W. J. Evans, K. J. Forrestal, J. T. Leman, J. W. Ziller, *Organometallics* **1996**, *15*, 527–531.

[31] W. J. Evans, T. J. Boyle, J. W. Ziller, *J. Am. Chem. Soc.* **1993**, *115*, 5084–5092.

[32] M. Schlosser, Ed. *Organometallic in Synthesis, A Manual*, Wiley, Chichester, **2002**.

[33] W. J. Evans, M. S.Sollberger, J. L. Shreeve, J. M. Olofson, J. H. Hain, Jr., J. W. Ziller, *Inorg. Chem*. **1992**, *31*, 2492 – 2501.

[34] H. E. Gottlieb, V. Kotlyar, A. Nudelman, *J. Org. Chem.* **1997**, *62*, 7512–7515.

[35] S. Ge, A. Meetsma, B. Hessen, *Organometallics* **2008**, *in press*.

[36] M. Elfferding, *private communication*, Philipps University Marburg, **2007**.

[37] W. J. Evans, J. C. Brady, J. W. Ziller, *J. Am Chem. Soc.* **2001**, *123*, 7711–7712.

[38] S. Bambirra, M. W. Bouwkamp, A. Meetsma, B. Hessen, *J. Am. Chem. Soc.* **2004**, *126*, 9182–9183.

[39] J.-C. Berthet, C. Riviere, Y. Miquel, M. Nierlich, C. Madic, M. Ephritikhine, *Eur. J. Inorg. Chem.* **2002**, 1439–1446.

[40] G. R. Giesbrecht, J. C. Gordon, D. L. Clark, B. L. Scott, *Appl. Organomet. Chem.* **2005**, *19*, 98–99.

[41] W. J. Evans, R. Dominguez, T. P. Hanusa, *Organometallics* **1986**, *5*, 1291–1296.

[42] S. Arndt, T. P. Spaniol, J. Okuda, *Organometallics* **2003**, *22*, 775–781.

[43] F. A. Riederer, *PhD. Thesis*: Technical University Munich, **2005**.

[44] D. V. Gribkov, K. C Hultzsch, *Chem. Commun.* **2004**, 730–731.

[45] K. A. Rufanov, B. H. Müller, A. Spannenberg, U. Rosenthal, *New J. Chem.* **2006**, 29–31.

[46] M. Booij, N. H. Kiers, A. Meetsma, J. H. Teuben, *Organometallics* **1989**, *8*, 2454–2461.

[47] O. Thomas, *Diploma Thesis*, Philipps University Marburg, **2008**.

[48] M. Hesse, H. Meier, B. Zee, *Spektroskopische Metoden in der organischen Chemie*; Georg Thieme Verlag, Stuttgart, **1979**, 155.

[49] F. Laquai, *Advanced inorganic research project in work group J. Sundermeyer (Forschungspraktikum)*, Philipps University Marburg, **2001**.

[50] J. Jin, S. Jin, W. Chen, *J. Organomet. Chem.* **1991**, *412*, 71–75.

[51] T. Jiang, Q. Shen, Y. Lin, S. Jin, *J. Organomet. Chem*. **1993**, *450*, 121–124.

[52] A. V. Khvostov, A. I. Sizov, B. M. Bulychev, S. Ya. Knjazhanski, V. K. Belsky, *J. Organomet. Chem*. **1998**, *559*, 97–105.

[53] M. Schultz, J. M. Boncella, D. J. Berg, T. D. Tilley, R. A. Andersen, *Organometallics* **2002**, *21*, 460–472.

[54] T. D. Tilley, R. A. Andersen, B. Spencer, A. Zalkin, *Inorg. Chem.* **1982**, *21*, 2647–.

[55] T. D. Tilley, R. A. Andersen, B. Spencer, A. Zalkin, *Inorg. Chim. Acta* **1998**, *280*, 138–142.

[56] T. D. Tilley, R. A. Andersen, A. Zalkin, *J. Am. Chem. Soc.* **1982**, *104*, 3725–3727.

[57] C. J. Kuehl, R. E. Da Re, B. L. Scott, D. E. Morris, K. D. John, *Chem. Commun*. **2003**, 2336–2337.

[58] G. Lin, W.-T. Wong, *J. Organomet. Chem.* **1995**, *495*, 203–208.

[59] T. D. Tilley, R. A. Andersen, B. Spencer, H. Ruben, D. H. Templeton, A. Zalkin, *Inorg. Chem.* **1980**, *19*, 2999–3003.

[60] J. H. Brownie, H. Schmider, M. C. Baird, *Organometallics* **2007,** *26,* 1433–1443.

[61] P. Laavanya, B. S. Krishnamoorthy, K. Panchanatheswaran, M. Manoharan, *J. Mol. Struct.* THEOCHEM **2005**, *716*, 149–158.

[62] F. A. Cotton, T. J. Marks, *J. Am. Chem. Soc*. **1970**, *92*, 5114–5117.

[63] L. Lettko, M. D. Rausch, *Organometallics* **2000**, *19*, 4060–4065.

[64] a) P. L. McGrane, M. D. Jensen, T. Livinghouse, *J. Am. Chem. Soc*. **1992**, *114*, 5459–5460.

[65] (a) G. A. Molander, E. D. Dowdy, *J. Org. Chem*. **1998**, *63*, 8983–8988 and references cited therein; (b) M. R. Gagné, C. L. Stern, T. J. Marks, *J. Am. Chem. Soc*. **1992**, *114*, 275–294.

[66] E. T. Muller, M. Beller, *Chem. Rev*. **1998**, *98*, 675–703.

[67] V. M. Arredondo, S. Tian, F. E. McDonald, T. J. Marks, *J. Am. Chem. Soc*. **1999**, *121*, 3633–3639.

[68] Complex synthesis: C. M. Fendrick, S. D. Schertz, V. M. Day, T. J. Marks, *Organometallics* **1988**, *7*, 1828–1838. For hydroamination tests see *Ref. 69b*.

[69] Complex synthesis: (a) D. Stern, M. Sabat, T. J. Marks, *J. Am. Chem. Soc*. **1990**, *112*, 9558–9575. (b) D. Stern, *Ph.D. Thesis*, Northwestern University, Evanston, IL, **1990**. For hydroamination tests see *Ref. 69b*.

[70] K. C. Hultzsch, F. Hampel, T. Wagner, *Organometallics* **2004**, *23*, 2601–2612.

[71] Y. K. Kim, T. Livinghouse, J, E. Bercaw, *Tetrahedron Lett.* **2001**, *42*, 2933–2935.

[72] a) b)N. C. Burton, F. G. N. Cloke, P. B. Hitchcock, H. C. de Lemos, A. A. Sameh, *J. Chem. Soc, Chem. Commun.* **1989**, 1462–1465.

Summary

This Thesis is dedicated to the synthesis and investigation of the rare-earth metal complexes with two particular types of chelating monoanionic ligand systems:

- *ortho*-deprotonated *N,N*-dimethyl-benzylamines $(dmba)^-$
- cyclopentadienyl-phosphazenes $(CpPN)^-$

The first ligand system is presented by a series of side-chain modified $(dmba)^-$ ligands that have been used to study the influence of present or absent benzylic protons on the stability of homoleptic rare-earth metal *tris*-aryl complexes. Discussion of their synthesis, thermal stability and crystal structures composes **Chapter II**. The second and novel ligand system is presented by a series of *CpPN*-ligands with different substituents on P- and N-atoms and at the Cp-ring. A discussion of their syntheses, prototropic equilibria and molecular structures is presented in **Chapter III**. Cyclopentadienyl-phosphoranes are the intermediates in the *CpPN* ligand synthesis. Thus a new highly crowded cyclopentadienyl-phosphane skeleton, some mechanistic aspects of its formation, its reactivity toward oxidants and some examples of coordination chemistry of this new ligand are reported in **Chapter IV**. Finally, a detailed study on the synthesis and analysis of the coordination modes of the rare-earth metal *CpPN*-complexes with different ligands and metals is presented in **Chapter V**. An additional contribution to this work is the development of a simple and versatile synthesis of anhydrous etherates $[LnBr_3(solv)_n]$ that are very promising precursors for the coordination and organometallic chemistry of the rare-earth metals. Combined with some general considerations on rare-earth metal chemistry this contribution is discussed in **Chapter I** of this Thesis.

Chapter I.

Anhydrous lanthanide trihalides are important starting materials in organolanthanide chemistry. Due to the large ionic radii of the early and middle lanthanides the corresponding tribromides and triiodides possess higher solubility and are superior to trichlorides as precursors.

A series of solvated lanthanide tribromides was prepared by a new and very convenient one-step protocol directly from their oxides. The developed method comprises the use of

molecular bromine and hexamethyldisilane, which are *in situ* forming Me_3SiBr, in the appropriate ethereal solvent. Thus high purity crystalline DME and THF solvated tribromides of neodymium and samarium were obtained in 64 – 88% isolated yield. Due to significant solubility of these tribromides in chlorinated solvents, the subsequent purification from traces of non-converted oxides was achieved by extraction with CH_2Cl_2.

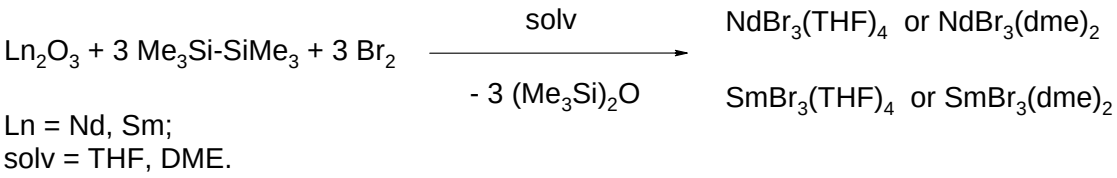

Chapter II.

In this Chapter the influence of the alkyl substituents in the (dmba)-ligand on the kinetic stability of corresponding lanthanide-aryl complexes was investigated. The aryllithium reagents were synthesized by *ortho*-directed lithiation of substituted benzylamines with BuLi.

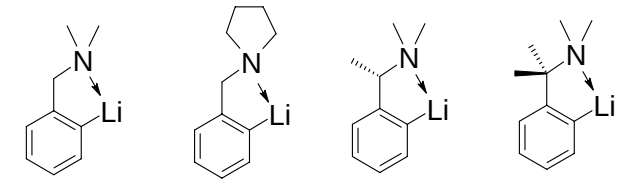

Li(dmba) Li(pyba) Li(tmba) Li(cuda)

The lanthanide complexes were prepared by the *salt-metathesis route* from anhydrous, solvated $[LnCl_3(dme)_n]$ (n = 1, 2) and the corresponding aryllithium reagent. The homoleptic complexes $[Ln(dmba)_3]$ of the late lanthanides (Ln = Er, Yb) and yttrium were for the first time crystallographically characterized. The analysis of the molecular structures show that the complexes are isostructural to the known lutetium complex $[Lu(dmba)_3]$. The molecular structure of $[Er(dmba)_3]$ is shown below.

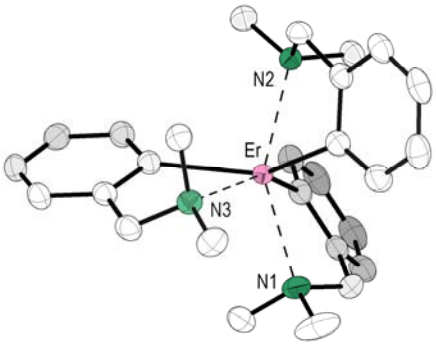

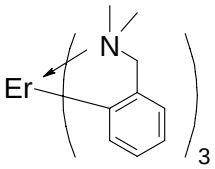

A VT NMR spectroscopic study of the diamagnetic yttrium complex $[Y(dmba)_3]$ reveals a coalescence temperature below 230 K and indicates a high conformational flexibility of (dmba) ligands in their complexes.

From an attempted reaction of $[GdCl_3(dme)_2]$ with 3 equiv Li(dmba) the only isolated compound was identified as an ate complex of the type $Li[Gd(dmba)_4]$. A similar result was obtained in case of the neodymium complex with (pyba) ligand. Molecular structures of both, $Li[Gd(dmba)_4]$ and $Li[Nd(pyba)_4]$, were confirmed by the single crystal X-ray diffraction.

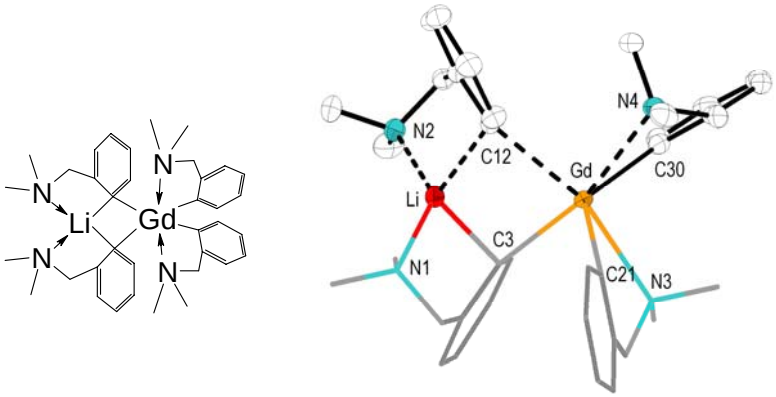

The coordination chemistry of the more rigid and bulkier ligands of the (dmba) type, (tmba) and (cuda), was further investigated.

The treatment of $[LuCl_3(thf)_3]$ with Li(tmba) leads to the formation of a heteroleptic complex $[(tmba)_2LuCl]$, even in 1:3 stoichiometry of reagents. No formation of homoleptic complex was observed under harsher reaction conditions.

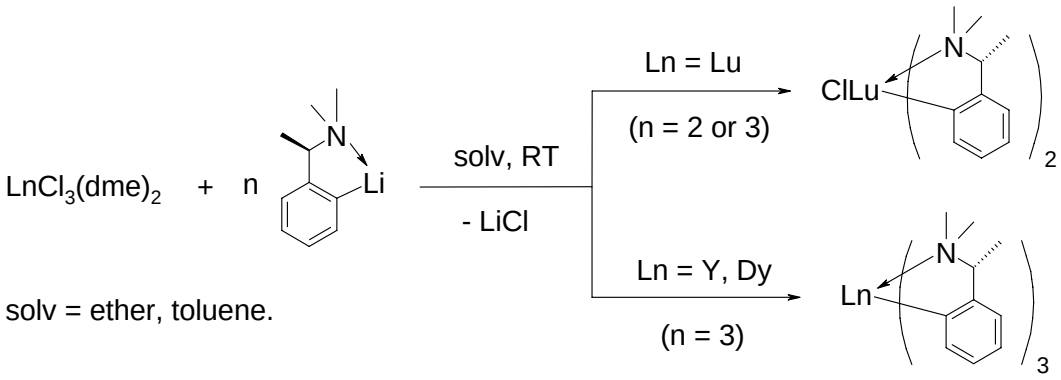

By its size the Y^{3+} ion occupies exactly the border position between middle and late lanthanides. Transmetallation of Li(tmba) with middle rare-earth elements trihalides dysprosium and yttrium leads to the formation of homoleptic aryl complexes of high thermal stability. The molecular structures of the complexes were determined by XRD analysis. The complexes of middle and early lanthanides, samarium and neodymium, with (tmba) ligand were also characterized. They possess a decreased thermal stability. The neodymium complex $[Nd(tmba)_3]$ was analysed by XRD.

The syntheses of complexes with the most bulky (cuda)-ligand were attempted with early lanthanides. The samarium complex [Sm(cuda)$_3$] was synthesized *via salt metathesis* reaction and was obtained as yellow crystalline solid. Compared to [Sm(tmba)$_3$] it has significantly higher thermal stability. The molecular structure was determined by XRD analysis.

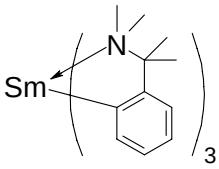

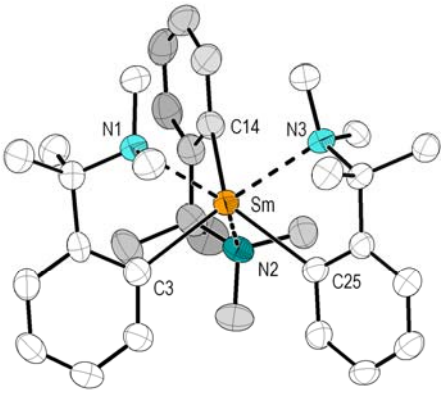

This investigations show that the formation of [LnAr$_3$] complexes is restricted to sterically unhindered (dmba) and (pyba) ligands in combination with relatively small late lanthanides or to fairly large early and middle lanthanides in combination with sterically demanding (tmba) and (cuda) ligands. The opposite combinations lead either to unstable species of early and middle lanthanides with unhindered ligands or to the formation of ate complexes Li[LnAr$_4$] or to incomplete substitution and formation of heteroleptic [Lu(tmba)$_2$Cl] complex. In this respect synthesis and structural characterization of first examples of one early lanthanide ate complex Li[Nd(pyba)$_4$]×½PhMe and one middle lanthanide ate complexes Li[Gd(dmba)$_4$] was achieved, but remains so far unverified for the sterically demanding (tmba) and (cuda) ligands.

Finally, it is worth to note that decomposition of all early Nd, Sm aryls takes place in THF and this is the reason why their syntheses could not be realized in THF as solvent or starting from analogues thf-solvated precursor [LnCl$_3$(thf)$_x$] (Ln = Nd, Sm). No ether cleavage was observed in Et$_2$O as solvent.

Chapter III.

The synthesis of phosphorus(V) ligands with a *CpPN*-binding was investigated. This class of monoanionic ligands has been deliberately designed for further application to the synthesis of "*constrained-geometry*" complexes (*CGCs*) of the rare-earth elements, isolobal with the well studied class of the group 4 metal *CGC* with the dianionic *CpSiN* ligand regime.

The best synthetic strategy towards this ligand class based on the *Staudinger* reaction of cyclopentadienyl-phosphanes with organic azides:

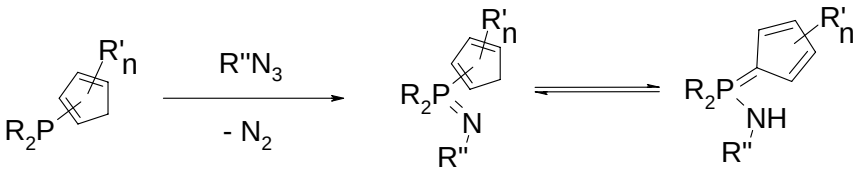

In a systematic manner a series of the cyclopentadienyl-phosphanes of increasing thermal stability – $C_5H_5PMe_2$, $C_5H_5PPh_2$, $HC_5Me_4PMe_2$ and $HC_5Me_4PPh_2$ – was investigated in the *Staudinger* reaction with three azides – Me_3SiN_3, AdN_3 and $DipN_3$ – of increasing reactivity.

Syntheses of the *CpPN*-H compounds from thermally labile phosphanes $C_5H_5PR_2$ (R = Me, Ph) were optimized by using CpTl as a Cp-precursor and THF as a solvent.

Scope and limitations of this synthetic approach were defined and are summarized in the following table:

	$C_5H_5PMe_2$	$C_5H_5PPh_2$	$HC_5Me_4PMe_2$	$HC_5Me_4PPh_2$
Me_3SiN_3	no reaction	no reaction	**L1**, 86%	no reaction
AdN_3	**L2**, traces	**L3**, 69%	**L4**, 95%	**L8**, 78 %
$DipN_3$	**L5**, 75%	**L6**, 85%	**L7**, 60%	no reaction

Most stable tautomers: *P*-amino-cyclopentadienyliden-phosphorane (light grey);
P-cyclopentadienyl-phosphazene (dark grey).

It was found that two both amenable tautomeric forms of the protonated *CpPN*-ligand can exist. For the *CpPN*-ligands bearing the $Me_2PC_5Me_4$-motiv, the position of the tautomeric equilibrium depends on the substituents at the nitrogen atom and the C5-ring:

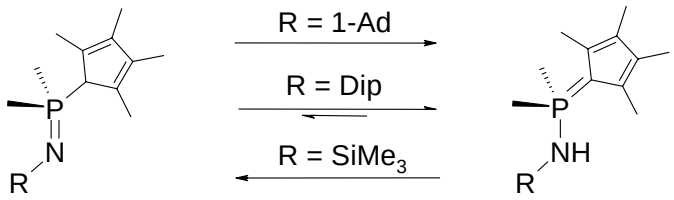

– all studied *CpPN*-H compounds bearing a Ad-group at the nitrogen atom along with those ones, having at the same time a *N*-Dip-group and an unsubstituted C5-ring moiety in the molecule, adopt the *P*-amino-cyclopentadienylidene-phosphorane form both in solution and in the solid state;

– the tautomeric *P*-cyclopentadienyl-iminophosphorane form is realized only in a limited number of representatives of this *CpPN* ligand family ($Me_2P(C_5Me_4H)NR$, R = $SiMe_3$, Dip) revealing a low CH-acidity and at the same time a low N-basicity. Besides of the predominant iminophosphorane form, small amounts of C5-ring isomers or *N*-amino-tautomer were observed to be present in solution equilibrium.

Chapter IV.

In order to enhance the thermal stability and diversity of Cp-phosphanes the synthesis of $Ph_2PC_5H_4$(*tert*-Bu) by the *fulvene route* was attempted. The *fulvene route* comprises the carbometallation of fulvenes, which can be obtained *via* the condensation of cyclopentadienes with carbonyl compounds.

In this chapter the synthesis of two sterically demanding fulvenes **F1** and **F2** is described.

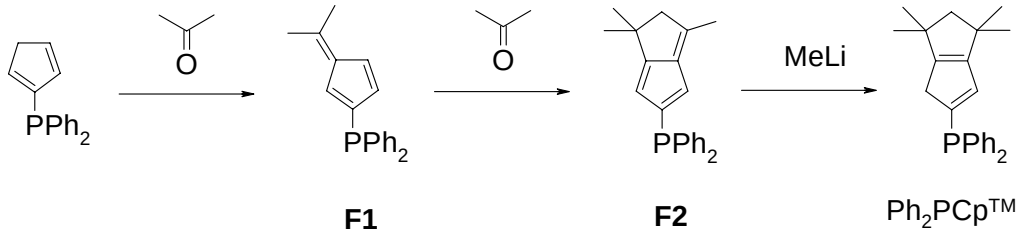

F1 **F2** $Ph_2PCp^{TM}H$

Using deuterated acetone as isotopically labeled reagent confirmed the assumption that **F1** acts as an intermediate in the pyrrolidine catalyzed formation of **F2**.

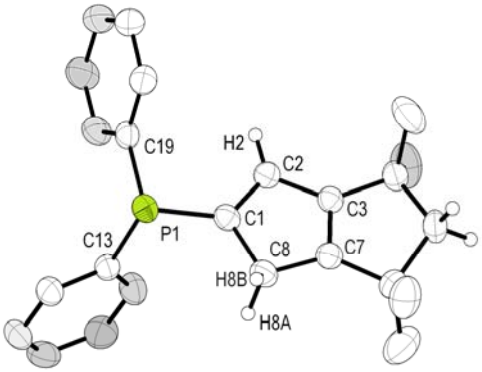

Subsequent carbometallation of **F2** with MeLi leads to the first air-stable, highly sterically crowded cyclopentadienyl phosphane $Ph_2PCp^{TM}H$ having an annelated 1,1,3,3-tetramethyl-cyclo-pentane moiety in its backbone. This cyclopentadienyl phosphane $Ph_2PCp^{TM}H$ appeared to be the first one in its class that was crystallographically characterized.

Oxidation reactions of $Ph_2PCp^{TM}H$ with H_2O_2, S_8 and selenium leads exclusively to corresponding chalcogenides $Ph_2P(X)Cp^{TM}H$ (X = O, X = S, X = Se).

The *Staudinger* reaction of $Ph_2PCp^{TM}H$ with AdN_3, *tert*-BuN_3, $DipN_3$ and Me_3SiN_3 leads to the *P*-amino-cyclopentadienylidene-phosphoranes $Ph_2P(Cp^{TM})NHR$ (R = Ad, *tert*-Bu) or tautomeric *P*-cyclopentadienyl-iminophosphoranes $Ph_2P(NR')Cp^{TM}H$ (R' = Dip, $SiMe_3$) respectively. The compound $Ph_2P(NDip)Cp^{TM}H$ is the first crystallographically characterized *P*-cyclopentadienyl-iminophosphorane.

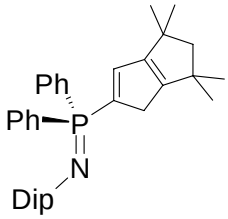

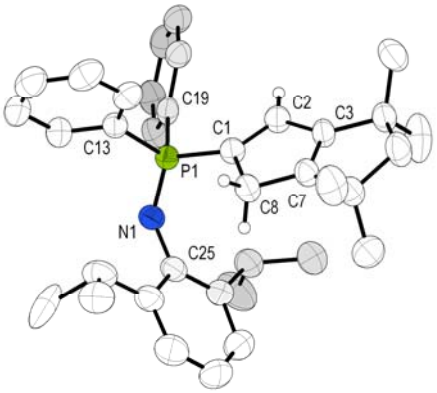

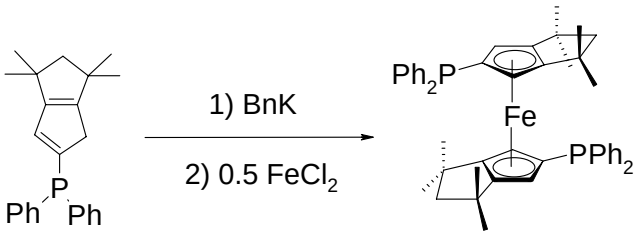

Finally, ferrocene $[(\eta^5\text{-}Cp^{TM}PPh_2)_2Fe]$ was synthesized by BnK metallation of $Ph_2PCp^{TM}H$ followed by transmetallation with $FeCl_2$. This extremely sterical demanding ferrocenyl diphosphane, named $dppf^{TM}$ in direct analogy to its known parent, has been applied as a bidentate phosphane ligand in the synthesis of $[(dppf^{TM})PdCl_2]$ and $[(dppf^{TM})PdI_2]$. The complexes $[dppf^{TM}]$ and $[(dppf^{TM})PdI_2]$ have been characterized by X-ray crystallography as well.

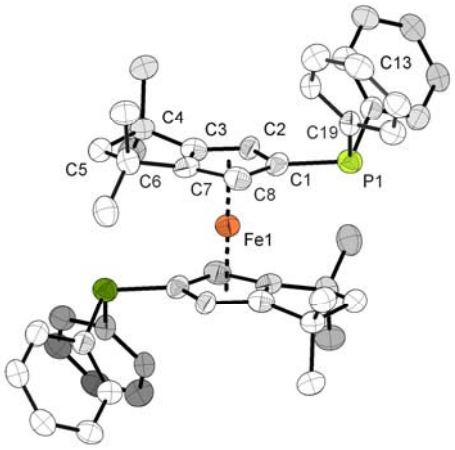

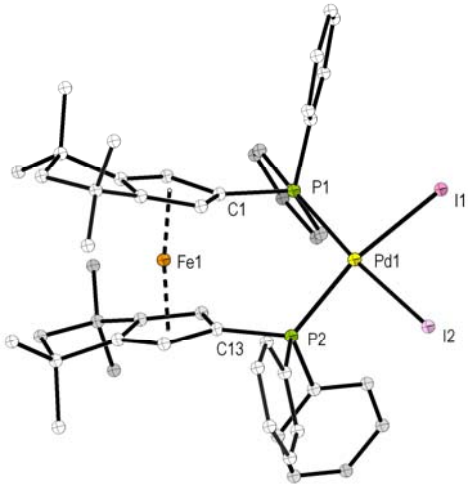

Chapter V.

In this chapter the synthesis and characterization of rare-earth metal complexes based on the *CpPN*-ligand is described. With one exception, all isolated *CpPN*-ligands exhibit the η^1,η^5-coordination.

A new, *one-pot* protocol that combines *deprotonation* and *salt-metathesis* has been developed in order to achieve the synthesis of CpPN-stabilized lanthanide-dialkyls of the type [{CpPN}LnR_2] for which the typical precursor complexes [(CpPN)$LnHal_2$] or [LnR_3] are not known so far.

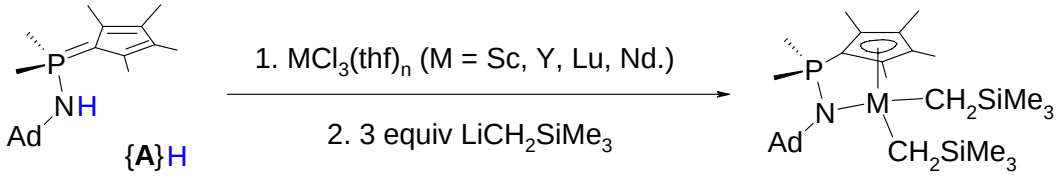

Using this protocol, a series of rare-earth metal dialkyl-*CpPN* complexes was synthesized with the following *CpPN*-ligands:

$Me_2P(C_5Me_4)NHAd$	{**A**}H
$Ph_2P(C_5H_4)NHDip$	{**B**}H
$Ph_2P(Cp^{TM})NHAd$	{**C**}H
$Ph_2P(NDip)Cp^{TM}H$	{**D**}H

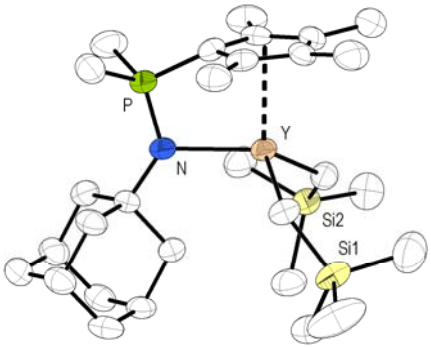

In general, the complexes with the ligand {**A**} possess the highest thermal stability within this series. For the paramagnetic neodymium complex [{**A**}$Nd(CH_2SiMe_3)_2$] a detailed analysis of the ^1H and ^{13}C NMR spectra and resonance assignment using 2D NMR techniques was accomplished. Its high reactivity was shown by the unexpected isolation of two decomposition products – a binuclear heteroleptic *trans*-[{**A**}$Nd(\mu^2\text{-}OMe)(CH_2SiMe_3)]_2$ and a tetranuclear hydroxy-species [{**A**}$Nd(\mu^2\text{-}OH)_2]_4$. Both complexes were structurally analyzed by XRD. Formation of the first complex can be rationalized by assumption of ether cleavage of DME, which retains from the starting neodymium source [$NdCl_3$(dme)], formation of the second by partial hydrolysis of [{**A**}$Nd(CH_2SiMe_3)_2$].

The rare-earth metal dialkyl complexes of yttrium and neodymium with the less bulky ligand $Ph_2P(C_5H_4)NHDip$ {**B**}H were isolated as THF complexes of the type [{**B**}$M(CH_2SiMe_3)_2(thf)$]. Both complexes were characterized by XRD analysis. The complexes are isostructural and reveal only a weak coordinative bond of the ligand nitrogen atom at the metal center.

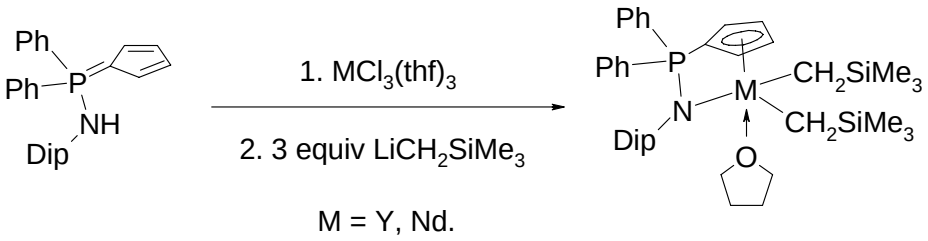

For the dialkyl complexes with smaller rare-earth metals – scandium and yttrium– corresponding solvent-free species with ligand {**B**}H were isolated and characterized.

Sterically most demanding ligands {**C**}H and {**D**}H could be directly metallated by $[Lu(CH_2SiMe_3)_3(thf)_2]$.

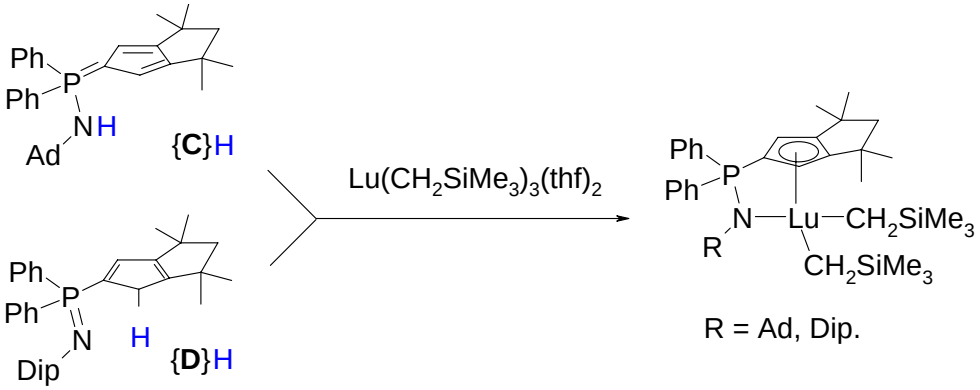

The NMR spectroscopy of both dialkyl complexes show their high conformational rigidity in solution.

The equimolar reaction of the ligand {**B**}H with homoleptic complex $[Y(dmba)_3]$ (dmba = *o*-dimethylaminomethyl-phenyl) leads to the selective formation of [{**B**}$Y(dmba)_2$]:

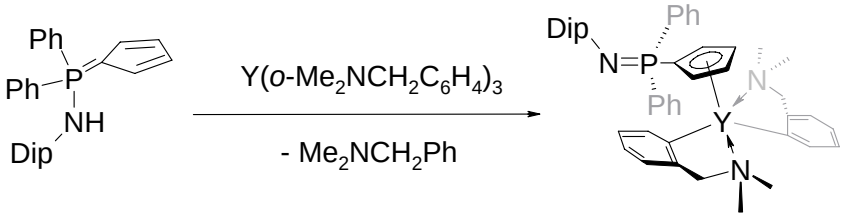

This complex represents the only example of a *CpPN*-lanthanide complex with an uncoordinated phosphazene arm.

Two homoleptic ytterbium(II) complexes of the type [Yb{*CpPN*}$_2$] with the ligands {**A**}H and its phenyl analog Ph$_2$P(C$_5$Me$_4$)NHAd were synthesized by the *salt-metathesis* route from the potassium salt of the appropriate ligand and [YbI$_2$(thf)$_2$].

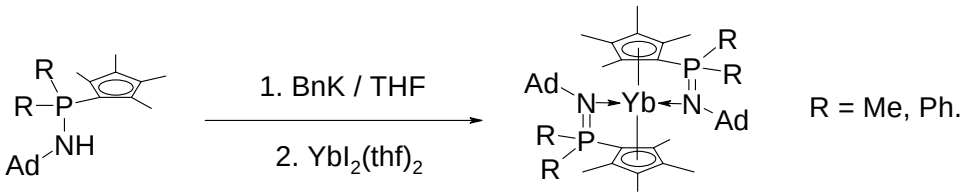

These ytterbocenes(II) were isolated as surprisingly moderate air-sensitive, crystalline solids. The complex [Yb{η^5,η^1-(Me$_4$C$_5$)PPh$_2$(NAd)}$_2$] was analyzed by XRD. In the solid state this complex reveals distorted tetrahedral geometry with a crystallographic C_2-axis and a chiral helix-like ligand arrangement.

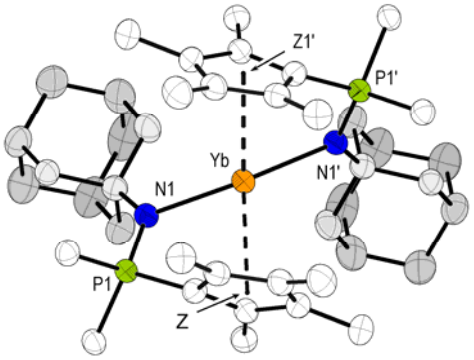

Finally, the catalytic activity of the dialkyl complexes of Sc, Lu, Y and Nd with ligand {**A**}H, which possess higher thermal stability, in intramolecular hydroamination/cyclization reactions of two *gem*-substituted penten-4-ylamines was investigated. The yttrium complex was found to be the most promising catalyst in the whole series showing an activity (TOF) of 15.2 and 70.3 h^{-1} for both substrates and yields up to 95%. The neodymium complex has comparable initial TON in the hydroamination/cyclization reaction, but only moderate conversions (< 33%), due to high reactivity and instability of the catalyst, were achieved.

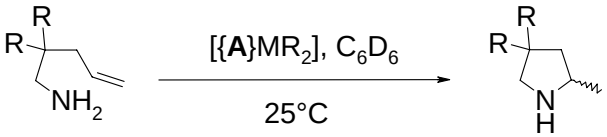

R = Me, Ph.

	TON	
M \ R	Ph	Me
Y	70.3	15.2
Nd	78.0	17.9

Scandium and lutetium dialkyl complexes were found to be completely inactive in these reactions, even at prolonged heating at higher temperatures (80°C).

The activity of *CpPN*-lanthanide complexes is comparable to that of *CpSiN*-lanthanide complexes recently reported by *Marks*. Thus, lanthanide alkyls and aryls reported in this Thesis offer a perfect pool of precursor complexes for further catalytic studies.

Zusammenfassung

Die vorliegende Arbeit beschäftigt sich mit der Synthese und Untersuchung von Seltenerdmetall-Komplexen, welche auf zwei speziellen Typen von chelatisierenden, monoanionischen Ligandensystemen basieren:

- *Ortho*-deprotonierte *N,N*-dimethyl-benzylamine $(dmba)^-$
- Cyclopentadienyl-phosphazene $(CpPN)^-$

Das erste Ligandensystem ist auf Basis von *ortho*-deprotoniertem *N,N*-Dimethylbenzylamin (dmba) und seiner Derivate aufgebaut. Diese wurden verwendet um den Einfluß der Ab- bzw. Anwesenheit benzylischer Protonen auf die Stabilität der Seltenerdmetalltrisalkyl-Komplexe zu untersuchen. Die Synthese homoleptischer Seltenerdmetall-Komplexe des Typs $[LnAr_3]$, ihre Stabilität und Kristallstrukturen werden in **Kapitel II** diskutiert. Das zweite neue Ligandensystem basiert auf einer Reihe von *CpPN*-Liganden mit unterschiedlichen Substituenten an den P- und N-Atomen, sowie am Cp-Ring. Die Diskussion der Synthese, beobachteter prototropischer Gleichgewichte und deren Molekülstrukturen erfolgt in **Kapitel III**. Cyclopentadienyl-phosphorane sind Zwischenstufen in der *CpPN*-Ligandensynthese. Daher werden anhand eines neuen, sehr anspruchsvollen Cyclopentadienyl-phosphans in **Kapitel IV** einige mechanistische Aspekte der Bildung, der Reaktivität gegen Oxidationsmittel, sowie einige Beispiele für dessen Koordinationschemie diskutiert. Abschließend folgt in **Kapitel V** eine Studie der Synthese und Charakterisierung, sowie möglicher Koordinationsmodi der Seltenerdmetall-*CpPN*-Komplexe. Über die Ergebnisse der schnellen, effizienten und einfachen Synthese von wasserfreien Lanthanoidbromiden wird im **Kapitel I** berichtet.

Kapitel I.

Wasserfreie Lanthanoidtrihalogenide stellen wichtige Ausgangstoffe für die Lanthanoidchemie dar. Dank der großen Ionenradien der frühen und mittleren Lanthanoide sind die entsprechenden Bromide und Iodide im Allgemeinen gut lösliche Präkursoren für deren Koordinationschemie.

Eine Serie von solvatisierten Lanthanoidbromiden wurde durch ein neues und einfaches *Eintopfverfahren* dargestellt. In diesem Verfahren wird von den relativ kostengünstigen

Lanthanoidoxiden ausgegangen, was den großen Vorteil des Verfahrens darstellt. Das eigentlich wirkende Reagenz – Me_3SiBr – wird aus dem viel leichter handhabbaren elementaren Brom und Hexamethyldisilan *in situ* erzeugt. Nach diesem Verfahren wurden die DME- und THF-solvatisierten Bromide des Neodyms und Samariums hochrein und kristallin in Ausbeuten von 64 - 88% dargestellt. Eine einfache Abtrennung der nicht vollständig umgesetzten Ausgangsstoffe kann durch Ausnutzung der hohen Löslichkeit dieser molekularen Salze in chlorierten Lösungsmitteln (CH_2Cl_2) realisiert werden.

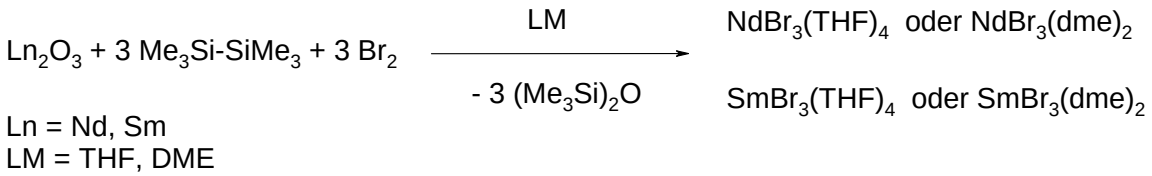

Kapitel II.

In diesem Kapitel wurde untersucht, welchen Einfluss die Modifizierung des (dmba)-Liganden mit alkylischen Resten hat. Es wurde beobachtet, dass diese die Entstehung eines Produkts und seine kinetische Stabilität stark beeinflussen. Die benötigten Aryllithiumreagenzien wurden durch Lithiierung der entsprechenden tertiären Amine synthetisiert.

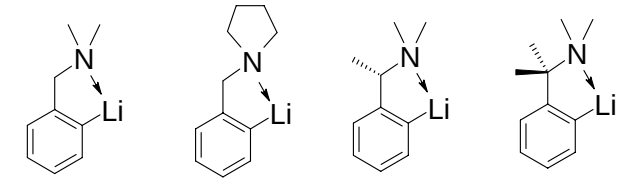

Li(dmba) Li(pyba) Li(tmba) Li(cuda)

Die Lanthanoidkomplexe wurden durch *Salzmetathese* aus den wasserfreien, solvatisierten Chloriden $[LnCl_3(dme)_n]$ (n = 1, 2) und den entsprechenden Aryllithiumreagenzien dargestellt. Die homoleptischen Komplexe $[Ln(dmba)_3]$ der späten Lanthanoide (Ln = Er, Yb) und Yttrium wurden synthetisiert und ein erstes Mal vollständig röntgenographisch charakterisiert. Die Analyse der Molekülstrukturen zeigt, dass alle zum bekannten Lutetiumkomplex $[Lu(dmba)_3]$ isostrukturell sind.

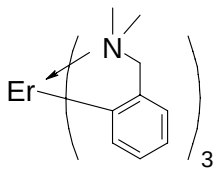

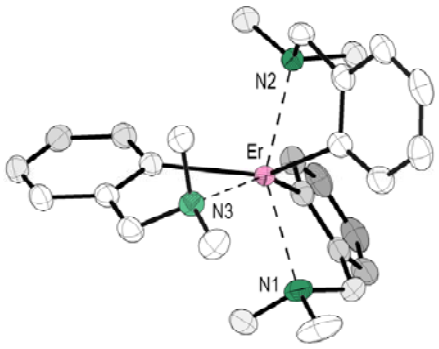

Die VT-NMR-Spektroskopie des diamagnetischen Yttriumkomplexes [Y(dmba)$_3$] zeigt eine sehr niedrige Koaleszenztemperatur (< 230 K). Damit wird die hohe konformationelle Labilität des (dmba)-Liganden in diesem Komplex bestätigt.

Die versuchte Transmetallierung von [GdCl$_3$(dme)$_2$] mit 3 Eq. [Li(dmba)] führt zur Isolierung der ersten Aryl-at-Komplexe des Typs [LiGd(dmba)$_4$]. Ähnliche Ergebnisse wurden auch für Neodym mit dem Liganden (pyba) erhalten. Die erhaltenen Komplexverbindungen wurden durch Elementaranalyse und röntgenographisch charakterisiert.

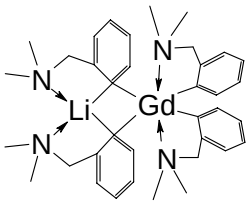

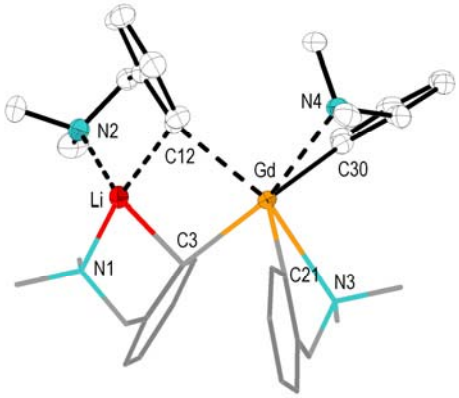

Des Weiteren wurde die Koordinationschemie der deutlich anspruchsvolleren Liganden (tmba) und (cuda) untersucht. Die Einführung von ein bzw. zwei Methylgruppen an den benzylischen Positionen des (dmba)-Liganden führt auch zu einer wesentlichen Erhöhung der Starrheit dieses Linkers. Zum Beispiel konnte aus der Reaktion von [LuCl$_3$(thf)$_3$] mit [Li(tmba)] lediglich ein heteroleptischer Komplex [LuCl(tmba)$_2$] isoliert werden. Eine Einführung eines dritten (dmba)-Liganden gelingt auch bei 1:3-Stöchiometrie, Erhitzen unter Rückfluss und längeren Reaktionszeiten nicht.

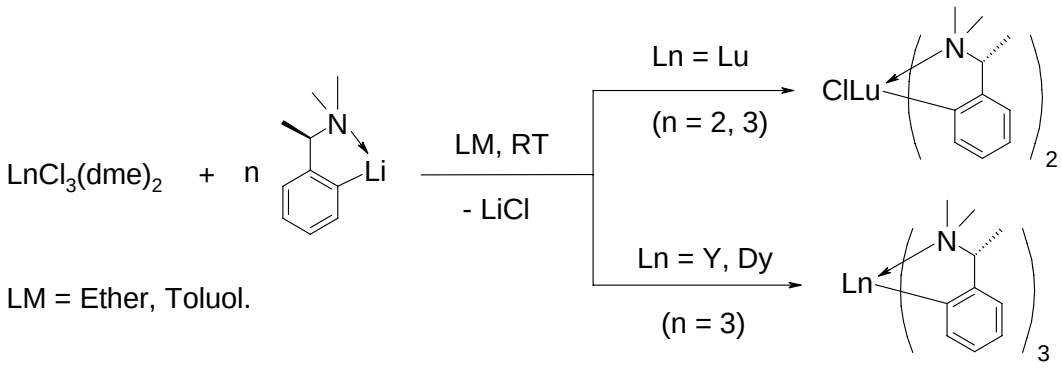

Bezüglich seines Ionenradius entspricht das Y^{3+}-Kation (KZ = 6) exakt der Grenzposition zwischen den mittleren und späten Lanthanoiden. Trotz des Unterschieds der Ionenradien von lediglich 0.04 Å im Vergleich mit einem Lu^{3+}-Kation, erfolgt eine erfolgreiche Transmetallierung von [YCl$_3$(dme)$_2$] mit [Li(tmba)]. Der farblose, homoleptische Yttriumkomplex [Y(tmba)$_3$], als auch der gelbliche Dysprosiumkomplex [Dy(tmba)$_3$],

konnten als kristalline Stoffe in hohen Ausbeuten isoliert werden. Der molekulare Aufbau der Komplexe wurde röntgenographisch nachgewiesen. Des Weiteren konnten ähnliche Komplexe des Samariums und Neodyms dargestellt werden. Die wesentlich niedrige thermische Stabilität, welche dennoch höher ist als mit dem (dmba)-Liganden, machte eine röntgenographische Charakterisierung leider unmöglich.

Eine weitere Erhöhung der Stabilität der Komplexe mit früheren Lanthanoiden konnte durch die Verwendung des (cuda)-Liganden erreicht werden. Der Samarium-Komplex [Sm(cuda)$_3$] wurde erfolgreich durch *Salzmetathese* dargestellt und in Form eines gelben kristallinen Stoffes isoliert. Verglichen mit [Sm(tmba)$_3$] ist dieser Komplex unzersetzt bei -30°C für Monate lagerfähig. Die Molekülstruktur wurde röntgenographisch bestätigt.

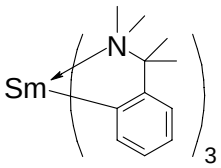

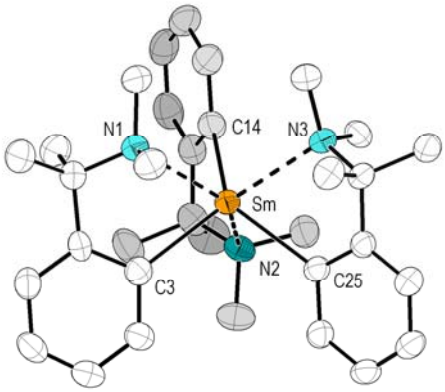

Es ist offensichtlich, dass die Bildung homoleptischer Aryl-Komplexe einerseits beschränkt ist auf sterisch ungehinderte (dmba)- und (pyba)-Liganden mit den kleinen, späten Lanthanoiden, und andererseits auf die sehr großen, frühen und mittleren Lanthanoide mit den sterisch anspruchsvollen (tmba)- und (cuda)-Liganden. Dies führt dazu, dass die frühen und mittleren Lanthanoide mit sterisch ungehinderten Liganden instabile Komplexe bilden, oder zu einer unvollständigen Umsetzung unter Bildung heteroleptischer Komplexe [LuCl(tmba)$_2$] führen. Die Bildung stabiler Komplexe vom Typ [Ln(tmba)$_3$] mit größeren, späten Lanthanoiden und vom Typ [Ln(cuda)$_3$] mit mittleren Lanthanoiden bleibt leider unverifiziert.

Die Existenz homoleptischer Komplexe von späten Lanthanoiden mit dem (cuda)-Liganden ist sehr unwahrscheinlich. Erstmalig wurde die Synthese und röntgenographische Charakterisierung diverser at-Komplexe des Typs Li[LnAr$_4$] durchgeführt. Zum Beispiel konnten für ein frühes und ein mittleres Lanthanoid die Komplexe [LiNd(pyba)$_4$]×½PhMe und [LiGd(dmba)$_4$] isoliert werden. Für Komplexe mit sterisch gehinderten (tmba)- und (cuda)-Liganden sind entsprechende Ergebnisse noch nicht verfügbar.

Alle beschriebenen Komplexe der früheren Lanthanoiden (Nd, Sm) besitzen eine sehr hohe Reaktivität und zersetzen sich rasch in THF. Es ist denkbar, dass dies der Grund ist, weswegen die früheren Versuche zur Darstellung der Komplexe fehlgeschlagen sind.

Kapitel III.

In diesem Kapitel wurde die Synthese von Phosphor(V)-Verbindungen, die eine *CpPN*-Einheit besitzen, untersucht. Dieses monoanionische Ligandensystem wurde zur weiteren Anwendung in der Synthese von Seltenerd-„Constrained-Geometry"-Komplexen (*CGC*) absichtlich gestaltet, welche isolobal zu den gut untersuchten dianionischen *CpSiN*-Komplexen der Metalle der 4. Gruppe sind.

Die retrosynthetische Analyse bietet mehrere mögliche Strategien zur Synthese von *CpPN*-Ligandensystemen. Es wurde festgestellt, dass unter den vielen Möglichkeiten die getestet wurden, die Anwendung einer *Staudinger* Reaktion – die Oxidation von Cyclopentadienyl-phosphanen mit organischen Aziden – die einzige synthetische Strategie ist, die erfolgreich zum gewünschten Ziel führt.

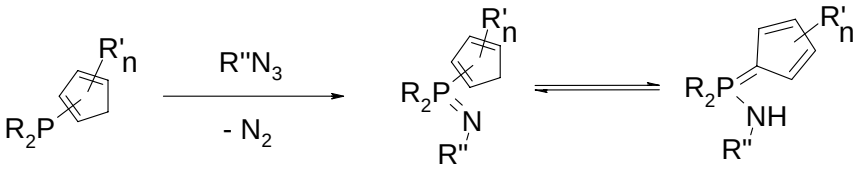

Die Synthese von *CpPN*-H Verbindungen aus den thermisch labilen Phosphanen C_5H_5-PR_2 (R = Me, Ph) wurde durch Verwendung von CpTl als effektivem Cp-Präkursor in THF als Lösungsmittel optimiert. Die Anwendbarkeit dieses synthetischen Ansatzes ist in folgender Tabelle zusammengefaßt:

	$C_5H_5PMe_2$	$C_5H_5PPh_2$	$HC_5Me_4PMe_2$	$HC_5Me_4PPh_2$
Me_3SiN_3	keine Reaktion	keine Reaktion	**L1**, 86%	keine Reaktion
AdN_3	**L2**, Spuren	**L3**, 69%	**L4**, 95%	**L8**, 78 %
$DipN_3$	**L5**, 75%	**L6**, 85%	**L7**, 60%	keine Reaktion

Stabilere Isomere sind: *P*-Amino-cyclopentadienyliden-phosphoran (helles Grau);
P-Cyclopentadienyl-phosphazene (dunkles Grau).

Es konnte gezeigt werden, dass bei *CpPN*-H-Verbindungen beide vorstellbaren Tautomerenformen vorliegen können. Dies wurde für die *CpPN*-Liganden die eine $Me_2PC_5Me_4$-Einheit enthalten beobachtet.

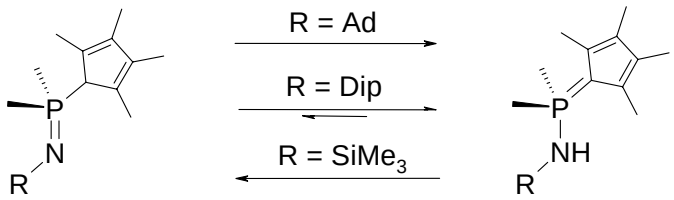

Das tautomere Gleichgewicht hängt stark von den Substituenten am Stickstoffatom und dem C5-Ring ab:

- Alle untersuchten *CpPN*-H-Verbindungen, die eine Ad-Gruppe am Stickstoffatom besitzen, und diejenigen, die gleichzeitig eine Dip- und C_5H_4-Gruppen enthalten, liegen als *P*-Amino-cyclopentadienyliden-phosphorane vor;
- die tautomere *P*-Cyclopentadienyl-iminophosphoran-Form wurde nur bei zwei Vertretern der *CpPN*-Liganden ($Me_2P(C_5Me_4H)NR$, R = $SiMe_3$, Dip) gefunden, die eine niedrigere CH-Acidität und N-Basizität besitzen. Für $Me_2P(C_5Me_4H)NSiMe_3$ wurde durch NMR-Spektroskopie neben dem überwiegenden Imino-phosphoran-Tautomer die Anwesenheit kleiner Mengen eines C5-Ring-Isomeren, und für $Me_2P(C_5Me_4H)NDip$ ein *N*-Amino-phosphoran-Tautomer nachgewiesen.

Kapitel IV.

Um die thermische Stabilität von Cp-Phosphanen zu erhöhen, werden solche benötigt, die mit sterisch anspruchsvollen Gruppen am C5-Ring, z. B. *tert*-Bu, modifiziert sind. Eine der Methoden, nach denen die *tert*-Bu-Gruppe eingefügt werden kann, ist die sogenannte *Fulven-Route*. Die *Fulven-Route* zur Synthese von Cyclopentadienen basiert auf der Carbometallierung von Fulvenen, welche bequem durch eine Kondensation von Cyclopentadienen mit Carbonylverbindungen dargestellt werden können. Das eigentliche Ziel der Untersuchung war die Synthese von $Ph_2PC_5H_4$(*tert*-Bu) und die weitere Verwendung in der Synthese von *CpPN*-Liganden.

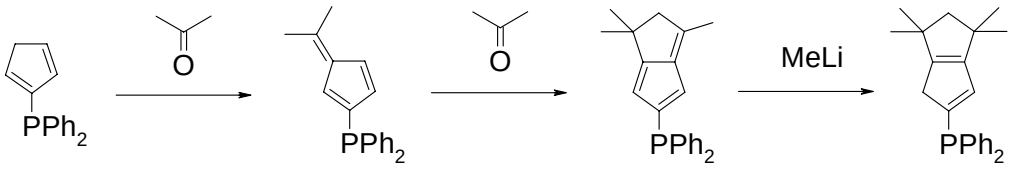

F1 **F2** $Ph_2PCp^{TM}H$

Die Synthese des Fulvens erfolgte nach dem *Little/Stone* Verfahren (in Methanol / Pyrrolidin als Katalysator) und führte zur Isolierung des gewünschten Stoffes. Zur Optimierung der Reaktionsbedingungen, wurde die Reaktion in reinem Aceton, als Reagenz und Lösungsmittel gleichzeitig, durchführt. Unerwarteter Weise führte die Reaktion zur ausschließlichen Bildung eines bizyklischen Fulvens (**F2**). Dieses Fulven wurde als Schlüsselverbindung in der Synthese eines attraktiven Cp-Phosphans angewendet. Das Kapitel beschreibt die Synthese und Reaktivität dieses eleganten Cp-Phosphans.

Die Durchführung der Reaktion in Aceton-d_6 ermöglichte die Gewinnung des entsprechenden isotopenmarkierten Produktes. Dieser Versuch bestätigte die Hypothese, dass das Fulven **F1** als ein Intermediat in dem Bildungsmechanismus von **F2** fungiert.

Die Carbometallierung des bizyklischen Fulvens **F2** mit MeLi eröffnet eine Methode zur Darstellung des ersten luftstabilen, kristallinen Cp-Phosphans, welches am C5-Ring eine sterisch sehr anspruchsvolle, 1,2-verknüpfte aliphatische Tetramethyl-trimethylen-Einheit (Cp^{TM}) besitzt. Dieses Cp-Phosphan $Ph_2PCp^{TM}H$ ist thermodynamisch sehr stabil und stellt den ersten Vertreter in seiner Klasse dar, der röntgenographisch charakterisiert ist.

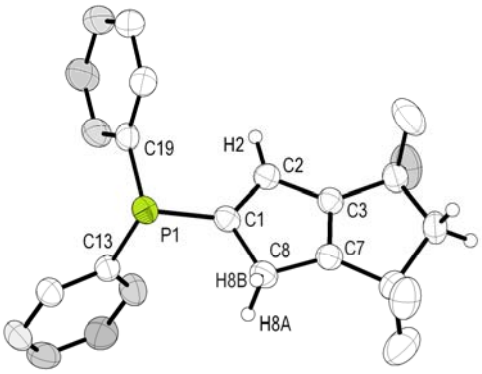

Die Oxidationsreaktionen von $Ph_2PCp^{TM}H$ mit H_2O_2, S_8 und Selen führen exklusiv zur Bildung von entsprechenden Phosphin-Chalkogeniden $Ph_2P(X)Cp^{TM}H$ (X = O, X = S, X = Se).

Mit dem Ziel *CpPN*-Liganden zu gewinnen, wurde die *Staudinger* Reaktion von $Ph_2PCp^{TM}H$ mit AdN_3, *tert*-BuN_3, $DipN_3$ und Me_3SiN_3 untersucht. Die Reaktionen verlaufen mit hohen Selektivitäten und in hohen Ausbeuten. Es wurde beobachtet, dass jede der Verbindungen in ihrer eigenen, fixierten, tautomeren Form existiert – im Falle R = Ad, *tert*-Bu führt dies zu *P*-Amino-cyclopentadienyliden-phosphoranen $Ph_2P(Cp^{TM})NHR$, und im Fall R' = Dip, $SiMe_3$ zu *P*-Cyclopentadienyl-iminophosphoranen $Ph_2P(NR')Cp^{TM}H$. Die Verbindungen $Ph_2P(Cp^{TM})NHAd$ und $Ph_2P(NDip)Cp^{TM}H$ wurden röntgenographisch charakterisiert, wobei letztere das erste charakterisierte *P*-Cyclopentadienyl-iminophosphoran darstellt.

Aus der *Staudinger* Reaktion mit und in Me_3SiN_3 (als Reagenz und Lösungsmittel gleichzeitig) wurde $Ph_2P(NSiMe_3)Cp^{TM}H$ als eine chemisch sehr labile Verbindung isoliert. Bei Hydrolyse mit Luftfeuchtigkeit, wurde $Ph_2P(Cp^{TM})NH_2$ als neues *N*-unsub-

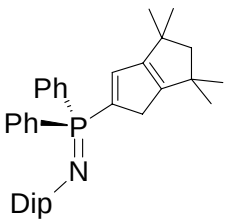

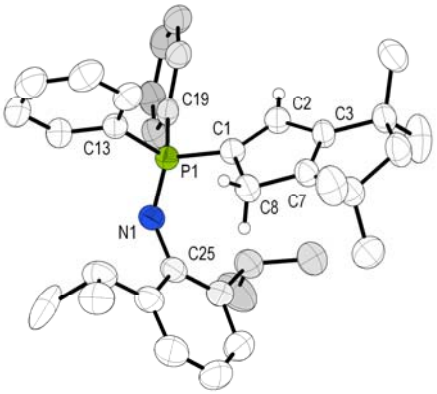

stituiertes *P*-Amino-cyclopentadienyliden-phosphoran, erhalten. Interessanterweise führt die Verwendung von *tert*-BuN_3 als "NH"-Synthon in einer direkte Reaktion mit $Ph_2P(Cp^{TM})NH_2$ zu dem regulären, dennoch neuen, *Staudinger* Produkt $Ph_2P(Cp^{TM})NH(tert\text{-}Bu)$.

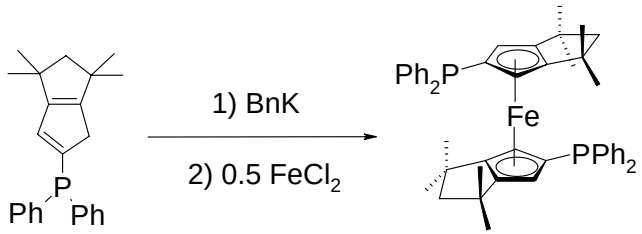

Weiterhin konnte ein darauf basierendes Ferrocen [(η^5-$Cp^{TM}PPh_2)_2Fe$] durch Deprotonierung von $Ph_2PCp^{TM}H$ mit BnK und folgender Transmetallierung mit $FeCl_2$ synthetisiert werden. In dieser Arbeit wird es in Analogie zum bekannten Vorläufer als [$dppf^{TM}$] bezeichnet. Dieses bidentate Phosphan wurde zur Synthese der Palladiumkomplexe [($dppf^{TM}$)$PdCl_2$] und [($dppf^{TM}$)PdI_2] verwendet. Die Komplexe [$dppf^{TM}$] und [($dppf^{TM}$)PdI_2] wurden ebenfalls röntgenographisch charakterisiert.

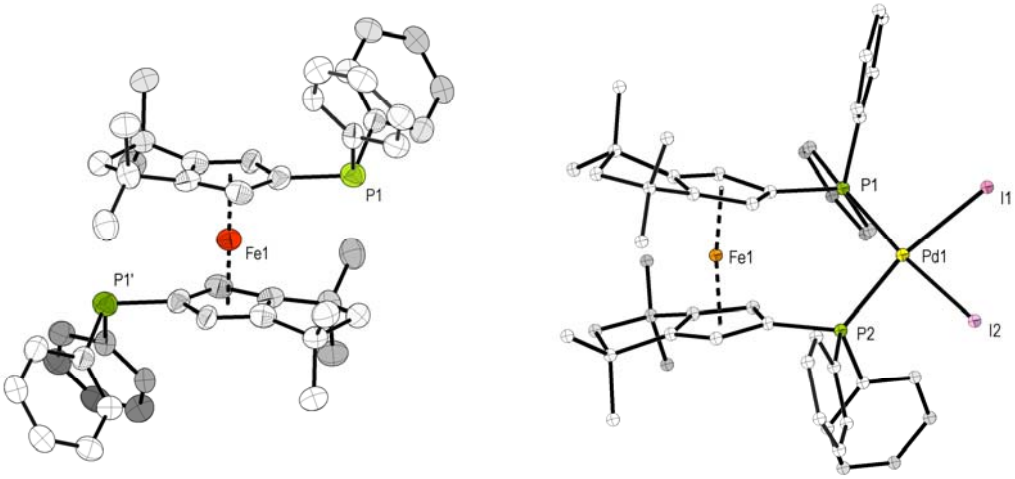

Kapitel V.

Dieses Kapitel befaßt sich mit der Beschreibung der Synthese und Charakterisierung der auf der Basis des *CpPN*-Liganden dargestellten Seltenerdmetall-Komplexe. Mit nur einer Ausnahme zeigen die *CpPN*-Liganden eine η^1,η^5-Koordination in den Komplexverbindungen.

Ein neuartiges *Eintopfverfahren* wurde entwickelt, welches Deprotonierung und Salzmetathese vereint. Damit konnte ein Zugangsweg zu *CpPN*-stabilisierten Lanthanoid-dialkylen des Typs [{*CpPN*}LnR_2] geschaffen werden, da die ansonsten üblichen Präkursor-Komplexe - [{*CpPN*}$LnHal_2$] oder [LnR_3] - nicht verfügbar sind.

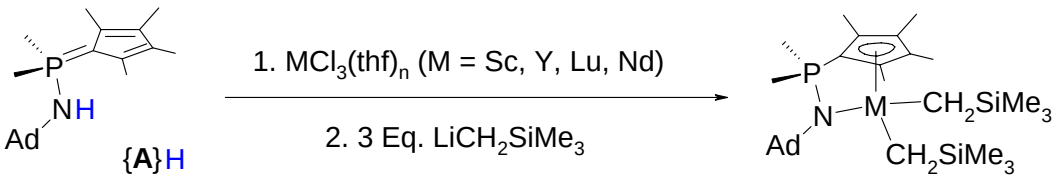

Auf Basis dieses Verfahrens wurde eine Serie von Seltenerdmetalldialkyl-*CpPN*-Komplexen synthetisiert, welche die folgenden *CpPN*-Liganden enthalten:

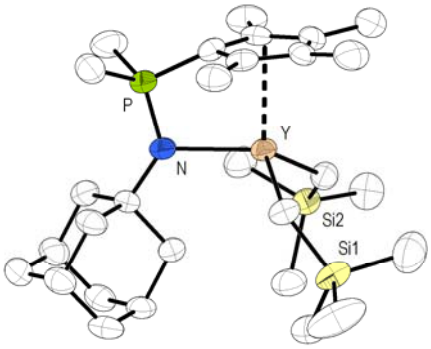

$Me_2P(C_5Me_4)NHAd$	{**A**}H
$Ph_2P(C_5H_4)NHDip$	{**B**}H
$Ph_2P(Cp^{TM})NHAd$	{**C**}H
$Ph_2P(NDip)Cp^{TM}H$	{**D**}H

Generell besitzen dabei Komplexe mit dem Liganden {**A**} die höchste thermische Stabilität innerhalb dieser Reihe. Für den paramagnetischen Neodym-Komplex [{**A**}$Nd(CH_2SiMe_3)_2$] konnte eine detaillierte Analyse der ^{1}H- und ^{13}C-NMR-Spektren, sowie eine Resonanzzuordnung durch 2D-NMR-Untersuchungen durchgeführt werden. Die hohe Reaktivität wurde durch die Isolierung zweier unerwarteter Zersetzungsprodukte demonstriert. Dabei handelte es sich um das binukleare heteroleptische *trans*-[{**A**}$Nd(\mu^2$-$OMe)(CH_2SiMe_3)]_2$ und eine tetranukleare Hydroxy-Spezies [{**A**}$Nd(\mu^2$-$OH)_2]_4$, wobei beide Verbindungen durch XRD analysiert werden konnten. Es kann vermutet werden, dass die Bildung des ersten Komplexes durch eine Etherabspaltung aus enthaltenem DME erfolgt, welches noch aus der Vorläuferverbindung [$NdCl_3$(dme)] stammt. Der zweite Komplex entsteht dabei offensichtlich durch partielle Hydrolyse von [{**A**}$Nd(CH_2SiMe_3)_2$].

Die Seltenerdmetalldialkyl-Komplexe des Yttriums und Neodyms mit dem sterisch weniger anspruchsvollen Liganden $Ph_2P(C_5H_4)$NHDip {**B**}H wurden als THF-Komplexe des Typs [{**B**}$M(CH_2SiMe_3)_2$(thf)] isoliert und durch XRD charakterisiert. Die Komplexe sind isostrukturell und weisen nur eine sehr schwache koordinative Wechselwirkung des Stickstoffatoms mit dem Metallatom auf.

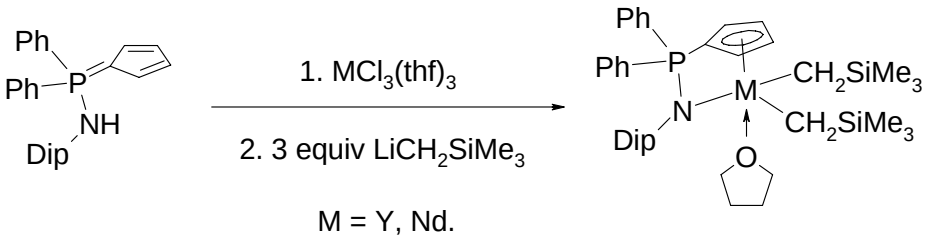

M = Y, Nd.

Die Dialkyl-Komplexe der Seltenerdmetalle mit kleinerem Ionenradius – Scandium and Yttrium – mit dem Liganden {**B**}H wurden als die entsprechenden lösungsmittelfreien Spezies isoliert und charakterisiert. Eine direkte Metallierung der sterisch höchst anspruchsvollen Liganden {**C**}H and {**D**}H durch $[Lu(CH_2SiMe_3)_3(thf)_2]$ war nicht möglich.

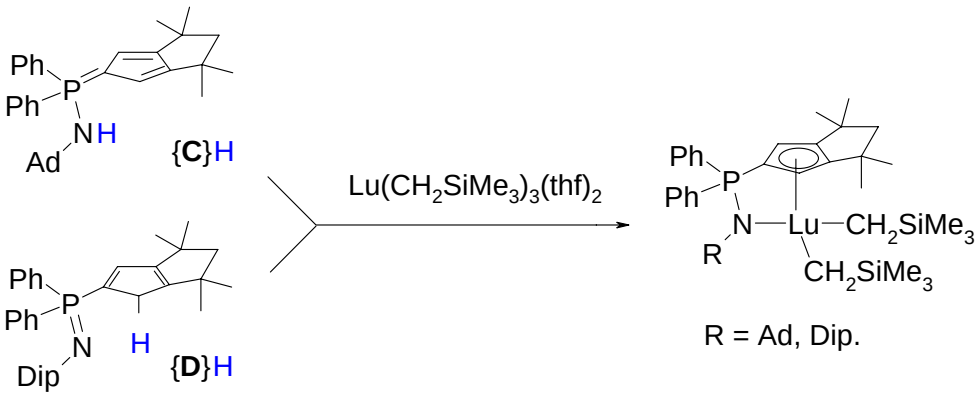

Anhand NMR-spektroskopischer Untersuchungen zeigt sich dabei für beide Dialkyl-Komplexe eine hohe konformelle Starre in Lösung.

Eine äquimolare Reaktion des Liganden {**B**}H mit dem homoleptischen Komplex $[Y(dmba)_3]$ (dmba = *o*-dimethylaminomethyl-phenyl) führt selektiv zur Bildung von $[\{\mathbf{B}\}Y(dmba)_2]$:

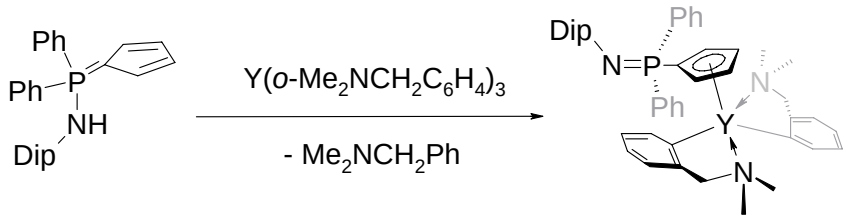

Dieser Komplex ist das einzige Beispiel für einen *CpPN*-Lanthanoid-Komplex mit einem an der Koordination unbeteiligtem Phosphazenarm.

Zwei homoleptische Ytterbium(II)-Komplexe des Typs $[Yb\{CpPN\}_2]$ mit dem Liganden {**A**}H und dessen Phenylanalogon $\underline{Ph}_2P(C_5Me_4)NHAd$ wurden durch *Salzmetathese* aus den entsprechenden Kaliumsalzen der Liganden und $[YbI_2(thf)_2]$ synthetisiert.

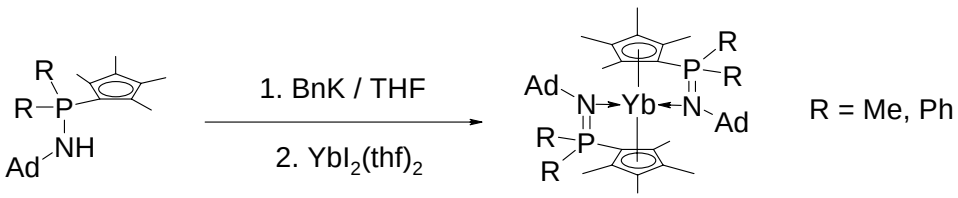

Diese Ytterbocene(II) wurden als überraschend wenig luftempfindliche kristalline Feststoffe erhalten. Der Komplex [Yb{η^5,η^1-(Me_4C_5)-PPh_2(NAd)}$_2$] konnte durch XRD charakterisiert werden. Im Feststoff zeigt dieser Komplex eine gestörte tetrahedrale Geometrie mit einer kristallographischen C_2-Achse und eine chirale, helixförmige Ligandanordnung.

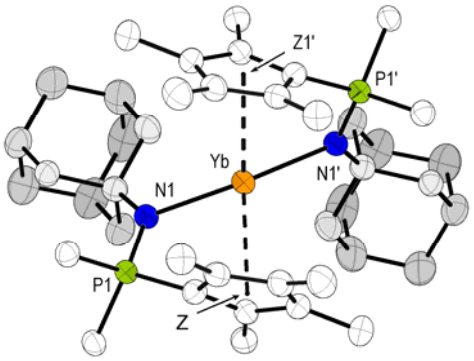

Die katalytische Aktivität der Dialkyl-Komplexe von Sc, Lu, Y und Nd mit dem Liganden {**A**}H – welcher die höchste thermische Stabilität zeigt - in intramolekularen Hydroaminierungs-/Cyclisierungs-Reaktionen zweier *gem*-substituierter Penten-4-ylamine wurde untersucht. Dabei zeigte sich, dass von allen untersuchten Verbindungen der Yttrium-Komplex die vielversprechendsten Ergebnisse lieferte. Dieser zeigte eine Aktivität (TOF) von 15.2 h^{-1} bzw. 70.3 h^{-1} für beide Substrate mit Ausbeuten von bis zu 95%. Der Neodym-Komplex weist vergleichbare Aktivitäten auf, jedoch nur geringe Umsätze (< 33%), was vermutlich auf die hohe Reaktivität bzw. Instabilität zurückzuführen ist.

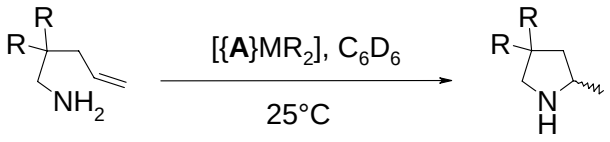

R = Me, Ph

M \ R	TOF Ph	TOF Me
Y	70.3	15.2
Nd	78.0	17.9

Die entsprechenden Scandium- and Lutetiumdialkyl-Komplexe zeigten dabei, selbst bei höheren Temperaturen (80°C) keinerlei Aktivität. Die Aktivität der *CpPN*-Lanthanoid-Komplexe ist vergleichbar mit den Aktivitäten entsprechender *CpSiN*-Lanthanoid-Komplexe, welche bereits von *Marks* vorgestellt wurden.

Demzufolge machen die im Rahmen dieser Arbeit vorgestellten Lanthanoid-Alkyle und -Aryle ein breites Spektrum von Präkursor-Komplexen für weitere katalytische Studien zugänglich.

Crystallographic Data

Dr. K. Harms (Chemistry Department, University of Marburg)

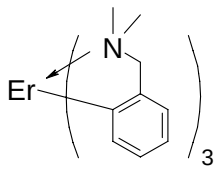

Table 1. Crystal data and structure refinement for [Er(dmba)$_3$] (**H1**).

Crystal data:

Identification code	aper1	
Habitus, color	irregular, red brown	
Crystal size	0.3 x 0.23 x 0.15 mm^3	
Crystal system	Monoclinic	
Space group	C 2/c	Z = 8
Unit cell dimensions	a = 24.1766(16) Å	α = 90°
	b = 9.3438(5) Å	β = 113.567(5)°
	c = 23.8596(15) Å	γ = 90°
Volume	4940.4(5) Å^3	
Cell determination	20330 peaks with Theta 1.8 to 27.1°	
Empirical formula	$C_{27}H_{36}ErN_3$	
Formula weight	569.85	
Density (calculated)	1.532 Mg/m^3	
Absorption coefficient	3.415 mm^{-1}	
F(000)	2296	

Data collection:

Diffractometer type	IPDS2
Wavelength	0.71073 Å
Temperature	173(2) K
Theta range for data collection	1.84 to 26.74°
Index ranges	-30<=h<=28, -11<=k<=11, -29<=l<=30
Data collection software	STOE WinXpose (X-Area)
Cell refinement software	STOE WinCell (X-Area)
Data reduction software	STOE WinIntegrate (X-Area)

Solution and refinement:

Reflections collected	18448
Independent reflections	5237 [R(int)= 0.0286]
Completeness to theta = 25.00°	100.0%
Observed reflections	4583 [I > 2sigma(I)]
Reflections used for refinement	5237
Extinction coefficient	X = 0.00019(2)
Absorption correction	Integration
Max. and min. transmission	0.6736 and 0.4673
Largest diff. peak and hole	0.512 and -0.774 e.Å^{-3}
Solution	Direct methods
Refinement	Full-matrix least-squares on F^2
Treatment of hydrogen atoms	Located, isotropic refinement
Programs used	SIR2004 (Giacovazzo, 2004)
	SHELXL-97 (Sheldrick, 1997)
	Diamond 3.1, STOE IPDS2 software
Data / restraints / parameters	5237 / 0 / 425
Goodness-of-fit on F^2	1.025
R index (all data)	wR2 = 0.0388
R index conventional [I > 2sigma(I)]	R1 = 0.0173

Table 2. Atomic coordinates and equivalent isotropic displacement parameters ($Å^2$)for aper1. U(eq)is defined as one third of the trace of the orthogonalized U^{ij} tensor.

	x	y	z	U(eq)	Occupancy
C1	6290(1)	4324(2)	7499(1)	28(1)	1
C2	6293(1)	5817(3)	7583(1)	34(1)	1
C3	6549(1)	6471(3)	8153(1)	38(1)	1
C4	6829(1)	5658(3)	8674(1)	41(1)	1
C5	6853(1)	4185(3)	8618(1)	37(1)	1
C6	6587(1)	3548(2)	8046(1)	29(1)	1
C7	6599(1)	1934(3)	8006(1)	34(1)	1
C8	7254(1)	1907(4)	7458(1)	47(1)	1
C9	6666(2)	-159(3)	7472(2)	60(1)	1
C10	5026(1)	1189(2)	6387(1)	31(1)	1
C11	4974(1)	-206(3)	6589(1)	38(1)	1
C12	4429(1)	-929(3)	6424(1)	41(1)	1
C13	3899(1)	-299(3)	6039(1)	39(1)	1
C14	3918(1)	1074(3)	5825(1)	35(1)	1
C15	4468(1)	1793(2)	5996(1)	28(1)	1
C16	4467(1)	3287(3)	5746(1)	30(1)	1
C17	4777(1)	4514(3)	6711(1)	31(1)	1
C18	4963(1)	5570(3)	5887(1)	36(1)	1
C19	6389(1)	4079(2)	6006(1)	26(1)	1
C20	6494(1)	5564(2)	5999(1)	30(1)	1
C21	6838(1)	6172(3)	5713(1)	33(1)	1
C22	7097(1)	5309(3)	5415(1)	36(1)	1
C23	7011(1)	3846(3)	5406(1)	35(1)	1
C24	6666(1)	3241(2)	5698(1)	28(1)	1
C25	6606(1)	1633(3)	5697(1)	32(1)	1
C26	6072(1)	-417(3)	5835(1)	39(1)	1
C27	5521(1)	1558(3)	5240(1)	31(1)	1
N1	6670(1)	1427(2)	7449(1)	33(1)	1
N2	4944(1)	4204(2)	6190(1)	26(1)	1
N3	6064(1)	1162(2)	5785(1)	28(1)	1
Er	5901(1)	2797(1)	6585(1)	21(1)	1

Dr. B. Ziemer (Chemical Department, Humboldt-University Berlin)

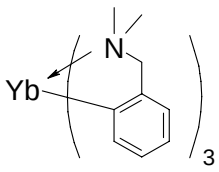

Table 3. Crystal data and structure refinement for [Yb(dmba)$_3$] (**H2**).

Crystal data:

Identification code	ruf22	
Habitus, color	prism, yellow	
Crystal size	0.92 x 0.80 x 0.40 mm^3	
Crystal system	Monoclinic	
Space group	C 2/c	Z = 8
Unit cell dimensions	a = 24.098(11) Å	α = 90°
	b = 9.312(4) Å	β = 123.880(3)°
	c = 26.247(9) Å	γ = 90°
Volume	4890(3) Å^3	
Cell determination	8000 peaks with Theta 2.0 to 26.0°	
Empirical formula	$C_{27}H_{36}N_3Yb$	
Formula weight	575.63	
Density (calculated)	1.564 Mg/m^3	
Absorption coefficient	3.843 mm^{-1}	
F(000)	2312	

Data collection:

Diffractometer type	IPDS2.87
Wavelength	0.71073 Å
Temperature	150(2) K
Theta range for data collection	1.84 to 25.99°
Index ranges	-29<=h<=29, 0<=k<=11, -32<=l<=32
Data Collection Software	IPDS2.87 (Stoe & Cie, 1997)
Cell Refinement Software	IPDS2.87 (Stoe & Cie, 1997)
Data Reduction Software	IPDS2.87 (Stoe & Cie, 1997)

Solution and Refinement:

Reflections collected	8466
Independent reflections	4780 [R(int)= 0.0345]
Completeness to theta = 25.99°	99.3%
Observed reflections	4201 [I > 2sigma(I)]
Reflection used for refinement	4780
Extinction coefficient	0.009(3)
Absorption correction	None
Max. and min. transmission	0.3086 and 0.1260
Largest diff. peak and hole	1.349 and -2.134 e.Å^{-3}
Solution	direct
Refinement	Full-matrix least-squares on F^2
Programs used	SHELXS-97 (Sheldrick, 1990)
	SHELXL-97 (Sheldrick, 1997)
	DIAMOND (Brandenburg, 1999)
Data / restraints / parameters	4780 / 0 / 280
Goodness-of-fit on F^2	0.935
R index (all data)	wR2 = 0.1129
R index conventional [I > 2sigma(I)]	R1 = 0.0332

Table 4. Atomic coordinates (x 10^4)and equivalent isotropic displacement parameters ($Å^2$x 10^3)for ruf22. U(eq)is defined as one third of the trace of the orthogonalized U^{ij} tensor.

	x	y	z	U(eq)	Occupancy
C1	-1283(3)	-9303(7)	7507(3)	21(1)	1
C2	-1282(3)	-10801(7)	7426(3)	26(1)	1
C3	-1544(3)	-11471(8)	6854(3)	31(2)	1
C4	-1829(3)	-10643(9)	6332(3)	33(2)	1
C5	-1849(3)	-9169(8)	6387(3)	30(2)	1
C6	-1584(3)	-8526(7)	6962(3)	22(1)	1
C7	-1595(3)	-6911(7)	6999(3)	25(1)	1
C8	-1680(5)	-4820(9)	7536(4)	54(3)	1
C9	-2249(3)	-6908(10)	7544(3)	42(2)	1
C10	-33(3)	-6195(7)	8603(3)	23(1)	1
C11	16(3)	-4793(7)	8395(3)	29(1)	1
C12	562(3)	-4057(7)	8559(3)	30(2)	1
C13	1090(3)	-4676(8)	8950(3)	30(2)	1
C14	1071(3)	-6055(8)	9167(3)	27(1)	1
C15	521(3)	-6795(7)	8998(2)	20(1)	1
C16	530(3)	-8271(7)	9252(2)	20(1)	1
C17	227(3)	-9521(7)	8288(3)	22(1)	1
C18	33(3)	-10561(7)	9115(3)	27(1)	1
C19	-1396(3)	-9070(6)	8979(2)	18(1)	1
C20	-1501(3)	-10558(7)	8984(3)	20(1)	1
C21	-1840(3)	-11172(7)	9278(3)	25(1)	1
C22	-2096(3)	-10299(8)	9583(3)	29(2)	1
C23	-2006(3)	-8840(8)	9592(3)	26(1)	1
C24	-1670(3)	-8220(7)	9296(2)	20(1)	1
C25	-1606(3)	-6616(7)	9299(3)	24(1)	1
C26	-514(3)	-6572(7)	9765(3)	23(1)	1
C27	-1059(3)	-4584(7)	9165(3)	30(2)	1
N1	-1669(3)	-6418(6)	7558(2)	26(1)	1
N2	51(2)	-9196(5)	8811(2)	17(1)	1
N3	-1055(2)	-6164(5)	9214(2)	20(1)	1
Yb	-901(1)	-7784(1)	8415(1)	13(1)	1

T. Linder (Chemistry Department, University of Marburg)

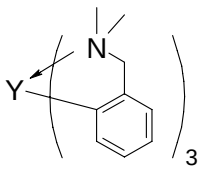

Table 5. Crystal data and structure refinement for [Y(dmba)$_3$] (**H4**).

Crystal data

Identification code	oth561	
Habitus, color	prism, colorless	
Crystal size	0.3 x 0.12 x 0.09 mm^3	
Crystal system	Monoclinic	
Space group	C 2/c	Z = 4
Unit cell dimensions	a = 24.170(3) Å	α= 90°
	b = 9.3613(7) Å	β= 113.474(11)°
	c = 23.880(2) Å	γ = 90°
Volume	4955.9(8) Å^3	
Cell determination	8000 peaks with Theta 1.9 to 26.0°	
Empirical formula	$C_{27}H_{36}N_3Y$	
Formula weight	491.50	
Density (calculated)	1.317 Mg/m^3	
Absorption coefficient	2.372 mm^{-1}	
F(000)	2064	

Data collection:

Diffractometer type	IPDS1
Wavelength	0.71069 Å
Temperature	193(2) K
Theta range for data collection	1.84 to 26.03°
Index ranges	-29<=h<=29, -11<=k<=11, -27<=l<=28
Data collection software	STOE WinXpose (X-Area)
Cell refinement software	STOE WinCell (X-Area)
Data reduction software	STOE WinIntegrate (X-Area)

Solution and Refinement:

Reflections collected	19038
Independent reflections	4794 [R(int)= 0.0944]
Completeness to theta = 25.00°	98.9%
Observed reflections	3147 [I > 2sigma(I)]
Reflections used for refinement	4794
Extinction coefficient	X = 0.00019(2)
Absorption correction	Semi-empirical from equivalents
Max. and min. transmission	0.7399 and 0.5989
Largest diff. peak and hole	1.125 and -0.533 e.Å^{-3}
Solution	direct/ difmap
Refinement	Full-matrix least-squares on F^2
Treatment of hydrogen atoms	geom.., mixed
Programs used	SHELXS-86 (Sheldrick, 1986)
	SHELXL-97 (Sheldrick, 1997)
	Ortep-3 for Windows (Farrugia, 1997)
Data / restraints / parameters	4794 / 0 / 280
Goodness-of-fit on F^2	0.914
R index (all data)	wR2 = 0.1048
R index [I>2sigma(I)]	R1 = 0.0415

Table 6. Atomic coordinates (x 10^4)and equivalent isotropic displacement parameters ($Å^2$x 10^3)for oth561. U(eq)is defined as one third of the trace of the orthogonalized U^{ij} tensor.

	x	y	z	U(eq)	Occupancy
C1	6391(2)	909(4)	1001(2)	24(1)	1
C2	6496(2)	-563(4)	991(2)	27(1)	1
C3	6836(2)	-1174(5)	709(2)	33(1)	1
C4	7093(2)	-313(5)	412(2)	39(1)	1
C5	7007(2)	1156(5)	404(2)	35(1)	1
C6	6665(2)	1749(4)	693(2)	26(1)	1
C7	6611(2)	3355(4)	696(2)	31(1)	1
C8	5525(2)	3450(4)	241(2)	32(1)	1
C9	6079(2)	5409(4)	837(2)	41(1)	1
C10	6298(2)	677(4)	2505(2)	26(1)	1
C11	6295(2)	-808(4)	2588(2)	31(1)	1
C12	6552(2)	-1463(5)	3157(2)	39(1)	1
C13	6834(2)	-651(5)	3674(2)	41(1)	1
C14	6859(2)	818(5)	3618(2)	37(1)	1
C15	6593(2)	1450(4)	3044(2)	28(1)	1
C16	6609(2)	3059(4)	3010(2)	31(1)	1
C17	7256(2)	3107(6)	2463(2)	47(1)	1
C18	6671(3)	5149(5)	2474(3)	61(2)	1
C19	5018(2)	3831(4)	1380(2)	29(1)	1
C20	4967(2)	5214(5)	1580(2)	38(1)	1
C21	4420(2)	5939(5)	1417(2)	41(1)	1
C22	3897(2)	5298(5)	1038(2)	39(1)	1
C23	3918(2)	3934(5)	831(2)	34(1)	1
C24	4461(2)	3222(4)	996(2)	26(1)	1
C25	4459(2)	1731(4)	749(2)	29(1)	1
C26	4955(2)	-556(4)	884(2)	38(1)	1
C27	4772(2)	506(4)	1708(2)	31(1)	1
N1	6069(2)	3836(3)	781(2)	26(1)	1
N2	6678(2)	3567(3)	2457(2)	32(1)	1
N3	4935(2)	807(3)	1187(2)	26(1)	1
Y	5901(1)	2210(1)	1583(1)	20(1)	1

Dr. K. Harms (Chemistry Department, University of Marburg)

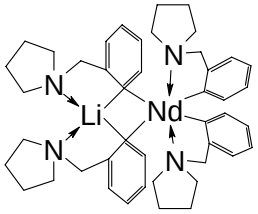

Table 7. Crystal data and structure refinement for [LiNd(pyba)$_4$]x ½C_7H_8 (**H5**).

Crystal data:

Identification code	apr01	
Habitus, color	prism, pale blue	
Crystal size	0.24 x 0.09 x 0.06 mm^3	
Crystal system	Monoclinic	
Space group	P 2_1/n	Z = 4
Unit cell dimensions	a = 12.5989(11) Å	α = 90°
	b = 24.3261(19) Å	β = 95.336(11)°
	c = 13.6311(13) Å	γ = 90°
Volume	4159.6(6) Å^3	
Cell determination	8000 peaks with Theta 2 to 25°	
Empirical formula	$C_{47.50}H_{60}LiN_4Nd$	
Formula weight	838.17	
Density (calculated)	1.338 Mg/m^3	
Absorption coefficient	1.285 mm^{-1}	
F(000)	1744	

Data collection:

Diffractometer type	IPDS1
Wavelength	0.71073 Å
Temperature	193(2) K
Theta range for data collection	1.72 to 25.00°
Index ranges	-14<=h<=14, -28<=k<=28, -16<=l<=16
Data collection software	STOE WinXpose (X-Area)
Cell refinement software	STOE WinCell (X-Area)
Data reduction software	STOE WinIntegrate (X-Area)

Solution and refinement:

Reflections collected	27227
Independent reflections	7312 [R(int)= 0.2045]
Completeness to theta = 25.00°	99.9%
Observed reflections	2799[I > 2sigma(I)]
Reflections used for refinement	7312
Extinction coefficient	X = 0.00019(2)
Absorption correction	Gaussian
Max. and min. transmission	0.9248 and 0.8144
Largest diff. peak and hole	0.815 and -0.606 e.Å^{-3}
Solution	Direct methods
Refinement	Full-matrix least-squares on F^2
Treatment of hydrogen atoms	Calculated, fixed isotropic U's
Programs used	SIR92 (Giacovazzo, 1993)
	SHELXL-97 (Sheldrick, 1997)
	Diamond 3.1, STOE IPDS1 software
Data / restraints / parameters	7312 / 72 / 502
Goodness-of-fit on F^2	0.723
R index (all data)	wR2 = 0.1054
R index conventional [I > 2sigma(I)]	R1 = 0.0570

Table 8. Atomic coordinates and equivalent isotropic displacement parameters ($Å^2$)for apr01. U(eq)is defined as one third of the trace of the orthogonalized U^{ij} tensor.

	x	y	z	U(eq)	Occupancy
C2	0.6103(10)	0.0653(7)	0.1235(9)	0.098(6)	1
C3	0.4999(10)	0.0727(7)	0.1182(9)	0.091(5)	1
C4	0.4685(9)	0.0975(8)	0.0209(11)	0.136(8)	1
C5	0.5618(8)	0.1097(5)	-0.0238(8)	0.063(4)	1
C6	0.7116(8)	0.0484(4)	-0.0178(7)	0.048(3)	1
C7	0.7631(7)	0.0727(4)	-0.1029(6)	0.030(2)	1
C8	0.8153(7)	0.1223(4)	-0.0899(5)	0.028(2)	1
C9	0.8628(7)	0.1422(4)	-0.1736(6)	0.042(3)	1
C10	0.8554(8)	0.1126(4)	-0.2627(7)	0.044(3)	1
C11	0.8004(9)	0.0660(5)	-0.2736(7)	0.046(3)	1
C12	0.7512(8)	0.0453(4)	-0.1924(8)	0.051(3)	1
C14	1.0912(7)	0.1277(6)	0.1666(7)	0.092(5)	1
C15	1.1842(11)	0.1195(6)	0.1154(10)	0.096(5)	1
C16	1.1463(16)	0.0902(8)	0.0236(13)	0.149(9)	1
C17	1.0492(12)	0.0803(10)	0.0201(10)	0.170(11)	1
C18	0.9661(11)	0.0506(7)	0.1630(11)	0.100(7)	1
C19	0.9165(8)	0.0674(5)	0.2575(9)	0.053(3)	1
C20	0.8527(8)	0.1139(4)	0.2536(6)	0.039(3)	1
C21	0.8200(7)	0.1288(4)	0.3433(7)	0.048(3)	1
C22	0.8427(9)	0.0999(6)	0.4302(8)	0.068(4)	1
C23	0.8999(11)	0.0534(6)	0.4314(9)	0.080(4)	1
C24	0.9414(9)	0.0363(5)	0.3427(10)	0.076(4)	1
C26	0.6633(8)	0.3695(5)	-0.0448(7)	0.052(3)	1
C27	0.7499(10)	0.4103(5)	-0.0681(8)	0.068(4)	1
C28	0.8329(11)	0.3732(6)	-0.1097(9)	0.087(4)	1
C29	0.7795(8)	0.3192(5)	-0.1271(7)	0.058(3)	1
C30	0.6302(8)	0.2716(4)	-0.0649(7)	0.052(3)	1
C31	0.5849(7)	0.2541(4)	0.0289(6)	0.038(2)	1
C32	0.6553(7)	0.2271(4)	0.0989(7)	0.037(3)	1
C33	0.6067(8)	0.2134(4)	0.1845(6)	0.042(3)	1
C34	0.5053(8)	0.2253(5)	0.2020(7)	0.053(3)	1
C35	0.4400(8)	0.2507(5)	0.1336(9)	0.063(4)	1
C36	0.4790(8)	0.2663(4)	0.0455(8)	0.052(3)	1
C38	0.7374(7)	0.3324(6)	0.2945(6)	0.062(3)	1
C39	0.6689(9)	0.3790(6)	0.2533(8)	0.071(4)	1
C40	0.7507(10)	0.4198(6)	0.2215(8)	0.076(4)	1
C41	0.8518(9)	0.3856(5)	0.2122(7)	0.047(3)	1
C42	0.9116(8)	0.2927(4)	0.2562(7)	0.043(3)	1
C43	0.9786(7)	0.2826(4)	0.1750(6)	0.038(3)	1
C44	0.9387(7)	0.2510(4)	0.0916(7)	0.039(3)	1
C45	1.0036(7)	0.2467(5)	0.0185(8)	0.056(3)	1
C46	1.1011(8)	0.2728(5)	0.0183(8)	0.057(3)	1
C47	1.1382(8)	0.3031(4)	0.0969(8)	0.056(3)	1
C48	1.0796(7)	0.3077(4)	0.1770(6)	0.043(3)	1
C901	0.4696(16)	-0.0158(10)	0.5432(14)	0.074(7)	0.50
C902	0.4511(13)	-0.0324(7)	0.4456(17)	0.057(9)	0.50
C903	0.5020(17)	-0.0058(10)	0.3728(11)	0.076(8)	0.50
C904	0.5714(18)	0.0375(10)	0.3977(16)	0.091(13)	0.50
C905	0.5899(16)	0.0541(8)	0.495(2)	0.091(9)	0.50
C906	0.5390(18)	0.0275(10)	0.5681(12)	0.095(12)	0.50
C907	0.418(4)	-0.038(2)	0.619(4)	0.19(3)	0.50
N1	0.6562(6)	0.0897(4)	0.0375(6)	0.048(3)	1
N13	1.0006(8)	0.0995(7)	0.1086(8)	0.089(5)	1
N26	0.7094(6)	0.3155(4)	-0.0486(5)	0.041(2)	1
N37	0.8196(5)	0.3290(4)	0.2248(4)	0.041(2)	1
Nd1	0.81952(4)	0.16190(2)	0.08584(4)	0.03359(15)	1
Li1	0.7855(10)	0.2896(7)	0.0892(10)	0.042(4)	1

Dr. K. Harms (Chemistry Department, University of Marburg)

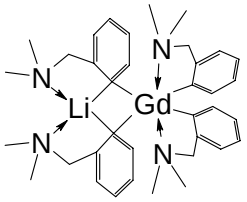

Table 9. Crystal data and structure refinement for [LiGd(dmba)$_4$] (**H6**).

Crystal data:

Identification code	apgd1	
Habitus, color	prism, colorless	
Crystal size	0.18 x 0.12 x 0.03 mm^3	
Crystal system	Triclinic	
Space group	P -1	Z = 2
Unit cell dimensions	a = 9.7595(12) Å	α= 82.535(10)°
	b = 12.0826(16) Å	β= 75.095(9)°
	c = 15.8362(19) Å	γ = 70.257(10)°
Volume	1696.6(4) Å^3	
Cell determination	14265 peaks with Theta 1.3 to 25°	
Empirical formula	$C_{36}H_{48}GdLiN_4$	
Formula weight	700.97	
Density (calculated)	1.372 Mg/m^3	
Absorption coefficient	1.983 mm^{-1}	
F(000)	718	

Data collection:

Diffractometer type	IPDS2
Wavelength	0.71073 Å
Temperature	173(2) K
Theta range for data collection	1.33 to 25.93°
Index ranges	-11<=h<=11, -14<=k<=14, -19<=l<=19
Data collection software	STOE WinXpose (X-Area)
Cell refinement software	STOE WinCell (X-Area)
Data reduction software	STOE WinIntegrate (X-Area)

Solution and refinement:

Reflections collected	14409
Independent reflections	6549 [R(int)= 0.0382]
Completeness to theta = 25.00°	99.7%
Observed reflections	5479 [I > 2sigma(I)]
Reflections used for refinement	6549
Extinction coefficient	X = 0.00019(2)
Absorption correction	Integration
Max. and min. transmission	0.9164 and 0.7277
Largest diff. peak and hole	0.749 and -0.573 e.Å^{-3}
Solution	Direct methods
Refinement	Full-matrix least-squares on F^2
Treatment of hydrogen atoms	Located, isotropic refinement
Programs used	SIR-2004
	SHELXL-97 (Sheldrick, 1997)
	Diamond 3.1, STOE IPDS2 software
Data / restraints / parameters	6549 / 0 / 571
Goodness-of-fit on F^2	0.905
R index (all data)	wR2 = 0.0471
R index conventional [I > 2sigma(I)]	R1 = 0.0252

Table 10. Atomic coordinates and equivalent isotropic displacement parameters ($Å^2$)for apgd1. U(eq)is defined as one third of the trace of the orthogonalized U^{ij} tensor.

	x	y	z	U(eq)	Occupancy
C1	0.8781(4)	0.0086(3)	0.2488(2)	0.0371(7)	1
C2	0.7125(3)	0.0597(2)	0.25127(18)	0.0323(6)	1
C3	0.6434(3)	0.1813(2)	0.26465(19)	0.0315(6)	1
C4	0.4872(4)	0.2197(3)	0.2745(2)	0.0369(7)	1
C5	0.4065(4)	0.1463(3)	0.2691(2)	0.0436(8)	1
C6	0.4787(4)	0.0299(3)	0.2527(2)	0.0444(8)	1
C7	0.6317(4)	-0.0136(3)	0.2445(2)	0.0406(8)	1
C8	1.0604(4)	0.0084(4)	0.3291(3)	0.0553(10)	1
C9	0.8676(6)	-0.0786(4)	0.3956(3)	0.0569(10)	1
C10	0.5792(4)	0.3476(3)	0.4822(2)	0.0385(7)	1
C11	0.7361(3)	0.3542(2)	0.45525(19)	0.0331(6)	1
C12	0.8188(3)	0.3235(2)	0.36955(19)	0.0316(6)	1
C13	0.9697(4)	0.3181(3)	0.3538(2)	0.0404(7)	1
C14	1.0325(4)	0.3443(3)	0.4158(3)	0.0480(9)	1
C15	0.9465(5)	0.3768(3)	0.4966(3)	0.0530(10)	1
C16	0.7976(4)	0.3815(3)	0.5174(2)	0.0438(8)	1
C17	0.6439(6)	0.1630(4)	0.5660(3)	0.0550(10)	1
C18	0.4337(5)	0.2146(4)	0.5009(3)	0.0573(10)	1
C19	0.8145(3)	0.2059(3)	0.0388(2)	0.0349(7)	1
C20	0.9709(3)	0.1937(2)	0.04655(18)	0.0321(6)	1
C21	0.9910(3)	0.2556(2)	0.11044(19)	0.0339(7)	1
C22	1.1421(4)	0.2307(3)	0.1128(2)	0.0384(7)	1
C23	1.2614(4)	0.1517(3)	0.0604(2)	0.0436(8)	1
C24	1.2351(4)	0.0926(3)	-0.0004(2)	0.0436(8)	1
C25	1.0902(4)	0.1160(3)	-0.0083(2)	0.0382(7)	1
C26	0.7327(5)	0.4157(3)	0.0096(2)	0.0439(8)	1
C27	0.5530(4)	0.3159(4)	0.0686(2)	0.0457(8)	1
C28	0.7520(4)	0.6249(3)	0.1466(2)	0.0434(8)	1
C29	0.5873(4)	0.6397(2)	0.17262(19)	0.0380(7)	1
C30	0.5403(4)	0.5419(3)	0.20911(19)	0.0367(7)	1
C31	0.3850(4)	0.5659(3)	0.2320(2)	0.0408(7)	1
C32	0.2838(4)	0.6775(3)	0.2190(2)	0.0483(9)	1
C33	0.3356(5)	0.7686(3)	0.1821(2)	0.0513(10)	1
C34	0.4866(5)	0.7501(3)	0.1590(2)	0.0473(9)	1
C35	0.9954(4)	0.5308(3)	0.1761(3)	0.0510(9)	1
C36	0.7852(5)	0.6048(3)	0.2936(2)	0.0441(8)	1
Li1	0.7413(6)	0.1722(4)	0.3756(3)	0.0348(11)	1
N1	0.9042(3)	0.0150(2)	0.33649(17)	0.0369(6)	1
N2	0.5834(3)	0.2231(2)	0.49017(16)	0.0377(6)	1
N3	0.7032(3)	0.3192(2)	0.06928(16)	0.0339(6)	1
N4	0.8351(3)	0.5472(2)	0.21018(17)	0.0381(6)	1
Gd1	0.75264(2)	0.35394(1)	0.21771(1)	0.02643(5)	1

Dr. K. Harms (Chemistry Department, University of Marburg)

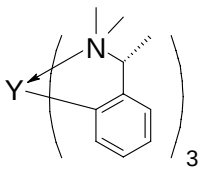

Table 11. Crystal data and structure refinement for [Y(tmba)$_3$] (**H8**).

Crystal data:

Identification code	oth28	
Habitus, color	prism, colorless	
Crystal size	0.30 x 0.20 x 0.10 mm^3	
Crystal system	Monoclinic	
Space group	P 2_1	Z = 4
Unit cell dimensions	a = 10.3760(10) Å	α= 90°
	b = 23.851(2) Å	β= 90.324(11)°
	c = 11.1035(9) Å	γ = 90°
Volume	2747.8(4) Å^3	
Cell determination	8000 peaks with Theta 2 to 26°	
Empirical formula	$C_{30}H_{42}N_3Y$	
Formula weight	533.58	
Density (calculated)	1.290 Mg/m^3	
Absorption coefficient	2.144 mm^{-1}	
F(000)	1128	

Data collection:

Diffractometer type	IPDS1
Wavelength	0.71073 Å
Temperature	193(2) K
Theta range for data collection	1.71 to 25.99°
Index ranges	-12<=h<=12, -29<=k<=28, -13<=l<=12
Data collection software	STOE WinXpose (X-Area)
Cell refinement software	STOE WinCell (X-Area)
Data reduction software	STOE WinIntegrate (X-Area)

Solution and refinement:

Reflections collected	18697
Independent reflections	10212 [R(int)= 0.0548]
Completeness to theta = 25.00°	99.3%
Observed reflections	7027 [I > 2sigma(I)]
Reflections used for refinement	10212
Extinction coefficient	X = 0.00019(2)
Absorption correction	None
Flack parameter (absolute struct.)	-0.028(6)
Largest diff. peak and hole	0.584 and -0.589 e.Å^{-3}
Solution	Direct methods
Refinement	Full-matrix least-squares on F^2
Treatment of hydrogen atoms	Calculated, riding model
Programs used	SIR2004 (Giacovazzo, 2004) SHELXL-97 (Sheldrick, 1997) Diamond 3.1, STOE IPDS1 software
Data / restraints / parameters	10212 / 1 / 632
Goodness-of-fit on F^2	0.848
R index (all data)	wR2 = 0.0746
R index conventional [I > 2sigma(I)]	R1 = 0.0417

Table 12. Atomic coordinates and equivalent isotropic displacement parameters ($Å^2$)for oth28. U(eq)is defined as one third of the trace of the orthogonalized U^{ij} tensor.

	x	y	z	U(eq)	Occupancy
C1	0.7150(7)	-0.0732(3)	0.2285(7)	0.0323(19)	1
C2	0.8023(9)	-0.1144(4)	0.1643(7)	0.036(2)	1
C3	0.9178(8)	-0.0948(3)	0.1136(7)	0.029(2)	1
C4	0.9953(9)	-0.1354(3)	0.0623(8)	0.040(2)	1
C5	0.9672(11)	-0.1924(4)	0.0658(7)	0.048(3)	1
C6	0.8573(11)	-0.2112(4)	0.1155(8)	0.064(3)	1
C7	0.7781(9)	-0.1719(4)	0.1655(9)	0.055(3)	1
C8	0.5876(7)	-0.0966(3)	0.2692(8)	0.054(2)	1
C9	0.6348(9)	0.0227(4)	0.2155(9)	0.046(3)	1
C10	0.6305(9)	-0.0337(4)	0.0398(8)	0.054(3)	1
C11	1.0676(9)	-0.0158(3)	0.3891(7)	0.0270(19)	1
C12	1.0021(8)	0.0419(3)	0.4080(7)	0.028(2)	1
C13	0.9382(9)	0.0629(3)	0.3044(7)	0.031(2)	1
C14	0.8828(9)	0.1175(3)	0.3237(8)	0.039(2)	1
C15	0.8888(9)	0.1462(3)	0.4324(8)	0.037(2)	1
C16	0.9505(9)	0.1208(4)	0.5276(8)	0.039(2)	1
C17	1.0044(8)	0.0681(3)	0.5166(7)	0.035(2)	1
C18	1.1503(10)	-0.0340(4)	0.4962(7)	0.045(2)	1
C19	1.2362(9)	0.0304(4)	0.2696(8)	0.035(2)	1
C20	1.2023(9)	-0.0687(3)	0.2499(9)	0.045(3)	1
C21	0.9931(8)	0.1082(3)	-0.0722(7)	0.037(2)	1
C22	1.1030(9)	0.0714(3)	-0.1041(7)	0.033(2)	1
C23	1.1223(7)	0.0222(3)	-0.0307(7)	0.0264(19)	1
C24	1.2338(9)	-0.0094(3)	-0.0647(7)	0.038(2)	1
C25	1.3124(9)	0.0057(5)	-0.1573(7)	0.042(2)	1
C26	1.2894(9)	0.0523(4)	-0.2225(8)	0.037(2)	1
C27	1.1859(9)	0.0848(4)	-0.1971(7)	0.036(2)	1
C28	1.0294(10)	0.1476(3)	0.0326(8)	0.045(2)	1
C29	0.7673(10)	0.1130(4)	-0.0215(9)	0.058(3)	1
C30	0.8437(10)	0.0427(5)	-0.1586(9)	0.052(3)	1
C31	0.4988(8)	0.1706(3)	0.5322(7)	0.032(2)	1
C32	0.6060(7)	0.2123(3)	0.5704(7)	0.0269(19)	1
C33	0.6128(9)	0.2631(3)	0.5038(7)	0.038(2)	1
C34	0.7177(8)	0.2952(3)	0.5488(7)	0.035(2)	1
C35	0.8058(8)	0.2821(5)	0.6419(7)	0.037(2)	1
C36	0.7871(10)	0.2316(4)	0.7001(8)	0.043(3)	1
C37	0.6858(8)	0.1962(3)	0.6637(7)	0.0334(19)	1
C38	0.5389(10)	0.1358(3)	0.4247(7)	0.042(2)	1
C39	0.3399(11)	0.2312(5)	0.6189(9)	0.053(3)	1
C40	0.2721(9)	0.1644(4)	0.4773(9)	0.052(3)	1
C41	0.1664(6)	0.3572(3)	0.3584(10)	0.055(2)	1
C42	0.2732(10)	0.3999(4)	0.3826(9)	0.042(2)	1
C43	0.4038(9)	0.3792(4)	0.3912(8)	0.034(2)	1
C44	0.4908(9)	0.4224(4)	0.4248(8)	0.043(2)	1
C45	0.4571(12)	0.4780(4)	0.4442(7)	0.050(2)	1
C46	0.3316(9)	0.4935(3)	0.4318(8)	0.048(2)	1
C47	0.2405(9)	0.4544(4)	0.4024(9)	0.050(2)	1
C48	0.1119(10)	0.3355(5)	0.4798(10)	0.073(3)	1
C49	0.1179(9)	0.2644(4)	0.2689(10)	0.062(3)	1
C50	0.2446(8)	0.3338(4)	0.1722(9)	0.066(3)	1
C51	0.5699(9)	0.2992(3)	0.0804(7)	0.034(2)	1
C52	0.5023(8)	0.2436(4)	0.0673(8)	0.034(2)	1
C53	0.4346(8)	0.2212(3)	0.1678(7)	0.0306(19)	1
C54	0.3757(9)	0.1686(4)	0.1435(7)	0.035(2)	1
C55	0.3845(9)	0.1416(4)	0.0351(8)	0.040(2)	1
C56	0.4493(9)	0.1631(4)	-0.0588(8)	0.043(2)	1
C57	0.5077(9)	0.2154(4)	-0.0409(8)	0.041(2)	1

C58	0.6572(10)	0.3166(4)	-0.0204(9)	0.058(3)	1
C59	0.7326(9)	0.2560(4)	0.2142(8)	0.039(2)	1
C60	0.6924(11)	0.3550(4)	0.2327(9)	0.054(3)	1
N1	0.7056(6)	-0.0211(3)	0.1508(6)	0.0344(16)	1
N2	1.1362(7)	-0.0150(3)	0.2710(5)	0.0264(16)	1
N3	0.8763(7)	0.0739(3)	-0.0454(6)	0.0371(18)	1
N4	0.3782(7)	0.2041(3)	0.5059(6)	0.0348(17)	1
N5	0.2143(7)	0.3082(3)	0.2965(7)	0.050(2)	1
N6	0.6321(7)	0.2993(3)	0.2034(7)	0.0345(18)	1
Y1	0.95246(9)	0.00611(2)	0.12015(7)	0.02809(18)	1
Y2	0.44875(9)	0.27927(2)	0.35174(7)	0.02783(18)	1

T. Linder (Chemistry Department, University of Marburg)

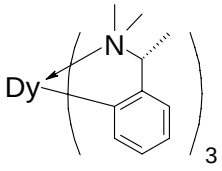

Table 13. Crystal data and structure refinement for [Dy(tmba)$_3$] (**H9**).

Crystal data:

Identification code	oth31	
Habitus, color	plate, yellow	
Crystal size	0.18 x 0.09 x 0.03 mm^3	
Crystal system	Orthorhombic	
Space group	P $2_12_12_1$	Z = 4
Unit cell dimensions	a = 9.1297(16) Å	α= 90°
	b = 22.055(6) Å	β= 90°
	c = 27.588(6) Å	γ = 90°
Volume	5555(2) Å^3	
Cell determination	1300 peaks with Theta 3.8 to 26.3°	
Empirical formula	$C_{30}H_{42}DyN_3$	
Formula weight	607.16	
Density (calculated)	1.452 Mg/m^3	
Absorption coefficient	2.712 mm^{-1}	
F(000)	2472	

Data collection:

Diffractometer type	IPDS2
Wavelength	0.71069 Å
Temperature	173(2) K
Theta range for data collection	1.18 to 25.98°
Index ranges	-11<=h<=11, -27<=k<=27, -31<=l<=33
Data collection software	STOE WinXpose (X-Area)
Cell refinement software	STOE WinCell (X-Area)
Data reduction software	STOE WinIntegrate (X-Area)

Solution and refinement:

Reflections collected	33898
Independent reflections	9998 [R(int)= 0.0837]
Completeness to theta = 25.00°	92.8%
Observed reflections	6660 [I > 2sigma(I)]
Reflections used for refinement	9998
Extinction coefficient	X = 0.00019(2)
Absorption correction	Semi-empirical from equivalents
Max. and min. transmission	0.8205 and 0.7068
Flack parameter (absolute struct.)	0.011(14)
Largest diff. peak and hole	0.776 and -0.902 e.Å^{-3}
Solution	direct/ difmap
Refinement	Full-matrix least-squares on F^2
Treatment of hydrogen atoms	geom., mixed
Programs used	SIR97 (Giacovazzo, 1997)
	SHELXL-97 (Sheldrick, 1997)
	Diamond 3.1, STOE IPDS2 software
Data / restraints / parameters	9998 / 0 / 613
Goodness-of-fit on F^2	0.727
R index (all data)	wR2 = 0.0702
R index conventional [I > 2sigma(I)]	R1 = 0.0372

Table 14. Atomic coordinates and equivalent isotropic displacement parameters ($Å^2$)for OTH31. U(eq)is defined as one third of the trace of the orthogonalized U^{ij} tensor.

	x	y	z	U(eq)	Occupancy
C00	1.1128(9)	0.7040(3)	0.8543(3)	0.0295(19)	1
C01	1.2619(9)	0.7179(3)	0.8489(3)	0.038(2)	1
C02	1.3145(9)	0.7702(3)	0.8264(3)	0.041(2)	1
C03	1.2163(9)	0.8122(3)	0.8075(3)	0.040(2)	1
C04	1.0680(8)	0.8009(3)	0.8126(3)	0.038(2)	1
C05	1.0213(10)	0.7485(3)	0.8364(3)	0.0322(17)	1
C06	0.8565(9)	0.7414(3)	0.8457(3)	0.0317(19)	1
C07	0.8166(8)	0.7666(3)	0.8954(3)	0.0371(19)	1
C08	0.8315(10)	0.6605(4)	0.7887(3)	0.042(2)	1
C09	0.6528(9)	0.6684(4)	0.8522(3)	0.044(2)	1
C10	0.8432(11)	0.5292(5)	0.8540(4)	0.041(3)	1
C11	0.7097(9)	0.5054(4)	0.8707(4)	0.048(3)	1
C12	0.7190(13)	0.4211(4)	0.8159(4)	0.066(3)	1
C13	0.6479(12)	0.4527(4)	0.8520(4)	0.062(3)	1
C14	0.8521(13)	0.4425(4)	0.7968(4)	0.064(3)	1
C15	0.9106(11)	0.4952(4)	0.8159(4)	0.052(3)	1
C16	1.0547(10)	0.5210(4)	0.7969(4)	0.053(3)	1
C17	1.1262(14)	0.4854(5)	0.7549(4)	0.080(4)	1
C18	1.2917(11)	0.5642(4)	0.8229(4)	0.063(3)	1
C19	1.1958(10)	0.4769(4)	0.8630(4)	0.056(3)	1
C20	0.8580(8)	0.6256(4)	0.9654(3)	0.038(2)	1
C21	0.7059(9)	0.6245(4)	0.9773(3)	0.043(2)	1
C22	0.6497(10)	0.6376(4)	1.0230(4)	0.048(2)	1
C23	0.7436(10)	0.6525(3)	1.0606(4)	0.049(2)	1
C24	0.8947(9)	0.6527(3)	1.0519(3)	0.040(2)	1
C25	0.9493(8)	0.6385(3)	1.0065(4)	0.034(2)	1
C26	1.1136(9)	0.6408(4)	0.9989(4)	0.038(2)	1
C27	1.1634(10)	0.7047(4)	0.9850(3)	0.048(2)	1
C28	1.1217(9)	0.5331(3)	0.9828(3)	0.044(2)	1
C29	1.3192(9)	0.5959(4)	0.9546(4)	0.055(3)	1
C30	0.3950(9)	0.5288(3)	0.6316(3)	0.0364(19)	1
C31	0.2530(9)	0.5062(4)	0.6199(3)	0.038(2)	1
C32	0.2059(9)	0.4485(3)	0.6325(3)	0.043(2)	1
C33	0.2973(9)	0.4099(3)	0.6585(3)	0.043(2)	1
C34	0.4382(9)	0.4301(3)	0.6691(3)	0.045(2)	1
C35	0.4825(10)	0.4877(3)	0.6570(3)	0.0346(17)	1
C36	0.6370(9)	0.5073(3)	0.6718(4)	0.044(2)	1
C37	0.6337(10)	0.5419(4)	0.7192(4)	0.057(3)	1
C38	0.7321(10)	0.5011(4)	0.5906(4)	0.058(3)	1
C39	0.8510(9)	0.5672(4)	0.6471(4)	0.058(3)	1
C40	0.6199(9)	0.7020(4)	0.6571(3)	0.035(2)	1
C41	0.7664(9)	0.7234(3)	0.6616(3)	0.040(2)	1
C42	0.8055(10)	0.7736(3)	0.6888(3)	0.044(2)	1
C43	0.7028(10)	0.8049(3)	0.7146(3)	0.045(2)	1
C44	0.5583(8)	0.7846(3)	0.7141(3)	0.0377(19)	1
C45	0.5209(9)	0.7347(3)	0.6857(3)	0.0356(18)	1
C46	0.3597(9)	0.7138(3)	0.6868(3)	0.0336(19)	1
C47	0.3362(9)	0.6640(4)	0.7238(3)	0.049(2)	1
C48	0.3089(10)	0.7484(3)	0.6062(4)	0.055(3)	1
C49	0.1640(8)	0.6663(4)	0.6378(4)	0.048(2)	1
C50	0.3806(9)	0.6241(4)	0.5242(3)	0.041(2)	1
C51	0.2281(9)	0.6138(3)	0.5143(3)	0.042(2)	1
C52	0.1637(9)	0.6194(4)	0.4689(3)	0.046(2)	1
C53	0.2446(10)	0.6370(4)	0.4298(4)	0.051(2)	1
C54	0.3949(10)	0.6471(3)	0.4357(3)	0.047(2)	1
C55	0.4582(9)	0.6389(3)	0.4814(3)	0.039(2)	1
C56	0.6262(9)	0.6396(4)	0.4841(4)	0.046(2)	1

C57	0.6840(9)	0.5773(4)	0.4723(4)	0.062(3)	1
C58	0.6338(10)	0.7280(3)	0.5356(3)	0.049(2)	1
C59	0.8367(9)	0.6605(4)	0.5356(4)	0.057(3)	1
N1	0.8136(7)	0.6776(3)	0.8404(3)	0.0341(16)	1
N2	1.1539(9)	0.5337(4)	0.8387(3)	0.041(2)	1
N3	1.1574(7)	0.5940(3)	0.9621(3)	0.0403(19)	1
N4	0.7067(7)	0.5433(3)	0.6316(3)	0.0413(19)	1
N5	0.3162(7)	0.6938(3)	0.6378(3)	0.0357(18)	1
N6	0.6744(7)	0.6635(3)	0.5326(3)	0.0439(19)	1
Dy1	0.98958(5)	0.61146(1)	0.88883(1)	0.03269(9)	1
Dy2	0.51202(5)	0.62232(1)	0.60298(1)	0.03460(9)	1

Dr. Klaus Harms (Chemistry Department, University of Marburg)

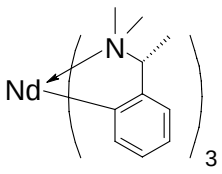

Table 15. Crystal data and structure refinement for $[Nd(tmba)_3]$ (**H10)**.

Crystal data:

Identification code	apndar3	
Habitus, color	prism, green	
Crystal size	0.27 x 0.27 x 0.17 mm^3	
Crystal system	Orthorhombic	
Space group	$P\ 2_12_12_1$	Z = 4
Unit cell dimensions	a = 10.4845(9) Å	α= 90°
	b = 11.2139(10) Å	β= 90°
	c = 23.7959(17) Å	γ = 90°
Volume	2797.7(4) $Å^3$	
Cell determination	8000 peaks with Theta 2 to 25°	
Empirical formula	$C_{30}H_{42}N_3Nd$	
Formula weight	588.91	
Density (calculated)	1.398 Mg/m^3	
Absorption coefficient	1.877 mm^{-1}	
F(000)	1212	

Data collection:

Diffractometer type	IPDS1
Wavelength	0.71073 Å
Temperature	193(2) K
Theta range for data collection	2.01 to 25.49°
Index ranges	-12<=h<=12, -13<=k<=13, -28<=l<=26
Data collection software	STOE Expose
Cell refinement software	STOE Cell
Data reduction software	STOE Integrate

Solution and refinement:

Reflections collected	16292
Independent reflections	5150 [R(int) = 0.0315]
Completeness to theta = 25.00°	99.9 %
Observed reflections	4755[I > 2sigma(I)]
Reflections used for refinement	5150
Absorption correction	Gaussian
Max. and min. transmission	0.7876 and 0.6745
Flack parameter (absolute struct.)	-0.017(18)
Largest diff. peak and hole	1.070 and -0.952 $e.Å^{-3}$
Solution	Direct methods
Refinement	Full-matrix least-squares on F^2
Treatment of hydrogen atoms	Calculated, riding model
Programs used	SIR92 (Giacovazzo et al, 1993)
	SHELXL-97 (Sheldrick, 1997)
	Diamond 2.1, STOE IPDS1 software
Data / restraints / parameters	5150 / 76 / 311
Goodness-of-fit on F^2	1.002
R index (all data)	wR2 = 0.0699
R index conventional [I > 2sigma(I)]	R1 = 0.0291

Table 16. Atomic coordinates and equivalent isotropic displacement parameters (Å^2) for apndar3. U(eq) is defined as one third of the trace of the orthogonalized U^{ij} tensor.

	x	y	z	U(eq)	Occupancy
C1	0.7481(5)	1.0514(5)	0.9703(2)	0.0410(12)	1
C2	0.6407(4)	1.0866(5)	0.9303(2)	0.0327(10)	1
C3	0.6246(5)	1.0205(4)	0.8801(2)	0.0328(10)	1
C4	0.5209(5)	1.0573(5)	0.8481(2)	0.0412(13)	1
C5	0.4385(5)	1.1497(5)	0.8623(3)	0.0442(11)	1
C6	0.4570(5)	1.2105(5)	0.9115(3)	0.0406(12)	1
C7	0.5608(5)	1.1800(5)	0.9457(2)	0.0372(11)	1
C8	0.7117(6)	0.9436(5)	1.0048(2)	0.0486(13)	1
C9	0.9014(6)	1.1439(7)	0.9080(3)	0.0633(16)	1
C10	0.9729(6)	0.9993(7)	0.9768(3)	0.064(2)	1
C11	0.6724(4)	0.5941(4)	0.8430(2)	0.0342(11)	1
C12	0.7391(4)	0.5769(4)	0.8993(2)	0.0283(10)	1
C13	0.8081(5)	0.6730(4)	0.9207(2)	0.0332(10)	1
C14	0.8656(5)	0.6537(5)	0.9734(2)	0.0402(12)	1
C15	0.8579(5)	0.5463(5)	1.0024(2)	0.0420(12)	1
C16	0.7916(5)	0.4534(4)	0.9785(2)	0.0398(11)	1
C17	0.7331(4)	0.4676(4)	0.9268(2)	0.0351(11)	1
C18	0.5889(6)	0.4916(6)	0.8243(3)	0.0549(16)	1
C19	0.5108(5)	0.7191(5)	0.8878(3)	0.0426(13)	1
C20	0.5487(3)	0.7393(3)	0.78900(16)	0.0452(14)	1
C22	0.9628(3)	0.8260(3)	0.73905(16)	0.0365(19)	0.604(5)
C23	0.8432(3)	0.8673(3)	0.75515(16)	0.027(2)	0.604(5)
C24	0.7635(3)	0.9209(3)	0.71585(16)	0.0419(12)	1
C25	0.8000(7)	0.9331(5)	0.6599(2)	0.0517(13)	1
C26	0.9204(7)	0.8966(6)	0.6448(4)	0.045(3)	0.604(5)
C27	1.0000(7)	0.8430(6)	0.6841(4)	0.051(3)	0.604(5)
C28	1.1789(7)	0.7343(6)	0.7622(4)	0.059(3)	0.604(5)
C29	1.1218(6)	0.7704(6)	0.8788(3)	0.0617(18)	1
C30	1.12113(2)	0.95600(2)	0.83959(1)	0.075(4)	0.604(5)
N1	0.86704(2)	1.03086(2)	0.93673(1)	0.0421(11)	1
N2	0.60826(2)	0.71271(2)	0.84359(1)	0.0314(9)	1
Nd1	0.79827(2)	0.86396(2)	0.86212(1)	0.02665(7)	1
N3	1.05022(2)	0.83160(2)	0.83385(1)	0.040(2)	0.604(5)
N3A	1.03111(2)	0.77073(2)	0.82627(1)	0.040(2)	0.396(5)
C21	1.04750(2)	0.76894(2)	0.78205(1)	0.036(2)	0.604(5)
C21A	1.0825(11)	0.8574(11)	0.7882(5)	0.054(3)	0.396(5)
C22A	0.9792(14)	0.8833(12)	0.7404(6)	0.0365(19)	0.396(5)
C23A	0.8473(13)	0.8980(17)	0.7632(6)	0.027(2)	0.396(5)
C26A	0.9336(19)	0.9363(18)	0.6447(9)	0.045(3)	0.396(5)
C27A	1.0187(19)	0.9007(16)	0.6854(8)	0.051(3)	0.396(5)
C28A	1.1285(19)	0.974(2)	0.8070(10)	0.075(4)	0.396(5)
C30A	1.0021(17)	0.6414(9)	0.8037(9)	0.110(9)	0.396(5)

Dr. Klaus Harms (Chemistry Department, University of Marburg)

Table 17. Crystal data and structure refinement for aryllithium reagent $[Li_2(cuda)_2(Et_2O)_{0.68}(dme)_{0.32}]$ **R4**.

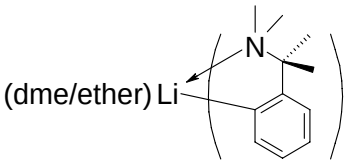

Crystal data

Identification code	apcear_2	
Habitus, color	prism, colorless	
Crystal size	0.30 x 0.24 x 0.21 mm^3	
Crystal system	Monoclinic	
Space group	P $2_1/c$	Z = 4
Unit cell dimensions	a = 9.5086(7) Å	α= 90°
	b = 17.2830(19) Å	β= 102.409(9)°
	c = 16.2434(12) Å	γ = 90°
Volume	2607.0(4) $Å^3$	
Cell determination	6428 peaks with Theta 1.8 to 25.5°	
Empirical formula	$C_{26}\ H_{42}\ Li_2\ N_2\ O_{1.32}$	
Formula weight	417.62	
Density (calculated)	1.064 Mg/m^3	
Absorption coefficient	0.063 mm^{-1}	
F(000)	914	

Data collection:

Diffractometer type	IPDS1
Wavelength	0.71073 Å
Temperature	193(2) K
Theta range for data collection	1.74 to 25.00°
Index ranges	-10<=h<=11, -20<=k<=20, -18<=l<=17
Data collection software	STOE Expose
Cell refinement software	STOE Cell
Data reduction software	STOE Integrate

Solution and refinement:

Reflections collected	15880
Independent reflections	4341 [R(int) = 0.0538]
Completeness to theta = 25.00°	94.2%
Observed reflections	2379[I > 2sigma(I)]
Reflections used for refinement	4341
Absorption correction	None
Largest diff. peak and hole	0.155 and -0.121 e.$Å^{-3}$
Solution	Direct methods
Refinement	Full-matrix least-squares on F^2
Treatment of hydrogen atoms	Calculated, riding model
Programs used	SIR2004 (Giacovazzo et al, 2004) SHELXL-97 (Sheldrick, 1997) Diamond 3.1, STOE IPDS1 software
Data / restraints / parameters	4341 / 0 / 325
Goodness-of-fit on F^2	0.799
R index (all data)	wR2 = 0.0840
R index conventional [I > 2sigma(I)]	R1 = 0.0377

Table 18. Atomic coordinates and equivalent isotropic displacement parameters ($Å^2$) for **R4**. U(eq) is defined as one third of the trace of the orthogonalized U^{ij} tensor.

	x	y	z	U(eq)	Occupancy
C1	0.84326(17)	0.01874(9)	0.30303(12)	0.0371(4)	1
C2	0.98353(17)	0.06646(9)	0.31646(11)	0.0342(4)	1
C3	0.98671(17)	0.13188(9)	0.26386(11)	0.0363(4)	1
C4	1.12049(18)	0.17008(10)	0.27869(12)	0.0415(4)	1
C5	1.24185(18)	0.14666(11)	0.33678(13)	0.0460(5)	1
C6	1.23390(19)	0.08261(11)	0.38528(13)	0.0472(5)	1
C7	1.10465(18)	0.04293(10)	0.37572(12)	0.0420(5)	1
C8	0.82320(18)	-0.02207(10)	0.21790(13)	0.0449(5)	1
C9	0.8453(2)	-0.04378(11)	0.37055(14)	0.0560(6)	1
C10	0.7275(2)	0.11116(12)	0.38253(14)	0.0598(6)	1
C11	0.57682(19)	0.04206(11)	0.26872(16)	0.0612(6)	1
C12	0.66059(17)	0.29788(9)	0.12470(12)	0.0349(4)	1
C13	0.61391(16)	0.22993(9)	0.06328(11)	0.0304(4)	1
C14	0.69142(16)	0.15922(9)	0.08031(11)	0.0340(4)	1
C15	0.63820(18)	0.09984(9)	0.02306(12)	0.0384(4)	1
C16	0.52236(18)	0.10701(10)	-0.04479(12)	0.0433(5)	1
C17	0.45284(18)	0.17668(10)	-0.05922(12)	0.0434(5)	1
C18	0.49872(18)	0.23791(10)	-0.00493(12)	0.0387(4)	1
C19	0.81886(18)	0.31709(10)	0.12682(13)	0.0445(5)	1
C20	0.5737(2)	0.37219(10)	0.09879(14)	0.0500(5)	1
C21	0.7124(2)	0.32254(11)	0.28033(14)	0.0605(6)	1
C22	0.49977(19)	0.25466(11)	0.21553(14)	0.0513(5)	1
C23	1.0146(11)	0.1835(4)	-0.0159(7)	0.065(2)	0.678(4)
C24	1.1070(3)	0.25824(15)	0.0143(2)	0.1069(11)	1
C25	1.1770(4)	0.0901(2)	0.0641(3)	0.0658(13)	0.678(4)
C23A	1.014(3)	0.1515(9)	-0.0298(17)	0.068(5)	0.322(4)
C25A	1.1129(10)	0.0905(5)	0.0110(6)	0.062(2)	0.322(4)
C26	1.1792(2)	0.02214(13)	0.12774(17)	0.0768(7)	1
N1	0.64940(14)	0.26984(8)	0.21078(9)	0.0375(4)	1
N2	0.72135(14)	0.07526(8)	0.29998(10)	0.0394(4)	1
O1	1.04062(19)	0.12727(12)	0.05211(13)	0.0464(8)	0.678(4)
O2A	1.0698(4)	0.0665(2)	0.0853(3)	0.0459(16)	0.322(4)
O1A	1.0063(6)	0.2120(3)	0.0288(4)	0.0529(18)	0.322(4)
Li1	0.7600(3)	0.16266(16)	0.21898(19)	0.0397(7)	1
Li2	0.9199(3)	0.13803(18)	0.1269(2)	0.0492(8)	1

Dr. K. Harms (Chemistry Department, University of Marburg)

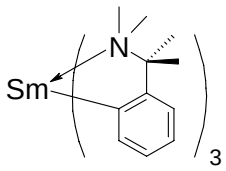

Table 19. Crystal data and structure refinement for [Sm(cuba)$_3$] (**H12**).

Crystal data:

Identification code	apsm1	
Habitus, color	cube, yellow	
Crystal size	0.27 x 0.06 x 0.01 mm^3	
Crystal system	Monoclinic	
Space group	P 2$_1$/c	Z = 4
Unit cell dimensions	a = 15.2069(10) Å	α = 90°
	b = 11.7296(6) Å	β = 90.816(6)°
	c = 17.1648(12) Å	γ = 90°
Volume	3061.4(3) Å^3	
Cell determination	15346 peaks with Theta 1.3 to 26.1°	
Empirical formula	$C_{33}H_{48}N_3Sm$	
Formula weight	637.09	
Density (calculated)	1.382 Mg/m^3	
Absorption coefficient	1.943 mm^{-1}	
F(000)	1316	

Data collection:

Diffractometer type	IPDS2
Wavelength	0.71073 Å
Temperature	173(2) K
Theta range for data collection	1.34 to 25.00°
Index ranges	-18<=h<=18, -13<=k<=13, -20<=l<=20
Data collection software	STOE WinXpose (X-Area)
Cell refinement software	STOE WinCell (X-Area)
Data reduction software	STOE WinIntegrate (X-Area)

Solution and refinement:

Reflections collected	38844
Independent reflections	5388 [R(int)= 0.1007]
Completeness to theta = 25.00°	100.0%
Observed reflections	3521 [I > 2sigma(I)]
Reflections used for refinement	5388
Extinction coefficient	X = 0.00019(2)
Absorption correction	Gaussian
Max. and min. transmission	0.9588 and 0.7367
Largest diff. peak and hole	0.492 and -0.649 e.Å^{-3}
Solution	Direct methods
Refinement	Full-matrix least-squares on F^2
Treatment of hydrogen atoms	Calculated positions, riding model
Programs used	SIR92 (Giacovazzo, 1993) SHELXL-97 (Sheldrick, 1997) Diamond 3.1, STOE IPDS2 software
Data / restraints / parameters	5388 / 0 / 346
Goodness-of-fit on F^2	0.818
R index (all data)	wR2 = 0.0522
R index conventional [I > 2sigma(I)]	R1 = 0.0332

Table 20. Atomic coordinates and equivalent isotropic displacement parameters ($Å^2$)for apsm1. U(eq)is defined as one third of the trace of the orthogonalized U^{ij} tensor.

	x	y	z	U(eq)	Occupancy
C1	0.2459(3)	-0.0355(4)	0.0127(3)	0.0394(11)	1
C2	0.2383(3)	-0.1192(4)	0.0811(2)	0.0364(10)	1
C3	0.2328(3)	-0.0750(4)	0.1575(2)	0.0378(11)	1
C4	0.2270(3)	-0.1594(4)	0.2160(3)	0.0406(13)	1
C5	0.2302(3)	-0.2754(4)	0.2023(3)	0.0431(13)	1
C6	0.2389(3)	-0.3134(4)	0.1281(3)	0.0476(13)	1
C7	0.2413(3)	-0.2365(4)	0.0669(3)	0.0452(13)	1
C8	0.2155(3)	0.1675(4)	-0.0225(2)	0.0437(12)	1
C9	0.1031(3)	0.0554(4)	0.0363(3)	0.0480(14)	1
C10	0.3439(3)	-0.0085(4)	0.0006(3)	0.0519(13)	1
C11	0.2097(4)	-0.0872(4)	-0.0643(3)	0.0584(15)	1
C12	0.4649(3)	0.1064(4)	0.2260(3)	0.0429(13)	1
C13	0.4595(3)	0.1947(4)	0.1608(3)	0.0411(11)	1
C14	0.3768(3)	0.2376(4)	0.1346(3)	0.0392(11)	1
C15	0.3821(3)	0.3170(4)	0.0732(3)	0.0451(12)	1
C16	0.4589(3)	0.3507(5)	0.0378(3)	0.0504(13)	1
C17	0.5366(4)	0.3037(4)	0.0631(3)	0.0540(14)	1
C18	0.5377(4)	0.2280(4)	0.1245(3)	0.0528(14)	1
C19	0.3804(4)	0.2232(4)	0.3194(3)	0.0462(13)	1
C20	0.3725(4)	0.0204(4)	0.3295(3)	0.0499(15)	1
C21	0.5481(3)	0.1229(6)	0.2782(3)	0.0665(15)	1
C22	0.4680(4)	-0.0138(4)	0.1905(3)	0.0582(15)	1
C23	0.0583(3)	0.3120(4)	0.2342(2)	0.0343(11)	1
C24	0.0734(3)	0.2284(4)	0.3019(2)	0.0336(10)	1
C25	0.1419(3)	0.1477(4)	0.2995(2)	0.0330(10)	1
C26	0.1415(3)	0.0679(4)	0.3614(3)	0.0384(12)	1
C27	0.0806(3)	0.0686(4)	0.4216(3)	0.0404(12)	1
C28	0.0155(3)	0.1508(4)	0.4216(2)	0.0416(12)	1
C29	0.0117(3)	0.2296(4)	0.3618(2)	0.0396(11)	1
C30	0.1309(3)	0.3796(4)	0.1130(2)	0.0433(11)	1
C31	0.2084(3)	0.3896(4)	0.2346(2)	0.0372(11)	1
C32	-0.0131(3)	0.2594(4)	0.1813(3)	0.0451(12)	1
C33	0.0255(3)	0.4299(4)	0.2621(3)	0.0437(12)	1
N1	0.1994(2)	0.0740(3)	0.0337(2)	0.0381(9)	1
N2	0.3813(2)	0.1159(3)	0.2736(2)	0.0387(9)	1
N3	0.1434(2)	0.3220(3)	0.18934(18)	0.0327(9)	1
Sm1	0.24201(2)	0.13384(2)	0.18200(1)	0.03197(7)	1

Dr. B. Ziemer (Chemical Department, Humboldt-University Berlin)

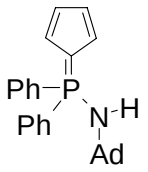

Table 21. Crystal data and structure refinement for $Ph_2P(C_5H_4)NHAd$ (**L3**).

Crystal data:

Identification code	ruf10	
Habitus, color	prism, pale yellow	
Crystal size	0.32 x 0.28 x 0.24 mm^3	
Crystal system	Monoclinic	
Space group	P $2_1/c$	Z = 4
Unit cell dimensions	a = 11.4180(16) Å	α = 90°
	b = 9.7728(13) Å	β = 99.072(18)°
	c = 19.444(3) Å	γ = 90°
Volume	2142.5(5) $Å^3$	
Cell determination	8000 peaks with Theta 2.3 to 25.0	
Empirical formula	$C_{27}H_{30}NP$	
Formula weight	399.49	
Density (calculated)	1.238 Mg/m^3	
Absorption coefficient	0.142 mm^{-1}	
F(000)	856	

Data collection:

Diffractometer type	IPDS2.87
Wavelength	0.71073 Å
Temperature	180(2) K
Theta range for data collection	2.56 to 25.25°
Index ranges	-13<=h<=13, -11<=k<=11, -23<=l<=23
Data Collection Software	IPDS2.87 (Stoe & Cie, 1997)
Cell Refinement Software	IPDS2.87 (Stoe & Cie, 1997)
Data Reduction Software	IPDS2.87 (Stoe & Cie, 1997)

Solution and Refinement:

Reflections collected	13689
Independent reflections	3872 [R(int)= 0.0571]
Completeness to theta = 25.25°	99.9%
Observed reflections	2567 [I > 2sigma(I)]
Reflections used for refinement	3872
Extinction coefficient	0.0045(4)
Absorption correction	None
Max. and min. transmission	0.9668 and 0.9561
Largest diff. peak and hole	0.291 and -0.324 e.$Å^{-3}$
Solution	direct
Refinement	Full-matrix least-squares on F^2
Programs used	SHELXS-97 (Sheldrick, 1990)
	SHELXL-97 (Sheldrick, 1997)
	Diamond 3.1
Data / restraints / parameters	3872 / 0 / 383
Goodness-of-fit on F^2	0.861
R index (all data)	wR2 = 0.0699
R index conventional [I > 2sigma(I)]	R1 = 0.0343

Table 22. Atomic coordinates (x 10^4)and equivalent isotropic displacement parameters ($Å^2$x 10^3)for ruf10. U(eq)is defined as one third of the trace of the orthogonalized U^{ij} tensor.

	x	y	z	U(eq)	Occupancy
C1	5757(1)	7886(2)	8956(1)	20(1)	1
C2	5279(2)	6590(2)	9042(1)	29(1)	1
C3	4442(2)	6058(3)	8512(1)	40(1)	1
C4	4072(2)	6792(3)	7912(1)	41(1)	1
C5	4532(2)	8074(2)	7830(1)	34(1)	1
C6	5371(2)	8631(2)	8350(1)	24(1)	1
C7	7047(2)	10359(2)	9487(1)	19(1)	1
C8	6448(1)	11326(2)	9860(1)	22(1)	1
C9	6568(2)	12603(2)	9566(1)	29(1)	1
C10	7215(2)	12458(2)	9011(1)	28(1)	1
C11	7513(2)	11088(2)	8957(1)	24(1)	1
C12	8283(1)	7744(2)	9437(1)	17(1)	1
C13	9351(2)	8467(2)	9504(1)	20(1)	1
C14	10400(2)	7787(2)	9466(1)	24(1)	1
C15	10394(2)	6397(2)	9333(1)	25(1)	1
C16	9337(2)	5671(2)	9247(1)	23(1)	1
C17	8285(2)	6341(2)	9301(1)	20(1)	1
C18	7401(1)	8096(2)	11035(1)	18(1)	1
C19	8302(2)	9273(2)	11110(1)	23(1)	1
C20	9064(2)	9233(2)	11834(1)	29(1)	1
C21	9721(2)	7871(3)	11941(1)	35(1)	1
C22	8815(2)	6698(2)	11880(1)	30(1)	1
C23	8008(2)	6875(2)	12429(1)	33(1)	1
C24	7356(2)	8244(2)	12321(1)	27(1)	1
C25	6601(2)	8267(2)	11592(1)	22(1)	1
C26	8261(2)	9419(2)	12384(1)	31(1)	1
C27	8070(2)	6735(2)	11148(1)	23(1)	1
N	6616(1)	8092(2)	10344(1)	18(1)	1
P	6937(1)	8602(1)	9587(1)	16(1)	1

Dr. B. Ziemer (Chemical Department, Humboldt-University Berlin)

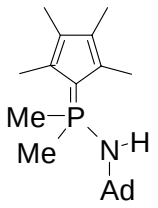

Table 23. Crystal data and structure refinement for $Me_2P(C_5Me4)NHAd$ (**L4**).

Crystal data:

Identification code	ruf12a	
Habitus, color	block, colorless	
Crystal size	0.52 x 0.40 x 0.28 mm^3	
Crystal system	Orthorhombic	
Space group	P $2_12_12_1$	Z = 4
Unit cell dimensions	a = 10.5823(16) Å	α = 90°
	b = 13.135(3) Å	β = 90°
	c = 13.845(2) Å	γ = 90°
Volume	1924.5(6) $Å^3$	
Cell determination	8000 peaks with Theta 2.6 to 25.1	
Empirical formula	$C_{21}H_{34}NP$	
Formula weight	331.46	
Density (calculated)	1.144 Mg/m^3	
Absorption coefficient	0.144 mm^{-1}	
F(000)	728	

Data collection:

Diffractometer type	IPDS2.87
Wavelength	0.71073 Å
Temperature	180(2) K
Theta range for data collection	2.94 to 25.24°
Index ranges	-12<=h<=12, -15<=k<=15, -16<=l<=16
Data Collection Software	IPDS2.87 (Stoe & Cie, 1997)
Cell Refinement Software	IPDS2.87 (Stoe & Cie, 1997)
Data Reduction Software	IPDS2.87 (Stoe & Cie, 1997)

Solution and Refinement:

Reflections collected	12951
Independent reflections	[R(int)= 0.0332]
Completeness to theta = 25.24°	99.1%
Observed reflections	3170 [I > 2sigma(I)]
Reflections used for refinement	3468
Extinction coefficient	0.009(3)
Absorption correction	None
Max. and min. transmission	0.9608 and 0.9289
Largest diff. peak and hole	0.153 and -0.196 e.$Å^3$
Solution	direct
Refinement method	Full-matrix least-squares on F^2
Absolute structure parameter	-0.02(7)
Programs used	SHELXS-97 (Sheldrick, 1990)
	SHELXL-97 (Sheldrick, 1997)
	DIAMOND (Brandenburg, 1999)
Data / restraints / parameters	3468 / 0 / 345
Goodness-of-fit on F^2	0.995
R index (all data)	wR2 = 0.0627
R index [I > 2sigma(I)]	R1 = 0.0270

Table 24. Atomic coordinates (x 10^4)and equivalent isotropic displacement parameters ($Å^2$x 10^3)for ruf12a. U(eq)is defined as one third of the trace of the orthogonalized U^{ij} tensor.

	x	y	z	U(eq)	Occupancy
C1	8084(1)	7571(1)	-640(1)	21(1)	1
C2	8285(1)	8353(1)	-1357(1)	22(1)	1
C3	8726(1)	7880(1)	-2180(1)	23(1)	1
C4	8806(1)	6809(1)	-2005(1)	25(1)	1
C5	8440(1)	6614(1)	-1068(1)	24(1)	1
C6	8084(2)	9480(1)	-1246(2)	36(1)	1
C7	9126(2)	8372(1)	-3113(1)	34(1)	1
C8	9208(2)	6042(2)	-2752(2)	40(1)	1
C9	8414(2)	5584(1)	-588(2)	36(1)	1
C10	6501(2)	6797(2)	951(2)	37(1)	1
C11	6913(2)	8918(2)	799(2)	38(1)	1
C12	9188(1)	7475(1)	2272(1)	22(1)	1
C13	8251(2)	8090(1)	2882(1)	29(1)	1
C14	8572(2)	7974(1)	3962(1)	33(1)	1
C15	9913(2)	8371(2)	4144(1)	40(1)	1
C16	10859(2)	7759(2)	3544(1)	38(1)	1
C17	10526(2)	7884(1)	2467(1)	30(1)	1
C18	9125(2)	6348(1)	2562(1)	30(1)	1
C19	9445(2)	6231(1)	3642(1)	35(1)	1
C20	8489(2)	6849(1)	4233(1)	36(1)	1
C21	10783(2)	6633(2)	3813(2)	41(1)	1
N	8958(1)	7600(1)	1223(1)	26(1)	1
P	7663(1)	7711(1)	555(1)	22(1)	1

T. Linder (Chemistry Department, University of Marburg)

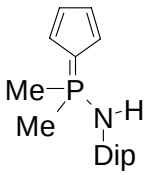

Table 25. Crystal data and structure refinement for $Me_2P(C_5H_4)NHDip$ ¼C_7H_8 (**C5**).

Crystal data:

Identification code	eq51	
Habitus, color	rod, colorless	
Crystal size	0.56 x 0.16 x 0.16 mm^3	
Crystal system	Triclinic	
Space group	P -1	Z = 2
Unit cell dimensions	a = 10.3038(11) Å	α= 101.477(14)°
	b = 17.697(2) Å	β= 100.780(13)°
	c = 23.576(3) Å	γ = 105.486(13)°
Volume	3926.5(8) $Å^3$	
Cell determination	8000 peaks with Theta 1.8 to 26.0°	
Empirical formula	$C_{20.75}H_{30}NP$	
Formula weight	324.43	
Density (calculated)	1.098 Mg/m^3	
Absorption coefficient	0.140 mm^{-1}	
F(000)	1412	

Data collection:

Diffractometer type	IPDS1
Wavelength	0.71069 Å
Temperature	193(2) K
Theta range for data collection	1.72 to 26.10°
Index ranges	-12<=h<=12, -21<=k<=21, -29<=l<=28
Data collection software	STOE WinXpose (X-Area)
Cell refinement software	STOE WinCell (X-Area)
Data reduction software	STOE WinIntegrate (X-Area)

Solution and refinement:

Reflections collected	39332
Independent reflections	14466 [R(int)= 0.0625]
Completeness to theta = 25.00°	94.3%
Observed reflections	7011 [I > 2sigma(I)]
Reflections used for refinement	14466
Absorption correction	Semi-empirical from equivalents
Max. and min. transmission	0.9678 and 0.9547
Largest diff. peak and hole	0.359 and -0.258 e.$Å^{-3}$
Solution	direct/ difmap
Refinement	Full-matrix least-squares on F^2
Treatment of hydrogen atoms	geom.., mixed
Programs used	SIR-97 (Giacovezzo, 1997)
	Diamond 3.1, STOE IPDS1 software
Data / restraints / parameters	14466 / 0 / 836
Goodness-of-fit on F^2	0.760
R index (all data)	wR2 = 0.0944
R index conventional [I > 2sigma(I)]	R1 = 0.0424

Table 26. Atomic coordinates and equivalent isotropic displacement parameters ($Å^2$)for eq51. U(eq)is defined as one third of the trace of the orthogonalized U^{ij} tensor.

	x	y	z	U(eq)	Occupancy
C101	-0.4019(2)	0.12426(15)	0.97199(10)	0.0306(6)	1
C102	-0.5159(3)	0.15490(15)	0.96127(11)	0.0371(6)	1
C103	-0.4971(3)	0.21872(16)	1.01011(13)	0.0466(7)	1
C104	-0.3730(3)	0.22925(17)	1.05146(12)	0.0475(8)	1
C105	-0.3135(3)	0.17235(16)	1.02880(11)	0.0402(6)	1
C106	-0.5484(3)	-0.02379(16)	0.88383(11)	0.0418(7)	1
C107	-0.3023(3)	-0.01250(16)	0.97034(11)	0.0399(6)	1
C108	-0.1628(2)	0.03199(14)	0.87641(9)	0.0268(5)	1
C109	-0.0311(2)	0.07729(14)	0.91400(9)	0.0279(5)	1
C110	0.0777(3)	0.04560(16)	0.91093(10)	0.0363(6)	1
C111	0.0570(3)	-0.02872(16)	0.87191(11)	0.0412(7)	1
C112	-0.0715(3)	-0.07173(16)	0.83467(11)	0.0392(6)	1
C113	-0.1843(3)	-0.04254(15)	0.83541(10)	0.0317(6)	1
C114	-0.0038(3)	0.15934(14)	0.95668(10)	0.0320(6)	1
C115	0.0780(3)	0.16748(17)	1.01973(10)	0.0485(7)	1
C116	0.0700(3)	0.22673(16)	0.93092(12)	0.0486(7)	1
C117	-0.3250(3)	-0.09318(16)	0.79418(10)	0.0391(6)	1
C118	-0.3836(3)	-0.17123(17)	0.81221(13)	0.0603(9)	1
C119	-0.3201(3)	-0.11291(19)	0.72843(11)	0.0542(8)	1
C201	-0.3919(3)	0.20808(15)	0.80598(11)	0.0379(6)	1
C202	-0.5043(3)	0.13712(17)	0.79868(11)	0.0463(7)	1
C203	-0.4894(3)	0.07336(18)	0.75862(12)	0.0554(8)	1
C204	-0.3687(3)	0.10215(18)	0.74084(13)	0.0570(8)	1
C205	-0.3080(3)	0.18370(17)	0.76932(12)	0.0506(7)	1
C206	-0.2416(3)	0.31436(17)	0.92600(11)	0.0451(7)	1
C207	-0.5188(3)	0.30561(18)	0.87147(13)	0.0526(8)	1
C208	-0.1745(3)	0.45027(15)	0.86125(10)	0.0352(6)	1
C209	-0.2048(3)	0.51764(16)	0.89128(10)	0.0425(7)	1
C210	-0.0942(4)	0.58821(18)	0.92061(11)	0.0558(8)	1
C211	0.0406(4)	0.5934(2)	0.92028(13)	0.0619(9)	1
C212	0.0677(3)	0.52742(19)	0.88975(12)	0.0554(8)	1
C213	-0.0358(3)	0.45471(16)	0.85992(11)	0.0405(7)	1
C214	-0.3505(3)	0.51744(18)	0.89380(12)	0.0511(8)	1
C215	-0.3694(4)	0.5216(2)	0.95699(14)	0.0837(12)	1
C216	-0.3889(4)	0.5873(2)	0.87249(14)	0.0698(10)	1
C217	-0.0028(3)	0.38475(18)	0.82397(12)	0.0468(7)	1
C218	0.1448(3)	0.3828(2)	0.84627(15)	0.0707(10)	1
C219	-0.0311(4)	0.3854(2)	0.75772(12)	0.0670(9)	1
C301	0.4355(3)	0.30065(14)	0.67883(10)	0.0322(6)	1
C302	0.3506(3)	0.33109(16)	0.71275(10)	0.0387(6)	1
C303	0.4203(3)	0.41240(16)	0.74097(11)	0.0444(7)	1
C304	0.5476(3)	0.43449(16)	0.72539(10)	0.0447(7)	1
C305	0.5567(3)	0.36697(15)	0.68736(10)	0.0380(6)	1
C306	0.2502(3)	0.19069(16)	0.56712(10)	0.0394(6)	1
C307	0.5383(3)	0.20077(16)	0.60254(12)	0.0472(7)	1
C308	0.2159(3)	0.06079(15)	0.63777(10)	0.0327(6)	1
C309	0.2125(3)	-0.00531(16)	0.59310(11)	0.0463(7)	1
C310	0.0906(3)	-0.07084(19)	0.57186(13)	0.0627(9)	1
C311	-0.0221(3)	-0.0729(2)	0.59434(13)	0.0646(10)	1
C312	-0.0151(3)	-0.00941(19)	0.63999(14)	0.0587(9)	1
C313	0.1029(3)	0.05804(16)	0.66264(12)	0.0454(7)	1
C314	0.3359(3)	-0.01058(18)	0.56763(15)	0.0653(10)	1
C315	0.3873(4)	-0.0782(2)	0.58437(19)	0.0924(13)	1
C316	0.3017(5)	-0.0201(2)	0.49984(17)	0.1023(15)	1
C317	0.1111(4)	0.1241(2)	0.71722(16)	0.0754(11)	1
C318	0.1072(4)	0.0929(3)	0.77205(14)	0.0927(13)	1
C319	-0.0060(6)	0.1588(3)	0.7033(2)	0.140(2)	1

C401	0.3677(2)	0.37722(14)	0.51604(9)	0.0287(6)	1
C402	0.2732(3)	0.32356(15)	0.46217(10)	0.0347(6)	1
C403	0.3370(3)	0.27067(16)	0.43732(11)	0.0392(7)	1
C404	0.4702(3)	0.28880(16)	0.47426(11)	0.0418(7)	1
C405	0.4899(3)	0.35351(15)	0.52273(10)	0.0347(6)	1
C406	0.5109(3)	0.53074(16)	0.59874(11)	0.0399(6)	1
C407	0.2446(3)	0.50425(16)	0.51958(10)	0.0393(6)	1
C408	0.1413(2)	0.45945(14)	0.62330(9)	0.0268(5)	1
C409	0.1582(3)	0.53269(15)	0.66453(10)	0.0341(6)	1
C410	0.0389(3)	0.55259(18)	0.67134(12)	0.0460(7)	1
C411	-0.0909(3)	0.50198(19)	0.63964(12)	0.0499(7)	1
C412	-0.1058(3)	0.42988(18)	0.60032(11)	0.0441(7)	1
C413	0.0089(2)	0.40723(14)	0.59087(10)	0.0309(6)	1
C414	0.2996(3)	0.59108(16)	0.70025(11)	0.0419(7)	1
C415	0.3082(3)	0.61502(18)	0.76709(11)	0.0544(8)	1
C416	0.3365(4)	0.66625(18)	0.67650(13)	0.0646(9)	1
C417	-0.0127(3)	0.32589(15)	0.54828(10)	0.0359(6)	1
C418	-0.0766(3)	0.25744(18)	0.57450(14)	0.0619(9)	1
C419	-0.0992(3)	0.31599(19)	0.48544(11)	0.0541(8)	1
C501	0.0887(3)	0.79879(18)	0.73882(13)	0.0526(8)	1
C502	0.1173(4)	0.77969(19)	0.79273(12)	0.0553(8)	1
C503	0.0209(5)	0.7249(2)	0.80832(16)	0.0720(10)	1
C504	-0.1116(5)	0.6869(2)	0.7690(2)	0.0857(13)	1
C505	-0.1395(4)	0.7066(2)	0.71431(18)	0.0755(10)	1
C506	-0.0407(4)	0.7608(2)	0.70045(14)	0.0612(9)	1
C507	0.1963(4)	0.8601(2)	0.72262(17)	0.0863(11)	1
N1	-0.2789(2)	0.06244(12)	0.88113(8)	0.0263(4)	1
N2	-0.2844(2)	0.37514(12)	0.82927(9)	0.0338(5)	1
N3	0.3371(2)	0.13207(12)	0.66005(9)	0.0340(5)	1
N4	0.2615(2)	0.43688(12)	0.61350(8)	0.0256(4)	1
P1	-0.37964(6)	0.04233(4)	0.92633(3)	0.02843(15)	1
P2	-0.35761(7)	0.30065(4)	0.85610(3)	0.03573(17)	1
P3	0.38989(7)	0.20626(4)	0.62953(3)	0.03028(15)	1
P4	0.34454(6)	0.45799(4)	0.56254(3)	0.02750(15)	1

Dr. B. Ziemer (Chemical Department, Humboldt-University Berlin)

Table 27. Crystal data and structure refinement for $Ph_2P(C_5H_4)NHDip$ (**L6**).

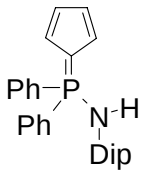

Crystal data:

Identification code	ruf20	
Crystal size	0.32 x 0.28 x 0.16 mm^3	
Crystal system	Monoclinic	
Space group	P $2_1/c$	Z = 4
Unit cell dimensions	a = 9.7757(9) Å	α = 90°
	b = 23.448(2) Å	β = 99.521(10)°
	c = 10.6991(8) Å	γ = 90°
Volume	2418.6(4) $Å^3$	
Cell determination	5000 peaks with Theta 3.0 to 25.0°	
Empirical formula	$C_{29}H_{32}NP$	
Formula weight	425.53	
Density (calculated)	1.169 Mg/m^3	
Absorption coefficient	0.130 mm^{-1}	
F(000)	912	

Data collection:

Diffractometer	IPDS2.87
Wavelength	0.71073 Å
Temperature	180(2) K
Theta range for data collection	2.60 to 25.25°
Index ranges	-11<=h<=6, -28<=k<=28, -12<=l<=12
Data Collection Software	IPDS2.87 (Stoe & Cie, 1997)
Cell Refinement Software	IPDS2.87 (Stoe & Cie, 1997)
Data Reduction Software	IPDS2.87 (Stoe & Cie, 1997)

Solution and Refinement:

Reflections collected	8539
Independent reflections	3726 [R(int)= 0.0541]
Completeness to theta = 25.25°	84.9%
Observed reflections	2735 [I > 2sigma(I)]
Reflections used for refinement	3726
Extinction coefficient	X = 0.0021(10)
Absorption correction	None
Max. and min. transmission	0.9796 and 0.9597
Largest diff. peak and hole	0.247 and -0.234 e.$Å^{-3}$
Solution	direct
Refinement	Full-matrix least-squares on F^2
Programs used	SHELXS-97 (Sheldrick, 1990)
	SHELXL-97 (Sheldrick, 1997)
	DIAMOND (Brandenburg, 1999)
Data / restraints / parameters	3726 / 0 / 361
Goodness-of-fit on F^2	0.901
R index (all data)	wR2 = 0.0790
R index conventional [I > 2sigma(I)]	R1 = 0.0370

Table 28. Atomic coordinates (x 10^4)and equivalent isotropic displacement parameters ($Å^2$x 10^3)for ruf20. U(eq)is defined as one third of the trace of the orthogonalized U^{ij} tensor.

	x	y	z	U(eq)	Occupancy
C1	4389(2)	5800(1)	10205(2)	17(1)	1
C2	3083(2)	5560(1)	9672(2)	22(1)	1
C3	2376(2)	5436(1)	10653(2)	24(1)	1
C4	3229(2)	5595(1)	11802(2)	27(1)	1
C5	4454(2)	5820(1)	11533(2)	22(1)	1
C6	4609(2)	6803(1)	8599(2)	17(1)	1
C7	3302(2)	6934(1)	8848(2)	23(1)	1
C8	2586(3)	7408(1)	8285(2)	32(1)	1
C9	3199(2)	7753(1)	7485(2)	32(1)	1
C10	4507(2)	7632(1)	7249(2)	29(1)	1
C11	5229(2)	7159(1)	7799(2)	23(1)	1
C12	6969(2)	6390(1)	10404(2)	19(1)	1
C13	7339(2)	6964(1)	10622(2)	28(1)	1
C14	8494(3)	7105(1)	11497(2)	41(1)	1
C15	9302(3)	6683(1)	12169(2)	45(1)	1
C16	8949(3)	6115(1)	11959(2)	40(1)	1
C17	7796(2)	5969(1)	11090(2)	29(1)	1
C18	6082(2)	5944(1)	6967(2)	16(1)	1
C19	7458(2)	6038(1)	6822(2)	19(1)	1
C20	7706(2)	6262(1)	5663(2)	24(1)	1
C21	6626(2)	6386(1)	4698(2)	28(1)	1
C22	5273(2)	6272(1)	4844(2)	24(1)	1
C23	4961(2)	6044(1)	5967(2)	18(1)	1
C24	8680(2)	5887(1)	7842(2)	23(1)	1
C25	9601(2)	6402(1)	8283(2)	33(1)	1
C26	9557(2)	5412(1)	7373(2)	32(1)	1
C27	3484(2)	5885(1)	6093(2)	22(1)	1
C28	3250(2)	5246(1)	5828(2)	34(1)	1
C29	2381(2)	6245(1)	5265(2)	33(1)	1
N	5755(2)	5751(1)	8166(1)	16(1)	1
P	5438(1)	6162(1)	9333(1)	14(1)	1

Dr. K. Harms (Chemistry Department, University of Marburg)

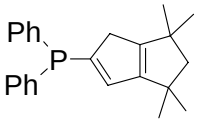

Table 29. Crystal data and structure refinement for compound $Ph_2PCp^{TM}H$ (**P6**)

Crystal data:

Identification code	app1	
Habitus, color	prism, colorless	
Crystal size	0.30 x 0.18 x 0.12 mm^3	
Crystal system	Monoclinic	
Space group	P $2_1/c$	Z = 4
Unit cell dimensions	a = 6.4001(3) Å	α = 90°
	b = 37.8489(13) Å	β = 96.017(6)°
	c = 8.4024(4) Å	γ = 90°
Volume	2024.16(15) $Å^3$	
Cell determination	8000 peaks with Theta 2.1 to 25.9°	
Empirical formula	$C_{24}H_{27}P$	
Formula weight	346.43	
Density (calculated)	1.137 Mg/m^3	
Absorption coefficient	0.139 mm^{-1}	
F(000)	744	

Data collection:

Diffractometer type	IPDS1
Wavelength	0.71073 Å
Temperature	173(2) K
Theta range for data collection	2.50 to 25.93°
Index ranges	-7<=h<=7, -46<=k<=44, -10<=l<=9
Data collection software	STOE WinXpose (X-Area)
Cell refinement software	STOE WinCell (X-Area)
Data reduction software	STOE WinIntegrate (X-Area)

Solution and refinement:

Reflections collected	12322
Independent reflections	3874 [R(int)= 0.0510]
Completeness to theta = 25.00°	98.6%
Observed reflections	2745 [I > 2sigma(I)]
Reflections used for refinement	3874
Absorption correction	Semi-empirical from equivalents
Max. and min. transmission	0.9903 and 0.9509
Largest diff. peak and hole	0.270 and -0.189 e.$Å^{-3}$
Solution	Direct methods
Refinement	Full-matrix least-squares on F^2
Treatment of hydrogen atoms	Mixture of restr. and free refinement
Programs used	SIR2004 (Giacovazzo, 2004)
	SHELXL-97 (Sheldrick, 1997)
	Diamond 3.1, STOE IPDS1 software
Data / restraints / parameters	3874 / 2 / 252
Goodness-of-fit on F^2	0.956
R index (all data)	wR2 = 0.0953
R index conventional [I > 2sigma(I)]	R1 = 0.0379

Table 30. Atomic coordinates and equivalent isotropic displacement parameters ($Å^2$)for app1. U(eq)is defined as one third of the trace of the orthogonalized U^{ij} tensor.

	x	y	z	U(eq)	Occupancy
C1	-0.0493(2)	0.11401(4)	0.60143(17)	0.0327(3)	1
C2	-0.0170(2)	0.11591(4)	0.76234(18)	0.0321(3)	1
C3	0.1304(2)	0.08837(4)	0.82121(17)	0.0318(3)	1
C4	0.2221(2)	0.07486(4)	0.98114(18)	0.0381(4)	1
C5A	0.378(2)	0.0463(4)	0.9295(12)	0.052(2)	0.49(2)
C5B	0.321(2)	0.0396(3)	0.9314(10)	0.0435(19)	0.51(2)
C6	0.3340(2)	0.03968(4)	0.7462(2)	0.0392(4)	1
C7	0.1879(2)	0.06979(4)	0.69813(18)	0.0342(3)	1
C8	0.0806(3)	0.08379(5)	0.54550(19)	0.0378(4)	1
C9	0.0498(3)	0.06362(7)	1.0830(2)	0.0674(6)	1
C10	0.3609(3)	0.10188(6)	1.0737(3)	0.0648(6)	1
C11	0.2395(3)	0.00450(5)	0.6876(3)	0.0626(5)	1
C12	0.5467(3)	0.04413(6)	0.6839(3)	0.0728(7)	1
C13	-0.0888(2)	0.16207(4)	0.33896(17)	0.0328(3)	1
C14	0.1124(2)	0.17374(5)	0.3885(2)	0.0434(4)	1
C15	0.2209(3)	0.19457(5)	0.2896(2)	0.0512(5)	1
C16	0.1293(3)	0.20382(5)	0.1407(2)	0.0502(5)	1
C17	-0.0682(3)	0.19177(5)	0.08771(19)	0.0487(4)	1
C18	-0.1772(3)	0.17081(4)	0.18615(18)	0.0397(4)	1
C19	-0.3395(2)	0.16954(4)	0.59852(18)	0.0338(3)	1
C20	-0.2829(3)	0.20491(4)	0.6013(2)	0.0425(4)	1
C21	-0.3709(3)	0.22861(5)	0.7003(2)	0.0521(5)	1
C22	-0.5162(3)	0.21724(5)	0.7988(2)	0.0497(4)	1
C23	-0.5726(2)	0.18218(5)	0.7987(2)	0.0434(4)	1
C24	-0.4870(2)	0.15862(5)	0.69923(19)	0.0380(4)	1
P1	-0.24590(6)	0.13592(1)	0.46598(5)	0.03453(13)	1

T. Linder (Chemistry Department, University of Marburg)

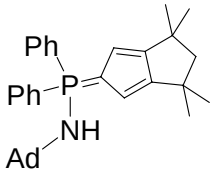

Table 31. Crystal data and structure refinement for compound $Ph_2P(Cp^{TM})NHAd$ (**L9**)

Crystal data:

Identification code	eq24	
Habitus, color	prism, bright yellow	
Crystal size	0.3 x 0.15 x 0.12 mm^3	
Crystal system	Monoclinic	
Space group	P -1	Z = 4
Unit cell dimensions	a = 10.6538(10) Å	α = 90°
	b = 10.6835(7) Å	β = 97.266(12)°
	c = 33.496(3) Å	γ = 90°
Volume	3781.9(6) $Å^3$	
Cell determination	7998 peaks with Theta 2.0 to 26.0°	
Empirical formula	$C_{46}H_{54}NP$	
Formula weight	651.87	
Density (calculated)	1.145 Mg/m^3	
Absorption coefficient	0.105 mm^{-1}	
F(000)	1408	

Data collection:

Diffractometer type	IPDS1
Wavelength	0.71069 Å
Temperature	193(2) K
Theta range for data collection	1.95 to 26.04°
Index ranges	-13<=h<=12, -13<=k<=12, -41<=l<=40
Data collection software	STOE WinXpose (X-Area)
Cell refinement software	STOE WinCell (X-Area)
Data reduction software	STOE WinIntegrate (X-Area)

Solution and refinement:

Reflections collected	29263
Independent reflections	7415 [R(int)= 0.1086]
Completeness to theta = 25.00°	100.0%
Observed reflections	4457 [I > 2sigma(I)]
Reflections used for refinement	7415
Extinction coefficient	0.00019(2)
Absorption correction	Semi-empirical from equivalents
Max. and min. transmission	1.2106 and 0.8853
Largest diff. peak and hole	0.503 and -0.521 e.$Å^{-3}$
Solution	direct/ difmap
Refinement	Full-matrix least-squares on F^2
Treatment of hydrogen atoms	geom.., mixed
Programs used	SHELXS-86 (Sheldrick, 1986) SHELXL-97 (Sheldrick, 1997) Diamond 3.1, STOE IPDS1 software
Data / restraints / parameters	7415 / 0 / 437
Goodness-of-fit on F^2	0.941
R index (all data)	wR2 = 0.1528
R index conventional [I > 2sigma(I)]	R1 = 0.0603

Table 32. Atomic coordinates and equivalent isotropic displacement parameters ($Å^2$)for eq24. U(eq)is defined as one third of the trace of the orthogonalized U^{ij} tensor.

	x	y	z	U(eq)	Occupancy
C01	0.4941(2)	0.2573(2)	0.33263(6)	0.0269(5)	1
C02	0.5699(2)	0.2408(2)	0.30033(7)	0.0282(5)	1
C03	0.6504(2)	0.3431(2)	0.30125(6)	0.0275(5)	1
C04	0.7578(2)	0.3899(2)	0.28000(7)	0.0339(5)	1
C05	0.7749(3)	0.5255(2)	0.29738(8)	0.0399(6)	1
C06	0.7142(2)	0.5346(2)	0.33705(7)	0.0351(6)	1
C07	0.6278(2)	0.4222(2)	0.33316(6)	0.0272(5)	1
C08	0.5338(2)	0.3724(2)	0.35296(7)	0.0285(5)	1
C09	0.8761(3)	0.3097(3)	0.29155(10)	0.0529(8)	1
C10	0.7273(3)	0.3925(3)	0.23407(8)	0.0471(7)	1
C11	0.8131(3)	0.5217(3)	0.37438(9)	0.0599(9)	1
C12	0.6432(3)	0.6574(3)	0.33964(9)	0.0516(7)	1
C13	0.3048(2)	0.0663(2)	0.30817(7)	0.0285(5)	1
C14	0.1800(2)	0.1009(2)	0.29579(7)	0.0343(5)	1
C15	0.1122(2)	0.0453(3)	0.26209(7)	0.0409(6)	1
C16	0.1669(3)	-0.0444(3)	0.24100(8)	0.0432(7)	1
C17	0.2903(3)	-0.0795(3)	0.25275(8)	0.0460(7)	1
C18	0.3601(2)	-0.0247(2)	0.28649(7)	0.0385(6)	1
C19	0.2860(2)	0.2217(2)	0.37755(6)	0.0282(5)	1
C20	0.2374(2)	0.3414(2)	0.36733(7)	0.0318(5)	1
C21	0.1463(2)	0.3932(2)	0.38796(8)	0.0387(6)	1
C22	0.1012(2)	0.3289(3)	0.41874(7)	0.0390(6)	1
C23	0.1482(2)	0.2104(3)	0.42917(7)	0.0397(6)	1
C24	0.2392(2)	0.1578(2)	0.40884(7)	0.0331(5)	1
C25	0.5858(2)	0.0382(2)	0.40526(7)	0.0286(5)	1
C26	0.5770(2)	0.1448(2)	0.43546(7)	0.0316(5)	1
C27	0.5954(2)	-0.0856(2)	0.42876(7)	0.0358(6)	1
C28	0.7032(2)	0.0548(3)	0.38424(7)	0.0355(6)	1
C29	0.6970(2)	0.1458(2)	0.46633(7)	0.0355(6)	1
C30	0.7069(3)	0.0222(3)	0.48943(7)	0.0428(6)	1
C31	0.7151(2)	-0.0852(2)	0.45994(8)	0.0409(6)	1
C32	0.8312(3)	-0.0688(3)	0.43840(8)	0.0457(7)	1
C33	0.8222(2)	0.0555(3)	0.41549(7)	0.0387(6)	1
C34	0.8127(2)	0.1628(3)	0.44476(8)	0.0410(6)	1
C101	0.1267(4)	0.8254(4)	0.39192(13)	0.0741(10)	1
C102	0.2398(3)	0.7705(4)	0.39955(12)	0.0691(10)	1
C103	0.2919(4)	0.7090(4)	0.37139(16)	0.0821(12)	1
C104	0.2215(6)	0.7021(4)	0.33138(16)	0.1020(18)	1
C105	0.1040(5)	0.7615(4)	0.32537(13)	0.0831(12)	1
C106	0.0596(4)	0.8212(4)	0.35518(13)	0.0801(11)	1
N02	0.46927(19)	0.03090(19)	0.37532(6)	0.0299(4)	1
P01	0.39720(6)	0.14693(6)	0.34901(2)	0.02606(16)	1
C202	0.4301(4)	0.3999(4)	0.48676(16)	0.0811(12)	1
C203	0.4425(4)	0.4952(5)	0.46203(10)	0.0814(13)	1
C205	0.9129(9)	0.5697(7)	0.47892(15)	0.111(2)	1
C201	0.4888(4)	0.4048(4)	0.52499(15)	0.0912(14)	1
C204	0.8787(5)	0.4689(8)	0.4973(3)	0.113(2)	1
C206	1.0332(11)	0.6016(4)	0.48164(18)	0.111(2)	1

Dr. K. Harms (Chemistry Department University of Marburg)

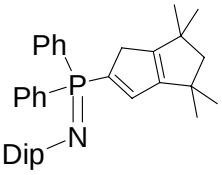

Table 33. Crystal data and structure refinement for compound $Ph_2P(Cp^{TM}H)NDip$ (**L10**).

Crystal data:

Identification code	apc	
Habitus, color	block, nugget	
Crystal size	0.24 x 0.15 x 0.12 mm^3	
Crystal system	Monoclinic	
Space group	P $2_1/c$	Z = 4
Unit cell dimensions	a = 9.3612(7) Å	α = 90°
	b = 23.389(2) Å	β = 96.201(6)°
	c = 14.7440(11) Å	γ = 90°
Volume	3209.3(4) $Å^3$	
Cell determination	10355 peaks with Theta 1.6 to 26.2°	
Empirical formula	$C_{36}H_{44}NP$	
Formula weight	521.69	
Density (calculated)	1.080 Mg/m^3	
Absorption coefficient	0.109 mm^{-1}	
F(000)	1128	

Data collection:

Diffractometer type	IPDS2
Wavelength	0.71073 Å
Temperature	193(2) K
Theta range for data collection	1.64 to 26.02°
Index ranges	-11<=h<=11, -28<=k<=28, -17<=l<=18
Data collection software	STOE WinXpose (X-Area)
Cell refinement software	STOE WinCell (X-Area)
Data reduction software	STOE WinIntegrate (X-Area)

Solution and refinement:

Reflections collected	28046
Independent reflections	6267 [R(int)= 0.0796]
Completeness to theta = 25.00°	100.0%
Observed reflections	3290 [I > 2sigma(I)]
Reflections used for refinement	6267
Extinction coefficient	0.00019(2)
Absorption correction	Semi-empirical from equivalents
Max. and min. transmission	1.0055 and 0.9664
Largest diff. peak and hole	0.147 and -0.193 e.$Å^{-3}$
Solution	Direct
Refinement	Full-matrix least-squares on F^2
Treatment of hydrogen atoms	Calculated, riding model
Programs used	SIR92 (Giacovazzo, 1993) SHELXL-97 (Sheldrick, 1997) Diamond 3.1, STOE IPDS2 software
Data / restraints / parameters	6267 / 7 / 371
Goodness-of-fit on F^2	0.805
R index (all data)	wR2 = 0.0824
R index conventional [I > 2sigma(I)]	R1 = 0.0415

Table 34. Atomic coordinates and equivalent isotropic displacement parameters ($Å^2$)for apc. U(eq)is defined as one third of the trace of the orthogonalized U^{ij} tensor.

	x	y	z	U(eq)	Occupancy
C1	0.7270(2)	0.16848(8)	0.33552(13)	0.0378(5)	1
C2	0.8026(2)	0.20215(8)	0.39863(13)	0.0407(5)	1
C3	0.8020(2)	0.26067(8)	0.36377(13)	0.0409(5)	1
C4	0.8565(2)	0.31852(8)	0.39714(14)	0.0472(5)	1
C5	0.8170(3)	0.35505(9)	0.30951(16)	0.0628(7)	1
C6	0.7135(2)	0.32080(9)	0.23982(14)	0.0510(6)	1
C7	0.7261(2)	0.26234(8)	0.28170(14)	0.0419(5)	1
C8	0.6692(2)	0.20461(8)	0.25476(13)	0.0443(5)	1
C9	0.7793(3)	0.33821(11)	0.47700(19)	0.0898(10)	1
C10	1.0178(3)	0.31930(10)	0.42443(19)	0.0750(8)	1
C11	0.5586(3)	0.34297(10)	0.23441(19)	0.0762(8)	1
C12	0.7639(3)	0.32061(10)	0.14489(16)	0.0724(8)	1
C13	0.7736(2)	0.05503(8)	0.26657(13)	0.0397(5)	1
C14	0.7367(2)	-0.00227(9)	0.25120(15)	0.0520(6)	1
C15	0.8044(3)	-0.03449(10)	0.18950(17)	0.0642(7)	1
C16	0.9090(3)	-0.01052(12)	0.14326(16)	0.0647(7)	1
C17	0.9473(3)	0.04561(11)	0.15819(16)	0.0635(7)	1
C18	0.8809(2)	0.07822(9)	0.22007(14)	0.0495(5)	1
C19	0.7502(2)	0.06939(8)	0.45543(13)	0.0383(5)	1
C20	0.6598(2)	0.04363(8)	0.51166(13)	0.0456(5)	1
C21	0.7163(3)	0.02052(9)	0.59533(14)	0.0541(6)	1
C22	0.8608(3)	0.02492(9)	0.62265(15)	0.0542(6)	1
C23	0.9519(3)	0.05121(9)	0.56801(15)	0.0518(6)	1
C24	0.8968(2)	0.07239(8)	0.48340(14)	0.0438(5)	1
C25	0.3986(2)	0.11919(8)	0.29149(14)	0.0415(5)	1
C26	0.3300(2)	0.15832(9)	0.34564(15)	0.0506(5)	1
C27	0.2158(3)	0.19045(11)	0.30523(18)	0.0693(7)	1
C28	0.1701(3)	0.18678(11)	0.21362(19)	0.0768(8)	1
C29	0.2378(3)	0.14936(11)	0.16103(17)	0.0666(7)	1
C30	0.3499(2)	0.11483(9)	0.19720(14)	0.0490(5)	1
C31	0.3779(2)	0.16630(9)	0.44624(15)	0.0542(6)	1
C32	0.4091(3)	0.22929(10)	0.47070(17)	0.0734(7)	1
C33	0.2685(3)	0.14103(13)	0.50440(18)	0.0880(9)	1
C34	0.4213(3)	0.07353(11)	0.13731(15)	0.0618(7)	1
C35	0.4031(7)	0.0936(3)	0.0363(3)	0.0628(18)	0.633(14)
C36	0.3721(9)	0.0140(3)	0.1469(5)	0.0600(18)	0.633(14)
N1	0.51031(17)	0.08411(6)	0.33147(11)	0.0410(4)	1
P1	0.67511(6)	0.09533(2)	0.34508(4)	0.03651(13)	1
C35A	0.489(3)	0.0904(7)	0.0582(13)	0.178(10)	0.367(14)
C36A	0.3202(16)	0.0206(5)	0.1129(14)	0.091(5)	0.367(14)

Dr. K. Harms (Chemistry Department, University of Marburg)

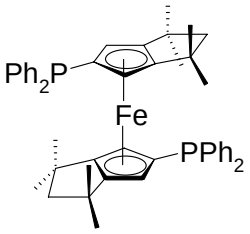

Table 35. Crystal data and structure refinement for compound [dppf^{TM}] (**S7**).

Crystal data:

Identification code	apfctm	
Habitus, color	prism, dark	
Crystal size	0.08 x 0.05 x 0.03 mm^3	
Crystal system	Triclinic	
Space group	P -1	Z = 1
Unit cell dimensions	a = 8.8276(18) Å	α = 80.50(2)°
	b = 11.002(3) Å	β = 71.261(17)°
	c = 11.123(3) Å	γ = 84.658(19)°
Volume	1008.0(4) Å^3	
Cell determination	3435 peaks with Theta 1.8 to 24.5°	
Empirical formula	$C_{48}H_{52}FeP_2$	
Formula weight	746.69	
Density (calculated)	1.230 Mg/m^3	
Absorption coefficient	0.486 mm^{-1}	
F(000)	396	

Data collection:

Diffractometer type	IPDS2
Wavelength	0.71073 Å
Temperature	130(2) K
Theta range for data collection	1.88 to 25.00°
Index ranges	-10<=h<=10, -13<=k<=13, -11<=l<=13
Data collection software	STOE WinXpose (X-Area)
Cell refinement software	STOE WinCell (X-Area)
Data reduction software	STOE WinIntegrate (X-Area)

Solution and refinement:

Reflections collected	8283
Independent reflections	3532 [R(int)= 0.1276]
Completeness to theta = 25.00°	99.7%
Observed reflections	1590 [I > 2sigma(I)]
Reflections used for refinement	3532
Extinction coefficient	0.00019(2)
Absorption correction	Integration
Max. and min. transmission	0.9865 and 0.9584
Largest diff. peak and hole	0.290 and -0.605 e.Å^{-3}
Solution	Direct methods
Refinement	Full-matrix least-squares on F^2
Treatment of hydrogen atoms	Calculated, riding
Programs used	SIR2004 (Giacovazzo, 2004)
	SHELXL-97 (Sheldrick, 1997)
	Diamond 3.1, STOE IPDS2 software
Data / restraints / parameters	3532 / 0 / 236
Goodness-of-fit on F^2	0.763
R index (all data)	wR2 = 0.0980
R index conventional [I > 2sigma(I)]	R1 = 0.0551

Table 36. Atomic coordinates and equivalent isotropic displacement parameters ($Å^2$)for apfctm. U(eq)is defined as one third of the trace of the orthogonalized U^{ij} tensor.

	x	y	z	U(eq)	Occupancy
C1	0.9215(5)	0.1436(4)	0.3838(4)	0.0343(11)	1
C2	1.0584(5)	0.1768(4)	0.4131(4)	0.0325(11)	1
C3	1.0154(5)	0.1716(4)	0.5470(5)	0.0362(12)	1
C4	1.0791(5)	0.2167(4)	0.6431(4)	0.0360(11)	1
C5	0.9483(5)	0.1685(4)	0.7715(4)	0.0401(12)	1
C6	0.7919(5)	0.1472(4)	0.7440(4)	0.0388(12)	1
C7	0.8575(5)	0.1346(4)	0.6023(5)	0.0360(11)	1
C8	0.7980(5)	0.1119(4)	0.5034(5)	0.0395(13)	1
C9	1.0836(5)	0.3570(4)	0.6180(5)	0.0449(13)	1
C10	1.2483(5)	0.1612(4)	0.6390(5)	0.0449(13)	1
C11	0.6725(5)	0.2598(4)	0.7595(5)	0.0484(13)	1
C12	0.7050(5)	0.0335(5)	0.8288(5)	0.0489(14)	1
C13	1.0334(5)	0.2737(4)	0.1306(4)	0.0348(11)	1
C14	1.1331(5)	0.2529(5)	0.0095(5)	0.0407(12)	1
C15	1.2358(5)	0.3437(5)	-0.0698(5)	0.0413(12)	1
C16	1.2390(5)	0.4548(5)	-0.0289(5)	0.0430(13)	1
C17	1.1411(5)	0.4771(5)	0.0926(5)	0.0401(13)	1
C18	1.0411(5)	0.3865(4)	0.1712(5)	0.0363(12)	1
C19	0.7031(5)	0.2444(4)	0.2520(4)	0.0346(12)	1
C20	0.6473(5)	0.3297(4)	0.3391(4)	0.0361(11)	1
C21	0.5044(5)	0.3973(5)	0.3469(5)	0.0444(13)	1
C22	0.4138(6)	0.3798(5)	0.2720(5)	0.0463(13)	1
C23	0.4639(5)	0.2937(4)	0.1886(5)	0.0434(13)	1
C24	0.6075(5)	0.2267(4)	0.1787(5)	0.0405(12)	1
P1	0.89545(14)	0.15348(12)	0.22548(13)	0.0384(4)	1
Fe1	1.0000	0.0000	0.5000	0.0352(3)	1

Dr. K. Harms (Chemistry Department, University of Marburg)

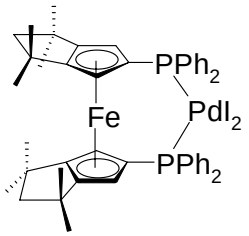

Table 37. Crystal data and structure refinement for palladium complex [(dppf)PdI_2] (**S9**).

Crystal data:

Identification code:	appd1	
Habitus, color	plate, light red	
Crystal size	0.21 x 0.06 x 0.03 mm^3	
Crystal system	Orthorhombic	
Space group	P $ca2_1$	Z = 4
Unit cell dimensions	a = 26.3109(17) Å	α = 90°
	b = 11.4236(7) Å	β = 90°
	c = 14.8667(7) Å	γ = 90°
Volume	4468.4(5) $Å^3$	
Cell determination	12673 peaks with Theta 1.8 to 25°	
Empirical formula	$C_{48}H_{52}FeI_2P_2Pd$	
Formula weight	1106.89	
Density (calculated)	1.645 Mg/m^3	
Absorption coefficient	2.212 mm^{-1}	
F(000)	2192	

Data collection:

Diffractometer type	IPDS2
Wavelength	0.71073 Å
Temperature	100(2) K
Theta range for data collection	1.78 to 25.00°
Index ranges	-25<=h<=31, -13<=k<=13, -17<=l<=17
Data collection software	STOE WinXpose (X-Area)
Cell refinement software	STOE WinCell (X-Area)
Data reduction software	STOE WinIntegrate (X-Area)

Solution and refinement:

Reflections collected	20064
Independent reflections	7797 [R(int)= 0.0745]
Completeness to theta = 25.00°	99.8%
Observed reflections	5930 [I > 2sigma(I)]
Reflections used for refinement	7797
Extinction coefficient	0.00019(2)
Absorption correction	Semi-empirical from equivalents
Max. and min. transmission	0.7367 and 0.7023
Flack parameter (absolute struct.)	0.03(3)
Largest diff. peak and hole	0.735 and -0.823 e.$Å^{-3}$
Solution	Direct methods
Refinement	Full-matrix least-squares on F^2
Treatment of hydrogen atoms	Calculated positions, constr. ref.
Programs used	SIR92 (Giacovazzo, 1993) SHELXL-97 (Sheldrick, 1997) Diamond 3.1, STOE IPDS2 software
Data / restraints / parameters	7797 / 1 / 496
Goodness-of-fit on F^2	0.898
R index (all data)	wR2 = 0.0767
R index conventional [I > 2sigma(I)]	R1 = 0.0439

Table 38. Atomic coordinates and equivalent isotropic displacement parameters ($Å^2$)for appd1. U(eq)is defined as one third of the trace of the orthogonalized U^{ij} tensor.

	x	y	z	U(eq)	Occupancy
C1	0.1327(3)	0.1776(7)	0.1739(5)	0.023(2)	1
C2	0.1270(3)	0.2033(7)	0.0799(6)	0.026(2)	1
C3	0.0805(3)	0.1560(8)	0.0488(6)	0.0233(19)	1
C4	0.0548(4)	0.1313(8)	-0.0392(6)	0.026(2)	1
C5	0.0058(4)	0.0718(8)	-0.0053(5)	0.027(2)	1
C6	0.0135(4)	0.0242(7)	0.0922(5)	0.026(2)	1
C7	0.0564(4)	0.1031(8)	0.1235(5)	0.026(2)	1
C8	0.0867(3)	0.1122(7)	0.1998(7)	0.0266(19)	1
C9	0.0888(3)	0.0491(9)	-0.0939(6)	0.032(2)	1
C10	0.0439(4)	0.2420(8)	-0.0947(6)	0.031(2)	1
C11	0.0312(4)	-0.1028(8)	0.0937(6)	0.034(2)	1
C12	-0.0352(3)	0.0329(8)	0.1485(8)	0.035(2)	1
C13	0.1008(3)	0.4401(7)	0.1823(5)	0.022(2)	1
C14	0.0603(3)	0.4508(8)	0.1172(5)	0.0238(19)	1
C15	0.0148(3)	0.4130(7)	0.1597(7)	0.0267(19)	1
C16	-0.0422(3)	0.4249(7)	0.1452(7)	0.025(2)	1
C17	-0.0622(3)	0.3582(9)	0.2302(5)	0.028(2)	1
C18	-0.0194(4)	0.3489(7)	0.3045(5)	0.025(2)	1
C19	0.0267(3)	0.3741(8)	0.2477(6)	0.026(2)	1
C20	0.0795(3)	0.3912(8)	0.2631(6)	0.029(2)	1
C21	-0.0643(3)	0.3744(9)	0.0583(6)	0.029(2)	1
C22	-0.0544(3)	0.5567(8)	0.1501(8)	0.0320(19)	1
C23	-0.0178(4)	0.2324(8)	0.3509(6)	0.032(2)	1
C24	-0.0251(4)	0.4467(9)	0.3747(6)	0.033(2)	1
C25	0.2253(4)	0.0729(8)	0.1997(7)	0.028(2)	1
C26	0.2387(4)	-0.0175(8)	0.2568(7)	0.042(3)	1
C27	0.2640(5)	-0.1157(9)	0.2205(9)	0.055(3)	1
C28	0.2755(4)	-0.1217(9)	0.1304(6)	0.041(3)	1
C29	0.2617(4)	-0.0333(9)	0.0758(7)	0.041(3)	1
C30	0.2377(4)	0.0650(9)	0.1096(7)	0.036(2)	1
C31	0.1727(3)	0.1866(7)	0.3541(6)	0.025(2)	1
C32	0.1483(4)	0.0860(7)	0.3859(6)	0.028(2)	1
C33	0.1308(4)	0.0822(7)	0.4736(6)	0.030(2)	1
C34	0.1379(4)	0.1766(9)	0.5302(7)	0.034(2)	1
C35	0.1636(4)	0.2746(10)	0.5005(6)	0.037(2)	1
C36	0.1807(4)	0.2794(9)	0.4127(6)	0.031(2)	1
C37	0.1663(3)	0.5756(8)	0.0733(5)	0.023(2)	1
C38	0.1682(3)	0.5149(9)	-0.0073(6)	0.029(2)	1
C39	0.1662(4)	0.5709(9)	-0.0889(6)	0.034(2)	1
C40	0.1645(3)	0.6925(9)	-0.0904(6)	0.035(2)	1
C41	0.1645(4)	0.7556(9)	-0.0106(6)	0.035(2)	1
C42	0.1654(4)	0.6969(8)	0.0715(6)	0.028(2)	1
C43	0.1614(3)	0.5999(7)	0.2689(6)	0.0217(19)	1
C44	0.1998(3)	0.6086(7)	0.3341(5)	0.026(2)	1
C45	0.1947(4)	0.6902(7)	0.4046(6)	0.030(2)	1
C46	0.1523(4)	0.7597(8)	0.4108(6)	0.031(2)	1
C47	0.1147(4)	0.7513(8)	0.3462(6)	0.032(2)	1
C48	0.1187(3)	0.6720(7)	0.2772(7)	0.030(2)	1
P1	0.19032(10)	0.20209(19)	0.23659(14)	0.0246(5)	1
P2	0.16546(9)	0.49342(19)	0.17859(13)	0.0223(5)	1
Fe1	0.07257(4)	0.27998(10)	0.15636(9)	0.0234(3)	1
I1	0.31338(2)	0.27001(5)	0.28120(4)	0.03280(14)	1
I2	0.29109(2)	0.54773(5)	0.15269(4)	0.02658(12)	1
Pd1	0.23337(2)	0.37212(5)	0.20624(4)	0.02273(14)	1

Dr. B. Ziemer (Chemical Department, Humboldt-University Berlin)

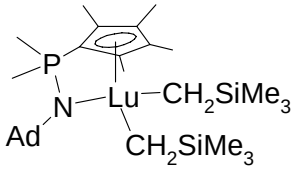

Table 39. Crystal data and structure refinement for complex [{$Me_2P(C_5Me_4)NAd$}$Lu(CH_2SiMe_3)_2$] (**C1**).

Crystal data:

Identification code	ruf16	
Habitus, color	block, colorless	
Crystal size	0.32 x 0.20 x 0.16 mm^3	
Crystal system	Monoclinic	
Space group	P $2_1/c$	Z = 4
Unit cell dimensions	a = 15.284(2) Å	α = 90°
	b = 10.4561(7) Å	β = 91.974(15)°
	c = 21.092(2) Å	γ = 90°
Volume	3368.7(7) $Å^3$	
Cell determination	5000 peaks with 2.5 to 25.0°	
Empirical formula	$C_{29}H_{55}LuNPSi_2$	
Formula weight	679.86	
Density (calculated)	1.340 Mg/m^3	
Absorption coefficient	3.066 mm^{-1}	
F(000)	1400	

Data collection:

Diffractometer type	IPDS2.87
Wavelength	0.71073 Å
Temperature	180(2) K
Theta range for data collection	2.31 to 25.97°
Index ranges	-18<=h<=18, -12<=k<=12, -25<=l<=25
Data Collection Software	IPDS2.87 (Stoe & Cie, 1997)
Cell Refinement Software	IPDS2.87 (Stoe & Cie, 1997)
Data Reduction Software	IPDS2.87 (Stoe & Cie, 1997)

Solution and Refinement:

Reflections collected	30805
Independent reflections	6383 [R(int)= 0.1009]
Completeness to theta = 25.97°	96.9%
Observed reflections	5621 [I > 2sigma(I)]
Reflections used for refinement	6383
Extinction coefficient	0.0060(3)
Absorption correction	Empirical (DIFABS)
Max. and min. transmission	0.6398 and 0.4404
Largest diff. peak and hole	2.952 and -2.465 e.$Å^{-3}$
Solution	direct
Refinement	Full-matrix least-squares on F^2
Treatment of hydrogen atoms	0.00019(2)
Programs used	SHELXS-97 (Sheldrick, 1990)
	SHELXL-97 (Sheldrick, 1997)
	DIAMOND (Brandenburg, 1999)
Data / restraints / parameters	6383 / 0 / 319
Goodness-of-fit on F^2	1.012
R index (all data)	wR2 = 0.1034
R index conventional [I > 2sigma(I)]	R1 = 0.0398

Table 40. Atomic coordinates (x 10^4)and equivalent isotropic displacement parameters ($Å^2$x 10^3)for ruf16. U(eq)is defined as one third of the trace of the orthogonalized U^{ij} tensor.

	x	y	z	U(eq)	Occupancy
C1	7571(3)	10623(4)	7618(2)	31(1)	1
C2	6668(3)	10839(4)	7740(2)	30(1)	1
C3	6621(3)	11385(4)	8346(2)	36(1)	1
C4	7493(3)	11495(4)	8614(2)	38(1)	1
C5	8089(3)	11041(4)	8170(2)	35(1)	1
C6	5868(3)	10551(5)	7316(2)	41(1)	1
C7	5815(4)	11890(5)	8655(2)	49(1)	1
C8	7732(4)	12104(6)	9246(2)	55(1)	1
C9	9073(4)	11078(5)	8266(3)	52(1)	1
C10	8153(3)	8493(6)	9319(2)	51(1)	1
C11	9635(5)	7696(9)	10267(3)	89(2)	1
C12	8580(8)	5708(8)	9579(4)	101(3)	1
C13	9857(5)	7356(8)	8868(3)	77(2)	1
C14	5768(3)	8286(5)	8660(2)	41(1)	1
C15	5908(6)	7959(15)	10101(3)	162(6)	1
C16	5775(6)	5645(8)	9232(5)	111(4)	1
C17	4210(3)	7324(5)	9442(2)	41(1)	1
C18	9056(4)	9470(6)	6965(3)	60(2)	1
C19	7410(5)	9582(5)	6319(2)	60(2)	1
C20	7588(3)	6784(4)	7283(2)	28(1)	1
C21	7513(4)	5955(4)	7879(2)	44(1)	1
C22	7479(4)	4541(5)	7715(2)	54(1)	1
C23	6678(4)	4280(5)	7272(3)	50(1)	1
C24	6746(4)	5074(5)	6678(2)	48(1)	1
C25	6777(3)	6485(4)	6851(2)	38(1)	1
C26	8418(4)	6402(5)	6946(3)	51(1)	1
C27	8309(5)	4182(6)	7374(4)	80(2)	1
C28	8380(4)	4968(6)	6774(4)	70(2)	1
C29	7569(5)	4719(6)	6334(3)	65(2)	1
Lu1	7202(1)	8951(1)	8444(1)	25(1)	1
N1	7602(2)	8141(3)	7494(1)	27(1)	1
P	7895(1)	9376(1)	7106(1)	33(1)	1
Si1	9028(1)	7383(2)	9497(1)	45(1)	1
Si2	5428(1)	7372(1)	9342(1)	41(1)	1

Dr. K. Harms (Chemistry Department University of Marburg)

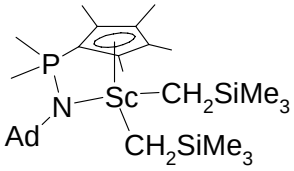

Table 41. Crystal data and structure refinement for complex $[(Me_2P(C_5Me_4)NAd)ScCH_2SiMe_3)_2]$ (**C2**).

Crystal data:

Identification code	apr03	
Habitus, color	prism, colorless	
Crystal size	0.45 x 0.21 x 0.12 mm^3	
Crystal system	Monoclinic	
Space group	P $2_1/c$	Z = 4
Unit cell dimensions	a = 15.1796(11) Å	$\alpha = 90°$
	b = 10.3440(8) Å	$\beta = 92.523(8)°$
	c = 20.9795(13) Å	$\gamma = 90°$
Volume	3291.0(4) $Å^3$	
Cell determination	8000 peaks with Theta 1.7 to 26.0°	
Empirical formula	$C_{29}H_{55}NPScSi_2$	
Formula weight	549.85	
Density (calculated)	1.110 Mg/m^3	
Absorption coefficient	0.362 mm^{-1}	
F(000)	1200	

Data collection:

Diffractometer type	IPDS1
Wavelength	0.71073 Å
Temperature	193(2) K
Theta range for data collection	2.20 to 26.08°
Index ranges	-18<=h<=18, -12<=k<=12, -25<=l<=25
Data collection software	STOE WinXpose (X-Area)
Cell refinement software	STOE WinCell (X-Area)
Data reduction software	STOE WinIntegrate (X-Area)

Solution and refinement:

Reflections collected	25584
Independent reflections	6113 [R(int)= 0.0667]
Completeness to theta = 25.00°	94.9%
Observed reflections	4192 [I > 2sigma(I)]
Reflections used for refinement	6113
Extinction coefficient	0.00019(2)
Absorption correction	Semi-empirical from equivalents
Max. and min. transmission	0.9834 and 0.8651
Largest diff. peak and hole	0.567 and -0.437 $e.Å^{-3}$
Solution	Direct methods
Refinement	Full-matrix least-squares on F^2
Treatment of hydrogen atoms	Calculated, fixed isotropic U's
Programs used	SIR92 (Giacovazzo, 1993)
	SHELXL-97 (Sheldrick, 1997)
	Diamond 3.1, STOE IPDS1 software
Data / restraints / parameters	6113 / 31 / 329
Goodness-of-fit on F^2	0.913
R index (all data)	wR2 = 0.1185
R index conventional [I > 2sigma(I)]	R1 = 0.0462

Table 42. Atomic coordinates and equivalent isotropic displacement parameters ($Å^2$)for apr03. U(eq)is defined as one third of the trace of the orthogonalized U^{ij} tensor.

	x	y	z	U(eq)	Occupancy
C1	0.75832(15)	0.1724(2)	0.23039(12)	0.0265(5)	1
C2	0.67574(17)	0.1450(2)	0.18865(14)	0.0354(6)	1
C3	0.67196(19)	0.0016(3)	0.16916(15)	0.0448(7)	1
C4	0.7526(2)	-0.0304(3)	0.13181(17)	0.0563(9)	1
C5	0.8356(2)	-0.0069(3)	0.17377(18)	0.0536(9)	1
C6	0.8339(2)	-0.0902(3)	0.2334(2)	0.0601(10)	1
C7	0.7521(2)	-0.0569(3)	0.27033(16)	0.0484(8)	1
C8	0.75621(19)	0.0862(2)	0.28938(14)	0.0384(6)	1
C9	0.83945(17)	0.1365(2)	0.19363(15)	0.0423(7)	1
C10	0.6704(2)	-0.0819(3)	0.22835(17)	0.0483(8)	1
C11	0.75625(16)	0.5571(2)	0.26618(12)	0.0302(6)	1
C12	0.80678(17)	0.5965(2)	0.32240(14)	0.0358(6)	1
C13	0.74798(18)	0.6383(2)	0.36737(14)	0.0378(6)	1
C14	0.66119(17)	0.6274(2)	0.34024(13)	0.0338(6)	1
C15	0.66496(16)	0.5766(2)	0.27870(13)	0.0304(6)	1
C16	0.90601(19)	0.6018(3)	0.33222(18)	0.0542(8)	1
C17	0.7706(2)	0.6953(3)	0.43213(17)	0.0570(9)	1
C18	0.5800(2)	0.6743(3)	0.37162(17)	0.0503(8)	1
C19	0.58639(18)	0.5483(3)	0.23535(14)	0.0403(6)	1
C20	0.9049(2)	0.4452(3)	0.19942(19)	0.0585(10)	1
C21	0.7401(3)	0.4569(3)	0.13487(15)	0.0568(9)	1
C22	0.58551(16)	0.3207(2)	0.36276(13)	0.0351(6)	1
C23	0.5934(3)	0.3021(9)	0.5080(2)	0.178(4)	1
C24	0.5839(4)	0.0593(5)	0.4264(3)	0.142(3)	1
C25	0.42720(18)	0.2311(3)	0.44006(14)	0.0419(7)	1
C26	0.8097(2)	0.3385(3)	0.42722(15)	0.0502(8)	1
C27	0.8593(4)	0.0601(4)	0.4563(3)	0.0937(18)	0.885(5)
C28	0.9835(2)	0.2274(4)	0.3851(2)	0.0756(12)	1
C29	0.9589(3)	0.2714(6)	0.5243(2)	0.0933(19)	0.885(5)
N1	0.75997(13)	0.30835(17)	0.25272(10)	0.0263(4)	1
Si1	0.54996(5)	0.23283(8)	0.43258(4)	0.0408(2)	1
Si2	0.89973(8)	0.23015(15)	0.44695(5)	0.0404(4)	0.885(5)
P1	0.78874(4)	0.43387(6)	0.21367(3)	0.03273(18)	1
Sc1	0.72144(3)	0.39112(4)	0.34318(2)	0.02502(13)	1
Si2A	0.9186(7)	0.2805(12)	0.4529(5)	0.054(3)	0.115(5)
C29A	0.973(2)	0.4288(19)	0.4858(11)	0.070(9)	0.115(5)
C27A	0.929(2)	0.155(2)	0.5160(9)	0.073(10)	0.115(5)

Dr. K. Harms (Chemistry Department, University of Marburg)

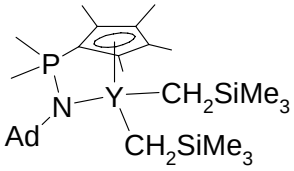

Table 43. Crystal data and structure refinement for complex [($Me_2P(C_5Me_4)$NAd)Y(CH_2SiMe_3)$_2$] (**C3**).

Crystal data:

Identification code	ruf28	
Habitus, color	prism, colorless	
Crystal size	0.48 x 0.40 x 0.32 mm^3	
Crystal system	Monoclinic	
Space group	P 2_1/n	Z = 4
Unit cell dimensions	a = 13.360(3) Å	α = 90°
	b = 17.293(3) Å	β = 91.26(2)°
	c = 14.497(3) Å	γ = 90°
Volume	3348.4(11) $Å^3$	
Cell determination	5000 peaks with Theta 2.5 to 25.0°	
Empirical formula	$C_{29}H_{55}NPSi_2Y$	
Formula weight	593.80	
Density (calculated)	1.178 Mg/m^3	
Absorption coefficient	1.878 mm^{-1}	
F(000)	1272	

Data collection:

Diffractometer type	IPDS1
Wavelength	0.71073 Å
Temperature	180(2) K
Theta range for data collection	2.36 to 24.50°
Index ranges	-15<=h<=15, -20<=k<=20, -16<=l<=16
Data collection software	STOE WinXpose (X-Area)
Cell refinement software	STOE WinCell (X-Area)
Data reduction software	STOE WinIntegrate (X-Area)

Solution and refinement:

Reflections collected	30437
Independent reflections	5486 [R(int)= 0.1239]
Completeness to theta = 24.50°	98.4%
Observed reflections	3510 [I > 2sigma(I)]
Reflections used for refinement	5486
Extinction coefficient	0.00019(2)
Absorption correction	Integration
Max. and min. transmission	0.5849 and 0.4660
Largest diff. peak and hole	0.434 and -1.028 e.$Å^{-3}$
Solution	direct/ difmap
Refinement	Full-matrix least-squares on F^2
Treatment of hydrogen atoms	geom.., noref
Programs used	SHELXS97 (Sheldrick, 1990)
	SHELXL97 (Sheldrick, 1997)
	Diamond 2.1, STOE IPDS1 software
Data / restraints / parameters	5486 / 0 / 319
Goodness-of-fit on F^2	0.872
R index (all data)	wR2 = 0.1156
R index conventional [I > 2sigma(I)]	R1 = 0.0490

Table 44. Atomic coordinates and equivalent isotropic displacement parameters ($Å^2$)for ruf_28. U(eq)is defined as one third of the trace of the orthogonalized U^{ij} tensor.

	x	y	z	U(eq)	Occupancy
C1	0.6923(4)	0.7389(3)	0.7821(2)	0.0347(10)	1
C2	0.6054(4)	0.7031(3)	0.7384(3)	0.0378(11)	1
C3	0.5399(4)	0.7616(3)	0.7061(3)	0.0411(11)	1
C4	0.5853(4)	0.8346(3)	0.7294(3)	0.0374(11)	1
C5	0.6758(4)	0.8216(3)	0.7756(3)	0.0404(12)	1
C6	0.5855(5)	0.6172(3)	0.7294(3)	0.0587(16)	1
C7	0.4382(4)	0.7508(4)	0.6623(3)	0.0613(16)	1
C8	0.5324(5)	0.9110(3)	0.7139(4)	0.0617(16)	1
C9	0.7470(4)	0.8841(3)	0.8100(3)	0.0533(14)	1
C10	0.8870(4)	0.7396(4)	0.8798(3)	0.0672(18)	1
C11	0.8056(5)	0.5979(3)	0.8271(4)	0.0701(18)	1
C12	0.7706(4)	0.8968(3)	0.5639(3)	0.0426(12)	1
C13	0.6348(6)	0.9393(4)	0.4022(4)	0.087(2)	1
C14	0.8237(8)	1.0319(4)	0.4303(4)	0.114(3)	1
C15	0.8373(5)	0.8687(3)	0.3666(3)	0.0613(16)	1
C16	0.6353(4)	0.7014(3)	0.4796(3)	0.0420(12)	1
C17	0.7683(5)	0.6250(3)	0.3357(3)	0.0570(15)	1
C18	0.7074(5)	0.5334(3)	0.5045(3)	0.0557(14)	1
C19	0.5576(5)	0.5673(3)	0.3534(4)	0.0617(15)	1
C20	0.9460(4)	0.6949(3)	0.6422(3)	0.0344(10)	1
C21	0.9280(4)	0.7086(3)	0.5383(3)	0.0381(11)	1
C22	1.0232(4)	0.6939(3)	0.4840(3)	0.0413(11)	1
C23	1.0549(4)	0.6092(3)	0.4988(3)	0.0474(13)	1
C24	1.0760(4)	0.5959(3)	0.6021(3)	0.0502(13)	1
C25	0.9806(4)	0.6106(3)	0.6560(3)	0.0442(12)	1
C26	1.0292(4)	0.7495(3)	0.6760(3)	0.0454(13)	1
C27	1.1259(4)	0.7347(3)	0.6216(3)	0.0505(13)	1
C28	1.1052(4)	0.7485(3)	0.5183(3)	0.0504(14)	1
C29	1.1589(4)	0.6510(4)	0.6362(3)	0.0585(15)	1
N	0.8488(3)	0.7112(2)	0.6852(2)	0.0356(9)	1
P	0.81197(10)	0.69746(8)	0.78855(7)	0.0413(3)	1
Si1	0.76710(13)	0.93400(8)	0.44527(8)	0.0517(4)	1
Si2	0.66522(11)	0.61057(8)	0.42085(8)	0.0403(3)	1
Y	0.71489(4)	0.76949(3)	0.60854(2)	0.03338(14)	1

M. Elfferding (Chemistry Department, University of Marburg)

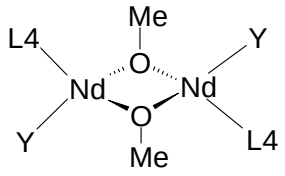

Table 45. Crystal data and structure refinement for binuclear complex $[(Me_2P(C_5Me_4)NAd)Nd(CH_2SiMe_3)(\mu\text{-}OMe)]_2$ (**C5** x $2C_7H_8$).

Crystal data:

Identification code	eq127	
Habitus, color	prism, green	
Crystal size	0.30 x 0.30 x 0.05 mm^3	
Crystal system	triclinic	
Space group	P -1	Z = 1
Unit cell dimensions	a = 11.5382(13) Å	α = 100.313(5)°
	b = 11.8124(15) Å	β = 96.935(5)°
	c = 13.6095(15) Å	γ = 109.057(5)°
Volume	1692.6(3) $Å^3$	
Cell determination	7998 peaks with Theta 2.0 to 26.1°	
Empirical formula	$C_{56}H_{110}N_2Nd_2O_2P_2Si_2$	
Formula weight	1250.11	
Density (calculated)	1.305 Mg/m^3	
Absorption coefficient	1.703 mm^{-1}	
F(000)	694	

Data collection:

Diffractometer type	IPDS1
Wavelength	0.71069 Å
Temperature	193(2) K
Theta range for data collection	1.88 to 26.08°
Index ranges	-13<=h<=14, -14<=k<=14, -16<=l<=16
Data collection software	STOE WinXpose (X-Area)
Cell refinement software	STOE WinCell (X-Area)
Data reduction software	STOE WinIntegrate (X-Area)

Solution and refinement:

Reflections collected	16929
Independent reflections	6230 [R(int)= 0.0396]
Completeness to theta = 25.00°	94.1 %
Observed reflections	5505 [I > 2sigma(I)]
Reflections used for refinement	6230
Extinction coefficient	0.00019(2)
Absorption correction	None
Largest diff. peak and hole	1.446 and -1.877 e.$Å^{-3}$
Solution	direct/ difmap
Refinement	Full-matrix least-squares on F^2
Treatment of hydrogen atoms	geom.., mixed
Programs used	SHELXS-97 (Sheldrick, 1990)
	SHELXL-97 (Sheldrick, 1997)
	Diamond 3.1, STOE IPDS1 software
Data / restraints / parameters	6230 / 0 / 343
Goodness-of-fit on F^2	1.038
R index (all data)	wR2 = 0.1206
R index conventional [I > 2sigma(I)]	R1 = 0.0414

Table 46. Atomic coordinates and equivalent isotropic displacement parameters ($Å^2$)for eq127. U(eq)is defined as one third of the trace of the orthogonalized U^{ij} tensor.

	x	y	z	U(eq)	Occupancy
C1	0.4328(4)	0.1226(4)	0.4546(3)	0.0267(9)	1
C2	0.5229(5)	0.2116(4)	0.5378(3)	0.0307(9)	1
C3	0.3118(5)	0.1020(4)	0.4799(3)	0.0315(10)	1
C4	0.3278(5)	0.1761(4)	0.5769(3)	0.0341(10)	1
C5	0.4574(5)	0.2443(4)	0.6126(3)	0.0347(10)	1
N1	0.4295(4)	0.1974(3)	0.2838(2)	0.0272(8)	1
C6	0.1878(5)	0.0161(5)	0.4150(5)	0.0454(12)	1
C7	0.2292(6)	0.1728(6)	0.6404(4)	0.0497(14)	1
C8	0.5159(7)	0.3318(5)	0.7161(4)	0.0497(14)	1
C9	0.6635(5)	0.2635(5)	0.5491(4)	0.0412(11)	1
C10	0.3613(6)	-0.0677(4)	0.2634(4)	0.0410(12)	1
C11	0.6125(5)	0.0822(5)	0.3305(4)	0.0424(12)	1
C12	0.4169(4)	0.2058(4)	0.1757(3)	0.0281(9)	1
C13	0.2849(5)	0.1229(5)	0.1160(4)	0.0409(11)	1
C14	0.5151(5)	0.1706(5)	0.1221(3)	0.0405(12)	1
C15	0.4350(5)	0.3398(4)	0.1738(3)	0.0377(11)	1
C16	0.2684(6)	0.1394(5)	0.0053(4)	0.0498(14)	1
C17	0.4972(7)	0.1858(6)	0.0107(4)	0.0513(15)	1
C18	0.4183(7)	0.3562(5)	0.0642(4)	0.0492(14)	1
C19	0.3693(7)	0.1035(6)	-0.0458(4)	0.0554(16)	1
C20	0.5176(7)	0.3222(6)	0.0138(4)	0.0598(17)	1
C22	0.1962(5)	0.3508(5)	0.3482(4)	0.0409(11)	1
C23	-0.0348(8)	0.1249(7)	0.2440(7)	0.078(2)	1
C24	-0.0153(7)	0.2545(9)	0.4648(6)	0.080(2)	1
C25	-0.0691(7)	0.3678(8)	0.2930(7)	0.0698(19)	1
C37	0.2872(7)	0.2734(6)	0.0070(4)	0.0559(16)	1
C34	0.0246(19)	0.8073(16)	0.117(3)	0.195(16)	1
C32	0.1331(13)	0.6982(12)	0.0325(10)	0.126(5)	1
Si1	0.02752(14)	0.27920(15)	0.33903(12)	0.0436(3)	1
P1	0.45674(12)	0.08962(10)	0.32799(8)	0.0275(2)	1
Nd1	0.39573(2)	0.33240(2)	0.43378(1)	0.02479(10)	1
C31	0.1222(8)	0.6340(8)	0.1017(9)	0.088(3)	1
C36	0.0674(11)	0.6564(13)	0.1827(10)	0.126(5)	1
C35	0.0136(16)	0.740(2)	0.2043(18)	0.208(13)	1
C30	0.1772(14)	0.5331(16)	0.0879(19)	0.214(12)	1
C33	0.092(2)	0.7825(17)	0.0390(18)	0.200(13)	1
O1	0.5781(3)	0.4927(3)	0.4359(2)	0.0297(7)	1
C200	0.6840(5)	0.4952(5)	0.3904(4)	0.0434(12)	1

Dr. K. Harms (Chemistry Department, University of Marburg)

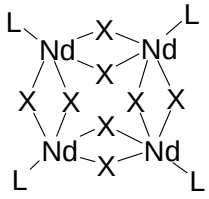

Table 47. Crystal data and structure refinement for tetranuclear neodymium complex $[(Me_2P(C_5Me_4)NAd)Nd(OH)_2]_4$ (**C6** x $6C_6H_6$).

Crystal data:

Identification code	apn	
Habitus, color	prism, pale blue	
Crystal size	0.20 x 0.10 x 0.10 mm^3	
Crystal system	Triclinic	
Space group	P -1	Z = 2
Unit cell dimensions	a = 15.2703(19) Å	α = 78.539(13)°
	b = 19.073(2) Å	β = 82.008(14)°
	c = 20.551(3) Å	γ = 84.326(14)°
Volume	5793.5(12) $Å^3$	
Cell determination	8000 peaks with Theta 2.0 to 25.9°	
Empirical formula	$C_{126}H_{188}N_4Nd_4O_8P_4$	
Formula weight	2587.77	
Density (calculated)	1.435 Mg/m^3	
Absorption coefficient	1.873 mm^{-1}	
F(000)	2576	

Data collection:

Diffractometer type	IPDS1
Wavelength	0.71069 Å
Temperature	193(2) K
Theta range for data collection	2.05 to 25.00°
Index ranges	-18<=h<=18, -22<=k<=22, -24<=l<=24
Data collection software	STOE WinXpose (X-Area)
Cell refinement software	STOE WinCell (X-Area)
Data reduction software	STOE WinIntegrate (X-Area)

Solution and refinement:

Reflections collected	52778
Independent reflections	19255 [R(int)= 0.1241]
Completeness to theta = 25.00°	94.3%
Observed reflections	7713 [I > 2sigma(I)]
Reflections used for refinement	19255
Extinction coefficient	X = 0.00019(2)
Absorption correction	Semi-empirical from equivalents
Largest diff. peak and hole	1.054 and -1.406 e.$Å^{-3}$
Solution	direct / difmap
Refinement	Full-matrix least-squares on F^2
Programs used	SHELXS-97 (Sheldrick, 1997)
	SHELXL-97 (Sheldrick, 1997)
	Diamond 2.1, STOE IPDS1 software
Data / restraints / parameters	19255 / 840 / 1213
Goodness-of-fit on F^2	0.714
R index (all data)	wR2 = 0.1056
R index conventional [I > 2sigma(I)]	R1 = 0.0481

Table 48. Atomic coordinates and equivalent isotropic displacement parameters ($Å^2$)for apn. U(eq)is defined as one third of the trace of the orthogonalized U^{ij} tensor.

	x	y	z	U(eq)	Occupancy
C1	0.6235(10)	0.1934(9)	0.3398(7)	0.075(4)	1
C2	0.5322(10)	0.1791(8)	0.3712(6)	0.066(4)	1
C3	0.6804(11)	0.1290(9)	0.3242(7)	0.074(4)	1
C4	0.6799(11)	0.0760(9)	0.3849(7)	0.081(5)	1
C5	0.5889(10)	0.0547(8)	0.4164(6)	0.068(4)	1
C6	0.5378(11)	0.1182(9)	0.4320(7)	0.076(4)	1
C7	0.6307(9)	0.1047(8)	0.2714(6)	0.066(4)	1
C8	0.5438(9)	0.0266(7)	0.3647(6)	0.055(3)	1
C9	0.4860(10)	0.1490(8)	0.3215(7)	0.067(4)	1
C10	0.5380(8)	0.0822(7)	0.3002(5)	0.038(3)	1
C11	0.6122(8)	-0.0562(8)	0.2135(6)	0.057(4)	1
C12	0.4550(8)	-0.0882(6)	0.2917(6)	0.049(3)	1
C13	0.4507(7)	-0.0032(6)	0.1575(5)	0.029(2)	1
C14	-0.0531(8)	-0.0695(7)	0.1301(5)	0.045(3)	1
C15	0.3453(7)	0.0188(6)	0.0855(5)	0.031(3)	1
C16	0.4196(7)	0.0570(6)	0.0536(5)	0.036(3)	1
C17	0.4852(7)	0.0447(6)	0.0975(5)	0.033(3)	1
C18	0.5722(8)	0.0774(7)	0.0836(6)	0.043(3)	1
C19	0.4304(8)	0.0992(6)	-0.0157(5)	0.048(3)	1
C20	0.2623(8)	0.0208(8)	0.0537(5)	0.052(4)	1
C22	0.2413(7)	0.1245(7)	0.4550(5)	0.043(3)	1
C23	0.2259(8)	-0.0256(6)	0.4216(5)	0.043(3)	1
C24	0.0532(9)	0.2123(7)	0.4479(5)	0.056(4)	1
C25	-0.0777(8)	0.1210(7)	0.4037(6)	0.043(3)	1
C26	0.0767(7)	0.1410(6)	0.4304(5)	0.033(3)	1
C27	0.0179(7)	0.0967(6)	0.4120(4)	0.030(2)	1
C28	0.1599(7)	0.1007(6)	0.4347(5)	0.032(3)	1
C29	0.1541(7)	0.0317(6)	0.4191(4)	0.032(3)	1
C30	0.0627(7)	0.0307(6)	0.4036(4)	0.027(2)	1
C31	0.0898(8)	-0.1070(6)	0.3597(6)	0.042(3)	1
C32	-0.0817(8)	-0.0517(7)	0.3992(5)	0.052(4)	1
C33	-0.0125(7)	0.0171(6)	0.2248(4)	0.026(2)	1
C34	-0.0909(7)	-0.0303(6)	0.2398(4)	0.030(2)	1
C35	0.0587(7)	-0.0173(6)	0.1783(5)	0.034(3)	1
C36	0.0240(7)	-0.0218(6)	0.1142(5)	0.037(3)	1
C37	-0.1270(7)	-0.0347(6)	0.1746(5)	0.039(3)	1
C38	-0.1584(8)	0.0365(7)	0.1398(6)	0.047(3)	1
C39	-0.0070(8)	0.0523(7)	0.0790(5)	0.043(3)	1
C40	-0.0444(7)	0.0890(6)	0.1872(4)	0.030(2)	1
C41	0.2844(8)	0.3621(7)	0.4304(5)	0.049(3)	1
C42	0.2234(8)	0.3561(7)	0.4971(5)	0.048(3)	1
C43	0.3294(9)	0.4330(8)	0.4158(6)	0.059(4)	1
C44	0.1530(9)	0.4177(7)	0.4946(6)	0.050(3)	1
C45	0.1972(10)	0.4887(8)	0.4807(6)	0.064(4)	1
C46	0.2594(9)	0.4946(7)	0.4150(6)	0.055(3)	1
C47	0.0960(7)	0.4181(6)	0.4375(5)	0.040(3)	1
C48	0.1999(8)	0.4948(7)	0.3586(5)	0.043(3)	1
C49	0.2282(7)	0.3621(6)	0.3733(5)	0.039(3)	1
C50	0.1560(7)	0.4247(6)	0.3706(5)	0.031(3)	1
C51	-0.0321(8)	0.5364(7)	0.3282(5)	0.051(3)	1
C52	0.1026(7)	0.5560(6)	0.2205(5)	0.041(3)	1
C53	-0.0187(7)	0.4438(6)	0.2312(5)	0.027(2)	1
C54	-0.0749(7)	0.3881(6)	0.2638(5)	0.035(3)	1
C55	-0.0964(7)	0.3558(6)	0.2159(5)	0.042(3)	1
C56	-0.0533(7)	0.3863(6)	0.1531(5)	0.036(3)	1
C57	-0.0032(7)	0.4403(6)	0.1604(5)	0.034(3)	1

C58	0.0533(7)	0.4841(7)	0.1037(5)	0.045(3)	1
C59	-0.0650(9)	0.3630(8)	0.0882(6)	0.053(4)	1
C60	-0.1610(9)	0.2966(7)	0.2257(7)	0.062(4)	1
C61	-0.1048(8)	0.3691(7)	0.3382(5)	0.046(3)	1
C62	0.4364(9)	0.4238(7)	0.2102(5)	0.056(4)	1
C63	0.5552(8)	0.3052(8)	0.1510(6)	0.066(4)	1
C64	0.5204(7)	0.3126(7)	0.0021(5)	0.038(3)	1
C65	0.3312(8)	0.5176(6)	0.0972(5)	0.042(3)	1
C66	0.4403(7)	0.4109(6)	0.1399(5)	0.033(3)	1
C67	0.4937(7)	0.3558(6)	0.1139(5)	0.036(3)	1
C68	0.4795(7)	0.3613(6)	0.0455(5)	0.036(3)	1
C69	0.4167(6)	0.4208(5)	0.0311(4)	0.022(2)	1
C70	0.3917(7)	0.4537(6)	0.0901(5)	0.028(2)	1
C71	0.2965(9)	0.5171(7)	-0.0523(6)	0.057(4)	1
C72	0.4300(8)	0.4339(7)	-0.1116(5)	0.046(3)	1
C73	0.2372(7)	0.3363(6)	-0.0554(5)	0.030(3)	1
C74	0.1383(10)	0.3613(9)	-0.0366(7)	0.073(4)	1
C75	0.0753(10)	0.3303(8)	-0.0776(6)	0.062(4)	1
C76	0.1041(9)	0.3504(8)	-0.1470(6)	0.061(4)	1
C77	0.1980(8)	0.3233(7)	-0.1708(6)	0.052(3)	1
C78	0.2071(12)	0.2419(9)	-0.1429(7)	0.085(5)	1
C79	0.1792(9)	0.2198(8)	-0.0729(6)	0.065(4)	1
C80	0.0887(9)	0.2503(7)	-0.0523(6)	0.054(3)	1
C81	0.2367(10)	0.2546(8)	-0.0337(7)	0.073(4)	1
C82	0.2580(10)	0.3511(9)	-0.1271(6)	0.076(4)	1
C83	0.8162(6)	0.3134(4)	-0.0411(4)	0.067(4)	1
C84	0.8497(5)	0.2716(5)	-0.0885(3)	0.057(3)	1
C85	0.8329(6)	0.1996(5)	-0.0770(4)	0.065(4)	1
C86	0.7826(6)	0.1694(4)	-0.0183(4)	0.067(4)	1
C87	0.7491(5)	0.2112(5)	0.0290(3)	0.061(4)	1
C88	0.7660(6)	0.2832(5)	0.0176(4)	0.061(4)	1
C89	0.6533(7)	0.3577(5)	0.5116(5)	0.089(5)	1
C90	0.6221(6)	0.3372(5)	0.5789(5)	0.071(4)	1
C91	0.6389(6)	0.2670(5)	0.6115(3)	0.067(4)	1
C92	0.6869(7)	0.2172(4)	0.5767(5)	0.080(5)	1
C93	0.7181(7)	0.2377(6)	0.5094(5)	0.087(5)	1
C94	0.7013(7)	0.3080(6)	0.4768(3)	0.088(5)	1
C95	0.4181(5)	0.2224(5)	0.5754(4)	0.071(4)	1
C96	0.3988(6)	0.2635(5)	0.6251(5)	0.077(4)	1
C97	0.3251(7)	0.2510(5)	0.6726(4)	0.074(4)	1
C98	0.2708(5)	0.1973(5)	0.6705(4)	0.074(4)	1
C99	0.2902(6)	0.1562(5)	0.6209(5)	0.076(4)	1
C100	0.3638(7)	0.1688(5)	0.5733(4)	0.081(5)	1
C101	0.3752(8)	0.4574(5)	0.6176(5)	0.091(5)	1
C102	0.4341(6)	0.5080(6)	0.6191(5)	0.095(5)	1
C103	0.4153(7)	0.5537(5)	0.6650(6)	0.094(5)	1
C104	0.3378(8)	0.5487(5)	0.7094(5)	0.104(6)	1
C105	0.2790(6)	0.4981(6)	0.7079(5)	0.081(5)	1
C106	0.2977(7)	0.4524(5)	0.6621(5)	0.085(5)	1
C110	-0.0789(7)	0.0847(6)	0.1231(5)	0.039(3)	1
C121	0.3634(7)	-0.0188(6)	0.1476(5)	0.034(3)	1
C131	0.2999(7)	-0.0664(6)	0.1957(5)	0.038(3)	1
C151	0.1240(6)	0.6932(6)	0.3777(5)	0.086(5)	1
C152	0.0344(7)	0.6955(5)	0.4024(4)	0.067(4)	1
C153	-0.0289(5)	0.7218(6)	0.3595(5)	0.087(5)	1
C154	-0.0027(7)	0.7458(6)	0.2918(5)	0.089(5)	1
C155	0.0868(8)	0.7435(6)	0.2671(4)	0.092(5)	1
C156	0.1501(6)	0.7173(6)	0.3101(5)	0.090(5)	1
C161	0.5106(7)	0.3385(6)	0.7543(5)	0.089(5)	1
C162	0.4930(6)	0.2710(6)	0.7914(5)	0.091(5)	1
C163	0.5528(8)	0.2338(5)	0.8334(5)	0.091(5)	1
C164	0.6303(7)	0.2640(6)	0.8383(5)	0.099(6)	1

C165	0.6479(6)	0.3315(6)	0.8012(5)	0.091(5)	1
C166	0.5880(8)	0.3687(5)	0.7592(5)	0.086(5)	1
N1	0.0263(5)	0.0251(4)	0.2853(3)	0.0233(19)	1
N2	0.4936(6)	0.0598(5)	0.2494(4)	0.032(2)	1
N3	0.2929(5)	0.3646(4)	-0.0148(3)	0.0249(19)	1
N4	0.1039(5)	0.4203(5)	0.3156(4)	0.029(2)	1
O1	0.2844(4)	0.0738(4)	0.2842(3)	0.0318(17)	1
O2	0.2002(4)	0.1311(4)	0.1800(3)	0.0296(17)	1
O3	0.3527(4)	0.2331(4)	0.2059(3)	0.0293(16)	1
O4	0.3641(5)	0.2121(4)	0.0839(3)	0.0404(19)	1
O5	0.2248(4)	0.3865(4)	0.1866(3)	0.0312(17)	1
O6	0.1615(4)	0.2879(4)	0.1356(3)	0.0286(16)	1
O7	0.1870(4)	0.2353(4)	0.2947(3)	0.0297(16)	1
O8	0.0287(4)	0.2151(4)	0.2625(3)	0.0298(17)	1
P1	0.35479(19)	0.42973(16)	-0.03652(12)	0.0310(7)	1
P2	0.0437(2)	0.48493(17)	0.27741(14)	0.0368(7)	1
P3	0.02383(18)	-0.02313(15)	0.35643(12)	0.0294(7)	1
P4	0.50267(19)	-0.01608(16)	0.22985(14)	0.0352(7)	1
Nd1	0.31121(4)	0.32216(4)	0.11215(3)	0.02377(17)	1
Nd2	0.13530(4)	0.12139(4)	0.29337(3)	0.02188(16)	1
Nd3	0.35795(4)	0.12045(3)	0.17754(3)	0.02502(16)	1
Nd4	0.09650(4)	0.32413(3)	0.23543(3)	0.02495(16)	1

Dr. K. Harms (Chemistry Department University of Marburg)

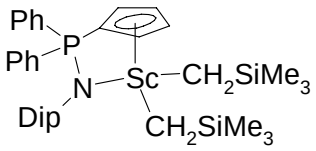

Table 49. Crystal data and structure refinement for complex $[(Ph_2P(C_5H_4)NDip)SCCH_2SiMe_3)_2]$ (**C7**).

Crystal data:

Identification code	apr02	
Habitus, color	block, colorless	
Crystal size	0.41 x 0.39 x 0.19 mm^3	
Crystal system	Monoclinic	
Space group	P $2_1/n$	Z = 4
Unit cell dimensions	a = 12.8408(8) Å	α = 90°
	b = 19.0640(9) Å	β = 102.747(4)°
	c = 16.0056(8) Å	γ = 90°
Volume	3821.6(4) $Å^3$	
Cell determination	30951 peaks with Theta 1.7 to 26.2°	
Empirical formula	$C_{37}H_{53}NPScSi_2$	
Formula weight	643.91	
Density (calculated)	1.119 Mg/m^3	
Absorption coefficient	0.321 mm^{-1}	
F(000)	1384	

Data collection:

Diffractometer type	IPDS2
Wavelength	0.71073 Å
Temperature	193(2) K
Theta range for data collection	1.69 to 25.00°
Index ranges	-15<=h<=15, -22<=k<=22, -19<=l<=19
Data collection software	STOE WinXpose (X-Area)
Cell refinement software	STOE WinCell (X-Area)
Data reduction software	STOE WinIntegrate (X-Area)

Solution and refinement:

Reflections collected	48835
Independent reflections	6735 [R(int)= 0.0410]
Completeness to theta = 25.00°	100.0%
Observed reflections	4854 [I > 2sigma(I)]
Reflections used for refinement	6735
Extinction coefficient	0.00019(2)
Absorption correction	Integration
Max. and min. transmission	0.9561 and 0.8937
Largest diff. peak and hole	0.378 and -0.545 e.$Å^{-3}$
Solution	Direct
Refinement	Full-matrix least-squares on F^2
Treatment of hydrogen atoms	Calculate, fixed isotropic U's
Programs used	SIR-92
	SHELXL-97 (Sheldrick, 1997)
	Diamond 3.1, STOE IPDS2 software
Data / restraints / parameters	6735 / 204 / 487
Goodness-of-fit on F^2	0.922
R index (all data)	wR2 = 0.0834
R index conventional [I > 2sigma(I)]	R1 = 0.0355

Table 50. Atomic coordinates and equivalent isotropic displacement parameters ($Å^2$)for apr02. U(eq)is defined as one third of the trace of the orthogonalized U^{ij} tensor.

	x	y	z	U(eq)	Occupancy
Sc1	0.40351(3)	0.12410(2)	0.22788(2)	0.04318(12)	1
P1	0.36054(3)	0.08553(2)	0.39910(3)	0.02787(11)	1
Si1	0.2723(3)	0.08830(13)	0.0014(2)	0.0511(5)	0.795(5)
Si2	0.6017(2)	0.24416(15)	0.16788(16)	0.0520(5)	0.615(5)
N1	0.30053(11)	0.13571(8)	0.32140(9)	0.0315(3)	1
C1	0.44146(14)	0.03665(10)	0.34359(11)	0.0337(4)	1
C2	0.54585(16)	0.05609(10)	0.33698(13)	0.0410(5)	1
C3	0.56206(18)	0.03077(12)	0.25908(14)	0.0526(6)	1
C4	0.4698(2)	-0.00421(12)	0.21683(14)	0.0544(6)	1
C5	0.39459(17)	-0.00052(11)	0.26761(13)	0.0428(5)	1
C6	0.44420(13)	0.13042(9)	0.48943(11)	0.0303(4)	1
C7	0.43706(15)	0.11801(10)	0.57401(11)	0.0349(4)	1
C8	0.49886(17)	0.15610(11)	0.64042(13)	0.0457(5)	1
C9	0.56946(18)	0.20557(11)	0.62423(14)	0.0501(6)	1
C10	0.57986(16)	0.21723(11)	0.54129(14)	0.0461(5)	1
C11	0.51724(14)	0.18048(10)	0.47421(13)	0.0366(4)	1
C12	0.27452(14)	0.03012(10)	0.44519(11)	0.0329(4)	1
C13	0.28010(15)	-0.04274(10)	0.43935(13)	0.0408(5)	1
C14	0.21563(16)	-0.08413(12)	0.47808(16)	0.0530(6)	1
C15	0.14784(17)	-0.05406(13)	0.52338(16)	0.0557(6)	1
C16	0.14165(16)	0.01781(13)	0.52960(14)	0.0513(6)	1
C17	0.20392(15)	0.06036(11)	0.48997(13)	0.0406(5)	1
C18	0.20364(14)	0.17350(10)	0.32390(11)	0.0336(4)	1
C19	0.10342(15)	0.14065(11)	0.29393(12)	0.0407(5)	1
C20	0.01234(17)	0.17711(13)	0.30217(14)	0.0523(6)	1
C21	0.01723(19)	0.24327(13)	0.33698(15)	0.0578(6)	1
C22	0.11416(17)	0.27614(12)	0.36170(13)	0.0487(5)	1
C23	0.20882(16)	0.24304(10)	0.35472(11)	0.0381(5)	1
C24	0.08879(16)	0.07029(12)	0.24787(14)	0.0487(5)	1
C25	0.02908(19)	0.01583(13)	0.28982(16)	0.0621(6)	1
C26	0.0287(2)	0.08061(15)	0.15381(15)	0.0696(7)	1
C27	0.31207(16)	0.28408(10)	0.37776(12)	0.0412(5)	1
C28	0.3372(2)	0.30862(12)	0.47089(14)	0.0577(6)	1
C29	0.3103(2)	0.34632(12)	0.31676(16)	0.0608(6)	1
C30	0.3010(3)	0.13991(19)	0.10083(17)	0.0444(8)	0.795(5)
C31	0.1516(6)	0.1203(5)	-0.0783(6)	0.108(3)	0.795(5)
C32	0.3882(5)	0.0882(3)	-0.0495(4)	0.112(2)	0.795(5)
C33	0.2403(3)	-0.00452(17)	0.0232(2)	0.0844(13)	0.795(5)
C34	0.5221(4)	0.2167(3)	0.2453(3)	0.0434(12)	0.615(5)
C35	0.6759(8)	0.1666(4)	0.1398(8)	0.193(7)	0.615(5)
C36	0.7040(5)	0.3131(4)	0.2057(4)	0.132(3)	0.615(5)
C37	0.5167(4)	0.2807(3)	0.0689(3)	0.0927(19)	0.615(5)
C30A	0.2676(8)	0.1024(7)	0.1073(6)	0.038(3)	0.205(5)
C31A	0.1277(13)	0.1006(13)	-0.082(2)	0.076(9)	0.205(5)
C32A	0.3474(19)	0.0383(11)	-0.0395(16)	0.198(16)	0.205(5)
C33A	0.3149(13)	0.1941(8)	-0.0332(10)	0.122(8)	0.205(5)
C34A	0.4805(7)	0.2215(5)	0.2218(7)	0.067(3)	0.385(5)
C35A	0.6352(9)	0.3148(5)	0.1597(9)	0.144(5)	0.385(5)
C36A	0.6117(11)	0.1630(7)	0.1012(8)	0.144(7)	0.385(5)
C37A	0.7162(6)	0.2001(5)	0.2828(7)	0.145(6)	0.385(5)
Si1A	0.2623(12)	0.1062(6)	-0.0072(8)	0.081(4)	0.205(5)
Si2A	0.6058(4)	0.2237(3)	0.1910(4)	0.0821(14)	0.385(5)

Dr. B. Ziemer (Chemistry department, Humboldt-University Berlin)

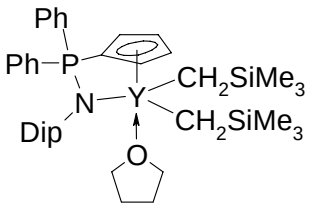

Table 51. Crystal data and structure refinement for yttrium complex [{$Ph_2P(C_5H_4)NDip$}$Y(CH_2SiMe_3)_2(thf)$] (**C9**)

Crystal data:

Identification code	ruf30	
Habitus, color	block, colorless	
Crystal size	0.50 x 0.40 x 0.30 mm^3	
Crystal system,	Triclinic	
Space group	P -1	Z = 2
Unit cell dimensions	a = 10.3990(6) Å	a = 102.967(5)°
	b = 11.2979(7) Å	b = 103.107(5)°
	c = 18.8584(11) Å	g = 100.256(5)°
Volume	2040.8(2) $Å^3$	
Cell determination	5000 peaks with 3.0 to 27.0°	
Empirical formula	$C_{41}H_{61}NOPSi_2Y$	
Formula weight	759.97	
Density (calculated)	1.237 Mg/m^3	
Absorption coefficient	1.557 mm^{-1}	
F(000)	808	

Data collection:

Diffractometer type	IPDS2.87
Wavelength	0.71073 Å
Temperature	100(2) K
Theta range for data collection	3.67 to 27.50°
Index ranges	-13<=h<=13, -14<=k<=14, 0<=l<=24
Data Collection Software	IPDS2.87 (Stoe & Cie, 1997)
Cell Refinement Software	IPDS2.87 (Stoe & Cie, 1997)
Data Reduction Software	IPDS2.87 (Stoe & Cie, 1997)

Solution and refinement:

Reflections collected	32491
Independent reflections	9297 [R(int)= 0.0655]
Completeness to theta = 27.50	98.9%
Observed reflections	8299 [I > 2sigma(I)]
Reflections used for refinement	9297
Extinction coefficient	0.0003(4)
Absorption collection	numerical
Max. and min. transmission	0.6523 and 0.5098
Largest diff. peak and hole	0.576 and -0.560 e.$Å^{-3}$
Refinement	Full-matrix least-squares on F^2
Programs used	SHELXS-97 (Sheldrick, 1990) SHELXL-97 (Sheldrick, 1997) DIAMOND (Brandenburg, 1999)
Data / restraints / parameters	9297 / 0 / 435
Goodness-of-fit on F^2	1.116
R indices (all data)	wR2 = 0.0799
R indices conventional [I > 2sigma(I)]	R1 = 0.0389

Table 52. Atomic coordinates (x 10^4)and equivalent isotropic displacement parameters ($Å^2$x 10^3) for ruf30. U(eq)is defined as one third of the trace of the orthogonalized U^{ij} tensor.

	x	y	z	U(eq)	Occupancy
C1	8506(2)	8812(2)	8376(1)	9(1)	1
C2	7319(2)	8921(2)	7859(1)	11(1)	1
C3	7737(2)	9750(2)	7462(1)	13(1)	1
C4	9174(2)	10153(2)	7713(1)	12(1)	1
C5	9655(2)	9583(2)	8277(1)	10(1)	1
C6	7015(2)	7599(2)	5867(1)	13(1)	1
C7	5871(3)	8398(3)	4421(2)	26(1)	1
C8	8090(4)	10231(3)	5693(2)	45(1)	1
C9	8659(4)	7916(4)	4743(2)	53(1)	1
C10	10882(2)	7827(2)	6889(1)	13(1)	1
C11	12242(3)	10660(2)	7217(2)	24(1)	1
C12	13548(2)	8752(2)	6483(1)	18(1)	1
C13	13612(2)	9106(2)	8113(1)	21(1)	1
C14	7462(2)	7339(2)	9334(1)	11(1)	1
C15	7307(2)	6273(2)	9604(1)	14(1)	1
C16	6598(2)	6207(2)	10143(1)	21(1)	1
C17	6063(2)	7197(3)	10424(1)	23(1)	1
C18	6214(2)	8247(2)	10155(1)	22(1)	1
C19	6908(2)	8324(2)	9611(1)	16(1)	1
C20	10214(2)	7714(2)	9335(1)	10(1)	1
C21	11317(2)	7603(2)	9042(1)	13(1)	1
C22	12605(2)	7787(2)	9525(1)	16(1)	1
C23	12802(2)	8099(2)	10305(1)	16(1)	1
C24	11722(2)	8249(2)	10605(1)	16(1)	1
C25	10431(2)	8057(2)	10122(1)	12(1)	1
C26	6996(2)	4522(2)	6014(1)	15(1)	1
C27	6792(3)	3938(2)	5184(1)	24(1)	1
C28	8218(3)	3878(2)	5155(2)	26(1)	1
C29	9062(2)	5116(2)	5704(1)	18(1)	1
C30	7442(2)	5106(2)	7849(1)	8(1)	1
C31	6017(2)	4740(2)	7748(1)	11(1)	1
C32	5423(2)	3484(2)	7646(1)	15(1)	1
C33	6187(2)	2596(2)	7640(1)	19(1)	1
C34	7567(2)	2955(2)	7730(1)	16(1)	1
C35	8216(2)	4198(2)	7832(1)	12(1)	1
C36	5088(2)	5643(2)	7716(1)	13(1)	1
C37	4263(3)	5480(3)	6904(2)	28(1)	1
C38	4111(2)	5496(2)	8209(1)	21(1)	1
C39	9731(2)	4520(2)	7914(1)	15(1)	1
C40	10531(2)	4446(2)	8686(2)	24(1)	1
C41	10113(3)	3676(2)	7274(2)	24(1)	1
N	8069(2)	6384(2)	7924(1)	9(1)	1
O	8329(2)	5415(1)	6273(1)	12(1)	1
P	8525(1)	7480(1)	8709(1)	7(1)	1
Si1	7392(1)	8508(1)	5211(1)	20(1)	1
Si2	12487(1)	9037(1)	7163(1)	11(1)	1
Y	8588(1)	7554(1)	7024(1)	6(1)	1

Dr. B. Ziemer (Chemical Department, Humboldt-University Berlin)

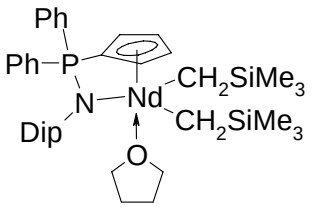

Table 53. Crystal data and structure refinement for complex [{$Ph_2P(C_5H_4)$NDip}Nd(CH_2SiMe_3)$_2$(thf)] (**C10**).

Crystal data:

Identification code	ruf21	
Habitus, color	block, green	
Crystal size	0.72 x 0.60 x 0.40 mm^3	
Crystal system	Triclinic	
Space group	P -1	Z = 2
Unit cell dimensions	a = 10.5185(15) Å	α = 103.105(17)°
	b = 11.4565(16) Å	β = 103.463(17)°
	c = 19.097(3) Å	γ = 100.589(16)°
Volume	2110.7(5) $Å^3$	
Cell determination	5000 peaks with 3.0 to 25.0°	
Empirical formula	$C_{41}H_{61}NNdOPSi_2$	
Formula weight	815.30	
Density (calculated)	1.283 Mg/m^3	
Absorption coefficient	1.354 mm^{-1}	
F(000)	850	

Data collection:

Diffractometer type	IPDS2.87
Temperature	180(2) K
Wavelength	0.71073 Å
Theta range for data collection	2.29 to 25.92°
Index ranges	-12<=h<=12, -14<=k<=14, -23<=l<=23
Data Collection Software	IPDS2.87 (Stoe & Cie, 1997)
Cell Refinement Software	IPDS2.87 (Stoe & Cie, 1997)
Data Reduction Software	IPDS2.87 (Stoe & Cie, 1997)

Solution and Refinement:

Reflections collected	21546
Independent reflections	7630 [R(int)= 0.0404]
Completeness to theta = 25.92°	92.8%
Observed reflections	6949 [I > 2sigma(I)]
Reflections used for refinement	7630
Extinction coefficient	0.009(3)
Absorption correction	None
Max. and min. transmission	0.6134 and 0.4422
Largest diff. peak and hole	0.517 and -0.463 e.$Å^{-3}$
Solution	direct
Refinement	Full-matrix least-squares on F^2
Programs used	SHELXS-97 (Sheldrick, 1990)
	SHELXL-97 (Sheldrick, 1997)
	DIAMOND (Brandenburg, 1999)
Data / restraints / parameters	7630 / 0 / 424
Goodness-of-fit on F^2	1.026
R index (all data)	wR2 = 0.0572
R index conventional [I > 2sigma(I)]	R1 = 0.0232

Table 54. Atomic coordinates (x 10^4)and equivalent isotropic displacement parameters ($Å^2$x 10^3)for ruf21. U(eq)is defined as one third of the trace of the orthogonalized U^{ij} tensor.

	x	y	z	U(eq)	Occupancy
C1	2490(2)	2646(2)	-4349(1)	23(1)	1
C2	2675(2)	3695(3)	-4610(1)	31(1)	1
C3	3392(3)	3753(3)	-5135(2)	41(1)	1
C4	3900(3)	2769(4)	-5401(2)	48(1)	1
C5	3732(3)	1734(3)	-5144(2)	43(1)	1
C6	3023(2)	1660(3)	-4617(1)	31(1)	1
C7	-238(2)	2272(2)	-4345(1)	21(1)	1
C8	-488(2)	1929(2)	-5123(1)	26(1)	1
C9	-1768(3)	1731(3)	-5590(1)	33(1)	1
C10	-2828(2)	1882(3)	-5291(1)	33(1)	1
C11	-2607(2)	2197(3)	-4520(1)	32(1)	1
C12	-1324(2)	2387(2)	-4046(1)	27(1)	1
C13	1469(2)	1211(2)	-3391(1)	20(1)	1
C14	334(2)	423(2)	-3305(1)	22(1)	1
C15	814(2)	-149(2)	-2756(1)	26(1)	1
C16	2237(2)	256(2)	-2505(1)	26(1)	1
C17	2642(2)	1097(2)	-2885(1)	22(1)	1
C18	-950(2)	2143(2)	-1882(1)	29(1)	1
C19	-3627(3)	877(3)	-3112(2)	47(1)	1
C20	-2261(3)	-653(3)	-2231(2)	55(1)	1
C21	-3621(3)	1180(3)	-1517(2)	37(1)	1
C22	3019(3)	2415(2)	-846(1)	30(1)	1
C23	1871(5)	-162(4)	-696(2)	82(1)	1
C24	1394(5)	2147(5)	264(3)	90(2)	1
C25	4097(3)	1590(4)	590(2)	60(1)	1
C26	995(3)	4946(3)	-662(2)	50(1)	1
C27	1866(4)	6087(5)	-84(3)	108(2)	1
C28	3062(4)	6368(5)	-240(2)	111(2)	1
C29	2985(3)	5615(3)	-983(1)	35(1)	1
C30	2530(2)	4897(2)	-2883(1)	20(1)	1
C31	3947(2)	5266(2)	-2764(1)	24(1)	1
C32	4540(3)	6500(2)	-2661(2)	33(1)	1
C33	3797(3)	7386(3)	-2655(2)	41(1)	1
C34	2430(3)	7030(2)	-2759(2)	36(1)	1
C35	1777(2)	5804(2)	-2870(1)	26(1)	1
C36	4839(2)	4354(2)	-2726(1)	27(1)	1
C37	5554(4)	4451(3)	-1917(2)	52(1)	1
C38	5880(3)	4523(3)	-3165(2)	46(1)	1
C39	264(3)	5480(3)	-2966(2)	36(1)	1
C40	-512(3)	5567(4)	-3718(2)	60(1)	1
C41	-105(3)	6303(3)	-2320(2)	56(1)	1
N	1898(2)	3636(2)	-2965(1)	18(1)	1
Nd	1393(1)	2480(1)	-2013(1)	17(1)	1
O	1702(2)	4681(2)	-1229(1)	30(1)	1
P	1443(1)	2525(1)	-3727(1)	17(1)	1
Si1	-2540(1)	933(1)	-2169(1)	26(1)	1
Si2	2620(1)	1522(1)	-200(1)	41(1)	1

Dr. B. Ziemer (Chemical Department, Humboldt-University Berlin)

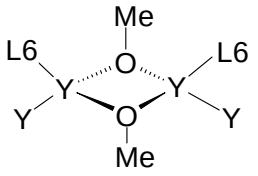

Table 55. Crystal data and structure refinement for binuclear complex $[\{Ph_2P(C_5H_4)NDip\}Y(CH_2SiMe_3)(\mu\text{-}OMe)]_2$ (**C11** x Et_2O).

Crystal data:

Identification code	ruf29neu	
Habitus, color	prism, pale yellow	
Crystal size	0.35 x 0.30 x 0.20 mm^3	
Crystal system	Monoclinic	
Space group	P $2_1/n$	Z = 4
Unit cell dimensions	a = 16.8339(9) Å	α = 90°
	b = 23.9480(18) Å	β = 100.137(4)°
	c = 18.0138(10) Å	γ = 90°
Volume	7148.7(8) $Å^3$	
Cell determination	5000 peaks with 4 to 25.0°	
Empirical formula	$C_{72}H_{100}N_2O_3P_2Si_2Y_2$	
Formula weight	1337.48	
Density (calculated)	1.243 Mg/m^3	
Absorption coefficient	1.738 mm^{-1}	
F(000)	2824	

Data collection:

Diffractometer type	IPDS2.87
Wavelength	0.71073 Å
Temperature	100(2) K
Theta range for data collection	3.50 to 26.00°
Index ranges	-20<=h<=20, -29<=k<=29, -22<=l<=22
Data Collection Software	IPDS2.87 (Stoe & Cie, 1997)
Cell Refinement Software	IPDS2.87 (Stoe & Cie, 1997)
Data Reduction Software	IPDS2.87 (Stoe & Cie, 1997)

Solution and Refinement:

Reflections collected	56916
Independent reflections	13828 [R(int)= 0.2386]
Completeness to theta = 26.00°	98.4%
Observed reflections	9490 [I > 2sigma(I)]
Reflections used for refinement	13828
Extinction coefficient	0.009(2)
Absorption correction	Numerical
Max. and min. transmission	0.7225 and 0.5813
Largest diff. peak and hole	0.969 and -0.849 e.$Å^{-3}$
Solution	direct
Refinement	Full-matrix least-squares on F^2
Programs used	SHELXS-97 (Sheldrick, 1990)
	SHELXL-97 (Sheldrick, 1997)
	DIAMOND (Brandenburg, 1999)
Data / restraints / parameters	13828 / 31 / 748
Goodness-of-fit on F^2	1.110
R index (all data)	wR2 = 0.2080
R index conventional [I > 2sigma(I)]	R1 = 0.0906

Table 56. Atomic coordinates (x 10^4)and equivalent isotropic displacement parameters ($Å^2$x 10^3)for ruf29neu. U(eq)is defined as one third of the trace of the orthogonalized U^{ij} tensor.

	x	y	z	U(eq)	Occupancy
C1	1077(4)	5305(3)	4112(4)	19(1)	1
C2	1158(4)	5861(3)	4377(4)	18(1)	1
C3	1972(4)	5980(3)	4596(4)	24(2)	1
C4	2410(4)	5501(3)	4463(4)	26(2)	1
C5	1872(4)	5087(3)	4162(4)	23(2)	1
C6	1097(5)	6665(3)	2592(4)	25(2)	1
C7	862(7)	7949(4)	2336(6)	56(3)	1
C8	374(5)	7394(3)	3674(5)	38(2)	1
C9	2140(5)	7523(4)	3565(6)	40(2)	1
C10	-642(4)	5435(3)	3627(4)	17(1)	1
C11	-1266(4)	5183(3)	3938(4)	20(2)	1
C12	-1952(4)	5484(3)	4020(4)	28(2)	1
C13	-1994(5)	6047(3)	3842(5)	32(2)	1
C14	-1379(4)	6303(3)	3545(4)	28(2)	1
C15	-709(4)	6005(3)	3454(4)	19(1)	1
C16	-3(4)	4334(3)	3643(4)	20(2)	1
C17	374(4)	4033(3)	4266(4)	20(2)	1
C18	142(5)	3487(3)	4368(5)	31(2)	1
C19	-486(5)	3247(3)	3863(5)	32(2)	1
C20	-863(5)	3540(3)	3253(5)	33(2)	1
C21	-627(4)	4076(3)	3130(5)	25(2)	1
C22	226(4)	4853(3)	1995(4)	16(1)	1
C23	626(4)	4352(3)	1844(4)	23(2)	1
C24	381(5)	4089(3)	1151(4)	28(2)	1
C25	-237(5)	4299(3)	620(5)	33(2)	1
C26	-629(4)	4782(3)	777(4)	26(2)	1
C27	-395(4)	5060(3)	1464(4)	19(1)	1
C28	1312(4)	4089(3)	2396(4)	23(2)	1
C29	1167(5)	3466(3)	2534(5)	35(2)	1
C30	2111(5)	4148(3)	2116(5)	33(2)	1
C31	-867(4)	5583(3)	1599(4)	21(2)	1
C32	-1699(4)	5440(4)	1759(5)	32(2)	1
C33	-948(5)	6002(3)	942(5)	34(2)	1
C34	1392(5)	5650(3)	1266(5)	31(2)	1
C35	3443(6)	6243(4)	3395(7)	55(3)	1
C36	2763(4)	4964(3)	653(4)	23(2)	1
C37	2856(4)	5404(3)	178(4)	23(2)	1
C38	3664(4)	5575(3)	312(4)	22(2)	1
C39	4086(4)	5230(3)	904(4)	19(1)	1
C40	3512(4)	4850(3)	1112(4)	20(2)	1
C41	3101(4)	6804(3)	1349(4)	23(2)	1
C42	2562(6)	7957(4)	626(6)	44(2)	1
C43	1587(6)	6943(5)	147(7)	63(3)	1
C44	3217(7)	7101(4)	-287(6)	57(3)	1
C45	5661(4)	4835(3)	1746(4)	22(2)	1
C46	5454(4)	4307(3)	1421(4)	24(2)	1
C47	5971(5)	3863(3)	1615(5)	33(2)	1
C48	6697(5)	3937(3)	2123(5)	32(2)	1
C49	6893(4)	4459(3)	2440(5)	29(2)	1
C50	6376(4)	4905(3)	2251(4)	22(2)	1
C51	5511(4)	5896(3)	984(4)	20(1)	1
C52	6241(4)	5750(3)	760(4)	23(2)	1
C53	6631(4)	6140(3)	370(4)	25(2)	1
C54	6289(4)	6644(3)	163(4)	26(2)	1
C55	5552(5)	6784(3)	359(4)	23(2)	1
C56	5172(4)	6412(3)	779(4)	21(2)	1

C57	5109(4)	5752(3)	2954(4)	16(1)	1
C58	5482(4)	6268(3)	3190(4)	16(1)	1
C59	5866(4)	6329(3)	3921(4)	21(2)	1
C60	5903(4)	5910(3)	4447(4)	23(2)	1
C61	5545(4)	5402(3)	4217(4)	23(2)	1
C62	5148(4)	5307(3)	3480(4)	19(1)	1
C63	5485(4)	6747(3)	2644(4)	23(2)	1
C64	6330(5)	6833(3)	2449(4)	30(2)	1
C65	5184(6)	7297(3)	2935(5)	43(2)	1
C66	4748(5)	4744(3)	3283(4)	24(2)	1
C67	3929(5)	4719(3)	3540(5)	30(2)	1
C68	5274(5)	4253(3)	3632(5)	34(2)	1
C69	-1756(11)	7450(5)	1971(8)	104(5)	1
C70	-1876(15)	7812(8)	1329(10)	170(9)	1
C71	-804(13)	7595(12)	592(11)	186(10)	1
C72	-640(11)	7543(10)	-195(10)	154(9)	1
N1	532(3)	5151(2)	2679(3)	16(1)	1
N2	4643(3)	5687(2)	2216(3)	17(1)	1
O1	1912(4)	5606(2)	1823(4)	32(1)	1
O2	3017(4)	5977(3)	2930(4)	36(2)	1
O3	-1558(12)	7718(9)	690(8)	231(9)	1
P1	243(1)	5049(1)	3472(1)	15(1)	1
P2	4982(1)	5420(1)	1510(1)	17(1)	1
Si1	1125(1)	7359(1)	3030(1)	26(1)	1
Si2	2637(1)	7185(1)	496(1)	28(1)	1
Y1	1684(1)	5783(1)	2989(1)	17(1)	1
Y2	3197(1)	5829(1)	1704(1)	18(1)	1

Dr. K. Harms (Chemistry Department, University of Marburg)

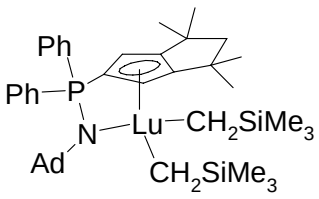

Table 57. Crystal data and structure refinement for complex $[(Ph_2PCp^{TM}NAd)Lu(CH_2SiMe_3)_2]$ (**C13**).

Crystal data:

Identification code	apc_tm	
Habitus, color	prism, colorless	
Crystal size	0.18 x 0.15 x 0.15 mm^3	
Crystal system	Tricinic	
Space group	P -1	Z =2
Unit cell dimensions	a = 10.8236(8) Å	α = 93.599(9)°
	b = 12.8149(9) Å	β = 103.167(8)°
	c = 17.0962(13) Å	γ = 91.998(8)°
Volume	2301.5(3) $Å^3$	
Cell determination	5000 peaks with 2.0 to 25.0°	
Empirical formula	$C_{48}H_{69}LuNPSi_2$	
Formula weight	922.16	
Density (calculated)	1.331 Mg/m^3	
Absorption coefficient	2.263 mm^{-1}	
F(000)	956	

Data collection:

Diffractometer type	IPDS1
Temperature	193(2) K
Wavelength	0.71073 Å
Theta range for data collection	2.08 to 25.00°
Index ranges	-12<=h<=12, -15<=k<=15, -20<=l<=20
Data collection software	STOE WinXpose (X-Area)
Cell refinement software	STOE WinCell (X-Area)
Data reduction software	STOE WinIntegrate (X-Area)

Solution and Refinement:

Reflections collected	20973
Independent reflections	7644 [R(int)= 0.0400]
Completeness to theta = 25.00°	94.2%
Observed reflections	6715 [I > 2sigma(I)]
Reflections used for refinement	7644
Extinction coefficient	0.00019(2)
Absorption correction	None
Max. and min. transmission	0.7277 and 0.6861
Largest diff. peak and hole	0.710 and -0.283 $e.Å^{-3}$
Solution	direct
Refinement	Full-matrix least-squares on F^2
Programs used	SHELXS-97 (Sheldrick, 1990)
	SHELXL-97 (Sheldrick, 1997)
	DIAMOND (Brandenburg, 1999)
Data / restraints / parameters	7644 / 0 / 478
Goodness-of-fit on F^2	0.925
R index (all data)	wR2 = 0.0370
R index conventional [I > 2sigma(I)]	R1 = 0.0182

Table 58. Atomic coordinates (x 10^4)and equivalent isotropic displacement parameters ($Å^2$x 10^3)for apc_tm. U(eq)is defined as one third of the trace of the orthogonalized U^{ij} tensor.

	x	y	z	U(eq)	Occupancy
C1	2518(3)	1254(2)	6276(1)	24(1)	1
C2	2939(3)	2004(2)	5790(1)	26(1)	1
C3	1850(3)	2477(2)	5386(1)	26(1)	1
C4	1476(3)	3169(2)	4692(1)	31(1)	1
C5	71(3)	3320(2)	4693(2)	35(1)	1
C6	-453(3)	2411(2)	5117(2)	33(1)	1
C7	792(3)	2060(2)	5619(1)	26(1)	1
C8	1180(3)	1298(2)	6169(1)	26(1)	1
C9	1638(3)	2590(2)	3912(2)	46(1)	1
C10	2246(3)	4212(2)	4811(2)	39(1)	1
C11	-1108(3)	1518(2)	4523(2)	53(1)	1
C12	-1374(3)	2814(2)	5601(2)	43(1)	1
C13	4395(2)	2090(2)	8613(1)	21(1)	1
C14	5149(3)	1158(2)	8950(1)	28(1)	1
C15	5842(3)	1433(2)	9828(1)	33(1)	1
C16	4872(3)	1654(2)	10325(2)	35(1)	1
C17	4113(3)	2579(2)	10010(1)	33(1)	1
C18	5017(3)	3542(2)	10069(2)	38(1)	1
C19	5986(3)	3320(2)	9573(1)	32(1)	1
C20	5301(3)	3052(2)	8694(1)	27(1)	1
C21	3439(3)	2319(2)	9125(1)	27(1)	1
C22	6749(3)	2390(2)	9884(2)	36(1)	1
C23	2908(3)	-263(2)	7495(1)	25(1)	1
C24	3364(3)	-1258(2)	7440(1)	32(1)	1
C25	2722(3)	-2103(2)	7664(2)	41(1)	1
C26	1653(3)	-1959(2)	7951(2)	45(1)	1
C27	1213(3)	-970(2)	8030(2)	43(1)	1
C28	1843(3)	-125(2)	7801(2)	34(1)	1
C29	4993(3)	531(2)	6813(1)	30(1)	1
C30	6148(3)	1064(2)	7112(2)	40(1)	1
C31	7195(4)	821(3)	6812(2)	55(1)	1
C32	7087(4)	50(3)	6209(2)	61(1)	1
C33	5944(4)	-476(3)	5895(2)	59(1)	1
C34	4882(3)	-242(2)	6187(2)	44(1)	1
C35	3148(3)	4707(2)	7067(2)	28(1)	1
C36	5760(3)	5737(2)	7852(2)	50(1)	1
C37	4517(3)	6237(2)	6172(2)	48(1)	1
C38	5563(3)	4130(2)	6483(2)	44(1)	1
C39	649(3)	3017(2)	7697(1)	27(1)	1
C40	1465(3)	4783(2)	9039(2)	47(1)	1
C41	-266(3)	5198(2)	7447(2)	45(1)	1
C42	-1246(3)	3958(3)	8621(2)	57(1)	1
C43	1654(6)	2211(5)	1526(4)	104(2)	1
C44	2124(5)	1293(6)	1600(3)	96(2)	1
C45	1969(5)	606(4)	987(4)	91(2)	1
C46	1317(5)	814(4)	263(3)	86(1)	1
C47	800(4)	1772(6)	160(3)	97(2)	1
C48	987(6)	2477(4)	813(5)	110(2)	1
N1	3716(2)	1913(1)	7751(1)	21(1)	1
Si1	4678(1)	5180(1)	6897(1)	31(1)	1
Si2	172(1)	4189(1)	8193(1)	28(1)	1
P1	3589(1)	887(1)	7154(1)	22(1)	1
Lu1	2311(1)	2983(1)	7023(1)	19(1)	1

Dr. K. Harms (Chemistry Department, University of Marburg)

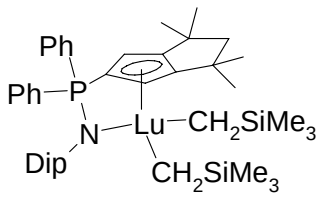

Table 59. Crystal data and structure refinement for complex [{$Ph_2PCp^{TM}NDip$}Lu(CH_2SiMe_3)$_2$] (**C14**).

Crystal data:

Identification code	apsk	
Habitus, color	prism, colorless	
Crystal size	0.18 x 0.12 x 0.09 mm^3	
Crystal system	Orthorhombic	
Space group	P bca	Z = 8
Unit cell dimensions	a = 19.2484(7) Å	α = 90°
	b = 20.4463(6) Å	β = 90°
	c = 23.1053(8) Å	γ = 90°
Volume	9093.3(5) $Å^3$	
Cell determination	28281 peaks with Theta 1.7 to 25.0°	
Empirical formula	$C_{44}H_{65}LuNPSi_2$	
Formula weight	870.09	
Density (calculated)	1.271 Mg/m^3	
Absorption coefficient	2.287 mm^{-1}	
F(000)	3600	

Data collection:

Diffractometer type	IPDS2
Wavelength	0.71073 Å
Temperature	173(2) K
Theta range for data collection	1.70 to 25.00°
Index ranges	-22<=h<=22, -24<=k<=24, -27<=l<=23
Data collection software	STOE WinXpose (X-Area)
Cell refinement software	STOE WinCell (X-Area)
Data reduction software	STOE WinIntegrate (X-Area)

Solution and refinement:

Reflections collected	48762
Independent reflections	8010 [R(int)= 0.0694]
Completeness to theta = 25.00°	100.0%
Observed reflections	5398 [I > 2sigma(I)]
Reflections used for refinement	8010
Extinction coefficient	0.00019(2)
Absorption correction	Semi-empirical from equivalents
Max. and min. transmission	0.762 and 0.7025
Largest diff. peak and hole	0.543 and -0.827 e.$Å^{-3}$
Solution	direct/ difmap
Refinement	Full-matrix least-squares on F^2
Treatment of hydrogen atoms	geom.., noref
Programs used	SIR-92
	SHELXL-97 (Sheldrick, 1997)
	Diamond 3.1, STOE IPDS2 software
Data / restraints / parameters	8010 / 0 / 485
Goodness-of-fit on F^2	0.866
R index (all data)	wR2 = 0.0452
R index conventional [I > 2sigma(I)]	R1 = 0.0309

Table 60. Atomic coordinates and equivalent isotropic displacement parameters ($Å^2$)for apsk. U(eq)is defined as one third of the trace of the orthogonalized U^{ij} tensor.

	x	y	z	U(eq)	Occupancy
C1	0.55538(18)	0.08989(18)	0.09156(16)	0.0263(9)	1
C2	0.59428(16)	0.1223(2)	0.04698(14)	0.0284(9)	1
C3	0.58930(18)	0.18988(19)	0.05746(17)	0.0290(9)	1
C4	0.6062(2)	0.2535(2)	0.02717(19)	0.0364(10)	1
C5	0.5823(2)	0.3038(2)	0.07293(19)	0.0405(10)	1
C6	0.52898(19)	0.27176(18)	0.11474(18)	0.0306(9)	1
C7	0.54704(18)	0.20009(18)	0.10641(16)	0.0265(8)	1
C8	0.52698(16)	0.13945(18)	0.12833(15)	0.0281(8)	1
C9	0.6839(2)	0.2618(2)	0.0135(2)	0.0518(13)	1
C10	0.5656(2)	0.2586(2)	-0.03004(19)	0.0504(12)	1
C11	0.5361(2)	0.2964(2)	0.17668(19)	0.0414(11)	1
C12	0.4534(2)	0.2841(2)	0.09510(19)	0.0414(10)	1
C13	0.77255(18)	0.1110(2)	0.11232(17)	0.0427(12)	1
C14	0.8642(6)	0.0102(7)	0.0579(5)	0.071(4)	0.439(9)
C15	0.9112(7)	0.1482(9)	0.0549(7)	0.094(7)	0.439(9)
C16	0.7923(2)	0.1123(3)	-0.02125(18)	0.0620(16)	1
C17	0.68708(19)	0.1971(2)	0.22722(16)	0.0351(9)	1
C18	0.7703(3)	0.0932(2)	0.2954(2)	0.0590(14)	1
C19	0.7477(2)	0.2258(2)	0.3484(2)	0.0499(11)	1
C20	0.8448(2)	0.2101(2)	0.2472(2)	0.0549(12)	1
C21	0.63717(18)	-0.01534(18)	0.21948(16)	0.0284(9)	1
C22	0.5977(2)	-0.0051(2)	0.27034(17)	0.0385(10)	1
C23	0.6093(2)	-0.0455(2)	0.31770(18)	0.0472(11)	1
C24	0.6582(3)	-0.0945(2)	0.31642(18)	0.0510(11)	1
C25	0.6978(2)	-0.1033(2)	0.26743(18)	0.0433(11)	1
C26	0.68893(18)	-0.0641(2)	0.21888(17)	0.0339(9)	1
C27	0.5441(2)	0.0492(2)	0.27568(19)	0.0530(13)	1
C28	0.5623(3)	0.0974(3)	0.3238(2)	0.0682(15)	1
C29	0.4710(2)	0.0225(3)	0.2863(2)	0.0734(17)	1
C30	0.7350(2)	-0.0753(2)	0.16695(18)	0.0396(10)	1
C31	0.8124(2)	-0.0727(3)	0.1833(2)	0.0594(14)	1
C32	0.7185(2)	-0.1397(2)	0.13667(18)	0.0531(12)	1
C33	0.60699(19)	-0.03656(19)	0.05778(17)	0.0304(9)	1
C34	0.5693(2)	-0.0878(2)	0.03235(17)	0.0387(10)	1
C35	0.5969(2)	-0.1236(2)	-0.01265(17)	0.0468(10)	1
C36	0.6624(3)	-0.1100(2)	-0.03288(17)	0.0512(11)	1
C37	0.7001(2)	-0.0587(2)	-0.00967(18)	0.0461(11)	1
C38	0.6730(2)	-0.0221(2)	0.03548(16)	0.0350(9)	1
C39	0.49554(18)	-0.03388(18)	0.13751(16)	0.0311(9)	1
C40	0.4301(2)	-0.0117(2)	0.12110(19)	0.0396(10)	1
C41	0.3723(2)	-0.0494(2)	0.1325(2)	0.0522(13)	1
C42	0.3785(2)	-0.1086(2)	0.15973(19)	0.0526(13)	1
C43	0.4426(2)	-0.1314(3)	0.17616(17)	0.0491(10)	1
C44	0.5014(2)	-0.0941(2)	0.16571(17)	0.0403(11)	1
N1	0.62574(14)	0.02601(14)	0.16993(12)	0.0258(7)	1
Si1	0.8321(3)	0.0959(4)	0.0516(2)	0.0500(15)	0.439(9)
Si2	0.75965(6)	0.18156(6)	0.27763(5)	0.0358(3)	1
P1	0.57239(5)	0.01014(5)	0.11740(4)	0.0267(2)	1
Lu1	0.66167(1)	0.12991(1)	0.14761(1)	0.02740(4)	1
C15A	0.8599(4)	0.2156(4)	0.0629(4)	0.058(3)	0.561(9)
C14A	0.9122(5)	0.0775(6)	0.0505(4)	0.066(3)	0.561(9)
Si1A	0.8314(2)	0.1287(2)	0.05347(16)	0.0388(8)	0.561(9)

M. Elfferding (Chemistry Department, Philipps-University Marburg)

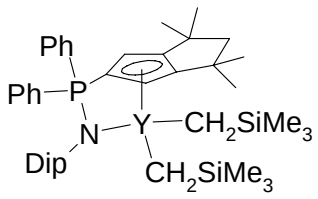

Table 61. Crystal data and structure refinement for complex $[(Ph_2P(Cp^{TM})NDip)Y(CH_2SiMe_3)_2]$ (**C15**).

Crystal data:

Identification code	hang11	
Habitus, color	prism, colorless	
Crystal size	0.30 x 0.27 x 0.15 mm^3	
Crystal system	orthorhombic	
Space group	P bca	Z = 1
Unit cell dimensions	a = 19.4018(13) Å	α = 90°
	b = 20.3212(12) Å	β = 90°
	c = 23.1462(14) Å	γ = 90°
Volume	9125.8(10) $Å^3$	
Cell determination	8000 peaks with Theta 1.75 to 25.9°	
Empirical formula	$C_{44}H_{65}NPSi_2Y$	
Formula weight	784.05	
Density (calculated)	1.141 Mg/m^3	
Absorption coefficient	1.394 mm^{-1}	
F(000)	3343	

Data collection:

Diffractometer type	IPDS1
Wavelength	0.71073 Å
Temperature	293(2) K
Theta range for data collection	1.70 to 26.10°
Index ranges	-23<=h<=23, -25<=k<=24, -28<=l<=28
Data collection software	STOE WinXpose (X-Area)
Cell refinement software	STOE WinCell (X-Area)
Data reduction software	STOE WinIntegrate (X-Area)

Solution and refinement:

Reflections collected	62596
Independent reflections	8995 [R(int)= 0.1237]
Completeness to theta = 26.10°	99.3%
Observed reflections	4850 [I > 2sigma(I)]
Reflections used for refinement	8995
Absorption correction	None
Largest diff. peak and hole	1.129 and -0.887 e.$Å^{-3}$
Solution	direct/ difmap
Refinement	Full-matrix least-squares on F^2
Treatment of hydrogen atoms	geom, mixed
Programs used	SHELSL-97 (Sheldrick, 1990) SHELXL-97 (Sheldrick, 1997) Diamond 3.1, STOE IPDS1 software
Data / restraints / parameters	8995 / 0 / 456
Goodness-of-fit on F^2	0.840
R index (all data)	wR2 = 0.1278
R index conventional [I > 2sigma(I)]	R1 = 0.0460

Table 62. Atomic coordinates and equivalent isotropic displacement parameters ($Å^2$)for hang11. U(eq)is defined as one third of the trace of the orthogonalized U^{ij} tensor.

	x	y	z	U(eq)	Occupancy
Y1	0.16181(2)	0.36864(2)	0.35049(2)	0.02763(11)	1
P1	0.07115(5)	0.48984(5)	0.38218(4)	0.0264(2)	1
Si1	0.33174(8)	0.38193(12)	0.44664(6)	0.0834(7)	1
Si2	0.25955(7)	0.31648(6)	0.22010(5)	0.0400(3)	1
N1	0.12341(16)	0.47520(16)	0.32975(13)	0.0262(7)	1
C4	0.3452(3)	0.2907(3)	0.2501(2)	0.0647(15)	1
C5	0.2492(3)	0.2729(2)	0.14927(19)	0.0542(13)	1
C6	0.2669(3)	0.4058(3)	0.2036(3)	0.0718(17)	1
C7	0.1884(2)	0.2984(2)	0.27017(17)	0.0373(10)	1
C8	0.2733(2)	0.3894(3)	0.38824(19)	0.0482(13)	1
C12	0.0354(2)	0.2028(2)	0.32368(18)	0.0431(11)	1
C11	-0.0467(2)	0.2152(2)	0.4047(2)	0.0441(11)	1
C10	0.0655(3)	0.2408(3)	0.52941(19)	0.0545(13)	1
C9	0.1824(3)	0.2375(3)	0.4854(2)	0.0570(14)	1
C13	0.0810(2)	0.1955(2)	0.42689(19)	0.0433(11)	1
C17	0.1050(2)	0.2460(2)	0.47263(17)	0.0357(10)	1
C14	0.0277(2)	0.2275(2)	0.38557(17)	0.0321(9)	1
C15	0.04580(19)	0.29923(19)	0.39316(15)	0.0264(9)	1
C16	0.08757(19)	0.3097(2)	0.44237(16)	0.0284(9)	1
C20	0.09344(19)	0.3773(2)	0.45208(15)	0.0287(9)	1
C19	0.05516(19)	0.41002(19)	0.40804(15)	0.0249(8)	1
C18	0.02598(19)	0.3600(2)	0.37146(16)	0.0281(9)	1
C21	0.1054(2)	0.5371(2)	0.44197(17)	0.0315(9)	1
C26	0.1710(2)	0.5228(2)	0.46307(16)	0.0371(10)	1
C25	0.1984(3)	0.5596(3)	0.50781(19)	0.0509(13)	1
C22	0.0679(2)	0.5879(2)	0.46723(17)	0.0388(11)	1
C23	0.0955(3)	0.6240(2)	0.51161(19)	0.0487(12)	1
C28	-0.0700(2)	0.5113(2)	0.3789(2)	0.0430(11)	1
C29	-0.1279(3)	0.5484(3)	0.3676(2)	0.0581(15)	1
C30	-0.1222(3)	0.6084(3)	0.3407(2)	0.0588(15)	1
C31	-0.0584(3)	0.6316(3)	0.3243(2)	0.0551(13)	1
C32	0.0000(2)	0.5939(2)	0.33492(18)	0.0427(11)	1
C33	0.1352(2)	0.51668(19)	0.28024(16)	0.0268(9)	1
C38	0.1871(2)	0.5645(2)	0.28043(17)	0.0334(10)	1
C37	0.1962(3)	0.6029(2)	0.2311(2)	0.0478(12)	1
C36	0.1574(3)	0.5939(3)	0.1828(2)	0.0540(13)	1
C35	0.1080(3)	0.5460(3)	0.18218(19)	0.0509(13)	1
C34	0.0951(2)	0.5063(2)	0.22982(18)	0.0397(11)	1
C42	0.2333(2)	0.5761(2)	0.33215(19)	0.0417(11)	1
C43	0.2158(3)	0.6403(3)	0.3622(2)	0.0571(14)	1
C44	0.3095(2)	0.5734(3)	0.3165(2)	0.0630(15)	1
C39	0.0408(3)	0.4536(3)	0.2257(2)	0.0572(15)	1
C41	-0.0309(3)	0.4810(3)	0.2123(3)	0.079(2)	1
C40	0.0590(3)	0.4020(3)	0.1798(3)	0.084(2)	1
C27	-0.0056(2)	0.5340(2)	0.36254(16)	0.0324(10)	1
C24	0.1604(3)	0.6100(3)	0.5318(2)	0.0562(14)	1
C2	0.2917(3)	0.3871(3)	0.5197(2)	0.0674(17)	1
C3	0.4026(7)	0.4368(11)	0.4482(4)	0.369(16)	1
C1	0.3698(7)	0.2962(8)	0.4397(4)	0.266(10)	1

Dr. K. Harms (Chemistry Department, University of Marburg)

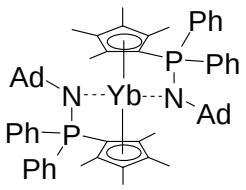

Table 63. Crystal data and structure refinement for complex of ytterbium (II)[($Ph_2P(C_5Me_4)NAd)_2Yb$] x ½Et_2O(**C18**).

Crystal data

Identification code	apryb1	
Habitus, color	prism, deep red	
Crystal size	0.24 x 0.24 x 0.15 mm^3	
Crystal system	Monoclinic	
Space group	P 2/n	Z = 2
Unit cell dimensions	a = 21.4860(9) Å	α = 90°
	b = 11.5448(3) Å	β = 106.194(3)°
	c = 23.6044(10) Å	γ = 90°
Volume	5622.8(4) $Å^3$	
Cell determination	62232 peaks with Theta 1.5 to 26.3°	
Empirical formula	$C_{66}H_{84}N_2OP_2Yb_2$	
Formula weight	1156.33	
Density (calculated)	1.366 Mg/m^3	
Absorption coefficient	1.764 mm^{-1}	
F(000)	2408	

Data collection:

Diffractometer type	IPDS2
Wavelength	0.71073 Å
Temperature	173(2) K
Theta range for data collection	1.51 to 25.94°
Index ranges	-26<=h<=26, -14<=k<=14, -29<=l<=29
Data collection software	STOE WinXpose (X-Area)
Cell refinement software	STOE WinCell (X-Area)
Data reduction software	STOE WinIntegrate (X-Area)

Solution and refinement:

Reflections collected	78030
Independent reflections	10932 [R(int)= 0.0465]
Completeness to theta = 25.00°	99.9%
Observed reflections	8915 [I > 2sigma(I)]
Reflections used for refinement	10932
Extinction coefficient	X = 0.00007(4)
Absorption correction	Integration
Max. and min. transmission	0.7579 and 0.6282
Largest diff. peak and hole	1.461 and -0.916 e.$Å^{-3}$
Solution	Direct methods
Refinement	Full-matrix least-squares on F^2
Treatment of hydrogen atoms	Calculated, riding, Ueq=1.2/1.5Ueq(C)
Programs used	SIR92 (Giacovazzo, 1993)
	SHELXL-97 (Sheldrick, 1997)
	Diamond 3.1, STOE IPDS2 software
Data / restraints / parameters	10932 / 0 / 661
Goodness-of-fit on F^2	0.947
R index (all data)	wR2 = 0.0598
R index conventional [I > 2sigma(I)]	R1 = 0.0258

Table 64. Atomic coordinates and equivalent isotropic displacement parameters ($Å^2$)for apryb1. U(eq)is defined as one third of the trace of the orthogonalized U^{ij} tensor.

	x	y	z	U(eq)	Occupancy
C1	0.27282(12)	0.1959(2)	0.36514(11)	0.0306(5)	1
C2	0.25754(13)	0.3090(2)	0.33927(11)	0.0334(6)	1
C3	0.18993(14)	0.3134(2)	0.31555(12)	0.0360(6)	1
C4	0.16258(13)	0.2058(3)	0.32639(11)	0.0343(6)	1
C5	0.21274(13)	0.1332(2)	0.35684(11)	0.0318(6)	1
C6	0.30138(15)	0.4115(2)	0.34344(13)	0.0425(7)	1
C7	0.15118(16)	0.4196(3)	0.29344(14)	0.0481(7)	1
C8	0.09130(14)	0.1841(3)	0.31611(14)	0.0449(7)	1
C9	0.20431(13)	0.0162(2)	0.38186(12)	0.0373(6)	1
C10	0.41407(13)	0.2205(2)	0.39561(11)	0.0325(6)	1
C11	0.44112(14)	0.2711(3)	0.45034(13)	0.0420(7)	1
C12	0.49039(17)	0.3517(3)	0.45803(15)	0.0518(8)	1
C13	0.51304(16)	0.3833(3)	0.41106(16)	0.0531(8)	1
C14	0.48694(16)	0.3335(3)	0.35628(15)	0.0471(7)	1
C15	0.43792(14)	0.2519(2)	0.34887(13)	0.0375(6)	1
C16	0.35926(12)	0.0597(2)	0.45719(11)	0.0314(6)	1
C17	0.40803(14)	-0.0188(3)	0.48271(12)	0.0381(6)	1
C18	0.41835(14)	-0.0548(3)	0.54044(12)	0.0424(7)	1
C19	0.38142(14)	-0.0096(3)	0.57464(12)	0.0415(7)	1
C20	0.33391(15)	0.0708(3)	0.55036(12)	0.0409(7)	1
C21	0.32301(13)	0.1054(2)	0.49250(11)	0.0348(6)	1
C22	0.37445(13)	-0.0690(2)	0.31963(11)	0.0322(6)	1
C23	0.35576(15)	-0.0959(3)	0.25375(12)	0.0432(7)	1
C24	0.38976(16)	-0.2057(3)	0.24115(15)	0.0566(9)	1
C25	0.37103(18)	-0.3084(3)	0.2736(2)	0.0720(12)	1
C26	0.39005(17)	-0.2836(3)	0.33974(18)	0.0590(9)	1
C27	0.46348(16)	-0.2650(3)	0.36194(17)	0.0561(9)	1
C28	0.48307(15)	-0.1639(3)	0.32857(14)	0.0431(7)	1
C29	0.44849(12)	-0.0536(2)	0.33960(12)	0.0333(6)	1
C30	0.46349(16)	-0.1881(3)	0.26223(15)	0.0535(8)	1
C31	0.35513(15)	-0.1738(2)	0.35121(15)	0.0434(7)	1
C32	0.25935(13)	0.8849(2)	0.64361(11)	0.0308(5)	1
C33	0.31738(13)	0.8180(2)	0.66681(11)	0.0313(6)	1
C34	0.36156(12)	0.8885(2)	0.70742(11)	0.0319(6)	1
C35	0.33207(12)	0.9982(2)	0.70966(11)	0.0313(5)	1
C36	0.26924(12)	0.9977(2)	0.67067(11)	0.0311(5)	1
C037	0.20101(17)	0.6983(3)	0.42278(13)	0.0486(8)	1
C37	0.33214(14)	0.6990(2)	0.64746(12)	0.0369(6)	1
C38	0.43181(13)	0.8614(3)	0.73480(13)	0.0385(6)	1
C39	0.36710(14)	1.1026(3)	0.74037(13)	0.0395(6)	1
C40	0.22629(14)	1.1033(2)	0.65773(13)	0.0379(6)	1
C41	0.12320(14)	0.9255(2)	0.58315(12)	0.0372(6)	1
C42	0.07972(14)	0.9430(3)	0.61557(14)	0.0435(7)	1
C43	0.03427(16)	1.0320(3)	0.60114(17)	0.0573(9)	1
C44	0.03323(19)	1.1035(3)	0.55437(19)	0.0676(12)	1
C45	0.07608(19)	1.0874(3)	0.52151(17)	0.0641(11)	1
C46	0.12116(16)	0.9977(3)	0.53498(14)	0.0485(8)	1
C47	0.19210(13)	0.7643(2)	0.53468(11)	0.0342(6)	1
C48	0.13947(15)	0.7130(3)	0.49338(12)	0.0410(6)	1
C49	0.14433(17)	0.6810(3)	0.43825(13)	0.0476(8)	1
C51	0.25283(16)	0.7511(3)	0.46247(13)	0.0462(7)	1
C52	0.24807(15)	0.7843(3)	0.51764(12)	0.0397(6)	1
C53	0.13527(13)	0.6209(2)	0.64740(11)	0.0311(5)	1
C54	0.13769(15)	0.5786(3)	0.70961(12)	0.0396(6)	1
C55	0.09812(16)	0.4672(3)	0.70744(13)	0.0488(8)	1
C56	0.02727(16)	0.4903(3)	0.67382(15)	0.0537(8)	1

C57	0.02377(15)	0.5298(3)	0.61107(14)	0.0452(7)	1
C58	0.05191(16)	0.4362(3)	0.57984(14)	0.0494(8)	1
C59	0.12243(16)	0.4122(3)	0.61394(13)	0.0456(7)	1
C60	0.16199(14)	0.5235(2)	0.61680(12)	0.0374(6)	1
C61	0.06332(13)	0.6418(2)	0.61483(13)	0.0369(6)	1
C62	0.12531(18)	0.3726(3)	0.67630(15)	0.0530(8)	1
C63	0.2285(2)	0.3934(4)	0.48433(16)	0.0720(11)	1
C64	0.1649(2)	0.3340(5)	0.46387(19)	0.0899(16)	1
C65	0.3225(2)	0.4072(4)	0.56329(19)	0.0720(11)	1
C66	0.3514(2)	0.3699(4)	0.6255(2)	0.0831(13)	1
N1	0.33780(10)	0.03558(18)	0.32659(9)	0.0302(5)	1
N2	0.17619(10)	0.72641(19)	0.65539(9)	0.0311(5)	1
P1	0.34613(3)	0.11841(6)	0.38241(3)	0.02790(14)	1
P2	0.18615(3)	0.81539(6)	0.60691(3)	0.03026(14)	1
Yb1	0.2500	0.14200(1)	0.2500	0.02955(5)	1
Yb2	0.2500	0.82621(1)	0.7500	0.02803(5)	1
O1	0.26201(13)	0.3533(2)	0.54107(10)	0.0567(6)	1

Dr. B. Ziemer (Chemical Department, Humboldt-University Berlin)

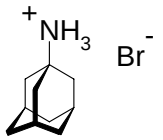

Table 65. Crystal data and structure refinement for 1-adamantylammonium bromide 1-AdNH_3^+ Br^-.

Crystal data:

Identification code	ruf15	
Habitus, color	needle, colorless	
Crystal size	0.68 x 0.28 x 0.24 mm^3	
Crystal system	Monoclinic	
Space group	P $2_1/n$	Z = 4
Unit cell dimensions	a = 11.300(3) Å	α = 90°
	b = 6.3301(9) Å	β = 103.54(3)°
	c = 14.778(3) Å	γ = 90°
Volume	1027.7(4) $Å^3$	
Cell determination	5000 peaks with 4 to 25°	
Empirical formula	$C_{10}H_{18}BrN$	
Formula weight	232.16	
Density (calculated)	1.501 Mg/m^3	
Absorption coefficient	3.949 mm^{-1}	
F(000)	480	

Data collection:

Diffractometer type	IPDS2.87
Wavelength	0.71073 Å
Temperature	180(2) K
Theta range for data collection	2.58 to 24.50°
Limiting indices	-13<=h<=13, -7<=k<=7, -17<=l<=17
Data Collection Software	IPDS2.87 (Stoe & Cie, 1997)
Cell Refinement Software	IPDS2.87 (Stoe & Cie, 1997)
Data Reduction Software	IPDS2.87 (Stoe & Cie, 1997)

Solution and refinement:

Reflections collected / unique	5961
Independent reflections	1693 [R(int)= 0.1017]
Completeness to theta = 24.50	98.9 %
Observed reflections	1126 [I > 2sigma(I)]
Reflections used for refinement	5961
Extinction coefficient	0.0040(17)
Absorption correction	numerical
Max. and min. transmission	0.4508 and 0.1743
Largest diff. peak and hole	1.154 and -1.084 e.$Å^{-3}$
Solution	direct
Refinement	Full-matrix least-squares on F^2
Treatment of hydrogen atoms	geom.., mixed
Programs used	SHELXS-97 (Sheldrick, 1990)
	SHELXL-97 (Sheldrick, 1997)
	DIAMOND (Brandenburg, 1999)
Data / restraints / parameters	1693 / 0 / 111
Goodness-of-fit on F^2	0.939
R index (all data)	wR2 = 0.1142
R index conventional [I > 2sigma(I)]	R1 = 0.0452

Table 66. Atomic coordinates (x 10^4)and equivalent isotropic displacement parameters ($Å^2$ x 10^3) for ruf15. U(eq) is defined as one third of the trace of the orthogonalized U^{ij} tensor.

	x	y	z	U(eq)	Occupancy
C1	10221(4)	2260(7)	-1890(3)	23(1)	1
C2	9313(4)	444(7)	-2104(3)	28(1)	1
C3	8922(4)	142(8)	-3163(3)	31(1)	1
C4	8309(5)	2194(7)	-3609(3)	36(1)	1
C5	9223(4)	4007(8)	-3380(3)	32(1)	1
C6	9611(4)	4301(7)	-2317(3)	28(1)	1
C7	11340(4)	1789(7)	-2257(3)	27(1)	1
C8	10953(4)	1505(8)	-3324(3)	30(1)	1
C9	10337(5)	3547(8)	-3763(3)	33(1)	1
C10	10033(5)	-337(7)	-3538(3)	33(1)	1
Br	8317(1)	2518(1)	184(1)	28(1)	1
N	10615(3)	2503(6)	-840(2)	27(1)	1